US-Korea Conference
Korean-American Scientists & Engineers Association (KSEA)

UKC 2023 Dallas

Discovery, Innovation and Dissemination for Transformative Impact

Proceeding

August 2-5, 2023
Hyatt Regency DFW
Dallas-Fort Worth, TX, USA
https://www.ukc.ksea.org

Co-Organized with
The Korean Federation of Science and Technology Societies (KOFST)
The Korea-U.S. Science Cooperation Center / National Research Foundation of Korea (KUSCO / NRF)

Papers from the 36th US-Korea Conference on Science, Technology and Entrepreneurship

Editors

Yongho Sohn, Conference Chair
University of Central Florida

Chang-Yong Nam, Program Chair
Brookhaven National Lab

Papers from the 36th US-Korea Conference on Science, Technology and Entrepreneurship
ISBN 978-1-958177-04-4

Published by KSEA (Korean-American Scientists and Engineers Association)
1952 Gallows Rd., Site 300, Vienna, VA 22182

Korean - American Scientists and Engineers
Association (KSEA)

UKC 2023

US - Korea Conference(UKC) 2023

https://www.ukc.ksea.org

Co-Organized with
The Korean Federation of Science and Technology Societies(KOFST) and
The Korea-U.S. Science Cooperation Center
National Research Foundation of Korea (KUSCO / NRF)

Table of Contents

UKC 2023 Organizers

Conference Chair / Co-chair

Yongho Sohn	University of Central Florida	UKC 2023 Chair
Tai Sik Lee	President of KOFST	UKC 2023 Co-Chair

Program, Executive, and Workshops

Chang-Yong Nam	Brookhaven National Lab	Program Chair
Sung Yun Jung	Baylor Medical College	Executive Director
Jayoung Kim	UCLA - CSMC	Executive Director 2
Soyoon Kum	Angelo State University	Financial Director
Juyoung Leem	University of Texas-Dallas	General Director
Taeyul Theo Choi	University of North Texas	Poster Session Chair
Sung-Hee Sonny Kim	University of Georgia	Sponsored Forum Director
Stella RH Kim	Data SC, Inc	Engagement Director
Sua Myong	Johns Hopkins University	SEED Director
Il Minn	Johns Hopkins University	IES Director
TJ (Tae Joong) Park	MIT	FIRE Director
Benjamin Lee	Weill Cornell Medicine	Data Science Workshop Chair

IT and Local Operations

Katie Sang Park		IT/Web Director
Jongwook Kim	University of Central Florida	IT/Web Assistance
Wooram Park	University of Texas-Dallas	Operation Director 1
In-Hyouk Song	Texas State University	Operation Director 2
Jung Hwan Kim	UT Health Houston	Operation Director 3
Nathan Han	Savills	Operation Director 4

Remarks from UKC 2023 Chair

Yongho Sohn Ph.D.

UKC 2023 Chair & President of KSEA (Korean-American Scientist and Engineers Association)

UCF Pegasus Professor & Lockheed Martin Professor of Engineering

Department of Materials Science and Engineering
University of Central Florida

Welcome to the 36th US-Korea Conference on Science, Technology, and Entrepreneurship (UKC 2023), jointly organized by the Korean-American Scientists and Engineers Association (KSEA), the Korean Federation of Science and Technology Societies (KOFST) and the Korea-US Science Cooperation Center (KUSCO) / National Research Foundation (NRF). As the Conference Chair, I am thrilled to host this extraordinary event where visionaries, innovators, and leaders from the United States and Korea gather to foster collaboration, exchange knowledge, and shape the future of our interconnected worlds. We embark on a journey that celebrates the spirit of collaboration, pushing the boundaries of knowledge and unleashing the power of innovation to create a transformative impact on our world.

Over the years, UKC has evolved into an iconic platform that celebrates the synergistic relationship between the United States and Korea, two nations renowned for their scientific advancements, technological breakthroughs, and entrepreneurial spirit. In Dallas, Texas, we gather to "*discover, innovate, and disseminate for transformative impact*" by converging brilliance and expertise of all invited and contributing participants who are at the forefront of scientific breakthroughs, technological advancements, entrepreneurial endeavors, and policy innovations. UKC 2023 offers unparalleled, cross-disciplinary platform of science, technology and entrepreneurship for participants to actively engage in various plenary sessions, keynote symposia, technical symposia, professional development workshops, and focused forums offered by conference sponsors and organizers.

The spirit of discovery drives our progress and plays pivotal role of the relentless pursuit of knowledge, the exploration of uncharted territories, and the curiosity that fuels our souls that cornerstones advancements. At the heart of our endeavors lies engineering and technological innovation that fuse creativity, expertise, and the courage to challenge conventions by driving transformative change that solve complex problems for the benefit of our lives. Dissemination by effective communication, collaboration, and the sharing of knowledge accelerates and amplifies our impact, while inspiring others to join our mission. Together, we will explore new frontiers, forge meaningful partnerships, and shape a future that is both prosperous and sustainable.

I extend my sincere gratitude to our co-organizers, sponsors, the organizing team members, and volunteers for their tireless efforts in making this conference a resounding success. Your unwavering support has enabled us to curate a program that promises to fulfill the vision and mission of UKC 2023.

I invite you to immerse yourself in the vibrant atmosphere of UKC 2023. Engage in stimulating conversations, form lasting connections, and embrace the spirit of collaboration that lies at the heart of this conference. Let us harness the power of discovery, innovation, and dissemination to create a transformative impact that will shape our world for generations to come.

Welcome to UKC 2023!

Yongho Sohn
UKC 2023 Chair and President of KSEA

Remarks from UKC 2023 Co-Chair

Tai Sik Lee

UKC 2023 Co-Chair &
President of KOFST
(Korean Federation of
Science and Technology
Societies)

It is truly an honor and pleasure to welcome all the scientists and engineers from home and abroad, who are joining us at the US-Korea Conference 2023 on Science, Technology, and Entrepreneurship (UKC-2023), bringing with them a passion as intense as the scorching summer in Texas.

As we commemorate the 70th anniversary of the ROK-U.S. alliance and the 120th anniversary of Korean immigration to the United States this year, I find it deeply meaningful that we are here to host the 36th UKC in Texas, which is emerging as a new hub for Korea-U.S. technological alliance. In order to survive in the accelerating race for technological hegemony, the world is putting forth every effort to secure competitiveness in science and technology. Consequently, the collaboration through international cooperation in science and technology has become more important than ever. Technology cooperation is being bolstered by technology alliance, and cooperative competition is taking place alongside technology competition.

Now, Korea and the U.S. are moving beyond a security alliance towards an advanced technology alliance. In line with this, I hope that Korean-American scientists and engineers can serve as a bridge of innovation which connects the two countries, and that the UKC will be further upgraded as a platform for joint research and collaboration in science and technology. The theme for this year's UKC is "*Discovery, Innovation and Dissemination for Transformative Impact*". I believe that the theme holds profound importance to the Korean economy, which is grappling with challenges after a phase of prosperity driven by the fast-follower model. Indeed, the essence and mission of science and technology is to spread innovation to the entire society through constant exploration and discovery. Nevertheless, we find ourselves in the midst of crisis as we turn away from challenges and innovation in a social atmosphere that feeds a fear of failure. Strangely enough, the science and technology community, which is unwilling to embrace uncertainty and risk, boasts an astonishing 100% success rate in national research and development.

However, a research that is predestined for success offers little promise for the future. We must boldly transition to become first movers who fearlessly venture into uncharted territories, utilizing numerous failures as stepping stones. The global triumph of K-pop and K-contents, exemplified by BTS and Squid Game, provides a clear indication of the path that K-science should strive towards.

I, myself, have dedicated significant time and effort to space construction, an area that initially garnered interest only from NASA. During my tenure as the President of the Korea Institute of Civil Engineering and Building Technology, we achieved a significant milestone by creating the largest lunar exploration technology and equipment test chamber (dusty thermal vacuum chamber), which was yet to be developed by NASA. It is worth noting that, only recently, other space power countries have commenced their research efforts in space construction. On the other hand, we have produced world-class research outcomes in this field as we took on the challenge as a first mover.

I hope that this year's UKC serves as a valuable opportunity for scientists and engineers to reflect on their mission, which is to fearlessly pioneer new territories, undaunted by the prospect of failure.

Lastly, I would like to express my deepest gratitude to the dedicated staff of the Korean-American Scientists and Engineers Association (KSEA), including President Yongho Sohn, for their tireless efforts in organizing this remarkable event. I hope that this conference will provide a meaningful venue to engage in intense discussions and share insightful ideas. Once again, I would like to extend a warm welcome to all of you who are with us today, and wish you all the best in your future endeavors.

Thank you.

Tai Sik Lee
President of the Korean Federation of Science and Technology Societies

Remarks from KUSCO/NRF President

Kwang Bok Lee

President of Korea-U.S. Science Cooperation Center

President of National Research Foundation of Korea

Dear Esteemed Guests, Ladies and Gentlemen,

It is my great honor to welcome you to the US-Korea Conference 2023. I would like to express my sincere appreciation to all the participants who have joined us for this year's Conference. I am truly grateful to the speakers, policymakers, and leaders of the academic and research communities for enhancing the significance of this event with their presence.

Furthermore, I extend my heartfelt gratitude to the Korean-American Scientists and Engineers Association and the Korean Federation of Science and Technology Societies, particularly President Yongho Sohn and President Taesik Lee, respectively, for their unwavering efforts in organizing this conference.

In today's world, international cooperation in science and technology plays a crucial role in addressing global challenges, driving innovation, and promoting sustainable development. By leveraging the strengths of different nations, sharing knowledge, and fostering collaboration, we can effectively tackle complex problems, accelerate scientific progress, and build a better future for the world.

This year we celebrate the 70th anniversary of the ROK-U.S. alliance. This partnership becomes even more critical in the face of a rapidly changing global landscape and intensifying technological competition. Recent State Visits and the Joint Committee Meeting on Science and Technology have further strengthened this collaboration. In this context, the role of Korean researchers in the United States holds utmost significance in promoting collaboration in science and technology.

The theme of UKC 2023 is "*Discovery, Innovation, and Dissemination for Transformative Impact*." In a world characterized by escalating competition and confrontation, we encounter various challenges and opportunities. In this era of transformation, it becomes imperative to seek innovative solutions that can profoundly impact our society and economy. Throughout this conference, we will explore the vital role of science, technology, and entrepreneurship in driving innovation and creating a transformative impact on our society.

I am truly confident that this conference will not only provide a platform for in-depth discussions and give us direction in this transformative era, but also offer an opportunity to strengthen the partnership between the two countries in the fields of science and technology. I hope that this event will offer you valuable insights and pave the way for fruitful collaborations.

Thank you once again for your participation in UKC 2023.

August 2023
Lee, Kwang Bok

President, Korea-U.S. Science Cooperation Center
President, National Research Foundation of Korea

Remarks from UKC 2023 Program Chair

Chang-Yong Nam

Scientist
Brookhaven National Laboratory

Greetings to all participants of the 36th US-Korea Conference on Science, Technology, and Entrepreneurship (UKC 2023).

As the annual flagship event of the Korean-American Scientists and Engineers Association (KSEA), UKC 2023 stands as a testament to the collaborative ties between the United States and Korea—two nations recognized for their contributions to scientific excellence, technological innovation, and enterprising spirit.

As the Program Chair, it is my great pleasure to extend a warm welcome to this distinguished gathering. At this event, esteemed experts, entrepreneurs, and policymakers from the United States and Korea come together to foster partnerships, exchange insights, and collectively shape the path of our interconnected world.

Set against the backdrop of the vibrant city of Dallas-Fort Worth, Texas, UKC 2023 centers around the theme, "*Discovery, Innovation, and Dissemination for Transformative Impact*", which aptly reflects the expertise of our invited participants and contributors, who are leaders in scientific advancements, technological progress, entrepreneurship, and policy innovation.

UKC 2023 presents a comprehensive program, featuring Plenary sessions, 4 Keynote Symposiums, and 14 Technical Group Symposiums. Additionally, it includes a dynamic Poster Session featuring nearly 130 poster presentations. Complemented by 9 Distinguished Forums, 8 Sponsor Forums, the Fostering Innovation in Rising Experts (FIRE) Symposium, the Innovation & Entrepreneurship Symposium (IES), the Data Science Workshop (DSW), and the Early Career Development (SEED) Workshop, this array captures the rich and diverse experience we aim to provide.

Lastly, I extend my heartfelt gratitude to our co-organizers, the dedicated members of the organizing team, the KSEA staff, and the volunteers. Their steadfast commitment has played a pivotal role in ensuring the success of UKC 2023.

With warm regards,
Chang-Yong Nam
UKC 2023 Program Chair

Technical Group A-1

Physics (PHY)

Spin Correlations and Bell's Inequality

Chueng-Ryong Ji[1]
[1]Department of Physics, North Carolina State University, Raleigh, NC 27695

I. SUMMARY

The orientation entanglement of the spins distinguishes quantum states of the particle. Currently, there are many practical applications of quantum orientation entanglement of the spins in the field of quantum technologies such as quantum computing and atomic clocks where the orientation of spin-state is squeezed to improve the precision.
I will discuss the foundation of the quantum mechanics with the spin correlation and the Bell's inequality as well as the debate on the quantum mechanical concept and the experimental evidence of quantum mechanical prediction defying the Bell's inequality based on the hidden variable theory as an alternative theory to the quantum mechanics.

II. BACKGROUND

Entanglement of spins is one of the most peculiar features which does not have a classical counterpart resulted in a debate in a series of conferences known as the Solvay conference over eight years (1927-1935). The final round of the debate was carried out in the so-called "EPR paradox"[1] and "Complementarity"[2] and the terminology "entanglement " was used to describe the correlation between the interacting particles.

Einstein, Podolsky, and Rosen considered the description of reality given by the wave function in the quantum mechanics is not complete[1] while Bohr's viewpoints the term "Complementarity" is explained from which quantum-mechanical description of phenomena is fulfilled within its scope. This debate ultimately led to formulate the Bell's inequality[3] that the local hidden-variable theory is satisfied but incompatible with quantum mechanics.

III. Bell's Inequality in "Hidden Variable Theory"

As alternative to quantum mechanics, the so called "Hidden Variable Theory" assumes that the dynamic behavior at the microscopic level appears probabilistic because some unknown parameters have not been specified. Do such theories make predictions different from those of quantum mechanics? John Stuart Bell in 1964 came up with a testable inequality relation known as the Bell's inequality. I will discuss how it can be derived from the spin correlation examples and how it doesn't hold in quantum mechanics as shown in Figure 1, where the quantum mechanical prediction shown by the blue curve goes over the maximally allowed upper bound from the Bell's inequality depicted by the yellow curve.

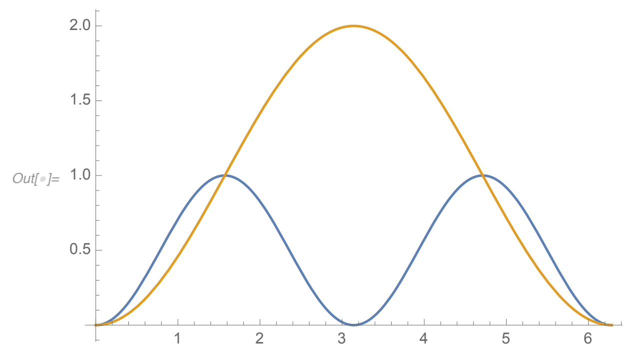

Figure 1: Violation of the Bell's Inequality in Quantum Mechanics

The Royal Swedish Academy of Sciences has decided to award the Nobel Prize in Physics 2022 to Alain Aspect, John F. Clauser and Anton Zeilinger "for experiments with entangled photons, establishing the violation of Bell inequalities and pioneering quantum information science". I'll discuss an example of experimental result[4] credited to the award of this Nobel Prize.

ACKNOWLEDGEMENTS

This work was supported in part by the U.S. Department of Energy under Grant No. DE-FG02-03ER41260.

REFERENCES

1. A. Einstein, B. Podolsky, and N. Rosen, Phys. Rev. 47 777 (1935)
2. N. Bohr, Phys. Rev. 48 696 (1935)
3. J.S. Bell,Physics Vol. 1, No.3, pp. 195-200(1964).
4. A. Aspect et al., Phys. Rev. Lett. 49, 91(1982).

From Quantum Physics to Quantum Computing

Alexander F. Kemper[1]
[1]North Carolina State University

Quantum computing has captured the imagination of scientists and engineers in industry and academia alike. The cloud accessible quantum computers have made it possible for anyone to go program a quantum computer, and the announcements of calculations that are beyond the capabilities of classical computers have inspired many to do so. In this talk, I'll give an introduction to the topic of quantum computing.

To start, I will motivate why we are working on quantum computers in the first place. Broadly speaking, we are starting to see the end of Moore's law, and new computational paradigms are starting to show promise in being able to tackle beyond-Moore problems. Quantum computing is one of these paradigms.

Quantum computation begins at the hardware level with a set of qubits – controllable two-level systems – that are made to interact. I will review some of the physical systems in use today, and some of the proposed future systems.

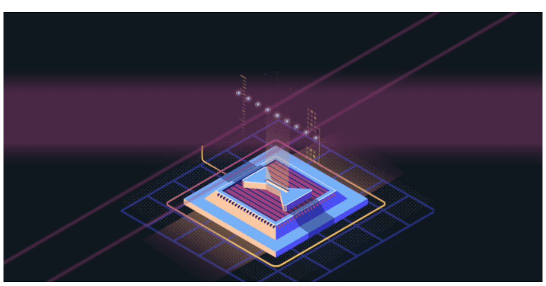

Figure 1: Artist illustration of a trapped ion quantum computer (courtesy of IonQ [1]).

The hardware is then used to run some software – a quantum program. Quantum program is quite different from classical programming; I will discuss some of the basics of quantum algorithms, including the circuit model of quantum computation.

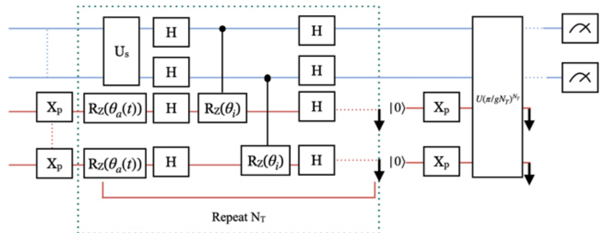

Figure 2: A quantum circuit (reproduced from Ref 2).

I will briefly discuss some of the basic quantum algorithms, and overview some of the standard algorithms in use today, and how they could potentially lead to speedups in computing.

REFERENCES

1. https://physicsworld.com/a/new-gate-optimization-strategy-could-boost-efficiency-in-trapped-ion-quantum-computers/
2. M. Metcalf, E. Stone, K. Klymko, A.F. Kemper, M. Sarovar, and W.A. de Jong, "Quantum Markov chain Monte Carlo with digital dissipative dynamics on quantum computers," *(2022) Quantum Science and Technology* ***7*** *025017*

DAMSA: A Novel Experiment Concept to Probe Dark Sector Particles

Wooyoung Jang and Jaehoon Yu
Department of Physics, University of Texas, Arlington, TX 76019, USA

I. Introduction

The search for dark sector particles has been a subject of significant interest in particle physics due to its potential to explain several long-standing mysteries in the universe. This paper introduces a novel experimental concept called Dump-produced Aboriginal Matter Searches at an Accelerator (DAMSA), a pioneering experimental challenge designed to tackle the dark sector particle searches at high-intensity proton accelerator facilities. Based on our benchmark physics model, searching for axion-like particle (ALP), I will discuss the overall key points of the experiment (See [1] for details).

II. DAMSA Experimental Setup

We describe the unique configuration of DAMSA, which involves strategically placing the detector in close proximity to a beam dump. This arrangement enhances the detection capabilities of signal events. DAMSA comprises three essential components: 1) the beam dump and neutron moderator, 2) the decay chamber and 3) a fast, precision angular resolution electromagnetic calorimeter. See Figure 1. for a visual representation of the experimental layout.

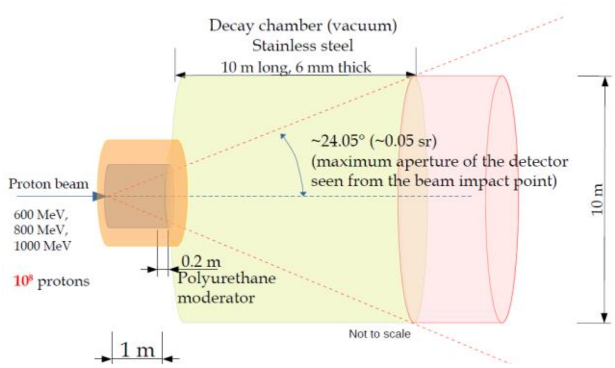

Figure 1: Experimental layout of DAMSA.

III. Beam-related Neutron Backgrounds Mitigation Strategies

The proximity of the detector to the target or interaction point introduces beam-related neutron (BRN) backgrounds. We analyze the BRN backgrounds and their potential impact on the detection of dark sector particles. Since the ALPs are unstable, they are decay into two photons. Therefore, we have investigated various physical quantities for all possible combinations of paired photon incidents to the detector. One such quantity is the distance of closest approach (DCA). The DCA is defined as the minimum distance between the trajectories of the two photons. A larger DCA indicates a higher likelihood of randomly paired photon pairs, while a smaller DCA suggests a higher possibility of a signal. In Table 1, we summarized the background mitigation strategies and their corresponding selection efficiencies that tells us background rejection capabilities.

Table 1. A summary of various selection cuts and their efficiencies that has been applied for BRN mitigation with different proton beam energy assumptions.

Cuts	Cut Efficiency		
	600 MeV	800 MeV	1 GeV
DCA < 10 cm	3.10e-3	2.98e-3	2.88e-3
dTOA < 0.1 ns	8.82e-3	9.38e-3	9.29e-3
Fiducial Volume	6.13e-1	6.13e-1	6.13e-1
Back Tracing	4.16e-2	4.18e-2	4.16e-2
Invariant Mass	1.88e-4	2.07e-4	2.61e-4

IV. Conclusion

We have presented an overview of the DAMSA experimental design and strategies to minimize the impact of BRN. The selection criteria introduced in Table 1, a rejection power of up to 10^{-13} can be expected for the ALP search program. Currently, efforts are underway to establish a collaboration and detailed simulation studies are being conducted.

REFERENCES

1. W. Jang et. al, “Search prospects for axionlike particles at rare nuclear isotope accelerator facilities”, Phys. Rev. D **107**, L031901 (2023).

COIFM Investigation of Self-Assembled Water Chains in Biomolecular Interactions

Byung I. Kim, Ryan D. Boehm, and Steven S. Heydendahl
Department of Physics, Boise State University

I. SUMMARY

We study one of the most challenging, but also one of the most important problems of sciences: the role of water in biomolecular functions. We measured the force-distance curves between biotin and avidin using the cantilever-based optical interfacial force microscope (COIFM) technology. The curves show large oscillatory forces as the tip approaches the surface. The oscillatory feature is analyzed with a model that describes a liquid crystal confined by two parallel planes. The analysis leads to the conclusion that both molecules are covered with hydration shells in the form of chain-like water.

II. Experiment, Data Analysis, and Discussion

A. Force-distance Measurement

We measured the force between biotin and avidin molecules to investigate their interactions in an aqueous environment. The molecules were tethered to a sample surface using bio-conjugate techniques utilizing glutaraldehyde for avidin and NHS-PEG for biotin. We used the COIFM to measure a force-distance curve of the biotinized tip approaching the avidinized silicon surface in liquid phosphate buffered saline (PBS). The force-distance curves show large oscillatory forces as the tip approaches the surface.

B. Analysis

The oscillatory force is analyzed with a model that describes the isotropic- smectic phase transition in liquid crystal systems. The smectic ordering contribution to the total free energy of an isotropic liquid crystal confined between parallel plates lying in the xy plane and located at $z = \pm d/2$ is calculated as follows:

$$F_{int}(d) = \frac{L_A A |\Psi_S|}{\xi_A}\left[\coth\left(\frac{d}{\xi_A}\right) - \frac{cos\left(\frac{2\pi d}{a_0}\right)}{\sinh\left(\frac{d}{\xi_A}\right)} - 1\right]$$

where L_A is the elastic coefficient, Ψ_S is the fixed smectic order parameter amplitude at z=0, A is the surface area of the plates, ξ_A is the smectic correlation length, and a_0 is the smectic period.

C. Discussion and Conclusion

The majority of biomolecular association reactions (e.g. protein associations) show a significant entropy increase upon association (a positive ΔS°). The entropy increase can be explained with a hydrogen bonded network known as a “hydration shell” that wraps each of two molecules. A biomolecular association reaction lowers the overall energy of the entire system because water molecules can be released from their entropically unfavorable intervening region to a favorable bulk region. Since the 1960s, the so-called iceberg model, proposed by Evans and Frank, has been a dominant mechanism to explain biomolecular interactions. The data and analysis lead to the following conclusion: Water in a hydration shell in the iceberg model should exist in the form of chain-like water.

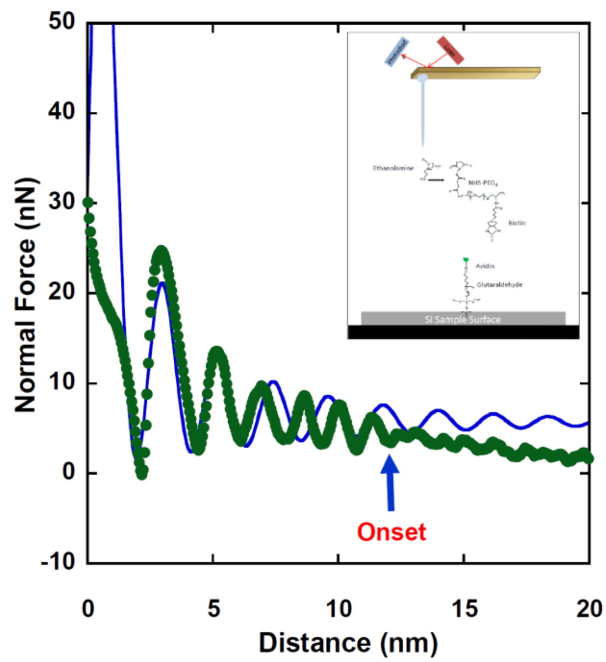

Figure 1: Force-distance curve with biotinized tip and avidinized surface. During approach, the oscillatory force with the periodicity of about 2.2 nm starts at the distance of 12 nm.

ACKNOWLEDGEMENTS

This research was supported by the Osher Faculty Grant.

Manipulation of Quantum Materials

Na Hyun Jo[1]

[1]Department of Physics, University of Michigan, Ann Arbor, MI 48109, USA, [2]Affiliation

I. SUMMARY

Manipulating the edge states of topological materials is of great interest as a way to realize novel many-body physics. Initial efforts included randomly distributing magnetic atoms on a topological insulator to open a gap in the dissipationless surface state [1]. But more recently, the intriguing physical properties of intrinsic magnetic topological materials have been studied [2]. Here, I will present theoretical, electrical transport, and angle-resolved photoemission spectroscopy (ARPES) results on two particularly promising systems. Antiferromagnetic $MnBi_{2n}Te_{3n+1}$ [3] is an intrinsic axion insulator with a single-gapped Dirac cone that provides the magnetic analog of the simplest time-reversal-symmetry-protected topological insulator. $EuCd_2As_2$ [4-6] is a tunable system for exploring the interplay of magnetic ordering and topology, potentially an ideal Weyl semimetal. I will also present very recent work [7] combining ARPES with *in situ* uniaxial stress tuning of a topological state.

II. Experimental approach

A. Crystal growth

Single crystals of $MnBi_6Te_{10}$ were grown using Bi-Te as flux following the procedure described in Ref. [8]. Single crystals of both FM-$EuCd_2As_2$ and AFM-$EuCd_2As_2$ were grown via solution growth using a salt mixture as flux. The difference in growth procedure between FM-$EuCd_2As_2$ and AFM-$EuCd_2As_2$ was the initial stoichiometry of Eu:Cd:As in the salt mixture. We also grew single crystals of $EuCd_2As_2$ using Sn flux and these crystals also manifest AFM order.

Single crystals of $HfTe_5$ were grown using tellurium flux. The growth was heated up to 650°C in 3 hours, dwell for 10 hours, and then slowly cooled to 460°C over 78 hours before decanting. Low temperature annealing was conducted at 380°C and 250°C for 5 days in a sealed silica tube for sample 1 and sample 2, respectively.

B. Electrical transport measurements

Temperature-dependent electrical transport measurement was carried out in a Quantum Design Physical Property Measurement System (PPMS) for $1.8\,K \leq T \leq 300\,K$. The samples for electrical transport measurements were prepared by attaching four Pt wires using DuPont 4929N silver paint. The current was applied in ab plane with $I = 1$ mA and $f = 17$ Hz.

C. Angle-resolved photoemission spectroscopy (ARPES)

Two ARPES systems were used. One is the laser-based ARPES system at Ames National Laboratory using a tunable VUV laser ARPES system that consists of Omicron Scienta DA30 electron analyzer, a picosecond Ti:Sapphire oscillator, and fourth harmonic generator. The other is the Beamline 7.0.2 (MAESTRO) at the Advanced Light Source. The data were acquired using the micro-ARPES end station, which consists of an Omicron Scienta R4000 electron analyzer. Samples were cleaved in situ by carefully knocking off an alumina post that is attached on top of each sample with silver epoxy.

ACKNOWLEDGEMENTS

* Collaborators include Omar A. Ashour, Zhixue Shu, Chris Jozwiak, Aaron Bostwick, Sae Hee Ryu, Tai Kong, Sin´ead M. Griffin, Eli Rotenberg, Yun Wu, Thaís V Trevisan, Lin-Lin Wang, Kyungchan Lee, Brinda Kuthanazhi, Benjamin Schrunk, Sergey L. Bud'ko, Paul C. Canfield, Peter P. Orth, Adam Kaminski, Robert-Jan Slager, Jiaqiang Yan, Ashvin Vishwanath, Erik Timmons, Tae-Hoo Kim, Lin Zhou, Benjamin G Ueland, Andriy Palasyuk, Dominic Ryan, Robert McQueeney, Anton Burkov, Ruslan Prozorov.

REFERENCES

1. Y. Chen *et. al.*, Science 329, 659 (2010)
2. B. A. Bernevig *et. al.*, Nature, 603, 41 (2022)
3. N. H. Jo *et. al.*, Phys. Rev. B 102 (4), 045130 (2020)
4. L. L. Wang, N. H. Jo *et. al.*, Phys. Rev. B 99 (24), 245147, 2020
5. N.H. Jo *et. al.*, Phys. Rev. B 101 (14), 140402, 2020
6. N.H.Jo *et.al.*, Nat. Comms. 12, 7169, 2021
7. N.H. Jo *et.al.*, arXiv.2303.10836
8. J.-Q. Yan *et. al.*, Phys. Rev. Materials 4, 054202 2020

Tunneling Andreev Reflection: Direct Access to the Superconductivity in the Atomic Resolution

Wonhee Ko[1], Sang Yong Song[2], Jose L. Lado[3], Petro Maksymovych[2]
[1] Department of Physics and Astronomy, University of Tennessee, Knoxville, [2]Center for Nanophase Materials Sciences, Oak Ridge National Laboratory, [3]Department of Applied Physics, Aalto University

I. SUMMARY

Andreev reflection (AR) is a physical process that occurs at the interface between a normal metal and a superconductor, where an electron from the normal metal transports into the superconductor and forms a Cooper pair with another electron while the hole is retroreflected to the normal metal with the opposite spin from the original electron. The process is not only essential to explain the electronic transport between the normal metal and the superconductor, but also extremely useful to probe the materials' superconductivity by direct interaction with the Cooper pairs.

Here, we present a new methodology, Tunneling Andreev Reflection (TAR), which utilizes the AR occurring at the tunneling junction between a normal metal and a superconductor (Fig. 1).[1,2] Incorporating TAR to the scanning tunneling microscope (STM) allows us to access superconductivity in the atomic resolution. The technique opens new opportunities for the development of future topological quantum computers based on superconductors, where the identification of quantum materials with unconventional order parameters is instrumental for the development of topological qubits.

II. EXPERIMENTAL METHODOLOGY

A. Decay rate spectroscopy

To distinguish normal electron tunneling from AR, we developed the decay rate spectroscopy, which measures the relative decay constant κ/κ_N from the tip-sample distance dependence of the tunneling current or tunneling conductance.[1] Since AR is a higher-order process compared to normal electron tunneling, it displays increased κ/κ_N that has specific shape for distinct superconducting order parameters.[2] Combining with the scanning capability of STM, decay rate spectroscopy provides the atomic-resolution map of the AR and visualizes the spatial distribution of inhomogeneous superconducting order parameters.

B. lowest- and higher-order AR

By controlling the tip height from tunneling regime all the way to the near-contact regime, we can access the AR from the lowest- to higher-order components.[1] This capability is critical for identification for nodal superconductors, whose lowest-order AR are suppressed by quasiparticle tunneling and quantum interference while higher-order AR still appears at near-contact regime.[2] The specific shapes of the spectra are highly dependent on the pairing symmetry, so we can determine one by comparing with theoretical calculations.

III. ILLUSTRATIONS

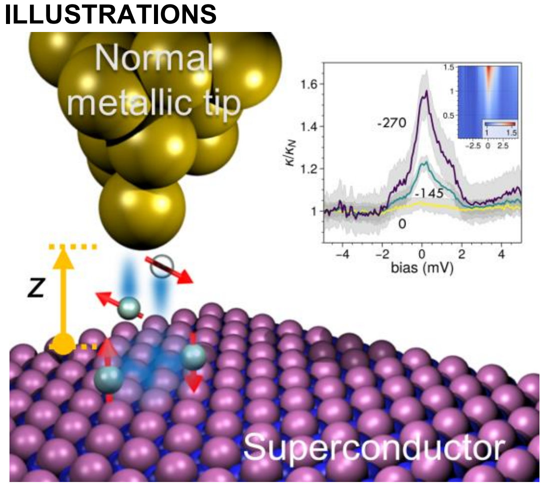

Figure 1: Experiment scheme of TAR. The inset shows representative decay rate spectra of FeSe.

REFERENCES

1. W. Ko *et al.*, “Non-contact Andreev reflection as a direct probe of superconductivity on the atomic scale,” *Nano Lett.*, 22 4042 (2022).
2. W. Ko *et al.*, “Atomic-scale Andreev probe of unconventional superconductivity,” *arXiv*: 2303.05301 (under review)

Quantum geometry for the optical properties of crystals

Junyeong Ahn[1], Guang-Yu Guo[2,3], Naoto Nagaosa[4,5], Ashvin Vishwanath[1]
[1]Department of Physics, Harvard University, Cambridge, MA, USA,
[2]Department of Physics and Center for Theoretical Physics, National Taiwan University, Taipei, Taiwan,
[3]Physics Division, National Center for Theoretical Sciences, Taipei, Taiwan,
[4]RIKEN Center for Emergent Matter Science (CEMS), Wako, Japan,
[5]Department of Applied Physics, The University of Tokyo, Tokyo, Japan.

I. SUMMARY

The geometry of quantum states is well established as a basis for understanding the response of electronic systems to static electromagnetic fields, as exemplified by the theory of the quantum and anomalous Hall effects. However, it has been challenging to relate quantum geometry to resonant optical responses. The main obstacle is that optical transitions involve a pair of states, whereas existing geometrical properties are defined for a single state. As a result, a concrete geometric understanding of optical responses has so far been limited to two-level systems, where the Hilbert space is completely determined by a single state and its orthogonal complement. Here, we construct a general theory of Riemannian geometry for resonant optical processes by identifying transition dipole moment matrix elements as tangent vectors. This theory applies to arbitrarily high-order responses, suggesting that optical responses can generally be thought of as manifestations of the Riemannian geometry of quantum states. We use our theory to show that third-order photovoltaic Hall effects are related to the Riemann curvature tensor and demonstrate an experimentally accessible regime where they dominate the response. Our work offers a new perspective on designing and controlling the functionality of quantum materials, especially topological materials.

II. THEORETICAL APPROACH

- Dipole matrix elements are shown to have the meaning of tangent basis vectors in the space of Bloch states. This allows understanding the full geometric meaning of optical response functions due to electric dipole transitions (Fig. 1).
- The optical meaning of the basic geometric quantities, metric, connection, and curvature of Bloch states are revealed, which are absorption, photovoltaic effect, and light-induced Hall effect, respectively.

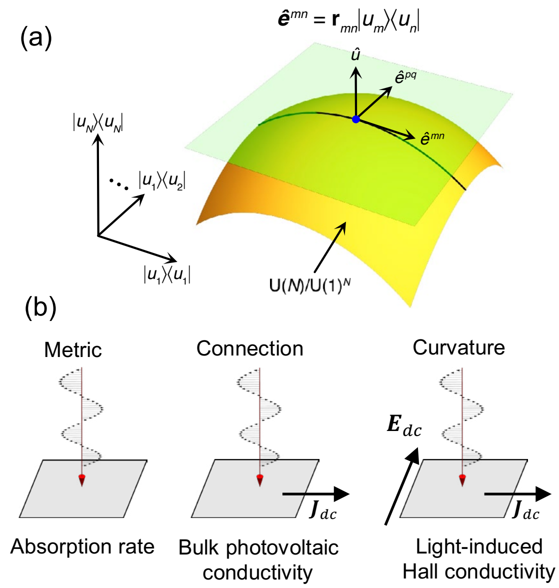

Figure 1: (a) Geometric meaning of dipole matrix elements in the space of Bloch states in terms of the tangent basis vectors. (b) Optical meaning of basic geometric quantities of the electronic wave functions.

ACKNOWLEDGEMENTS

J.A. was supported by the Basic Science Research Program through the National Research Foundation of Korea funded by the Ministry of Education (grant no. 2020R1A6A3A03037129) and by the Center for Advancement of Topological Semimetals, an Energy Frontier Research Center funded by the United States Department of Energy Office of Science, Office of Basic Energy Sciences, through the Ames Laboratory under contract no. DE-AC02-07CH11358.

REFERENCES

1. Junyeong Ahn, Guang-Yu Guo, Naoto Nagaosa, and Ashvin Vishwanath, “Riemannian geometry of resonant optical responses,” *Nature Physics* Vol. 18, No. 3, pp. 290-295, 2022.

Quantum Phases and Transitions under Decoherence: Many Body Physics of Information

Jong Yeon Lee
Kavli Institute of Theoretical Physics, Santa Barbara, CA 93106, USA

I. Introduction

The study of non-trivially entangled many-body quantum states has been an active area of research in both quantum information science and condensed matter physics. In particular, symmetry-protected topological (SPT) phases are of great importance since the SPT states provide a class of non-trivially entangled quantum systems that can be realized in the current experimental platforms, and they are also relevant to measurement-based quantum computation and measurement-based long-range entangled state preparations. However, whether SPT phases can be experimentally identified under noisy, decohering quantum circuits has not been addressed, which is important in the era of noisy intermediate-scale quantum devices.

II. Main results

In the series of work [1-3], we introduce a novel perspective for comprehending exotic quantum states and the practical utilization of quantum entanglement in quantum devices, which are inherently subject to decoherence.

In [1], we provide a protocol for generating long-range entangled (LRE) states utilizing finite-depth unitary circuits, measurements, and feedforward operations informed by measurement outcomes. Then, we examine the stability of the proposed protocol under decoherence and present a fundamental constraint on the potential to employ short-range entangled (SRE) states for creating LRE states.

Then, we reveal that one's capacity to create a LRE states from a decohered SRE state is closely connected to a fundamental limit on the potential to verify the presence of SRE topological states [2]. While doing so, we establish the explicit mapping between the properties of decohered density matrices and the topological features of the corresponding pure state in the doubled Hilbert space. This allows one to study various properties of the decohered topological states, including the information theoretic quantities, in terms of concepts from condensed matter physics.

Lastly, we investigate the emergence of critical physics within the system under decoherence, resulting in an information-theoretic phase transition [3]. This comprehensive analysis offers valuable insights into the behavior and properties of exotic quantum states in quantum devices, paving the way for future developments in the field.

III. Illustration

Figure 1 shown below: Protocol to create a mixed state with LRE from finite depth unitary circuits, measurement, and decoding procedure

REFERENCES
1. **JY Lee**, W Ji, Z Bi, M Fisher, arXiv:2208.11699
2. **JY Lee**, YZ You, C Xu, arXiv:2210.16323
3. **JY Lee**, CM Jian, C Xu, arXiv:2301.05238

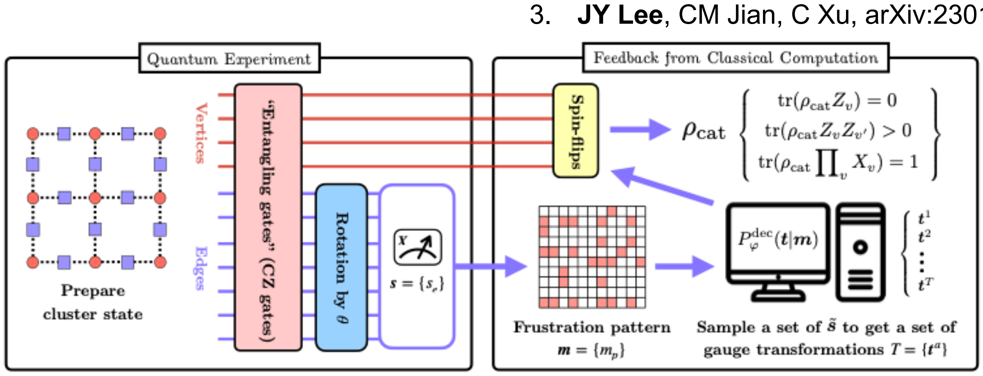

A Toolbox for Analog Quantum Simulation

Soonwon Choi
Center for Theoretical Physics, Massachusetts Institute of Technology, Cambridge, MA 02139, USA

I. Introduction

Quantum simulators—carefully engineered and programmable quantum systems—provide an exciting avenue to explore the laws of nature and to realize complex physical phenomena. However, current quantum simulators still lack the sophisticated controls needed to interrogate a prepared state in depth, limiting the information that can be extracted by measurements. Here, we propose a novel measurement protocol that completely overcomes this difficulty, allowing for the extraction of arbitrary physical information. Excitingly, the protocol can be implemented with present-day technologies.

II. Main results

Our protocol involves introducing ancillary degrees of freedom prepared in a known state to a system of interest, letting them evolve naturally under joint quantum dynamics, then performing global measurements in a standard basis. Even though only a single, fixed basis is measured, we show how our protocol enables any property of the original quantum state to be estimated. The key ingredient of our protocol is ergodicity—the natural randomness in general quantum dynamics—which ensures that all information of the original system, even complicated observables, manifest over the ancillary system and can be observed. We demonstrate our protocol with extensive numerical simulations showcasing the extraction of elusive properties like topological numbers and entanglement entropies, assuming only the capabilities of existing experimental platforms.

Our protocol empowers quantum simulators to make previously impossible measurements, significantly advancing near-term quantum technologies. Further, our work heralds a paradigm shift in quantum protocol design, where we harness ergodicity—a ubiquitous feature of quantum dynamics—to aid scientific discoveries.

III. Illustration

Figure 1: Artistic illustration of scientists interogating quantum devices to extract physically meaningful properties. This illustration has been generated by an AI algorithm with the prompt provided by the authors of Ref. [1].

ACKNOWLEDGEMENTS
This submission is based on the publication in Ref. [1].

REFERENCES

1. Minh C. Tran, Daniel K. Mark, Wen Wei Ho, and Soownon Choi "Measuring Arbitrary Physical Properties in Analog Quantum Simulation," *Physical Reivew X* **13**, 011049 2023.

Launching multiple modes in hyperbolic vdW heterostructures

Byung-Il Noh[1], Siyuan Dai[2]
[1]Materials Research and Education Center, Department of Mechanical Engineering, Auburn University, Auburn, Alabama 36849, USA

I. SUMMARY

Polaritons arise from the strong interaction between electromagnetic (EM) waves and the electric or magnetic dipole components of matter. Recently, low-dimensional van der Waals (vdW) materials have garnered considerable attention as promising candidates for nano-polaritonic devices.[1] These materials, consisting of weakly bonded atomic layers, offer unique properties, such as easy exfoliation to single or few layers and the ability to engineer them through stacking. Among these materials, hyperbolic vdW materials with opposite signs of in-plane and out-of-plane permittivity ($\varepsilon_d \varepsilon_z < 0$) are particularly intriguing as they support multiple branches of polaritons at deep subwavelength scales.[2] Hyperbolic polaritons are of great importance due to their highly confined light and high optical density of states (optical momenta k_p) beyond that of free space light (k_0). Notably, the higher-order branches enable extreme light confinement and higher energy density compared to the fundamental mode, making them suitable for nano-polaritonic devices spanning a wide range of spectroscopic fields. Despite the existing body of research focusing on the fundamental (0-order) branch, where polaritons manifest as fringes in near-field images with a dominant single period, our work addresses multiple branches of hyperbolic polaritons, particularly the higher-order branches, through vdW stacking. In contrast to conventional fringe oscillations, we have observed beat phenomena in a SNOM of a prototype natural hyperbolic hexagonal boron nitride (hBN). Our findings regarding the engineering of polariton reflection have the potential for further development in nano-polaritonic circuits, nano-optical communications, energy transfer, and other functional applications.

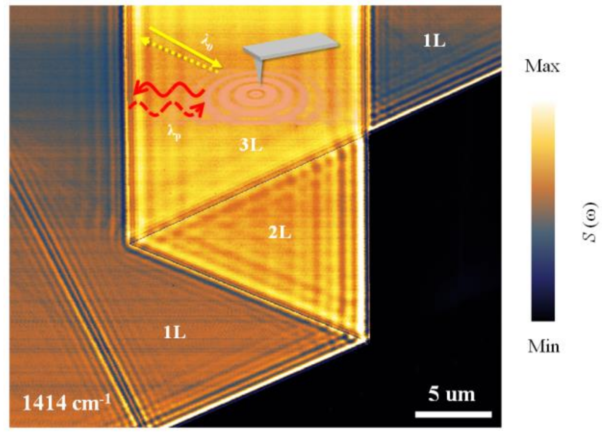

Figure 1: Near-field nano-imaging. Near field s-SNOM image of foldable hBN at IR beam frequency ω = 1414 cm^{-1}. The AFM tip and foldable hBN are illuminated by the IR beam (yellow arrow) from a QCL. Hyperbolic polaritons (red arrow) are launched by strong coupling between AFM tip and hBN. At the edge, the multiple polaritons are reflected back and then detected by s-SNOM.

ACKNOWLEDGEMENTS

This project was mainly supported by Auburn University Intramural Grants Program and National Science Foundation under grant no. DMR-2005194.

REFERENCES

1. D. N. Basov, M. M. Fogler, and F. J. Garcia De Abajo, “Polaritons in van der Waals materials”, Science, 354, 6309, aag1992-aag1998, 2016.
2. S. Dai, Z. Fei, Q. Ma, A. S. Rodin, M. Wagner, A. S. McLeod, M. K. Liu, W. Gannett, W. Regan, K. Watanabe, T. Taniguchi, M. Thiemens, G. Dominguez, A. H. Castro Neto, A. Zettl, F. Keilmann, P. Jarillo-Herrero, M. M. Fogler, D. N. Basov, “Tunable Phonon Polaritons in Atomically Thin van der Waals Crystals of Boron Nitride”, *Science*, 343, 6175, 1125-1129, 2014.

Research and Development of the multi-qubit superconducting quantum processor in SKKU

Yonuk Chong
SKKU Advanced Institute of Nano Technology (SAINT), Suwon 16419, Korea
Department of Nano Engineering, SungKyunKwan University (SKKU), Suwon 16419, Korea

I. SUMMARY

Here we present our recent progress in multi-qubit superconducting quantum processor development research activities in SKKU. We will present our design, fabrication and measurement flow in SKKU laboratory up to 10+ qubit scale devices. As the qubit number increases, calibration of the qubit parameters against the drift is a large overhead in operating quantum chips. We improved our measurement fidelities and we have automated calibration process to improve our system performance. Our result of entangling gate optimization and fidelity results will be presented. As simple examples, we demonstrate simple algorithms in small scale devices, in addition to the simple VQE iteration and CHSH inequality measurement.

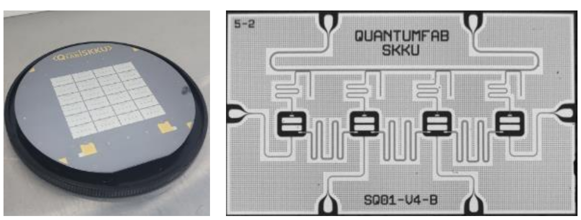

Figure 1: Example of 4-qubit device fabricated in SKKU. We currently run 3-inch wafer process.

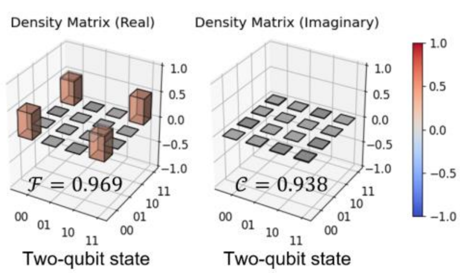

$$|\psi\rangle = \frac{1}{\sqrt{2}}(|00\rangle + |11\rangle)$$

Figure 2: 2-qubit entanglement gate example. Using the calibrated CNOT gate, the Bell state fidelity is about 0.97, which includes the SPAM error of (estimated) ~2%.

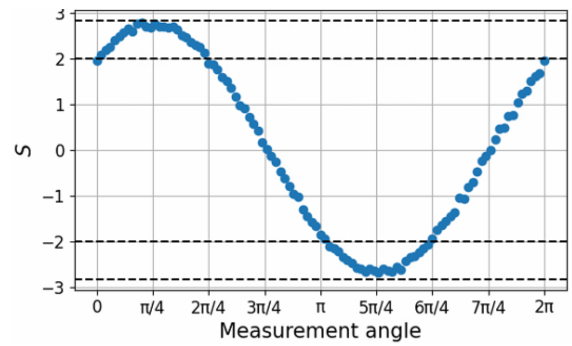

Figure 3: Test of CHSH inequality violation.

ACKNOWLEDGEMENTS

This work was supported by the National Research Foundation of Korea (grant nos. 2022M3K2A1084250, 2022M3E4A1077186, 2022M3E4A1083527, 2020M3H3A1110365 and 021M3H3A1036573.)

REFERENCES

1. H. S. Yeo *et al.,* “High-fidelity Multiplexed Single-shot Readout for Transmon Qubits with High-power Measurement”, to be published in IEEE Trans. Appl. Supercond. Vol. 33, Issue 5, Aug 2023.
DOI: 10.1109/TASC.2023.3254485

CONTRIBUTIONS

Hwan-Seop Yeo, Seungwook Woo, Jeongwon Kim, Youngdu Kim, Beomgyu Choi, Jongwon Park, Dongki Cho, Yonuk Chong*

* email : yonuk@skku.edu
* homepage : http://quantum.skku.edu

Magnetic-field-resilient niobium cavity electromechanical system and its optomechanical frequency comb generation

Junho Suh[1], Seung-Bo Shim[2], Jinwoong Cha[2]
[1]Pohang University of Science and Technology, Pohang, Korea
[2]Korea Research Institute of Standards and Science, Daejeon, Korea

I. SUMMARY

Mechanical oscillators provide a novel platform to harness phonons as a resource for quantum technology. In this talk, I describe our recent results on developing mechanical oscillator devices suitable for quantum sensing applications. We demonstrate a superconducting cavity electromechanical device with thin film niobium implementing optomechanical interactions at microwave frequency. The device demonstrates significant improvements in the operating temperature, magnetic fields, and microwave powers. At high microwave powers, it exhibits a microwave frequency comb emerging from nonlinear interactions between the microwave and mechanical oscillation. These results could lead to mechanical quantum sensors aided with precision comb-based frequency determination.

II. EXPERIMENTS

A. Device and experimental set-up

The fundamental flexural mode (8.4 MHz) of a niobium micro-membrane is the mechanical oscillator under study. The membrane is suspended above a bottom electrode by 130 nm forming a vacuum gap capacitor in a superconducting LC resonator. The LC resonator is the “cavity” for 3.8 GHz microwave photons, and the modulation of LC resonance frequency by the vibration of membrane provides the “optomechanical” coupling between the microwave photons and mechanical phonons. We perform all the measurements at the liquid helium temperature (Fig.1a-b).

B. Magnetic-field-resilience and optomechanical frequency comb

At 4.2 K, the electromechanically induced reflection of input microwave persists up to 0.8 T magnetic field (Fig.1c). We observe that the single-photon optomechanical coupling rate(~3.3 Hz) is independent of magnetic field strengths.

The niobium device pertains optomechanical interaction at high microwave powers and starts to show frequency comb above a threshold. The comb spacing matches exactly with mechanical resonance frequency. This is also confirmed with time-domain measurements of microwave powers and is explained by coupled equations of motion of microwave field and mechanical motion with a nonlinear coupling from radiation pressure (Fig. 1d-e).

III. ILLUSTRATIONS

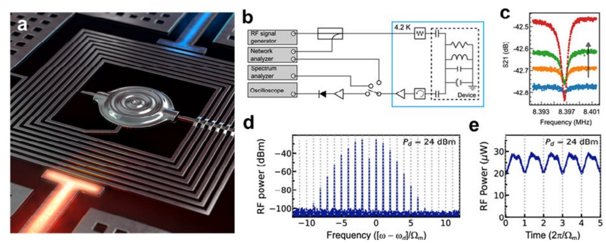

Figure 1: Device, experimental set-up, and measurement data. a: schematic of cavity electromechanical device. b: measurement circuit diagram. c: electromechanically induced reflection of input microwave at 0.8 T magnetic field. d: optomechanical frequency comb. e: time-domain measurement of microwave power when the frequency comb appears at high microwave powers.

ACKNOWLEDGEMENTS

The research is supported by the National Research Council of Science and Technology (CAP21031-100) and the National Research Foundation of Korea (NRF-2016R1A5A1008184, 2022R1C1C1011544).

REFERENCES

1. Jinwoong Cha *et. al.*, “Superconducting Nanoelectromechanical Transducer Resilient to Magnetic Fields,” *Nano Lett.* **21**, 1800-1806, 2021.
2. Junghyun Shin *et. al.*, “On-Chip Microwave Frequency Combs in a Superconducting Nanoelectromechanical Device,” *Nano Lett.* **22**, 5459-5465, 2022.

Deterministic Generation of Multidimensional Photonic Cluster States with a Single Quantum Emitter

Gihwan Kim
Thomas J. Watson, Sr., Laboratory of Applied Physics, California Institute of Technology, Pasadena, CA 91125, USA

I. SUMMARY

Multidimensional photonic cluster states hold great potential in various quantum information processing tasks, including quantum metrology and measurement-based quantum computation. However, the scalability of generating multidimensional photonic cluster states in optical systems has been limited due to the reliance on probabilistic photon sources and entangling gates.

We present an experimental implementation of a resource-efficient scheme in the microwave domain for the deterministic generation of two-dimensional (2D) photonic cluster states. Our method is based on a modified version of the protocol proposed by Pichler et al. [1]. In our setup, we utilize a coupled resonator array as a slow-light waveguide [2], a single flux-tunable transmon qubit as a quantum emitter, and a second auxiliary transmon qubit as a switchable mirror. This configuration enables us to achieve rapid and controlled emission of entangled photon wavepackets, as well as selective time-delayed feedback of photon wavepackets to the emitter qubit (refer to Figure 1). By leveraging these capabilities, we successfully generate a 2D cluster state composed of four photons and five photons [3].

II. EXPERIMENT

A. Qubit-Photon CZ Gate Implementation

We successfully implement a qubit-photon CZ gate between a previously emitted photon and the emitter qubit, achieving a fidelity of 90% as verified by quantum process tomography.

B. On-Demand Shaped Photon Emission

We demonstrate the emission of envelope-shaped photons with high efficiency of 97% within 30 ns.

C. Deterministic 2D Cluster State Generation

We demonstrate the generation of four-photon square cluster states with 70% fidelity and five-photon pentagon cluster states with 61% fidelity, as confirmed through tomographic reconstruction of the quantum state.

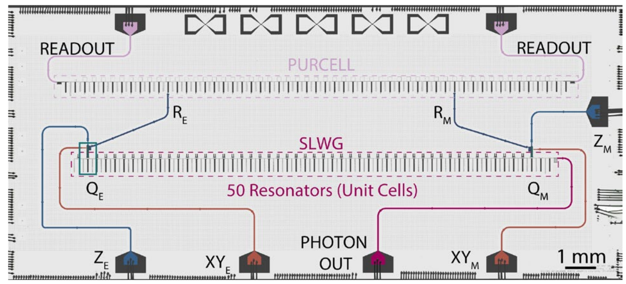

Figure 1: Optical micrograph of the fabricated device. A slow-light waveguide (SLWG), comprising 50 lumped-element resonators, functions as a delay line and a high-cooperativity waveguide. At the ends of the SLWG, two flux-tunable transmon qubits (Q_E and Q_M) are coupled. Q_E emits itinerant microwave photons, while Q_M selectively reflects photons for time-delayed feedback. The interactions between the qubits and the SLWG are dynamically tuned by adjusting the qubits' frequencies, which are controlled individually through flux lines.

ACKNOWLEDGEMENTS

This work was supported by the AFOSR MURI Quantum Photonic Matter (grant 16RT0696), through a grant from the Department of Energy (grant DE-SC0020152), and through a sponsored research agreement with Amazon Web Services.

REFERENCES

1. H. Pichler, S. Choi, P. Zoller, and M. D. Lukin, “Universal photonic quantum computation via time-delayed feedback”, *PNAS* 114, 11362, 2017.
2. V. S. Ferreira, J. Banker, A. Sipahigil, M. H. Matheny, A. J. Keller, E. Kim, M. Mirhosseini, and O. Painter, “Collapse and Revival of an Artificial Atom Coupled to a Structured Photonic Reservoir”, *Phys. Rev. X* 11, 041043, 2021.
3. V. S. Ferreira, G. Kim, A. Butler, H. Pichler, and O. Painter, “Deterministic Generation of Multidimensional Photonic Cluster States with a Single Quantum Emitter”, *arXiv preprint at* https://arxiv.org/abs/2206.10076, 2022.

Towards a practical quantum advantage with a high-fidelity Rydberg quantum simulator

Joonhee Choi
Department of Electrical Engineering, Stanford University, Stanford, CA 94305, USA

I. Introduction

Which is the better representation of some ideal quantum evolution, a classical computer using an approximate simulation algorithm, or a noisy quantum simulator? We experimentally test this question by producing maximum-entanglement entropy states with as many as 60 atoms using a Rydberg atom array with state-of-the-art fidelity, and compare against similarly state-of-the-art classical simulation algorithms.

II. Main results

Recently we discovered that universal statistics emerge from ergodic Hamiltonian dynamics of generic quantum systems. The signatures of these statistics were revealed by the observation of the so-called Porter-Thomas distribution that emerges in a wide variety of quantum computers and simulators. The presence of such universal properties plays an important role in quantum information science, for example allowing the development of an efficient, widely applicable benchmarking protocol. Via the new benchmarking method, here we demonstrate the fidelity estimation of a Rydberg atom-array quantum simulator with up to 60 atoms and discuss prospects for realizing practical quantum advantage with near-term quantum simulators. In particular, in the high-entanglement regime, neither the classical nor quantum device has perfect fidelity, but the classical algorithm's limited accuracy can be precisely controlled by varying the degree of classical resources employed. This allows us to define the equivalent classical cost to perform evolution with the same fidelity as the quantum experiment. We show that with incremental experimental improvements, the classical cost required to beat the quantum device increases by orders-of-magnitude, and even in the present day we find the quantum experiment can outperform the classical computer in finite sampling from these high-entanglement states. Our results shed light on the boundary between classical and quantum advantage.

III. Illustration

Figure 1 (below): Quantifying the boundary between classical and quantum advantage.

REFERENCES

1. Joonhee Choi, Adam L. Shaw, Ivaylo S. Madjarov, Xin Xie, Ran Finkelstein, Jacob P. Covey, Jordan S. Cotler, Daniel K. Mark, Hsin-Yuan Huang, Anant Kale, Hannes Pichler, Fernando G. S. L. Brandão, Soonwon Choi & Manuel Endres, "Preparing random states and benchmarking with many-body quantum chaos," Nature **613**, 468 (2023).

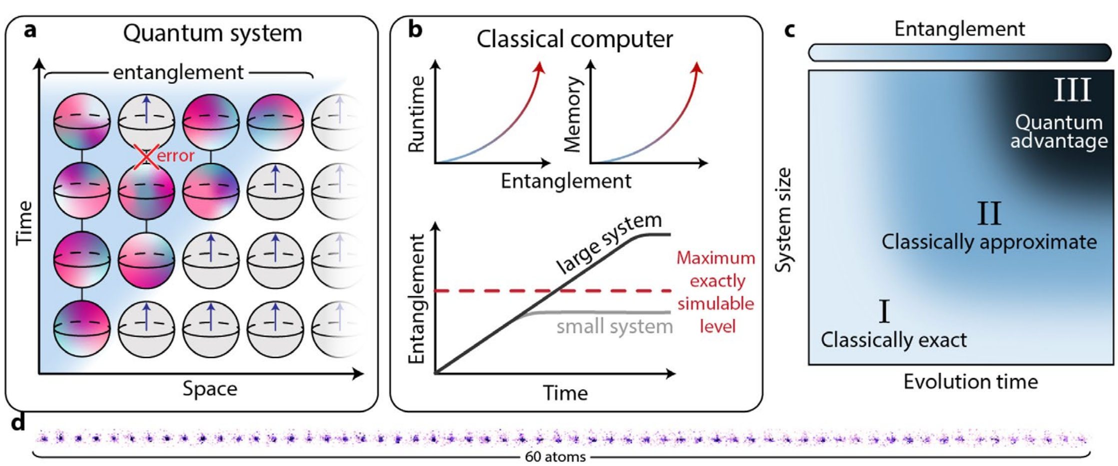

Scalable fault-tolerant quantum error correction with linear array of emitters

Isaac H. Kim[1], **Jintae Kim**[2]
[1]UC Davis, [2]Sungkyunkwan University

I. SUMMARY

Quantum error correction is essential for building a scalable fault-tolerant quantum computer, but existing schemes for quantum error correction suffer from an enormous experimental overhead. We introduce a fault-tolerant quantum error correction scheme using a linear array of emitters and waveguides, which can reduce this overhead substantially. The proposed scheme possesses a threshold of 0.39%, which is comparable to a prior scheme that uses a single emitter, while exhibiting improved resilience against the loss in the waveguide.

Our scheme improves upon the approach of Wan et al., which proposed to use a single emitter and waveguides to build a fault-tolerant qubit. This prior scheme stores photons in a waveguide, which sequentially interacts with the emitter. Our scheme evenly allocates the photons to shorter waveguides, thus reducing the effect of loss in the waveguide. Based on an extensive Monte Carlo simulation, we observe a logical error rate that decays exponentially with the number of emitters, while maintaining the same threshold.

In particular, even in an experimentally realistic setup in which the gates applied between emitters are substantially slower and noisier than the other gates, the threshold remains largely unchanged [Figure 1].

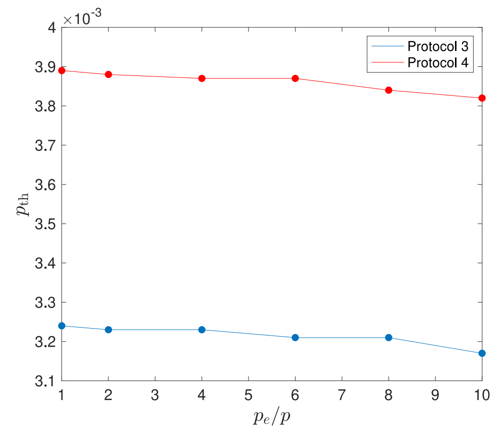

Figure 1: A plot of threshold under a different ratio of error rate between neighboring emitters (p_e) and gate error rate (p).

ACKNOWLEDGEMENTS

IK's work was supported by Cisco research. JK's work was supported by the education and training program of the Quantum Information Research Support Center, funded through the National research foundation of Korea (NRF).

REFERENCES

1. Kianna Wan, Soonwon Choi, Isaac H. Kim, Noah Shutty, Patrick Hayden, PRX Quantum **2**, 040345 (2021).

Fault-tolerant quantum computing with bosonic qubits

Kyungjoo Noh[1]
[1]AWS Center for Quantum Computing, Pasadena, CA, USA

I. INTRODUCTION
Implementing surface code quantum error correction (QEC) using transmons as qubits is one of the most popular approaches for building a fault-tolerant quantum computer. Here, we discuss the possibility of using oscillator-based bosonic qubits instead of transmon qubits.

II. BOSONIC QUBITS
Bosonic qubits are unique in the sense that they are protected by bosonic quantum error correction [1,2]. GKP qubits [3] and cat qubits [4] are among the most notable examples.

GKP qubits can offer advantages in that they are robust against small displacement errors in an arbitrary direction in the phase space and, depending on the implementation, the outer error-correcting codes can benefit from the soft analog information coming from the qubit-level GKP error correction [5,6,7].

The unique advantage of a cat qubit is that the bit-flip errors can be suppressed as the size of the cat qubit is increased due to the large separation of the two coherent states in the phase space. This means that the outer error-correcting codes can focus on correcting the dominant phase-flip errors on cat qubits, leading to an overall resource reduction [8,9,10]. In this submission we mostly focus on cat qubits.

III. CAT-TRANSMON ARCHITECTURE
In an all-cat architecture, all the qubits are implemented with cat qubits whose noise is biased towards phase-flip errors [8,9,10]. However, implementing high-fidelity and bias-preserving entangling gates between cat qubits is experimentally challenging, although it is not impossible. Here, we propose an alternative cat-qubit architecture, named cat-transmon architecture, in which cat qubits are used only as data qubits of an outer error-correcting codes and ancilla qubits are implemented by using transmons [11]. The use of transmons, instead of cat qubits, as ancilla qubits significantly relaxes experimental requirements.

REFERENCES
1. Victor V. Albert et al., “Performance and structure of single-mode bosonic codes,” *Phys. Rev. A* ***97**, 032346*, 2018.
2. Atharv Joshi, Kyungjoo Noh, and Yvonne Y Gao, “Quantum information processing with bosonic qubits in circuit QED,” *Quantum Science and Technology 6, 033001*, 2021.
3. Daniel Gottesman, Alexei Kitaev, and John Preskill, “Encoding a qubit in an oscillator,” *Phys. Rev. A* ***64**, 012310*, 2001.
4. P. T. Cochrane, G. J. Milburn, and W. J. Munro, “Macroscopically distinct quantum-superposition states as a bosonic code for amplitude damping,” *Phys. Rev. A* ***59**, 2631*, 1999.
5. Kosuke Fukui et al., “High-Threshold Fault-Tolerant Quantum Computation with Analog Quantum Error Correction,” *Phys. Rev. X* ***8**, 021054*, 2018.
6. Christophe Vuillot et al., “Quantum error correction with the toric Gottesman-Kitaev-Preskill code,” *Phys. Rev. A* ***99**, 032344*, 2019.
7. Kyungjoo Noh and Christopher Chamberland, “Fault-tolerant bosonic quantum error correction with the surface–Gottesman-Kitaev-Preskill code”, *Phys. Rev. A* ***101**, 012316*, 2020.
8. Jérémie Guillaud and Mazyar Mirrahimi, “Repetition Cat Qubits for Fault-Tolerant Quantum Computation,” *Phys. Rev. X* ***9**, 041053*, 2019.
9. Andrew S. Darmawan et al., “Practical Quantum Error Correction with the XZZX Code and Kerr-Cat Qubits,” *PRX Quantum* ***2**, 030345*, 2021.
10. Christopher Chamberland et al., “Building a Fault-Tolerant Quantum Computer Using Concatenated Cat Codes,” *PRX Quantum* ***3**, 010329*, 2022.
11. Connor T Hann et al., “Hybrid cat-transmon architecture for scalable, hardware-efficient quantum error correction,” APS March Meeting, 2023.

Technical Group A-2

Chemistry (CHM)

Towards single virus genomics

Hee-Sun Han[1, 2]
[1]University of Illinois, Chemistry, [2]Carl R. Woese Institute for Genomic Biology

I. SUMMARY

Single virus genomics enables the quantitative assessment of critical processes underlying virus evolution and infection. However, the unique challenges associated with processing single virus genomes make it impractical to adapt existing single cell technologies. These challenges arise from the limited genomic material present in each viral particle, which is 1K-1M-fold less than that of eukaryotic cells, as well as the presence of only a single copy of genomic RNA/DNA. These obstacles are even more pronounced for viruses with segmented genomes, such as influenza. In this talk, I will showcase our efforts to facilitate cell-free, direct profiling of single influenza genomes at high throughput. The new technology will, for the first time, allow large-scale reassortment studies of natural influenza strains, opening the door to characterizing their reassortment potential.

II. Passive restoration of drop spacing

Having evenly spaced drops is essential to achieve deterministic and reliable manipulation of drops, such as drop counting, sorting, and merging. However, drop spacing is often disturbed on chip, especially when drops are smaller than the flow channel. Restoring uniform drop spacing has required active manipulation of drops, either by repacking drops using an oil remover and adding back respacing oil or reinjection of drops. These approaches require extensive technical expertise and repeated optimization of chip designs. We developed a passive method to restore even spacing of drops using inertial forces. We showed flowing SE drops into an asymmetric serpentine channel quickly produce evenly spaced drops. This simple channel design can be easily integrated into other microfluidic modules and devices, making our strategy highly accessible.

III. Double emulsion strategies

SE drop stability remains a persistent challenge in the design of microfluidic assays. Despite considerable efforts, drop merging cannot be fully eliminated and varies substantially across experiments. Drop merging negatively affects workflows by mixing the contents of single cell compartments and causes spurious detection. It also increases size heterogeneity which causes highly variable reaction yields and disrupts drop-by-drop manipulations. To avoid the negative impact of merging, most SE-based technologies employ single-step reactions in drops. Single IAV genome profiling, however, requires multiple steps to be performed in drops. We have shown that DE drops address the stubborn challenges of SE drop merging. Instead of merging to form larger drops, DEs rupture releasing their contents into the continuous phase where they are effectively removed from downstream steps. By retaining only intact, monodisperse drops, reaction volumes remain constant, yields are uniform across drops, and assay results are consistent. This is particularly important for PCR amplification and barcoding, where variable yield reduces sequencing throughput by allocating excess reads to larger drops. Importantly, DE drops eliminate the risk of barcode mixing due to the exclusion of the released materials from downstream barcoding reactions.

IV. Flow cytometry analysis

DEs allow automated drop-by-drop interrogation using flow cytometry screening. Using single particle loading, TaqMan probes, and multi-color screening, individual IAV genomes can be characterized for the presence or absence of targeted genome segments. DE flow cytometry has gained attention for improving the throughput and data quality of drop-based assays. We have extended these methods to exclude similarly sized oil drops from ddPCR detection. We have also successfully injected and analyzed DE drops up to 80 um, surpassing the previous limit of 35-50 um. Multi-step drop reactions naturally lead to larger drop sizes. Through the exploration of injection strategies, we achieved comparable throughput analysis with larger drops.

Nanotechnology Approaches for Real-time Neurotransmitter Detection in Stem Cell-Derived Neural Interfaces

KiBum Lee

Dept. of Chemistry & Chemical Biology, Rutgers University

123 Bevier Road, Piscataway, NJ 08854-8087, USA

I. SUMMARY

This presentation aims to explore the intersection of nanobiosensing and stem cell therapies, focusing on the challenges faced in understanding the microenvironment and gene expression in stem cells, as well as the limitations of conventional methods and the lack of comprehensive knowledge of regulatory signals. Stem cells have the potential to differentiate into various cell types under specific cues, and stem cell therapy holds promise for regenerative treatments of neurological disorders. However, to fully harness the potential of stem cell therapeutics, advanced biosensors are urgently needed that can identify stem cell fate in a non-destructive, real-time, and quantitative manner.

To address these challenges, our research primarily focuses on developing nanotechnology-based biosensing methods. These methods aim to accurately detect key biomarkers like proteins, oligonucleotides, and small molecules in a real-time, non-destructive, and highly sensitive/selective way during stem cell fate transition. One approach involves the creation of a nanosensing platform with two essential components. The first component is an immunomagnetic module designed for exosome isolation, while the second component incorporates plasmonic/metal-enhanced fluorescence technology for the sensitive detection of exosomal miRNA. This platform enables the characterization of stem cell differentiation.

Another approach we explore is a novel cell-based sensing platform known as large-scale Nano-Electrode Arrays (NEAs). This platform demonstrates real-time and highly sensitive electrochemical/spectroscopic detection of neurotransmitters produced from stem cell-based neural interfaces. By utilizing NEAs, we can gain valuable insights into the dynamic changes of neurotransmitter release in stem cell systems.

These advancements in nanotechnology-based biosensing have the potential to revolutionize our understanding of stem cell behavior and facilitate the development of more effective stem cell therapies for neurological disorders. *In this presentation, a summary of the most updated results from these efforts and future directions will be discussed.*

II. ILLUSTRATIONS

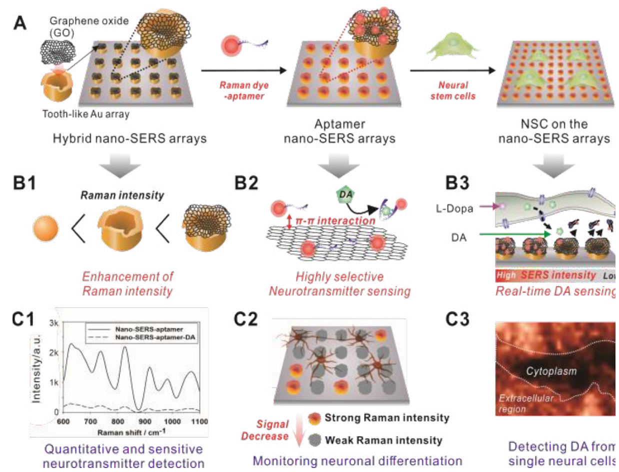

Figure 1: Schematic diagram illustrating the method to detect dopamine (DA) releasing from single live cells using graphene oxide (GO)-hybrid nano-SERS.

III. ACKNOWLEDGEMENTS

The presenter would like to acknowledge KBLEE group members and collaborators. http://kblee.rutgers.edu/

III. KEY REFERENCES (from KBLEE Group)

1. "Ultrasensitive Electrochemical Detection of Mutated Viral RNAs with Single Nucleotide Resolution Using a Nanoporous Electrode Array (NPEA)", *ACS Nano*, **2022.**
2. "CRSPR-Mediated Amplification-Free Detection of Viral DNAs Using Surface-Enhanced Raman Spectroscopy-Active Nanoarray", *ACS Nano*, **2021**
3. "Sensing Neurotransmitters From Stem Cell-derived Neural Interface at the Single-Cell Level Using Graphene Oxide-Hybrid Nano-SERS Array", *Nano Letter*, **2020.**
4. "NIR Biosensing of Neurotransmitters in Stem Cell-derived Neural Interface Using Advanced Core-shell Upconversion Nanoparticles", *Advanced Materials*, **2019**.
5. "Non-destructive Real-Time Monitoring of Enhanced Stem Cell Differentiation using a Graphene-Au Hybrid Nanoelectrode Array", *Advanced Materials*, **2018.**

Precision tumor cell death through targeting cancer-specific InDel mutations with CRISPR-Cas9

Taejoon Kwon, Seung Woo Cho, and Kyungjae Myung
Department of Biomedical Engineering, College of Information and Biotechnology,
Ulsan National Institute of Science and Technology, Ulsan, Republic of Korea
Center for Genomic Integrity, Institute for Basic Science, Ulsan, Republic of Korea

I. SUMMARY

We developed a novel therapeutic strategy to induce cancer cell death using the CRISPR-Cas system selectively. CINDELA utilizes a previously unexplored idea of introducing CRISPR-mediated DNA double-strand breaks (DSBs) in a cancer-specific fashion to facilitate specific cell death. In particular, CINDELA targets multiple InDels with CRISPR-Cas9 to produce many DNA DSBs that result in cancer-specific cell death.

II. RESULTS

To test whether DNA DSBs induced by CRISPR-Cas9 can also kill cancer cells, we selected well-known CRISPR-Cas9 targeting sequences that appear repeatedly that range from a single to 20,000 targets in the human genome. We observed that HEK293T cells started to die when the number of sgRNA targets increased to more than 10, which created 20 DSBs in the genomes of diploid cells. HEK293T cell death was further enhanced when the transfected plasmid expressed the sgRNA and targeted more genomic locations.

To prove that CINDELA treatment can be applied to actual tumor samples, we used the primary tumor cell line GBL-67 derived from a Korean glioblastoma patient. Based on whole-genome sequencing data, we designed 26 SaCas9 CINDELA guide RNAs that targeted specific GBL-67 InDels. Because we did not have access to normal cells from the same individual, NSC-10 neural stem cells, which do not have the targeted InDels, were used as the control. AAVs expressing sgRNA and SaCas9 were generated and simultaneously transduced into primary glioblastoma GBL-67 and NSC-10 cells. We found that approximately 50 cell-specific DSBs induced by CINDELA treatment were sufficient to enhance apoptosis and kill glioblastoma cells. In contrast, the NSC-10 cells did not exhibit any growth attenuation after the same transduction.

we tested CINDELA's efficacy in patient-derived xenografts (PDXs), which are predictive preclinical models for cancer treatment. After sequencing tissue from an established lung cancer PDX, we identified approximately 30 CINDELA targets. Xenograft tumor size was monitored for two weeks after the injection of AAVs (five times within a 3-day interval) that expressed SaCas9 with the targeted sgRNAs. PDX tumor growth was inhibited by the AAVs that expressed sgRNAs and SaCas9. In contrast, AAVs that only expressed SaCas9 did not inhibit tumor growth. In addition, the mice did not exhibit any significant symptoms during the AAV treatment.

III. SIGNIFICANCE

Targeted killing of cancer cells without affecting surrounding normal cells is the most desirable approach for cancer therapy; however, it cannot be easily achieved owing to the shared properties of normal and cancer cells. The novel concept proposed in this study may become a potential approach for personalized cancer treatments.

ACKNOWLEDGEMENTS
This work is supported by an IBS grant IBS-R022-D1, UNIST Research Fund (1.200094 and 1.190041)) and the National Research Foundation of Korea (NRF) grant (2018R1A6A1A03025810, 2020R1C1C1013242, 2023R1A2C100627511).

REFERENCES

1. Kwon T, et al., Proc Natl Acad Sci U S A. 2022 Mar 1;119(9):e2103532119.

Structure and mechanisms of DNA damage recognition and initiation in Nucleotide Excision Repair

Jennifer Le[1], Temilade Adeniran[1], Amir Tavakoli[1], Debamita Paul[1], Trevor van Eeuwen[2], Kenji Murakami[2] and Jung-Hyun Min[1]

[1]Department of Chemistry and Biochemistry, Baylor University

[1]Department of Biochemistry and Biophysics, Perelman School of Medicine, University of Pennsylvania

Nucleotide excision repair (NER) repairs DNA lesions caused by diverse environmental agents such as UV, pollutants, cigarette smoke, etc. The lesions, if left unrepaired, block essential cellular functions and lead to cell death or diseases. To initiate NER, the XPC protein complex (Rad4 in yeast) initially locates diverse lesions scattered around the genomic DNA and recruits downstream factors to the damaged sites. The recognition efficiency of the lesions can, however, vary widely depending on the lesion, and certain lesions can evade detection by XPC and thus become resistant to NER. Our research addresses how Rad4/XPC recognizes DNA lesions and how certain lesions evade Rad4/XPC by using multiple complementary approaches including X-ray crystallography/Cryo-EM, time-resolved fluorescence spectroscopy, chemical crosslinking, and molecular dynamics (MD) simulations. In this talk, I will summarize the current understanding of the mechanism of NER initiation based on our and others' studies. In particular, I will discuss the impact of DNA sequence context for the lesion recognition, how photoactive DNA may be used as a model lesion, and recent cryo-EM structures that provide insights into how Rad4/XPC recruits TFIIH to a lesion to initiate the DNA unwinding and lesion verification process in NER.

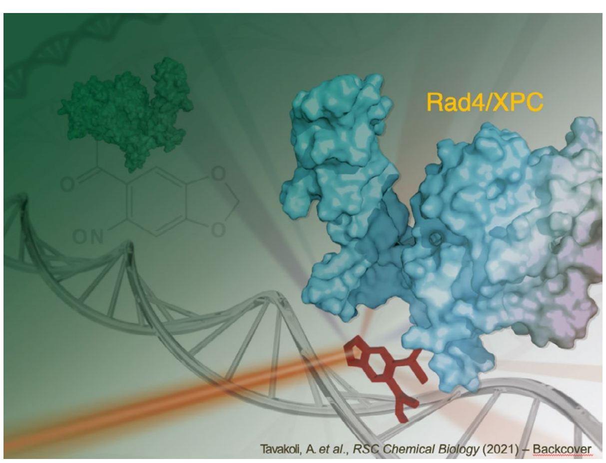

Figure 1: Rad4/XPC (blue) is a key DNA damage sensor that recognizes various types of DNA damage for the eukaryotic nucleotide excision repair pathway. Rad4/XPC can also recognize a photoactive nucleotide (red, NPOM) in a DNA duplex (grey) as a lesion, and this binding can be reversed using light as a trigger.

ACKNOWLEDGEMENTS

This work was funded by NSF MCB-2131806 and NIH 1R15 GM147899 to J.-H.M. and NIH R01-GM123233 to K.M.

REFERENCES

1. van Eeuwen, T., Shim, Y., Kim, H. J., Zhao, T., Basu, S., Garcia, B. A., Kaplan, C. D., Min, J. H. & Murakami, K. Cryo-EM structure of TFIIH/Rad4-Rad23-Rad33 in damaged DNA opening in nucleotide excision repair. *Nat. Comm.* **12**, 3338, doi:10.1038/s41467-021-23684-x (2021).
2. Paul, D., Mu, H., Tavakoli, A., Dai, Q., Chakraborty, S., He, C., Ansari, A., Broyde, S. & Min, J. H. Impact of DNA sequences on DNA 'opening' by the Rad4/XPC nucleotide excision repair complex. *DNA Repair (Amst)* **107**, 103194, doi:10.1016/j.dnarep.2021.103194 (2021).
3. Tavakoli, A. & Min, J. H. Photochemical modifications for DNA/RNA oligonucleotides. *RSC Adv* **12**, 6484-6507, doi:10.1039/d1ra05951c (2022).
4. Le, J. & Min, J. H. Structural modeling and analyses of genetic variations in the human XPC nucleotide excision repair protein. *J Biomol Struct Dyn*, 1-28, doi:10.1080/07391102.2023.2177349 (2023).

Transcription-Induced Active Forces Suppress Chromatin Motion by Inducing a Transient Disorder-To-Order Transition

Sucheol Shin[1], **Guang Shi**[1,2], **Hyun Woo Cho**[3], **Dave Thirumalai**[1,4]
[1]Department of Chemistry, The University of Texas at Austin, Austin, TX 78712, USA;
[2]Department of Materials Science, University of Illinois, Urbana, Illinois 61801, USA;
[3]Department of Fine Chemistry and Center for Functional Biomaterials, Seoul National University of Science and Technology, Seoul 01811, Republic of Korea;
[4]Department of Physics, The University of Texas at Austin, Austin, TX 78712, USA

I. INTRODUCTION

The organization of interphase chromosomes in a number of species is starting to emerge thanks to advances in a variety of experimental techniques. However, much less is known about the dynamics, especially in the functional states of chromatin. Recent experiments have shown that the mobility of individual loci in human interphase chromosome decreases during transcription, and increases upon inhibiting transcription.[1] This is a counter-intuitive finding because it is thought that the active mechanical force (*F*) on the order of ten piconewtons, generated by RNA polymerase II (RNAPII), that is presumably transmitted to the gene-rich region of the chromatin, would render it more open, thus enhancing the mobility.[2,3]

II. RESULTS

Inspired by the experimental observations, we develop a minimal active copolymer model for interphase chromosomes to investigate how *F* affects the dynamical properties of a single chromosome.[4] In the model, *F* is applied along each bond of gene-rich euchromatin (A-type) loci as an extensile force dipole. The movements of the A-type loci are suppressed in an intermediate range of *F*, and are enhanced at small and large *F* values. On the other hand, the dynamics of the inactive heterochromatin (B-type) loci is not affected by *F*. The intermediate *F* values accord well with forces exerted by RNAPII (3 to 16 pN)[3], and the relative change in the mean square displacement upon removing the activity is semi-quantitatively comparable to that from the experiments. Remarkably, this good agreement is obtained without adjusting parameters to fit the data. In the intermediate *F*, the bond length between consecutive loci increases, becoming commensurate with the pair distance at the minimum of the attractive interaction potential between non-bonded active loci. This results in a transient disorder-to-order transition, leading to the decreased mobility during transcription.

III. DISCUSSION

Notably, the *F*-dependent change in the locus dynamics does not alter the organization of the chromosome. Moreover, the *F*-induced structural transition is not observed in a copolymer chain whose A/B sequence is randomly shuffled. Hence, the activity-induced dynamical suppression occurs only in the interphase chromosomes which exhibit microphase separation between A and B loci. Our study suggests that transient ordering of the active loci might be a plausible mechanism for nucleating a dynamic network involving transcription factors, RNAPII, and chromatin.

ACKNOWLEDGEMENTS

This work was supported by the National Science Foundation (CHE19-000033) and the Welch Foundation through the Collie-Welch Chair (F-0019).

REFERENCES

1. Nagashima, R. *et al.* Single nucleosome imaging reveals loose genome chromatin networks via active RNA polymerase II. *J. Cell Biol.* **218**, 1511–1530 (2019).
2. Yin, H. *et al.* Transcription against an applied force. *Science.* **270**, 1653–1657 (1995).
3. Wang, M. D. *et al.* Force and velocity measured for single molecules of RNA polymerase. *Science.* **282**, 902–907 (1998).
4. Shin, S., Cho, H. W., Shi, G. & Thirumalai, D. Transcription-induced active forces suppress chromatin motion by inducing a transient disorder-to-order transition. arXiv:2205.00353 (2022).

Single-molecule characterization of the early phase of amyloid-β aggregation

Hoi Sung Chung, Fanjie Meng
Laboratory of Chemical Physics, National Institute of Diabetes and Digestive and Kidney Diseases, National Institutes of Health, Bethesda, MD, 20892-0520

I. SUMMARY

Protein aggregation is implicated in the development of various diseases. Although amyloid fibrils are known to be toxic, a number of experimental studies have shown that a subset of soluble oligomers formed during the aggregation process, can be more toxic than the fibrils. Structural studies using solid-state NMR and cryoEM have revealed polymorphism in amyloid fibril structures, suggesting that soluble oligomers are a dynamic mixture of various species with different sizes and conformations. Oligomers may also appear transiently during aggregation and their population is very low. These characteristics make it very difficult to quantitatively characterize oligomers using conventional biophysical and biochemical methods, and the identity of the toxic species remains unknown.

We studied the early phase of aggregation of amyloid-β (Aβ) including the dimerization and formation of stable oligomers using single-molecule Förster resonance energy transfer (FRET) spectroscopy. To enhance the dimerization, we designed three tandem Aβ dimer constructs of the two isoforms: 40-residue (Aβ40) and 42-residue (Aβ42). In all three cases of the homodimers (Aβ42-Aβ42 and Aβ40-Aβ40) and the heterodimer (Aβ40-Aβ42), dimerization is extremely rare with a high dissociation constant of > 15 mM, a value of non-specific interactions. More importantly, we found multiple dimer states with different FRET efficiencies and stabilities. We used a 6 dimer state model to determine the equilibrium constant and kinetic parameters between monomer and dimer equilibrium. This structural and kinetic diversities potentially result from the non-specific interactions between the monomers and can be the cause of the structural heterogeneity of the fibrils.

To detect the formation of larger and stable oligomers of Aβ42, we employed a single-molecule free diffusion experiment, in which fluorophore-labeled oligomers are detected by fluorescence bursts produced when the molecules pass through a focal spot. To accurately determine the size and concentration of oligomers and the difference in their conformations from the brightness (fluorescence intensity), number of fluorescence bursts, and FRET efficiency, we introduce a new method based on the maximum likelihood analysis of individual photons. The method is based on a rigorous description of diffusing molecules and explicitly takes burst selection criteria into account, which removes the burst selection bias in the parameter determination. We found that the concentration of stable Aβ42 oligomers is extremely low, less than 0.1% of all soluble species. The average size of the oligomers is large, about 70-mer, and they have a rod-like, elongated shape.

ACKNOWLEDGEMENTS

This work was supported by the Intramural Research Program of the National Institute of Diabetes and Digestive and Kidney Diseases, NIH.

Silver Chalcogenide Infrared Colloidal Quantum Dots

Gahyeon Kim[1], Haemin Song[1], So Young Eom[1], Mai Ngoc An[2], Dongsun Choi[1], Rajesh Bera[2], Kwang Seob Jeong[1,2]

[1] Department of Chemistry,Korea University,Seoul 02841, Republic of Korea

[2] Center for Molecular Spectroscopy and Dynamics, Institute for Basic Science (IBS), Korea University, Seoul 02841, Republic of Korea

I. SUMMARY

Infrared colloidal nanomaterials have generated a lot of interest due to their potential in various applications such as telecommunications, biosensing, gas sensing, crewless vehicles, etc. This talk will discuss the optical and electrical properties of the silver chalcogenide colloidal quantum dots and their potential in optoelectronic.[1-5] The silver chalcogenide colloidal quantum dots exhibit wide-tunable bandgap energy due to the quantum confinement effect, extending to the extended SWIR regime of 2.7 μm. [1] Moreover, the compositional versatility of the nanocrystal and the switchable electronic transitions between the bandgap transition and intraband transition provide maximum wavelength tunability over one order of magnitude, up to the MWIR regime of 6.7 μm. [2-5] With such tunable electronic transition and relatively low toxicity, the silver chalcogenide quantum dot could be an alternative to heavy metal materials embedded in infrared sensors requiring non-toxicity.

ACKNOWLEDGEMENTS

This research was supported by Creative Materials Discovery Program (NRF-2019M3D1A1078299), the Nano & Material Technology Development Program (NRF-2021M3H4A3A01062964 and NRF-2022M3H4A1A03076626), the Basic Science Research Program (NRF-2021R1A2C2092053) through the National Research Foundation of Korea (NRF) funded by the Ministry of Science and ICT, and the Institute for Basic Science (IBS-R023-D1).

REFERENCES

1. Gahyeon Kim, Dongsun Choi, So Young Eom, Haemin Song, and Kwang Seob Jeong "Extended- Short-Wavelength Infrared Photoluminescence and Photocurrent of Nonstoichiometric Silver Telluride Colloidal Nanocrystals", *Nano Lett.*, 21, 19, 8073-8079, 2021.
2. Juhee Son, Dongsun Choi, Mihyeon Park, Juyeong Kim, Kwang Seob Jeong "Transformation of Colloidal Quantum Dot: From Intraband to Localized Surface Plasmon Resonance", *Nano Lett.,* 20, 7, 4985-4992, 2020.
3. Mihyeon Park, Dongsun Choi, Yoonchang Choi, Hang-beum Shin, Kwang Seob Jeong "Mid-Infrared Intraband Transition of Metal Excess Colloidal Ag_2Se Nanocrystals" *ACS Photonics,* 5, 5, 1907-1911. 2018.
4. Rajesh Bera, Dongsun Choi, Yoon Seo Jung, Haemin Song, Kwang Seob Jeong "Intraband Transitions of Nanocrystals Transforming from Lead Selenide to Self-doped Silver Selenide Quantum Dots by Cation Exchange", *J. Phys. Chem. Lett.*, 13, 26, 6138–6146, 2022.
5. Joonhyung Lim, Yun Chang Choi, Dongsun Choi, I-Ya Chang, Kim Hyeon-Deuk, Kwang Seob Jeong, Kyungwon Kwak, Minhaeng Cho "Ultrafast Intraband Auger Process in Self-doped Colloidal Quantum Dots", *Matter*, 4, 3, 1072-1086, 2021.

Nature-inspired synthetic polymers for customized biomedical applications

Soon-Mi Lim[1,4], Shih-Guo Li[1], Yunchong Yang[1], Tan Nguyen[1], Kevin T. Wacker[1], Lauren A. Link[1], Sarosh Khan[1], Andrew C. Weems[1], and Karen L. Wooley[1,]

[1]Deparment of Chemistry, [2]Chemical Engineering, [3]Department of Materials Science & Engineering, [4]Laboratory for Synthetic-Biologic Interactions Texas A&M University, College Station, Tx, USA, [5]Department of Biomedical Engineering, Ohio University

Synthetic polymers are promising candidates for customized biomedical applications due to versatility of structural modifications to meet the need of specific applications. In this talk, we will be presenting our recent developments of nature-inspired polymers for artificial bones, cardiovascular applications, and tissue recovery. Poly(thioether-co-carbonate) materials were synthesized from tris(alloc)quinic acid (TAQA) and multifunctional thiols. Quinic acid is abundant in coffee beans and plant-based food and can be metabolized by bacteria in guts. The TAQA polymers showed storage modulus of 1.4 GPa, which can be comparable to moduli of cancellous bones, and provided viable environment for preosteoblast cells. Degradation compounds from the polymer were also tested to be benign to cells. Poly(honokiol carbonate) (PHC) and a series of thermosets were synthesized from tree-based honokiol and magnolol and tested for cardiovascular applications. 3D-printed PHC and magnolol thermosets were tested with vascular endothelial cells, which maintained a monolayer of viable cells on the substrate even after a month. Furthermore, magnolol thermosets showed scavenger effect for reactive oxygen species (ROS). Hydrolytic degradation and swelling properties of magnolol thermosets also exhibited great potential as a drug-eluting material for vascular stents and coatings. Soft polymers have different categories of biomedical applications such as artificial tissue for wound healing and tissue rejuvenation. A hydrogel system from poly(ethylene glycol)-block-poly(dl-allylglycine) (PEG-b-PDLAG) mixed with fibroblast cells were tested for viability. As the hydrogel degraded in cell culture medium, cells were released to the cell culture plate and proliferated on the substrate. Cells showed high viability even after captured for a week in the hydrogel due to the porous structure of the hydrogel that allows penetration of nutrition and air. Our study showed that nature-inspired synthetic polymers can be environment-friendly tools for on-demand materials to meet the need of specific applications with relatively simple and cost-effective synthesis methods.

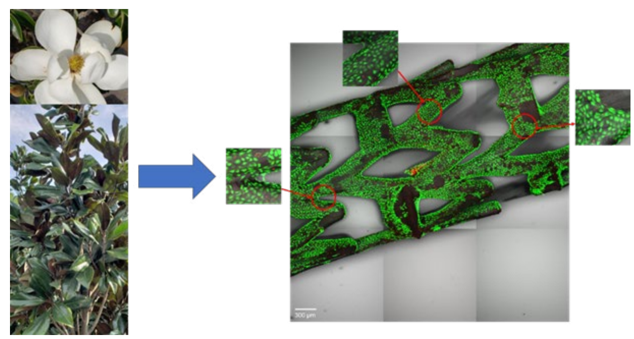

Figure 1: Poly-honokiol carbonate (PHC) based on honokiol from a magnolia tree and cell viability on PHC material.

ACKNOWLEDGEMENTS

This abstract is approved for 2023 ACS Fall National Meeting. We kindly thank Profs. Cynthia J. Meininger and Andreea Trache (Texas A&M Health Science Center) for providing coronary venular endothelial cells (CVECs) and gratefully acknowledge financial support from the National Science Foundation (CHE-1410272), and the Welch Foundation through the W. T. Doherty-Welch Chair in Chemistry (A-0001). All images were acquired at Laboratory for Synthetic-Biologic Interactions at Texas A&M University.

REFERENCES

1. Wacker, K. T.; Kristufek, S. L.; Lim, S.-M.; Kahn, S.; Wooley, K. L. "Bio-based Polycarbonates Derived from the Neolignan Honokiol", RSC Advances, 2016, 6(85), 81672-81679
2. Wacker, K. T.; Lim, S.-M.; Khan, S.; Weems, A. C.; and Wooley, K. L., "3D-printed poly-honoiol carbonate for scaffolding in vascular applications", *Manuscript in preparation.*

Photoemission of Upconverted Hot electrons from Doped Quantum Dots– Effect of Charge and Ligand

Dong Hee Son
Department of Chemistry Texas A&M University College Station, TX 77843

I. SUMMARY
Photogeneration of hot electrons via exciton-to-hot electron upconversion from Mn-doped semiconductor nanocrystals and the application of the upconverted hot electrons in catalysis have been successfully demonstrated in recent years.[1-6] The upconversion occurs via the two-step process involving the initial sensitization of Mn^{2+} by exciton followed by the Auger energy transfer from Mn^{2+} to the electrons in the host nanocrystals. Taking advantage of the long lifetime of the excited ligand field state of Mn^{2+}, the generation of hot electron via the upconversion can occur under weak continuous wave (cw) excitation. (Fig. 1) So far, hot electron upconversion has been demonstrated in several host nanocrystals doped with Mn^{2+} including II-VI and cesium lead halide quantum dots (QDs). In this work, the effect of introducing a hole transport layer between Mn-doped CdS/ZnS core/shell QDs and ITO/glass substrate on the photoemission of the upconverted hot electrons in vacuum was investigated.

II. RESULTS and DISCUSSIN

The Auger energy transfer in Mn-doped semiconductor QDs is considered to produce primarily hot electrons rather than hot holes, although further studies are needed to explore the possibility of hot holes generation. Therefore, we consider the hole transfer in Mn-doped CdS/ZnS QDs under hot electron upconversion condition to be similar to that of conventional undoped QDs that can be facilitated by the hole transport materials commonly used in solar cell and light-emitting devices. Here, we used poly(3,4-ethylenedioxythiophene): polystyrene sulfonate (PEDOT:PSS) as the hole transport material to fabricate the photocathode on ITO/glass substrate and measured the hot electron photoemission current as a function of the bias between the photocathode and anode that forms a simple vacuum tube structure. By comparing the bias-dependent hot electron photocurrents from several different photocathodes with and without PEDOT:PSS, we obtained evidence for the increased excess kinetic energy of the photoemitted hot electrons from more facile removal of holes by PEDOT:PSS. The decreased energy required to eject the electrons from the conduction band of the QDs by reducing the remaining positive charge (hole) in the QDs was discussed as the origin of the increased energy of the photoemitted hot electrons. The results demonstrate the importance of the hole transfer between Mn-doped QDs and the surroundings on the energy of the upconverted hot electrons that also bears an important practical implication in their applications.

Figure 1: (a) Hot electron upconversion mechanism. (b) Hot electron photoemission measurement setup.

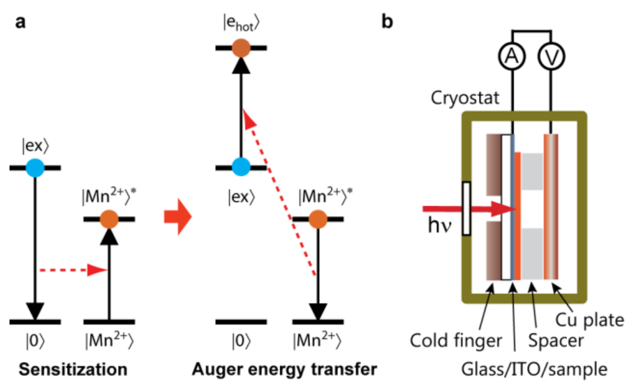

INFRARED SEES PROTEINS IN WATER, SENSITIVELY

Young Jong Lee, Bonghwan Chon, Seong-Min Kim
Biosystems and Biomaterials Division, National Institute of Standards and Technology

I. ABSTRACT

Infrared (IR) absorption spectroscopy has been widely used to characterize the secondary structure of proteins and polypeptides. In particular, the amide I band is extensively studied because its absorption cross section is high compared to other functional groups, and more importantly, its absorption peak width and position are unique for different secondary structures, such as α-helices, β-sheets, and random coils. The distinct spectral features of the amide I band are so well investigated that IR spectroscopy can be used to measure semi-quantitatively the fractions of mixed secondary structures. In addition to the amide I band, analysis of broader IR absorption spectra of other molecular vibrations enables label-free chemical identification with the help of extensively accumulated spectral libraries. This non-emission-based approach can also provide absolute concentrations of subcomponents from the Beer-Lambert law. The SI (international system of units)-traceable measurement can improve data reproducibility and inter-laboratory comparability significantly for measurement assurance.

Despite these many advantages, conventional IR approaches to protein in aqueous solutions have been significantly challenged because the strong IR absorption of water overwhelms the limited dynamic range of the detection system and thus allows only a short path length and poor concentration sensitivity. In this presentation, we demonstrate an adaptive solvent absorption compensation (SAC) approach can improve the concentration sensitivity and extend the available path length by distinguishing the analyte signal over the full dynamic range at each wavelength. We present QCL-based IR absorption spectra of hydrated proteins from >100 mg/mL to < 0.02 mg/mL protein concentration, allowing a three-orders of magnitude enhanced signal-to-noise ratio in the amide I band compared to the non-SAC results. We also present new advancements in spectral range and speed of absorption measurement. This simple optical technique can be applied to other absorption spectroscopies of analytes in strongly absorbing solvents, allowing for enhanced sensitivity without changing the detection system.

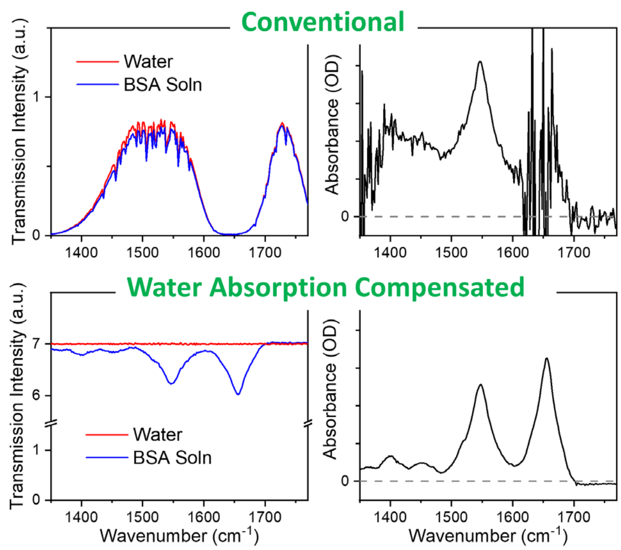

Figure 1: Comparison of IR transmission and absorbance spectra of an identical protein solution measured by conventional and new solvent absorption compensated (SAC) methods.[1]

REFERENCES

1. B. Chon, S. Xu, Y. J. Lee, "Compensation of strong water absorption in infrared spectroscopy reveals the secondary structure of proteins in dilute solutions," *Anal. Chem.* Vol. 93, pp. 2215, 2021.

Introduction advanced environmental risk assessment for pesticide residues in environmental and AISS

Hyo sub Lee[1], Geonhee Jung[1], Taekkyum Kim[1], Seojin Ki[2], Sangik Seo[2], Minho Son[3]
[1]Residual Agrochemical Assessment Division, Rural Development Administration(RDA), [2]Department of Environmental Engineering, Gyeongsan National University, [3]Digitalplatform HQ, podo inc.

Abstract

The focus on pesticide safety has evolved beyond food security and now encompasses considerations for sustainable environmental management. The monitoring for soil and water has carried out since 2018 more than 800 sites and appoximately 300 tested pesticides and metabolites in Korea. Risk assessement were conducted for detected compounds. Conventional methods for environmental risk assessment such as Toxicity Exposure Ratios (TER) and Risk Quotients (RQ) are commonly employed, but their precision is notably limited. Therefore methodological enhancements were needed. This study has implemented techniques such as principal component analysis and cluster analysis using physicochemical properties and toxicity data for pesticides, to refine environmental risk assessment. The advanced approach incorporates the identification and validation of critical hazardous pesticides, and compared to conventional methods, it offers improved correlation and simplicity. To facilitate the all of preocess, we have developed websystem "Agricultural environmental Integrated Safety management System(AISS)", designed to streamline the process with a single click. Our study marks a significant stride towards a more efficient and accurate environmental risk assessment of pesticides.

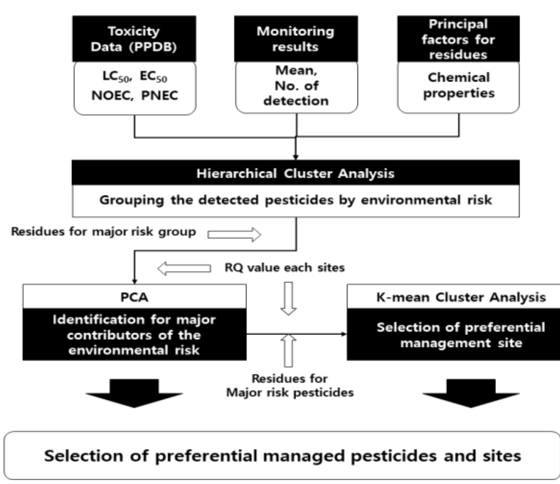

Figure 1: **Algorithm for developed environmental risk assessment by PCA and cluster analysis**

Figure 2: **Agricultural environmental Integrated Safety management System(AISS)**

ACKNOWLEDGEMENTS

This work was carried out with the support of "Co-operative Research Program for Agriculture Science and Technology Development (Project No. PJ014488)" Rural Development Administration, Republic of Korea.

REFERENCES

1 .Panizzi, S., Suciu, N. A. and GarmoM. 2017. Combined ecotoxicological risk assessment in the frame of European authorization of pesticides. Science of the Total Environment, 580, 136-146.
2 Hvězdová, M., Kosubová, P., Košíková, M., Scherr, K. E., Šimek, Z., Brodský, L. and Hofman, J. 2018. Currently and recently used pesticides in Central European arable soils. Science of the Total Environment, 613, 361-370.
3 Silva, V., Mol, H. G., Zomer, P., Tienstra, M., Ritsema, C. J. and Geissen, V. 2019. Pesticide residues in European agricultural soils–A hidden reality unfolded. Science of the Total Environment, 653, 1532-1545.

New 2D with atomically thin crystals

Jiwoong Park
University of Chicago

I. SUMMARY

Two dimensional (2D) electron transport has been one of the most important topics in science and technology for decades. It was originally studied in 3D semiconductors and then continued in 2D van der Waals (vdW) crystals. In this talk, I will start with the large-scale processes for generating 2D crystalline semiconductor films and superlattices that could be used to fabricate atomically thin integrated circuits [1-2]. Then we will discuss more recent directions. I will discuss how we use these 2D materials to realize non-electronic 2D transport phenomena observed from phonons [3], photons [4], and mass [5], which could empower the development of 2D phononics, 2D photonics, and 2D mechanics. I will end with discussing how one can realize these properties using molecule-based 2D polymers and crystals [6].

REFERENCES

1. J. Mannix, A. Ye, S. H. Sung, A. Ray, F. Mujid, C. Park, M. Lee, J.-H. Kang, R. Schreiner, A. High, D. A. Muller, R. Hovden, and J. Park, "Robotic four-dimensional pixel assembly of van der Waals solids", ***Nature Nanotechnology***, 17, 361-366 (2022).
2. K. Kang, S. Xie, L. Huang, Y. Han, P. Y. Huang, K. F. Mak, C.-J. Kim, D. A. Muller, and J. Park, "High-performance three-atom-thick semiconducting films with wafer scale homogeneity," ***Nature***, 520, 656-660 (2015).
3. S. E. Kim, F. Mujid, A. Rai, F. Eriksson, J. Suh, P. Poddar, A. Ray, C. Park, E. Fransson, Y. Zhong, D. A. Muller, P. Erhart, D. G. Cahill, and J. Park, "Extremely anisotropic van der Waals thermal conductors", ***Nature***, 597, 660-665 (2021).
4. M. Lee, H. Hong, J. Yu, F. Mujid, A. Ye, C. Liang, and J. Park, "Wafer-scale δ-waveguides for integrated two-dimensional photonics", under review, ***Science***.
5. J. Yu, C. Liang, M. Lee, S. Das, A. Ye, F. Mujid, P. Poddar, B. Cheng, N. L. Abbott, and J. Park, "Two-dimensional mechanics of atomically thin solids on water", ***Nano Letters***, 22, 7180-7186 (2022).
6. Y. Zhong, B. Cheng, C. Park, A. Ray, S. Brown, F. Mujid, J.-U. Lee, H. Zhou, J. Suh, K.-H. Lee, A. J. Mannix, K. Kang, S. J. Sibener, D. A. Muller and J. Park, "Wafer-scale synthesis of monolayer two-dimensional porphyrin polymers for hybrid superlattices", ***Science***, 366, 1379-1384 (2019).

Vapor-Phase Anisotropic Polymer Particle Synthesis through Condensed Droplet Polymerization

Kwang-Won Park[1], Rong Yang[1*]

[1]School of Chemical and Biomolecular Engineering, Cornell University, Ithaca, NY 14853

I. Abstract

Anisotropic polymer particles exhibit interesting physicochemical properties and can be assembled into complex structures, compared to isotropic, i.e., spherical polymer particles. However, polymer synthesis strategies, such as emulsion polymerization, currently known for polymer nanoparticles, cannot reliably create non-spherical particles and may not be practical due to solvent restrictions, low efficiency, and reaction time. Recently, our group developed a rapid, solvent-, and template-free synthesis of non-spherical polymer particles through condensed droplet polymerization (CDP).[1] Despite of the advantages of CDP technique, the efficacy of radical species based on different filament temperatures, which influences on polymerization kinetics and particle morphologies, were not fully understood.

Here, we present a systematic approach through the CDP process at different filament temperatures and working pressures to understand the role of the radical species, i.e., tert-butoxy (*t*-BuO$^\bullet$) and methyl ($CH_3^\bullet$) radicals originating from *tert*-butyl peroxide (TBPO). We find that higher filament temperatures lead to lower aspect ratio with larger diameter polymer domes, while lower filament temperatures result in higher aspect ratio with smaller diameter polymer domes. **Figure 1** illustrates the CDP process used to create various morphologies of poly(benzyl methacrylate) domes at different filament temperatures. This is attributed to the different kinetics of $CH_3^\bullet$ radical species generated at higher temperatures from the *β*-scission reaction of *t*-BuO$^\bullet$ radicals.

In addition to the morphological characterizations, chemical properties of polymer materials, such as FT-IR, GPC, and MALDI-TOF, provide more insight into free-radical polymerization kinetics. Notably, we realize the capability of fine tuning of polymer dome morphologies through different CDP conditions, meaning that our approach can be adapted to improve the industries, such as nano-lens with various focal lengths, drug delivery with enhanced hydrodynamic properties.

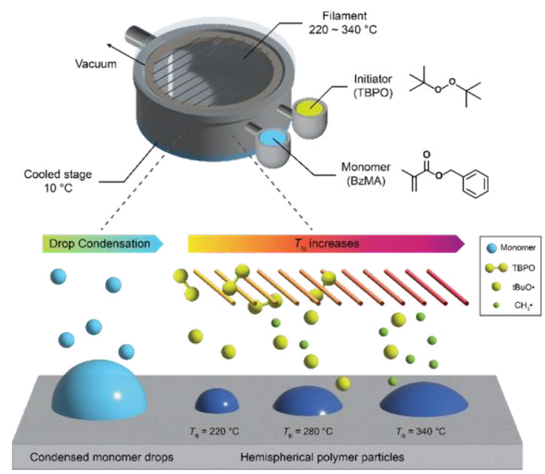

Figure 1: Schematic of CDP process to synthesis polymer domes with various morphologies at different filament temperatures (T_{fil}).

ACKNOWLEDGEMENTS

Analytical methods involved the use of the Cornell Center for Materials Research (CCMR) Shared Facilities which are supported through the NSF MRSEC program (DMR-1719875). This work is supported by the National Science Foundation Faculty Early Career Development Program under Grant no. CMMI-2144171.

REFERENCES

1. Franklin, T, Danielle L. S, and Yang, R. "Versatile and Rapid Synthesis of Polymer Nanodomes via Template-and Solvent-free Condensed Droplet Polymerization." *Chemistry of Materials* **2022**, 34, 5960-5970.

Iron-Gold Contacts: An Effective Linker for Ferrocene-Based Single-Molecule Electronics

Woojung Lee[1]
[1]Department of Chemistry, Columbia University, New York, New York, 10027, United States

The structure and geometry of the interfacial electrode-molecule contacts play a significant role in controlling the stability, conductance, and variability of single-molecule junctions. Though organic groups such as thioethers, amines, and phosphines are known to form robust linkages in measurements using the scanning tunneling microscope-based break-junction method, it is of significant interest to expand the known library of suitable contacting moieties to provide new opportunities in the tunability and functionality of molecular components. Recent studies have reported bonds between the ferrocene iron center and other metals (Pd, Co, etc.) in derivatives where there are additional coordinating groups attached to the cyclopentadienyl rings. Here we explore the electron transport properties of ferrocene-containing wires and show evidence that the iron atom can itself function effectively as a contact group through direct metal-electrode binding, but only when it is in the formal 3+ oxidized state. Through a series of control measurements and density functional theory calculations, we confirm that the iron-gold bond can provide a chemical link between the metal electrodes and the molecular backbone in ferrocene junctions. These findings also provide a robust method of controlling the bond between the ferrocene iron center and the Au electrode using simple electrochemical manipulations.

We have measured the conductance of single-molecule junctions formed with a Fe-Au in ferrocene derivatives using the scanning tunneling microscope-based break-junction (STM-BJ) method. Through this study, we confirm that the Fe-Au bond is formed only when the ferrocene is in an oxidized state. Our calculations suggest that the half-filled frontier orbital of oxidized ferrocene derivatives enables a Au atom to share an electron covalently. Remarkably, molecular junctions through the Fe-Au bond exhibit a high conductance that may be switched on and off through electrochemical methods, offering new avenues to control and switch the geometry of a molecule in a junction. This work sets the path to achieving versatile and higher-conducting ferrocene-based electronics that were previously inaccessible with organic linkers.

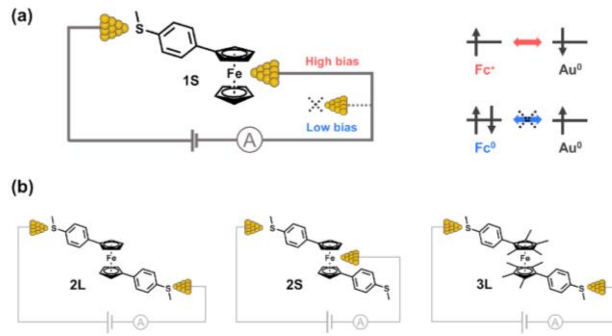

Figure 1: (a) *Left:* Schematic of a single-molecule junction formed with **1** between two Au electrodes during scanning tunneling microscope-based break junction (STM-BJ) measurements. *Right:* The electron configurations within frontier orbitals of a ferrocene (Fc) and a Au atom (Au^0) for a neutral (blue) and oxidized (red) Fc. (b) Chemical structures of **2** and **3**, and their experimentally accessible junction geometries; **S** and **L** denote "short" and "long" junction geometries of each derivative, respectively.

ACKNOWLEDGEMENTS

This work was supported in part by the NSF CCI Phase I: Center for Chemistry with Electric Fields (CHE-2023568), the NSF MRSEC on Precision-Assembled Quantum Materials (DMR-2011738), and the National Science Foundation under grant DMR-1807580.

REFERENCES

1. Yamaguchi, Y. *et al.* "Electronic structure, spectroscopy, and photochemistry of group 8 metallocenes", *Coordination chemistry reviews* **251**, 515-524 (2007)
2. Pick, F. S., Thompson, J. R., Savard, D. S., Leznoff, D. B. & Fryzuk, M. D. "Synthesis of Iron and Cobalt Complexes of a Ferrocene-Linked Diphosphinoamide Ligand and Characterization of a Weak Iron–Cobalt Interaction", *Inorganic Chemistry* **55**, 4059-4067 (2016)

Generalized Understanding of Double Layer for Concentrated Aqueous Electrolytes and Ionic Liquids

Suehyun Park[1], Jesse McDaniel[1]

[1]Department of Chemistry and Biochemistry, Georgia Institute of Technology, Atlanta, GA 30332

I. SUMMARY

Electrical double layer (EDL) is a unique structure found at the interface of electrolyte and electrode. EDL modulates its structure in response to the applied voltage, and the structural change alters the charge/electron transfer required for electrosynthesis and electrocatalysis[1]. To probe the structural response of EDL with respect to applied voltage, the differential capacitance measurement is one of the oldest and still most widely used techniques. The standard model of the capacitance profile for aqueous solutions is the Gouy-Chapman-Stern (GCS) theory[2], which successfully predicts the key feature, the minimum near the potential of zero charge (PZC) at dilute solutions (~ 1mM). At high ion concentration, the voltage-independent capacitance profile predicted by the GCS theory doesn't resemble experimentally observed profiles of disappearing minimum near the PZC. Here, we propose and validate the generalized Helmholtz model that well describes the capacitance profiles for concentrated aqueous electrolytes and ionic liquids.

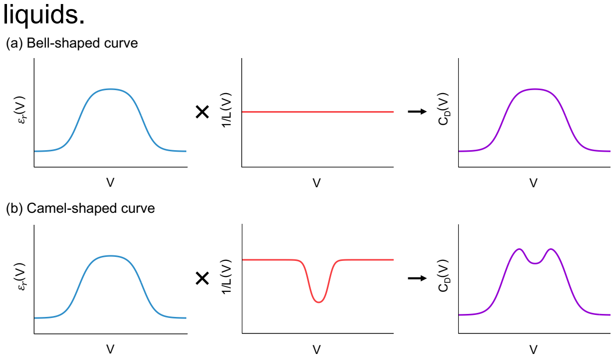

Figure 1: Generalized Helmholtz model. (a) Bell-shaped capacitance curve (b) Camel-shaped capacitance curve.

The generalized Helmholtz model explains the two most representative capacitance curves, bell-shaped and camel-shaped curve, for concentrated aqueous electrolytes and ionic liquids by incorporating the voltage-dependent dielectric response and the voltage-dependent thickness of the inner layer.

$$C(V) = \frac{A\varepsilon(V)}{L(V)}$$

where A is the surface area of the electrode, $\varepsilon(V)$ is the voltage-dependent dielectric response, and $L(V)$ is the voltage-dependent thickness of the inner layer.

To validate the model, we ran molecular dynamics simulations of three different electrochemical interfaces: Au(100)/1M $[Na^+][Cl^-]$ interface, Au(100)/$[BMIM^+][BF_4^-]$ interface and graphite/$[BMIM^+][BF_4^-]$ interface. The Au(100)/ 1M $[Na^+][Cl^-]$ interface exhibits the bell-shaped capacitance curve, with a peak at negative voltage and the decrease of the capacitance value at positive voltage. The trend of $\varepsilon(V)$ is consistent with the capacitance profiles, while $L(V)$ is invariant to the applied voltage. The Au(100)/$[BMIM^+][BF_4^-]$ interface also exhibits the bell-shaped capacitance profile near the PZC and the invariant thickness of the inner layer. Lastly, the graphite/$[BMIM^+][BF_4^-]$ interface shows the camel-shaped capacitance curve with a local minimum near the PZC and two peaks on either side of the minimum. The local minimum of the capacitance curve is induced by the maximum of the inner layer thickness near the PZC, which results in the camel-shaped capacitance curve. Therefore, three electrochemical interfaces that we investigated follow the generalized Helmholtz model.

ACKNOWLEDGEMENTS

Computational resources and services were provided by the Partnership for an Advanced Computing Environment (PACE) at Georgia Tech.

REFERENCES

1. Sun, L., Ramesha, G. K., Kamat, P. V., Brennecke, J. F., “Switching the reaction course of electrochemical CO_2 reduction with ionic liquids.” *Langmuir*, 30, 6302-6308, 2014.
2. Stern, O., “The theory of the electrolytic double-layer.” *Z. Elektrochem. Angew. Phys. Chem.*, 30, 508-516, 1924.

Technical Group A-3

Mathematics, Applied Math and Statistics (MAS)

GMsHDG method for nonlinear porous media

Minam Moon[1]
[1]Korea Military Academy

I. SUMMARY

We present a generalized multiscale hybridizable discontinuous Galerkin method for nonlinear porous media. We give projection-based error analysis on the GMsHDG method to numerically solve a nonlinear parabolic problem. Through representative numerical experiments, we confirm the reliability of the error estimations and show that the proposed method is practical and efficient.

II. Analysis on GMsHDG method

A. Model problem

$$u_t(x,t) - \nabla \cdot \left(\kappa\,(x,u)\nabla\, u(x,t)\right) = f(x,t)$$

with the homogeneous boundary condition and initial condition.

B. Assumptions

Assumption 1. A is chosen in such a way that there exist constants $\mathrm{C}_1, \mathrm{C}_2, C_3$, and C_4 such that for all $\mathrm{u} \in \mathrm{R}$, we have the following inequalities:

(1) $0 < \mathrm{C}_1 \leq \alpha\,(u) \leq C_2 < \infty$,

(2) $-\infty < C_3 \leq \partial_t \alpha(u) \leq C_4 < \infty$

We further assume that both $\alpha(u)$ and $\partial_t \alpha(u)$ are Lipschitz continuous.

Assumption 2. On each coarse-grid edge $\mathrm{F_i} \in e_H$, we assume that the exact solution u and time derivative $\partial_t u$ have spectral expansions as:

$$u(\mathrm{x},t) \cong \sum_j u_{ij}(t)\psi_j^i(x),\ \partial_t u(\mathrm{x},t) \cong \sum_j u_{ij}'(t)\psi_j^i(x)$$

where ψ_j^i is *j*-th eigenfunction of the local problem.

C. Main results

Theorem 3. Under Assumptions 1 and 2, for all $0 \leq \mathrm{s} \leq \mathrm{k}+1$, we have

$$\begin{aligned}\|e_u\|_{L^\infty(L^2)} \leq\ & C\mathrm{h}^s\left(\|u\|_{H^1(H^s)} + \|\boldsymbol{q}\|_{H^1(H^s)}\right)\\ &+ C\mathrm{h}^s H^{-\frac{1}{2}}\left(\|u\|_{L^2(H^{s+1})} + \|\boldsymbol{q}\|_{H^2(H^{s+1})}\right)\\ &+ \mathrm{C}\left(\frac{H}{\Lambda \mathrm{h}}\right)^{\frac{1}{2}} \left\|\kappa^{\frac{1}{2}}\,\nabla u\right\|_{L^2(L^2)}\end{aligned}$$

$$\begin{aligned}\|\boldsymbol{e}_q\|_{L^\infty(L^2)} \leq\ & C\mathrm{h}^s\left(\|\boldsymbol{q}(0)\|_s + \|u\|_{H^2(H^s)} + \|q\|_{H^2(H^s)}\right)\\ &+ C\mathrm{h}^s H^{-\frac{1}{2}}\left(\|\boldsymbol{q}(0)\|_{s+1} + \|u\|_{L^2(H^{s+1})} + \|q\|_{H^2(H^{s+1})}\right)\\ &+ \mathrm{C}\left(\frac{H}{\Lambda \mathrm{h}}\right)^{\frac{1}{2}} \left\|\kappa^{\frac{1}{2}}\,\nabla u\right\|_{H^1(L^2)} + C\left(\frac{H}{\Lambda}\right)^{\frac{1}{2}} \left\|\kappa^{\frac{1}{2}}\,\nabla u\right\|_{L^\infty(L^2)}\end{aligned}$$

where $\Lambda = \min_i \lambda_{L_i+1}$.

III. Numerical Results

We present representative numerical results to illustrate the applicability of the GMsHDG method for nonlinear equations.

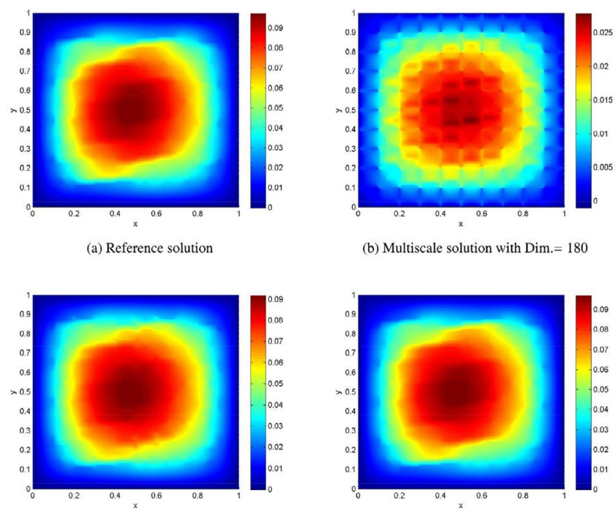

(a) Reference solution (b) Multiscale solution with Dim.= 180

(c) Multiscale solution with Dim.= 720 (d) Multiscale solution with Dim.= 1800

Figure 1: Comparison of the multiscale solutions with the reference (fine-scale) solution

Table 1 : Error table

Dim.	$\|u_\mathrm{h}^* - u_H\|_{L^\infty(L^2)}$	$\|\boldsymbol{q}_\mathrm{h}^* - \boldsymbol{q}_H\|_{L^\infty(L^2)}$
180	0.7157	0.8655
360	0.0750	0.3537
540	0.0350	0.2902
720	0.0320	0.2460

ACKNOWLEDGEMENTS

The work was supported by the NRF grant funded by the Korea government (MSIT) (No. NRF-2020R1 F1A1A01072414, NRF-2022R1F1A1069217)

REFERENCES

1. Minam Moon, “Generalized multiscale hybridizable discontinuous Galerkin (GMsHDG) method for flows in nonlinear porous media,” Journal of Computational and Applied Mathematics, Vol. 415, 2022.

An Efficient K-way Constrained Normalized Cut and its Connection to Algebraic Multigrid Method

Young Ju Lee[1], Ivan Ojeda-Ruiz[1] and Jia Jiwei[2]
[1]Texas State University, [2]Jilin University

I. SUMMARY

Normalized Cut (NCut) discourages the isolated segmentation that may result from the standard minimum Cut by adding a volume constraint. Such a volume constraint introduces a significant computational challenge. In this paper, we propose the K-way constrained Normalized Cut (K-way CNCut). It is formulated as the minimum Cut with a priori chosen constraints or representatives for the cluster. We provide a measure that can assess if the selected constraints can replace the volume constraint as well. For a special case when a single constraint is given as a representative of a single cluster, the K-way CNCut is discovered to have a link with the construction of the prolongation operator in the algebraic multigrid method[1] for the normalized Graph Laplacian. We show how successful multiscale image segmentation[2,3] can be understood in the framework of the K-way CNCut as well. In particular, we show how the multiscale graph coarsening algorithm can be used to construct a set of constraints for the K-way CNCut. A number of numerical experiments are presented to demonstrate the effectiveness of the proposed framework.

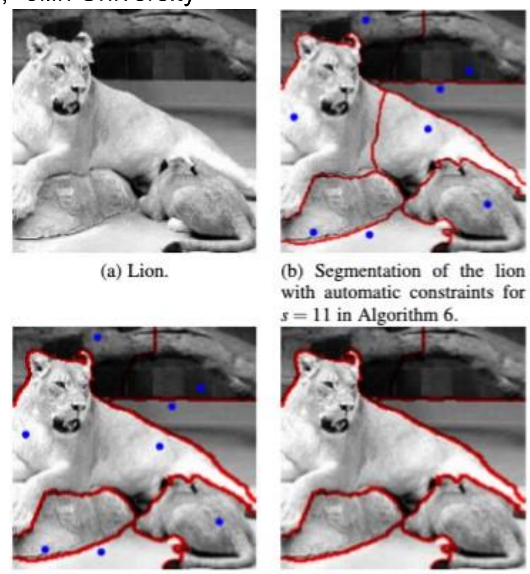

(a) Lion.

(b) Segmentation of the lion with automatic constraints for $s = 11$ in Algorithm 6.

(c) Segmentation of the lion with removed boundaries (constraints included).

(d) Segmentation of the lion with removed boundaries (constraints not included).

Figure 1: Sample results from K-way CNcut

ACKNOWLEDGEMENTS
Lee would like to thank a partial support of NSF-DMS 2208499.

REFERENCES

1. **J. Xu and L. Zikatanov, "Algebraic multigrid methods", Acta Numerica, Vol 26, 2017**
2. **E. Sharon, A. Brandt, and R. Basri, "Fast multiscale image segmentation", Proceedings of the IEEE Computer Society Conference on Computer Vision and Pattern Recognition, 2000.**
3. **E. Sharon, M. Galun, D. Sharon, R. Basri, A. Brandt, "Hierarchy and adaptivity, in segmenting visual scenes", Nature, 2006.**

The moduli space of holomorphic chains of rank one over a compact Riemann surface

JinHyung To
Indiana University Bloomington

I. SUMMARY

A holomorphic chain on a compact Riemann surface is a tuple of vector bundles together with homomorphisms between them. We show that the moduli space of holomorphic chains of rank one is identified with a fiber product of projective space bundles.

II. INTRODUCTION

Let X be a compact Riemann surface of genus $g \geq 0$.

Definition A holomorphic chain C on X is a tuple $(E_0, ..., E_n; \phi_1, ..., \phi_n)$ of vector bundles together with the homomorphisms $\phi_i : E_i \to E_{i-1}$ for $i = 1, ..., n$. The tuple $\boldsymbol{t} = (\mathrm{rk}(E_0), ..., \mathrm{rk}(E_n); \deg(E_0), ..., \deg(E_n))$ is called the type of the holomorphic chain C. A subchain of C is a holomorphic chain $(F_0, ..., F_n; \phi_1|F_1, ..., \phi_n|F_n)$, where $F_i \subseteq E_i$ is a subsheaf such that $\phi_i(F_i) \subseteq F_{i-1}$ for $1 \leq i \leq n$.

A map from $C = (E_0, ..., E_n; \phi_1, ..., \phi_n)$ to $C' = (F_0, ..., F_n; \psi_1, ..., \psi_n)$ is a tuple of vertical maps $f_i : E_i \to F_i$ for $i = 0, ..., n$ such that $\psi_i f_i = f_{i-1}\phi_i$ for $i = 1, ..., n$. It is an isomorphism if all f_i's are isomorphisms.

Given a chain C of type $(r_0, ..., r_n; d_0, ..., d_n)$ and a vector $\boldsymbol{\alpha} = (\alpha_0, \alpha_1, ..., \alpha_n) \in \mathbb{R}^{n+1}$, the $\boldsymbol{\alpha}$-slope of C is the fraction $\mu_{\boldsymbol{\alpha}}(C) = \frac{\sum_{i=0}^{n}(d_i + \alpha_i r_i)}{\sum_{i=0}^{n} r_i}$. A chain C is $\boldsymbol{\alpha}$-stable ($\boldsymbol{\alpha}$-semistable) if $\mu_{\boldsymbol{\alpha}}(C') < \mu_{\boldsymbol{\alpha}}(C)$ ($\mu_{\boldsymbol{\alpha}}(C') \leq \mu_{\boldsymbol{\alpha}}(C)$) for all proper subchains C', i.e., $C' \neq (0, \cdots, 0; 0, \cdots, 0)$ and $C' \neq C$.
The moduli spaces of holomorphic chains are constructed in [Sch]. As a set the moduli space of holomorphic chains is the set of isomorphism classes of holomorphic chains. It is a projective variety.

III. MAIN RESULT

Let $\mathcal{M}^s_{\boldsymbol{\alpha}}(\boldsymbol{t})$ be the moduli space of $\boldsymbol{\alpha}$-stable chains of type $\boldsymbol{t} = (r_0, ..., r_n; d_0, ..., d_n)$ over a compact Riemann surface X of genus g.

By the deformation theory of holomorphic chains ([AGS], Theorem 3.8), the dimension of $\mathcal{M}^s_{\boldsymbol{\alpha}}(\boldsymbol{t})$ at a smooth point C in $\mathcal{M}^s_{\boldsymbol{\alpha}}(\boldsymbol{t})$ is given by the formula $\dim_C \mathcal{M}^s_{\boldsymbol{\alpha}}(\boldsymbol{t}) = (g-1)\left(\sum_{i=0}^{n} r_i^2 - \sum_{i=1}^{n} r_i r_{i-1}\right)$
$+ \sum_{i=1}^{n}(r_i d_{i-1} - r_{i-1} d_i) + 1$.

From now on we assume that $\boldsymbol{t} = (1, ..., 1; d_0, ..., d_n)$ unless otherwise stated. Then the open convex polyhedral cone $H \subset \mathbb{R}^n$ is determined by the inequalities $(n-i)\sum_{k=1}^{i} \alpha_k - (i+1)\sum_{k=i+1}^{n} \alpha_k < (i+1)\sum_{k=i+1}^{n} d_k - (n-i)\sum_{k=0}^{i} d_k$ for $i = 0, ..., n-1$.

Let $\mathcal{L}_i$ be the poincaré bundle over $\mathrm{Pic}^{d_{i-1}-d_i}(X) \times X$. The pushforward $\nu^i_*\mathcal{L}_i$ is a coherent sheaf over $\mathrm{Pic}^{d_{i-1}-d_i}(X)$, where ν^i is the projection map $\mathrm{Pic}^{d_{i-1}-d_i}(X) \times X \to \mathrm{Pic}^{d_{i-1}-d_i}(X)$. Now consider the pullback sheaf $\varphi_i^*\nu^i_*\mathcal{L}_i$, where $\varphi_i : \mathrm{Pic}^{d_0}(X) \times \mathrm{Pic}^{d_1}(X) \times \cdots \times \mathrm{Pic}^{d_n}(X) \to \mathrm{Pic}^{d_{i-1}-d_i}(X)$ is the map defined by $\varphi_i(L_0, ..., L_n) = L_{i-1}L_i^{-1}$.

Theorem Let $\boldsymbol{t} = (1, 1, ..., 1; d_0, d_1, ..., d_n)$. Assume that $d_{i-1} - d_i > 2g - 2$ for all $i = 1, ..., n$. Then for $\boldsymbol{\alpha}$ in H, $\mathcal{M}^s_{\boldsymbol{\alpha}}(\boldsymbol{t}) = \mathbb{P}E_1 \times_Z \mathbb{P}E_2 \times_Z \cdots \times_Z \mathbb{P}E_n$, where $E_i = \varphi_i^*\nu^i_*\mathcal{L}_i$ for $i = 1, 2, ..., n$ and $Z = \mathrm{Pic}^{d_0}(X) \times \mathrm{Pic}^{d_1}(X) \times \cdots \times \mathrm{Pic}^{d_n}(X)$.

ACKNOWLEDGEMENTS

I would like to thank my advisor Steven Bradlow for proposing this question and for valuable discussions.

REFERENCES

[Sch] A. H. W. Schmitt: *Moduli problems of sheaves associates with oriented trees.* Algebras Represent. Theory 6(2003), 1–32.

[AGS] L. Álvarez-Cónsul, O. García-Prada, A. H. W. Schmitt: *On the geometry of moduli spaces of holomorphic chains over compact Riemann surfaces.* IMRP Int. Math. Res. Pap., pages Art. ID 73597, 82, (2006).

Inference about differences in predictive skill between infectious disease forecasting models

Dongah Kim[1], Nicholas G. Reich, Evan L. Ray[1]
[1]University of Massachusetts, Amherst

I. SUMMARY
We introduce inferential procedures for comparison of predictive accuracy of forecasts from a pair of models for multiple locations, multiple forecast creation dates, and multiple horizon forecasts. In the past, hypothesis test methods have been developed in the literature to compare the predictive accuracy for cross-sectional or multi-horizon forecasts. However, there are no test methods that compare cross-sectional and multi-horizon forecasts together. For this task, we adopted both Autoregressive Heteroskedasticity (ARH) and Bayesian dynamic factor analysis (DFA). Since ARH model is for time series data and dynamic factor analysis only considers time and location, we expanded the analysis by incorporating a horizon.

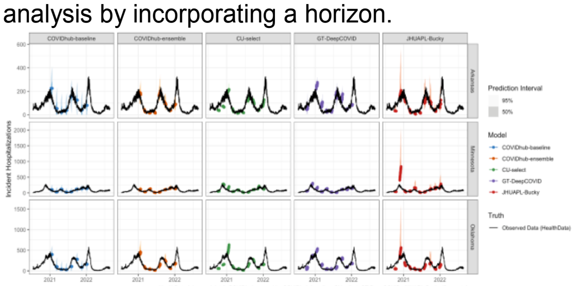

Figure 1 : Daily COVID-19 Incident Hospitalization : observed and forecasted – We can observe the presence of heteroskedasticity in the scores across various locations and horizons.

II. Methods

we propose two approaches for comparing forecast performance. The first approach is relatively straightforward and allows for the application of various test methods. In this approach, we aggregate the data by forecast date, simplifying the analysis to one-dimensional data instead of three-dimensional data. However, this approach may result in the loss of valuable information and statistical power. We are using Diebold and Mariano test (Diebold & Mariano, 2002) and Multi-Horizon Forecast Comparison (Quaedvlieg, 2021).

To address this limitation, we also explore a more complex method for comparing forecast performance. We employ a Bayesian autoregressive heteroskedasticity dynamic factor analysis model (ARH DFA) to estimate the mean difference in the data (Engle, 1982). Although this method is more intricate and computationally intensive, it enables us to account for correlations across all three factors: time, location, and horizon.

III. Simulation Study

Our simulations were conducted to assess the performance of the proposed methods in various scenarios. We performed two simulations: one to evaluate the performance of the Diebold-Mariano (DM) test and bootstrap-based test, and the other to estimate the intercept using the Bayesian ARH DFA model. In order to create complex and realistic data, we generated data from the Bayesian ARH DFA model.

Table 1: Type I error rate with nominal $\alpha = 0.05$ from 1000 simulations

df	3	5	10	15	20	25	30
2	0.272	0.234	0.164	0.129	0.050	0.023	0.130
10	0.266	0.241	0.169	0.137	0.055	0.021	0.140

ACKNOWLEDGEMENTS
Add appropriate acknowledgements as needed.

REFERENCES
Diebold, F. X., & Mariano, R. S. (2002). Comparing predictive accuracy. *Journal of Business & Economic Statistics*, *20*(1), 134–144.

Engle, R. F. (1982). Autoregressive Conditional Heteroscedasticity with Estimates of the Variance of United Kingdom Inflation. *Econometrica*, *50*(4), 987–1007. http://www.jstor.org/stable/1912773

Quaedvlieg, R. (2021). Multi-horizon forecast comparison. *Journal of Business & Economic Statistics*, *39*(1), 40–53.

Exploring Dynamics of HIV Infections: An Analysis of the Susceptible-Infected-Virus Model in Deterministic and Stochastic Forms

Jangwoon Lee
University of Mary Washington

SUMMARY

In this paper, we explore the application of the Susceptible-Infected-Virus (SIV) model to study the dynamics of Human Immunodeficiency Virus (HIV) infections. The SIV model is a compartmental model that describes the within-host dynamics of viral infections. We analyze the model in both its deterministic and stochastic forms. Initially, we provide analytical solutions for two simplified versions of the deterministic model. Subsequently, we utilize numerical methods to investigate the complete deterministic and stochastic systems. The obtained results offer an illustrative depiction of the population dynamics of HIV within the host in the absence of treatment. Furthermore, they highlight the influence of randomness on the progression of the disease.

I. HIV MODEL

$$\frac{dS}{dt} = \lambda - dS - kVS,$$
$$\frac{dI}{dt} = kVS - \delta I,$$
$$\frac{dV}{dt} = N_T\delta I - cV,$$

where *S* is the number of healthy cells, *I* is the number of infected cells, *V* is the number of free virus particles, λ is the healthy T-cell growth rate, *d* is the healthy T-cell death rate constant, *k* is the infection rate constant, δ is the infected cell death rate constant, N_T is the virus production rate constant (per infected cell), and *c* is the viral clearance rate constant.

II. ANALYTICAL SOLUTIONS

$$t = \int_{V_0}^{V} e^{\phi(\xi)} d\xi.$$

$$S = S_0 \exp\left[-k\int_0^t V(\xi)d\xi\right].$$

$$I = P - S_0 \exp\left[-k\int_0^t V(\xi)d\xi\right] - \frac{V(t)}{N_T}.$$

Here, *V* is given implicitly, $\phi = ln\,\frac{dt}{dV}$, and *P*= *S*+*I*+$\frac{V}{N_T}$

III. NUMERICAL SOLUTIONS

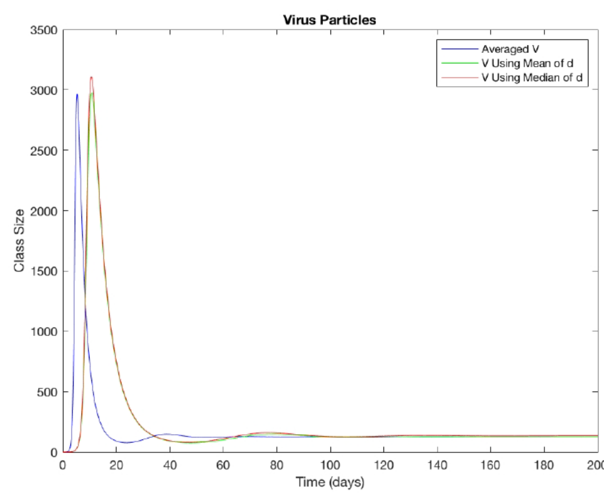

REFERENCES

1. E. Jones and P. Roemer, Analysis and Simulation of the Three-Component Model of HIV Dynamics, SIAM Undergraduate Research Online Vol 7 (2014), pp. 89-106

2. T. Harko, F. Lobo, and M. Mak, Exact Analytical Solutions of the Susceptible-Infected-Recovered (SIR) Epidemic Model and of the SIR Model with Equal Death and Birth Rates}, Appl. Math. Comput., Vol. 236 (2014), pp. 184-194

Rigidity of Steady Solutions to the Navier-Stokes Equations in High Dimensions

Jeaheang Bang[1], Changfeng Gui[1], Hao Liu[2], Yun Wang[3], Chunjing Xie[2]
[1]The Department of Mathematics, the University of Texas at San Antonio,
[2]School of Mathematical Sciences and Institute of Natural Sciences, Shanghai Jia Tong University,
[3]School of Mathematics, Soochow University

I. SUMMARY

Solutions with scaling-invariant bounds, such as self-similar solutions, play an important role in the understanding of the regularity and the asymptotic structure of solutions for the Navier-Stokes problem. I will present our recent work where we prove that any steady solutions satisfying $|u(x)| \leq \frac{C}{|x|}$ in $R^n \setminus \{0\}, n \geq 4$, are trivial.

Our main idea is to analyze the velocity field and the total head pressure via weighted energy estimates with suitable multipliers. The proof is somewhat elementary and short. These results not only give a Liouville-type theorem for steady solutions in higher dimensions with neither smallness nor self-similarity assumptions but also help remove possible singularities of solutions.

II. A Scaling Property

The Navier-Stokes equations are one of the most important equations in fluid mechanics, and it has attracted so much attention from many researchers.

Due to its nonlinear character, the equations satisfy a scaling property. Motivated by it, one can assign scaling dimensions to the spatial variables, time variable, velocity and pressure fields. According to the scaling-dimensions, the stationary five-dimensional case has the same scaling dimensions as the non-stationary three-dimensional case. Hence it is meaningful to consider the stationary five-dimensional case, or even higher-dimensional case.

Again, motivated by the scaling property, one can consider self-similar solutions, or scaling-invariant solutions, to the Navier-Stokes equations in order to study the regularity of a solution in general.

III. Rigidity of Steady Solutions

Tsai and Sverak proved the triviality of stationary self-similar solutions to the Navier-Stokes equations in higher dimensions removing a possible scenario of singularity.
We extended this result to a more general class of solutions.

ACKNOWLEDGEMENTS

The research of Gui is partially supported by NSF grant DMS-1901914. The research of Wang is partially supported by NSFC grants 12171349 and 11671289. The research of Xie is partially supported by NSFC grants 11971307 and 1221101620, Natural Science Foundation of Shanghai 21ZR1433300, and Program of Shanghai Academic Research Leader 22XD1421400.

REFERENCES

1. Tai-Peng Tsai, “On problems arising in the regularity theory for the Navier-Stokes equations.” *ProQuest LLC*, Ann Arbor, MI, 1998, Thesis (Ph.D.)-University of Minnesota.
2. Vladimir Sverak, “On Landau’s solutions of the Navier-Stokes equations.” Volume 179, pages 208-228, 2011, *Problems in mathematical analysis*, No. 61.

Reconstruction of the shape and boundary condition in inverse scattering for an obstacle with partial generalized impedance boundary

Heejin Lee[1]
[1]Department of Mathematics, Purdue University, West Lafayette, IN, 47906, USA

I. Introduction
Inverse scattering theory is concerned with determining properties of an object, such as its shape and boundary coefficients, based on the measured data of how it scatters incoming waves. This type of problem occurs in various areas of application, such as medical imaging, geophysical exploration, and non-destructive testing. Mathematical methods such as linearization, nonlinear optimization, and qualitative methods have been developed to solve the inverse scattering problems, which are nonlinear and ill-posed in nature.

II. Theoretical Background
Linearization methods such as the Born approximation were considered to stabilize the problem and approximate solution by reducing the nonlinear inverse problem to a set of linear integral equations under some conditions that are not generally satisfied. These methods are easy to implement due to their mathematical simplicity, but the nonlinear nature of the problem, such as multiple scattering effects, is ignored, and hence the model may be incorrect.
Efforts to avoid linearizing the problem gave rise to the development of nonlinear optimization methods, which are iterative and typically reconstruct all the unknowns with possible little data. They require the solution of the direct problem at each iteration and, in addition, strong a priori information and accurate models that are generally not possible and numerically expensive.
Qualitative methods such as the linear sampling method, the factorization method and the generalized linear sampling method have been developed to overcome these drawbacks, which avoid incorrect model assumptions and require little a priori information about the scattering object such as its shape or estimates on its constitutive material properties.

III. Summary
We consider the inverse problem of recovering the shape and boundary coefficients of an obstacle from far-field measurements of the scattered field. More specifically, the scatterer is impenetrable with Dirichlet boundary condition on a part of its boundary and anisotropic generalized impedance boundary condition on the complementary boundary(see Figure 1). The latter is an approximate model for complicated thin anisotropic, absorbing layer and is given as a second-order surface differential operator. A deep analysis of the far-field operator (otherwise known as the relative scattering operator) for this scattering problem leads to unique determination results and reconstruction methods for the shape of the scatterer as well as the boundary coefficients. Our reconstruction method is non-iterative and uses no a priori information on the topology and physics of the unknown object. This inversion approach is mathematically rigorous, it resolves nonlinear information from the range properties of the linear far-field operator, and it is easy to implement.

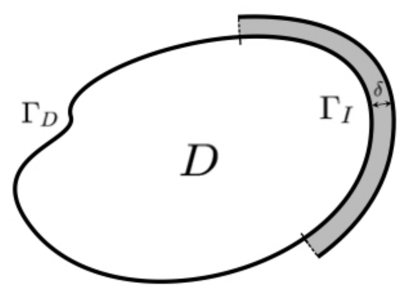

Figure 1: An obstacle partially coated by a thin layer

REFERENCES

1. Heejin Lee, “Inverse Scattering Problems for Obstacles with Higher Order Boundary Conditions," *ProQuest Dissertations Publishing, 2022.*

Recent Development of Bayesian Joint Modeling for Medical Sciences

Seongho Song[1], **Anushka Palipana[2]**, **Chen Zhou[3]**, **Rhonda Szczesniak[2]**
[1]Division of Statistics and Data Science, University of Cincinnati, [2]Division of Biostatistics & Epidemiology, Cincinnati Children's Hospital Medical Center

I. SUMMARY
Joint modeling has been a useful strategy for incorporating latent associations between different types of outcomes simultaneously, often focusing on a longitudinal continuous outcome characterized by a Linear Mixed Effect (LME) sub-model (i) with a terminal-event subject to a Cox proportional hazard or parametric survival sub-mode, and (ii) with a binary process, which is commonly specified by a Generalized linear Mixed Model (GLMM). In addition to (ii), only some joint models have allowed for investigations of nested effects, such as those arising from multi-center studies. In this talk, we will discuss the recent development of Joint model in Bayesian Statistics perspective for medical studies.

II. Models
A. Joint Model with LME sub-model and Survival sub-model
We propose the joint modeling with a longitudinal sub-model for the biomarker measurements and a survival sub-model for assessing the hazard of events can alleviate measurement error issues, and to estimate both between and within-patient heterogeneity in biomarker trajectories, we use longitudinal sub-model with scaled integrated fractional Brownian motion (IFBM).
B. Joint Model with LME sub-model and GLMM for hierarchically structured data
We propose a multi-level joint model that encompasses the LME sub-model and GLMM through a Bayesian approach. Motivated by the need for timely detection of pulmonary exacerbation and characterization of irregularly observed lung function measurements in people living with cystic fibrosis (CF) receiving care across multiple centers, we apply the model to the data arising from US CF Foundation Patient Registry.

III. Applications
A. NHLBI LAM registry data
We apply the proposed model to the NHLBI Lymphangioleiomyomatosis (LAM) registry, which enrolled women with LAM (98-03). Select demographic and clinical characteristics were collected approximately every 12 months. Among the 246 participants, 16 (6.5%) were excluded from our application due to a partially substantiated or unverified LAM diagnosis, and another 13 (5.3%) who received a lung transplant prior to follow-up were omitted from the analysis.

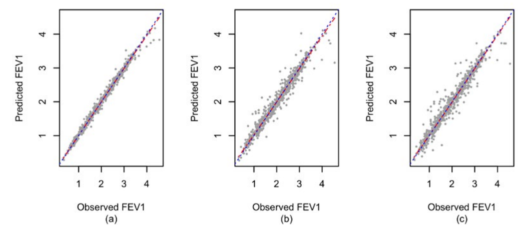

Figure 1: Plot of observed vs. predicted FEV1 values using a) IFBM, b) IOU, and c) random effects models for NHLBI LAM registry data.

B. CF registry data
The analysis cohort for this application consists of 381 CF patients who contributed a total of 9,209 observations across five centers from CF Foundation Patient Registry.

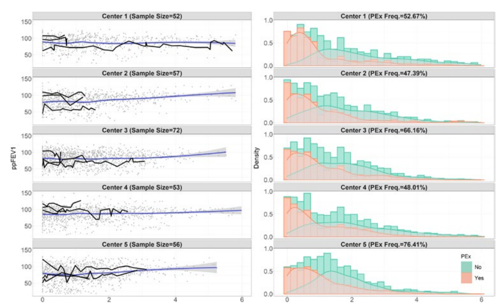
Figure 2: Observed ppFEV1 (left panel) and density of PEx (right panel) against time since the first PEx occurrence in years for Model B.

ACKNOWLEDGEMENTS
Supported by grant R01 HL141286 from the NIH

REFERENCES
1. Zhou, C., Song, S. and Szczesniak, R.D., "Multilevel joint model of Longitudinal continuous and binary outcomes for hierarchically structured data," *Statistics in Medicine*, in press, 2023.
2. Palipana, A., Song, S., Gupta, N. and Szczesniak, R.D., "Bayesian Two-stage Modeling of Longitudinal and Time-to-Event Data with an Integrated Brownian Motion Covariance Structure", *Biostatistics*, under review, 2023.

Bayesian Clustering Factor Model

Hwasoo Shin, Marco A. R. Ferreira, Allison N. Tegge
Virginia Tech

I. Introduction

Factor models are useful tools to reduce dimensionality of a multivariate dataset. In addition, Gaussian mixture models may find latent clusters among the observations. In our paper, we introduce the Bayesian Clustering Factor Model (BCFM) that performs at the same time dimension reduction and clustering.

II. i. Model Description

The data we consider has n observations and R variables. The ith observation $\mathbf{y}_i$ follows the factor model

$$\mathbf{y}_\mathrm{i} = \mathbf{B}\mathbf{x}_i + \mathbf{v}_i,$$

where **B** is the matrix of factor loadings of size $R \times F$, $\mathbf{x}_i$ is the F-dimensional vector of common factors of the ith data, and $\mathbf{v}_i$ is the error vector of length R. We assume the data points are independent, and therefore $\mathbf{v}_i \sim N(0, \mathbf{V})$, where $\mathbf{V} = diag(\sigma_1^2, \ldots, \sigma_R^2)$. Given the cluster assignment $z_i = k$, the ith $\mathbf{x}_i$ common factor follows

$$\mathbf{x}_i | z_i = k \sim N(\boldsymbol{\mu}_k, \boldsymbol{\Omega}_\mathrm{k})\ , x_i \sim \sum_{\{k=1\}}^{K} p_k N(\boldsymbol{\mu}_k, \boldsymbol{\Omega}_k)$$

where $p(z_i = k) = p_k$, $\boldsymbol{\mu}_k$ is the cluster mean, and $\boldsymbol{\Omega}_k$ is the cluster covariance.

II. ii. Model Identifiability

To guarantee that the BCFM is identifiable, we assume the following constraints: (i) The matrix of factor loadings respects a structural hierarchical constraint (Aguilar and West, 2000); (ii) The cluster probabilities are in descending order $p_1 > \cdots > p_K$ and (iii) the covariance of the first cluster $\boldsymbol{\Omega}_1$ is diagonal.

III. Model Selection

We use the Metropolis-Laplace estimator of marginal density (Lewis and Raftery, 1997) to select the numbers of factors and clusters. Here, we integrate out $\mathbf{x}_i$ and $\mathbf{z}_i$ to obtain the integrated likelihood. The approximate marginal density is

$$(2\pi)^{\frac{d}{2}} |\boldsymbol{\Psi}|^{\frac{1}{2}} p(\mathbf{Y}|\widehat{\mathbf{B}}, \widehat{\mathbf{V}}, \widehat{\boldsymbol{\mu}}, \widehat{\boldsymbol{\Omega}}, \widehat{\mathbf{p}}) p(\widehat{\mathbf{B}}, \widehat{\mathbf{V}}, \widehat{\boldsymbol{\mu}}, \widehat{\boldsymbol{\Omega}}, \widehat{\mathbf{p}}),$$

where $p(\mathbf{Y}|\widehat{\mathbf{B}}, \widehat{\mathbf{V}}, \widehat{\boldsymbol{\mu}}, \widehat{\boldsymbol{\Omega}}, \widehat{\mathbf{p}})$ is the integrated likelihood, $p(\widehat{\mathbf{B}}, \widehat{\mathbf{V}}, \widehat{\boldsymbol{\mu}}, \widehat{\boldsymbol{\Omega}}, \widehat{\mathbf{p}})$ is the prior, d is the number of free parameters, and $\boldsymbol{\Psi}$ is the posterior covariance matrix of the parameters.

IV. Simulation Results

We simulated a dataset with K = 4 clusters and F = 3 factors. We then fitted BCFMs with 1 to 4 factors and 1 to 5 clusters.

Model	1 Factor	2 Factors	3 Factors	4 Factors
1 Cluster	-41792	-21875	-14974	-14971
2 Clusters	-41822	-21259	-13943	-13948
3 Clusters	-41741	-20688	-13255	-13254
4 Clusters	NA	-20625	**-13172**	-13183
5 Clusters	NA	-21441	-13221	-13189

Table 1: Simulated dataset – marginal density

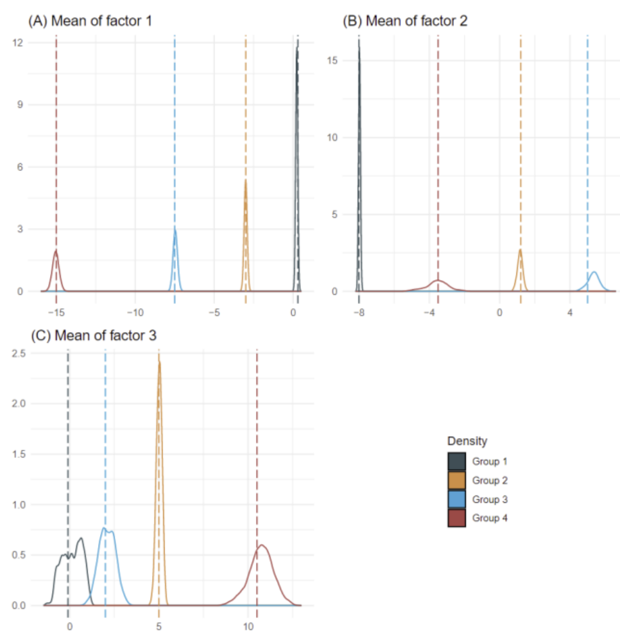

Figure 1: Simulated dataset- cluster means $\boldsymbol{\mu}$

REFERENCES

1. Aguilar, O. and West, M. (2000). "Bayesian Dynamic Factor Models and Portfolio Allocation." Journal of Business Economic Statistics, 18, 3, 338–357.

2. Lewis, S. M. and Raftery, A. E. (1997). "Estimating Bayes Factors via Posterior Simulation With the Laplace-Metropolis Estimator." Journal of the American Statistical Association, 92, 438, 648–655.

Rational approximation for the fractional diffusion

Seungil Kim[1], Thomas Hagstrom[2]
[1]Kyung Hee University, [2]Southern Methodist University

I. SUMMARY

In this talk we study a numerical method to solve the fractional Poisson equation in a bounded Lipschitz domain. Since the fractional power is a Markov function, we can use the rational approximation theory to find rational approximants converging to the fractional power function exponentially at the optimal rate e^{-cn} for some positive constant c in terms of the order n of rational functions. By replacing the fractional power of the Laplacian with rational approximants, we end up with a set of simple elliptic boundary value problems, which can be solved efficiently due to the parallel structure. We present the algorithm to solve the fractional Laplace equation and the convergence analysis together with numerical examples confirming the convergence theory.

II. RATIONAL APPROXIMATION FOR THE FRACTIONAL LAPLACE OPERATOR

A. Optimal rational approximation

For $0 < \alpha < 1$, the fractional function $f(\lambda) = \lambda^{-\alpha}$ can be written as a Markov-type function

$$\lambda^{-\alpha} = \frac{\sin(\pi\alpha)}{\pi}\int_{-\infty}^{0}\frac{|x|^{-\alpha}}{\lambda - x}dx,$$

which is called Balakrishnan formula. It is shown in [1] that there exists a sequence of rational approximants r_n in R_n (the set of rational functions whose numerators and denominators are of degree $\leq n$), which converge at the optimal rate

$$\lim_{n\to\infty}\|f - r_n\|_{[a,b]}^{1/2n} = \rho,$$

where $[a, b]$ is a spectral interval of interest and ρ is a positive constant determined by the conformal mapping from the doubly connected domain $\bar{\mathbb{C}} \setminus ([a, b] \cup (-\infty, 0])$. The interpolating nodes for the optimal rational approximants can be found by using elliptic functions analytically or by using Remez algorithm numerically.

B. Algorithm

To find the solution $u = \mathrm{f}(-\Delta)\mathrm{g}$ to the fractional diffusion problem

$$(-\Delta)^{\alpha}u = g \text{ in } \Omega$$
$$u = 0 \text{ on } \partial\Omega,$$

we replace $\mathrm{f}(\lambda)$ with $r_n(\lambda)$ and rewrite it as a sum-of-poles representation

$$u = (\gamma_0 + \sum_{j=1}^{n}\gamma_j(-\Delta + \sigma_j)^{-1})g,$$

for some constant poles $-\sigma_j$ and residues γ_j. The obvious advantage of this algorithm is that the nonlocal problem is transformed into decoupled elliptic boundary value problems, which are embarrassingly parallel.

III. NUMERICAL EXPERIMENTS

As an example we consider a fractional diffusion problem in $\Omega = (0,1)^2$ with $\alpha = 1/3$. We set g to be

$$g(x, y) = \sum_{n,m=1}^{9}\frac{((m^2+n^2)\pi^2)^{1/3}}{m+n}\sin(m\pi x)\sin(n\pi y)$$

so that the exact solution u is given by

$$u(x, y) = \sum_{n,m=1}^{9}\frac{1}{m+n}\sin(m\pi x)\sin(n\pi y)$$

The following plots illustrate the convergence of relative L^2 errors of finite element approximations of mesh size h with respect to order n of optimal rational approximations.

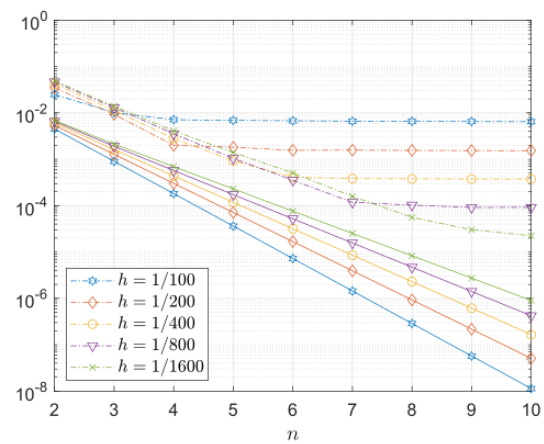

Figure 1: Relative L^2 errors of finite element approximations vs. order n of rational approximations.

REFERENCES

1. A. A. Gonchar, “On the speed of rational approximation of some analytic functions,” Mathematics of the USSR-Sbornik, 34(2), pp. 131-145, 1978.

Technical Group B-1

Medical Science, Pharmaceutical Science, Veterinary Medicine, Physical Education (MPS)

Herbal Extracts from Lycii Radicis Corex and Achyranthes Japonica Prevent Multiple Myeloma.

Donghoon Yoon
Myeloma Center, the University of Arkansas for Medical Sciences, Little Rock, AR

Multiple Myeloma (MM) is a plasma cell malignancy that, despite advances in treatment, remains incurable. In over 90% of MM patients, aberrant bone remodeling occurs and results in osteolytic lesions. Korean traditional medicine has a long-standing interest in healthy foods to enhance the immune system, energy-boost, and Yin-and-Yang balance. Traditional medicine has used herbal extracts (HE) from natural plants with fewer side effects and long-term treatment tolerance. In earlier studies, lycii radices cortex (LRC) and achyranthes japonica (AJ) containing herbal extracts (HE) have demonstrated the ability to enhance cell growth and mineralization of osteoblast cells while also inhibiting osteoclast differentiation.

The current study investigated the effects of LRC+AJ containing HE on murine 5TGM1 MM-bearing mice. Our data demonstrated that the HE significantly increased the mouse survivals of both treatment conditions (Treatment before Transplant, (TbT), and Treatment after Transplant, (TaT), with median survivals of undetermined and 52.5 days, respectively, while MM control had a median survival of 42 days. The Mantel-Cox test found that TbT and TaT mice were significantly different from the control group ($P=0.0014$ and 0.0182, respectively). In histomorphometric analysis, the spines were scanned by micro-CT and revealed that TbT and TaT groups had significantly increased bone volume over total volume (BV/TV) than control. To see if HE affects the cell growth of myeloma cells and osteoblast cells, we further investigated the HE on preosteoblast cell line MC3T3-E1, mouse MM cell line 5TGM1-Luc, and human MM cell line U-266. Cells were treated with HE, and viability was assessed at 48 and 96 hours post-treatment. HE increased MC3T3-E1 cell growth while it decreased 5TGM1 and U-266 cell viability. We identified the DAP3G in HE, which was found as a responsible factor for bone formation in the previous study. Furthermore, we identified unique changes in the gut microbiome and short-chain fatty acids of the survived mice.

Our results demonstrated that LRC+AJ HE delays/inhibits MM progression that three different mechanisms may drive; i) promotes bone formation, ii) suppresses myeloma cell growth and enhances osteoblast cell survival/differentiation, and iii) changes in the gut microbiome.

High extracellular glucose promotes cell motility by modulating cell deformability and contractility via cAMP-RhoA-ROCK axis in human breast cancer cells

Mijung Oh[1], Skylar Batty[2,4,&], Nayan Banerjee[5], and Tae-Hyung Kim[1,3,#]

[1]Department of Pathology, School of Medicine

[2]Undergraduate Pipeline Network Summer Research Program, University of New Mexico Health Sciences Center

[3]University of New Mexico Comprehensive Cancer Center, Albuquerque, NM 87131, USA

[4]Department of Molecular and Cellular Biology, University of Arizona, Tucson, AZ 85721, USA

[5]School of Chemical Sciences, Indian Association for the Cultivation of Science, 2A & 2B Raja S. C. Mullick Road, Jadavpur, Kolkata 700032, West Bengal, India

[&]Current address: Biomedical Sciences Graduate Program, University of California San Diego, La Jolla, CA 92093, USA

I. ABSTRACT

The mechanical properties, or mechanotypes, of cells are largely determined by their deformability and contractility. The ability of cancer cells to deform and generate contractile force is critical in multiple steps of metastasis. Identifying soluble cues that regulate cancer cell mechanotypes and understanding the underlying molecular mechanisms regulating these cellular mechanotypes could provide novel therapeutic targets to prevent metastasis.

Glucose levels vary from blood circulation (5.5 mM) to normal tissues (1 – 3 mM) to tumor tissues (<0.5 mM). Cancer cells adapt to these different glucose levels by reprogramming their metabolism. Such metabolic reprogramming can impact cancer cell behaviors including growth, epithelial-mesenchymal transition, and invasion. Several clinical studies of breast cancer patients also have shown that high glucose levels (>7 mM) are associated with poor prognosis. Although a strong correlation between high glucose level and cancer metastasis has been demonstrated, the causality is not elucidated, and the underlying molecular mechanisms remain largely unknown.

In this study, using novel high-throughput mechanotyping assays, we show that human breast cancer cells become less deformable and more contractile with increased extracellular glucose levels (>5 mM) in a concentration-dependent manner. These altered cell mechanotypes are due to increased F-actin rearrangement and non-muscle myosin II (NMII) activity. We identify the cAMP-RhoA-ROCK-NMII axis to play a major role in regulating cell mechanotypes at high extracellular glucose levels, whereas calcium and myosin light chain kinase (MLCK) are not required. The altered mechanotypes are also associated with increased cell migration and invasion.

Our study identifies key components in breast cancer cells that convert high extracellular glucose levels into changes in cellular mechanotype and behaviors relevant in cancer metastasis. Such mechanistic understanding will provide a framework for integrating drugs for glucose control and mechanotype regulation into existing treatment strategies to control metastatic cancers.

II. SUMMARY ILLUSTRATION

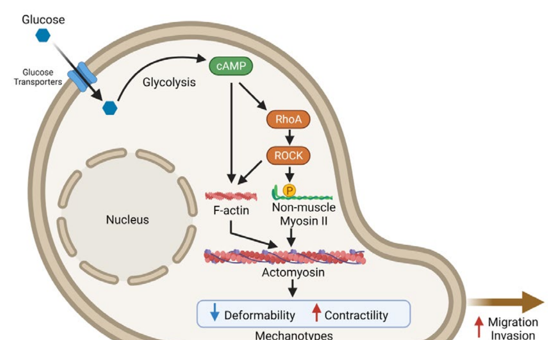

III. ACKNOWLEDGEMENTS

This work was supported by NIH grants P30CA118100 (UPN fellow to S. Batty) and P20GM121176 (mPI to T.-H. Kim), UNM Department of Pathology Start-up fund to T.-H. Kim, and METAvivor Early Career Investigator Award to T.-H. Kim.

Dysregulated 24-dehydrocholesterol reductase (DHCR24) in Head and Neck Squamous Cell Carcinoma (HNSCC)

Bok-Soon Lee[1,2], Ji-Hye Choi[3], Hyun Goo Woo[3], Chul-Ho Kim[2], and Jiyoung Lee[1,4]*

[1] Department of Biochemistry and Molecular Medicine, School of Medicine and Health Sciences, The George Washington University, Washington, DC 20037, USA

[2] Department of Otolaryngology, Ajou University School of Medicine, Suwon, Republic of Korea

[3] Department of Physiology, Ajou University School of Medicine, Suwon, Republic of Korea

[4] GW Cancer Center, School of Medicine and Health Sciences, The George Washington University, Washington, DC 20037, USA

I. Introduction

Head and Neck Squamous Cell Carcinoma (HNSCC) is the 6th most abundant cancer type in the world and is responsible for upwards of 270,000 annual deaths globally. Fewer than 10% of patients with metastatic HNSCC survive beyond 5 years, indicating metastatic and recurrent HNSCC needs clinical attentions. Here we investigate altered transcriptional networks in HNSCC compared with normal tissues in order to understand fundamental biology of HNSCC, focused on tumor metabolism.

Methods: Transcriptomic profiling using high throughput RNA-sequencing of HNSCC tumor tissues and paired normal tissues isolated from cancer patients (n=16) identified a de novo cholesterol/sterol biosynthesis pathway by Gene Set Enrichment Analysis (GSEA). Silencing of 24-dehydrocholesterol reductase (DHCR24) that are enriched in the cholesterol/sterol biosynthesis pathway was achieved by introducing siRNA, shRNA, and small inhibitory molecules in human HNSCC cells for functional studies.

Results: Genes expression of DHCR7/24 involved in de novo cholesterol pathway is associated with poor prognosis of head and neck cancer patients using The Cancer Genome Atlas (TCGA) data. Enriched expression of DHCR7 and DHCR24 was validated by immunohistochemistry (IHC) assays in tumor tissues from patients. In parallel, single cell RNA-sequencing (ssRNA-seq) analysis of HNSCC tumors (n=24) supported that DHCR7/24 expression is exclusively high in tumors not in immune cells. Silencing of DHCR24 by siRNA or a small inhibitory molecule Triparanol and SH-42 decreased cell viability and proliferation of HNSCC cells.

Conclusions: We observed that HNSCC tumors shows enriched cholesterol biosynthesis pathways. HNSCC expresses higher DHCR7/24 mRNA than normal tissues and indicate poor prognosis of patients. Targeting DHCR7/24 using genetic or pharmacological tools impairs viability of HNSCC, suggesting DHCR7/24 is a potential therapeutic target to manage patients with HNSCC.

II. ILLUSTRATIONS

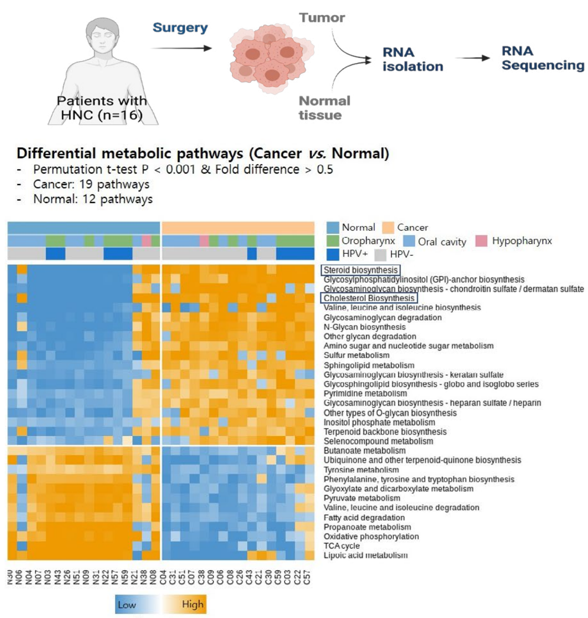

Figure 1: Transcriptomic profiling indicating altered metabolic pathways in HNSCC and normal control tissues from patients (n=16).

ACKNOWLEDGEMENTS

1. CDMRP DOD Breakthrough Award (BC161588, JL)
2. NIH NCI 1R37CA270536 (JL)

Metabolic Vulnerabilities of Squamous Cell Carcinoma

Jung-whan Kim
University of Oklahoma Health Science Center, Oklahoma City, OK 73117 USA

Squamous cell carcinoma (SCC), a malignancy arising across multiple anatomical sites, is responsible for significant cancer mortality due to insufficient therapeutic options. Here, we identify exceptional glucose reliance among SCCs dictated by hyperactive GLUT1-mediated glucose influx. Mechanistically, squamous lineage transcription factors p63 and SOX2 transactivate the intronic enhancer cluster of *SLC2A1*. Elevated glucose influx fuels generation of NADPH and GSH, thereby heightening the anti-oxidative capacity in SCC tumors. Systemic glucose restriction by ketogenic diet and inhibiting renal glucose reabsorption with SGLT2 inhibitor precipitate intratumoral oxidative stress and tumor growth inhibition. Furthermore, reduction of blood glucose lowers blood insulin levels, which suppresses PI3K/AKT signaling in SCC cells. Clinically, we demonstrate a robust correlation between blood glucose concentration and worse survival among SCC patients.

Targeting altered glucose metabolism in cancer cells has resulted in varied and unsatisfactory outcomes Among multiple factors preventing effective therapeutic responses, a poorly understood tumor-intrinsic metabolic heterogeneity across different cancers may preclude effective therapeutic strategies to target cancer metabolism. Here, we uncover a previously unrecognized metabolic reliance and vulnerability distinctively embedded across all SCCs, in which the major glucose transporter GLUT1 is exceptionally overexpressed through the squamous lineage-specific transcriptional network, p63 and SOX2. Enhanced GLUT1 expression is linked to an exquisite reliance on glucose for survival and tumor growth in SCC. This strongly argues that hyperactive GLUT1 activity and dramatically enhanced glucose influx is not a uniform metabolic hallmark of all cancers but rather a potent and unique characteristic of SCC, thereby rendering SCC the most susceptible tumor type to glucose restriction and may present an actionable therapeutic window.

Collectively, this study identifies the exceptional glucose reliance of SCC and suggests its candidacy as a highly vulnerable cancer type to be targeted by systemic glucose restriction.

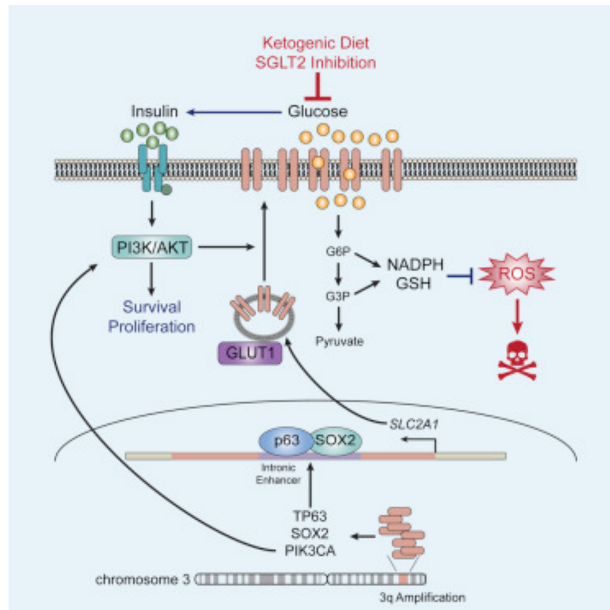

Figure 1: p63 and SOX2-mediated GLUT1 overexpression in squamous cell carcinomas

ACKNOWLDGEMENTS
This work was supported by American Lung Association, LCD-400239; DOD, W81XWH-18-1-0439; CPRIT, RP180670; and NIH, 5R21CA208746 and P50CA70907

REFERENCES
Hsieh MH, Choe JH, Gadhvi J, Kim YJ, Arguez MA, Palmer M, Gerold H, Nowak C, Do H, Mazambani S, Knighton JK, Cha M, Goodwin J, Kang MK, Jeong JY, Lee SY, Faubert B, Xuan Z, Abel ED, Scafoglio C, Shackelford DB, Minna JD, Singh PK, Shulaev V, Bleris L, Hoyt K, Kim J, Inoue M, DeBerardinis RJ, Kim TH, **Kim JW***. p63 and SOX2 Dictate Glucose Reliance and Metabolic Vulnerabilities in Squamous Cell Carcinomas. **Cell Reports. 2019;28(7):1860-78 e9**. doi: 10.1016/j.celrep.2019.07.027.

Sex difference in the profile of extracellular bioactive lipids of conjunctival epithelial cells during allergic inflammation

Changrim Lee[1,2], **Darlene A. Dartt**[1,2]
[1]Department of Ophthalmology, Harvard Medical School, [2]Massachusetts Eye and Ear Infirmary

SUMMARY

Ocular allergy affects about 40% of the North American population, of which comorbidities include allergic rhinitis, asthma, eczema, food allergy, and eosinophilic esophagitis, making daily life even more debilitating[1]. In Korea, about 0.23 million people per month are treated for allergic conjunctivitis, which is one of the most common ocular allergies[2]. Allergen sensitization activates mast cells to release histamine to initiate an ocular allergic response. One of the ocular surface tissues affected is the conjunctival epithelium that lines the inside of the eyelids and covers the sclera, thus providing stability to the transparent cornea and anterior segment of the eye[3]. The conjunctival goblet cells (CGCs) that secrete mucins to wet and protect the ocular surface over-secrete mucins in response to histamine stimulation, which causes ocular surface instability and visual disturbance. To better understand the molecular basis of allergic response in CGCs, our research team has been investigating the role of bioactive lipid mediators, especially specialized pro-resolving mediators (SPMs) and proinflammatory mediators (PIMs), in the cellular response of CGCs during histamine-mediated allergic inflammation[4,5].

Our exciting preliminary data show, for the first time, that human primary CGCs biosynthesize SPMs and PIMs, load them into extracellular vesicles (EVs), and secrete them into the extracellular space during health and disease. Interestingly, the amount of SPMs dramatically increases in EVs secreted by female CGCs, but decreases in males during a histamine-mediated allergic response, suggesting that the sex of the CGCs results in the differences in CGC response. This is in line with our recent publication showing that human female CGCs increase intracellular Ca^{2+} concentration ($[Ca^{2+}]_i$) more sensitively (at lower histamine concentrations) than males[6]. To further investigate this observation, we hypothesize that in human CGCs there are sex differences in the cellular response to histamine-mediated allergic inflammation, which results in the differential secretion of SPMs and PIMs. We will test this hypothesis by quantifying and comparing the type and amount of SPMs and PIMs in EVs, and their time course of secretion in histamine-stimulated CGCs from both sexes (**Fig. 1**).

The success of this study will provide new insights into the bioactive lipid-mediated ocular surface protective mechanism generated by the conjunctiva and the basis for a tailored sex-dependent, lipid-based therapeutic approach in the management of vision-debilitating ocular surface diseases.

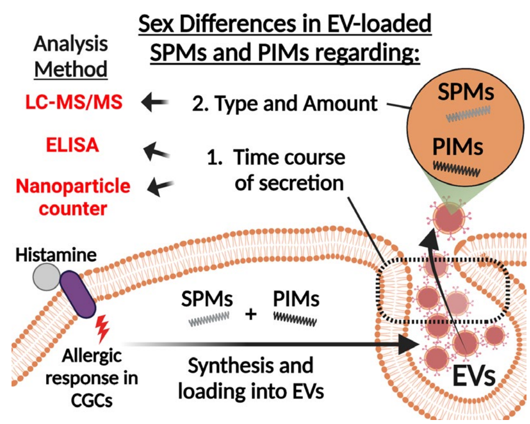

Fig 1. Schematic illustration of the proposed research. Sex differences in EV-loaded specialized pro-resolving mediators (SPMs) and proinflammatory mediators (PIMs) in terms of the (1) time course of secretion and (2) type and amount will be investigated in histamine stimulated human conjunctival goblet cells (CGCs).

REFERENCES

1. Dupuis P, *et al*. A contemporary look at allergic conjunctivitis. Allergy Asthma Clin Immunol. 2020;16:5.
2. Choi HG, *et al*. Changes in the Mean and Variance of the Numbers of Medical Visits for Allergic Diseases before and during the COVID-19 Pandemic in Korea. J Clin Med. 2022;11(15).
3. Craig JP, *et al*. TFOS DEWS II Definition and Classification Report. Ocul Surf. 2017;15(3):276-83.
4. Hayashi D, *et al*. Role of histamine and its receptor subtypes in stimulation of conjunctival goblet cell secretion. Invest Ophthalmol Vis Sci. 2012;53(6):2993-3003.
5. Serhan CN. Discovery of specialized pro-resolving mediators marks the dawn of resolution physiology and pharmacology. Mol Aspects Med. 2017;58:1-11.
6. Yang M, *et al*. Sex-based differences in conjunctival goblet cell responses to pro-inflammatory and pro-resolving mediators. Sci Rep. 2022;12(1):16305.

Modulating the Host's Immune Response for Preventing Peri-implantitis in Mice

Yejin Ki[1], Anastasiya Badziai[2], Anu Viswanathan[2], Charles Sfeir[1,2]
[1]Department of Oral and Craniofacial Sciences, [2]Department of Periodontics and Preventive Dentistry

I. SUMMARY

Peri-implantitis is an inflammatory disease of the soft tissue and bone around dental implants, which is mediated by the host's immune response. In this study, we propose to develop a novel therapeutic method to prevent peri-implantitis by modulating the host's immune response. C–C motif chemokine ligand 2 (CCL2) is a chemoattractant for macrophages that is reported to drive macrophage polarization toward the anti-inflammatory M2 phenotype in periodontal disease (1). The goal of this study was to test the feasibility of local delivery of CCL2-releasing microparticles (CCL2 MPs) as a preventive therapy for bone loss in peri-implantitis. Our Micro-CT analysis showed that there was a statistically significant reduction of bone loss around implants treated with CCL2 MPs compared to diseased and blank MPs treated implants. The preliminary data demonstrated the feasibility of our CCL2 local delivery as a preventive therapy in peri-implantitis.

II. METHODS

A. CCL2-releasing Microparticles

PLGA microparticles encapsulating CCL2 (CCL2 MPs) were fabricated in our collaborator's laboratory, Dr. Steve Little in the Department of Chemical Engineering at the University of Pittsburgh. The release profile and morphology of CCL2 MPs were characterized by ELISA and SEM respectively.

B. Ligature-induced Peri-implantitis

Maxillary left first molars were extracted on 4-week-old C57BL/6J male mice. After 8 weeks of healing, 6AL4V titanium implants (1 mm long and 0.5 mm in diameter) were placed at the healed extraction sites. Following implant placement, osseointegration was allowed for 4 weeks. After osseointegration, 6-0 silk ligatures were tied under each implant head for disease induction, and simultaneously, particles were locally injected into the soft tissues around dental implants. For this study, four different groups were compared (n=5 per group): healthy control (implant only), diseased control (implant with ligature), blank group (PLGA only), and treatment group (CCL2 MPs). The ligatures were maintained for 7 days to induce bone loss around the implants. At the end of the experiments, mice maxillae were harvested and fixed in formalin. Micro-CT analysis was performed to compare bone loss around implants in the experiment and control groups.

III. ILLUSTRATIONS

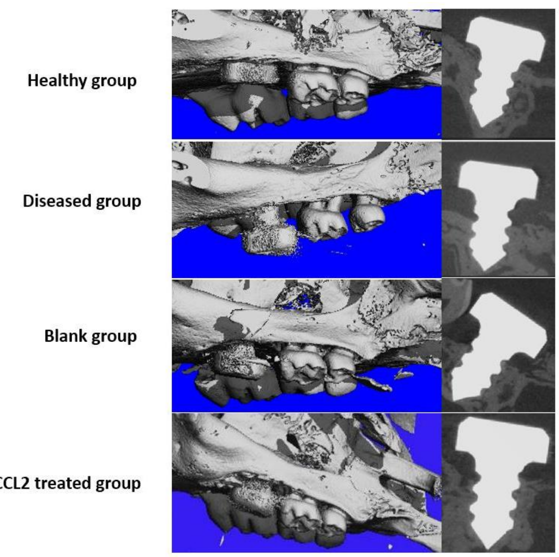

Figure 1: Micro-CT images (3D and 2D) of each group: healthy implant, ligature placed implant, blank treated ligatured implant, and CCL2 treated ligatured implant.

ACKNOWLEDGEMENTS

We thank Konstantinos Verdelis and Lyudmila Lukashova at the Micro-CT Core and Center for Craniofacial Regeneration at the University of Pittsburgh

REFERENCES

1. Zhuang, Z., et al., "Induction of M2 Macrophages Prevents Bone Loss in Murine Periodontitis Models," *Journal of dental research*, *98*(2), 200–208, 2019.

Ets-1 as a Negative Regulator of Peripherally Induced Regulatory T Cells and its implications in autoimmune diseases

Choong-Gu Lee[1,2,3]

[1]Natural Product Informatics Research Center, Korea Institute of Science and Technology (KIST), Gangneung Institute of Natural Products, Gangneung 25451, Korea.

[2]Division of Bio-Medical Science and Technology, Korea Institute of Science and Technology (KIST) School, University of Science and Technology (UST), Seoul 02792, Korea.

[3]Department of Convergence Medicine, Wonju College of Medicine, Yonsei University, Wonju 26493, Korea.

SUMMARY

E26 transformation-specific-1 (Ets-1), a member of the Ets family of transcription factors, controls a wide variety of cellular processes and plays an important role in autoimmune diseases. Previous studies in Ets-1 deficient (Ets1-/-) mice have demonstrated the important functions of Ets-1 in the development, proliferation, and survival of T cells. Regulatory T cells (Treg cells) constitute a population of CD4+ T cells that limits immune responses. Transcription factor Foxp3 plays key roles in determining the development and function of Treg cells. However, the molecular mechanisms that trigger or maintain its expression remain incompletely understood. Though Ets1-/- mice developed T cell-mediated splenomegaly and lupus-like autoimmune phenotype, the mice showed no severe autoimmune disease symptoms in steady state in the aged mice. We unexpectedly found considerable amount of CD4+ Foxp3+ T cells in the peripheral lymphoid tissues of Ets1-/- mice. Interestingly, most of them were CD25-Nrp1-, suggesting the possibility of peripherally induced Foxp3+ T cells. These Foxp3+ T cells express reduced levels of Treg phenotypic markers such as ICOS, GITR and CTLA4 and exhibit naïve-like T cell phenotypes (CD44lo CD62L+), suggesting they are in the transition of becoming pTregs from naïve T cells. In addition, naïve T cells from Ets1-/- mice were more prone to become induced Treg cells *in vitro* and *in vivo*. We have also confirmed the negative role of Ets1 in Foxp3 regulation through the ETS domain (known for DNA binding). In summary, our data suggests that Ets-1 may repress Foxp3 expression in naïve CD4+ T cells, thereby acting as an important negative regulator of peripherally induced regulatory T cells.

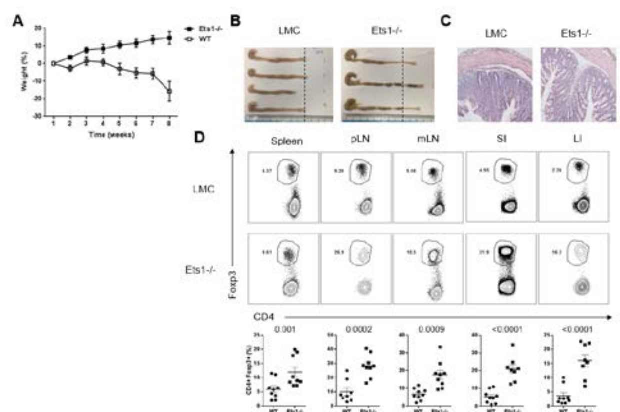

Figure 1: Enhanced pTreg generation from Ets1-/- T naïve cells prevent colitis induction

ACKNOWLEDGEMENTS

This study was supported by grants from the National Research Foundation of Korea (2021R1C1C1007040), and an intramural grant of Korea Institute of Science and Technology (2Z06822).

Removing the root cause of Fragile X syndrome by Inducing the contraction of CGG repeats and FMR1 restoration

Hun-Goo Lee [1,2], Sachiko Imaichi [1,2], Elizabeth Kraeutler [1,2], Rodrigo Aguilar [1,2], Yong-Woo Lee [1,2], Steven D. Sheridan[3,4], and Jeannie T. Lee [1,2]

[1]Department of Molecular Biology, Massachusetts General Hospital, Boston, MA 02114, USA
[2]Department of Genetics, Harvard Medical School, Boston, MA 02114, USA
[3]Center for Genomic Medicine, Massachusetts General Hospital, Boston, MA 02114, USA
[4]Department of Psychiatry, Harvard Medical School, Boston, MA 02114, USA

SUMMARY

Fragile X syndrome (FXS) is one of the most common monogenic causes of autism spectrum disorders (ASD). Here I describe potential methods for correcting the genetic cause of FXS without introducing gene-editing nucleases in cellular models. In FXS patients, very long expansion of CGG trinucleotide repeats (>200 times) at the 5' UTR of the FMR1 gene causes epigenetic silencing of FMR1, a crucial gene for brain development. By investigating conditions favorable to FMR1 reactivation, I have found that certain sets of small molecules can strongly reactivate FMR1 mRNA and its protein FMRP expression in human embryonic stem (ES) and induced pluripotent stem (iPS) cells with FXS full mutation. Surprisingly, it also entails the shortening of the long CGG repeats. I traced the mechanism to a site-specific R-loop — a 3-stranded RNA-DNA structure — that is both necessary and sufficient for repeat contraction. The R-loop formation triggers DNA demethylation and FMR1 transcription, which in turn fortifies R-loop formation. Repeat contraction is specific to FMR1, restores production of FMRP protein. Collectively, these data implicate a positive feedback loop of DNA demethylation, de novo transcription, R-loop formation, and DNA repair in CGG contraction and FMR1 reactivation.

METHODS: To identify the conditions for reversing epigenetic silencing of FMR1, we explored the methods for global epigenetic reprogramming that induces the naïve state of the human pluripotent cells. We tested multiple combinations of kinase inhibitors and found one of the combinations that successfully reactivates FMR1 mRNA and its protein FMRP levels. To analyze the long CGG repeat lengths, we utilized a specialized PCR method - Repeat PCR and combined it with Bioanalyzer analysis for quantitative estimation of the repeat size distributions.

RESULTS: By investigating conditions favorable to *FMR1* reactivation, we have found that a certain combination of small molecules (**five kinase inhibitors: 5i**) can **trigger DNA demethylation and strongly reactivate FMR1** mRNA and protein FMRP expression in FXS cells. Surprisingly, FMR1 transcription reactivation induced **a strong repeat contraction**. We traced the mechanisms to **DNA demethylation and site-specific R-loops** (RNA and DNA hybrid), which are necessary and sufficient for repeat contraction. A **positive feedback cycle** comprising demethylation, de novo *FMR1* transcription, and R-loop formation results in the recruitment of endogenous DNA repair mechanisms that then drive excision of the long CGG repeat. Repeat contraction is specific to *FMR1* and restores the production of FMRP protein.

CONCLUSIONS: Here we have identified methods of *FMR1* gene editing without exogenous nucleases. We demonstrate FMRP restoration can be induced by CpG demethylation and R-loop formation, which together recruit endogenous DNA repair mechanisms to correct the long CGG repeat length. Our study therefore identifies a potential method of treating FXS in the future. (Lee *et al*., Cell in press)

ACKNOWLEDGEMENTS

This research was funded by FRAXA Foundation.

REFERENCES

Hun-Goo Lee, Sachiko Imaichi, Elizabeth Kraeutler, Rodrigo Aguilar, Yong-Woo Lee, Steven D. Sheridan, and Jeannie T. Lee. "Site-specific R-loops induce CGG repeat contraction and Fragile X gene reactivation" Cell (in press)

Slow Myosin Binding Protein-C and Congenital Muscle Disease

Taejeong Song[1], James McNamara[2], Sadayappan Sakthivel[1]
[1]Heart, Lung and Vascular Institute, Division of Cardiovascular Health and Disease, Department of Internal Medicine, University of Cincinnati, Cincinnati, OH, USA
[2]Murdoch Children's Research Institute, The Royal Children's Hospital, Parkville, Victoria, Australia

Myosin binding protein-C (MyBP-C) is a sarcomere-thick filament-associated protein that plays a crucial role in regulating the contractility of striated muscles by interacting with actin and myosin. One of its isoforms, slow myosin binding protein-C (sMyBP-C), is expressed in all muscle fibers. Mutations in the sMyBP-C gene, encoded by MYBPC1, have been linked to the emergence of congenital muscle disorders known as distal arthrogryposis (DA) and lethal congenital contracture syndrome (LCCS). These conditions are estimated to affect approximately 1 in every 3,000 newborns. However, our understanding of the mechanisms behind disease development caused by Mybpc1 mutations and the functional and structural roles of sMyBP-C in skeletal muscle is still incomplete. Hence, the primary objective of this study is to explore the roles of sMyBP-C in skeletal muscles during various developmental stages and introduce a comprehensive experimental model for DA and LCCS.

First, we investigated the structural and functional roles of sMyBP-C during various developmental stages using three recently created sMyBP-C knock-out (KO) mouse models. These models included the *Mybpc*1 global KO (gKO) for the embryonic stage, *Mybpc*1 early conditional KO (Mybpc1$^{fl/fl}$ MCK^{Cre}) for the post-natal stage, and *Mybpc*1 adult conditional KO (Mybpc1$^{fl/fl}$ HSA^{Cre}) for the adult stage. The *Mybpc*1gKO resulted in a range of severe symptoms, including whole-body tremors, pronounced skeletal deformities, muscle atrophy, impaired respiratory function, muscle weakness, and early postnatal mortality. These observations underscore the crucial role of sMyBP-C expression in postnatal survival and its vital contribution to the formation and maturation of the musculoskeletal structure. The phenotypes observed in the *Mybpc*1gKO mice closely resemble the symptoms associated with LCCS. Furthermore, two conditional knockout mouse models of Mybpc1 exhibited impaired muscle growth and reduced functional capacity after birth, primarily attributed to disrupted actomyosin interaction and sarcomere structure, as well as muscle fiber atrophy and a shift in fiber type. These findings emphasize the fundamental significance of sMyBP-C in both embryonic musculoskeletal development and postnatal muscle growth and function.

In addition to the sMyBP-C knockout mouse models, we have also developed three knock-in (KI) mouse models (W198R, P295L, E335K) with skeletal phenotype to study DA. These three *Mybpc*1 mutations, which have been documented in human patients, are known to be associated with the development of DA. Illustrated in Figure 1, our research employs a comprehensive approach to examine the underlying mechanisms of DA, encompassing multiple aspects of contractile function and muscle structure. By utilizing these Mybpc1 KO and KI mouse models, we aim to establish fundamental tools for investigating the disease mechanisms underlying DA and LCCS, which will aid in the development of potential therapeutic interventions. Furthermore, our systemic research model holds great potential as a valuable tool for exploring other muscle-related disorders and evaluating the effects of novel drugs and gene therapy on muscle function and structure.

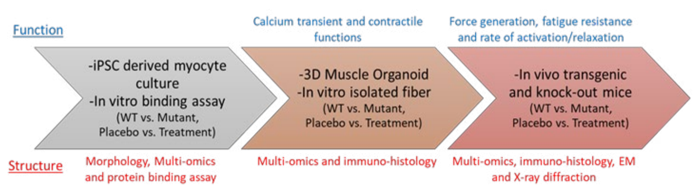

Figure1. Multi-level systemic approach to muscle function and structure assessment

Funding: NIH NIMS, RO1 AR078001 and AHA CDA1046498

Expression and Characterization of MYO7A Isoforms Localized to the Stereocilia Upper Tip-link Density

Jinho Park[1,2], Sihan Li[3,4], Jung-bum Shin[3,4], Jonathan E. Bird[1,2]

[1]Department of Pharmacology and Therapeutics, [2]Myology Institute, University of Florida, Gainesville, FL 32610. [3]Department of Neuroscience, [4]Department of Biochemistry and Molecular Genetics, University of Virginia, Charlottesville, VA, USA.

I. INTRODUCTION

The mutations in MYO7A cause Usher Syndrome type 1 (USH1B) and autosomal recessive hearing loss, DFNB2. MYO7A has multiple functions in cochlear hair cells, being essential for normal development of hair bundle architecture, as well as concentrating at the upper tip link density (UTLD) where it helps tension the mechanoelectrical transduction (MET) complex. Hair cells produce multiple isoforms of MYO7A that contribute to these diverse and essential functions. At the UTLD, a canonical isoform (MYO7A-C) is detected in addition to an isoform (MYO7A-N) that has an additional exon in the ATPase motor domain. In this study, we explore the hypothesis that altered ATPase activities of MYO7A-C and MYO7A-N contribute towards tuning mechanical activity at the UTLD.

II. METHODS

Testing this hypothesis using biophysical approaches requires the isolation of highly pure MYO7A protein in milligram quantities. This is challenging to obtain from primary tissues, and thus recombinant expression systems are needed. Expression of MYO7A poses additional challenges as it has five light chain binding sites (LCBS) that bind to an unknown assortment of light chain proteins. These light chains likely regulate MYO7A motor activity and are thus key for understanding functional differences between MYO7A-C and MYO7A-N at the UTLD. We have addressed this problem using a multiple promoter baculovirus system (biGBac) to express MYO7A in Sf9 insect cells. Utilizing the biGBac expression system, we engineered baculovirus that contains the ATPase domain of either MYO7A-C or MYO7A-N, in addition to co-expressing a myosin specific chaperone (UNC45A), and candidate light chains: calmodulin (CALM1), calmodulin-like protein 4 (CALML4), essential light chain (MYL6) and regulatory light chain (MYL12B).

III. RESULTS AND CONCLUSION

MYO7A-C protein was captured from whole cell lysates using FLAG-affinity chromatography and further purified with sequential anion exchange and size exclusion chromatography. SDS-PAGE shows that recombinant MYO7A-C is > 99% pure and forms a pentamer, stably binding to all four light chains (CALM, CALML4, MYL6, MYL12B). These results confirm previous co-immunoprecipitation of endogenous MYO7A from hair cells (Morgan, 2016), by showing that CALM and CALML4 bind to MYO7A. We performed functional assays to compare the activity of MYO7A-C and MYO7A-N fraction B using a steady-state NADH ATPase assay. MYO7A-N has reduced maximal ATPase activity (k_{cat}) compared with MYO7A-C, indicating the N-terminal domain regulates motor activity.

In conclusion, we have established a scalable pipeline to express MYO7A protein isoforms present at the UTLD. This will allow us to perform biophysical and structural studies to understand its contribution to MET, and the effects of pathogenic USH1B / DFNB2 deafness mutations.

ACKNOWLEDGEMENTS

Funded by R01 DC018842

REFERENCES

1. Li, Sihan et al. “Myosin-VIIa is expressed in multiple isoforms and essential for tensioning the hair cell mechanotransduction complex." *Nature communications* Vol. 11, No. 1, pp 2066, 2020.

Sex Differences in Amino Acid Kinetics in Older Adults with Chronic Morbidities.

Chloe Minchae Kang
[1]A Center for Translational Research in Aging & Longevity, Texas A&M University

I. INTRODUCTION

It has long been reported that women live longer than men and have lower mortality at all ages, but higher rates of disability and spend a larger portion of life expectancy in worse health due to higher rates of illness, immobility, frailty, and more comorbidities. Muscle weakness and loss are associated with aging and mortality and are even more prevalent when chronic morbidities are present. Therefore, investigating protein and amino acid profiles in the elderly is of clinical importance. Previous studies observed decreased plasma essential amino acids and branched-chain amino acids concentrations in older adults and sarcopenic older adults respectively. Moreover, females have shown to have lower levels of tryptophan, tyrosine, branched-chain amino acids, methionine, ornithine, citrulline, phenylalanine, but a higher level of glycine. Previously, greater whole body protein breakdown in males but no sex difference in muscle protein synthesis rate in young men and women. However, It remains unclear whether age-related protein amino acid metabolic perturbations in older adults with chronic morbidities are different between men and women.

II. METHODS

Subjects and Study Protocol

444 participants with chronic morbidities (Charlson comorbidity score ≥1) over the age of 50 (MEDIT database). We divided the selected subjects into two age groups (the young-older adults (age50-70y) and the middle-older adults (age70-90y)/old-older adults (age ≥90). We stratified two age groups based on birth sex to create four subgroups: young-older adults (age 50-70y: n=139/111 (f/m)), and 194 middle/old-older adults (age 70-95y: n= 94/100 (f/m)). Body composition was measured by DXA. Peak handgrip force and single-leg muscle strength were measured using dynamometry (Vernier) and (Kincom).

Stable Isotope Tracer Infusion and Analysis

After an overnight fast, participants visited the clinic early in the morning for blood draw. After a blood sample was collected for baseline enrichment analysis and plasm amino acid concentrations, a single pulse of a mixture of 18 stable amino acid tracers was administered followed by subsequent blood sampling at times t=10, 20, 30, 60, and 120 min for tracer enrichments analysis (Cambridge Isotope Laboratories, Woburn, USA). Tracer enrichments was analyzed by LC-MS/MS to calculate whole body production (WBP) rate.

Statistics

Statistic was performed by two-way ANOVA on decay curves corrected for sex and age group. Data were adjusted for total lean mass for amino acid kinetic data. Significance set at P<0.05.

III. RESULTS

Aging was associated with lower extremity lean mass (p=0.046) and muscle function (p=0.017). Lean mass and muscle function were lower in females than in males (p<0.001). Females also had lower WBP of phenylalanine, hydroxyproline, tau-methylhistidine (markers of protein, - collagen,- and myofibrillar breakdown), tyrosine, all BCAA(valine, leucine, isoleucine), arginine, citrulline (p<0.001) as compared to males. The older group showed lower WBP of phenylalanine, tyrosine, arginine, citrulline, leucine, valine and higher tau-methylhistidine (p<0.001) than young older adults. Sex*age interactions were found for WBP of arginine, citrulline, valine (p<0.001), indicating that age-related decrease in males was higher for WBP arginine and citrulline and lower for WBP valine.

REFERENCES

1. Deutz, N.E.P., et al., *Comprehensive metabolic amino acid flux analysis in critically ill patients.* Clin Nutr, 2021. **40**(5): p. 2876-2897.
2. Fujita, S., et al., *Basal muscle intracellular amino acid kinetics in women and men.* American Journal of Physiology-Endocrinology and Metabolism, 2007. **292**(1): p. E77-E83.

Sigma Anti-Bonding Calcium Carbonate (SAC) cream enhances the wound-healing process in C57/BL6 mouse

YEONJU KANG[1,2*], Jihwan Song[2*], Syed Hassan Mehdi[1*], Sae Woong Oh[3], Jongsung Lee[3], Paul K Lee[4], Alex Lee[4], Yong Gu Lee[2], Wondong Kim[2], and Donghoon Yoon[1]

[1]Myeloma Center, the University of Arkansas for Medical Sciences, Little Rock, Arkansas, USA; [2]College of Pharmacy and Institute of Pharmaceutical Sciences and Technology, Hanyang University, Ansan, Republic of Korea; [3]Molecular Dermatology Lab, Dep. of Integrative Biotechnology, Sungkyunkwan Univ., Suwon, Republic of Korea; [4]CBHI (Calcium & Bone Health Institute, Canada), Coquitlam, British Colombia, Canada.

** Represents that these authors equally contributed to this work.*

I. INTRODUCTION

Wound healing includes replacing destroyed/damaged tissues with newly generated tissue. Once the injury occurs, the epidermis and dermis form a protective barrier against the external environment. The wound is repaired through sequential steps with overlaps; hemostasis, inflammation, cell proliferation, and tissue remodeling (maturation and cell differentiation). Wound healing is a calcium-mediated process. Calcium regulates inflammatory cell infiltration, migration/proliferation, and differentiation of dermal fibroblast and keratinocytes. Sigma Anti-Bonding Calcium Carbonate (SAC) is a chemically modified calcium carbonate with a unique weak bonding that becomes SAC water-soluble and stable at room temperature. In the body, SAC behaves as ionic calcium but also helps dissociate protein-bound calcium into ionized calcium. In turn, SAC significantly increases active ionized calcium in the body. Collectively, we hypothesized that the topical treatment of SAC enhances wound healing.

II. MATERIAL AND METHOD

To study the effects of the SAC on wound healing, we took 32, 8~10-month-old, C57/BL6 mice and singly housed them. Two bilateral circular wounds were created on the dorsum using a 5-mm punch biopsy. About 0.8mg of Control or SAC cream was applied to each circular wound twice a day for wound treatment. The SAC cream contains 0.12% SAC in a control dermatology cream provided by the company. The wound size was measured using CellSens software (Olympus Co.). In addition, skin biopsies were taken before the wound was created and after the wound closed. The skin biopsy was fixed in 4% paraformaldehyde and underwent hematoxylin & eosin immunohistology staining (Vector, H-3502) and collagen staining (Abcam, ab270993). The skin tissue was measured using a Zeiss AXIO Imager M2 microscope. The MTT cell proliferation assays were performed using HDFa and HaCaT cells in 24, 48, and 72 hours at 0.032, 0.32, and 1.6μg/ml SAC.

III. Result

We found that the SAC -treatment rapidly reduced the wound size in the early healing phase and closed wounds earlier than the control. Furthermore, SAC increased in epidermal thickness during wound healing, which eventually returned to its basal level. SAC-derived epidermis and dermis showed an increased synthesis of loricrin and collagen, suggesting that SAC-promoted skin layers are functional. The *in vitro* experiments in adult human dermal fibroblast (HDFa) and keratinocyte (HaCaT) showed that i) SAC does not induce cytotoxicity at any tested concentrations, ii) SAC enhanced HDFa and HaCaT growth in a dose-dependent manner, and iii) SAC promotes HaCaT migration than $CaCl_2$.

IV. CONCLUSION

SAC cream improves wound healing by enhancing re-epithelialization and proliferation of epithermal keratinocytes and dermal fibroblasts with no toxicity. The SAC effect is transient as the effects gradually return to normal once the treatment is terminated. These results suggested that SAC cream can be a good therapeutic intervention for skin injury healing.

ACKNOWLEDGEMENTS

This research was supported by the Calcium and Bone Health Institute (CBHI; CBHI CRA C23992). Y.K. and J.S. were supported by a grant from the Korea Health Technology R&D Project through the Korea Health Industry Development Institute (KHIDI), funded by the Ministry of Health & Welfare, Republic of Korea (grant number: HI19C0748).

Development of Humanized Diffuse large B-cell Lymphoma Mouse Models.

HYEJEONG JEONG[1,2], Syed Hassan Mehdi[1], Leonard Shultz[3], Yong Gu Lee[2], and DongHoon Yoon[1]

1 Myeloma Center, the University of Arkansas for Medical Sciences, Little Rock, Arkansas, USA; 2 College of Pharmacy and Institute of Pharmaceutical Sciences and Technology, Hanyang University, Ansan, Republic of Korea; 3 The Jackson Laboratory, Bar Harbor, ME

I. INTRODUCTION

Diffuse Large B-cell Lymphoma (DLBCL) is the most common type of non-Hodgkin's lymphoma, with ~40% of patients developing relapsed or refractory disease. There are two subtypes of DLBCL; i) a germinal center B cell-like subtype; ii) an activated B cell-like subtype. The development of alternative therapies that target molecular features defining these unresponsive tumors is an active area of research.

In the current study, we try to establish a pipeline for the rapid, reliable generation of *in vivo* DLBCL models with easy accession of lymphoma progression.

II. Method

We transduced the well-established human ABC DLBCL cells (U2932 and HBL-1) and human GCB DLBCL cells (SUDHL-5 and Val) with the luciferase (Luc)-EGFP gene. The Luc-expressing (U2932-Luc, HBL-1-Luc, SUDHL-5-Luc or Val-Luc) tumor cells were sorted for GFP positivity and expanded. The U2932-Luc, HBL-1-Luc, SUDHL-5-Luc and Val-Luc cells (0.5x106/100µl PBS) were injected via tail vein into 8-12 weeks old mice of various humanized NSG strains (representing same sex). NSG mice were humanized by transgenic expression of human cytokines (SCF, GM-CSF, and IL3 or human IL6 alone or IL6 plus SCF, GM-CSF, and IL3) with the CMV promoter. We assessed engraftment and growth by weekly in vivo imaging (IVIS 200 imager, Perkin Elmer). To evaluate organ-specific engraftment and progression, ex vivo IVIS imaging was performed weekly. The spleen, lungs, gut, brain, stomach, spine, kidney, heart, and liver were fixed with 10% formalin and embedded in paraffin. Sections were stained with an anti-human CD20 antibody to evaluate the tumor morphology using a Zeiss AXIO imager M2 microscope (Zeiss, Nashville, TN)

III. RESULTS

We found that the IL-6 strain exhibited a uniform expansion of U2932 cells relative to the IL-6/SGM3 mice. Engraftment rates were 68% at IL6 30% in IL6/SGM3. The survival graph shows IL-6 mice have consistent and uniform progression of U2932. The organ-specific evaluation demonstrated that U2932-Luc cells were initially engrafted and grew in the lung, liver, and spleen, subsequently found in the skeleton, ovary, and brain. In the case of HBL-1, NSG, SGM-3, and IL-6 mice showed 60, 60, and 56% engraftment rates, while IL-6/SGM3 showed 18%. However, in the ex vivo evaluation, all three strains showed inconsistent tissue infiltrations on the examined organs.

SUDHL-5 cells were not engrafted in any humanized NSG mice. How about, Val cells were well engrafted in IL6 and IL6/GM3 with 100% and 50% engraftment rate, respectively. The engraftments and progression were uniform. In the ex vivo evaluation, IL6 injected Val cells showed consistent tissue infiltrations on the examined organs.

IV. CONCUSIONS

We tried to develop human DLBCL animal models using two different ABC-type DLBCL cells, U2932 and HLB-1 and two different ABC-type DLBCL cells, SUDHL-5 and VAL. While HBL-1 showed inconsistent tumor infiltration and SUDHL-5 was not well engrafted, the U2932 and VAL DLBCL cells in the NSG-IL-6 mouse reproduced the clinical features of an aggressive DLBCL with consistent tumor infiltration. This model will provide a new tool to enable the expansion of patient samples while overcoming the current limitations of DLBCL xenografts and transgenic mice. Furthermore, the ability to maintain the growth of patient-derived samples within clinically relevant locations has excellent potential to test patient-specific, personalized treatment strategies more accurately.

V. ACKNOWLEDGEMENTS

This work was supported by Seed-of-Science Award from Winthrop P. Rockefeller Cancer Institute at the UAMS, and Hyejeong was supported by a grant from the Korea Health Technology R&D Project through KHIDI, funded by the Ministry of Health & Welfare, Republic of Korea (grant number: HI19C0748).

Multiple Sclerosis Research Across the African Continent: A Systematic Review

Soonmyung Hwang[1], Ilena George[2], Maria A. Garcia-Dominguez[3], Vanessa Salasky[4], Anastasia Vishnevetsky[2,5], Dhanashri Miskin[6], Andy Tran[7], Brian C. Chiluba[8], Deanna Saylor[1,8,9]

[1]Department of Neurology, Johns Hopkins University School of Medicine, Baltimore, MD, USA, [2]Department of Neurology, Massachusetts General Hospital, Boston, MA, USA, [3]Department of Biostastistics, Johns Hopkins Bloomberg School of Public Health, Baltimore, MD, USA, [4]Department of Neurology, University of Maryland Medical Center, Baltimore, MD, USA, [5]Department of Neurology, Brigham and Women's Hospital, Boston, MA, USA, [6]Department of Neurology, Thomas Jefferson University Hospital, Philadelphia, PA, USA, [7]University of Iowa Carver College of Medicine, Iowa City, IA, USA, [8]University of Zambia, Lusaka, Zambia, [9]University Teaching Hospital, Lusaka, Zambia

Background: The global prevalence of multiple sclerosis (MS) has increase substantially from previous years, with a current estimate of approximately 2.8 million people.[1] However, MS remains considered a rare neurological disorder among African populations, despite the fact that original MS-related research based in African countries is extremely limited or non-existent.[2]

Objective: To summarize the contemporary state of MS-related research across the African continent and to identify knowledge gaps from the current research landscape.

Methods: Boolean searches on the PubMed, SCOPUS and Embase databases were conducted for articles published from 1990 to February 2022. Two reviewers evaluated the title and abstract of each identified record for inclusion based on pre-defined eligibility criteria. Discrepancies between reviewers were resolved by discussion until consensus was reached. Full-text review and, where applicable, data extraction were conducted by a single reviewer for all articles which passed the initial title and abstract screening process.

Results: After removal of duplicates, 2491 records were initially identified and underwent screening, of which 332 records were selected for full-text review and 251 were ultimately deemed eligible for inclusion. The majority of included studies were from the Northern African region (n=204; 81%), particularly from Egypt (n=166; 66%), and had a case-control study design (n=145; 58%). Yet, there were no original studies from 36 African countries, whereas Egypt, Tunisia and South Africa accounted for >90% of included studies. Over 50% (n=150) of selected studies were published from 2016-2022, highlighting the substantial increase in research output in recent years. Studies investigating the utility of diagnostic tools such as blood/serum biomarkers and neuroimaging technology were most common (n=105; 42%), followed by studies investigating MS risk factors (n=41; 16%).

Conclusion: The MS research landscape across the African continent has grown substantially over the past few decades and especially in the past seven years. Yet, the majority of the output comes from only a few countries with virtually no data from the majority of African countries. In particular, longitudinal cohort studies and randomized controlled trials are lacking. As such, notable gaps and barriers in our knowledge of the burden of MS in Africa remain, and further efforts to promote clinical and epidemiological MS research in sub-Saharan Africa are needed to improve our understanding of the burden of MS amongst African patients.

III. ILLUSTRATIONS

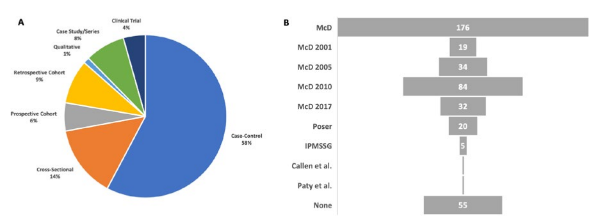

Figure 2. A) Type of study design distribution among included studies. B) Number of studies indicating the utilization of specific diagnostic MS criteria. Abbreviations: McD, McDonald; IPMSSG, International Pediatric Multiple Sclerosis Study Group.

REFERENCES

1. Multiple Sclerosis International Federation, "Atlas of MS 3rd Edition," *Multiple Sclerosis International Federation,* 2020.
2. GBD 2016 Multiple Sclerosis Collaborators, "Global, regional, and national burden of multiple sclerosis 1990-2016: a systematic analysis for the Global Burden of Disease Study 2016," *Lancet Neurol.* 2019;18(3):269-285. doi:S1474-4422(18)30443-5 [pii].

Multi-Omics Profiling for Evaluating Carcinogenic Exposure and Health Effects in Firefighters during Emergency Fires

Jooyeon Hwang[1]

[1] Department of Epidemiology, Human Genetics and Environmental Sciences, School of Public Health, University of Texas Health Science Center, Houston, TX 77030, USA

I. STUDY RATIONALE

Firefighters are covered with smoke-derived organic compounds, including polycyclic aromatic hydrocarbons (PAH), from fire-related activities and their turnout gear.[1] Although the inhalation of PAH from off-gassing after a fire activity or accumulated PAH when donning or doffing turnout gear cannot be ignored, transdermal absorption forms the major route of exposure. Many firefighter studies have investigated transdermal absorption; however, they have not employed multi-omics in applied industrial hygiene and occupational health to further explicate their findings. The goal of this study is to conduct multi-omics profiling to examine alterations in exposure-associated omics in healthy firefighters before and after engaging in fire suppression activities.

II. STUDY DESIGN

We conducted a comprehensive multi-omics analysis, including epigenome, transcriptome, proteome, and microbiome analyses, using biospecimen samples such as blood and urine from participants. The recruitment of study participants was a collaborative effort between our research team and local/regional fire departments. With this partnership, we conducted field exposure assessments to collect PAH wipe samples from firefighters' turnout gear and skin as well as biospecimens at emergency firefighting events. The baseline pre-assessment was conducted over at least two days without intervening fire activity (see Figure 1).

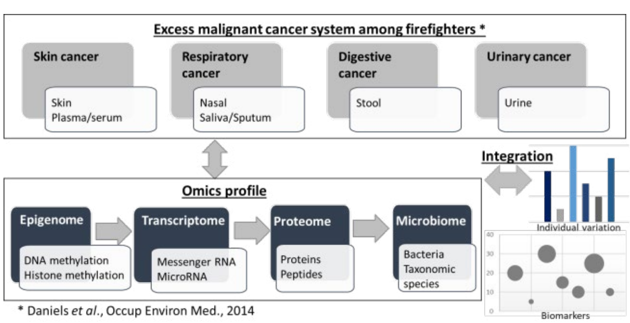

Figure 1: A range of complex high-dimensional biomarkers for this study. Based on the firefighters cancer mortality and incidence study,[2] a selected malignant cancer that poses a high risk was explored using a combination of biospecimen and omics profile.

III. FUTURE DIRECTIONS

We plan to incorporate practical guidelines for monitoring the health of firefighters into the manual for their required annual training. Currently, the training does not specify the learning outcomes or lesson outlines. As the study moves through its various stages, we will collect copious information on omics (e.g., gene expression) profiling and pathways. That information can be used for a wide range of purposes, from identifying biomarkers such as miRNA for early cancer diagnosis to detecting reversible health symptoms such as oxidative stress and immune/ inflammatory disease. The data collected could potentially contribute to individual, precise diagnoses for firefighters—a unique occupational group.

ACKNOWLEDGEMENTS

We would like to thank both the firefighters who participated in the study and the individuals who provided valuable support and assistance in study planning, data collection, and dissemination: Robert Agnew, Chao Xu, Mingze Zhu, Willard M. Freeman, Jenny Gipson, Timothy VanWagoner, Pauline Norris, Nagib Ahsan, Paul Grunsted, Jake Mitchell, Brittany Karfonta, Gina Herbert, Krista Thompson, and Xin Xu. Funding for this project was provided by the Centers for Disease Control and Prevention/National Institute for Occupational Safety and Health (CDC/ NIOSH K01OH011891).

REFERENCES

1. Hwang, J., Xu, C., Agnew, R., Clifton, S. & Malone, T. Health Risks of Structural Firefighters from Exposure to Polycyclic Aromatic Hydrocarbons: A Systematic Review and Meta-Analysis. *Int. J. Environ. Res. Public Heal.* **18:8**, (2021).
2. Daniels, R. D. *et al.* Mortality and cancer incidence in a pooled cohort of US firefighters from San Francisco, Chicago and Philadelphia (1950-2009). *Occup. Environ. Med.* **71**, 388–97 (2014).

Bridging the Gap: A Community Approach to Addressing Health Disparities in North Nashville through Food Access Community Mapping

Wansoo Im, Ph.D.
Meharry Medical College

I. SUMMARY

North Nashville, an underserved community with significant health disparities, faces alarming rates of hypertension and diabetes. Socioeconomic factors and social determinants of health contribute to these disparities. This proposal emphasizes the importance of food accessibility as a crucial social determinant of health and explores how community mapping can effectively tackle this issue.

Food accessibility, the availability and affordability of nutritious food options, profoundly impacts community health. While the USDA has developed methods to assess food accessibility, such as mapping food deserts, these approaches have limitations that hinder a comprehensive understanding of challenges faced by communities like North Nashville.

To bridge this gap, we propose a comprehensive community mapping project integrating data analysis, community education, engagement, and empowerment. Community mapping, a participatory approach leveraging local knowledge to identify and address community needs, offers various benefits, including fostering ownership and facilitating data-driven decision-making.

The North Nashville Community Mapping Project (https://www.communitymap.net/nashvillefood) combines geospatial data, community surveys, and feedback to create a detailed and accurate representation of the area's food accessibility landscape. The project took place on April 15th, 2023, in a central location in North Nashville. Attendees actively participated in mapping, attended educational workshops, and provided valuable feedback through surveys.

The collected data will inform the development of actionable strategies to enhance food accessibility and improve health outcomes in North Nashville. This conference proposal aims to showcase the potential of community mapping as an effective tool for addressing health disparities and promoting health equity in underserved communities.

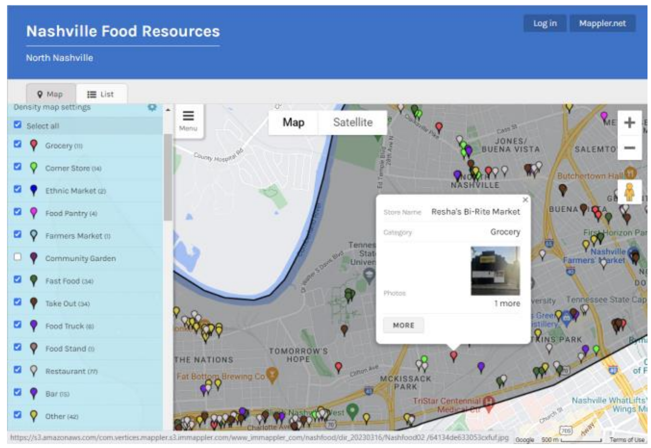

Figure1: Screenshot from http://www.immappler.com/nashfood

REFERENCES

Heerman, W. J., Wallston, K. A., Osborn, C. Y., Bian, A., Schlundt, D. G., Barto, S. D., & Rothman, R. L. (2016). Food insecurity is associated with diabetes self-care behaviours and glycaemic control. Diabetic medicine : a journal of the British Diabetic Association, 33(6), 844–850.

Coleman-Jensen, Alisha, Matthew P. Rabbitt, Christian A. Gregory, and Anita Singh. 2020. Household Food Security in the United States in 2019, ERR-275, U.S. Department of Agriculture, Economic Research Service.

Beltrán, S., Pharel, M., Montgomery, C. T., López-Hinojosa, I. J., Arenas, D. J., & DeLisser, H. M. (2020). Food insecurity and hypertension: A systematic review and meta-analysis. PloS one, 15(11), e0241628.

Augmented Reality Glasses for Enhancing Coaching Abilities of Exercise Instructors

Jeeyoung Hong, PhD[1,2], Hyoun-Joong Kong, PhD[3,4,5]
[1]Medical Big Data Research Center, Seoul National University Medical Research Center, Seoul, Korea
[2]Institute of Exercise Prescription, Kongju National University, Kongju, Korea
[3]Department of Transdisciplinary Medicine, Seoul National University Hospital, Seoul, Korea
[4]Department of Medicine, Seoul National University College of Medicine, Seoul, Korea
[5]Innovative Medical Technology Research Institute, Seoul National University Hospital

I. INTRODUCTION

The aim of this study is to investigate the efficacy of utilizing augmented reality (AR) glasses in an exercise coaching platform for enhancing the coaching abilities of exercise instructors during exercise instruction.

II. METHODS

This study recruited a total of thirty-five novice exercise instructors with less than two years of experience in guiding exercise, who expressed their agreement with the study's objective. A crossover design was employed to investigate the effects of augmented reality glasses on exercise instruction abilities. The participants were randomly assigned to two groups. In one group, participants provided exercise instruction to elderly individuals without wearing AR glasses, and their performance was assessed using the Elderly Exercise Instruction Questionnaire. After a one-month washout period, the same group of participants wore AR glasses and provided exercise instruction again, followed by evaluation using the same questionnaire. The procedure was reversed for the other group, where participants initially wore AR glasses and then provided exercise instruction without them after one month. To determine if there were any differences in exercise instruction abilities for elderly individuals before and after wearing AR glasses, a paired-sample t-test was conducted in this study.

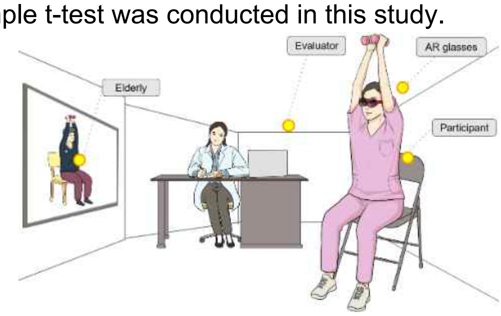

Figure 1: Guidance for elderly individuals using augmented reality glasses.

III. RESULTS

The significant differences were observed in professionalism (p=.009), emotional communication ability (p=.018), and safety (p<.001).

Table 1: Results of the t-test examining differences in exercise instruction abilities before and after the use of augmented reality glasses

Item	Pre	Post	t	p
Professionalism	23.45±4.35	25.85±4.49	-2.778	**.009**
Emotional communication ability	13.28±4.82	15.77±6.44	-2.495	**.018**
Fidelity	29.28±6.87	29.62±5.65	-.281	.781
Safety	29.31±4.6	35.37±4.8	-6.965	**.000**
Total	95.34±17.00	106.62±16.98	-3.799	**.001**

IV. Discussion

This study enhances our understanding of AR glasses effectiveness in improving exercise instruction abilities and guides innovative approaches for exercise coaching.

ACKNOWLEDGEMENTS

This work was supported by Institute of Information & communications Technology Planning & Evaluation (IITP) grant funded by the Korea government (MSIT) (No. 2021-0-0052, Cloud-based XR content conversion and service technology development that changes according to device performance) and Ministry of Education of the Republic of Korea and the National Research Foundation of Korea (NRF-2021S1A5B5A16078226).

REFERENCES

1. ACSM. (2018). ACSM's Guidelines for exercise testing and prescription, Tenth Edition. Baltimore: Lippincott Williams & Wilkins.
2. Hong JY, Kim HR, Kong HJ. Development of a Scale for Quantitative Evaluation of Exercise Instructors for Older People. Exercise science. 2022;31(4):438-443.

Associations between Binge Eating Severity and Factors from Social Comparison among Korean American women

Bo Ra Kim[1], Gayle M Timmerman[2]
[1]MSN, RN, Doctoral student, [2]PhD, RN, CNS, FNAP, FAAN, Professor, School of Nursing,
The University of Texas at Austin

I. BACKGROUND

Binge-eating behavior, uncontrolled consumption of large amounts of food, commonly occurs in the general public, especially in women. It is associated with psychological, as well as physical problems (e.g. obesity). Social comparison may promote personal relative deprivation (i.e., feelings of resentment and unfairness from social comparison), being over-concerned with their body image (thin-ideal internalization), which may lead to binge-eating behavior. Yet, little is known about the relationship among factors from social comparison and binge eating severity, especially in Korean American populations. The purpose of this study was to examine the relationships between binge eating severity and social comparison factors (personal relative deprivation and thin-ideal internalization) among Korean American women.

II. METHODS

A convenience sample (n= 136) was recruited from Korean churches, community organizations, universities and student groups. Inclusion criteria were women at least 18 years old, who read English, and are not pregnant or breastfeeding. Participants completed on-line questionnaires [Background Information, Personal Relative Deprivation Scale (PRDS), Thin-ideal Internalization Scale (Sociocultural Attitudes Towards Appearance Questionnaire, SATAQ-3) and Binge Eating Scale (BES)]. SATAQ-3 consists of four subscales: Information, Pressures, General, and Athlete.

III. RESULTS

The participants' average age was 31.1 (SD = 12.2), BMI 22.1 (SD = 2.5), and 57.4% were born in South Korea. Out of 136 participants, 57.4% had little to no binge eating (BES score ≤ 17), 22.1% had mild to moderate binge eating (BES score 18-26), and 20.5% had severe binge eating (BES score ≥ 27). Binge eating severity (total score of BES) was significantly related to PRDS (r = .51, p < .001) and SATAQ-3 (r = .40, p < .001). Also, the level of binge eating had significant relationships with all subscales of SATAQ-3 with Information (r = .34, p < .001), Pressures (r = .45, p < .001), General (r = .36, p < .001), and Athlete (r = .31, p < .001).

Table 1: Correlations between BES, PRDS, SATAQ-3 (N = 136)

P(r)

Variables	1	2	3	4	5	6	7
1.BES	1						
2.PRDS	.51***	1					
3.SATAQ3	.40***	.56***	1				
4.Information	.34***	.54***	.94***	1			
5.Pressures	.45***	.52***	.91***	.81***	1		
6.General	.36***	.54***	.96***	.86***	.84***	1	
7.Athlete	.31***	.56***	.85***	.72***	.70***	.79***	1

Note: ***p<.001

IV. Conclusions

In this sample, participants with higher personal relative deprivation and thin-ideal internalization were more likely to have greater levels of binge eating. Also, the increased level of acknowledgement of body image information from media sources (Information), pressure of appearance from media (Pressures), internalization of ideal beauty from media (General), and internalization of athletic ideals (Athlete) were associated with the higher level of binge eating. Further examination of binge eating severity and other risk factors among the Korean American women population is warranted.

REFERENCES

1. Festinger, L. "A theory of social comparison processes," *Human relations,* Vol. 7, No. 2, pp. 117-140, 1954.

ACKNOWLEDGEMENTS Funded by The Epsilon Theta chapter of Sigma Theta Tau Honor Society.

Differential Moderating Roles of the Salience Network and Central Executive Network in Internalizing Psychopathology and Fluctuating Negative Affect

Ha Jeong Park[1] & Annmarie MacNamara[1, 2]

[1]Department of Psychological and Brain Sciences, Texas A&M University, College Station, TX

[2] Institute for Neuroscience, Texas AM University, College Station, TX

I. INTRODUCTION

Internalizing psychopathology such as anxiety and depression has been associated with higher levels of negative affect instability (AI), suggesting greater sensitivity and/or deficient affect regulation in response to events. The salience network (SN) detects and responds to emotional stimuli, and the central executive network (CEN) exerts top-down control over attention toward salient stimuli. General functional connectivity (GFC) within these networks might further understanding of the mechanisms behind AI, and why some individuals with internalizing psychopathology are more likely to be characterized by negative AI than others.

II. METHODOLOGY

Individuals with mixed internalizing psychopathology (N = 54, M_{age} = 25, SD_{age} = 9.14, 38 female) completed self-report measures, underwent fMRI scans, and then completed 10 days of ecological momentary assessment to assess negative AI. We used GFC from 32 minutes of resting state and task fMRI, a latent variable reflecting transdiagnostic internalizing symptoms, and their interaction to predict daily negative AI.

III. RESULTS

In one regression model, participants with higher internalizing symptoms showed greater negative AI, β = .324, p = .015, but only when SN connectivity was high, β = .303, p =.023. In another model, participants with higher levels of internalizing symptoms also showed higher negative AI, β = .340, p = .010, but only when CEN connectivity was low, β = -.380, p = .004.

IV. CONCLUSION

SN and CEN connectivity may play a role in increased negative AI in internalizing psychopathology. Stronger connectivity in the SN is associated with enhanced emotional reactivity, which may cause difficulty in regulating emotional fluctuations in internalizing patients. In parallel, weaker connectivity in the CEN is associated with deficits in cognitive control over emotion, which may cause difficulty in regulating emotional fluctuations in internalizing psychopathology. Thus, individual differences in negative AI may depend on variability in SN and/or CEN connectivity.

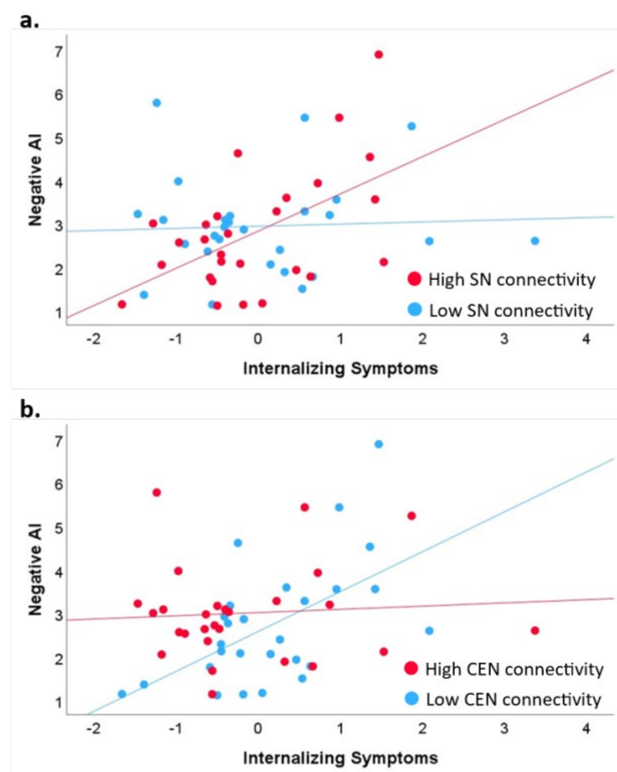

Figure 1: Scatterplots depicting the moderating role of SN (a) and CEN (b) connectivity on the association between internalizing symptoms and negative AI.

ACKNOWLEDGEMENTS

This work was supported by National Institute of Mental Health grant, R01MH125083 (to AM)

Clinical and Environmental Effects of Healthy Home Interventions

Insung Kang
Civil, Architectural, and Environmental Engineering, Illinois Institute of Technology, Chicago, IL USA

I. BACKGROUND

Human exposure to indoor air pollutants is an important risk factor for asthma and the exacerbation of respiratory symptoms. Healthy home interventions, including ventilation and filtration, have the potential to improve indoor air quality (IAQ) and respiratory health outcomes, although empirical evidence of their effectiveness remains limited. This paper describes two home intervention research projects to improve IAQ and respiratory diseases among high-risk population in existing homes in Chicago, IL. One is installation of residential mechanical ventilation systems among 53 adults with asthma and the other is deployment of stand-alone air filtration systems among 80 U.S. military veterans with chronic obstructive pulmonary disease (COPD).

II. METHODS

For homes with asthmatic participants received one of three types of ventilation systems half-way through the study: continuous exhaust-only system, intermittent central-fan-integrated-supply (CFIS) system, or continuous balanced system with an energy recovery ventilator (ERV). For homes with COPD participants received one of two types of stand-alone air cleaners, with a real or sham filter. We conducted approximately weeklong field measurements on a quarterly basis throughout the study to monitor indoor and outdoor size-resolved particles (0.3-10 μm) and other gaseous pollutants, if applicable.

III. RESULTS AND DISCUSSION

The following parameters were significantly lower across all homes after the ventilation system retrofits, treating all system types as one: I/O ratios of CO_2, NO_2, PM_1, $PM_{2.5}$, and PM_{10} (Figure 1). In addition, asthma control test scores increased after the installation of residential mechanical ventilation systems ($p < 0.001$). Examined separately, all three types of ventilation systems also showed statistically significant improvements on asthma control test score (*Figure 2*).

Air cleaner study with COPD patients is still ongoing and we expect stand-alone air filtration for improving IAQ and COPD outcomes. There will be housing-related factors that may contribute to COPD exacerbation. To this end, we will evaluate the utility of using low-cost sensors for indoor air pollution epidemiology studies and for providing actionable or useful information on the quality of their indoor air to patients and their physicians.

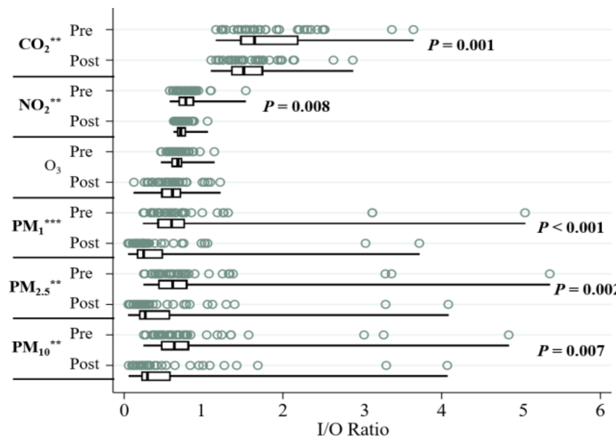

Figure 1. I/O ratios of pollutants measured during pre- and post-intervention periods.

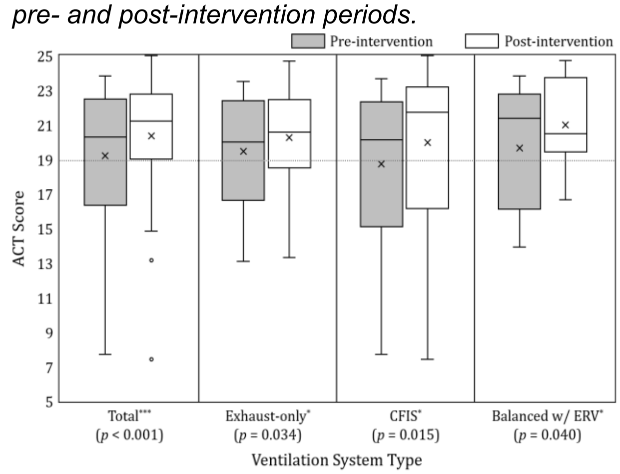

Figure 2. Impact of all and specific ventilation system types on ACT score.

REFERENCES

1. Kang et al., "Indoor air quality impacts of residential mechanical ventilation system retrofits in existing homes in Chicago, IL" *Science of The Total Environment* 804, 2022.

Mutations in the UBIAD1 gene, the vitamin K2 synthesizing enzyme, cause Schnyder Corneal Dystrophy (SCD) by inhibiting ER-associated degradation of HMG CoA reductase.

Dong-Jae Jun[1], Marc Schumacher[1], Youngah Jo[1], and Russell DeBose-Boyd[1]

[1]UTSouthwestern Medical Center, Dallas TX

I. SUMMARY

1. UBIAD1 is the causative gene for Schnyder corneal dystrophy(SCD).

Schnyder corneal dystrophy (SCD) is a rare autosomal dominant human genetic eye disease characterized by bilateral corneal opacification resulting from an abnormal accumulation of cholesterol and lipid. The sole causative gene for this disease is UbiA prenyltransferase domain-containing protein-1 (**UBIAD1**), which synthesizes the vitamin K2 by transferring a geranylgeranyl group onto menadione. Mutations that alter 20 amino acid residues in UBIAD1 have been identified in ~50 SCD families.

2. UBIAD1 regulates ER-associated degradation of HMG CoA reductase

A link between UBIAD1 and cholesterol metabolism was first provided by co-immunoprecipitation studies that showed an association of UBIAD1 with the rate-limiting cholesterol biosynthetic enzyme HMG-CoA reductase. Recently, our group showed that UBIAD1 temporarily keeps the reductase from the complete sterol-accelerated endoplasmic reticulum (ER)-associated degradation (ERAD) until the reductase produces sufficient geranylgeranyl pyrophosphate (GGpp), the direct substrate of UBIAD1 for the synthesis of Vitamin K2. We also discovered that GGpp stimulates translocation of UBIAD1 from the ER to the Golgi, and subsequently, the reductase gets fully degraded by the co-works of sterol and ERAD complex. This exquisite regulation illustrates how UBIAD1 ensures the protein stability of reductase for the sufficient production of non-sterol isoprenoids, including GGPP, and contributes to the feedback regulation of non-sterol isoprenoids and sterol metabolism.

3. All 20 SCD mutant UBIAD1s failed to localize in Golgi and ended up in ER where they increased the stability of HMGCR's protein level.

We found the common feature of all 20 Schnyder corneal dystrophy (SCD)-associated UBIAD1 mutants. All SCD-associated UBIAD1 mutants fail to respond to GGpp-induced Golgi transport and abnormally translocate to the ER, where they stabilize HMG CoA reductase (**1**). The resulting stabilization of reductase by mutant UBIAD1s is the causative cellular mechanism that leads to the overproduction of cholesterol in the cornea of SCD patients.

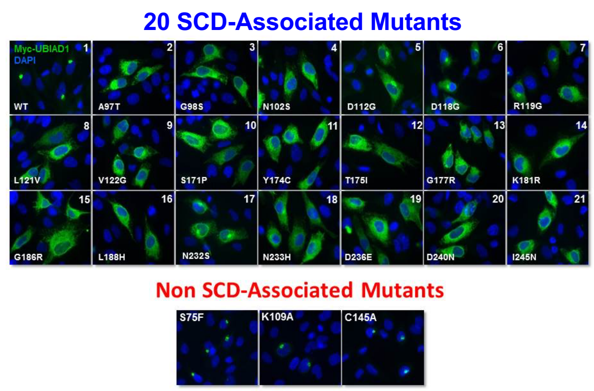

Figure 1. *This figure shows the subcellular localization of wild-type UBIAD1 and all SCD-associated mutants of the prenyltransferase. The results reveal that wild-type Myc-UBIAD1 localized to the Golgi of SV-589 cells cultured in FCS (Panel 1). In contrast, the remaining SCD-associated mutants of UBIAD1 were defective in transport to the Golgi and localized to the ER (Panels 2-21). UBIAD1 (S75F), which is not associated with SCD and results from a moderately common polymorphism in the UBIAD1 gene, and other arbitrary missense mutants (K109A, C145A) also localized to the Golgi (bottom panels).*

REFERENCES

1. Schumacher MM, Jun DJ, and Russell DeBose-Boyd, "Geranylgeranyl-regulated transport of the prenyltransferase UBIAD1 between membranes of the ER and Golgi." Journal of Lipid Res. 2016 Jul;57(7):1286-99

Technical Group B-2

Agriculture, Ecology, Food, Nutrition (FAN)

Metabolomics in food and agricultural science

Joonhyuk Suh

Department of Food Science and Technology, University of Georgia, Athens, GA, USA

I. SUMMARY

In the post-genomic era, metabolomics, a newly emerging toolbox in omics science, has been introduced with analysis of small molecules (metabolites) in biological systems to understand in-depth biochemical mechanisms of organisms at the chemical level. Since metabolites are the end product of cellular signaling processes, the profiling of metabolites can give us direct information on phenotypes and changes in biological functions of the organisms. With these merits, metabolomics has been intensively used in clinical and pharmaceutical science, and gradually expanded to other areas including food and agricultural science.

In this presentation, metabolomics approach (concept, methodology) will be introduced, and its applications in the field of food and agricultural science will be discussed with case studies[1,2].

II. ILLUSTRATIONS

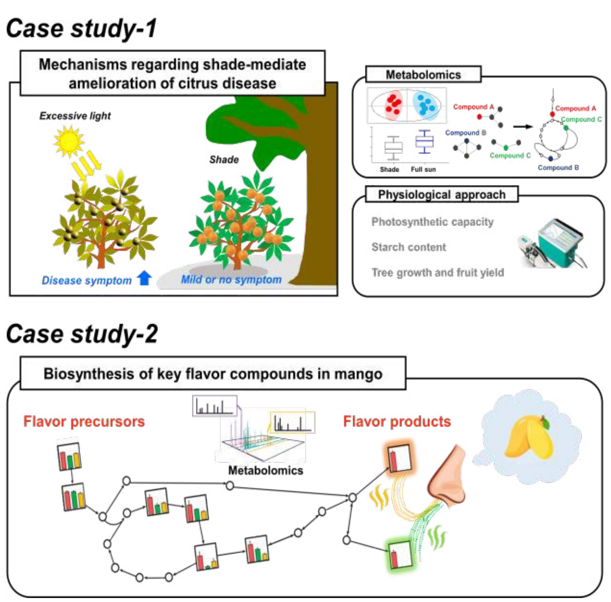

Figure 1: Case studies of metabolomics in food and agricultural science

ACKNOWLEDGEMENTS

The case studies were supported by USDA-NIFA (2018-51181-28375) and Citrus Initiative of the University of Florida. The author thanks research teams at the Citrus Research and Education Center and the Tropical Research and Education Center, University of Florida.

REFERENCES

1. Suh JH, Guha A, Wang Z, Li S-Y, Killiny N, Vincent C, Wang Y, “Metabolomic analysis elucidates how shade conditions ameliorate the deleterious effects of greening (Huanglongbing) disease in citrus”, *The Plant Journal*, Vol. 108, pp. 1798-1814, 2021.
2. Suh JH, Madden RT, Sung J, Chambers AH, Crane J, Wang Y, “Pathway-based metabolomics analysis reveals biosynthesis of key flavor compounds in mango”, *Journal of Agricultural and Food Chemistry*, Vol. 70, No. 34, pp. 10389-10399, 2022.

New antioxidants for frying oil developed in NCAUR, ARS, USDA

Hong-Sik Hwang
USDA, ARS, NCAUR, Peoria, IL, USA

I. SUMMARY

Although vegetable oils rich in polyunsaturated fatty acids are beneficial to human health, they are highly prone to oxidation. Strong antioxidants, preferably natural antioxidants, are needed to prevent oxidation of these oils, especially, for deep frying that is done at high temperatures. We recently developed new natural antioxidants that can replace synthetic antioxidants. This presentation will summarize the antioxidant activities of amino acids, amino acid salts, and inorganic bases.

II. METHODS and RESULTS

A. Heating and Frying Experiments

The heating study was conducted with vegetable oils containing an antioxidant (typically 5.5 mM) in vials heated at 180 ºC for 7 or 8 h. The frying study was done with potato cubes (about 0.6 cm x 0.6 cm x 0.6 cm) at 180 ºC for 8 h.

B. Results

It was found that some amino acids had strong antioxidant activity. When they were converted to sodium or potassium salts, the activity increased. Potassium salts had higher activity than sodium salts. It was also found that inorganic bases such as sodium and potassium carbonates and bicarbonates had significant antioxidant activity. It should be noted that these new antioxidants at 5.5 mM had stronger activity than a synthetic antioxidant, *tert*-butylhydroquinone (TBHQ) at 1.1 mM (0.02%) (Fig. 1).

C. Interaction with tocopherols

The synergistic effect with tocopherols was found to be the major mechanism for the antioxidant activity of amino acids, amino acid salts, and inorganic bases (Fig. 2). The antioxidant activity of these compounds may also be attributed to other mechanisms such radical scavenging activity, retention of tocopherols, negation of prooxidant activity of free fatty acids, stabilization of hydroperoxides, and formation of antioxidant compounds by reactions with oxidation products.

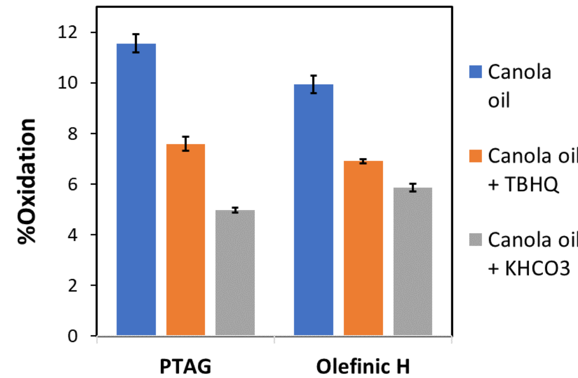

Figure 1: Antioxidant activity of $KHCO_3$ (0.06%) in canola oil in comparison with TBHQ (0.02%) during 8-h frying at 180 ºC.

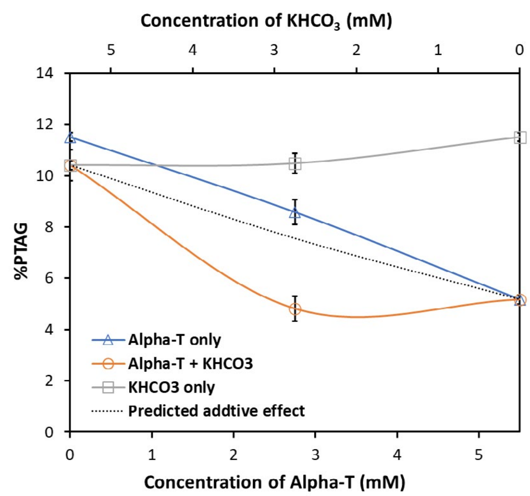

Figure 2: Antioxidant activity of KHCO3 (0.06%) in canola oil in comparison with TBHQ (0.02%) during 8-h frying at 180 ºC.

ACKNOWLEDGEMENTS

Add appropriate acknowledgements as needed.

REFERENCES

1. H.-S. Hwang, J. K. Winkler-Moser. Authors, “Bicarbonates and carbonates as antioxidants in vegetable oils at frying temperatures,” *J. Food Sic.* 88:717-731, 2023.

R&D Direction for Plant-based Meat and Cultivated Meat: Critical Variables for Consumer's Sensory Acceptance

Jung Hoon Han, Bouhee Kang
EAT JUST

I. SUMMARY
Consumers believe that the plant-based meats do not deliver the same sensory qualities of animal-based meats and taste remains a significant barrier for trial and repeated purchase. For the cultivated meats, the lack of sensorial quality is also the critical issue. From the sensory test with plant-base chicken and beef meats available from market, it is identified that the most critical variables affecting the overall sensorial acceptance are texture acceptance for beef patty, while the flavor acceptance and texture acceptance are equally significant for chicken breast meat. For the cultivated meat products, through the internal large sensory test, the lack of umami flavor was obtained for both cultivated chicken and beef. In summary, for the successful alternative meat business, it is important to improve texture and flavor acceptances for plant-based meat products and the umami taste enhancement for the cultivated meats.

II. QUALTY EVALUATION OF PLANT-BASED AND CULTIVATED MEATS

A. Materials and Methods
All data of plant-based meat products were analyzed using regression analysis after data normalization with mean and standard deviation. For cultivated chicken, 80 panelists were tasted the GOOD Meat cultivated chicken with real chicken thigh as a reference sample (difference test). For cultivated beef, 11 internal panelists joined the descriptive test after tasting the GOOD Meat cell paste in gelatin gels.

B. Sensory Results with Plant-based Meat Products
Figure 1 shows the results of the test. Both flavor and texture acceptances were significant to overall acceptance, while the appearance acceptance was insignificant for both beef and chicken. The most significant variable affecting the overall acceptance of beef patty was the texture acceptance, while the flavor and texture acceptances of chicken were equally significant to the overall acceptance.

$$Overall\ acceptance\ Y = f(A, F, T)$$
$$\text{where,}\quad A = Appearance\ acceptance$$
$$F = Flavor\ acceptance$$
$$T = Texture\ acceptance$$

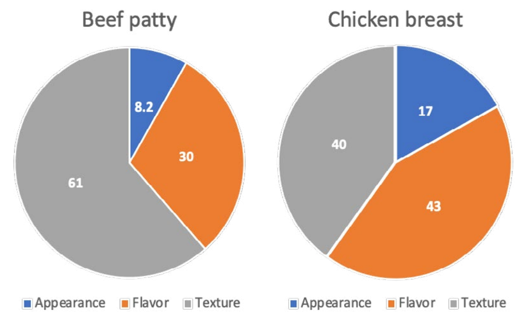

Figure 1: Effects of Appearance, Flavor, and Texture Acceptances on Overall Acceptance of Plant-based Beef Patty and Chicken Breast Meat

C. Sensory Evaluation Results with Cultivated Meats
The difference test for the cultivated chicken products and the descriptive test for the cultivated beef prototype both identified the lack of umami taste in the cultivated meats. This result was agreed to the umami taste measurement by Joo et al. (2022) which concluded that the cultivated beef and chicken meats have significantly lower glutamic acid and inositol monophosphate than those in traditional meats.

Table 1: Umami Taste Related Amino Acids % in Cultivated and Traditional Meats (data from 1)

	Chicken		Beef	
	Cultivated	Traditional	Cultivated	Traditional
Aspartic acid	9.37	9.93	8.59	9.76
Glutamic acid	15.42	17.3	14.56	15.89
Alanine	6.88	6.41	7.92	6.53
Methaonine	1.8	2.44	3.49	2.52
Lysin	8.46	9.5	7.43	9.73

REFERENCES

1. Joo ST, Choi JS, Hur SJ, Kim GD, Kim CJ, Lee EY, Bakhsh A, Hwang YH. "A Comparative Study on the Taste Characteristics of Satellite Cell Cultured Meat Derived from Chicken and Cattle Muscles" Food Sci Anim Resour 2022; 42(1):175-185

Comparative Study of the Susceptibility to Blue Light Inactivation of Foodborne Pathogens and Spoilage Bacteria

Minji Hur[1], **Francisco Diez-Gonzalez**[2]

[1,2]Center for Food Safety, Department of Food Science and Technology, University of Georgia, Griffin, GA

SUMMARY

Introduction

Antimicrobial Blue Light (aBL) in the visible spectrum of 400–470 nm could be a potential intervention technology for treating surfaces. Several microbial species are susceptible to aBL, but a systematic comparison for efficacy of aBL against food related bacteria is largely missing in the literature. This study was conducted to determine the broad-spectrum effect of aBL against selected foodborne pathogenic and food spoilage bacteria.

Methods

Strains of *Listeria monocytogenes* (Lm), *Salmonella*, *Cronobacter, E. coli,* and *Pseudomonas* were inoculated in tryptic soy broth (TSB), phosphate buffered saline (PBS), and on stainless steel (SS) coupons. Coupons were dried overnight. Viability was determined after exposure to 405 nm aBL at 4 °C and room temperature. Time of exposure was based on irradiation dose, 1,500 and 1,700 J/cm^2 for liquid cultures and dry cells, respectively. Dry cells were resuspended by sonication before plating. Counts were calculated by standard plating on tryptic soy agar after incubation at 37 °C for 24–48 h. Statistical analysis were conducted using ANOVA.

Results

Viable counts of all species were reduced > 6 Log CFU/ml when incubated in TSB during aBL treatment, but in PBS, except for *Pseudomonas*, viability decreases of < 2.1 Log CFU/ml were observed. *Pseudomonas* was the most susceptible bacteria to aBL at all conditions, inactivated more than 6 Log CFU/ml or coupon. The viability of *Cronobacter* and *Salmonella* dried cells remained within 1.5 Log CFU less than controls after treatment. In contrast, viability reductions of *L. monocytogenes* and *Pseudomonas* dried cells were > 3 Log CFU (p<0.05). No significant temperature effect was determined at any experimental condition. (p>0.05).

Significance

These findings suggest that the susceptibility to aBL may be variable among different food-relevant bacterial species.

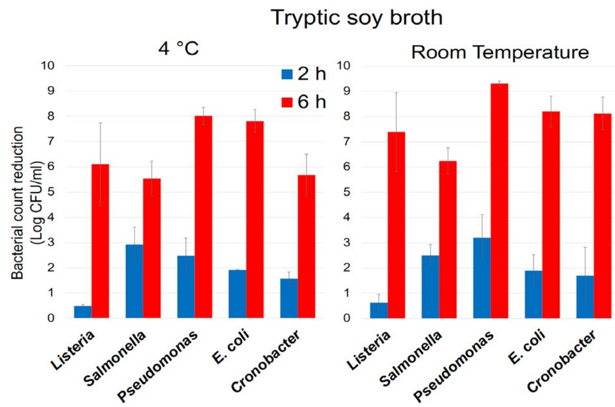

Figure 1. Viability reduction of bacterial cells suspended in tryptic soy broth after exposure to aBL (Irradiation intensity = 70 mW/cm2).

Table 1. Statistical analysis of cell reductions after 3 h of exposure of dried cells on SS coupons: effect of species (ABCDE) or temperature (ab), at p < 0.05.

	Reductions (Log CFU/ml)	
	4 °C	Room temp.
Pseudomonas	7.6 ^{Aa}	7.6 ^{Aa}
E. coli	3.6 ^{Ca}	4.3 ^{Ba}
Listeria	4.9 ^{Ba}	3.1 ^{Cb}
Salmonella	1.5 ^{Da}	1.4 ^{Da}
Cronobacter	0.3 ^{Ea}	0.6 ^{Da}

ACKNOWLEDGEMENTS

The support for this grant was provided by a Center for Food Safety internal grant and by the National Institute of Food and Agriculture, U.S. Department of Agriculture, award number “2022-67017-36307”.

REFERENCES

1. Yoon, J. H., Chu, H., Jeong, D. Y., Choi, S., Hwang, I. J., Lee, S. Y., & Kim, S. R. (2020). Decontamination of *Listeria monocytogenes* in enoki mushrooms using a 405-nm light-emitting diode illumination combined with organic acid dipping. *LWT*, *133*, 110048.
2. Kim, M. J., & Yuk, H. G. (2017). Antibacterial mechanism of 405-nanometer light-emitting diode against *Salmonella* at refrigeration temperature. *Appl. Environ. Microbiol. 83*, e02582-16.

Pathway-based metabolomics reveals the biosynthesis of key flavor compounds in apple

Min Jeong Kang[1], Keono Kim[2], Aria Grace Morrill[1], Jeehye Sung[2], Joon Hyuk Suh[1]
[1] Department of Food Science and Technology, College of Agricultural and Environmental Sciences, University of Georgia, Athens, GA 30602, USA
[2] Department of Food Science and Biotechnology, Andong National University, Andong 36729, South Korea

I. SUMMARY

Apple (*Malus domestica Borkh.*) is globally consumed fruits, with production in the U.S, surpassing 11 billion pounds in the 2010s[1]. The flavor of apples is a crucial factor in determining consumer acceptance and market price. Our previous research had identified key flavor compounds significantly influencing sensory attributes and consumer preference of apples[2]. As a follow-up, the present study aimed to elucidate the formation (biosynthetic pathways) of those key flavor compounds in different cultivars of apples using a pathway-based metabolomics.

Through this work, we identified major metabolic pathways for apple flavor synthesis. Pathways including tricarboxylic acid (TCA) cycle, amino acids metabolism, and butanoate metabolisms were associated with key aroma compounds (e.g. butyl acetate, 2-methylbutyl acetate) of apple. Ascorbate, myo-inositol, and carbon fixation pathways were linked to key taste compounds (e.g. tartaric acid, sucrose) of apple.

Our result demonstrated metabolic flux towards pivotal metabolic pathways, contributing to the formation and regulation of key flavor compounds in apple. Collected information will be used as preliminary data for the quality control of apple in the field. The identified pathways will also provide insights into the selection of related genes/proteins (breeding markers) within the pathways for the breeding of apple cultivars with desirable flavor traits.

II. ILLUSTRATIONS

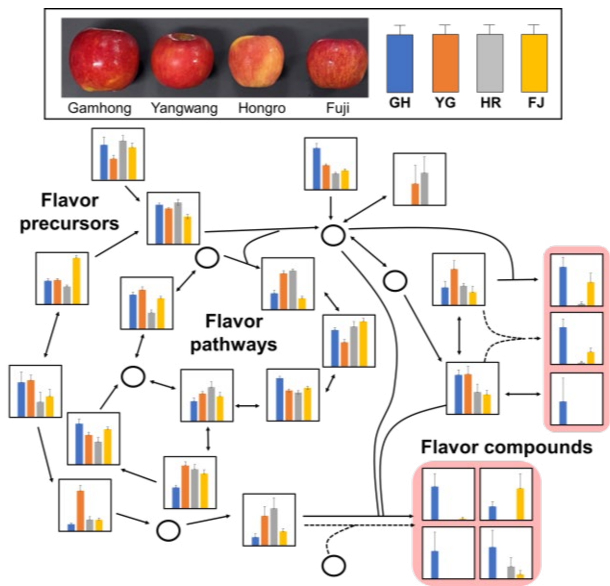

Figure 1. Metabolite mapping on the key flavor formation pathways from different apple cultivars.

ACKNOWLEDGEMENTS

This research was supported by the Basic Science Research Program through the National Research Foundation of Korea funded by the Ministry Education, Science and Technology (project number 2020R1C1C1003766)

REFERENCES

1. Weber C, Simnitt S, Lucier G, Davis WV, “Fruit and tree nuts outlook: March 2023”, U.S. Department of Agriculture, Economic Research Service. Vol. FTS-376, pp 34, 2023.
2. Kim K, Chun I-J, Suh JH, Sung J., “Relationships between sensory properties and metabolomic profiles of different apple cultivars”, *Food Chemistry: X*, Vol. 18, pp 100641, 2023

Influence of stunning methods on sensory characteristics of chicken breast meat using electronic senses

Sungeun Cho, Linda Barahona, Michelle Hayden, Md Shakir Moazzem
Department of Poultry Science, Auburn University, 260 Lem Morrison Drive, Auburn, AL, 36849

I. INTRODUCTION

Electrical water bath stunning (ES) is the most common method for poultry stunning prior to slaughter in the United States. However, from an animal welfare standpoint, the ES performs poorly due to stressful and painful shackling before moving to the electrified water bath. Controlled atmosphere stunning (CAS) method, involving a variety of gas mixtures, is considered the ideal stunning method in that it causes the minimum of avoidable pain and suffering to the birds. In this study, we evaluated the aroma and taste of ES and CAS chicken breast meat using Electronic Tongue (e-tongue, α-Astree II E-tongue, Alpha MOS, Toulouse, France) and Electronic Nose (e-nose, Heracles Neo E-nose, Alpha MOS).

III. MATERIALS AND METHODS

The aroma and taste of ES and CAS chicken breast meat at 0, 2, 4, and 6 hr post-mortem were evaluated. Furthermore, the ES and CAS samples were stored at -20°C and analyzed for four consecutive days (Days 1 to 4) to investigate the changes in aroma and taste over time using e-tongue and e-nose, respectively. The chicken breast samples (20 g) for e-tongue were homogenized with distilled water (200 mL), filtered with cheesecloth, and then centrifuged at 1500 rpm x 20 min. The samples were filtered again using 0.4 μm vacuum filters. Two grams of chicken breast were minced and placed in 20 mL vials for e-nose analysis. The vial was incubated for 20 min at 60°C for headspace analysis. Hydrogen gas was used at 1 mL/min flow rate to carry the volatile compounds into the two capillary columns (MXT-5 and MXT-1701) with two Flame Ionization Detectors. The final temperature of the analysis sequence was increased up to 250°C at 10°C/s temperature increment from the initial 40°C temperature.

IV. RESULTS

The results showed that the aroma and taste of ES and CAS stunned chicken breast at 0, 2, 4, and 6 hr post-mortem were not distinguishable as no separations were found on the aroma and taste maps obtained through the Alpha MOS proprietary software. Similarly, the aroma and taste of ES and CAS samples were not distinguished over the four days. The only difference we found was that the aromas of both ES and CAS samples on Day 1 were clearly separated from Days 2 to 4. This means that the aroma of never-frozen chicken breast meat was well distinguished from the chicken breast meat stored at -20°C for at least one day or longer.

V. CONCLUSIONS

CAS chicken breast meat showed no differences in aroma and taste quality compared to ES stunned meat.

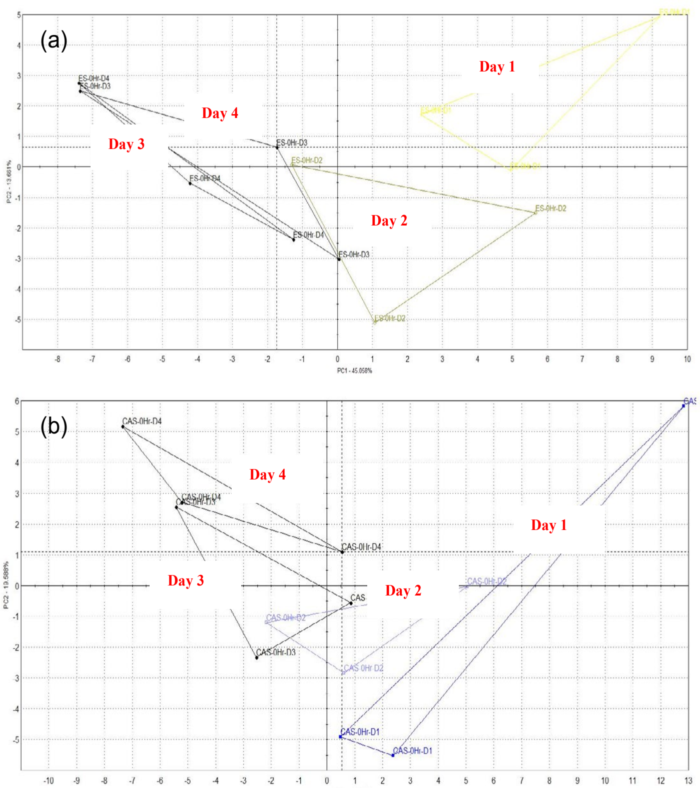

Figure 1: Aroma map of electrical stunned chicken breast (a) and gas stunned chicken (b) stored at -20°C for four days using an electronic nose.

ACKNOWLEDGEMENTS

This work is supported by the USDA ARS-Sustainability Project # 6040-42440-001-011-5.

Advancing Sustainable Food Production Through Synthetic Biology

Eun Joong Oh[1]
[1]Department of Food Science, Purdue University, West Lafayette, IN 47907, USA

I. INTRODUCTION

For centuries, the chemical and pharmaceutical manufacturing industries, driven by chemical synthesis, have significantly contributed to the rapid growth of the global economy. However, this progress has come at the cost of environmental pollution and degradation, posing threats to human health and well-being. As awareness of environmental conservation grows and petroleum resources dwindle, the pursuit of sustainable, green production methods using renewable raw materials has emerged as a crucial pathway for sustainable development. In this context, microbial cell factories offer a promising alternative, boasting rapid growth, environmentally friendly processes, and no competition with land or food resources.

II. OBJECTIVES

In recent times, yeast cell factories have gained widespread use in the synthesis of food ingredients and value-added chemicals, owing to its demonstrated suitability for industrial-scale production of various products.

A. Engineering yeast strains capable of converting carbon sources from cellulosic biomass into value-added products

Conversion of agricultural biomass to value-added products using microbial fermentation is an attractive option to substitute petroleum-based production economically and sustainably. Therefore, sustainable and cost-effective feedstocks for bioconversion are critical for industrial fermentation strategies. Since widely used cell factories such as *Saccharomyces cerevisiae* cannot ferment carbon sources in agricultural residues, research efforts have been focused on developing engineered yeast strains capable of co-utilizing carbon sources in the hydrolysates of biomass. Dr. Oh explored the potential of heterologous pathways to enable the assimilation of non-glucose carbon sources, such as cellobiose and xylose, as a strategy for enhancing cellular metabolism and increasing the yield of desired compounds.

B. Developing a bioengineered probiotic yeast-based precision therapeutic platform for gut health

Advanced engineered probiotics present distinctive characteristics for potential therapeutic applications in disease management. *Saccharomyces boulardii*, a probiotic yeast, demonstrates rapid proliferation at 37°C, allows for straightforward transformation, and possesses the ability to synthesize therapeutic proteins within the gastrointestinal tract. Dr. Oh's lab constructed engineered probiotic yeast strains capable of producing the ketone body (R)-3-hydroxybutyrate (3HB). 3-HB is the predominant constituent of ketone bodies in animals, acting as an energy substrate during starvation or exercise. In addition to its role in energy provision, 3-HB is regarded as a therapeutic agent.

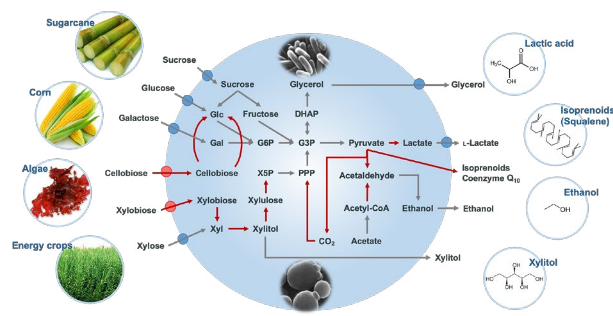

Figure 1: Production of food ingredients by engineered microorganisms.

ACKNOWLEDGEMENTS

This work was supported by funding from USDA.

REFERENCES

1. Oh et al., "Multiplex Evolution of Antibody Fragments Utilizing a Yeast Surface Display Platform", *ACS Synthetic Biology*, Vol. 9, pp. 2197-2202, 2020.
2. Oh et al., "Enhanced Xylitol Production Through Simultaneous Co-utilization of Cellobiose and Xylose by Engineered *Saccharomyces Cerevisiae*", *Metabolic Engineering*, Vol 15, pp. 226-234, 2013.

Dietary Curcumin Attenuates Hepatic Cellular Senescence by Suppressing MAPK/NF-κB Signaling Pathway in Aged Mice

Da-Yeon Lee[1], Su-Jeong Lee[1], Yoo Kim[1]
[1]Department of Nutritional Sciences, Oklahoma State University, Stillwater, OK 74078, USA

I. SUMMARY
This study provides a potent anti-aging mechanism of curcumin in which gene and protein expression levels related to the hepatic cellular senescence pathway are suppressed.

II. OBJECTIVES
Aging is a time-dependent functional decline that causes cellular senescence in metabolic organs, eventually inducing age-related metabolic disorders. Curcumin (CUR), the primary curcuminoid from the spice *Curcuma longa* L. (turmeric), is well-known for its antioxidant and anti-inflammatory properties, but it is still unclear whether CUR has anti-aging properties. This study aimed to explore the role of CUR on hepatic cellular senescence in a diet-induced obesity (DIO) aged mouse model.

III. METHODS
18 to 20-month-old male C57BL/6 mice were fed a normal chow diet (NCD), an NCD with 0.4 % (w/w) CUR (NCD+CUR), a high-fat high-sugar diet (HFHSD), or an HFHSD+CUR (n = 7–9 each) for 15 weeks. To identify the differentially expressed genes (DEGs) in the liver, we used RNA-Seq based on the Gene Ontology (GO) terms and Kyoto Encyclopedia of Genes and Genomes (KEGG) pathway analysis. For validation of hepatic transcriptomic data, we conducted qPCR to analyze senescence-associated secretory phenotypes (SASPs) and immunoblotting to detect proinflammatory proteins.

IV. RESULTS

A. Curcumin alters hepatic senescence-related gene profiling
Of 157 combined senescence gene lists from GO term and KEGG pathway analysis, 75 genes showed significant changes in CUR-fed mice compared to the controls, and most of these genes were downregulated in the HFHSD+CUR group.

B. Curcumin suppresses MAPK signaling pathways in aged mice
Our results showed that CUR supplementation suppressed mitogen-activated protein kinase (MAPK) signaling cascades in the liver, particularly c-Jun N-terminal kinase (JNK) in aged mice and p38 in DIO aged mice.

C. Curcumin regulates senescence-associated inflammatory pathways in aged mice
Dietary CUR decreased the phosphorylation of nuclear factor-κB (NF-κB), a downstream transcription factor of JNK and p38,[1] and inhibited mRNA expression of proinflammatory cytokines (*Cxcl2*, *Cxcl10*, *IL-6*, *FoxO3*) and SASPs.

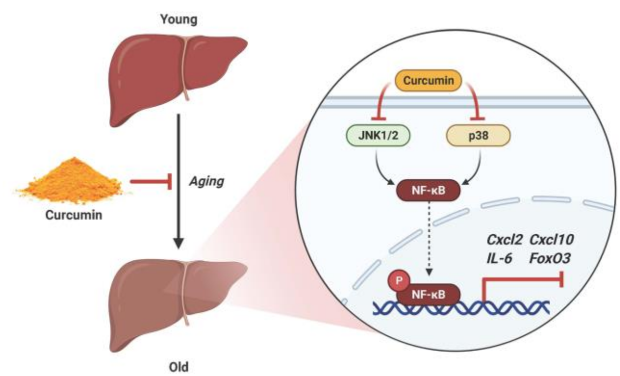

Figure 1: A schematic diagram regarding the role of curcumin in hepatic cellular senescence pathways.

ACKNOWLEDGEMENTS
This study was supported by the National Institute on Aging (NIA) Intramural Research Program (IRP) and the OTTOGI HAM TAIHO Foundation.

REFERENCES
1. Torres, J. et al. "Activation of MAPK signaling pathway and NF-κB activation in pterygium and ipsilateral pterygium-free conjunctival specimens." *Invest. Ophthalmol. Visual Sci.* Vol.52, pp. 5842-5852, 2011.

Systems Genetic Analysis of Atherosclerosis and Gut Microbiota in a Diet-induced Hyperlipidemic Diversity Outbred F1 Mouse Population

Myungsuk Kim[1,2], M. Nazmul Huda[1], Excel Que[1], Erik R. Gertz[1], Brian J. Bennett[1]
[1]Department of Nutrition, University of California, Davis, CA, USA
[2]Korea Institute of Science and Technology (KIST), Gangneung, Gangwon-do, Republic of Korea

I. BACKGROUNDS & AIMS

Atherosclerosis is a precipitating event in the development of cardiovascular disease. Recent studies report that gut microbiota contributes to the pathogenesis of cardiovascular disease, including metabolic syndrome. While host genetic variants are known factors that affect atherosclerosis development and gut microbiota composition, the mechanisms underlying genetic variations are not yet clear. Here, we interrogated atherosclerosis regulatory networks in hyperlipidemic Diversity Outbred mice to reveal key insights into control of atherosclerosis using system genetic approaches of cardio-metabolic traits, microbiome and liver transcriptome.

II. STUDY DESIGN & METHODS

We collected offspring (238 female and 234 male mice) from a cross between transgenic male C57BL/6J mice, which were made susceptible to atherosclerosis by microinjection of human apolipoprotein E-Leiden and cholesterol ester transfer protein genes, and ~200 female DO mice, a population derived from 8 inbred strains. We fed the offspring a high fat/cholesterol diet for 12 weeks. We then examined over 30 cardio-metabolic traits, fecal microbiota compositions using 16S rRNA gene sequencing, and global liver gene expression using RNA-sequencing. To elucidate the association of genetic factors and phenotype, we performed quantitative trait locus (QTL) analysis.

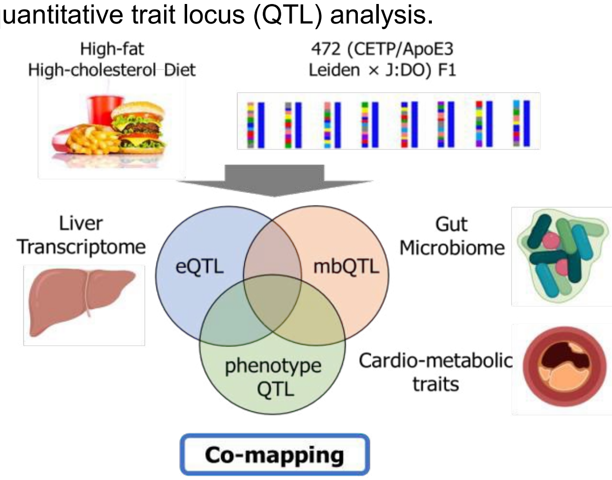

III. RESULTS

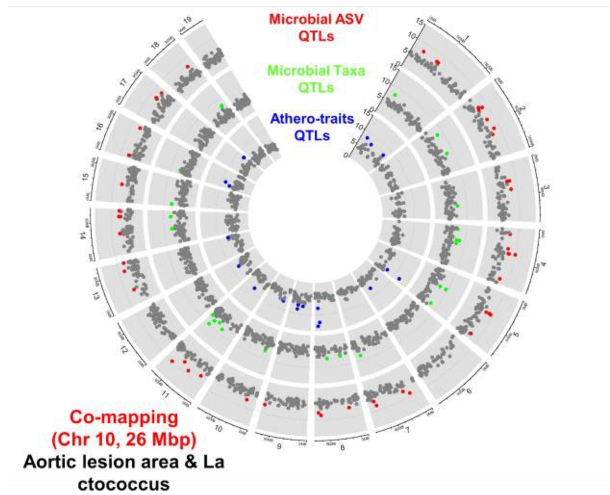

Figure 1: Circos plot showing an overview of genetic regulation of cardio-metabolic traits and microbial taxa abundance at 24 weeks. The outermost track shows the LOD profiles of microbial ASV levels on chromosomes. The middle track represents the LOD profiles of microbial taxa. The innermost track represents LOD profiles of cardio-metabolic traits.

ACKNOWLEDGEMENTS

This research was supported in part by R01HL128572 (to B. J. Bennett) and by USDA/ARS/Western Human Nutrition Research Center project funds 2032-51000-022-00D (to B. J. Bennett) and a Korea Institute of Science and Technology intramural research grant.

REFERENCES

Bennett, B.J., et al. (2015). Genetic Architecture of Atherosclerosis in Mice: A Systems Genetics Analysis of Common Inbred Strains. PLOS Genetics 11.

New insights into the role of piceatannol in cancer-associated cachexia

Kee-Hong Kim[1], Jonathan C. Kershaw[2]
[1]Department of Food Science, Purdue University, West Lafayette, IN, USA, [2]Department of Public and Allied Health, Bowling Green State University, Bowling Green, OH, USA

Cancer-associated cachexia (CAC) is a progressive metabolic disorder associated with adipose tissue and skeletal muscle wasting, thereby contributing to the devastating impact on patient quality of life. CAC is highly associated with cancers of the pancreas, esophagus, stomach, lung, and liver. Moreover, a side-effect of chemotherapy regimens is often associated with cachexia (i.e., anticancer drug-induced cachexia). A growing body of literature suggests that depletion of adipose tissue in cancer patients is an early event of CAC followed by muscle loss, and it has been attributed to an aberrant increase in adipose lipolysis. While lipolytic enzyme-catalyzed lipolysis of triglycerides in adipocytes is known to supply the body with free fatty acids in periods of high-energy demand and nutrient deficiency, cancer- and anticancer drug-induced lipolysis plays a key role, in part, in promoting energy expenditure, inflammation and tumor metastasis in the patients. This in turn weakens the treatment efficacy of the chemotherapy and compromises patients' quality of life and mortality. Despite significant efforts being given to translational research and clinical trials with cancer patients, efforts on treating CAC, and relieving chemotherapy-induced cachexia are less appreciated. This seminar will primarily focus on the biochemical investigation of the role of piceatannol, a dietary stilbene found in various fruits such as passion fruits and grape, in adipose lipolysis. The therapeutic potential of piceatannol-inhibited adipose lipolysis in CAC and anticancer drug-induced cachexia will also be discussed. Collectively, our data presented in this seminar will support the novel function of piceatannol in the treatment of cachexia induced by cancer cells and chemotherapy.

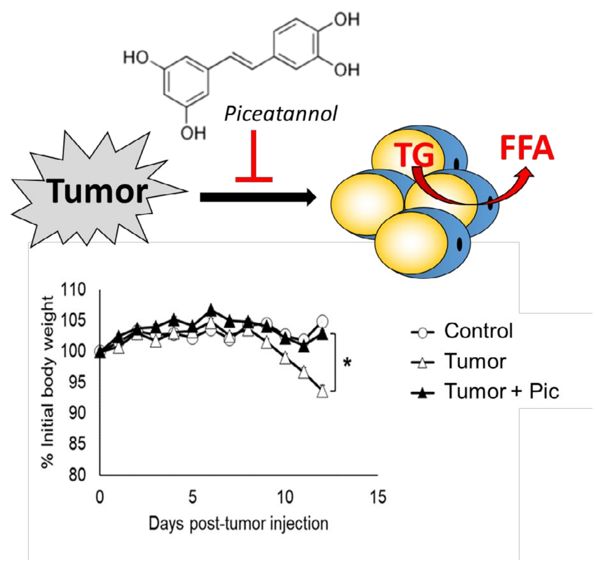

Figure 1: Piceatannol prevents cancer-associated lipolysis by inhibiting adipose lipolysis. This, in turn, protects C26 colon carcinoma-bearing mice from cancer-induced weight loss.

ACKNOWLEDGEMENTS
This study was supported, in whole or in part, by the National Institutes of Health (5R03CA184544), the Purdue University Center for Cancer Research, NIH grant (P30 CA023168) and the USDA National Institute of Food and Agriculture Hatch project (1013613) (K.-H.K.).

REFERENCE

1. Kershaw, J.C., Elzey, B.D., Guo, X, Kim, K.H. 2022, Piceatannol, a dietary polyphenol, protects adipose tissue from cancer-associated wasting via inhibiting lipolysis, *Nutrients* (doi.org/10.3390/nu14112306)

Protective Effects of Dietary Curcumin on Type 3 Diabetes

Gopal Lamichhane[1], Jing Liu[2], Su-Jeong Lee[2], Da-Yeon Lee[1] and Yoo Kim[1]
[1]Department of Nutritional Sciences, Oklahoma State University, Stillwater, OK 74078,
[2] Department of Animal and Food Sciences, Oklahoma State University, Stillwater, OK 74078

I. INTRODUCTION

Increased burden of metabolic diseases and aging population comes with an alarming incidence of Alzheimer's disease. In this study, we aim to evaluate the protective effect of curcumin, a bioactive flavonoid, in cognitive and metabolic functions, and regulation of gut microbiome using high-fat high-sugar diet (HFHSD) fed Alzheimer's disease-induced 3xTg mice and cross-interaction between brain/liver and gut microbiome.

II. MATERIALS AND METHODS

Eight months old 3xTg mice were divided into 4 groups fed with a normal chow diet (NCD) or a HFHSD alone and supplemented with curcumin and control mice were divided into 2 groups with NCD and HFHSD as dietary controls for 14 weeks. Phenotypic parameters, behavioral changes were evaluated for all groups. After 14 weeks, RNA sequencing for the hippocampus and liver was conducted to evaluate transcriptomic changes among the groups and analyzed for differential expression of gene using Kyoto Encyclopedia of Genes and Genomes (KEGG) pathway analysis and gene ontology (GO) terms. Feces samples were analyzed for 16s rRNA to investigate alteration in microbiota by curcumin supplementation.

III. Results and Discussion

HFHSD fed 3xTg mice showed higher body weight gain than HFHSD fed control mice. Curcumin supplementation in HFHSD-fed group significantly lowered body weight gain compared to non-supplemented group. For evaluating a cognitive function in the neurodegenerative mice, we performed spatial memory test using a Y-maze. We observed that HFHSD feeding aggravated cognitive dysfunction compared to NCD feeding in 3xTg mice. However, curcumin supplemented HFHSD-fed 3xTg mice attenuated memory impairment than mice fed HFHSD alone, implying curcumin prevents spatial memory loss. Transcriptomic analysis data support these results: 1) curcumin supplementation changes genes related to fatty acid metabolism, microbody, and peroxisome in the liver and 2) dietary curcumin alters calcium signaling pathway related genes in the hippocampus. Furthermore, curcumin increased microbial diversity and richness in gut of mice as represented by increased amplicon sequence variants (ASVs), Pielou's evenness index, and Shannon index in treated animals, which is also supported by weighted and unweighted UniFrac analysis. Of particular, group of Muribaculaceae, Acetatifactor, Lachnospiraceae, Ruminococcaceae and Flintibacter bacteria were increased in curcumin supplemented group compared to non-treated 3xTG mice.

Curcumin protects neurodegenerative-associated weight gain and memory impairment by altering signaling in the liver and brain combining with changing gut microbiota compositions.

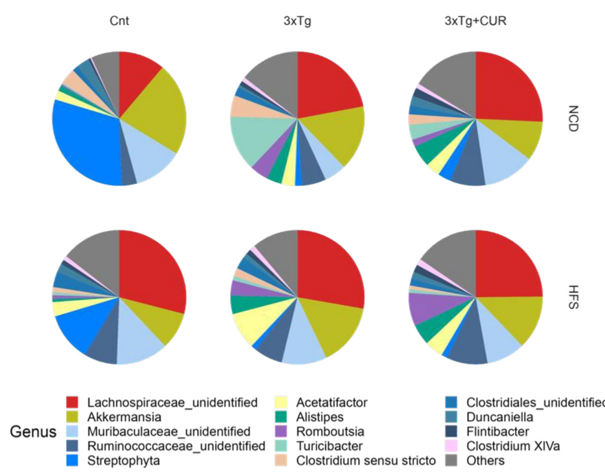

Figure: RNA sequencing analysis of liver samples

ACKNOWLEDGEMENTS

This work was supported by Oklahoma State University Research Start-up Funding (Stillwater, OK) and OTTOGI HAM TAIHO Foundation Research Funding (Seoul, South Korea).

Development of a method for risk assessment of organic pollutant exposure using monitoring data in the agricultural sector

Sang-Ik Suh[1], Hyo Sub Lee[2], Minho Son[3], Gunwoo Nam[1], Jinuk Jang[1], Seo Jin Ki[4]
[1]Department of Environmental Engineering, Gyeongsang National University, [2]Rural Development Administration (RDA), Residual Agrochemical Assessment Division, [3]Digitalplatform HQ, Podo inc., [4]Department of Environmental Engineering, Gyeongsang National University

ABSTRACT

Pesticides have become indispensable in modern agriculture; nonetheless, their application also presents probable hazards to human health and the ecosystem. Hence, it is essential to formulate proficient approaches for assessing the risks associated with the use of pesticides to determine their potential adverse impacts, This study was conducted to develop an initial hazard assessment method for agricultural organic pollutants in Korean soil and agricultural water using monitoring data. The input data used for analysis included nationwide monitoring data of 118 agricultural contaminants collected from 300 monitoring sites of orchards and soils in 2018 with pesticide properties and toxicity information collected from the Pesticide Properties Database (PPDB), which composed 12 input variables. Principal Components Analysis (PCA) was applied to extract the main components of the monitored agricultural pollutants to identify pesticides with relatively high hazardous levels in the initial screening phase. Furthermore, cluster analysis was utilized to classify the investigated pesticides into more precise categories based on their level of risk. Based on the collected data, the risk quotient (RQ) of each pesticide was calculated. Then, the total RQ of all detected pesticides at each site and the total RQ of the group of highly hazardous contaminants were separately computed. The time taken for each RQ reached below 1 was calculated to compare their relative levels of toxicity. The PCA revealed 3 principal components, which accounted for 61.2% of the total variance. From the 118 organic pollutants, 34 pesticides were identified as having relatively high environmental toxicity. Through cluster analysis, it was found that classifying into three clusters according to the relative level of environmental risk was statistically the most significant Further detailed classification of the clusters revealed that seven pesticides had the highest relative environmental risk among the 118 organic pollutants examined. Based on the RQ at Chungnam 21, it was found that the time required for the RQ of the total group of detected pesticides and the group of pollutants with high risk levels to decrease to 1 or less was the same. The findings of this study suggest that the selected pesticide risk index derived from PCA analysis and cluster analysis can be used as an initial screening model to assess the environmental risk of an area more efficiently. Moreover, it is expected to be useful for the development of a Korean future integrated risk assessment system that incorporates exposure models (such as FOCUS) and artificial intelligence algorithms with continuous monitoring data.

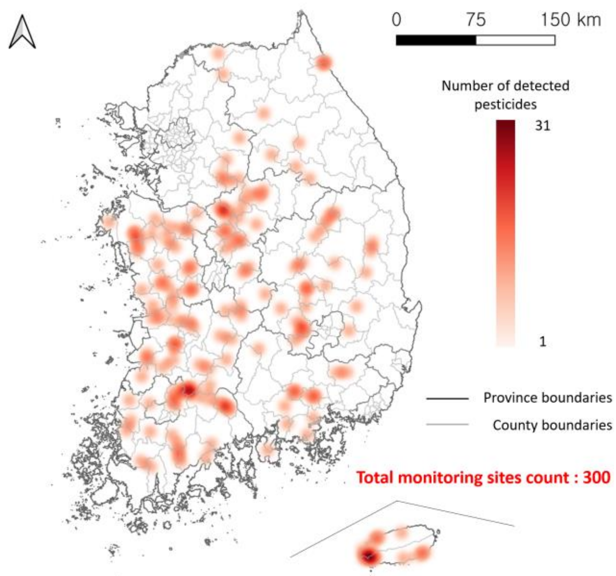

Figure 1: The total amount of residual pesticides detected in agricultural water by each monitoring site in Korea (2018).

ACKNOWLEDGEMENTS

This work was carried out with the support of "Cooperative Research Program for Agriculture Science and Technology Development (Project No. PJ015845)" Rural Development Administration, Republic of Korea.

REFERENCES

1. Weisner, O., et al., "Risk from pesticide mixtures–The gap between risk assessment and reality," *Science of The Total Environment*, Vol. 796, pp. 149017, 2021.

Autonomous Stand Counting in Field Pea using Aerial Imagery

Jeong-Hwa Kim[1], Aliasghar Bazrafkan[2], Harry Navasca[1], Mario Morales[1], Josephine Princy Johnson[1], Paulo Flores[2], and Nonoy Bandillo[1]
[1]Plant Sciences, North Dakota State University, Fargo, ND, 58108,
[2]Agricultural Biosystems Engineering, North Dakota State University, Fargo, ND, 58108

I. BACKGROUND

Early-season stand count in field pea is critical to evaluate the germination and emergence of the planted seed and can potentially alert farmers to potential issues due to planting, insects, diseases, and/or environmental factors. In addition, timely stand counting can guide farmers for any replanting decision. However, manual counting of pea seedlings is time consuming, costly, destructive, and subject to human error, which evoke the necessity to develop a robust and high-throughput phenotyping tool to better predict this complex trait under field condition.

II. HIGHLIGHTS

This study aims to develop a robust and high-throughput phenotyping platform for measuring stand count in field pea using deep leaning algorithms and unmanned aerial systems (UASs) collected data. A field-based trial with 300 genetically diverse field pea genotypes was conducted. The aerial view of each plot using red–green–blue (RGB) cameras. Aerial view of each plot was imaged using red–green–blue (RGB) cameras and the image-derived indices were compared with manually collected stand count data.

Our preliminary results show that estimated stand count had a modest positive correlation with manual stand count with Pearson's correlation coefficient (r = 0.44), and comparatively high correlation with approximate stand count and canopy height (r = 0.76 and 0.57, respectively). Further evaluation of other image-derived parameters is necessary to select indices for better prediction of stand count of field pea seedlings.

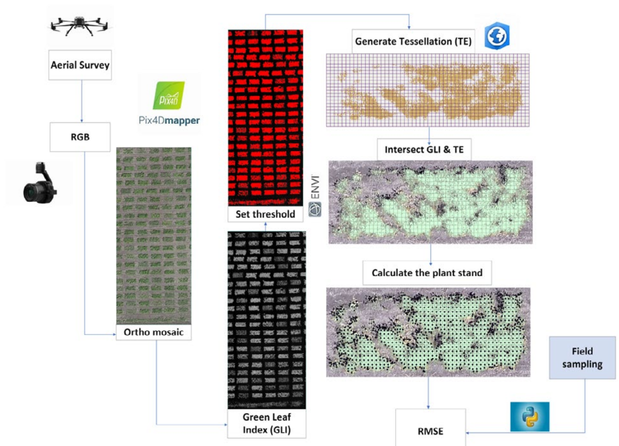

Figure 1: Workflow of image acquisition and analysis.

REFERENCES

1. Lin Z and Guo W. "Cotton stand counting from unmanned aerial system imagery using mobilenet and centernet deep learning models." *Remote Sensing*. 13(14), p.2822. 2021.
2. Moeinizade S, Pham H, Han Y, Dobbels A, and Hu G. "An applied deep learning approach for estimating soybean relative maturity from UAV imagery to aid plant breeding decisions." *Machine Learning with Applications.* 15;7:100233. 2022.
3. Nguyen GN, Norton SL, Rosewarne GM, James LE, and Slater AT. "Automated phenotyping for early vigour of field pea seedlings in controlled environment by colour imaging technology." *PLoS One.* 19;13(11):e0207788. 2018.

Effects of Berry Volatile Extracts on LPS-induced Intestinal Inflammation in a Caco-2/RAW264.7 Co-culture Model

Inah Gu[1], Cindi Brownmiller[1], Luke Howard[1], Sun-Ok Lee[1]
[1]Department of Food Science, Division of Agriculture, University of Arkansas

INTRODUCTION

Berry volatiles are responsible for the aroma of berries. However, their impacts on intestinal inflammation are unclear. Intestinal inflammation can alter gut microbiota composition, leading to gastrointestinal inflammatory diseases.

OBJECTIVES

This study investigated the impact of black raspberry, blueberry, and blackberry volatile extracts on intestinal inflammation using a co-culture model of Caco-2/RAW264.7 cells.

MATERIALS & METHODS

Caco-2 cells were seeded onto 12-well transwell apical side and fully differentiated. RAW264.7 cells were seeded onto basolateral side and co-cultured with Caco-2 cells after 24 h incubation. Berry volatile extracts with 25-fold dilution were pretreated to Caco-2 cells for 1 h, and lipopolysaccharide (LPS) was used to induce inflammation in RAW264.7 cells for 24 h. Cell culture supernatants from basolateral side were collected for analyzing the production of pro-inflammatory mediator and cytokines, such as nitric oxide (NO), interleukin-6 (IL-6), and tumor necrosis factor-α (TNF-α).

RESULTS

The results showed that LPS stimulation significantly increased the production of pro-inflammatory mediator and cytokines, NO, IL-6, and TNF-α. However, blueberry and blackberry volatile extract treatments significantly suppressed the LPS-induced overproduction of NO, IL-6, and TNF-α. Berry volatile extracts with 25-fold dilution did not affect the cell cytotoxicity of Caco-2 cells.

SUMMARY

These findings suggest that blueberry and blackberry volatiles have the potential as functional food components with gastrointestinal protective effects due to their anti-inflammatory properties.

ACKNOWLEDGEMENTS

The research was supported by the Arkansas Bioscience Institute.

REFERENCES

1. Gu, I., Brownmiller, C., Stebbins, N. B., Mauromoustakos, A., Howard, L., & Lee, S.-O, “Berry Phenolic and Volatile Extracts Inhibit Pro-Inflammatory Cytokine Secretion in LPS-Stimulated RAW264.7 Cells through Suppression of NF-κB Signaling Pathway,” *Antioxidants*, *9*(9), Article 9, 2020.

System Dynamics Model for Autonomous and Controlled Environment Potato Production System

Jae Ryu[1], Zarin Subah[2] Jeonghyun Baek[3]

[1]Associate Professor of Water Resources Engineering, University of Idaho; [2]Dept. of Agricultural Engineering, National Institute of Agricultural Sciences, RDA, Jeonju 54875, Korea;[3]Graduate Research Assistant, College of Natural Resources, University of Idaho

I. INTRODUCTION

Smart farming using technology-monitored controlled environment agriculture (CEA) has recently evolved to optimize crop growth while minimizing land use and environmental impacts, especially for climate-threatened regions. This study focuses on the development of an autonomous and small-scale CEA using system dynamics modeling to provide alternative food resources in a changing climate. The designed CEA is equipped with Internet of Things (IoT) to monitor the physiological parameters, including (pH, electric conductivity (EC), PH, and water temperature) (WT) associated with plant growth. Two varieties of tomato (Solanum lycopersicum) plants were used in this study with using two nutrients input (with N-P-K ratios of 2-1-6 and 5-5-5) to assess the nutrient application impact on the plants. Repeated measure analysis was conducted to investigate the effects of the environmental factors in response to changing plant nutrients. Based on the analysis, the proposed CEA was simulated and improved using a system dynamics (SD) approach by exploring managing the optimum ranges of the environmental factors.

II. SYSTEM DESIGN AND OPERATION

The experiment was conducted in a controlled environment hydroponic set-up at the facility of the University of Idaho, Boise, US (43°36'32.2"N 116°11'37.8" W). An autonomous and economically feasible hydroponic system was designed for sustainable tomato production. Two types of tomato (Solanum lycopersicum) plants used in this experiment: regular-size cherry tomato (CT: heirloom indeterminate), and dwarf-size traditional tomato (DT: heirloom determinate). Non-genetically modified organism (Non-GMO) and certified seeds of the two tomato plants were sown in rock wool grow plugs for germination and transplanted to the CEA system later. Basically, seeds were sown in a 25-millimeter (mm) width, 25 mm length, and 25 mm height grow plugs where each grow plug contains 3 seeds. The grow plugs were placed in a plastic dome of 508 mm length, 245 mm width, and 177 mm height. The dome was placed on a heat mat and T5 fluorescent grow light was provided to facilitate germination processes. The amount of water provided for seed germination is about 2 liters with no nutrients added to the system. The seeds were sown on July 27, 2022, for cherry tomato (CT: heirloom indeterminate) plants and on September 27, 2022, for dwarf-size traditional tomato (DT: heirloom determinate) plants. Seedlings were noticed to emerge on July 29, 2022, for CT and September 30, 2022, for DT and were ready to be transplanted within 7 days.

quired.

III. RESULTS & DISCUSSION

The result shows that different nutrient compositions have a significant effect on both pH and WT ($p < 0.001$) as opposed to EC. Since EC, pH, and WT were found to be close to the optimum value with the 5-5-5 nutrient, the study indicates that the proposed autonomous CEA would be a promising solution for high tomato yield. Based on the preliminary result, the SD model performs well to evaluate aquaponic simulations by maintaining the optimum value of the environmental factors, including water levels. We anticipate that the proposed CEA system will be widely adapted to promote urban indoor agriculture in a changing climate, ultimately contributing to a space farming initiative administrated by the National Aeronautics and Space Administration (NASA) in years to come.

Acknowledgements: This work was carried out with the support of “Cooperative Research Program for Agriculture Science and Technology Development (Project No. PJ015553)” Rural Development Administration, Republic of Korea. Jae Ryu is also supported partially by the National of Food and Agriculture, United States Department of Agriculture, under ID01654. Any opinions, findings, conclusions or recommendations expressed in this publication are those of the authors and do not necessarily reflect the view of the United States Department of Agriculture.

Technical Group B-3 / C-1

Biological and Biomedical Sciences (Biology, Molecular Biology, Cognitive Science, Botany, Zoology, Biomechanics, etc.) / Bioengineering and Biomedical Engineering (BME)

Progress and Trends in Artificial Intelligence for Colonoscopy

Dongheon Lee[1,2]

[1]Department of Biomedical Engineering, College of Medicine, Chungnam National University

[2] Department of Biomedical Engineering, College of Medicine, Chungnam National University Hospital

I. Introduction

In this paper, we aim to introduce the research trends on how the application of AI in the field of colonoscopy has evolved, mainly through three applications. We also wish to discuss how AI will develop and be applied in the future.

II. Computer-aided Diagnosis for Colonoscopy

A. Endoscopist vs AI-assisted Endoscopist[1]

We developed CNN for evaluation of NBIs of diminutive colorectal polyps, based on ENAS. We trained the CNN using images from 1,100 adenomatous polyps and 1,050 hyperplastic polyps from 1,379 patients, and then tested on 300 images of polyps. We compared the accuracy of 22 endoscopists of different skill levels vs the CNN in evaluation of images. The endoscopists then evaluated the polyp images with knowledge of the CNN-processed results.

As a result, the CNN distinguished diminutive polyps with 86.7% accuracy, and endoscopists distinguished diminutive polyps with 82.5% overall accuracy (novices, 73.8%; experts, 83.8%; and NBI-trained experts, 87.6%). With knowledge of the CNN-processed results, the accuracy of novice endoscopists increased to 85.6% (P < .05).

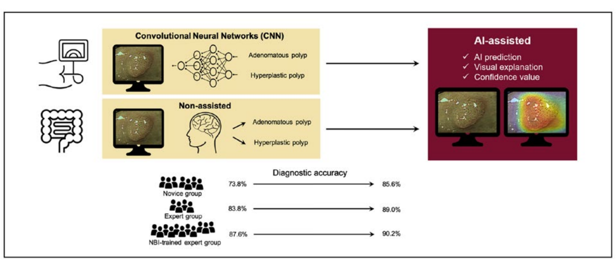

Figure 1. Overview of optical diagnosis of colorectal polyps using convolutional neural networks with visual explanations

B. Endoscopist vs AI-assisted (with uncertainty quantification) Endoscopist

Expanding upon the first study, we conducted research to validate uncertain polyp cases across multiple institutions using a type of bayesian deep learning method known as MC-dropout.

II. 3D Map Generation for Colonoscopy

Colonoscopic 3D map generation using monocular colonoscopy has emerged as a novel algorithm that transforms 2D colonoscopic images into a 3D map. The proposed algorithm consists of two steps: uninformative frame classification and deep visual SLAM. In the first step, to generate a continuous 3D map, non-informative frames, which are blurry or occluded by bubbles and other factors, are filtered out using a classification algorithm. In the second step, a MonoDepth2-based deep visual SLAM is trained through self-supervised depth and pose estimation using colonoscopic images.

III. Virtual Colonoscopy Simulator

For the effective delivery of endoscopic education, it is imperative to create naturalistic virtual images of colonoscopy. The VR-Caps simulator[2], although superior in quality to existing educational simulators, falls short in depicting consistent color and texture. The study proposed herein seeks to overcome these limitations by employing generative models to create high-resolution texture maps that reflect the anatomical characteristics of various colon segments, thereby enhancing the educational efficacy of the tool.

ACKNOWLEDGEMENTS

This work was supported by the National Research Foundation of Korea Grant funded by the Korean Government(NRF-2022M3J6A1084843).

REFERENCES

1. Jin, Eun Hyo, et al. "Improved accuracy in optical diagnosis of colorectal polyps using convolutional neural networks with visual explanations." *Gastroenterology* 158.8 (2020): 2169-2179.
2. İncetan, Kağan, et al. "VR-Caps: a virtual environment for capsule endoscopy." *Medical image analysis* 70 (2021): 101990.

Multimodal Interfaces for Immersive Virtual Reality

Jin Ryong Kim
The University of Texas at Dallas

I. SUMMARY

Humans perceive the world through multiple modalities, including the basic senses of sight, hearing, smell, taste, and touch. For example, a person in a coffee shop can see nearby people, hear the ambient noise in that setting, smell the coffee in their cup, and feel its warmth while holding it. These modalities work together to provide them with a rich and reliable sense of their surroundings. A multimodal human-computer interface is a user interface that offers different types of sensory stimuli at the same time (e.g., visual, auditory, haptic, olfactory, etc.). Multimodal interfaces are necessary to support multi-sensory experiences, which can benefit usability and user experience. They can lead to more “natural” interaction with digital environments, providing multiple types of sensory information similar to what we perceive when interacting with physical environments. It is challenging to create high-quality multimodal interfaces: This requires an in-depth understanding of human perception and device output capabilities and how these can be combined to make interactions with a convincing multi-sensory experience. In this talk, I will discuss how I have designed and engineered interactive multimodal interfaces and how they could impact the user experience by delivering multi-sensory experiences in an immersive virtual reality. I will also introduce MetaTwin, a collaborative Metaverse platform that supports one-to-one spatiotemporal synchrony between physical and virtual spaces, and how multimodal interfaces and platforms can play a significant role in medical applications.

II. MetaTwin Platform

MetaTwin is a collaborative Metaverse platform that supports one-to-one spatiotemporal synchrony between physical and virtual spaces. The users can interact with other users and surrounding IoT devices without being tied to physical spaces.

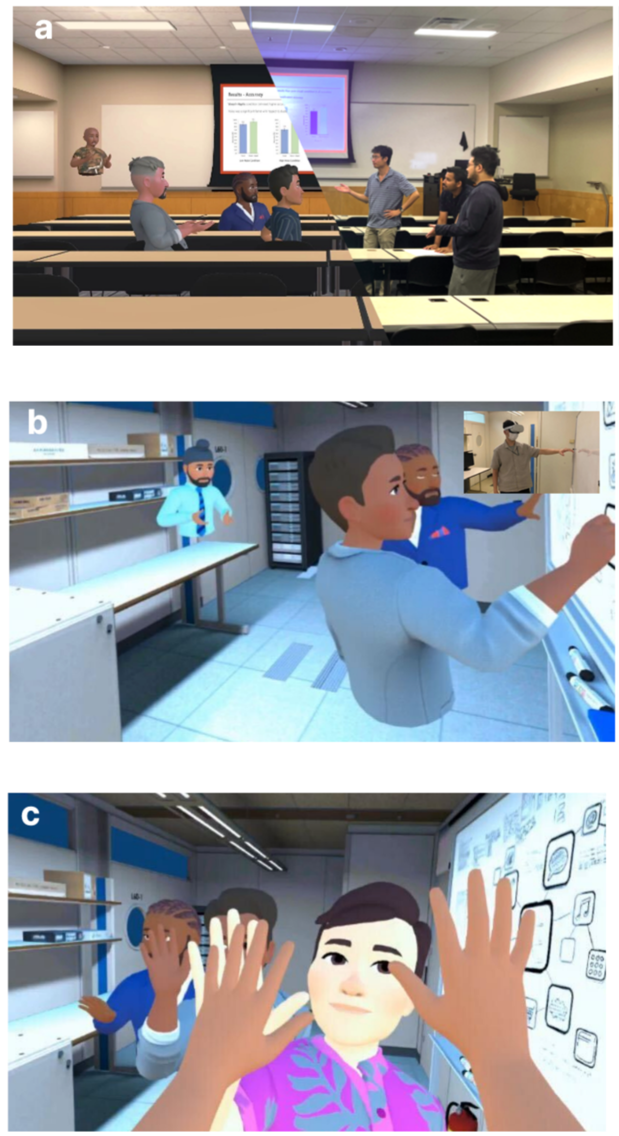

Figure 1: Metaverse Platform

Image-based Deep Survival Learning Model for Risk Stratification of Cardiovascular Disease using Retinal Fundus Image

Jooyoung Chang[1,2], Sang Min Park[1,2]

[1] Seoul National University [2]XAIMED Co. Ltd.

I. SUMMARY

Previously, deep learning(DL)-based retinal fundus image (RFI) cardiovascular disease (CVD) biomarkers have been developed by training models to predict coronary artery score, atherosclerosis, and other CVD biomarkers. In this work, we develop an RFI-based CVD biomarker by training a DL model to predict CVD events using a technique known as deep survival modelling. We validate the risk stratification ability of the resulting deep survival learning-based funduscopic cardiovascular disease incidence score (DL-FCVD) using a retrospective cohort.

II. METHODS

Using data from health examinees at Seoul National University Hospital – Health Promotion Center between 2004 and 2016, we constructed a retrospective cohort with non-mydriatic RFIs and follow up data of incident CVD events. A deep survival model was trained on 16,666 patients and validated using 11,100 patients. The resulting DL-based biomarker was used as an independent variable in a Cox Proportional Hazards model adjusting for Framingham Risk Score (FRS) and other CVD-related covariates.

III. FINDINGS

The cohort of 11,050 patients were followed between 2004 and 2017, for a total of 7·33x104 person-years resulting in 2,315 CVD events during a median follow-up of 6·41 years. After adjusting for age, sex, HDL, TC, SBP, smoking status, BMI, drinking habit, exercise frequency, diabetes, hypertension, and dyslipidemia, high DL-FCVD patients had significantly higher risk of CVD (HR, 95% CI; 2·62, 2·11-3·26) compared to low DL-FCVD.

IV. INTERPRETATION

DL-FCVD was developed using CVD event data and retinal fundus images using deep survival modelling. It improves CVD risk stratification beyond FRS. DL-FCVD may serve as a non-invasive diagnostic biomarker for risk stratification of CVD.

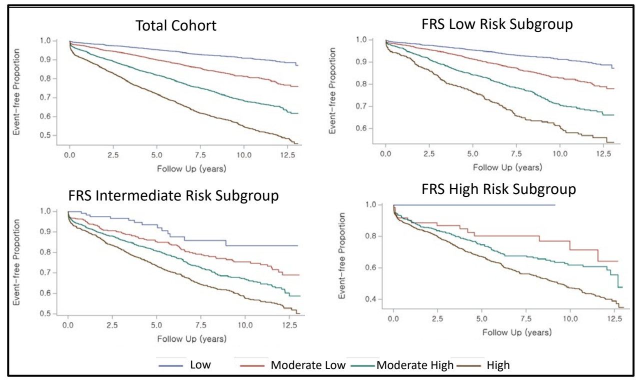

Figure 1: Survival Curves of Participants by DL-FCVD Groups among Total Cohort and Framingham Risk Score Risk Groups

Table 1: Association of DL-FCVD and CVD Incidence among health screening participants

	DL-FCVD Groups				
	Low	Moderate Low	Moderate High	High	p-trend
DL-FCVD	0·00-0·17	0·17-0·39	0·39-0·63	0·63-0·96	
Participants	2765	2766	2762	2757	
Cases	196	408	687	1024	
F/U 10^4PY	2·03	1·93	1·78	1·60	
Unadjusted	1·00 (Ref)	2·18 (1·84-2·59)	3·95 (3·37-4·63)	6·48 (5·56-7·55)	<0·001
Adjusted	1·00 (Ref)	1·57 (1·31-1·88)	2·22 (1·84-2·67)	2·62 (2·11-3·26)	<0·001

ACKNOWLEDGEMENTS

JC was supported by a grant of the Korea Health Technology R&D Project through the Korea Health Industry Development Institute (KHIDI), funded by the Ministry of Health & Welfare, Republic of Korea.

REFERENCES

1. D'Agostino RB, Russell MW, Huse DM, et al. Primary and subsequent coronary risk appraisal: New results from the Framingham study. American Heart Journal 2000; 139(2, Part 1): 272-81.
2. Chang J, Ko A, Park SM, et al. Association of Cardiovascular Mortality and Deep Learning-Funduscopic Atherosclerosis Score derived from Retinal Fundus Images. *American Journal of Ophthalmology* 2020; **217**: 121-30.

Machine Learning of Colors for mHealth Applications

Young L. Kim
Weldon School of Biomedical Engineering, Purdue University, West Lafayette, IN 47907, USA
Centers for Disease Control and Prevention, Atlanta, GA 30333, USA

I. Introduction

A photograph is more than merely a picture and contains detailed spectral information that can be used for digital diagnostic applications. Hyperspectral learning enables the recovery of high-resolution spectra from three RGB color values acquired by the built-in camera; a detailed full spectrum in the visible range of light is mathematically reconstructed from a red-green-blue (RGB) image. Several research communities (e.g., color science and digital imaging) deal with this an ill-posed problem using different, but related methods (e.g., sparse regularization, compressive sensing, machine learning, and deep learning). Our lab is one of the first groups to combine spectral learning with spectroscopic analyses of diagnostic applications. Importantly, this mHealth technology approach can eliminate the need for expensive optical components (e.g., spectrometer and bulky optical filter) that are commonly used in conventional hyperspectral imaging systems and spectrometers. We have all seen numerous mHealth sensing applications that require additional accessories and bulky components. Simply put, no additional hardware components are necessary for spectral learning.

II. Diagnostic applications of spectral learning

Spectral learning exploits the idea that a photograph is more than merely a picture and contains detailed diagnostic information. To overcome limitations of purely driven machine learning, the domain knowledge about tissue optics and machine vision are further incorporated into learning algorithms to ease the requirement of a large training dataset. We will discuss clinical applications with a focus of hemodynamic parameters, such as blood hemoglobin content and oxygen saturation, for several different diseases and disorders. We will also share our ongoing mHealth research in sub-Saharan Africa including Kenya and Rwanda. This approach has reciprocal innovation, allowing mHealth technologies developed in the resource-limited settings to be brought back to the US, as demonstrated in our mHealth surveillance study with Centers for Disease Control and Prevention.

III. Outlook

The COVID-19 pandemic has made clear that mHealth can be used to identify where there is illness in the community, to protect people from potential exposure, and to prevent our healthcare systems from potential collapse. We have all seen numerous mHealth sensing applications that require additional accessories and bulky components as a mandatory attachment to the smartphone. Now taking advantage of the onboard cameras, mHealth can offer novel ways to diagnose, track and trace diseases, improve treatments, and generate important health data. mHealth can potentially improve healthcare at a patient level as well a population level. Machine learning and big data approaches can increase patients' access to POC testing, aiding in treatment, and improving surveillance. Overall, machine learning powered mHealth technologies of spectral learning can potentially offer mobility, simplicity, and affordability for rapid and scalable adaptation in a variety of digital health applications, including telemedicine.

REFERENCES

PNAS Nexus, 2:pgad111, 2023, ACS Central Science 8:513, 2022, Advanced Functional Materials 32:2112479, 2022, Nature Communications 13:247, 2022, Nano Letters 21:921, 2021, 2020, Optica 7:563, 2020, Nature Communications 11:328, 2020, Annual Review of Biomedical Engineering 22:79, 2020, ACS Photonics 5:881, 2018, Nature Communications 9:452, 2018, Advanced Science 5:1700863, 2018.

Assessing the generalization of graph neural networks

Kijung Yoon[1]
[1]Hanyang University, Seoul, Korea

I. Abstract

Graph neural networks (GNNs) have become compelling models designed to perform learning and inference on graph-structured data. However, little work has been done to understand the fundamental limitations of GNNs for scaling to larger graphs and generalizing to out-of- distribution (OOD) inputs. In this paper, we use a random graph generator to systematically investigate how the graph size and structural properties affect the predictive performance of GNNs. We present specific evidence that the average node degree is a key feature in determining whether GNNs can generalize to unseen graphs, and that the use of multiple node update functions can improve the generalization performance of GNNs when dealing with graphs of multimodal degree distributions. Accordingly, we propose a multi-module GNN framework that allows the network to adapt flexibly to new graphs by generalizing a single canonical nonlinear transformation over aggregated inputs. Our results show that the multi-module GNNs improve the OOD generalization on a variety of inference tasks in the direction of diverse structural features.

II. Introduction

Graph neural networks (GNNs) have recently been established as an effective machine learning models for representation learning on graph-structured data. Graph is a powerful mathematical abstraction that can represent the structure of many complex data, and learning on graphs has been widely explored in many scientific domains.

Despite the growing empirical success of GNNs in various fields, the necessity of a deeper understanding of this model framework has arisen due to the inconsistent model efficiency across different tasks and experimental settings. Building large-scale graph benchmarks is one recent attempt to address this challenge, and there have also been significant theoretical studies on the expressivity of GNNs focused on the isomorphism task. However, little work has been conducted on understanding the fundamental limitations of GNNs for adapting to distribution shifts on graphs, where systematic differences between training and test data can significantly degrade model performance.

Recent approaches to OOD generalization concentrate primarily on images or structural equation models. However, the nature of the graph domain is fundamentally different from these works in that the inputs are not simple image features or variables, but full of complex irregularities and connectivity in topology. We hypothesize that the difference in underlying graph properties of training and testing datasets (i.e. structural distribution shift) presents a fundamental challenge to the extrapolation beyond the range of input distribution. We are particularly interested in the conditions under which we can expect GNNs to (not) perform well in predicting targets for unseen graphs. To study this question, we use a random graph generator that allows us to systematically investigate how the graph size and structural properties affect the predictive performance of GNNs.

III. Contributions

We argue that, among the many graph properties, the average node degree within each mode of the degree distribution is a key factor that determine whether GNNs can generalize to unseen graphs. Then, we propose and explore methods for using multiple node update functions as a way to generalize a single canonical nonlinear transformation over aggregated inputs. This approach enhances the flexibility of the network to handle shifts in graph properties, resulting in better control over structural distribution shifts. We evaluate the performance of the multi-module GNN framework on the task of approximating marginal inference for general graphs, solving graph theory multi-task problems, conducting CLRS algorithmic reasoning tasks, and benchmarking against OOD scenarios for real-world graphs.

ISOTROPIC CELLULAR RESOLUTION ACROSS CENTIMETER FIELD OF VIEW USING SUBVOXEL AXIALLY SWEEPING LIGHT SHEET MICROSCOPY (SV-ASLSM)

Juhyun Lee[1]
[1]Department of Bioengineering, The University of Texas at Arlington, Arlington, TX

<u>Introduction</u>: Light sheet microscopy (LSM) has emerged a prominent optical sectioning modality, due to millimeter penetration depth and ability to tune optical section thickness from single to several microns(>20um). However, LSM resolution and imaging Field-of-View (FOV) is dependent on the numerical aperture (NA) of the objective lens (OL) used for producing the light section[1]. Axially sweeping light sheet microscopy (AS-LSM), provides promising avenues for decoupling dependance of NA on FOV[1]. Original AS-SLM methods sweep the focus spot longitudinally across the sample, by beam refocusing via mechanical actuators and a rolling shutter (RS) camera pixel strategy for capturing extended FOV**.** However, a puzzling conundrum of choosing an appropriate NA without sacrificing resolution is still encountered. To address the resolution constraint, we propose a new generation of AS-LSM utilizing maximum likelihood estimation (MLE) based LSM[1], by off-axis sample detection with respect to beam propagation axis to improve voxel density and enable in silico resolution enhancement.

<u>Materials and Methods</u>: A Voice Coil Actuator (VCA) was used to offset the optical section at detection objective lens [2]. A cylindrical lens was used to focus 1D light sheet into a high working distance (WD) objective. Furthermore, we have designed a tilted scan stage for SV-LSM. The off axis scanned raw volume is split into multiple sub-stacks, that are treated as low-resolution (LR) volumes containing redundant information due to significant image overlap produced by oblique scan. Using MLE, LR stacks are modelled as probability distributions with subtle spatial correlations and furthermore, a cost function based on image degradation operators is minimized to produce a high-resolution estimate from LR image volumes[1].

<u>Results and Discussion</u>

Using AS-LSM, we extended the imaging FOV from 700 um **(Figure 1A)** to 1400 um by axially sweeping the light sheet beam waist using a remote refocusing actuator **(Figure 1B)**, enabling arbitrary FOV tuning (micron-centimeter) independent of NA. Furthermore, we quantified 5 um fluorescent bead resolution **(Figures 1C-D)** as 16 um laterally **(Figure 1G)** and 19 um axially **(Figure 1H)** using 1x air detection lens. Using SV-LSM **(Figures 1E-F)**, we improved lateral resolution 1.45x to 10 um **(Figure 1I)** and axial resolution 1.65x to 11 um **(Figure 1J)** *in silico,* using 1x detection and 4x excitation OL's. Consequently, MLE-based SV-LSM intrinsically improves 3D voxel density due to oblique sample scan, regardless of low lens NA.

<u>Conclusion:</u> We hypothesize integration of SV-LSM and AS-LSM can be used fully decouple dependance of resolution and confocal region on NA, and thereby enable isotropic cellular resolution using centimeter WD OL's.

<u>References</u>

[1] T. Teranikar, *et.al.*, "Development of Planar Illumination Strategies for Solving Mysteries in the Sub-Cellular Realm," *International Journal of Molecular Sciences*, vol. 23, no. 3, 2022, doi: 10.3390/ijms23031643.
[2] T. Chakraborty *et al.*, "Light-sheet microscopy of cleared tissues with isotropic, subcellular resolution," *Nature Methods*, vol. 16, no. 11, pp. 1109–1113, Nov. 2019, doi: 10.1038/s41592-019-0615-4.

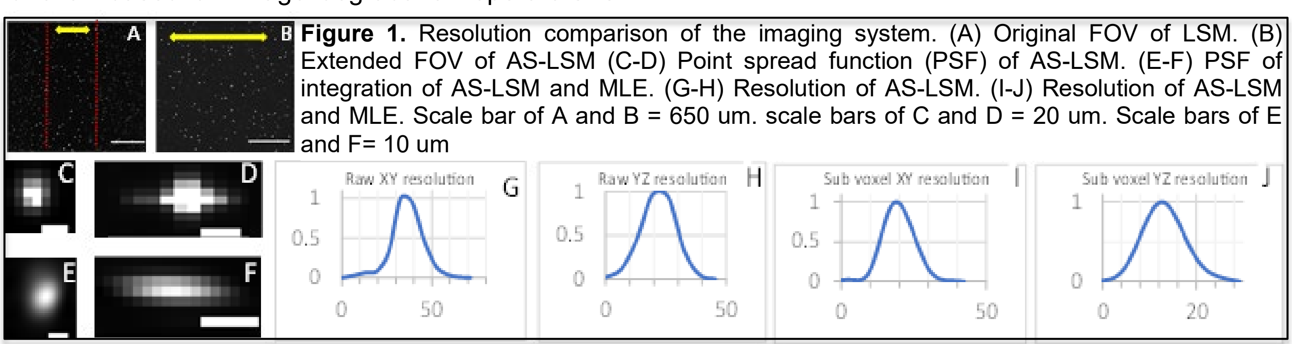

Figure 1. Resolution comparison of the imaging system. (A) Original FOV of LSM. (B) Extended FOV of AS-LSM (C-D) Point spread function (PSF) of AS-LSM. (E-F) PSF of integration of AS-LSM and MLE. (G-H) Resolution of AS-LSM. (I-J) Resolution of AS-LSM and MLE. Scale bar of A and B = 650 um. scale bars of C and D = 20 um. Scale bars of E and F= 10 um

Analysis of GAN Artifacts in Breast Screening Mammogram Simulation

Juhun Lee[1, 2]
[1]Department of Radiology, University of Pittsburgh, PA, USA, [2]Department of Bioengineering, University of `Pittsburgh, PA, USA

The number of developments and publications using Generative Models, such as Generative Adversarial Networks (GANs), is exponentially increasing every year. GAN models are now being used to solve various medical imaging tasks, primarily to augment the number of trainable images for deep network algorithms. The basic assumption of using GAN for augmentation is that it creates plausible-looking images. While this is generally true, it is well-known that GAN can create both visually apparent and subtle artifacts in the generated images. Depending on the task, such artifacts could result in negative impacts, such as false positive or even false negative detection of diseases. To minimize these negative impacts for various medical imaging tasks, it is important to define, categorize, and analyze GAN artifacts for medical image simulation. In this study, we focused on the GAN artifacts in breast screening mammogram simulation.

We adopted a conditional GAN (CGAN) or pix2pix [1] model to train a GAN that generates a mammogram with a normal appearance using the opposite mammogram as guidance [2]. We used screening mammograms of 1366 women with normal/healthy breasts to train the CGAN for mammogram simulation. Then, we tested the trained CGAN on an independent cancer dataset with 333 women with dense breasts (97 cancer cases).

We visually inspected the mammogram simulations generated by the trained CGAN to identify the artifacts present in the resulting simulations. We then defined different types of artifacts based on their possible reasons.

We found artifacts in the texture and shape of the simulated breast mammogram. Texture artifacts were similar to checkerboard artifacts that can be seen in GAN artifacts in natural scene simulations. Shape artifacts included deviations from the natural appearance of the simulation. We observed breast nipple artifacts as one type of shape artifact in the simulated mammograms. Texture artifacts, like checkerboard artifacts, appeared more frequently than shape artifacts.

We concluded that artifacts exist in mammogram simulation. As they look different from what we expect to observe in real mammograms, anyone who wants to use GAN to augment the mammogram dataset for training deep algorithms to analyze breast mammograms needs to understand the existence of artifacts and consider ways to minimize the possible negative impacts of these artifacts.

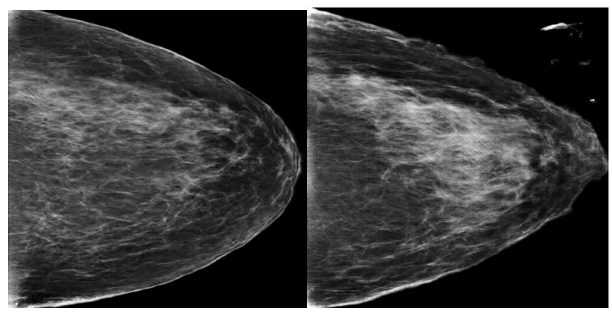

Figure 1. The CGAN simulated mammogram without artifacts (left) and with texture and shape artifacts (right)

ACKNOWLEDGEMENTS
This study has been supported in part by grants from the National Institutes of Health R37-CA248207. The author thanks Nvidia for providing a GPU for this research.

REFERENCES

1. P. Isola, J.-Y. Zhu, T. Zhou, *et al.*, "Image-to-image translation with conditional adversarial networks," in *Proceedings of the IEEE conference on computer vision and pattern recognition*, 1125–1134 (2017).
2. J. Lee and R. M. Nishikawa, "Identifying women with mammographically-occult breast cancer leveraging GAN-simulated mammograms," IEEE Transactions on Medical Imaging 41(1), 225–236 (2021).

Ultra-sensitive Silicon Photonic Opto-mechanical Ultrasound Sensor for Biomedical Photoacoustic Imaging: Proof-of-concept study

Jaesok Yu[1], Sangyoon Han[1]
[1]Department of Robotics Engineering, DGIST, 42988, South Korea

I. SUMMARY
The study proposes a new silicon photonic-based ultrasonic sensor with a thin membrane structure, allowing for easy fabrication. Compared to previous techniques, which used a 2 μm-thick membrane defined by wafer bonding, our approach utilizes lithography and etching, providing a broader design space. As a proof of concept, we successfully created a sensor with a 70 nm-thick membrane, resonating at 6.5 MHz, and demonstrating a sensitivity of 0.41μV/Pa and a fractional bandwidth of 62%.

II. MAIN BODY
A. Introduction
Optical ultrasound sensors have gained attention for their superior sensitivity and bandwidth compared to traditional piezoelectric ultrasound sensors [1-2]. However, integrating them into an array has been a major challenge. Photonics integrated circuits (PICs) offer a promising solution by fabricating large-scale optical systems on a single tiny silicon chip. Thus, a PICs-based acoustic sensor is a great candidate for high-performance photoacoustic imaging.

B. Methods
The sensor consisted of a bus waveguide, an optical ring resonator, and an acoustically sensitive membrane acting as an optical phase shifter. The mechanical resonance frequency shift of the ring resonator was detected when the acoustically sensitive membrane vibrated transversely. The Lorentzian resonance of the sensor was modulated by the acoustic pressure, resulting in a change in optical intensity transmitted through the bus waveguide. The sensor design, based on CMOS technology, allowed for an ultra-thin 70 nm membrane. This thickness was significantly thinner than previous reports using wafer-bonded acousto-optic membranes [3]. The sensor was evaluated immersion condition.

C. Results & Discussion
Fig. (e) shows the measured optical intensity, indicating the sensed acoustic pressure, and Fig. (f) shows the corresponding frequency spectrum of the measured signal. The sensor sensitivity and fractional bandwidth are 0.41 μV/Pa and 62%, respectively. The center frequency is 6.5 MHz, with the bandwidth at 3 dB of 3.1 MHz while the fractional bandwidth of the acoustic source is limited to 52%.

III. ILLUSTRATIONS

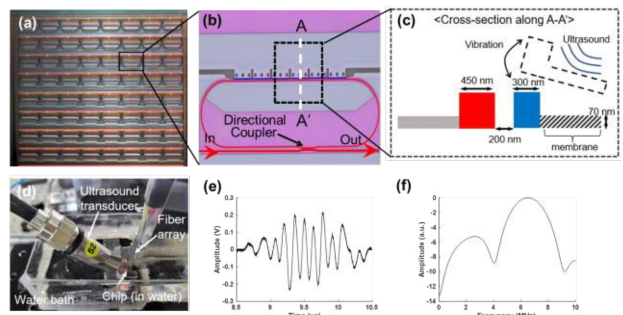

Fig. (a) Optical microscopic image of the sensor array, (b) Single cell structure **(c)** Cross -section along A-A' in (b), **(d)** Experimental setup, **(e)** Measured time-domain received signal of the sensor, **(f)** Frequency spectrum of the received signal

ACKNOWLEDGEMENTS
This work was supported by Samsung Research Funding & Incubation Center of Samsung Electronics under Project Number SRFC-IT2102-02.

REFERENCES
1. Dong B, Sun C, Li H, Zhang HF, Shu X. Quantifying melanin concentration in retinal pigment epithelium using broadband photoacoustic microscopy. Biomed Opt Express, Vol 8, Issue 6, pp 2851-2865. 2017;8(6):2851-2865. doi:10.1364/BOE.8.002851
2. Kim KH, Luo W, Zhang C, et al. Air-coupled ultrasound detection using capillary-based optical ring resonators. Sci Reports 2017 71. 2017;7(1):1-11. doi:10.1038/s41598-017-00134-7
3. Westerveld WJ, Mahmud-Ul-Hasan M, Shnaiderman R, et al. Sensitive, small, broadband and scalable optomechanical ultrasound sensor in silicon photonics. Nat Photonics 2021 155. 2021;15(5):341-345. doi:10.1038/s41566-021-00776-0

Smart Contact Lenses for Glaucoma Care

Chi Hwan Lee[1,2,3]
[1]Weldon School of Biomedical Engineering, [2]School of Mechanical Engineering, [3]School of Materials Engineering, Purdue University, West Lafayette, IN 47907 USA

I. INTRODUCTION

The continuous monitoring of intraocular pressure, especially during sleep, presents a significant challenge in the management of glaucoma. In this study, we introduce a novel category of smart soft contact lenses that enable uninterrupted monitoring of intraocular pressure for 24 hours, including during sleep. Importantly, these smart soft contact lenses are developed using existing commercial brands of soft contact lenses, without modifying their inherent properties such as lens power, biocompatibility, softness, transparency, wettability, oxygen transmissibility, and suitability for overnight wear. Our research demonstrates that these smart soft contact lenses can seamlessly adapt to various corneal curvatures and thicknesses in human eyes, enabling accurate measurements of absolute intraocular pressure in real-life conditions. To validate their performance, we conducted comprehensive in vivo evaluations using rabbit, dog, and human eyes, encompassing individuals with normal eye conditions as well as those with hypertension. The results confirmed the superior measurement accuracy, within-subject repeatability, and user comfort of the smart soft contact lenses, surpassing the capabilities of existing wearable ocular tonometers. Based on these findings, we anticipate that the implementation of smart soft contact lenses will significantly enhance glaucoma care by providing effective and reliable monitoring of intraocular pressure.

II. APPROAH

A. Device Design and Production

Our objective is to develop smart soft contact lenses capable of monitoring intraocular pressure for individuals with glaucoma or those at risk of developing it. The lenses are designed with a focus on enhancing comfort and usability in comparison to existing devices available in the market. To achieve this, we employed soft materials that are safe for human use to construct a ring-shaped wireless IOP sensor, which could be seamlessly integrated with commercially available contact lenses. To ensure the reliability and longevity of our lenses, we conducted extensive testing. Enucleated pig eyes, which closely resemble human eyes, were utilized to evaluate the wireless sensing capabilities of our lenses. These experiments provided valuable insights into the performance of our sensors in a realistic environment.

B. Clinical Studies in Human Eyes

We initiated pilot clinical tests involving healthy adult contact lens users to assess the comfort and effectiveness of our lenses. Throughout this process, we actively sought feedback from both users and clinicians, aiming to ensure that our lenses met their requirements and were user-friendly. The evaluation encompassed various key areas, including biosafety, user comfort, lens fit, visual field, overnight wearability, ease-of-use, and measurement accuracy of our scleral lenses in an ambulatory setting. To establish a comprehensive benchmark, the findings were compared with data obtained from existing ocular tonometers. Through this comparison, we sought to assess the performance of our lenses and identify potential areas for improvement. Throughout the process, valuable feedback was gathered from both end-users and clinicians, enabling us to refine and optimize the design of our scleral lenses.

III. ILLUSTRATIONS

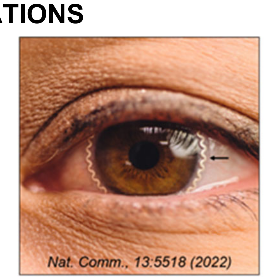

Figure 1: Smart soft contact lens in a human eye designed for continuous monitoring of glaucoma.

ACKNOWLEDGEMENTS

This work is published in *Nature Communications,* 13:5518 (2022).

Microbead-based Biomaterials for Cellular Immunotherapy

Kyung-Ho Roh[1]
[1]Chemical and Materials Engineering, University of Alabama in Huntsville, Huntsville, AL 35899

I. INTRODUCTION

Cellular immunotherapies using T lymphocytes exemplified by tumor-infiltrating lymphocytes and T cells engineered with exogenous receptors (T Cell Receptors or Chimeric Antigen Receptors) have achieved tremendous success and progress in various cancer treatments. However, these therapies are still hampered by a few remaining challenges such as inconsistent engraftment upon adoptive transfer, diminished efficacies in tumor microenvironments, toxicities, and astronomical manufacturing costs. In this presentation, two microbead-based biomaterial designs that have been recently proposed as innovative ways to alleviate some of these obstacles will be discussed. Lastly, we will also discuss B cell immunotherapy developed by the use of a similar strategy as one of the next cellular immunotherapies on the horizon.

II. OPTIMIZED T CELL ACTIVATION BY NOVEL PEPTIDE LIGANDS AGAINST CD3e PRESENTED ON MICROBEADS

Recently, we identified new peptide ligands that can specifically recognize and bind to human CD3e by screening peptide phage-display using a subtractive biopanning process.[1] Out of 13 identified phage clones expressing unique peptide sequences, one dominant phage clone demonstrated a superior binding behavior in the binding assays. Molecular modeling and docking simulation confirmed that the selected peptide ligand in an energetically stable conformation binds to a pocket of CD3e that is not hidden by either CD3g or CD3d. More importantly, the magnetic microbeads presenting the synthesized peptide ligands demonstrated a weak but specific association with a human T cell line, Jurkat cells, and induced the calcium flux, a hallmark indication of proximal T cell receptor signaling. This specific T cell activation signaling induced an enhancement of IL-2 section and cell proliferation. Thus, it indicates that this platform has great potential in applications of T cell immunotherapies by enabling proliferation of T cells without further induction of differentiation to terminal effector phenotypes which are venerable to exhaustion and premature apoptosis.

III. STANDARDIZED CAR-T CELL FUNCTIONAL ASSAY USING MICROBEADS

We recently have developed and reported a novel microbead-based biomaterial platform, acellular artificial target particles against CAR-T cells.[2] By devising a simple and standardized procedure, we precisely controlled the antigen surface densities presented on the microbeads for a wide range. Upon co-incubation of these microbeads with CAR-T cells followed by flow cytometry and cytokine assays, we were able to quantitatively determined the antigen-specific and dose-dependent activation of anti-HER2 CAR-T cells. This biomaterial platform was also able to serve as a clean target cell in in-vitro assays to prove the proposed mechanism of action of a next-generation CAR-T product. Overall, the simple, inexpensive, modular and precisely controllable synthetic biomaterials platform provides some critical advantages over the conventional assays using target cell lines, and thus has great potential as a standardized tool for the development and evaluation of both conventional and new CAR-T products in the context of regulatory approval and clinical translation.

REFERENCES

[1] A. Ahmadi, V. S. S. A. Ayyadevara, J. Baudry, and K. H. Roh, “Calcium signaling on Jurkat T cells induced by microbeads coated with novel peptide ligands specific to human CD3ε,” *J. Mater. Chem. B*, vol. 9, no. 6, pp. 1661–1675, 2021.

[2] R. Harari-Steinfeld, V. S. S. Abhinav Ayyadevara, L. Cuevas, F. Marincola, and K. H. Roh, “Standardized in-vitro evaluation of CAR-T cells using acellular artificial target particles,” *Front. Immunol.*, vol. 13, no. October, pp. 1–12, 2022.

In vivo evaluation of fractal microelectrodes for Vagus nerve stimulation

Hyowon Lee
Center for Implantable Devices, Weldon School of Biomedical Engineering, Birck Nanotechnology Center, Purdue University, West Lafayette, IN, USA

I. INTRODUCTION

Vagus nerve stimulation (VNS) has the potential to treat various peripheral dysfunctions, but the traditional cuff electrodes for VNS are susceptible to off-target effects. Microelectrodes may enable highly selective VNS that can mitigate off-target effects, but they suffer from the increased impedance. Recent studies on microelectrodes with non-Euclidean geometries have reported higher energy efficiency in neural stimulation applications. These previous studies use electrodes with mm/cm-scale dimensions, mostly targeted for myelinated fibers. This study evaluates fractal microelectrodes for VNS in a rodent model ($N = 3$). A thin-film device with fractal and circle microelectrodes is fabricated to compare their neural stimulation performance on the same radial coordinate of the nerve. The results show that fractal microelectrodes can activate C-fibers with up to 52% less energy ($p = 0.012$) compared to circle microelectrodes. To the best of the knowledge, this work is the first to demonstrate a geometric advantage of fractal microelectrodes for VNS in vivo [1].

II. Methods and Results

To evaluate the performance of the circle and the fractal microelectrodes in terms of their capability to recruit axon fibers and energy efficiency, we visualized the recruitment profile of $|V_{pp}|$ of the C-fiber volleys with respect to load energy (**Fig. 1**). Our results shows measured activation profiles for VNS using circle and fractal microelectrodes for each animal. The stimuli comprised 10 s train duration of 1 ms current-controlled pulses, 5 Hz of pulse repetition frequency alternating cathodic and anodic pulses: cathodic pulse for the charge injection and anodic pulse for the charge balancing. To mitigate the experimental variability in maximum $|V_{pp}|$ across animals, we normalized the $|V_{pp}|$ for microelectrodes to the maximum value for each animal and computed a grand mean (and 95% CI) across animals. The average normalized $|V_{pp}|$ profile from all three animals shows higher recruitment for fractal microelectrodes for pulse current amplitudes greater than 0.1 mA, but the 95% CI overlaps except for 0.4 and 0.8 mA. However, the 50% activation levels of the normalized $|V_{pp}|$ for the circle and the fractal are placed in the range where their 95% CIs do not overlap, which indicates the significant difference in activation level at this current range.

II. Conclusions

In this work, we have shown that the Vicsek fractal microelectrode can evoke neural responses from the rat vagus nerve to a 50% activation level with less energy consumption compared to the circle microelectrode. The normalized ECAP recruitment profile shows that fractal microelectrodes consumed 52% ± 33% ($p = 0.012$) less energy to activate 50% of maximum recruitable fibers. To the best of our knowledge, this is the highest energy saving among similar previous works that evaluated various electrode designs.

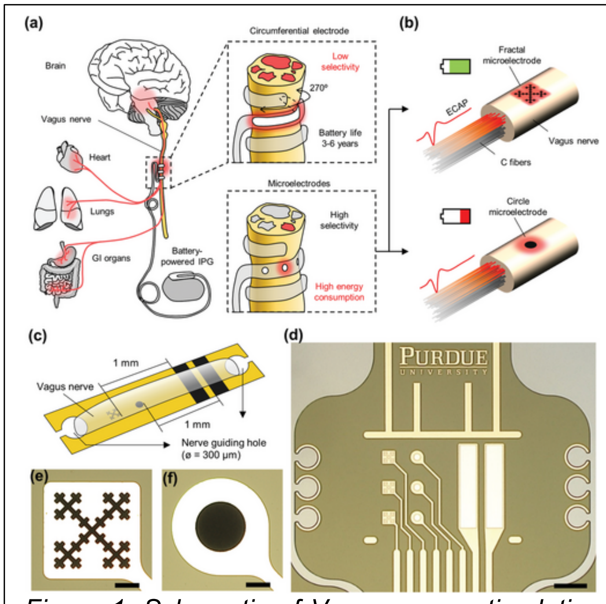

Figure 1: Schematic of Vagus nerve stimulation using microfabricated thin-film electrodes

ACKNOWLEDGEMENTS

This work was supported by the NIH SPARC OT2 OD023847.

REFERENCES

1. Lim et. al., Advanced Healthcare Materials, 2202619, 2023.

Advanced Cell and Gene Therapies For Effective CNS Repair Using Bionanomaterials

KiBum Lee

Dept. of Chemistry & Chemical Biology, Rutgers University

123 Bevier Road, Piscataway, NJ 08854-8087, USA

I. SUMMARY

Neurological disorders are a major cause of disability and death worldwide. These disorders are often caused by damage to the central nervous system (CNS), which is the part of the body that controls thought, movement, and sensation. The CNS is made up of a complex network of neurons, which are cells that send and receive signals. When neurons are damaged, they can no longer send or receive signals properly, leading to various symptoms, including paralysis, loss of sensation, and cognitive impairment. There are a number of potential therapies for neurological disorders, including gene therapy and stem cell therapy. Gene therapy is a treatment that uses genes to repair or replace damaged genes. Stem cell therapy is a treatment that uses stem cells to replace damaged or diseased cells.

Both gene therapy and stem cell therapy have the potential to be very effective treatments for neurological disorders. However, there are several challenges that need to be overcome before these therapies can be widely used. One challenge is that it is difficult to deliver genes or stem cells to the targeted CNS injury sites. The CNS is a very complex and protected system, and it is difficult to get genes or stem cells to the cells that need them.

Another challenge is that gene therapy and stem cell therapy can have side effects. Gene therapy can sometimes cause unwanted changes in the body, and stem cell therapy can sometimes cause the body to reject the stem cells.

Despite these challenges, gene therapy and stem cell therapy are still very promising treatments for neurological disorders. Researchers are working on ways to overcome the challenges of delivering genes and stem cells to the CNS, and they are also working on ways to reduce the side effects of these therapies.

In this presentation, I will discuss the interface between nanomedicine, chemical biology, and stem cell therapeutics. Moreover, a summary of the most updated results from these efforts and future directions will be discussed.

II. ILLUSTRATIONS

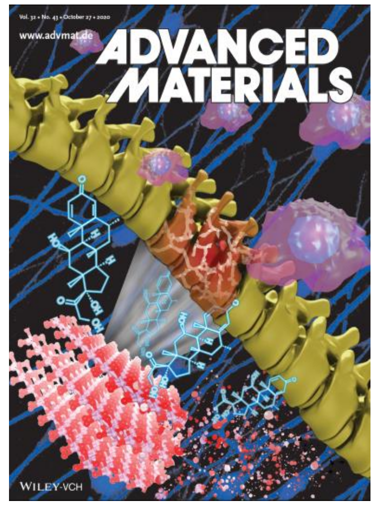

Figure 1: A novel in vivo drug delivery method: to effectively treat CNS injuries by delivering anti-inflammatory drugs in vivo and providing a permissive neural matrix using biodegradable nanoscaffolds. Implantation of drug-loaded nanoscaffolds to spinal-cord injury sites reduces macrophage infiltration, suppresses fibrotic scarring, and thereby promotes functional recovery.

III. ACKNOWLEDGEMENTS

The presenter would like to acknowledge KBLEE group members and collaborators. http://kblee.rutgers.edu/

III. KEY REFERENCES (from KBLEE Group)

1. "MitoScript: A Nanoparticle-based Effective Mitochondrial DNA Transcription Regulator", *Nano Letter*, **2023.**
2. "Advanced Theragnostics for the Central Nervous System (CNS) and Neurological Disorders Using Functional Inorganic Nanomaterials", *Advanced Drug Delivery Reviews*, **2023.**
3. "Predictive Biophysical Cue Mapping for Cellular Differentiation and Reprogramming Using Combinatorial Nanoarrays", *ACS Nano*, **2022.**
4. "Injectable hybrid inorganic nanoscaffold as rapid stem cell assembly template for cartilage repair", *National Science Review*, **2022**.
5. "Hybrid SMART Spheroids for Enhanced Stem Cell-based Cell Replacement Therapy", Science Advances, **2021.**
6. "Bioengineering Approaches for Advanced Organoid Research", Advanced Materials, **2021.**
7. "Effective Modulation of CNS Inhibitory Microenvironment using Bio-inspired Hybrid Nanoscaffold-based Therapeutic Interventions", *Advanced Materials*, **2020.**

Development of Novel Ultra-low Profile Coronary Stents to Treat Potential In-Stent Restenosis

Mohamed S. Ibrahim[1], Moataz Elsisy[2], Kara Nghiem[3], Chang Hun Kum[4], Jae Hwa Cho[4], Gyuhyun Jin[4], Sang Hyun An[5], and Youngjae Chun[1,3,6*]

[1]Department of Industrial Engineering, University of Pittsburgh, PA 15261, USA; [2]Department of Mechanical Design, Cairo University, Giza, Egypt; [3]Department of Bioengineering, University of Pittsburgh; [4]OSSTEM CARDIOTEC Co., Ltd., Seoul, South Korea; [5]Daegu-Gyeongbuk Medical Innovation Foundation Laboratory Animal Center, Daegu, South Korea; [6]McGowan Center for Regenerative Medicine, University of Pittsburgh Medical Center, PA 15213, USA (yjchun@pitt.edu)

Statement of Purpose: A leading cause of morbidity and mortality in the United States is cardiovascular disease, which accounts for >420,000 deaths per year, and epidemiological studies have estimated that approximately 44% of cardiovascular disease related deaths are attributable to coronary artery disease (CAD). Endovascular technologies such as percutaneous transluminal coronary angioplasty (PTCA) and stenting are currently more widely used since they are minimally invasive and less risky, however, there are still major complications called "*restenosis*" after these procedures. Recently, as the safety and efficacy of drug-eluting stents with thinner struts have been demonstrated by short-term clinical trials, it is necessary to develop a stent with the thinnest possible struts while maintaining the existing mechanical strength (diameter less than 70um). This study shows the structural analysis of the new CoCr stents for the thinner struts and improved biocompatibility. Finite Element Analysis with the necessary numerical calculations shows the optimized geometry and dimensions for the new device considering tensile and compressive strength of the stent strut, torsional stiffness, bending, and fracture due to fatigue.

Methods: Two unique designs of CoCr balloon-expandable coronary stents and a self-expanding pediatric valve frame made using iron wires and nitinol links were tested. Axial flexibility was tested using a 3-point bending test based on the standard guide from the ASTM International for balloon-expandable vascular stents and stent systems. Bending moment, midspan curvature, and bending stiffness were calculated based on the guide, and the plotted results were used to compare the bending stiffness of the stents and their commercial counterparts. Radial stiffness was evaluated by supporting the deployed coronary stent on a flat, stationary plate and applying force from a parallel plate. Stress and strain were calculated and plotted to compare the elastic recoil. Radial force was measured using a Dacron strip made into a tensile loop system around the self-expanding frame. This data was then used to calculate and plot stress and strain to show the elasticity of the stent.

Results: Mechanical test results of two types of newly developed coronary stents (Stent A and B shown in Fig. 1(A) and (B)) have demonstrated equivalent to commercially available coronary drug eluting stents widely used in clinics. Stent A showed an average of 31.6% lower bending stiffness compared to Stent B when collapsed, and 17.84% lower bending stiffness when in its deployed state. Stent A showed lower elastic recoil than Stent B, requiring 144% more force to achieve the same deformation, however, both stents had a similar permanent deformation of 500µm. Figure 1(C) shows the results from the radial stiffness of two stents. Stent A showed approximately double compared to the Stent B, demonstrating more ideal structural design compared to Stent A.

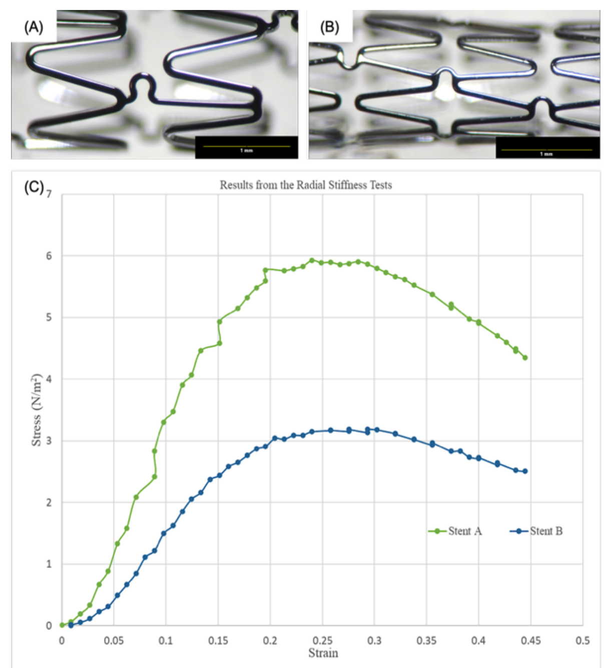

Figure 1. (A) Tested stent A, (B) tested stent B, and (C) radial stiffness results of two types of stents tested and calculated

Conclusions: A series of benchtop mechanical tests were conducted to validate the design of new ultra-thin coronary stents. Comprehensive mechanical test results have demonstrated that Stent A exhibits superior mechanical performance compared to the Stent B. Our recent outcomes will provide better solutions for new generation of coronary stents or other vascular diseases that require stents.

Acknowledgements: This work was supported by *South Korean Ministry of Trade, Industry and Energy*.

A Homozygous IER3IP1 Mutation Causes Secretory Protein Trafficking Defects in Neural Progenitor Cells

Lucie Yeongran Ahn[1], Ashleigh Schaffer[1]
[1]Case Western Reserve University School of Medicine

I. SUMMARY

Microcephaly with simplified gyration, generalized epilepsy, and permanent neonatal diabetes syndrome (MEDS) is a severe autosomal recessive disorder characterized by the aforementioned clinical features. It is caused by a deleterious bi-allelic variant in the immediate early response-3 interacting protein-1 (*IER3IP1*) gene. The role of IER3IP1 in secretory protein trafficking and the pathogenesis of MEDS remains elusive. Yos1p, a yeast homolog, has been reported to be involved in the anterograde transport of cargos from the endoplasmic reticulum (ER) to the Golgi via COPII vesicles. Based on prior research and the clinical presentations of MEDS patients, we hypothesize that IER3IP1 regulates secretory protein trafficking during neurogenesis.

II. RESULTS

A. Isogenic line generation and characterization of IER3IP1 homozygous p.L78P mutation

We first corrected IER3IP1 homozygous L78P mutation using CRISPR/Cas9 from induced pluripotent stem cells (iPSCs) reprogrammed from MEDS patient fibroblasts. Then we differentiated patient derived iPSCs and isogenic controls to neural progenitor cells (NPCs). The patient NPCs had reduced expression of IER3IP1 protein compared to isogenic controls, but the mRNA expression of *IER3IP1* was not reduced.

B. IER3IP1 p.L78P mutation causes structural abnormalities in organelles involved in secretory protein trafficking.

We show that IER3IP1$^{L78P/L78P}$ leads to structural abnormalities in ER and functional secretion defects in NPCs. IER3IP1 mutation leads to a reduction of Calnexin, ER marker, expression level and altered Golgi stacking in IER3IP1$^{L78P/L78P}$ NPCs compared to isogenic controls. Also, IER3IP1$^{L78P/L78P}$ NPCs had swollen ER morphologies and abnormally stacked Golgi in electron microscopy images compared to IER3IP1 wildtype NPCs.

C. IER3IP1 p.L78P mutation leads to functional defects in protein trafficking in NPCs.

Furthermore, I confirmed the variant causes a defect in secretion using a GFP trafficking reporter that utilizes FKBP domain. To investigate proteins that are differentially secreted in IER3IP1$^{L78P/L78P}$ NPCs, I performed a global quantitative protein analysis of secretome samples using Tandem Mass Tagging. The analysis showed that IER3IP1$^{L78P/L78P}$ NPCs have reduced secreted ECM proteins than isogenic controls. In summary, we demonstrated that IER3IP1$^{L78P/L78P}$ seen in MEDS patients lead to structural and functional defects in secretory protein trafficking in NPCs.

III. ILLUSTRATIONS

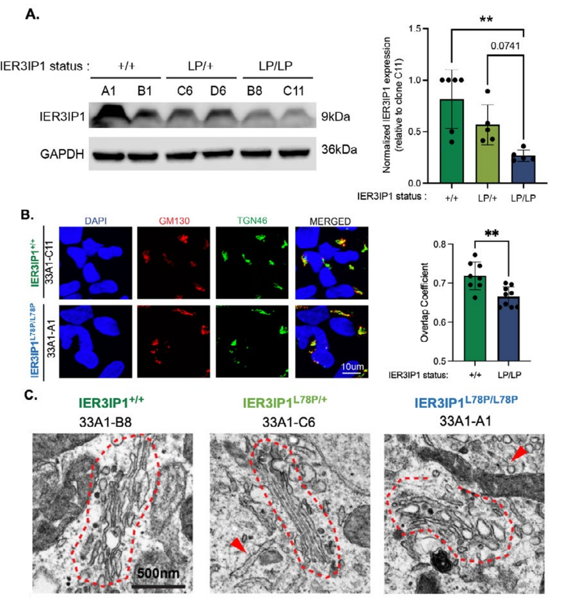

Figure 1: Characterization of IER3IP1 p.L78P mutation and its impact on secretory protein trafficking. (A) Western blot for IER3IP1 from NPC lysates shows p.L78P mutation impairs protein accumulation in a dose-dependent manner. GAPDH, loading control. Each dot represents an experimental replicate. ** $p<0.01$ (B) Co-immunocytochemistry showing altered *cis*-Golgi and *trans*-Golgi stacking in affected NPCs. Each dot represents a technical replicate. ** $p<0.01$ (C) Electron microscopy images showing IER3IP1 p.L78P mutation leads to shortened and swollen ER structures (arrows) and abnormal stacking of Golgi (dotted lines).

REFERENCES

1. Abdel-Salam, G. M. et al. A Homozygous IER3IP1 Mutation Causes Microcephaly With Simplified Gyral Pattern, Epilepsy, and Permanent Neonatal Diabetes Syndrome (MEDS). Am J Medical Genetics Part 158A, 2788–2796 (2012).
2. Barrowman, J., Wang, W., Zhang, Y. & Ferro-Novick, S. The Yip1p·Yif1p Complex Is Required for the Fusion Competence of Endoplasmic Reticulum-derived Vesicles*. J Biol Chem 278, 19878–19884 (2003).
3. Adolf, F. et al. Proteomic Profiling of Mammalian COPII and COPI Vesicles. Cell Reports 26, 250-265.e5 (2019).

Osteoporosis Drug Testing on Demineralized Bone Paper

Yongkuk Park[1], **Jungwoo Lee**[1]
[1]Department of Chemical Engineering, University of Massachusetts Amherst, Massachusetts, 01003

I. INTRODUCTION

Osteoclasts, multinucleated cells responsible for bone resorption during bone remodeling, play a crucial role in driving osteoporosis due to their heightened activity. In order to gain accurate insights into the regulation of bone remodeling and predict pharmacological responses, it is essential to recapitulate osteoclast differentiation and function in vitro. Recent animal studies have revealed the functional integration of osteoclasts and osteoblasts, as well as the recycling of osteoclasts following bone resorption. However, existing platforms have limitations when it comes to reproducing and investigating these newly identified osteoclast processes in vitro. To address this gap, we introduce a new in vitro osteoclast culture and assay platform that utilizes demineralized bone paper (DBP) inspired by osteoid.

II. Materials and Methods

A midsection of the femur containing mostly compact bone was demineralized through the rapid demineralization process that we devised previously. Briefly, after removing outer connective tissue and dissolving inner marrow fat in a 1:1 methanol-chloroform solution, the bovine compact bone block was demineralized in 1.2 N hydrochloric acid with cyclic pressure up to 4 bar with a 10-s on/off interval while replacing HCl solution each day for 5-7 days. A fully demineralized bone block was cryosectioned with 20 μm thickness. Bone cell assay was performed by using mouse osteoprogenitor and bone marrow mononuclear (BMM) cells from tibia.

III. Results and Discussion

The selection of biomaterials is crucial for accurately replicating in vivo-relevant bone remodeling processes in vitro, as bone-forming osteoblasts and bone-resorbing osteoclasts develop and function exclusively on the mineralized bone surface. By employing an osteoid-inspired demineralized bone paper (Fig. 1a), we have recreated the cellular and extracellular complexity of the bone tissue surface while preserving optical accessibility for fluorescent microscopy imaging. The process of osteoblastic bone formation involves the synthesis of a collagen-based structural framework called osteoid, followed by mineral deposition. Moreover, DBP is scalable for production and mechanically durable, facilitating easy experimental handling. Leveraging these enabling features, we first demonstrated longitudinal fluorescent monitoring of osteoclast differentiation in murine BMMs and subsequent bone resorption on remineralized DBP. Subsequently, we successfully recapitulated a bone remodeling cycle, encompassing osteoclast fusion, bone resorption, and fission, by stimulating cocultures of osteoblasts and BMMs on DBP with vitamin D3 and prostaglandin E2. Furthermore, we simulated the process of osteoclast-targeting bisphosphonate drug action on the coculture model using a fluorescent dye-conjugated bisphosphonate (Ostensese680) (Fig 1b). The established DBP-based in vitro osteoclast culture and assay platform holds significant promise in advancing scalable, functional, and analytical screening of other osteoporosis drugs. We envision that advanced in vitro bone models incorporating DBP will greatly contribute to a deeper understanding of various aspects of bone biology.

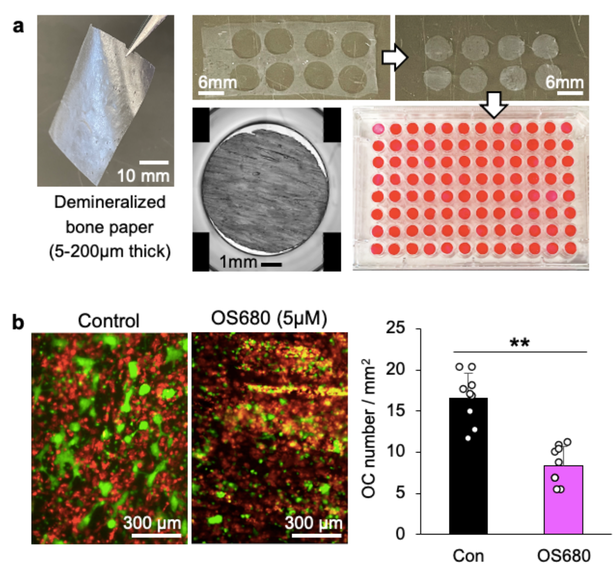

Figure 1: a, Demineralized bone paper stained with rhodamine dye. b, Bisphosphonate (OS680) testing with osteoblasts (red) and osteoclasts (green).

Spatial Phenotyping of the Glioblastoma Tumor Microenvironment

Jungmin Nam[1], **Rong Fan**[1,2]
[1]Department of Biomedical Engineering, Yale University, [2]Department of Pathology, Yale School of Medicine

I. Introduction

Glioblastoma, the most common primary malignant brain tumor, is an extremely aggressive cancer associated with dismal prognosis and poor quality of life. To improve patient treatment and survival, it is crucial to understand the heterogeneity in glioblastoma tissues. Compared to the genotypes of various subgroups of glioblastoma, the phenotypes of glioblastoma have been less extensively studied, especially in a spatial context. In this work, we use co-detection by indexing (CODEX) to spatially profile glioblastoma tissue and identify glioblastoma subtypes using a 46-plex immune and tissue marker panel.

II. Materials and Methods

Human formalin-fixed, paraffin-embedded (FFPE) glioblastoma tissue sections were profiled with the PhenoCycler-Fusion system, using a 46-plex immune marker panel to capture the complexity of the immune state. These antibodies are tagged with a unique DNA barcode. Tissues are then imaged corresponding DNA tags are used to cyclically image tissue via the addition, imaging, and removal of reporters. Following imaging, cell segmentation was performed using StarDist. Cell clustering and marker expression analysis was carried out using Seurat.

III. Results

We successfully imaged a comprehensive 46-plex panel of immune and tissue markers on FFPE glioblastoma tissue. Interestingly, distinct subtypes of glioblastoma were found spatially arranged in a ring-like distribution pattern. Further downstream analysis revealed notable differences amongst regions, characterized by varying levels of cell proliferation and leukocyte infiltration, which mirrored this ring-like structure. Moving forward, we anticipate that further exploration of the multiplex data, in conjunction with additional omics data, will provide deeper insights into the spatial phenotypic profile of glioblastoma subtypes.

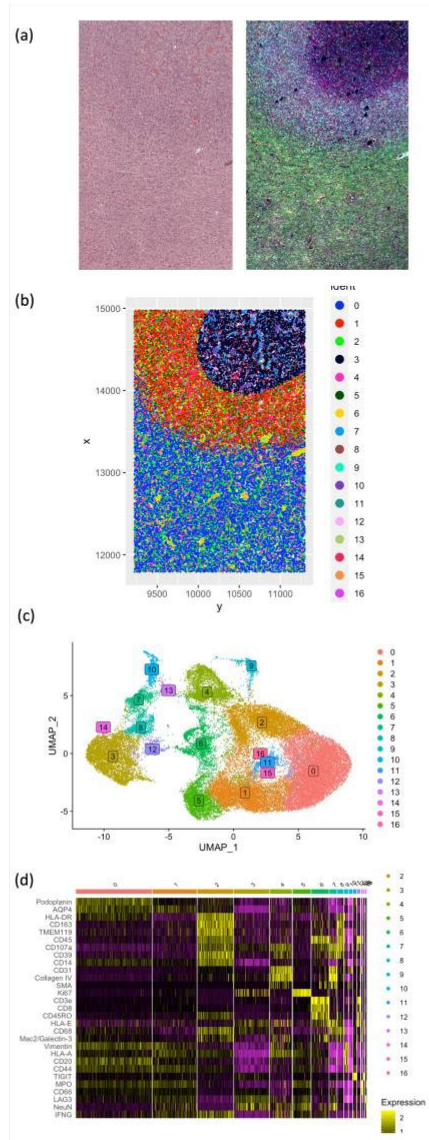

Figure 1: (a) H&E and multiplex image of glioblastoma. (b) Spatial map of cell clusters. (c) UMAP of cell clusters. (d) Expression heatmap.

REFERENCES

1. Stoyanov, George S., Deyan Dzhenkov, Peter Ghenev, Bogomil Iliev, Yavor Enchev, and Anton B. Tonchev. 2018. “Cell Biology of Glioblastoma Multiforme: From Basic Science to Diagnosis and Treatment.” *Medical Oncology* 35 (3): 27.

Production of animal stealth red cells by cell surface modulation

Hyung Kyu Kim[1], **Hee Young Kim**[2]
[1]Department of Oral Physiology, School of Dentistry, Kyungpook National University, 2177, Dalgubeol-daero, Jung-gu, Daegu 41940, Korea, [2]Department of Physiology, Yonsei University College of Medicine, 50-1 Yonsei-ro, Seodaemun-gu, Seoul 03722, Korea

I. INTRODUCTION

Blood transfusion has been practiced for centuries to save human and animal lives. As the pet market continues to expand, the demand for blood transfusions in animals is steadily increasing. However, similar to the situation in humans, there is a shortage of minor blood groups in animals. In the case of cats, the AB blood group system has reported three blood groups. Blood type A is the most prevalent, while blood type B is found in only 1 % of the feline population in Korea. Type B cats naturally develop antibodies against type A antigens, which can lead to potentially fatal hemolytic reactions if transfused with incompatible blood. To address this challenge, the manipulation of red blood cell surface antigens using methoxy polyethylene glycols (mPEGs) offers a promising approach to create "stealth" red cells that do not bind anti-A antibodies. This study aims to determine the optimal conditions for producing feline stealth red cells and validate their stealth effect in vitro.

II. METHODS

Feline red cells of type A were subjected to PEGylation using mPEG, and the PEGylation reaction conditions were optimized. Subsequently, the physical properties of the cell membrane and the biochemical properties of the pegylated red cells were assessed, followed by the evaluation of phagocytosis mediated by anti-A antibodies.

III. RESULTS

The feline stealth red cells were generated with mPEG of 2 mM, 20 kDa as determined by aggregation reaction. When reacted with feline A antibodies in vitro for up to 24 hours, the Stealth red cells showed minimal or no aggregation reaction. Cell membrane stability for cell viability and biochemical properties related to oxygen transport capacity of Stealth red cells were not different from normal feline A typed red cells.

IV. CONCLUSION

It is the first report in veterinary medicine showing that manipulation of feline A erythrocytes with activated mPEG can produce universal erythrocytes suitable for transfusion to B-typed cats.

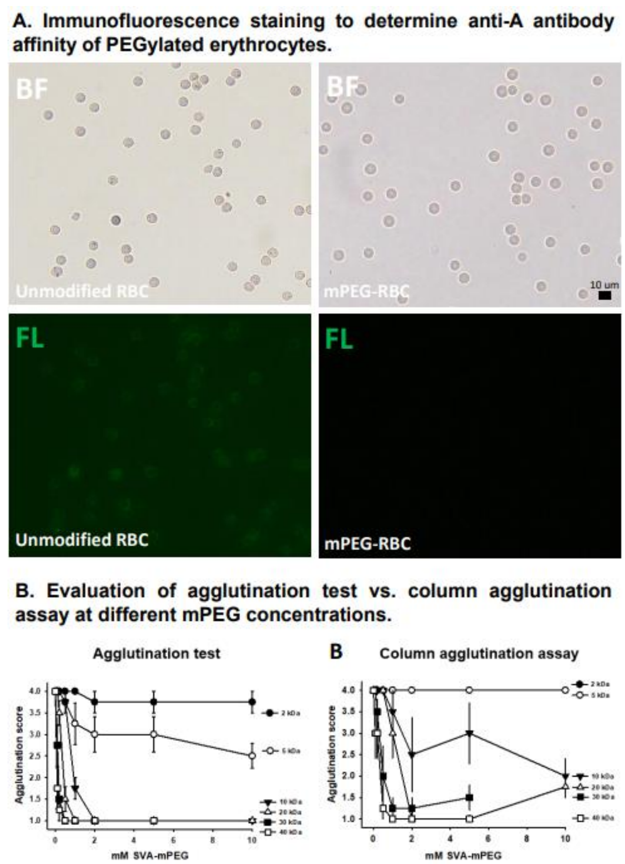

Figure 1: Effect of mPEGylation of feline A RBC on antibody- mediated agglutination

ACKNOWLEDGEMENTS

This research was supported by the National Research Foundation of Korea (NRF) grant funded by the Korea government (MSIT) (No.2019R1A2C1002555), Evaluation for Technology in Food, Agriculture and Forestry(IPET) through Companion Animal Life Cycle Industry Technology Development Program, funded by Ministry of Agriculture, Food and Rural Affairs(MAFRA)(322096-5)

A Pillar and Perfusion Plate Platform for Robust Human Organoid Culture and Analysis

Soo-Yeon Kang[1], Moo-Yeal Lee[1]
[1]Department of Biomedical Engineering, University of North Texas

I. SUMMARY

Human organoids have potential to revolutionize in vitro disease modeling by providing multicellular architecture and function that are similar to those in vivo. This innovative and evolving technology, however, still suffers from assay throughput and reproducibility to enable high-throughput screening (HTS) of compounds due to cumbersome organoid differentiation processes and difficulty in scale-up and quality control. Using organoids for HTS is further challenged by lack of easy-to-use fluidic systems that are compatible with relatively large organoids. Here, we overcome these challenges by engineering "microarray three-dimensional (3D) bioprinting" technology and associated pillar and perfusion plates for human organoid culture and analysis. High-precision, high-throughput stem cell printing and encapsulation techniques were demonstrated on a pillar plate, which was coupled with a complementary deep well plate and a perfusion well plate for static and dynamic organoid culture. Bioprinted cells and spheroids in hydrogels were differentiated into liver and intestine organoids for in situ functional assays. The pillar/perfusion plates are compatible with standard 384-well plates and HTS equipment, and thus may be easily adopted in current drug discovery efforts.

II. ILLUSTRATIONS

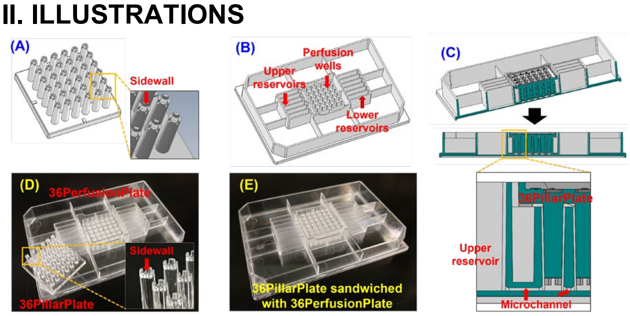

Figure 1: **The combination of a pillar plate and a perfusion well plate for dynamic organoid culture.** SolidWorks designs of (A) a 36PillarPlate, (B) a 36PerfusionPlate, and (C) the 36PillarPlate sandwiched onto the 36PerfusionPlate. Injection molding with polystyrene was performed to manufacture (D, E) the 36PillarPlate and the 36PerfusionPlate for dynamic organoid culture. The culture media added into the upper reservoirs (URs) can flow through the microchannels and the perfusion wells to reach the lower reservoirs (LRs) by gravity.

ACKNOWLEDGEMENTS

This study was supported by the National Institutes of Health (NIDDK UH3DK119982, NCATS R44TR003491, and NIEHS R01ES025779) and the Ohio Third Frontier Commission (TVSF Phase IB and Phase II).

REFERENCES

1. Soo-Yeon Kang, Masaki Kimura, Sunil Shrestha, Phillip Lewis, Sangjoon Lee, Yuqi Cai, Pranav Joshi, Prabha Acharya, Jiafeng Liu, Yong Yang, J. Guillermo Sanchez, Sriramya Ayyagari, Eben Alsberg, James M. Wells, Takanori Takebe, Moo-Yeal Lee, "A Pillar and Perfusion Plate Platform for Robust Human Organoid Culture and Analysis" *This article is a preprint and has not been certified by peer review.*

Studying depressive disorders with a 3D neurosphere model on a micropillar chip

NaYoung Choi[1,2], Minseong Lee[2], Soo-Yeon Kang[2], Anvitha Tharakesh[3], Moo-Yeal Lee[2], Sehoon Jeong[1]

[1]Department of Healthcare Information Technology Inje University, Gimhae, South Korea, 50834, [2]Department of Biomedical Engineering, University of North Texas, Denton, TX 76207, [3]Texas Academy of Mathematics and Science, University of North Texas, Denton, TX 76203

I. SUMMARY

This study aims to develop a depression research system based on the pillar plate platform to discover target proteins for the treatment of depression and to validate the interaction of antidepressants with target proteins.

II. INTRODUCTION

Depression refers to a wide range of mental health problems that causes persistent sadness and loss of interest[1]. The prevalence of depression in the US increased from 7.3% in 2015 to 9.2% in 2020[2]. Most studies investigating the mechanisms of depression have been conducted using two-dimensional (2D) cultures and animal models, while several theories of depression, such as the monoamine, neuroplasticity, and neurogenesis hypotheses, have been proposed[3]. However, animal models are time-consuming, expensive, and may not fully reflect the disease state of depressed patients due to differences in genetic, biochemical, and metabolic processes. Neurons cultured in 2D are limited in their ability to accurately reproduce the physiological functions of the real brain that occur in three-dimensional (3D) cell-to-cell interactions. To address these limitations, we developed a 3D culture system using micropillar chip platforms for human neural stem cells (hNSCs).

III. RESULT

NSCs were seeded in Aggrewell plates at specific densities to form uniformly sized spheroids, which were then collected and precisely printed onto the pillar plate using a 3D bioprinter. The neurospheres were cultured on the pillar plate for 5 days in a growth factor-containing culture medium and then differentiated for 14 days in the absence of growth factors. The dynamic culture conditions to enhance the drug delivery effect were established by changing the tilt of the rocker by 10 degrees at 1-minute intervals to induce culture fluid movement. Using dexamethasone (DEX)-treated neurospheres, we created a depression-like environment and performed analyses to assess brain-specific biomarkers. We found that most of the genes were significantly downregulated.

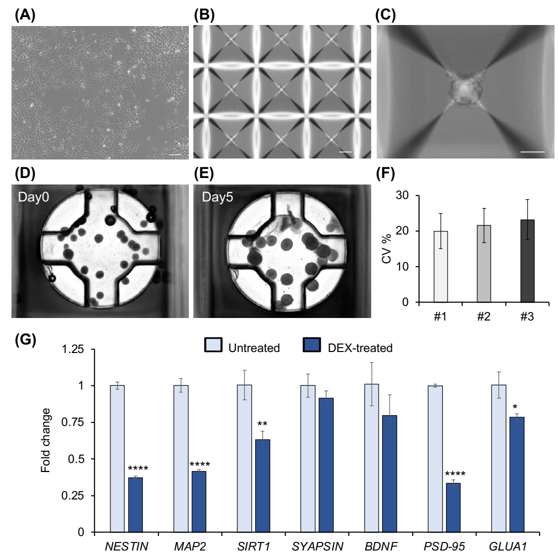

Figure 1: Bioprinted neurospheres on pillar plate and the effect of DEX treatment. (A) hNSCs, (B) and (C) formation of neural aggregates, (D) and (E) bioprinted neurospheres on pillar plate, (F) coefficient of variation (CV) for neurospheres printing on pillar plate, (G) qPCR analysis of gene expression in DEX treatment.

ACKNOWLEDGEMENTS

This work was supported by the National Research Foundation of Korea (NRF) grant funded by the Korea government (MSIT). (No. NRF-2021R1I1A3061265).

REFERENCES

1.Chand, S.P., and Arif, H. “Depression”. In StatPearls. 2023.
2.Goodwin, R.D., et al. “Trends in U.S. Depression Prevalence From 2015 to 2020: The Widening Treatment Gap”. Am J Prev Med *63*, 726-733. 2022.
3.Yang, T., et al. “The Role of BDNF on Neural Plasticity in Depression”. Front Cell Neurosci *14*, 82. 2020.

Estimation of Musculotendon Stiffness and Slack Length Using an Optimization Algorithm

Hwan Choi[1], Sepehr Ramezani[1]
[1]University of Central Florida, Orlando, FL, USA

I. INTRODUCTION

The level of muscle stiffness and slack length play an important role in dynamic performance and joint range of motion. Musculoskeletal modeling is a useful tool to evaluate the function of joint kinetics and kinematics that were driven by muscles. As this musculoskeletal model employs muscle stiffness and slack length to estimate the muscle forces and activation, it is important to use subject specific muscle stiffness parameters. However, the current musculoskeletal model uses an average muscle stiffness and slack length of unimpaired individuals, the outcome of modeling simulation result is often discrepant with directly measured outcomes. Thus, this study represents a new method that enables comprehensive and accurate muscle stiffness and slack length using an optimization algorithm.

II. METHOD

In this study, we recruited an unimpaired participant. The participant was sitting on the human dynamometers and positioned full knee extensions with three hip flexion angles (90°, 55°, and 15°). Then, we let knee flexion with low angular velocity (5°/sec) while participants were relaxing their muscles. From this experiment, we measured knee torques that were only induced by the stretched muscles by compensating the gravity and the human dynamometer's jig mass.

We used a recently developed musculoskeletal model [1] to use the Hill-type muscle model and joint definitions. All the muscles (were deactivated as we only validate muscle stiffness and slack length. The experimentally collected knee torques were implemented to the musculoskeletal model as a control input. Then, a virtual control actuator was generated on the musculoskeletal model that replicates the human dynamometer function to make isokinetic knee motion. We used an optimization algorithm in OpenSim Moco to allocate muscle passive parameters in the musculotendon model to replicate the experimentally collected passive net knee torque.

III. RESULTS & DISCUSSION

The muscle stiffness and slack length are shown in Table 1. The results are aligned with the previous direct measured results suggesting our experiment method and optimization algorithm provide reliable results.

Previous research on evaluating the level of muscle active estimation of muscle contracture that is characterized by short and tight muscle uses a generic musculotendon model. As a result, there are significant discrepancies between experimentally collected muscle activation from electromyography sensors and simulated results. This study can be used to people with movement disabilities with short and tight muscles and improve muscle activation in the future.

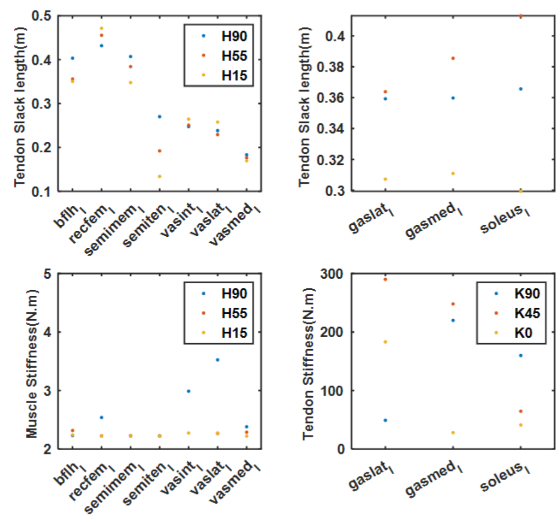

Figure 1: Musculotendon slack length and stiffness of biceps femoris long head (bflh), rectus femoris(rfem), semimembranosus (semimem), semitendinosus (semiten), vastus intermedius (vasint), vastus lateralis (vaslat), vastus medialis (vmed), gastrocnemius lateralis (gaslat), gastrocnemius medialis (gasmed) and soleus.

REFERENCES

1. De Groote F. et. al., "Evaluation of direct collocation optimal control problem formulations for solving the muscle redundancy problem," *Annals of biomedical engineering*, Vol. 44, pp. 2922-2936, 2016.

Frequency Analysis on Tissue Perfusion using a Laser Speckle Contrast Imaging *in vivo*

Yungjun Yoo[1], Yoseph Kim[1], and Richard Jaepyeong Cha[1,2,3]
[1]Optosurgical, LLC , [2]Children's National Hospital, [3]George Washington University School of Medicine

SUMMARY
This paper presents a way to classify the ischemic and normal tissue regions with laser speckle contrast imaging. In addition, we provide a frequency spectrum analysis to extract additional information such as breathing and the heartbeat rate.

I. INTRODUCTION
Objective tissue perfusion assessment is a longstanding unmet clinical need in medicine [1]. There are several equipment available for pre-operative diagnostic purposes but these devices are still suboptimal to be directly interpreted in the operating room. Laser speckle contrast imaging (LSCI) is a commonly employed optical imaging technique for non-invasively monitoring microcirculations in superficial tissues, without the need for contrast dye injections or near infrared indocyanine green (ICG) fluorescence imaging. Despite the noninvasiveness and its simplicity, an objective assessment of ischemic tissue regions solely through LSCI can be challenging, as the technique provides only the relative blood flow not the absolute and quantitative velocity. Consequently, supplementary analytic tools may help assist surgeons to make better decisions.

To address this challenge, we propose a method that involves performing Fourier Transform-based spectral analysis on LSCI dat. By applying this, we were able to clearly differentiate between live and ischemic tissue areas in the frequency domain. Moreover, we successfully extracted vital information such as heartbeat from breathing motion artifacts, which serve as valuable indicators of tissue viability. This new approach holds a potential for an adjunctive tool to LSCI by providing additional quantitative values and helping surgeons' decision-making processes during the surgery.

II. EXPERIMENT
To evaluate the performance of our analytic model, animal data acquired from the previous studies on swine (IACUC approved protocol #30591 at the Children's National Hospital) were used [1].

III. ANALYSIS
In Figure 1, the left side displays an image, while the right side shows a spectrum. The top portion represents ischemic tissue, while the bottom portion represents healthy tissue. By examining the spectrum graph of the ischemic region, we observe three peaks (30, 60, 90 beats/min) with decreasing intensities as the frequency rises. The peak at 30 beats/min corresponds to the breathing rate during the experiment, while the others are the second and third harmonics of the breathing. As this region is ischemic, we cannot detect high-frequency components aside from the higher harmonics of the breathing signal. However, in the spectrum graph of the live tissue, a distinct disparity is visible. We were able to observe a higher frequency peak, near the heartbeat rate, apart from the higher harmonics of the breathing. This discernible distinction in the spectral pattern holds potential for real-time classification of ischemic and live tissue regions.

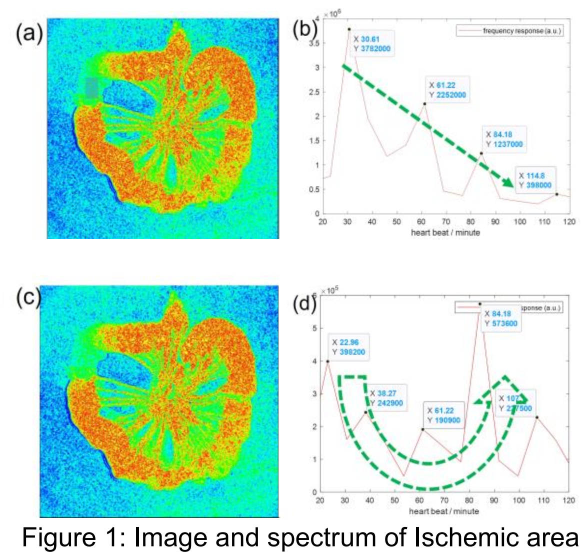

Figure 1: Image and spectrum of Ischemic area (top) and healthy region (bottom),

REFERENCES
1. Y. Wang, L. Tiusaba, S. Jacobs, M. Saruwatari, B. Ning, M. Levitt, A. D. Sandler, S-H. Nam, J. U. Kang, J. Cha, *J. Med. Imag.* **9**(6) 064502 (28 November 2022)

Fundamental Issues in Cognitive Workload Classification

Junho Park
Texas A&M University

I. INTRODUCTION

Severe functional disability in performing activities of daily living (ADLs) can result from limb amputation, and amputees often rely on prosthetic devices (PDs) to carry out these tasks. However, PDs can require a significant amount of cognitive resources, and some users rejected devices due to poor usability [1].

Despite this, there have been few studies investigating usability issues, and those that have been conducted have primarily relied on subjective methods such as questionnaires. Additionally, no previous studies have classified the cognitive workload (CWL) of PDs during the early stages of the design process. To address the research gaps, the objectives of this study were to develop a prediction model for CWL and to explore fundamental issues.

II. COGNITIVE WROKLOAD PREDICTION OF UPPER-LIMB PROSTHESES

A. METHOD

A human subject experiment was conducted with 30 able-bodied participants (Age: *M*=22.9 yrs.; *SD*=2.8 yrs.) [2]. Three types of electromyography-based (EMG) control schemes were used for clothespin relocation task. Random forest (RF), support vector classifier (SVC), and Naïve Bayes (NB) model were developed as they were heavily used to classify CWL in other domains. Task performance (the number of pins moved within 2 minutes), pupillometry data (pupil diameter and blink rate), and cognitive performance model (CPM) outcomes (e.g., motor operators) were used as features for machine learning models. NASA-TLX was collected to be used as a ground truth for the CWL classification. CWL was classified with two levels: “High” or “Low.”

B. RESULTS

It was found that SVC and NB models classified CWL with reasonable accuracy (>70%) under near real-time [2]. Experimental cost among several subset of features was compared, and subset of NB model seemed to be appropriate, considering accuracy and computational cost.

III. FUNDAMENTAL ISSUES

From practical point of view, several fundamental issues were identified. The first issue was the nature of interaction between physical workload (PWL) and CWL. Although there is a recent systematic review [3], it did not cover the domain for amputees, which requires more CWL than the able-bodied. The interaction between PWL and CWL should be investigated and modeled. Second, current study is the first study that used CPM outcomes as input for ML. It was not possible to fully replace all other features only with CPM outcomes (e.g., pupillometry data was required). Next step should involve establishing a theory or methodology to expand the impact of CPM. Lastly, individual differences should be reflected (e.g., age, gender, height, and weight).

Table 1: Summary of classification results ([2], © by IEEE)

Subset ID	Subset of features	Feature Selector	Test Accuracy (0-1)			Computational cost (sec)			Experimental cost
			RF	NB	SVM	RF	NB	SVM	
1-1	Pupil + TP + CPM	RFE	0.89	0.63	0.48	134.50	0.48	0.59	High
1-2		KBEST	0.89	0.7	0.7	65.24	2.26	0.70	High
1-3		SFS	0.89	0.7	0.7	917.74	16.22	9.60	High
2-1	Conf + TP + CPM	RFE	0.89	0.67	0.67	155.08	0.78	0.54	High
2-2		KBEST	0.89	0.63	0.7	72.41	1.52	0.73	High
2-3		SFS	0.89	0.59	0.7	1232.42	15.82	9.59	High
3-1	Conf + Pupil + CPM	RFE	0.59	0.59	0.7	132.78	0.42	0.44	High
3-2		KBEST	0.78	0.7	0.7	64.12	1.03	0.59	High
3-3		SFS	0.63	0.7	0.7	907.79	8.63	6.66	High
4-1	Conf + Pupil + TP	RFE	0.85	0.59	0.56	90.91	0.30	0.39	High
4-2		KBEST	0.89	0.67	0.7	48.25	0.59	0.50	High
4-3		SFS	0.89	0.7	0.7	475.59	4.52	3.87	High
5-1	TP + CPM	RFE	0.89	0.67	0.67	90.59	0.34	0.51	Moderate
5-2		KBEST	0.89	0.63	0.7	48.37	0.78	0.59	Moderate
5-3		SFS	0.89	0.59	0.7	463.60	6.54	5.82	Moderate
6-1	Pupil + CPM	RFE	0.56	0.59	0.7	85.08	0.34	0.47	High
6-2		KBEST	0.56	0.7	0.7	46.32	0.77	0.56	High
6-3		SFS	0.37	0.7	0.7	382.57	5.51	5.00	High
7-1	Pupil + TP	RFE	0.85	0.48	0.44	43.55	0.32	0.43	High
7-2		KBEST	0.89	0.67	0.7	27.49	0.61	0.52	High
7-3		SFS	0.89	0.59	0.7	116.16	3.00	2.82	High
8-1	Conf + CPM	RFE	0.56	0.7	0.7	89.18	0.29	0.35	Low
8-2		KBEST	0.56	0.7	0.7	47.66	0.61	0.51	Low
8-3		SFS	0.56	0.7	0.7	459.21	4.39	4.05	Low
9-1	Conf + TP	RFE	0.89	0.67	0.67	65.54	0.31	0.34	Moderate
9-2		KBEST	0.89	0.78	0.7	37.19	0.59	0.43	Moderate
9-3		SFS	0.89	0.59	0.7	217.95	2.71	2.29	Moderate
10-1	Conf + Pupil	RFE	0.59	0.56	0.7	43.42	0.30	0.29	High
10-2		KBEST	0.78	0.7	0.7	27.45	0.54	0.37	High
10-3		SFS	0.59	0.7	0.7	115.46	2.03	1.48	High
11-1	CPM	RFE	0.56	0.7	0.7	53.24	0.31	0.40	Low
11-2		KBEST	0.56	0.63	0.7	29.62	0.61	0.51	Low
11-3		SFS	0.56	0.7	0.7	131.22	2.99	2.56	Low
12-1	TP	RFE	0.81	0.59	0.7	19.54	0.32	0.39	Moderate
12-2		KBEST	0.81	0.7	0.7	14.27	0.52	0.48	Moderate
12-3		SFS	0.81	0.59	0.7	25.24	1.29	1.15	Moderate
13-1	Pupil	RFE	0.52	0.48	0.7	8.78	0.42	0.37	High
13-2		KBEST	0.59	0.7	0.7	6.78	0.55	0.37	High
13-3		SFS	0.48	0.7	0.7	6.37	0.80	0.66	High
14-1	Conf	RFE	0.56	0.7	0.7	19.50	0.25	0.25	Low
14-2		KBEST	0.56	0.7	0.7	15.39	0.38	0.31	Low
14-3		SFS	0.56	0.7	0.7	24.49	0.68	0.60	Low

*Note: Pupil features include: pupil diameter and blink rate. Task performance (TP) features include: number of moved pins from the experiment, shortest time to move one pin, and number of training trials. Device configuration (Conf) features include: DC, PR, and CC. Cognitive performance model (CPM) features include: estimated time to move one pin, number of cognitive, perceptual, or motor operators, and number of memory chunks

ACKNOWLEDGEMENTS

The funding for this study was provided by National Science Foundation (No. IIS-1900044).

REFERENCES

1. Park, J., & Zahabi, M. (2022). Cognitive Workload Assessment of Prosthetic Devices: A Review of Literature and Meta-Analysis. *IEEE Transactions on Human-Machine Systems*.
2. Park, J., Berman, J., Dodson, A., Liu, Y., Matthew, A., Huang, H., ... & Zahabi, M. (2022, November). Cognitive Workload Classification of Upper-limb Prosthetic Devices. In *2022 IEEE 3rd International Conference on Human-Machine Systems (ICHMS)* (pp. 1-6). IEEE.
3. Mixter, S., Mathiassen, S. E., Jahncke, H., Hygge, S., Lyskov, E., Hallman, D. M., & Lewis, C. (2023). Effects of combining occupationally relevant physical and cognitive tasks. a systematic review. *Annals of work exposures and health*, *67*(3), 303-319.

Integrated Edge-AI Based Closed-loop Stimulation System for Gait Rehabilitation after Spinal Cord Injury

Ahnsei Shon[1], Alex Stefanov,[2] Michelle Hook[2], and Hangue Park[1,3]

[1]Department of Multidisciplinary Engineering, Texas A&M University, College Station, TX 77843 USA,
[2]Department of Neuroscience and Experimental Therapeutics, Texas A&M University, Bryan, TX 77807 USA.
[3]Department of Biomedical Engineering and Department of Intelligent Precision Healthcare Convergence, Sungkyunkwan University, Suwon, South Korea

Abstract

Recently, closed-loop electrical stimulation (E-Stim) has been garnering a lot of attention to maximize stimulation effects on regaining locomotor function from various diseases such as spinal cord injury (SCI), stroke, Parkinson's disease, and multiple sclerosis. However, each subject has a different threshold to trigger an electrical stimulator, requiring human intervention or sophisticated complex algorithms generally operating in a certain condition. To maximize E-Stim efficacy without complex algorithms or human intervention, we developed edge-AI model which can be deployed on a commercial microprocessor on a closed-loop neural interface system. The developed edge-AI model was deployed on a customized single neural interface board and evaluated with a spinal cord injured rat.

I. Introduction

Globally, there are more than 6.2 million people suffering from spinal cord injury (SCI). A new SCI occurs every 1 to 2 minutes. SCI is commonly caused by car accidents, falls, violence, and sports injuries, among many other reasons. Because spinal cord plays a pivotal role in our body, connecting the brain to the peripheral nervous system, spinal cord injuries severely affect bodily functions. To regain the weakened functions after SCI, various electrical stimulations (E-Stim) have been used such as epidural stimulation, functional electrical stimulation (FES) with immediate effectiveness. However, there are still limitations requiring manual setting of threshold level because each individual has different threshold to extract maximum E-Stim effects. Therefore, there are increasing requirements for setting optimal threshold level to trigger stimulation pulses. For stable and effective E-Stim, in this study, we suggest an automated threshold method using edge-AI technology to maximize rehabilitation effects on gait rehabilitation after SCI with E-Stim.

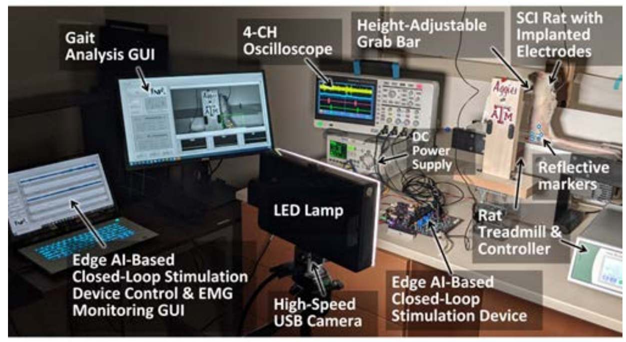

Figure 1: Experimental setup. The experiment was performed with an SCI rat holding a height-adjustable grab bar on a rat treadmill during bipedal locomotion [1].

II. RESULTS AND CONCLUSION

The system was integrated into a single board with three main components: real-time EMG recording for stance phase identification, edge AI-processing to automatically set threshold level, and stimulation pulse generation. Additionally, we developed a multi-site EMG recording electrode specifically designed for freely moving small animals, enabling continuous use for more than 28 days. The whole functionalities including edge-AI model was successfully evaluated through benchtop test and with a SCI rat.

ACKNOWLEDGEMENTS

This work was supported by Morton Cure Paralysis Fund.

REFERENCES

1. A. Shon, A. Stefanov, M. Hook, and H. Park, "Edge AI-Based Closed-Loop Peripheral Nerve Stimulation System for Gait Rehabilitation after Spinal Cord Injury," 2023 11th Int. IEEE/EMBS Conf. Neural Eng., pp. 1–4, doi: 10.1109/NER52421.2023.10123734.

Characterization of Decellularized Plant Leaf Biomaterials for Tissue Engineering

Chanul Kim[1], Junsu Yun[2], Padma Gopalan[2,3]*, William Murphy[1,2,4]*
[1]Department of Biomedical Engineering [2]Department of Materials Science and Engineering, [3]Department of Chemistry, [4]Department of Orthopedics and Rehabilitation, University of Wisconsin–Madison

Summary

Plants are sustainable sources as they are abundant in nature and can be used as a tissue culture scaffold after decellularization. Decellularized plants are comprised of biocompatible materials such as cellulose, hemicellulose, and lignin. In addition, they have highly porous structures with pre-vascularized channels, which have the potential for efficient oxygen and fluid transportation throughout the structure. Despite many studies on decellularized plants, their material properties need to be understood more. When cells are cultured on the materials, their behaviors are influenced by the properties of the materials. Thus, it is essential to comprehend the physical and chemical properties of the materials and the interactions between cells and materials. In this work, we studied decellularized monocot plant materials' physical and chemical properties to understand their compatibility in tissue engineering. Surface chemistry and topography were analyzed since they provide cell surface interactions such as cellular attachment, proliferation, and differentiation [1]. Then, microporosity was measured since it allows for the movement of nutrients and waste in and out of the scaffold. Lastly, plant fiber composition is measured. Plant fiber composition correlates with mechanical properties, one of the important properties of scaffolds; mechanical properties such as plants' tensile strength and stiffness depend on these compositions [4].

Introduction

Paradigm of Tissue Engineering

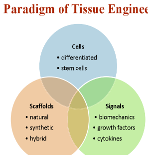

3D Scaffold
To serve complex functions (fill defect; provide structural support; take on mechanical responsibility; provide instructive signals) to guide cell behavior with spatial and temporal controls of materials and structural properties.

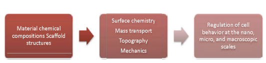

Decellularized Plant Leaf Material

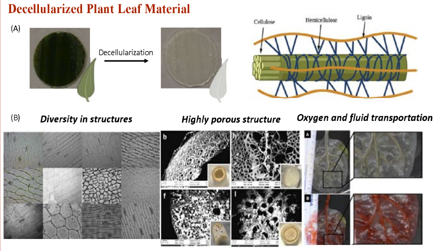

Fig 1. (A) Cell wall structure that was left after the removal of the cellular component of the plants throughout the decellularization process. (B) Plant leaf material has several advantages over conventional materials. Plant materials are sustainable and are made up of biocompatible materials such as cellulose, hemicellulose, and lignin. Highly porous structures with pre-vascularized channels of the material enable efficient oxygen and fluid transportation throughout the biomaterial [2, 3].

Decellularized plant material characterization

Decellularization of plant tissue

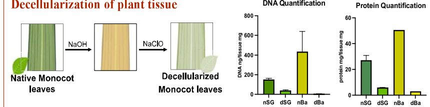

Fig 2. Schemes of decellularization process of monocot leaves. Decellularized sorghum and banana samples showed significantly less DNA and protein compared to native Sorghum samples.

Surface chemistry - Fourier-transform infrared spectroscopy (FTIR)

Fig 3. The surface chemistry of native and decellularized sorghum leaf material was assessed by FTIR, detecting a signal difference in 1200-1800 and 2300 cm^{-1} wavenumber.

Microporosity – Water uptake Test

$$WU\% = \frac{(W_o - W_s)}{W_s} * 100$$

	Thickness(mm)	diameter(mm)	Volume(mm^3)
dSG	0.13	12	14.703
dBa	0.41	8	20.609

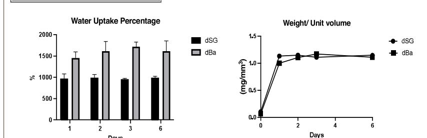

Fig 4. Water uptake analysis was done to determine the water-retaining capacity of plant materials. The Banana leaf showed a higher water uptake % since the Banana sample is 1.5 times thicker than Sorghum samples. However, when we calculated how much the samples could uptake water in their sample unit volume, the value of the both samples showed similar values.

Surface Topography – Scanning Electron Microscopy (SEM)

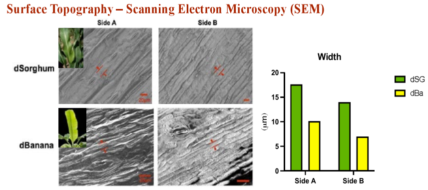

Fig 5. The monocot leaves showed parallel topography with a micro-pattern. The width of the dBanana material showed smaller width on both sides of the sample compared to that of the dSorghum material.

Plant fiber composition analysis

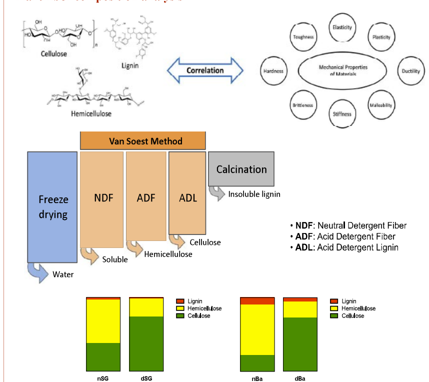

Fig 6. Plant fiber composition was determined using Van Soest Method. Ground and freeze-dried samples were treated with detergent in each step and calcinated in a crucible to isolate plant leaf chemical components in the order of hemicellulose, cellulose, and lignin. Decellularization significantly removes hemicellulose content percentage while slightly reducing lignin content [4, 5].

Conclusion

- Decellularization process using NaOH and NaClO significantly reduced cellular and protein components of plant leaf material regardless of plant species.
- Decellularization modifies the surface chemistry of the plant leaf material.
- Both decellularized sorghum and banana leaf material uptake fluid about twice the amount of their volume, allowing for fluid penetration with high microporosity.
- Surface topography of monocot plant species shows parallel micro-patterning on both sides of the surface, which can be useful for controlling cellular alignment.
- Decellularization significantly removes hemicellulose content percentage while slightly reducing lignin content.

Future work

- Determine the structural parameters of pores, including pore size, porosity, and pore interconnectivity, to figure out the ability of mass transport of our scaffold.
- Measure the mechanical properties of the scaffold using AFM for the indentation test and MTS machine for the uniaxial tensile test to further investigate the correlation between plant fiber composition and mechanical properties.
- Explore the differences in material characteristics by species and age.

References

1) Lanza RP, Langer RS, Vacanti J, Atala A, eds. Principles of Tissue Engineering. Academic Press, an imprint of Elsevier; 2020.
2) Gershlak JR, Hernandez S, Fontana G, Perreault LR, Hansen KJ, Larson SA, Binder BY, Dolivo DM, Yang T, Dominko T, Rolle MW. Crossing kingdoms: Using decellularized plants as perfusable tissue engineering scaffolds. Biomaterials. 2017 May 1;125:13-22.
3) Fontana G, Gershlak J, Adamski M, Lee JS, Matsumoto S, Le HD, Binder B, Wirth J, Gaudette G, Murphy WL. Biofunctionalized plants as diverse biomaterials for human cell culture. Advanced healthcare materials. 2017 Apr;6(8):1601225.
4) Karimah A, Ridho MR, Munawar SS, et al. A review on natural fibers for development of eco-friendly bio-composite: characteristics, and utilizations. Journal of Materials Research and Technology. 2021;13:2442-2458.
5) Viel M, Collet F, Prétot S, Lanos C. Hemp-Straw Composites: Gluing Study and Multi-Physical Characterizations. Materials (Basel). 2019;12(8):1199. Published 2019 Apr 12.

Acknowledgements

This research was funded by the National Science Foundation (NSF DMR 1709179) and the Wisconsin Alumni Research Foundation. The authors acknowledge support from staff and the use of equipment at the Materials Science Center at UW-Madison (NSF DMR-1121288 and DMR-1720415).

Development of Nanoparticle Inducing Device Through ML

Gawon Lim, Donggu Lee, Minkyu Kim, Seungjoon Heo, Yunsu Han, Inseo Hwang, Jisoo Kang, and Jaehong Park
University of Illinois, Urbana-Champaign, IL 61820, USA

I. INTRODUCTION

Nanoparticle-based treatments have emerged as a promising alternative to traditional medical treatments such as surgery, radiation, and chemotherapy, due to their potential to minimize side effects. One of the most critical factors for the success of these treatments is their targeting accuracy, which ensures that they reach the desired cells or tissues in the body. To address this challenge, researchers have proposed a nanoparticle-inducing device (NID) that utilizes a magnetic targeting method, thus enhancing the delivery functionality of nanoparticles and potentially improving the accuracy of treatment in various medical applications (Lee, 2017). This paper aims to further develop NID technology through machine learning methods.

II. PROPOSED NID PROTOTYPE

A. Hardware Design and Implementation

For the experiment, instead of using blood and nanoparticles, water and Iron Oxide (Fe_3O_4) were used for better-quality of data. The modified prototype of NID consists of an injection device, a moving bed, and C-arm. The injection device is responsible for applying fluid pressure to the tubes that are connected to the moving bed. A moving bed allows the tube to be positioned at the rotating center of the C-arm for nanoparticle induction experiments. The C-arm with neodymium magnets and the rotating motor generates various internal magnetic field conditions in the targeting area, depending on the speed and pattern of rotation. The optical density sensor was placed right above the moving bed to get the concentration of iron oxide inside the tube.

B. Software and Machine Learning

To optimize the NID, a machine learning approach utilizing data from an optical sensor was employed. During the given time, the device was programmed to find the optimal rotation pattern and speed through reinforced learning. This was done by rewarding the system when the change of concentration of Iron Oxide (Fe_3O_4) was greater.

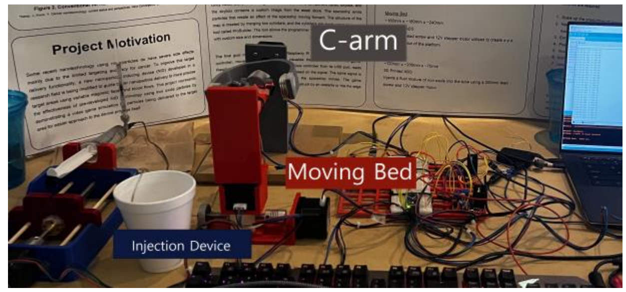

Figure 1: NID

III. EXPERIMENT AND DISCUSSION

Experiment was conducted using 2 Neodymium Magnets (5000 Gauss) ~11cm apart rotated 90° every 2 seconds. Throughout the process it was found that generated magnetic flux induced the Iron Oxide (Fe_3O_4) to a significant degree. However, it was challenging to achieve accurate outcomes through reinforcement learning. The continuous increase in Iron Oxide (Fe_3O_4) concentration led to unintended displacement of the device caused by the magnetic force. This prevented the device from obtaining consistent data from identical settings, ultimately resulting in unsuccessful learning.

The experimental setup in the figure lacks intermediary layers and does not consider crucial factors like fluid density and blood vessel structure. However, it demonstrated the potential of using machine learning to optimize nanoparticle-based treatments. Future research should create sustainable and enhanced test configurations that better emulate the complexities of the human body for accurate evaluation.

REFERENCES

1. A Lee, Chongmyeong, et al, “Nanoparticle Inducing Device for Effective Drug Delivery System,” Journal of Biomedical Engineering Research, Vol. 38, No. 3, pp. 102–110, 2017.

Modulating the corticospinal excitability using various non-invasive brain stimulation techniques

Hakjoo Kim[1], Yuming Lei[1], David L. Wright[1]
[1]Motor Neuroscience Laboratory, Texas A&M University

I. INTRODUCTION

The number of studies using non-invasive brain stimulation (NIBS) techniques, such as transcranial direct current stimulation, transcranial magnetic stimulation (TMS), and transcranial-focused ultrasound stimulation, continues to increase in basic and clinical research. NIBS techniques have been shown to modulate the excitability of the corticospinal tract, which is the pathway connecting the motor cortex to the spinal cord and controls voluntary movements. In this paper, the effects of various NIBS techniques on human corticospinal excitability will be discussed.

II. METHODS

A. Participants

In Experiment 1, single- and paired-pulse TMS (ppTMS) data from 21 undergraduate students were analyzed. In a second experiment, TMS theta burst stimulation was also administered to five undergraduate students. Before participating in either study, all participants provided written informed consent approved by the Texas A&M University Institutional Review Board.

B. Transcranial Magnetic Stimulation (TMS)

Single-pulse TMS was administered at the left primary motor cortex (M1) and induced motor-evoked potentials (MEPs) to assess corticospinal excitability. For ppTMS, stimulation at the supplementary motor area (SMA) occurred 7 ms prior to stimulation at M1. Single and ppTMS were administered randomly in a single block of trials (15 ppTMS at SMA and M1; 15 single-pulse TMS at M1) (Arai et al., 2012). For TBS in Experiment 2, intermittent TBS (iTBS) or continuous TBS (cTBS) was administered at SMA between baseline and post-measures (Huang et al., 2005).

C. Electromyography (EMG)

TMS-induced MEPs were recorded from the right first dorsal interosseous (FDI) muscle. EMG signals were sampled at about 5 kHz, amplified, and filtered.

III. RESULTS AND DISCUSSION

The conditioned stimulus (SMA prior to M1 stimulation) induced larger MEPs compared to the unconditioned stimulus only (M1 only) ($p = .0042$) (Fig. 1A). Application of iTBS at SMA facilitated MEPs, whereas cTBS at SMA inhibited MEPs (Fig. 1B).

Congruent with the proposed role for SMA during motor planning, these data demonstrate that the ongoing activation status at SMA has an impact on the excitability of the motor cortex.

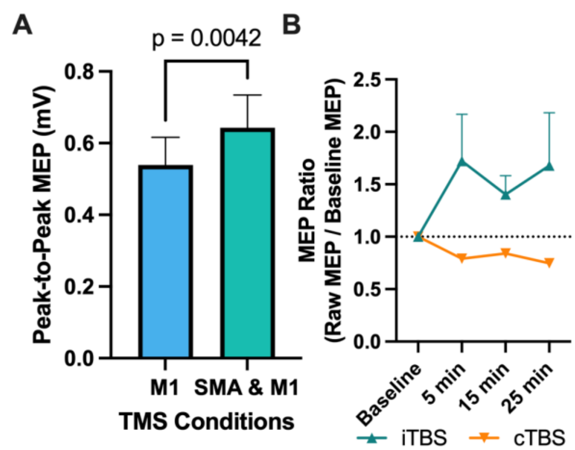

Figure 1: Effects of different TMS on MEPs. (A) ppTMS at SMA and M1. (B) iTBS and cTBS at SMA.

ACKNOWLEDGEMENTS

This work was supported by THE SYDNEY AND J.L. HUFFINES INSTITUTE FOR SPORTS MEDICINE AND HUMAN PERFORMANCE.

REFERENCES

1. Arai, N., Lu, M. K., Ugawa, Y., & Ziemann, U., "Effective connectivity between human supplementary motor area and primary motor cortex: a paired-coil TMS study," *Experimental brain research*, 220, 79-87, 2012.
2. Huang, Y.-Z., Edwards, M. J., Rounis, E., Bhatia, K. P., & Rothwell, J. C., "Theta Burst Stimulation of the Human Motor Cortex," *Neuron,* 45, 2, 201-206, 2005.

Organic Synthesis Reactions on Digital Microfluidic Device

Hyejin Moon[1], Junha Jeon[2]
[1]Meachinal and Aerospace Engineering, [2]Chemistry and Biochemistry, University of Texas at Arlington

I. ABSTRACT
This paper presents a microfluidic organic chemical reaction using an electrowetting-on-dielectric (EWOD) digital microfluidic (DMF) device. It demonstrates the promising potential of EWOD DMF as the high-data-throughput organic chemical reaction platform toward drug discovery and development.

II. INTRODUCTION
Although microchannel reactors have advantages such as fast reaction and automation capabilities [1-3], they suffer from limitations such as material incompatibilities, clogging of the channels by solid products, and cross-contaminations. EWOD digital microfluidic platforms can be an alternative and/or complement to microchannel reactors because it handles fluids in discrete droplet format which eliminates the need of mechanical pumps, cross-contamination, and clogging. EWOD devices are chemically inert and compatible with organic solvents. However, most organic solvents are non-polar, thus they are not movable in EWOD device. A simple solution without any modification of device architecture is needed.

II. METHODS
A. Engine-and-cargo system
An engine-and-cargo system is a compound droplet of two immiscible fluids. An engine refers to the fluid that has electrowetting properties. A cargo is the one without electrowetting properties. As illustrated in Figure 1(a), the motion of an engine droplet by electrowetting operation leads motion of an entire compound droplet, thus fluidic functionalities of cargo droplet, too.

B. Experimental
The electrowetting motion of an engine droplet generated a cargo droplet (A) and a polar reactants droplet (B). Merging droplets A and B initiated the esterification reaction. The reaction yield data were obtained by GC-MS. Total 60 reactions in 21 different conditions of esterification were carried out on-chip as shown in Figure 1(b).

III. RESULTS
The on-chip esterification reaction conversion data is shown in Figure 1(c). This result suggests that esterification with non-polar solvent gives higher yield than with polar counterpart. It suggests that the higher concentration of DMAP resulted better yield, but no higher than 1.0 mol%.

(a)
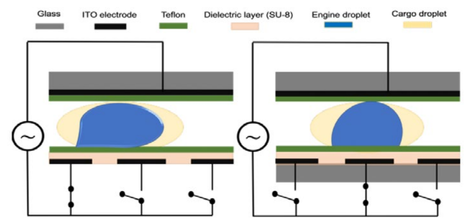

(b)

(g) Design of Experiment

Configuration / Reaction Characterization	Engine	Cargo solution			Other reactant		Quenching agent	Reaction time (s)
		Catalyst (Loading)	Reactant	Solvent	Reactant	Solvent		
Kinetic Study	$[bmim]PF_6$	DMAP (0.5 mol%)	menthol, Et_3N	toluene	Ac_2O	toluene	$NaHCO_3$	10 , 20 , 30 , 40, 50, 60, 70, 80, 90
Solvent Screening	$[bmim]PF_6$	DMAP (0.5 mol %)	menthol, Et_3N	toluene, dioxane, DMF, DCE	Ac_2O	toluene, dioxane, DMF, DCE	$NaHCO_3$	30
Optimize Catalyst Loading	$[bmim]PF_6$	0.1 %, 0.5 1.0 1.5 mol%	menthol, Et_3N	toluene	Ac_2O	toluene	$NaHCO_3$	30
Parallel esterification reactions	$[bmim]PF_6$	DMAP (0.5 mol%)	menthol, benzyl alcohol, phenol | Et_3N	toluene	Ac_2O	toluene	$NaHCO_3$	30

(c)
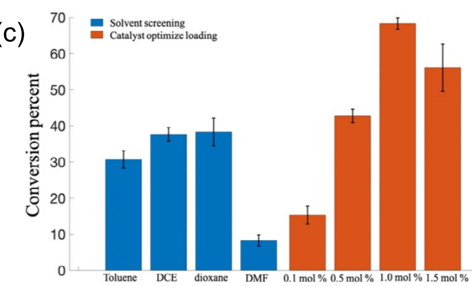

Figure 1: (a) Engine-and-cargo system, (b) conditions of all reactions tested in this study, and (c) conversion of on-chip esterification reactions.

REFERENCES
1. P. W. Miller et.al., “Rapid formation of amides via carbonylative coupling reactions using a microfluidic device,” *Chem. Comm.*, 546-548, 2006.
2. M. Torabinia et.al., “Electrochemical model to predict the movability of liquids in an electrowetting-on-dielectric microfluidic device,” J. App. Phys., 123, 15492, 2018.

Trans-Golgi protein TVP23B regulates host-microbe interactions via Paneth cell homeostasis and Goblet cell glycosylation

Ran Song, Bruce Beutler, Emre E. Turer

Center for the Genetics of Host Defense, University of Texas Southwestern Medical Center, Dallas, Texas, USA.

I. SUMMARY

A key feature in intestinal immunity is the dynamic intestinal barrier, which separates the host from resident and pathogenic microbiota through a mucus gel impregnated with antimicrobial peptides[1]. The mechanisms underlying the maintenance and function of this intestinal barrier are not completely understood. Using a mouse forward genetic screen for defects of intestinal homeostasis, we have found a mutation in *Tvp23b*, which conferred susceptibility to chemically induced and infectious colitis. Golgi apparatus membrane protein TVP23 homolog B (TVP23B) is a transmembrane protein conserved from yeast to humans. We found that TVP23B controls the homeostasis of Paneth cells and function of goblet cells *in vivo*. As a result, *Tvp23b*$^{-/-}$ mice displayed decreased barrier function and a loss of host-microbe separation. TVP23B-deficient colonocytes have a loss of core-3 O-glycosylation of colonic proteins, which is the major O-glycosylation present on gel forming mucins. TVP23B binds with another Golgi protein, YIPF6, which is similarly critical for intestinal homeostasis. The Golgi proteomes of YIPF6 and TVP23B-deficient colonocytes have a common deficiency of several critical glycosylation enzymes, including those necessary for core-3 glycosylation of mucins. Overall, TVP23B is necessary for the formation of the sterile mucin layer of the intestine and its absence disturbs the balance of host and microbe *in vivo*.

II. Results

A. TVP23B deficiency leads to colitis susceptibility

Tvp23b$^{-/-}$ were susceptible to DSS challenge, exhibiting greater than 20% weight loss by day 8 of treatment.

B. TVP23B required for Paneth cell and goblet cell form and function

C. TVP23B is essential for host-microbial segregation and intestinal glycosylation

Tvp23b$^{-/-}$ colons have a thinner, more penetrable mucus layer, which impacts host-microbe interactions. This appears to result from a primary defect in glycosylation.

D. TVP23B forms a complex with the Golgi protein YIPF6 and TVP23B and YIPF6 regulate the Golgi Proteome including B3GNT6

III. Figures

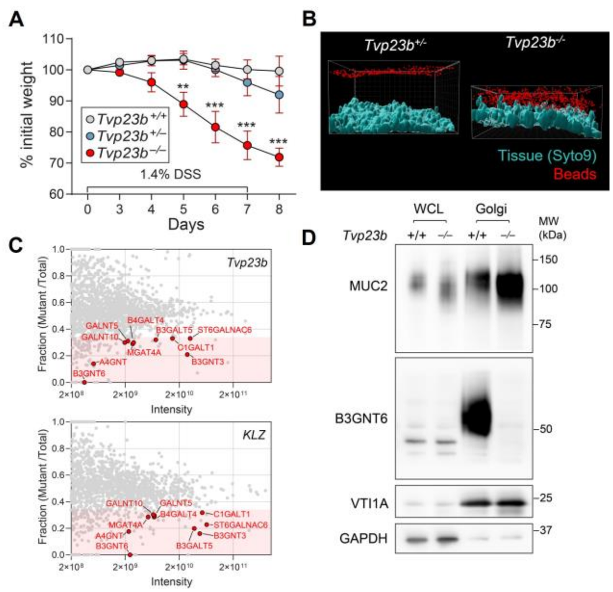

TVP23B is essential for host-microbe segregation and intestinal homeostasis maintenance by controlling intestinal glycosylation. (A) Weight loss analysis of mice of *Tvp23b*$^{+/+}$, *Tvp23b*$^{+/-}$, and *Tvp23b*$^{-/-}$ after DSS treatment. (B) Representative confocal z-stacks showing x/z-axis cross sections of tissue obtained from *Tvp23b*$^{+/-}$ and *Tvp23b*$^{-/-}$ littermates; tissue (blue), 1-μm beads (red). (C) Composite proteome of Golgi enriched fractions from *Tvp23b*$^{-/-}$ and *Yipf6*$^{Klz/Y}$ colonocytes compared to littermate control. (D) Immunoblot analysis of B3GNT6 in Golgi enriched fractions from *Tvp23b*$^{-/-}$ samples.

REFERENCES

1. Johansson, M., Hansson, G. Immunological aspects of intestinal mucus and mucins. *Nat Rev Immunol* 16, 639–649 (2016).

Effects of collagen fiber alignments in regulating osteoblasts and mineralization

Hyejin Yoon[1], **Jungwoo Lee**[1]
[1]Molecular and Cellular Biology Graduate Program, University of Massachusetts, Amherst

I. ABSTRACT
The structure and composition of the extracellular matrix are known to regulate tissue-specific cellular processes. Osteoblasts on the bone surface deposit collagen fibers and minerals in a sequential manner to form mature lamellar bone layer-by-layer. While the pre-established native collagen osteoid on the bone surface plays a critical role in regulating osteoblast to deposit new bone tissue, detailed investigation has been limited due to the lack of relevant biomaterial platforms. Recently, we have developed an osteoid-inspired demineralized bone paper (DBP) which retains the intrinsic complexity of lamellar collagen and is optically transparent facilitating microscopic imaging. DBP preserves the collagen alignment found in native bone which can be controlled depending on sectioning direction. Here, we report the effects of lamellar collagen fiber orientation on regulating osteoblast adhesion, growth, and mineralization using DBP.

II. Materials and Methods
frozen bovine femur blocks were subjected to demineralization using cyclic pressure in 1.2 N hydrochloric acid, which facilitated the penetration of the acidic solution. Subsequently, the demineralized bone was cryosectioned into two directions: a vertical section characterized by parallel lamellae structure, and a transverse section exhibiting concentric lamellae structure. To investigate the essential role of collagen as a template for mineral deposition, DsRed osteoblasts were cultured on TCP, vDBP, and tDBP in osteogenic differentiation medium. Fluorescent calcein staining revealed parallel mineral deposition on vDBP and concentric deposition on tDBP. Further characterization was conducted through thermal decomposition and SEM, confirming the alignment-dependent mineral structure.

III. Results and Discussion
Vertical and transverse sections of demineralized bovine compact bone generate concentric uniaxially aligned collagen structures on DBP that have significantly different optical and mechanical properties (Fig. 1A). Osteoblasts derived from DsRed reporter mice showed different growth kinetics, adhesion, and mineralization between vertical and transverse DBPs. Mineral deposition on DBP was quantitatively measured by fluorescent calcein (Fig. 1B), colorimetric alizarin red staining and scanning electron microscopy. These results reveal that the underlying collagen structure directs the amount of osteoblast mineral deposition and mineral growth pattern (Fig. 1C). Taken together, these observations suggest that the alignment of pre-existing lamellar collagen plays an important role in regulating osteoblasts and their subsequent formation of structural bone tissue. We anticipate that DBP will allow investigation of many aspects of bone extracellular matrix-related skeletal development and diseases.

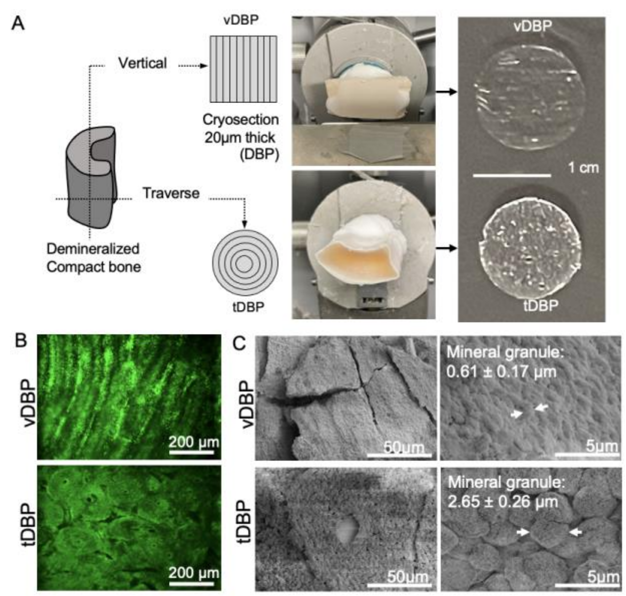

Figure 1: Morphological characterization of mineral deposition between tDBP and vDBP.
(A) Demineralized bone paper sectioned into 20 μm sheets in vertical and transverse directions. (B) Fluorescent calcein staining images of osteoblastic deposited minerals on tDBP and vDBP after 3 weeks of culture in osteogenic differentiation medium. **(C)** Scanning electron microscopy images of osteoblast deposited minerals on vDBP and tDBP with characterized mineral granule sizes (n=50).

Blood compatibility assessment of biomaterial surface chemistries to mitigate intrinsic coagulation pathway activation

Kyung-Hoon Kim[1], and Buddy D. Ratner[1,2]
[1]Department of Bioengineering, University of Washington, Seattle, WA, United States
[2]Department of Chemical Engineering, University of Washington, Seattle, WA, United States

SUMMARY
We assessed the blood compatibility of biomaterials for the intrinsic coagulation pathway to improve the understanding of how the protein-surface interactions vary across different surface chemistries. Intrinsic pathway is a dominant thrombus formation mechanism at the venous shear flow, relatively lower shear rate compared to the arterial flow. The trigger of intrinsic pathway is Factor XII (FXII) adsorption, leading to thrombin generation and crosslinked fibrin clot formation. Two different characteristic biomaterials outperformed other commercial polymers; zwitterionic poly(carboxybetaine) surface; and radio frequency glow discharge (RFGD) plasma-polymerized fluoropolymeric surface.

Keywords: *blood compatibility, intrinsic pathway, zwitterionic polymers, plasma-polymerized fluoropolymers*

INTRODUCTION
Blood compatibility has been remaining as a major challenge in the field of biomedical engineering and clinical applications for several decades. Surface thrombus formation is critical for blood-contacting medical devices since it can cause many lethal side effects. Because thrombogenesis is a significant complication, we still do not have a perfect blood compatible surface, as well as not been reached to the consensus on blood compatibility. One strategy to address this complication necessarily brings up the consideration of different hemodynamic shear rates with tailored approaches for venous and arterial shear flow, as the dominant thrombus formation mechanism is different between high and low shear hemodynamic flow. Intrinsic coagulation system is predominantly governing the low shear condition, triggered by FXII adsorption and activation, leading to the thrombin generation and crosslinked fibrin clot formation (**Figure 1**). In contrast, high shear flow is primarily associated with extrinsic system, initiated by platelet aggregation with adsorbed fibrinogen.

Two promising groups of polymers have been demonstrating improved blood compatibility; zwitterionic polymers and fluoropolymers. Notably, they have very distinct wettability even though their improved blood compatibility. Zwitterionic polymers are hydrophilic, while fluoropolymers are hydrophobic because of low surface energy attributed to the strong carbon-fluorine bonds.
We have investigated blood compatibility, specifically in relation to the intrinsic pathway. We have scrutinized a range of biomaterial groups with the aim of enhancing our comprehension of the variance in molecular events during clotting across diverse surface chemistries. This study has highlighted two biomaterial groups that show promising results, each based on unique hypotheses. Firstly, zwitterionic surfaces are perceived as blood-compatible owing to their ultralow protein fouling characteristics. Fluoropolymers represent another group studied in this research. We focused on RFGD plasma-polymerized hexafluoropropylene (ppC3F6) surfaces, which exhibit distinctive properties against proteins that may have a selective 'tight binding' affinity to the albumin, which may reduce the chance of FXII adsorption and activation. As we continue to examine these promising biomaterials, the knowledge gained will be instrumental in the development of better blood compatible surfaces. Such advances could potentially revolutionize the design of blood-contacting medical devices.

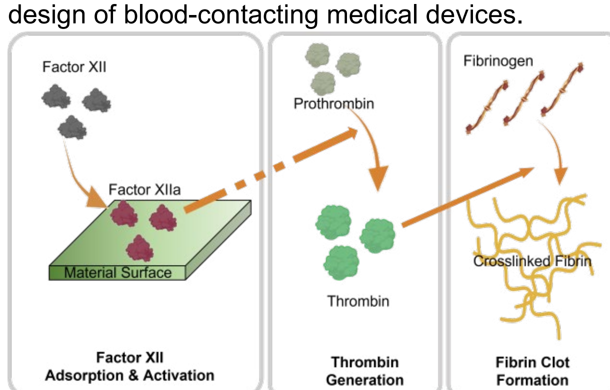

Figure 1. Schematic Illustration of Blood-Surface Interaction Intrinsic Pathway Activation

[SEED2023] Ectopic high endothelial venule-targeted nanodelivery for type 1 diabetes

Sungwook Jung*, Baharak Bahmami, Moufida Ben Nasr, Jing Zhao, Gianmarco Sabiu, Andy Joe Seelam, Said Movahedi Naini, Xiaofei Li, Vivek Kasinath, MacKenzie D. Williams, Ousama Rachid, Yousef Haik, Clive Wasserfall, Mark A. Atkinson, Jonathan S. Bromberg, Wei Tao, Paolo Fiorina, and Reza Abdi*

Transplantation Research Center and Renal Division, Brigham and Women's Hospital, Harvard Medical School, Boston, MA 02115, USA

Abstract

Targeted drug delivery systems hold the remarkable potential to improve the therapeutic index of diabetes medications. Herein, we developed a targeted delivery platform for type 1 diabetes (T1D) treatment using high endothelial venule (HEV)-targeted nanoparticles. We encapsulated anti-CD3 in PLGA nanoparticles (NPs) and conjugated mAb on the surface of NPs. Our mAb-NP localized to pancreatic lymph nodes (PLNs) and pancreata in NOD mice and encapsulation of anti-CD3 in MECA79-NP enhanced its delivery to these organs. Treatment of hyperglycermic NOD mouse model with mAb-anti-CD3-NP resulted in significant reversal of T1D, as compared to non-treatment, empty NP, and free anti-CD3. mAb-anti-CD3-NP treatment caused a marked increase of regulatory T (Treg) cells in pancreata. Our data suggested that ectopic HEV expressed in pancreata of T1D patients. Our study demonstrates that HEV-targeting nanovehicles constitute a novel drug delivery platform that can augment the effects of immunosuprression as well as reduce the inflammatory risk in treating T1D. Moreover, HEV-targeting therapeutics may be used as means by which drugs are delivered specifically to PLNs and pancreata, thereby prolonging the reversal of T1D patients.

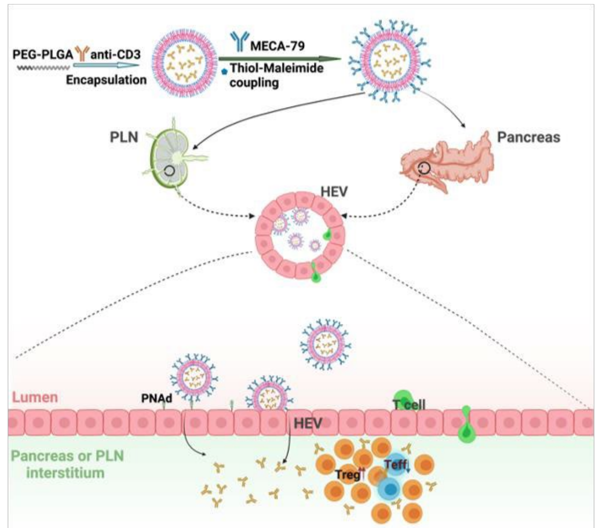

Figure 1: A scheme for the synthesis of MECA79-conjugated NP encapsulating anti-CD3 and the working mechanism of MECA79-anti-CD3-NP for T1D treatment.

[SEED2023] A Microengineered Organoid-on-a-Chip Model of Alveolar Development in the Human Lung

Sunghee Estelle Park[1], Dan D. Huh[1]
[1]Department of Bioengineering, University of Pennsylvania, Philadelphia, PA 19104

I. SUMMARY

Lung development is a complex process that involves highly coordinated, dynamic changes in the structural organization and mechanical environment of developing tissues. As a unique signature of this dynamic biomechanical process, the fetal breathing movements (FBMs) occur when contractions of the respiratory muscles cause the fetus to inhale and exhale amniotic fluid. However, current research on FBMs has focused primarily on early stages of lung development. To address this gap, we developed an approach by synergistically combining organoids with organ-on-a-chip technology. Our device enables integration of mechanical forces into human alveolar organoid culture to recapitulate FBMs and key aspects of the developing fetal lung at higher levels of tissue complexity.

II. MATERIALS AND METHODS

We developed a platform called the "alveologenesis-on-a-chip," which can mechanically actuate the extracellular matrix hydrogel scaffold during organoid culture (Fig. 1a). To establish alveolar organoid culture in this device, we inject a mixture of human pluripotent stem cell-derived alveolar type 2 (AT2) cells and a hydrogel precursor solution into the organoid culture chamber (Fig. 1b). Our platform allows for precise control of mechanical properties that accurately mimic FBMs through the vacuum chamber located at the bottom of the device (Fig. 1c).

III. RESULTS AND DISCUSSION

We first examined whether the alveologenesis chip supports extended development of alveolar organoids by culturing hPSC-derived AT2 cells in our device. hAT2s proliferated and self-assembled to form alveolar organoids within the first 10 days of culture. Interestingly, organoids stimulated with FBM-like mechanical forces from culture day 10 exhibited significantly increased size and number of buds, whereas organoids in the static chip showed arrested growth after 28 days (Fig. 2a). We analyzed the activation of mechanotransduction signaling pathways through immunocytochemical analysis and found that the continuous stretching motion allowed organoids to express significantly higher levels of MAPK and YAP/TAZ expression compared to organoids in static culture (Fig. 2b). Furthermore, we found that FBM-like mechanical forces result in extensive epithelial growth and branching morphology (Fig. 2c). By continuously culturing alveolar organoids on the alveologenesis chip for over a month, we observed significant formation of aerated space (Fig. 2d). In addition, the dynamic culture led to enhanced alveolar epithelial differentiation and maturation (Figs. 2f, 2g). Overall, these data suggest our advanced capabilities of i) engineering mechanical properties of the developing fetal lung and ii) using this model to study how mechanical forces regulate complex developmental program of epithelial differentiation and maturation for normal alveolar development and function.

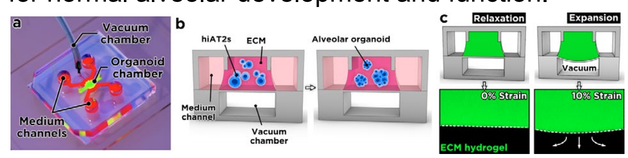

Figure 1: Alveologenesis-on-a-chip.

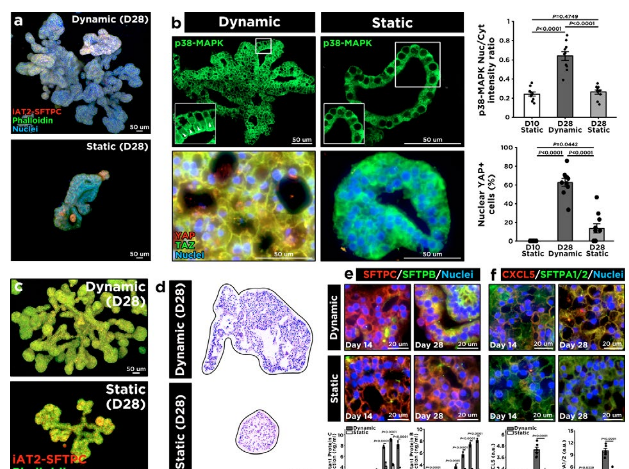

Figure 2: Effects of FBM-like mechanical forces.

ACKNOWLEDGEMENTS

This work was supported by the National Institutes of Health (NIH) (1DP2HL127720-01), the National Science Foundation (CMMI: 15-48571), the Ministry of Trade, Industry & Energy of the Republic of Korea and the University of Pennsylvania.

Injectable Lignin Composites to Improve Neovascularization and Healing of Diabetic Wounds

Jangwook P. Jung[1], Swathi Balaji[2]
[1]Department of Biological Engineering, Louisiana State University, Baton Rouge, LA
[2]Department of Pediatric Surgery, Texas Children's Hospital & Baylor College of Medicine, Houston, TX

SUMMARY
Engineered biomaterials with multiple wound healing-promotive functions, including pro-angiogenesis, sustained oxygenation and ROS (reactive oxygen species)–scavenging can promote wound healing. We engineered novel lignin (a natural antioxidant from lignocellulose)-based composites with ROS-scavenging and oxygen-releasing properties and hypothesized that they enhance neovascularization and attenuate fibrosis to promote diabetic wound healing.

A. Results and Discussion
Functional enrichment analysis revealed thyroid stimulating hormone as a key hub gene. The binding of thyroid hormone triiodothyronine (T3) through its nuclear receptors regulates the TGF-β/SMAD pathway. Our findings indicate a role for lignin composites in governing TGF-β signaling to attenuate fibrotic responses of fibroblasts[1,2]. The engineered lignin composites promoted granulation tissue deposition and $CD31^+$ capillary lumen density at d7 in full thickness db/db skin wounds. Quantification of VEGF expression in the homogenized wound tissue showed an increase in the VEGF expression at d7, suggesting dermal angiogenesis is promoted by the engineered lignin composites in diabetic wounds. Interestingly, decreased HIF-1α expression was noted in the leading wound epithelium, with reduced expression of wound homogenates in the wounds treated with the engineered lignin composites. To determine the effect of the lignin composite treatment in db/db wounds, we assessed the remodeling at d14 post wounding. We noted visibly improved healing in the wounds treated with the engineered lignin composites from gross images, which was supported by the presence of a robust granulating wound bed in representative hematoxylin and eosin stained wounds sections, along with an increase in the $CD31^+$ lumens.

B. Conclusions
Our data showed that the dual function of antioxidation and oxygen production capacity of the lignin composites improved wound healing associated with enhanced neovascularization, representing new frontiers in improving diabetic wound healing by engineered biomaterials.

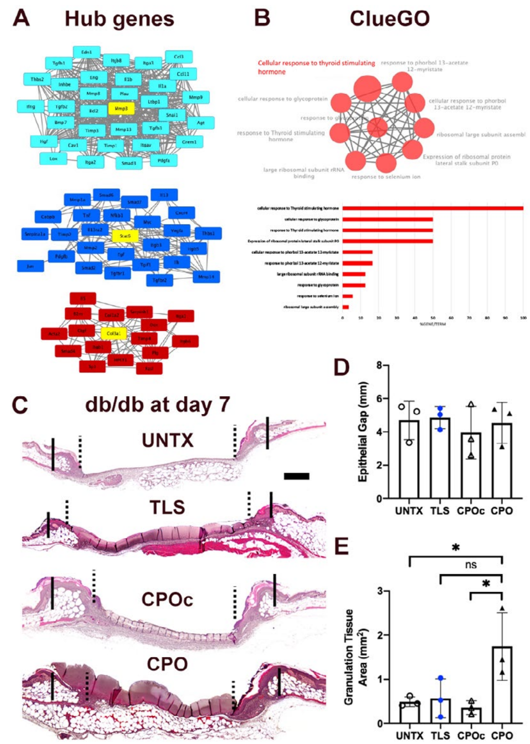

Figure 1. (A) A total of 88 genes[1] were used as input for WGCNA where three modules were identified. (B) Enrichment analysis of the entire gene list using ClueGO enrichment analysis showed overrepresentation of genes in cellular response to thyroid stimulating hormone: Bar chart represents the percentage of enriched genes in a term. (C) Wound healing in db/db mice. 6mm wounds in 8 wk old mice with blood glucose>350mg/dl were treated with lignin composites immediately after wounding. H&E staining of wound sections at day 7 show that compared to untreated (UNTX) wounds, wounds treated with engineered lignin composite had more granulation tissue. Quantification of epithelial gap (D) and granulation tissue area (E). Mean±SD, n=3 wounds per treatment group, *$p<0.05$ by one way ANOVA and Tukey's *post hoc* tests.

REFERENCES
1. Balaji et al. "Injectable Antioxidant and Oxygen-Releasing Lignin Composites to Promote Wound Healing," *ACS Appl Mater Interface* Vol. 15, pp.18639-18652, 2023. 2. Alonso-Merino et al. "Thyroid Hormones Inhibit TGF-β Signaling and Attenuate Fibrotic Responses," *PNAS* Vol. 113, pp. E3451-E3460, 2016.

Sex difference in the profile of extracellular bioactive lipids of conjunctival epithelial cells during allergic inflammation

Changrim Lee[1,2], **Darlene A. Dartt**[1,2]
[1]Department of Ophthalmology, Harvard Medical School, [2]Massachusetts Eye and Ear Infirmary

SUMMARY

Ocular allergy affects about 40% of the North American population, of which comorbidities include allergic rhinitis, asthma, eczema, food allergy, and eosinophilic esophagitis, making daily life even more debilitating[1]. In Korea, about 0.23 million people per month are treated for allergic conjunctivitis, which is one of the most common ocular allergies[2]. Allergen sensitization activates mast cells to release histamine to initiate an ocular allergic response. One of the ocular surface tissues affected is the conjunctival epithelium that lines the inside of the eyelids and covers the sclera, thus providing stability to the transparent cornea and anterior segment of the eye[3]. The conjunctival goblet cells (CGCs) that secrete mucins to wet and protect the ocular surface over-secrete mucins in response to histamine stimulation, which causes ocular surface instability and visual disturbance. To better understand the molecular basis of allergic response in CGCs, our research team has been investigating the role of bioactive lipid mediators, especially specialized pro-resolving mediators (SPMs) and proinflammatory mediators (PIMs), in the cellular response of CGCs during histamine-mediated allergic inflammation[4,5].

Our exciting preliminary data show, for the first time, that human primary CGCs biosynthesize SPMs and PIMs, load them into extracellular vesicles (EVs), and secrete them into the extracellular space during health and disease. Interestingly, the amount of SPMs dramatically increases in EVs secreted by female CGCs, but decreases in males during a histamine-mediated allergic response, suggesting that the sex of the CGCs results in the differences in CGC response. This is in line with our recent publication showing that human female CGCs increase intracellular Ca^{2+} concentration ($[Ca^{2+}]_i$) more sensitively (at lower histamine concentrations) than males[6]. To further investigate this observation, we hypothesize that in human CGCs there are sex differences in the cellular response to histamine-mediated allergic inflammation, which results in the differential secretion of SPMs and PIMs. We will test this hypothesis by quantifying and comparing the type and amount of SPMs and PIMs in EVs, and their time course of secretion in histamine-stimulated CGCs from both sexes (**Fig. 1**).

The success of this study will provide new insights into the bioactive lipid-mediated ocular surface protective mechanism generated by the conjunctiva and the basis for a tailored sex-dependent, lipid-based therapeutic approach in the management of vision-debilitating ocular surface diseases.

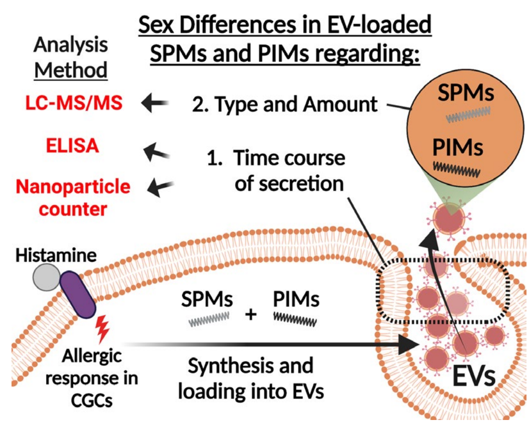

Fig 1. Schematic illustration of the proposed research. Sex differences in EV-loaded specialized pro-resolving mediators (SPMs) and proinflammatory mediators (PIMs) in terms of the (1) time course of secretion and (2) type and amount will be investigated in histamine stimulated human conjunctival goblet cells (CGCs).

REFERENCES

1. Dupuis P, *et al*. A contemporary look at allergic conjunctivitis. Allergy Asthma Clin Immunol. 2020;16:5.
2. Choi HG, *et al*. Changes in the Mean and Variance of the Numbers of Medical Visits for Allergic Diseases before and during the COVID-19 Pandemic in Korea. J Clin Med. 2022;11(15).
3. Craig JP, *et al*. TFOS DEWS II Definition and Classification Report. Ocul Surf. 2017;15(3):276-83.
4. Hayashi D, *et al*. Role of histamine and its receptor subtypes in stimulation of conjunctival goblet cell secretion. Invest Ophthalmol Vis Sci. 2012;53(6):2993-3003.
5. Serhan CN. Discovery of specialized pro-resolving mediators marks the dawn of resolution physiology and pharmacology. Mol Aspects Med. 2017;58:1-11.
6. Yang M, *et al*. Sex-based differences in conjunctival goblet cell responses to pro-inflammatory and pro-resolving mediators. Sci Rep. 2022;12(1):16305.

Creating a Therapeutic Application Plan through Research on Rare Genetic Disorders

Bokyeong Song, Myung-Jin Kim and Yonghwan Kim,
Department of Biological Sciences, Research Institute of Women's Health and Digital Humanity Center, Sookmyung Women's University, Seoul 04310, Republic of Korea

I. SUMMARY

Rare genetic diseases are a group of disorders that affect a small percentage of the population and are caused by variations in genes. The research on rare genetic diseases is crucial as it can provide insights into the mechanisms of the disease, improve diagnostic methods, and lead to the development of targeted therapies. Moreover, studying rare genetic diseases can also provide opportunity to develop novel therapeutic strategy for common diseases as many of the causative genetic variants lead to neomorph phenotypes. Recently, we have identified causative genetic variants leading to rare genetic skeletal dysplasia including a weak bone disorder and a heterotopic ossification. Firstly, the weak bone disorder is a rare, recessive skeletal dysplasia characterized by short stature, facial dysmorphism, and aberrant radiographic findings of the spine and long bone metaphysis. Using whole-exome sequencing (WES), we identified bi-allelic *MBP1* mutations in 10 individuals with the genetic disorder. Secondly, the heterotopic ossification, a pathological condition whereby soft tissues transform into skeletal bones, is rare but debilitating disease without any effective treatment. Here we report that *AVBP* is a previously unidentified genetic contributor of the congenital heterotopic ossification. We show that a rare gain of function mutation in *AVBP* leads to congenital heterotopic ossification. By elucidating molecular mechanism of pathophysiology, we would like to translate the findings to cure common diseases, which we will share the recent progress in the UKC meeting.

II. Results

A. Depletion of MBP1 leads to drug resistant cancer cells

MBP1 plays a diverse role in genome maintenance and replication. In the preliminary studies, we identified that biallelic mutations of MBP1 cause rare skeletal disorders presented with weak bone phenotypes. However, unexpectedly, we found that the MBP1 expression level is relatively high in various cancers, which implies that the MBP1 can be a therapeutic target for cancer therapy. In order to test the possibility, we established drug resistant HeLa cells of which the survival rate of the cells are severely decreased in the absence of MBP1 expressioin (Figure 1).

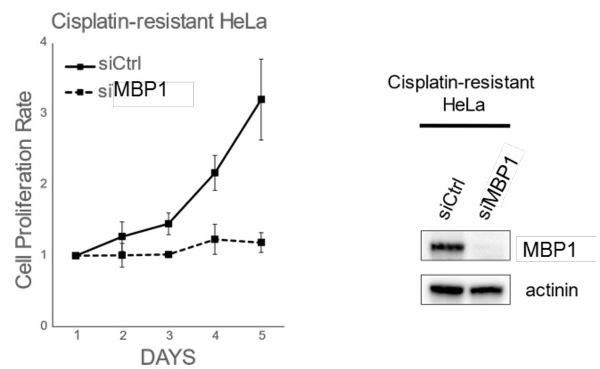

Figure1: Depletion of MBP1 leads to drug resistant cancer cells

B. Expression of mutant AVBP can be used to cure common diseases

Expression of the mutant form of AVMP in stem cells enhances multiple cellular differentiation, which can be used to cure various common diseases.

ACKNOWLEDGEMENTS

Sookmyung Women's University Research Grant, Research Institute of Women's Health and Digital Humanity Center at Sookmyung Women's University.

The Intervention of the Beta Amyloid Protein Dysfunction by Carbon Nanodots in Alzheimer's Disease

John Bang[1], Mikyoung Ji[1], Srivalli Mukkavilli[2], and Gordon Ibeanu[2]

[1]Department of Environmental, Earth & Geospatial Sciences, North Carolina Central University, Durham N.C.

[2]Department of Pharmaceutical Sciences, North Carolina Central University, Durham, N.C.

I. SUMMARY

Despite the focus of the treatment method development of Alzheimer's Disease has been on finding ways to remove the plaques and prevent plaque formation, more evidence indicates maintaining a normal Beta Amyloid (BA) metabolism[1] could be more relevant as a preventive measure or a treatment option. In our study, the hydrogen peroxide (H_2O_2) level was controlled by carbon nanodots (CNDs) in the presence of IMR-32 cells and Copper Nanoparticles(CuNPs), and the levels of aggregation of radicalized BA proteins were compared. Through this experiment, the roles of Reactive Oxygen Species and CNDs on BA aggregation were evaluated.

II. STUDY DESIGN, RESULTS, & CONCLUSIONS

A. Materials and Methods

Anti-DMPO Antibody assay was used for quantifying aggregated BA proteins in the presence of CuNPs and IMR-32 cells as a source of BA proteins. ELISA with primary and secondary antibodies was performed with Confocal imaging for confirmation of BA protein aggregation.

B. Results

The level of BA aggregation after protein radicalization was proportional to the level of CuNPs used, the main source of H_2O_2. The CNDs with different functional groups reduced the level of BA aggregation in a concentration-dependent manner. Aggregated BA proteins were observed in the presence of CuNPs and the level of aggregated proteins was reduced in the presence of CNDs. Different sizes of CuNPs smaller than 100nm didn't seem to make much difference in terms of the protein aggregation effects. Copper ions, compared to CuNPs, demonstrated comparable effects on BA aggregation.

C. Conclusions and Discussion

Quantification of aggregated BA proteins after radicalization is achievable by anti-DMPO antibody assay in a concentration-dependent mode. CuNPs used as a main source of ROS can induce aggregation of BA proteins from IMR-32 cells In Vitro conditions and lyophilized BA proteins. CNDs both in pristine form and with various types of functional groups carry a potential for their use in the treatment of AD as a ROS scavenger. Further investigation on the tuning method of CND's ROS controlling mechanisms will be able to provide potentially practical ways for CND application in the treatment of AD.

III. ILLUSTRATIONS

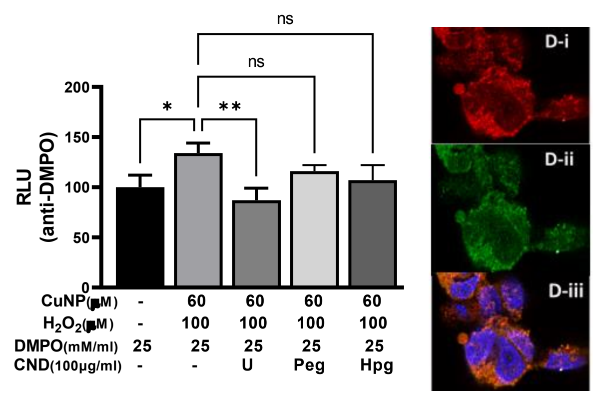

Figure 1: Intracellular BA protein aggregation and CND effects. Localization of DMPO Nitron adduct(D-i), Aggregated BA proteins (D-ii), and Hoechst test.

ACKNOWLEDGEMENTS

-NSF-EiR (Award #: 1832134).

-Drs. Ronald Mason (NIEHS Emeritus), Ashutosh Kumar (Altria Client Service), and Smritee Pokharel (BD) for technical support

REFERENCES

1. Heinz Hillen, "The Beta Amyloid Dysfunction (BAD) Hypothesis for Alzheimer's Disease " *Frontiers in Neuroscience*, Vol.13, 2019. doi.org/10.3389/fnins.2019.01154

Particulate Matter (PM) induced Beta Amyloid (BA) Protein Aggregation

Kevin Omar[1], Rodney Hawkins[1], Macie Bethea[2], Jeffery Shipman[2], Vijay Sivaraman[2], Mikyoung Ji[1], John Bang[1!],

[1]Department of Environmental, Earth & Geospatial Sciences, North Carolina Central University, Durham N.C.
[2]Department of Biological and Biomedical Sciences, North Carolina Central University, Durham, N.C.

I. SUMMARY

Alzheimer's Disease (AD) is one of the most debilitating illnesses that affect millions of people around the world[1]. The cause of AD is multifactorial including environmental effects that can build oxidative stress. One common causal mechanism is abnormal BA metabolism that induces the formation of increased levels of plaques[2], In this study, PMs from indoors and outdoors were tested by using BV2 microglial cells if they can induce oxidative stress leading to BA protein aggregation as well inflammatory responses (IL-6, TNF-a). Concentration-dependent inflammatory responses were observed for both indoor and outdoor PM extract. Nitrite-induced BA aggregation was PM concentration-dependent manner. Carbon nanodots were also used to see their efficacy in nitrite removal. The results indicate that PMs from both indoor and outdoor environments can induce BA protein aggregation and generate plaques. It is also noted that the BA aggregation process can be also influenced by the ROS scavenger like CNDs.

II. STUDY DESIGN, RESULTS, & CONCLUSIONS

A. Materials and Methods

PMs were collected from both indoor and outdoor. Stock solution for PM samples collected from both indoor and outdoor settings was prepared. Different concentrations of the diluted stock solution were used to BV2 cells for their inflammatory responses and Nitrie-induced Anti-DMPO Antibody assay which is an indicative value for the level of aggregated BA proteins. ELISA for quantifying aggregated BA proteins and Confocal for confirming the formation of aggregated BA proteins were conducted to obtain their responses.

B. Results

PMs from both indoors and outdoors caused inflammatory responses (IL-6, TNS-a). PMs also induced increased levels of Nitrite, LDH, and H_2O_2 in a concentration-dependent manner. CND's ROS scavenging effect was less prominent for Nitrite. Anti-DMPO assay, Confocal imaging with Hoechst indicated that PMs induce the aggregation of BA proteins in a concentration-dependent manner.

C. Conclusions and Discussion

PMs from both indoor and outdoor environment increases the oxidative stress levels in BV2 microglial cells in the form of nitrite formation. In both LPS-challenged and non-challenged conditions, BV2 cells showed increased inflammatory responses (IL-6 and TNF-a) after exposure to the PMs. Increased Oxidative Stress levels by the PMs influenced the aggregation level of BA proteins. CND's ROS scavenging role was less influential on nitrite compared to H_2O_2. Further analysis of the potential impacts of the PMs on AD is warranted.

III. ILLUSTRATIONS

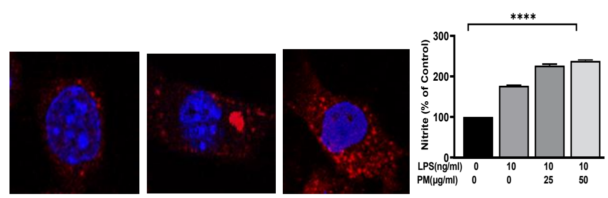

Figure 1: Confocal: BV2 microglial cells treated with PM for 24 hr. Cells were immuno-stained using an anti-DMPO antibody (red), and Hoechst (blue). Nitrite levels were measured by ELISA.

ACKNOWLEDGEMENTS

-NSF-EiR (Award #: 1832134).
-Drs.Jianjun Wei (UNC-G) and Smritee Pokharel (BD)
-Taste of Africa & Beth El Synagogue for sampling

REFERENCES

1. M. DeTure, D. Dickson, "The neuropathological diagnosis of Alzheimer's disease', Molecular Neurodegeneration. Vol14, 32, 2019.
2. Heinz Hillen, "The Beta Amyloid Dysfunction (BAD) Hypothesis for Alzheimer's Disease " *Frontiers in Neuroscience*, Vol.13, 2019. doi.org/10.3389/fnins.2019.01154

Polystyrene Microplastics and their GI Transmembrane Passage Capacity in Zebrafish Embryos

Majemite Iyangbe[1], TinChung Leung[2], Dereje Jima[3], John Bang[1‡]

[1]Department of Environmental, Earth and Geospatial Sciences, North Carolina Central University, N.C.27707
[2]Department of Biological and Biomedical Sciences, North Carolina Central University, N.C. 27707
[3]Center of Human Health and the Environment and Bioinformatics Research Center, North Carolina State University, Raleigh, N.C. 27606

I. SUMMARY

The use of plastic materials has received increased attention mainly due to their exposure-related potential to human health as well as ecological disruption issues. A recent study indicated that human plasma contains high levels of microplastic materials that can induce various types of pathological conditions1. However, it is not clear how microplastics (size smaller than 5mm), through various exposure mechanisms, end up showing up in the plasma. Our group began to investigate the relationship between transmembrane passing capacities and physical properties such as size, morphology, surface charges, and types of plastic polymers. The morphological effect of PS on the embryos was also sought. As a first step, Fluorescent-dyed polystyrene (PS), among five other subgroups of plastic polymers, of two different sizes and functional groups on the surface were tested on Zebrafish embryos of 3 – 7 days of. Visual localization of the fluorescent PS particles in Zebrafish embryos' GI tracks and other organs was taken for initial analysis.

II. Materials, Methods, Results, and Conclusions

A. Materials and Methods

Polystyrene (PS) FluoSpheres 1.0 μm size or FluoSpheres carboxylate-modified microspheres (PS-COOH) 1.0μm and 100nm sizes, with orange fluorescent (Ex/Em 540/560) were resuspended in zebrafish medium (0.3X Danieau's buffer). Zebrafish embryos (15 embryos/group) were exposed to PS nano- or micro-plastics from 3 days post-fertilization (dpf) to 7 dpf. Following exposure, embryos were washed and anesthetized with tricaine before imaging analysis.

B. Results

Microscopic imaging indicated that PS at the size of 100 μm stays inside the GI luminal space without crossing the membranes. The embryos with 3-7 dpf did not demonstrate any abnormal morphological development.

C. Conclusions and Discussion

We observed the fluorescent nano- and micro-plastics accumulated along the GI tract and were present in all 3 regions, the intestine bulb, the mid-intestine, and the posterior intestine regions. However, we did not observe fluorescent nano- or microplastics in another region of the zebrafish embryos. A possible reason is that the 1.0 μm size PS or PS-COOH and 100nm size PS plastics were not taken up from the GI tract to other tissues. Future studies are warranted with a focus on the effect of the smaller sizes of nano plastics with various surface conditions on transmembrane crossing potential. Further investigation into the behavioral characteristics of nano-range plastics is warranted.

III. ILLUSTRATIONS

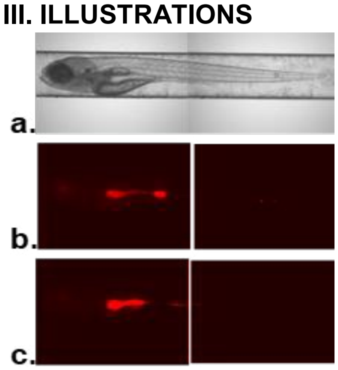

Figure 1: a) Brightfield Image of Zebrafish, b) PS iμm size at 200 μg/ml to Zebrafish 7 dpf, c) PS-COOH, 100nm size at 200 μg/ml to Zebrafish 7dpf

ACKNOWLEDGEMENTS

-NIEHS, Center of Human Health and Environment
-NSF-EiR (Award #: 1832134)

REFERENCES

1. H. Leslie, et al. "Discovery and quantification of plastic particle pollution in human blood". *Environment International*, Vol: 163, 107199, May 2022

Analysis of Clock-Controlled Genes (CCGs) in Human Intestinal Enteroids

Suengwon Lee[1], Danilo E Flores[2], Gang Wu[2], John Hogenesch[2], and Christian Hong[1]
[1]Department of Pharmacology & Systems Physiology, University of Cincinnati, Cincinnati, OH, USA.,
[2]Division of Human Genetics and Immunobiology, Center for Chronobiology, Department of Pediatrics, Cincinnati Children's Hospital Medical Center, Cincinnati, OH, USA.

I. Abstract

Since life has emerged on Earth, it has not been able to escape the environmental influence of the Sun, which creates diurnal cycles of approximately 24 hours. Hence, the behaviors of most living organisms are under the influence of 24-hour cycles, which are referred to as circadian rhythms. Previous studies established that most organisms possess molecular mechanisms that maintain endogenous circadian rhythms that entrain and adapt to their local environment regulating temporal organization of cellular and physiological functions from metabolism to sleep/wake cycles. In mammals, the circadian rhythm consists of master (suprachiasmatic nucleus in the hypothalamus) and peripheral (organs and tissues) clocks. However, recent findings indicate that peripheral clocks maintain circadian rhythms even in the absence of the master clock. Previously, we demonstrated that 3-dimensional mouse intestinal organoids or enteroids (*in vitro* mini gut) possess robust circadian rhythms [1, 2, 3]. In this report, we utilized biopsy-derived human intestinal enteroids (bHIE) to characterize clock-controlled genes (CCGs) and signaling pathways.

Our 48-hour time course RNA-Seq data were analyzed with RAIN algorithm to identify CCGs and phase set enrichment analysis (PSEA) to examine the circadian clock-dependent signaling pathways. Our analysis revealed the rhythmic patterns of more than 1700 CCGs and 146 rhythmic pathways, including metabolism, mRNA processing, cell cycle, cancer, and circadian clock. Thus, our findings suggest that the human patient-derived organoid model could be utilized to understand circadian rhythm in peripheral tissues, investigate the mechanisms of circadian-associated diseases, and explore potential therapeutic strategies using circadian medicine.

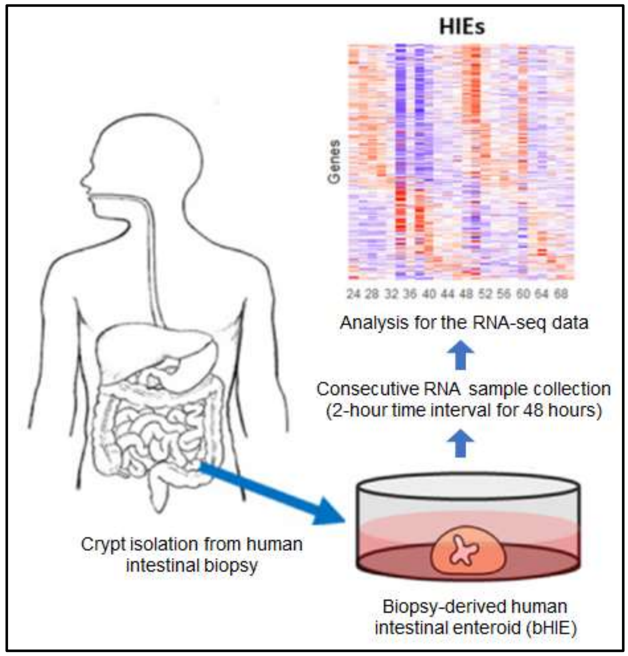

Figure 1. Schematic diagram of the study. The *in vitro* mini gut bHIEs were cultured and prepared for RNA-seq at every 2 hours over 48 hours. The image is cited from the previous article [2] and modified.

ACKNOWLEDGEMENTS

Biopsy-derived human intestinal enteroids (bHIEs) were provided by Noah Shroyer, PhD. from Baylor College of Medicine, Houston, TX, USA.

REFERENCES

1. Matsu-ura T et al., “Intercellular coupling of the cell cycle and circadian clock in adult stem cell culture,” Mol Cell 64: 900–912, 2016
2. Rosselot AE et al., “Ontogeny and function of the circadian clock in intestinal organoids,” EMBO J, 17;41(2):e106973, 2022
3. Moore, S.R., et al. “Robust circadian rhythms in organoid cultures from PERIOD2::LUCIFERASE mouse small intestine.” Dis Model Mech, **7**(9): p. 1123-30, 2014.

Toward Hyperplexed Immunohistochemistry using Hydrogel Staining, Chiral Nanoparticles, and Nanobodies

Kyung-Hak Choi[1], Woongsun Choi[1], Yoon Ho Lee[2], Hidde Ploegh[3], Kitea Nam[2]
[1]Noul Co., Ltd, Yongin-si, Gyeonggi-do, South Korea, [2]Dept. of Material Science & Engineering, Seoul National University, Seoul, South Korea, [3]Boston Children's Hospital & Harvard Medical School, Boston, MA, USA

I. INTRODUCTION

We present an on–going research project aiming to develop cancer profiling technology by employing hydrogel stamping staining, chiral gold nanoparticles and nanobodies. The technology is expected to provide highly multiplexed spatial information of cancer cells or tissues. To realize the technology, three breakthroughs should be made.

II. BREAKTHROUGHS-TO-BE-MADE

A. Chiral gold nanoparticles as signal reporters

According to particle size and shape, the chiral gold nanoparticles show distinct colors under the dark-field microscopy. Polarizing characteristics of chiral nanoparticles make the number of colors multiple, so that hyperplexed imaging can be implemented for immunohistochemistry.

B. Highly Specific Nanobodies with Strong Affinity

The affinity to specific protein biomarkers can be significantly enhanced by controlling the stability and orientation of nanobodies attached to the surface of nanoparticles.

C. Hydrogel Stamping for Immunostaining

Solution-free stain utilizing hydrogel-based stamping technology is being developed. The hydrogel contains nanobody-nanoparticle conjugates that can be released and absorbed by slightly squeezing it. This can lead faster staining and smaller amount of immunostaining reagents.

III. DISCUSSIONS

Nanoparticles can be easily aggregated each other. By applying surface treatment or controlling the size of the nanoparticles, it can reduce aggregations. Nanobodies are protein-based materials which can be degraded in the air at room temperature. For the prevention of the degradation, lyophilizing method for nanobody-nanoparticle conjugates should be developed.

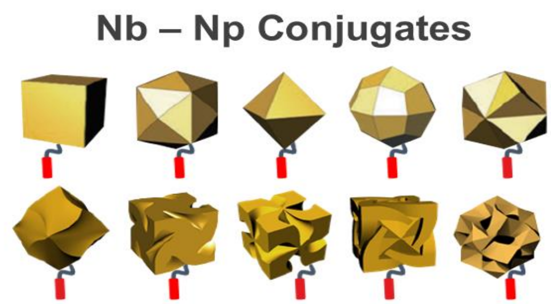

Figure 1: Nanobody-Nanoparticle Conjugates

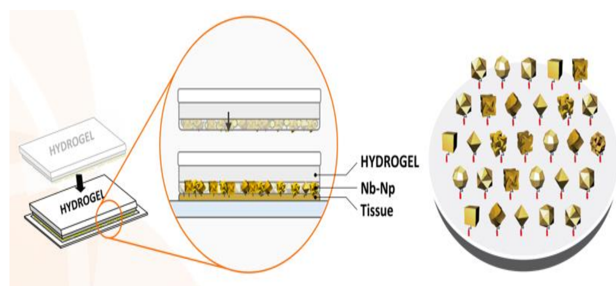

Figure 2: Hydrogel Immunostaining

ACKNOWLEDGEMENTS

This research is being supported by Korea Institute for Advancement of Technology grant funded by the Korea Government (MOTIE)(P0019783)

REFERENCES

1. H.-E. Lee, *et. al,.* Amino-acid- and peptide-directed synthesis of chiral plasmonic gold nanoparticles. *Nature,* Vol. **556**, pp. 360–365 2018
2. Y. J. Xie, *et al.*, Nanobody-based CAR T cells that target the tumor microenvironment inhibit the growth of solid tumors in immunocompetent mice, PNAS, Vol. 116, No. 16, pp. 7624-7631, 2019
3. J.-H. Choi, *et al.*, Hydrogel-Based Stamping Technology for Solution-Free Blood Cell Staining, *ACS Applied Materials & Interfaces,* Vol.13, No. 19, pp. 22124-22130, 2021

An AI-embedded and Fully Automated Device for Malaria Detection at Remote Setting

Kyung-Hak Choi[1], Chae Yun Bae[1], Younghoon Song[1], Young Min Shin[1]
[1]Noul Co., Ltd., Yongin-si, Gyeonggi-do, South Korea

I. INTRODUCTION

Malaria continues to be a severe and widespread disease with significant implications for global public health. Many malaria cases and fatalities, accounting for over 99%, transpire in low- and middle-income countries.

Microscopy, despite being the gold standard for malaria diagnosis, presents challenges in resource-limited and remote areas due to the lack of experts and insufficient laboratory infrastructure. To solve this problem, we introduce a deep learning embedded and fully automated diagnostic device for malaria detection that can be used in resource-limited remote settings.

II. DEVELOPMENT

A. Hydrogel Stamping Staining

Dye-containing hydrogel was developed. The dye can be released and absorbed by simply contacting hydrogel onto blood smears. A single-use cartridge facilitates three hydrogel patches containing eosin, methylene blue, and a buffer, respectively, all applied sequentially to the same location.

B. Digital Imaging System

For imaging malaria parasites within red blood cells, the optical system is equipped in the device with a 50x objective lens, providing a depth of field of less than 1μm and 10 different focal planes.

C. Embedded Convolutional Neural Network

Due to the limited resource of embedded hardware, we designed all neural network architectures with minimal computational complexity. For this, we opted for a semantic segmentation algorithm instead of a general object detection algorithm.

III. CLINICAL EVALUATION

The clinical evaluation of the device was assessed using 368 peripheral blood samples from patients with fever in Mzuzu, Malawi. The results were an overall percent agreement of 94.20%, positive percent agreement of 88.39%, and negative percent agreement of 98.95%.

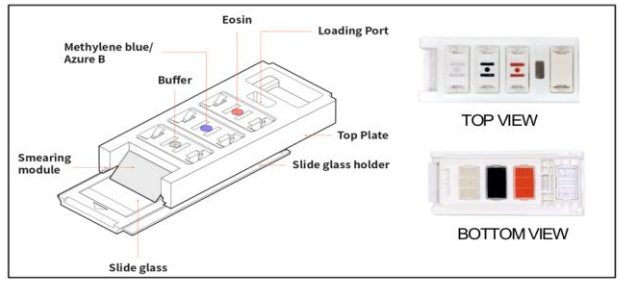

Figure 1: Embedded Deep Learning Algorithm

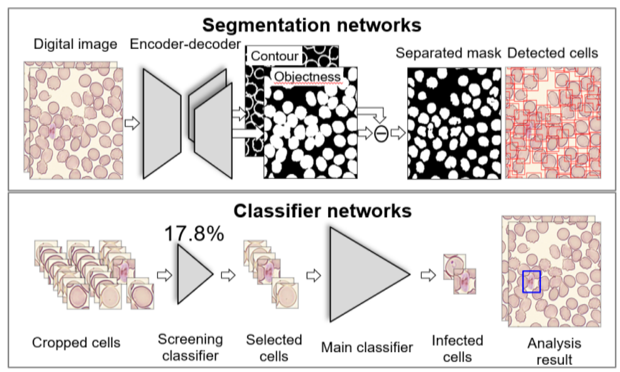

Figure 2: Embedded Deep Learning Algorithm

ACKNOWLEDGEMENTS

This work was supported by a grant of the Korea Health Technology R&D Project through the Korea Health Industry Development Institute, funded by the Ministry of Health & Welfare, Republic of Korea (grant number: HI18C1685).

REFERENCES

1. World Health Organization, World malaria report 2021
2. J.-H. Choi, *et al.*, Hydrogel-Based Stamping Technology for Solution-Free Blood Cell Staining, *ACS Applied Materials & Interfaces* Vol.13, No. 19, pp. 22124-22130, 2021
3. O. Bailo, *et Al.*, Red blood cell image generation for data augmentation using Conditional Generative Adversarial Networks, *IEEE/CVF Conference Proceedings*, pp. 1039-1048, 2019

Structural and biochemical characterization of the thiol-methyltransferase 1A and 1B

Taeyoon Jung[1], Drake Russell[1], Rheem Totah[1]
[1]University of Washington

Methyltransferase-like protein-7A and -7B (METTL7A and METTL7B) have been recently been identified as microsomal associated phase II methyl transferases that transfer a methyl group from S-adenosyl methionine to exogenous alkyl and phenyl thiols (Maldonato, Russell, & Totah, 2021). Both enzymes consist of 244 residues and share 60% sequence identity and 75% sequence homology. METTL7A (TMT1A) is potently inhibited by the historical microsomal thiol methyltransferase (TMT) inhibitor 2,3-dichloro-alpha-methylbenzylamine (DCMB), while the methylation activity of METTL7B (TMT1B) is not affected despite the high sequence homology and similar substrate specificity (Russell et al., 2023). In this work, we utilize AlphaFold generated models, binding site analysis software, and in silico small molecule binding prediction approaches to identify several unique residues in the active site that can explain the difference of DCMB inhibition in METTL7A and METTL7B.

Further more, two individual programs, DoGSiteScorer and AutoDock were used to identify active site in TMT1A and TMT1B and generated protein-ligand complex (Morris et al., 2009). Molecular dynamic (MD) simulation was performed for 50ns with the best interacting complex of TMT1A-SAM-DCMB and TMT1B-SAM-DCMB complex using GROMACS 2019. In TMT1A, we found three aromatic residues F39, F43, and Y47 that form pi bonds with DCMB. We then expressed and purified TMT1A triple mutant (F39L, F43L, and Y47S), and overexpressed in HeLa cells. Compared to the TMT1A wild type, TMT1A triple mutant is not inhibited by DCMB.

In this project, we first developed an in silico model to identify the residues that distinguish the active site in TMT1A and TMT1B, and identified three key residues that plays interacts with TMT inhibitor. We have proved our simulation model by purified TMT1A and TMT1A mutants which would help understanding of the DMPK properties of alkyl- or phenolic-thiol-containing therapeutics.

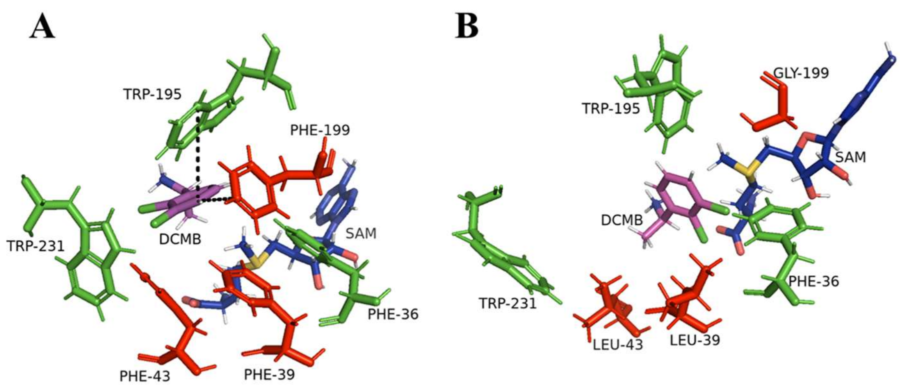

Figure 1. MD simulation results showed that residues in TMT1A form a parallel and T shape pi stacking

Maldonato, B. J., Russell, D. A., & Totah, R. A. (2021). Human METTL7B is an alkyl thiol methyltransferase that metabolizes hydrogen sulfide and captopril. *Sci Rep, 11*(1), 4857. doi:10.1038/s41598-021-84218-5

Morris, G. M., Huey, R., Lindstrom, W., Sanner, M. F., Belew, R. K., Goodsell, D. S., & Olson, A. J. (2009). AutoDock4 and AutoDockTools4: Automated docking with selective receptor flexibility. *J Comput Chem, 30*(16), 2785-2791. doi:10.1002/jcc.21256

Russell, D. A., Chau, M. K., Shi, Y., Levasseur, I. N., Maldonato, B. J., & Totah, R. A. (2023). METTL7A (TMT1A) and METTL7B (TMT1B) are responsible for alkyl S-thiol methyl transferase activity in liver. *Drug Metab Dispos*. doi:10.1124/dmd.123.001268

Numerical and Computational Analysis of Vascular Phantom Model for Sensor Design Validation

Youngjae Chun[1,2,3,*], Moataz Elsisy[1,4], and Woon-Hong Yeo[5]
[1]Department of Industrial Engineering, University of Pittsburgh, PA 15261, USA; [2]Department of Bioengineering, University of Pittsburgh, [3]McGowan Center for Regenerative Medicine, University of Pittsburgh Medical Center, PA 15213, USA; [4]Department of Mechanical Design, Cairo University, Giza, Egypt; [5]George W. Woodruff School of Mechanical Engineering, Center for Human-Centric Interfaces and Engineering, Georgia Institute of Technology, Atlanta, GA 30332, USA (yjchun@pitt.edu)

Statement of Purpose: A leading cause of morbidity and mortality in the United States is cardiovascular disease, which accounts for >420,000 deaths per year, and epidemiological studies have estimated that approximately 44% of cardiovascular disease related deaths are attributable to coronary artery disease (CAD). Endovascular technologies such as percutaneous transluminal coronary angioplasty (PTCA) and stenting are currently more widely used since they are minimally invasive and less risky, however, there are still major complications called "*restenosis*" after these procedures. Various imaging techniques are currently widely used to detect the progression of restenosis, but these are invasive, inconsistent, and entail relatively high hospital costs. Therefore, there is urgent clinical need for the development of a new technology on continuous non-invasive monitoring method or device technology to evaluate restenosis progression long term. This study shows a new low-profile strain sensor integrated coronary stent with its associated computational and preclinical *in vitro* study outcomes.

Methods: Finite element analysis (FEA) was used to predict the focal restenosis to model the coronary artery silicone elastomer models with varied thickness of neointimal layer mimicking in-stent restenosis. The model constituents, intima, media, adventitia, and plaque are modeled as hyperelastic material, to show the material behavior due to different loading. The hyperelastic behavior of the artery components was modeled using the 9-parameters Mooney-Rivilen equation. With the results artery models were fabricated using silicone (Ecoflex 00-30,), with mixed viscosity 3,000 cP, tensile strength 200 psi, 100% modulus 10 psi, elongation% at break 900%-, and 4-hours curing time. The wireless strain sensor consists of a soft, low-profile strain sensor and electronic stent. The strain sensor acts as a capacitor and the stent is the inductor, which forms an LC circuit with a detectable resonant frequency.

Results: A novel *in vitro* test platform with silicone coronary artery models has been fabricated to accurately evaluate the sensor's performance *in vitro* prior to animal studies. Both numerical analysis and computational fluid dynamics (CFD) were used to design the artery model with various levels of restenosis. Optically measured diameter changes under pulsatile cardiac flow represents the corresponding strain values as shown in Figure 1. (A). The higher restenosis levels (i.e., thicker neointima growth) shows reduced strain values from 0.2 to 0.048. Figure 1. (B) shows our newly developed low-profile capacitive strain sensor that contains polyimide substrate, transfer-printed nanomembrane electrodes, which can detect strains as low as 0.15% with a sensitivity of 3% per % linear strain. The relationship between the restenosis level and capacitance changes have been successfully demonstrated as shown in Figure. 1 (C). The sensor performance is suitable to detect small alterations produced in the coronary artery with the progression of restenosis under typical pulsatile flow. The sensor performance is suitable to detect small alterations produced in the coronary artery with the progression of restenosis under typical pulsatile flow. In addition to the development of strain sensors, an *in vitro* test platform has been constructed to accurately evaluate the sensor's performance. Both numerical analysis and computational fluid dynamics (CFD) were used to design the artery model with various levels of restenosis. The strain plots of artery models from both numerical and computational analyses have successfully shown the relationship between the strain and restenosis levels, varied pressures, artery lumens, and artery thicknesses.

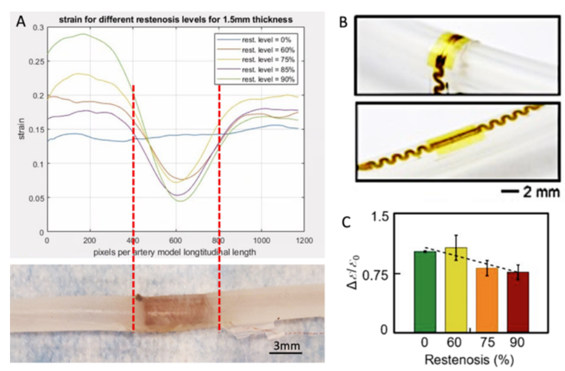

Figure 1. (A) Optically quantified strains using silicone restenosis model developed, (B) low-profile capacitive strain sensor, and (C) capacitance changes with varied restenosis conditions

Conclusions: Both computational modeling and *in vitro* benchtop mechanical tests were used to validate the silicone coronary artery model design with varied neointima thicknesses. A newly developed strain sensor showed its flexibility and capability of arterial strain sensing under physiological conditions *in vitro*. Our recent outcomes will provide better solutions for both diagnostic heart disease and many other vascular diseases that require stents.

Acknowledgements: This work was supported by the National Science Foundation (Grant No. 2152638).

Scalable manufacturing of skin-conformal, stretchable electrodes via screen-printing

Jong-Hoon Kim[1]

[1]School of Engineering and Computer Science, Washington State University, Vancouver, WA

I. SUMMARY

Various printing technologies have demonstrated efficiency and compatibility with soft materials for manufacturing wearable electronics.[1-4] However, wearable device manufacturing still involves a costly, complex, multi-step, and error-prone cleanroom process.[1] Here, we present fully screen-printable, skin-conformable electrodes with real-time electrocardiogram (ECG) recording for assessing arrhythmia. Flexible and stretchable electrodes are screen-printed with polyimide (PI) and silver/silver chloride (Ag/AgCl) multi-layers, which successfully demonstrate its excellent mechanical compliance during deformation, such as twisting, bending, and stretching (Figure 1a). PI layer printing is achieved with thixotropic additives. Several properties are ideal for screen printing inks. Screen printing inks generally have high viscosity, thixotropic, and viscoelastic properties. This thixotropic behavior helps the printing ink press through the screen opening (low viscosity at a high shear rate) and avoid spreading after printing (high viscosity at a low shear rate). Polyethylene-glycol (PEG) has been chosen as the thixotropic additive for biocompatibility. With 2% PEG, the PI layer can be printed as small as 150 μm while maintaining mechanical properties.

In addition, the flexible, wearable circuit with wireless communication allows conformal contact on human skin and real-time monitoring through a mobile device. Further, we have designed and demonstrated an algorithm for heartbeat rates (HR), respiration rates (RR), and heart rate variability (HRV), which are critical tools for analyzing the physiological information and early detection of arrhythmia (Figure 1b).

The scalable and cost-effective manufacturing of skin-conformable electrodes for continuous and wireless health monitoring will potentially offer wellness to patients with chronic or acute diseases. Future studies will focus on clinical applications of the electrode for machine-learning-enabled real-time diagnosis of acute heart diseases.

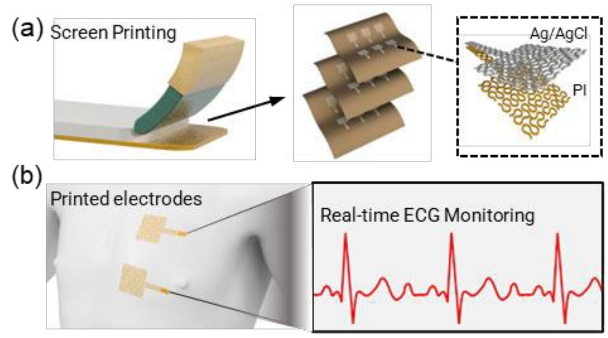

Figure 1 (a) Schematic illustration of PI-PEG, Silver ink screen-printing, and the electrode structure. (b) Real-time ECG collection with the calculated heart metrics related to arrhythmia.

ACKNOWLEDGEMENTS

JK acknowledges partial financial support from the National Science Foundation (NSF CBET-1707056).

REFERENCES

1. Velasco-Bosom, S.; Karam, N.; Carnicer-Lombarte, A.; Gurke, J.; Casado, N.; Tomé, L. C.; Mecerreyes, D.; Malliaras, G. G. Conducting Polymer-Ionic Liquid Electrode Arrays for High-Density Surface Electromyography. Advanced Healthcare Materials 2021, 10 (17), 2100374.
2. Cui, Z.; Han, Y.; Huang, Q.; Dong, J.; Zhu, Y. Electrohydrodynamic Printing of Silver Nanowires for Flexible and Stretchable Electronics. Nanoscale 2018, 10 (15), 6806–6811.
3. Ferri, J.; Llinares, R.; Segarra, I.; Cebrián, A.; Garcia-Breijo, E.; Millet, J. A New Method for Manufacturing Dry Electrodes on Textiles. Validation for Wearable ECG Monitoring. Electrochemistry Communications 2022, 136, 107244.
4. Yoo, J.; Long Yan; Seulki Lee; Hyejung Kim; Hoi-Jun Yoo. A Wearable ECG Acquisition System With Compact Planar-Fashionable Circuit Board-Based Shirt. IEEE Trans. Inform. Technol. Biomed. 2009, 13 (6), 897–902.

Multi-responsive injectable ECM-based embolic delivering therapeutic agents for treating cerebral saccular aneurysms

Seungil Kim[1,2], **Kamil W Nowicki[3]**, **Sangho Ye[1,2]**, **Robert M. Friedlander[3]**, **William R Wagner[1,2,4,5]**
[1] McGowan Institute for Regenerative Medicine, [2] Department of Surgery, [3] Department of Neurosurgery, [4] Department of Bioengineering, and [5] Department of Chemical and Petroleum Engineering, University of Pittsburgh, Pittsburgh, PA, USA

I. INTRODUCTION

Aneurysms are vascular lesions resulting from the vessel wall's biomechanical failure related to hemodynamic stress and inflammation. Aneurysm rupture can result in subarachnoid hemorrhage often leading to death or disability. Embolization using a metallic coil (e.g. platinum) is a current clinical first choice for saccular aneurysm treatment, but it has limitations including coil compaction, coil migration, and recanalization, leading to a need for retreatment.[1,2] Injectable embolic agents and hydrogels (e.g., Onyx™, TRUfill™ n-butyl cyanoacrylate, and EmboGel™) are entering the clinical arena and showing positive results. However, these injectable embolics also have shown recanalization after treatment. In this regard, an alternative material inducing rapid embolization of the aneurysmal sac and stimulating tissue ingrowth as the material is absorbed might provide a more permanent treatment. An injectable hydrogel delivering therapeutic agents could isolate the aneurysm by embolization and stabilize the sac through in vivo tissue engineering.

II. APPROACH

An extracellular matrix (ECM) based thermo-/pH responsive injectable gel system consisting of thiolated gelatin (Gel-SH) and vinyl sulfonated hyaluronic acid (HA-VS) was prepared. Chemical structures were confirmed by proton nuclear magnetic resonance. Contrast agent iohexol and therapeutic agents (Monocyte Chemoattractant Protein-1 (MCP-1) or substance p (SP)) were incorporated in the injectable embolic and their morphology, hemocompatibility, thrombogenicity, cell penetration and proliferation, von Willebrand factor (VWF) or α-smooth muscle actin (αSMA) expression were evaluated in vitro. At three weeks following the injection into a murine carotid aneurysm model, pro-inflammatory cytokine production assay and immunohistochemistry including H&E staining were performed to evaluate the potential physiologic response in cerebral aneurysm treatment.

The Gel-SH and HA-VS gelled after injection through 30-gauge needles at pH 7.4 and 36°C within 30 sec and the gel exhibited a porous structure with scanning electron microscopy. The iohexol-incorporated gel had moderate thrombogenicity, and rat smooth muscle cell penetration and proliferation. VWF and αSMA expressions were greater when SP was incorporated. In the animal study, the injectables demonstrated potential for use in the treatment of aneurysms in terms of successful embolization of the sac with subsequent tissue ingrowth (**Fig. 1**).

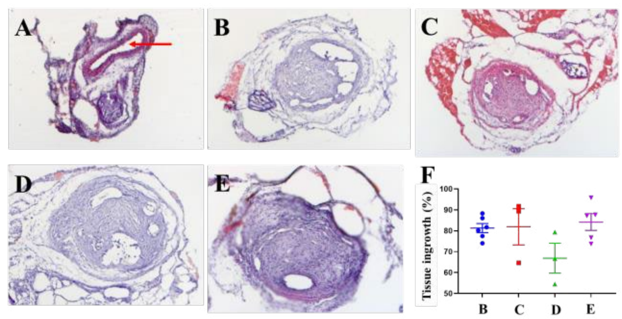

Figure 1. *H&E staining of mouse carotid aneurysms post-embolization with different gel combinations: (A) carotid artery without embolic, (B) HA-VS/Gel-SH with 10% iohexol, (C) HA-VS/Gel-SH with 10% iohexol and MCP-1, (D) HA-VS/Gel-SH with 10% iohexol and RSDA-SP, and (E) HA-VS/Gel-SH with 10% iohexol, RADA-SP, and MCP-1; (F) tissue in growth in the sac of the aneurysm with the injected embolic*.

III. CONCLUSION

The proposed ECM-based injectable embolic demonstrated potential use in aneurysm embolization, delivering therapeutics, and treating saccular aneurysms. Long-term animal studies are planned for the next step of the project.

REFERENCES

1. Kim, S., Nowicki, K. W., Gross, B. A. & Wagner, W. R. Injectable hydrogels for vascular embolization and cell delivery: The potential for advances in cerebral aneurysm treatment. *Biomaterials* **277**, 121109 (2021).
2. Kim, S. *et al.* Bioabsorbable, elastomer-coated magnesium alloy coils for treating saccular cerebrovascular aneurysms. *Biomaterials* **290**, 121857 (2022).

Co-transcriptional folding of nascent RNA in the presence of RNA-binding proteins

Sunghyun Cho[1], **Chun-Ying Lee**[1], **Sua Myong**[1]
[1]Department of Biophysics, Johns Hopkins University, Baltimore, MD 21218

I. SUMMARY

During transcription, RNA is folded with the assistance of RNA-binding proteins (RBPs). However, typical RNA-folding experiments are conducted without RBPs, and RNA-protein binding experiments employ RNAs that have already been well-folded. In this study, we imitated the co-transcriptional binding of RBP and its effect on RNA folding during transcription via a helicase-mediated RNA folding method. We discovered that the presence of RBPs during transcription produces novel intermediate states in the folding of the G-quadruplex and halts the folding of the hairpin structure.

II. Introduction

The transcription process generates nascent RNA, which requires a co-transcriptional process to mature. Numerous RNA-binding proteins (RBPs) are involved in this co-transcriptional process, in which RNA folds in the presence of RBP bindings. However, conventional in vitro RNA folding experiments were conducted without RBPs in solution; consequently, the binding effect of RBPs during RNA folding has not been thoroughly comprehended. In this study, we utilized a helicase-mediated RNA folding method[1] that enables us to mimic the co-transcriptional binding of RBP and its effect on RNA folding during transcription.

III. Methods

Using biotin, we affixed a DNA-RNA hybrid construct to a PEG-coated glass slide (Figure 1a, c). The construct for post-folded (i.e., RNA folds before RBP injection) has one DNA oligo with biotin and a G-quadruplex (TERRA) sequence containing RNA which can be combined with DNA oligo. So, the RNA overhang is well-folded to the Gq structure. However, the construct for vectorial-folded (i.e., RNA folds simultaneously with RBPs) has one more DNA oligo that can bind to overhang RNA sequence to prevent RNA folding. The injection of super helicase, RepX[1], unwinds the additional DNA strand and enables RNA to fold. With Cy3 and Cy5 dyes at each RNA and DNA oligos, we can figure out the folding state by FRET signals.

IV. Results and Discussion

We identified a newly emerged intermediate folding state in the vectorial-folded case based on the FRET histogram of each construct (Figure 1b, d). It describes how the Gq-binding protein, FUS, can bind to RNA during its folding to generate a new folding state. The vectorial folding experiment can provide a more realistic environment for RNA folding and expand our knowledge of co-transcriptional RNA folding.

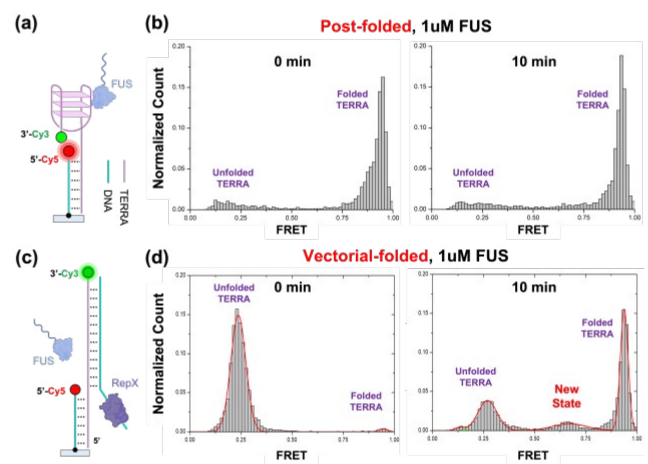

Figure 1: DNA-RNA hybrid FRET constructs for mimicking (a) post-folded and (b) vectorial-folded RNAs with the presence of RNA-binding protein, FUS. (c-d) The FRET histograms of each condition show the novel state in the vectorial folded state.

ACKNOWLEDGEMENTS

I would like to acknowledge Prof. Myong and Dr. Lee's mentoring and insightful advice.

REFERENCES

1. Hua, Boyang, et al., “Mimicking co-transcriptional RNA folding using a superhelicase.”, *Journal of the American Chemical Society*, Vol. 140, No. 32, pp. 10067-10070, 2018.

Towards Robotic Knee Prosthesis Personalization: Impedance Control With PCA-Based Tuning Methodology

Woolim Hong[1], **He (Helen) Huang**[1]
[1]Joint Department of Biomedical Engineering, NC State University, Raleigh, NC, USA

I. INTRODUCTION

Robotic prostheses, designed to mimic natural human walking as closely as possible, have been studied over the years to address mobility and agility issues in the lower-limb amputee population [1-3]. However, a common drawback is the lack of personalized control for each individual amputee [2]. Furthermore, these prosthetics often require a complex and time-consuming tuning process to optimize walking performance for each user and different walking scenarios [2]. This study introduces a novel framework for robotic knee prostheses aimed at offering personalized control to each amputee, potentially improving the interaction between the user and the prosthesis. The goal of our study is to enable personalized control of knee prostheses while also minimizing the required tuning efforts.

II. METHOD

We propose a continuous impedance control for knee prosthetics, requiring varying stiffness, damping, and equilibrium angle throughout human ambulation [3], termed 'Continuous Impedance Functions' (CIFs). We use a convex optimization problem to create individual CIF sets, fitting estimated knee joint torque to healthy human data. For personalization, we adjust CIFs using a new lower-dimensional tuning space (i.e., Principal Components (PCs)) developed via Principal Component Analysis (PCA) to capture common features. By adjusting the weights of the PCs, we can reconstruct the CIFs to refine the initial CIFs for each individual.

III. RESULTS & DISCUSSIONS

Fig. 1(A) illustrates the CIFs for ten healthy subjects obtained through convex optimization. As shown in Fig. 1(B), PCA was used to extract the first two PCs, reducing the dimensionality of the CIF dataset. To assess the feasibility of using PC weight modulation to fine-tune the impedance functions, we adjusted the weights of PC1 and PC2 and observed the resulting variations in impedance functions. Fig. 1(C) presents the reconstructed impedance functions based on different weights of the PCs. The weights of PC1 ($W_{S,1}$, $W_{D,1}$, $W_{Eq,1}$) were modulated from 0 to 1 in increments of 0.1, while the weights of PC2 ($W_{S,2}$, $W_{D,2}$, $W_{Eq,2}$) were modulated between -1 and 1 in increments of 0.1. The newly generated impedance functions cover the actual impedance functions, showing their potential for fine-tuning by adjusting the weights of the PCs. Consequently, our framework requires only six tuning parameters, in contrast to the current finite state machine-based impedance control framework, which necessitates 12 parameters for the knee joint [2].

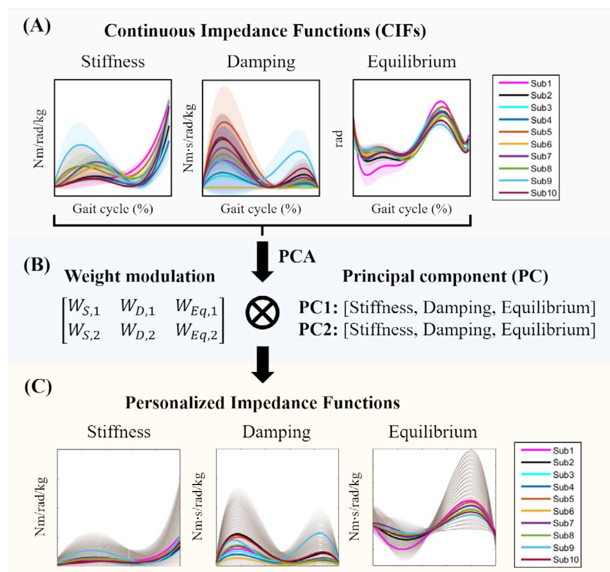

Figure 1: Study overview: (A) CIFs. (B) PCs and their weights modulation. (C) Personalized CIFs.

REFERENCES

1. Best et al., "Data-Driven Variable Impedance Control of a Powered Knee-Ankle Prosthesis for Adaptive Speed and Incline Walking," IEEE Transactions on Robotics, pp. 1-19, 2023.
2. Li et al. "Hierarchical Optimization for Control of Robotic Knee Prostheses Toward Improved Symmetry of Propulsive Impulse," IEEE Transactions on Biomedical Engineering, 2022.
3. Anil Kumar et al. "Control framework for sloped walking with a powered transfemoral prosthesis," Frontiers in Neurorobotics, Vol. 15, pp. 790060, 2022.

Skin-interfaced wireless device for fetal and maternal monitoring to minimize unnecessary C-section

Hyoyoung Jeong[1]
[1]University of California Davis, Electrical and Computer Engineering department

I. SUMMARY

For nearly 50 years, intrapartum fetal monitoring has relied on cardiotocography (CTG), but this method has limitations, including false positives that often lead to unnecessary interventions. To address this issue, I aim to develop an integrated monitoring system that utilizes advanced flexible electronics for continuous sensing and autonomous analysis[1,2]. This platform will enable extensive monitoring of vital signs for both women and fetuses, incorporating non-invasive measurements of fetal and maternal heart rates, as well as uterine contraction activity.

II. DESIGN AND IMPLEMENTATION

A. Skin-like continuous and seamless monitoring

E-tattoos are thin and flexible sensors that conform to the skin to monitor various biomarkers, such as ECG, skin temperature, and blood oxygen saturation. Integrated with wireless technologies, they provide comfortable and robust monitoring capabilities, even under mechanical stress, ensuring soft and non-irritating interfaces with the skin (Figure 1).

Figure 1: Mechanical and electrical robustness of battery-free E-tattoo under severe deformation during power and data transmission.

B. E-Tattoo as a Personalized Sensor

The modular and reconfigurable NFC and Bluetooth-enabled E-tattoo, consisting of four layers, including NFC, BT, Functional, and electrodes layers, can be powered by an interrogator or a rechargeable coin cell battery, enabling multiple sensing modalities such as ECG, SpO_2, heart rate, skin temperature, and skin hydration[3]. The e-tattoo's design allows for reusability and customization based on user requirements, offering flexibility in choosing the tracked biomarkers according to personal needs.

C. Multichannel ambulatory platform for pregnancy monitoring

In our research, we have developed a wearable system that monitors maternal and fetal vital signs, including continuous maternal/fetal heart rates, uterine contraction activity. The system utilizes flexible sensors and a cloud platform, allowing for data analysis and prediction of maternal and neonatal outcomes, and has been successfully validated in both high and low-resource settings with positive usability and effectiveness results (Figure 2).

III. DISCUSSION

The device design and implementation method proposed here offers a new value of continuous fetal-maternal monitoring, collecting continuous fetal and maternal ECGs, oximetry, uterine activity, and mapping. Further research will be conducted to validate the system using an animal model enhancing our understanding of labor dynamics.

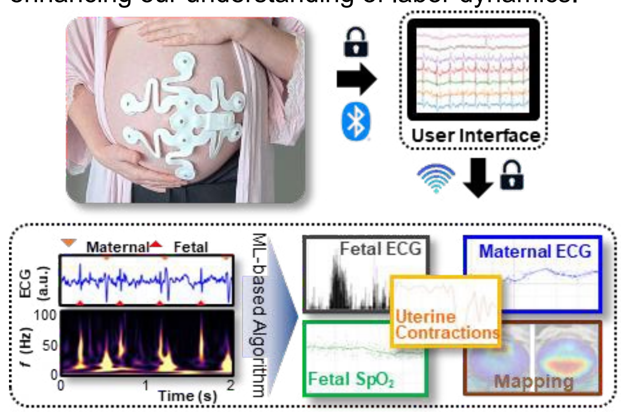

Figure 2: Proposed system operation including sensors, user interface, and cloud-based analysis.

ACKNOWLEDGEMENTS

Thanks to collaborators, especially Drs. John Rogers, Steve Xu, Soheil Ghiasi, and Satyan Lakshminrusimha.

REFERENCES

1. Jeong, H. et al. Miniaturized wireless, skin-integrated sensor networks for quantifying full-body movement behaviors and vital signs in infants. Proc. Natl. Acad. Sci. U.S.A. 118, e2104925118, 2021.
2. Choi, Y. S. Jeong, H. et al. A transient, closed-loop network of wireless, body-integrated devices for autonomous electrotherapy. Science 376, 1006–1012, 2022.
3. Jeong, H. et al. Modular and Reconfigurable Wireless E-Tattoos for Personalized Sensing. Adv. Mater. Technol. 4, 1900117, 2019.

Genome-wide epigenetic editing of human microsatellite repeats using engineered zinc finger transcription factors

Y. Esther Tak[1,2,3], **Gaylor Boulay**[1,3,4], **Miguel N. Rivera**[1,3,4], **J. Keith Joung**[1,2,3]

[1]Molecular Pathology Unit and Center for Cancer Research, Massachusetts General Hospital, Charlestown, MA, USA
[2]Center for Computational and Integrative Biology, Massachusetts General Hospital, Charlestown, MA, USA
[3]Department of Pathology, Harvard Medical School, Boston, MA, USA
[4]Broad Institute of MIT and Harvard, Cambridge, MA, USA

Microsatellite repeats are short tandem repeats that are widely distributed throughout the human genome and, like many other types of repetitive elements, have been shown to be dysregulated in a variety of human diseases. For example, in the pediatric tumor Ewing sarcoma, hundreds of inert GGAA repeat sequences can be converted into *de novo* transcriptional enhancers when bound by the oncogenic EWS-FLI1 translocation protein. However, studying the mechanistic role of any given class of microsatellite is challenging both because of the highly repetitive nature of their DNA sequence and their distribution at hundreds to thousands of sites genome-wide. Recent targetable DNA-binding technologies such as engineered zinc finger (ZFs) and CRISPR-Cas9 provide attractive tools for studying microsatellites but, to our knowledge, their efficacies have not yet been determined.

To address this, we engineered ZF arrays (ZFAs) and targeted an RNA-guided catalytically inactive "dead" Cas9 (dCas9) to bind to GGAA microsatellite repeats. Unexpectedly, we found that when fused to the EWS domain, engineered ZFAs substantially outperformed dCas9 in epigenetically editing a GGAA repeat into a *de novo* enhancer. Moreover, when assessed genome-wide, we found that expression of an individual EWS-ZFA fusion was at least as efficient as that of EWS-FLI1 for binding and converting hundreds of normally inert GGAA repeats into *de novo* transcriptional enhancers in mesenchymal stem cells (MSCs), a precursor cell model for Ewing sarcoma.

In addition, we also found that a KRAB transcriptional repression domain fused to a GGAA repeat-targeted ZFA could silence GGAA microsatellite enhancers genome-wide in Ewing sarcoma cells, resulting in a marked reduction of EWS-FLI1-activated genes. Remarkably, this KRAB-ZFA fusion also showed selective toxicity in Ewing sarcoma cell lines compared with other non-Ewing cancer cell lines, consistent with its expected Ewing sarcoma-specific editing impact on the transcriptome.

These results demonstrate that a single engineered ZFA, in contrast to dCas9, can efficiently bind GGAA microsatellites genome-wide in human cells and that recruitment of fused functional domains to these repeats can profoundly alter chromatin states and transcriptional signatures. These studies provide important proofs-of-concept for how engineered ZF technology can be used to study the function of microsatellites in gene regulation at a genome-wide scale and to edit the abnormal activity of these elements in pathogenic states for potential therapeutic applications.

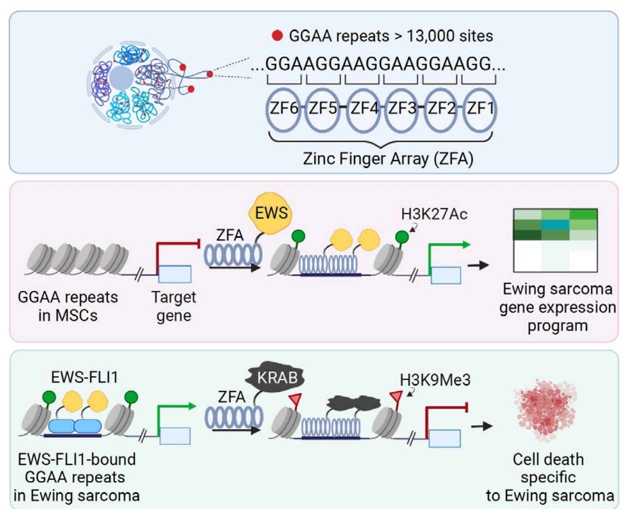

Figure1: Engineered ZFA-based fusions can efficiently target thousands of microsatellites 1) recapitulating the genome-wide activation of GGAA microsatellites and 2) silencing GGAA microsatellites inducing selective toxicity in Ewing sarcoma cells.

Intelligent Upper-limb Exoskeleton using Deep Learning to predict Human Intention for Sensory-Feedback Augmentation

Kangkyu Kwon[1,2], **Woon-Hong Yeo**[1,2]
[1]Georgia Institute of Technology, [2]IEN Center for Human-Centric Interfaces and Engineering

I. SUMMARY

The decline in musculoskeletal strength from age or stroke impacts individuals with neuromotor disorders, with current exoskeleton robots limited by insufficient human intention prediction, sensory feedback, and support for upper limb joint movements. This study introduces an intent-driven robotic exoskeleton with cloud-based intention prediction, sensory feedback via skin-like bioelectronics, and soft pneumatics for upper-limb assistance, achieving 96.2% accuracy in determining movement and augmenting strength by 5.15 times, providing a promising solution for neuromotor disorders.

II. Materials and Methods

A. Exoskeleton and Soft EMG Sensor Fabrication

The actuator consists of silicone tubing, polyester mesh, and aluminum fittings. Quasistatic testing evaluates performance at various pressures. The exoskeleton uses carbon fiber, aluminum connectors, and steel fasteners. It features telescoping collets and 3D-printed arm mounts for adjustability. Fabrication process of EMG sensor involves fabric substrate, circuit development, nanomembrane electrodes. Stretchable sensors are made with Silbione, gold/chromium electrodes, and PDMS. Mechanical and electrical tests measure sensor properties, including cyclic stretching, circuit bending, and electrode-skin impedance, and Finite Element Analysis.

B. Cloud Computing Interface and Deep-learning Motion Classifications

A microcontroller and Bluetooth system enable wireless EMG recording. Data is transmitted to Google Cloud for real-time applications. Cloud software hosts the machine learning algorithm for motion classifications. For Deep-Learning algorithm, CNN+LSTM model is used for motion classification, with optimized hyperparameters selected via random search. Performance is evaluated using accuracy metrics.

III. Results, Conclusions, and Discussions

The fully-intent driven robotic exoskeleton combines a motion-predicting cloud computing platform, strength augmentation, and soft bioelectronics-enabled sensory feedback to assist human upper-extremity joint movements. The lightweight exoskeleton, powered by a PAM module, substantially reduces EMG activity (6.9 and 3.4 times for elbow and shoulder flexion) and assists loaded movements (1.7 and 2.1 times for elbow and shoulder flexion). Skin-like bioelectronics monitor EMG signals, which are processed via a cloud-based deep-learning algorithm to predict users' intended movements with 95.4% accuracy for biceps/triceps and 97.0% for medial deltoid/latissimus dorsi movements. The exoskeleton's response time for movement assistance is 300-350 ms, offering a transformative solution for individuals with neuromotor disorders.

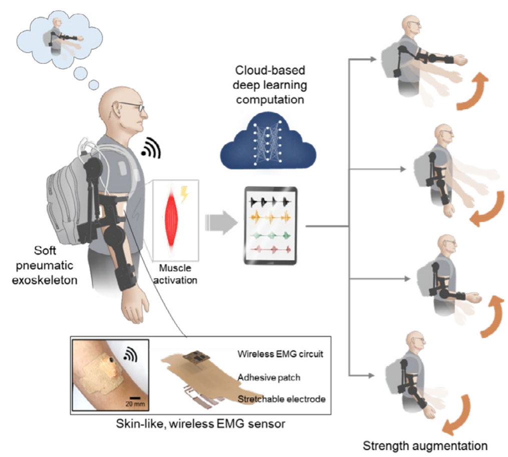

Figure 1: Overview of System

ACKNOWLEDGEMENTS

The authors acknowledge the support from the SEMI-FlexTech and the IEN Center for Human-Centric Interfaces and Engineering at Georgia Tech.

REFERENCES

1. Kwon, Y.-T. et al. Printed, wireless, soft bioelectronics and deep learning algorithm for smart human–machine interfaces. ACS Applied Materials & Interfaces 12, 49398-49406 (2020).

[SEED2023] Engineered Helicase Replaces Thermocycler in DNA Amplification While Retaining Desired PCR Characteristics

Jimin Kang[1], Momčilo Gavrilov[2], Taekjip Ha[1,3,4,5]

[1]Department of Biophysics, Johns Hopkins University, Baltimore, MD, USA, [2]Honeywell International, 500 Brooksbank Ave, North Vancouver, BC, Canada [3]Department of Biophysics and Biophysical Chemistry, Johns Hopkins University School of Medicine, Baltimore, MD, USA [4]Department of Biomedical Engineering, Johns Hopkins University School of Medicine, Baltimore, MD, USA [5]Howard Hughes Medical Institute, Baltimore, MD, USA

I. SUMMARY

Our study introduces a significant innovation in molecular diagnostics and life sciences. We have developed an engineered PcrA M6 helicase that exhibits increased speed and processivity, effectively replacing the heat cycling step in the Polymerase Chain Reaction (PCR) process with enzymatic DNA unwinding. This has led to the establishment of an isothermal amplification technique, termed SHARP (SSB/helicase-assisted rapid PCR), which maintains the essential characteristics of PCR.

II. METHODOLOGY AND RESULTS

SHARP is an isothermal nucleic acid amplification technique that utilizes an engineered helicase PcrA M6 and single-stranded DNA binding protein (SSB) alongside standard PCR reagents. SHARP is capable of generating amplicons up to 6000 base pairs in length and producing functional DNA. Moreover, SHARP has the ability to amplify specific fragments from the genomic DNA of human cells. We have used SHARP to evaluate the results of CRISPR/Cas9 editing at endogenous genomic sites and for the straightforward detection and quantification of genome editing outcomes at these sites.

III. APPLICATIONS AND FUTURE WORK

Our findings indicate that SHARP can reliably amplify genomic DNA, establishing it as a feasible PCR-free method for targeted quantification of genome editing outcomes. We have also examined SHARP's capacity to amplify sequences that are susceptible to secondary structure formation, such as trinucleotide CAG repeats. Furthermore, we have shown that SHARP can operate effectively at 37°C. Looking ahead, we plan to investigate further applications of SHARP within the realms of molecular diagnostics and life sciences.

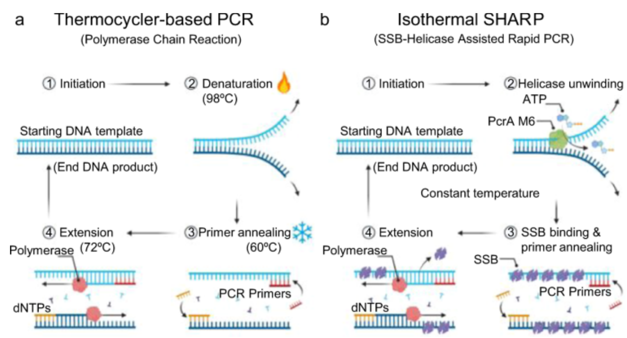

Figure 1: Comparison of PCR and SHARP. **a**. PCR uses temperature cycling to unwind DNA. **b**. SHARP uses PcrA M6 helicase and SSB for DNA unwinding at a constant temperature. Created with BioRender.com.

Table 1: SHARP Components for 20 µL Reaction

Reagent	Volume (µl)
PcrA M6 (0.2mg/ml)	1
SSB (9mg/ml)	0.25
Bst-LF (1.5mg/ml)	0.1
dNTPs (10mM)	0.25 each
ATP (100mM)	1
DTT (100mM)	2
Primers (10µM)	0.5 each
10x Buffer	1x

ACKNOWLEDGEMENTS

This work was supported by grants from the JHU COVID-19 Research Response Program, National Institutes of Health (R35 GM 122569 to T.H.), and the National Science Foundation (MCB 2031094 to T.H.).

REFERENCES

1. Gavrilov, M., et al. (2022). "Engineered helicase replaces thermocycler in DNA amplification while retaining desired PCR characteristics," *Nature Communications, Vol. 13, No. 6312, pp. 1-14.*

Noninvasive estimation of intracranial pressure via diffuse correlation spectroscopy

John Sunwoo[1], Samuel Snider[2], and Maria Angela Franceschini[1]

[1]Athinoula A. Martinos Center for Biomedical Imaging, Massachusetts General Hospital, Harvard Medical School, Charlestown, MA, USA, [2]Department of Neurology, Neurocritical Care and Stroke, Brigham and Women's Hospital, Harvard Medical School, Boston, MA, USA

I. INTRODUCTION

Intracranial pressure (ICP) monitoring is crucial for assessing cerebral perfusion in traumatic brain injury (TBI) patients. The prevailing method, though invasive and risk-laden due to surgical drilling and probe insertion, remains the gold standard. We've previously demonstrated that non-invasive critical closing pressure (CrCP) estimates via diffuse correlation spectroscopy (DCS) hold promise, given CrCP's direct correlation with ICP. However, the non-linear relationship between the flow and pressure measurements involved in CrCP estimation often undermines its accuracy, thereby necessitating optimization of the processing/estimating algorithm. We hereby propose a systematic approach to enhance the CrCP and ICP correlation.

II. Method

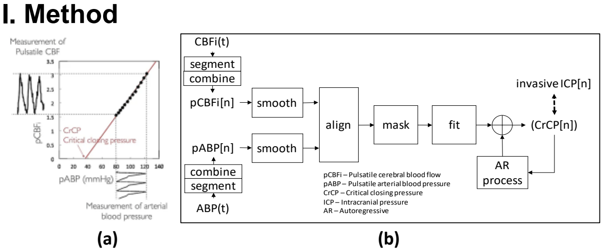

Figure 1. Proposed CrCP algorithm to best match with invasive ICP measurements. (a) DCS-based CrCP principle, (b) The CrCP algorithm

A. DCS and CrCP

DCS employs a non-invasive optical technique to provide a cerebral blood flow index (CBFi) based on fluctuations in light intensity scattered by moving red blood cells [1]. CrCP hinges on the linear correlation between changes in pulsatile arterial pressure (pABP) and blood flow (pCBFi) during a cardiac cycle. The zero-flow intercept is CrCP, which several studies have confirmed correlates with ICP [2].

B. Algorithm Optimization

The traditional CrCP fitting algorithm necessitates optimization to better align the CrCP estimates with actual ICP measurements. Issues like a low signal-to-noise ratio in pCBFi and non-linear physiological relationship between flow and pressure considerably affect the linearity assumption in the CrCP fitting method. The proposed optimization involves parameter adjustments (as outlined in Table 1) to improve the CrCP-ICP match.

C. Subject Recruitment, Study Procedure, Analysis

Under an active, approved protocol, we are collecting DCS data from TBI patients with clinically placed ICP and arterial blood pressure monitors. Although we are conducting individualized data analyses, further measurements are necessary to enhance the efficacy in CrCP algorithm optimization.

ACKNOWLEDGEMENTS

I express my gratitude to Dr. Tony Wu for his contribution to DCS pulsatile blood flow beat-averaging analysis, and to Alyssa Martin and Stephanie Jordan for their administrative support.

REFERENCES

[1] K.C. Wu, J. Sunwoo, et al., Validation of diffuse correlation spectroscopy measures of critical closing pressure against transcranial Doppler ultrasound in stroke patients. Journal of Biomedical Optics, 26 (03), 2021

[2] D. Boas, J. Sutin, and M.A. Franceschini, "SYSTEM AND METHOD FOR NON-INVASIVELY MONITORING INTRACRANIAL PRESSURE," WO 2016/164891 Al, 2016.

Table 1. CrCP parameters in Figure 1.

	Combine	Smooth	Align	Mask	AR process	CrCP-ICP
Parameters to sweep (min:step: max)	• Cardiac cycle averaging (1:5:50 cycles)	• Sliding window average (size = 1:10:500 msec) • Low-pass cut-off (10:10:100 Hz)	• By cardiac peaks (systole or diastole) • At the best cross-correlation (lag of 0:10:200 msec)	• Which cardiac cycle (systole or diastole) • % cardiac cycle (Last 30-100 %)	• Autoregressive (AR) memory size (0-5 minutes)	• Transfer function (0-5 minutes long)

Technical Group C-2

Chemical, Textile, Energy, and Nuclear Engineering (CHE)

Next-Generation Hybrid Models: Combining Attention Mechanisms and LSTM for Improved Predictions and Process Control in the Chemical Industry

Parth Shah[1], and Joseph Sang-Il Kwon[1]
[1]Artie McFerrin Department of Chemical Engineering, Texas A&M University, Texas

I. SUMMARY

The chemical industry is undergoing a significant transformation, which is driven by recent advancements in artificial intelligence (AI) and machine learning (ML) techniques that harness large quantities of process data from chemical plants. At the forefront of this revolution are hybrid models, which have gained substantial popularity over purely data-driven approaches such as deep neural networks (DNN) and long short-term memory (LSTM) networks [1]. This is because hybrid models combine a first-principles (FP) model with a suitable data-driven approach to synergistically provide better predictions than purely data-driven ML models [2]. DNN-based hybrid models developed in the literature for various chemical processes show good predictions [3]. But most chemical systems exhibit process uncertainties, such as sensor noise, feed and temperature fluctuations, and changing kinetics, distorting the measurements fed to the hybrid model and resulting in a noticeable plant-model mismatch. As a result, a DNN-based hybrid model that does not accurately capture these temporal dependencies will display a plant-model mismatch with process operation. Therefore, the development of next-generation hybrid models that can (a) account for these process uncertainties and (b) accurately predict these time-varying parameters is necessary.

Recently, attention-based ML models have been in the spotlight due to their remarkable ability to establish strong correlations between input and outputs, even in the presence of system noise or uncertainties. These models adeptly focus on short-term (e.g., sudden change in temperature due to control actions) and long-term (e.g., concentration evolution) dependencies in the evolution of system states [3,4]. On the other hand, LSTM-based sequential time-series models have shown superior predictive performance due to their ability to consider the time evolution of system states explicitly.

To this end, we propose a novel attention-LSTM-based hybrid model for a complex, non-trivial fed-batch fermentation process. Here, the input (past state measurements) is sent through an encoder module to lift the states into higher dimensions. Then an attention mechanism with a subsequent LSTM layer is applied to obtain time-series predictions of uncertain parameters. Next, the predicted uncertain parameters are then fed to the FP model to obtain state predictions. The training and validation dataset is generated by simulating a FP model of a fermenter system for over 100 different operating conditions. Additionally, the prediction results (i.e., biomass, substrate, and product) were compared against an existing DNN-based hybrid model to highlight the superior performance of the proposed model. Finally, the developed hybrid model is incorporated within a model predictive controller (MPC) to achieve set-point targets for product and operating cost by determining optimal input profiles for flow rate and temperature. In a nutshell, the combined benefits of attention mechanism and LSTM-based sequential modeling give rise to the next generation of hybrid models that can regulate process uncertainties while providing accurate process predictions.

REFERENCES

1. *Sansana, J., Joswiak, M. N., Castillo, I., Wang, Z., Rendall, R., Chiang, L. H., & Reis, M. S. (2021). Recent trends on hybrid modeling for Industry 4.0. Computers & Chemical Engineering, 151, 107365.*
2. *Thompson, M. L., & Kramer, M. A. (1994). Modeling chemical processes using prior knowledge and neural networks. AIChE Journal, 40(8), 1328-1340.*
3. *Devlin, Jacob, et al. "Bert: Pre-training of deep bidirectional transformers for language understanding." arXiv preprint (2018).*
4. *Vaswani, Ashish, et al. "Attention is all you need." Advances in neural information processing systems 30 (2017).*

CO2 EOR and Carbon Capture Utilization and Storage (CCUS): Field-Scale Application of Mobility-Control CO2 Foams

SEUNG IHL KAM

Professor, Craft & Hawkins Department of Petroleum Engineering, Louisiana State University, Baton Rouge, LA

(ph) 1-225-578-5216, (fax) 1-225-578-6039, (email) kam@lsu.edu

I. SUMMARY

In addition to CO2 Enhanced Oil Recovery (EOR), underground petroleum-bearing geological formation has long been recognized as a safe and effective means of sequestrating carbon dioxide (CO2) in Carbon Capture Utilization and Storage (CCUS) processes. Among numerous projects (more than 10 projects in 3 different continents) that we have carried out during the last decades, this study presents an example of field-scale project (4 layers with differing petrophysical properties) – how field-scale evaluation of CO2 EOR and CCUS treatment can be performed.

II. INTRODUCTION

A typical gas injection process often suffers from gravity segregation, viscous fingering, and channeling, resulting in early breakthrough and poor volumetric sweep efficiency (meaning low oil production and poor CO2 storage). By injecting foamed CO2, the process can significantly improve both aerial and vertical sweep efficiency in actual field processes [1, 2].

III. METHODOLOGY

This study first utilizes small laboratory-scale experiments conducted to extract the non-Newtonian behavior of CO2 foams. The experimental data is extended afterwards to construct a mechanistic foam rheology model and evaluate field-scale oil recovery and CO2 storage capacities.

IV. RESULTS AND DISCUSSIONS

Although the result from the field pilot test is field-specific, there seems a consensus that the outcome of using stable foams in this particular field example with 4 layers with differing petrophysical properties proves the effectiveness of mobility control foams.

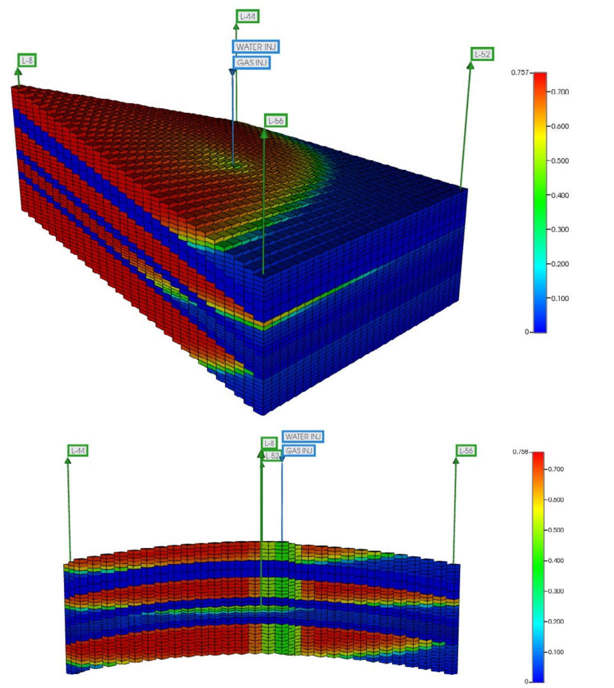

Figure 1: FIELD INJECTION EXAMPLE

REFERENCES

1. S. Lee and S.I. Kam, “Enhanced Oil Recovery by Using CO2 Foams: Fundamentals and Field Applications,” *a book chapter in “Enhanced Oil Recovery Field Case Studies” (James Sheng), Gulf Professional Publishing (Elsevier), ISBN: 9780123865458*, May 2013.
2. M. Izadi, P. Nguyen, D.P. Ortiz Maestre, H. Fleifel, and S.I. Kam, “An Investigation of Mechanistic Foam Modeling for Optimum Field Development of CO2 Foam EOR Application,” *SPE Reservoir Evaluation and Engineering*, p. 475–494, Vol. 24, Issue 3, 2021.

Valorization of Nutrients in Surface Waters Through the Sustainable Biomass Production of the Attached Algae Flow-way for Biofuels

Sungwhan Kim[1] and Ryan W. Davis[1]
[1]Sandia National Laboratories, 7011 East Ave., Livermore, CA 94550, United States

I. SUMMARY

A. Research background

Energy needs and climate change have increased the demand for algal research as a promising solution to produce clean and sustainable products and services in various industries including food, energy, and environment. Sandia National Laboratories (SNL) has been studying attached periphytic algae flow-ways to couple environmental remediation, particularly wasted nutrients from agricultural runoff, with sustainable biomass production for the applications of biofuels and other biomaterials.

B. Field deployments

SNL has concentrated on an application for environmental remediation on nutrient recovery from non-point source water through the employment of the attached periphytic algae flow-way. Our study consists of an in-depth assessment of multi-year-long field deployments of the attached algae flow-way in different US territories with various compromised surface water. Key environmental factors, which had a significant impact on biomass productivity, were determined and their predictive capability were assessed[1,2].

B. Pilot-scale study

SNL built and operated two pilot-scale attached algae flow-ways to test and optimize various operating parameters and understand microbial community change throughout the cultivation period. As a result, dynamics of microbial consortia during continuous cultivation were observed. Diversity changes over the cultivation period were analyzed as well as relative abundance of associated microbes with respect to key events were analyzed to determine key microbes that are associated with positive impacts such as high biomass productivity, low ash contents, and low sloughing.

II. ILLUSTRATIONS

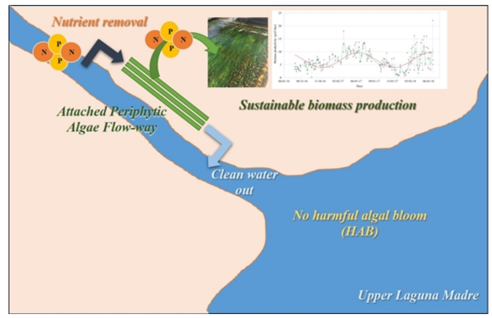

Figure 1. Illustration of field deployment of attached algae flowway to remediate surface water while producing algal biomass

ACKNOWLEDGEMENTS

Funding is supported by the U.S. Department of Energy's Office of Energy Efficiency and Renewable Energy (EERE), BioEnergy Technologies Office (BETO), Advanced Algae Systems program under agreement 27375, Sandia National Laboratories is a multimission laboratory managed and operated by National Technology and Engineering Solutions of Sandia LLC, a wholly owned subsidiary of Honeywell International Inc. for the U.S. Department of Energy's National Nuclear Security Administration under contract DE-NA0003525.

REFERENCES

1. Kim, S., Quiroz-Arita, C., Monroe, E.A., Siccardi, A., Mitchell, J., Huysman, N., Davis, R.W., "Application of attached algae flow-ways for coupling biomass production with the utilization of dilute non-point source nutrients in the Upper Laguna Madre, TX.," *Water Research*, 191, 116816, 2021.
2. Hennequin, L.M., Kim, S., Monroe, E.A., Eckles, T.P., Beck, N., Mays, W.D., Fennell, P.S., Hallett, J.P., George, A. and Davis, R.W., "Reclamation of nutrients, carbon, and metals from compromised surface waters fated to the Salton Sea: Biomass production and ecosystem services using an attached periphytic algae flow-way.", *Algal Research*, *66*, p.102757, 2022.

Solid-State Hydrolysis of Sodium Borohydride for Hydrogen Generation

Hyun Tae Hwang[1], Geo Jong Kim[2], Savannah G. Hunt[1], Allison Millspaugh[3], Byeong Uk Kim[4], Sang Bum Kim[4]

[1] b Department of Chemical and Materials Engineering, University of Kentucky, [2] Korea Research Institute of Chemical Technology, Daejeon, South Korea, [3] Department of Mechanical Engineering, University of Kentucky, [4] Green and Sustainable Materials R&D Department, Korea Institute of Industrial Technology

I. SUMMARY

We proposed the hydrolysis of sodium borohydride ($NaBH_4$, SBH) and water formed by thermal dehydration of sodium metaborate tetrahydrate ($NaBO_2{\cdot}4H_2O$, SMBH). The safety hazards due to self-hydrolysis of SBH are eliminated as the mixture of SBH and SMBH is stable at ambient temperature. In addition, SMBH is a product of the hydrolysis of SBH. Since the final products are homogeneous with SMBH, therefore, there is no need for post-reaction separation for the regeneration of the spent fuel. Using this approach, maximum overall H_2 yields of 4.7 and 5.1wt% were obtained at 200 and 250°C, respectively.

II. RESULTS

A. Hydrogen Release Kinetics

The effect of molar ratio of SMBH to SBH (SMBH/SBH) was investigated at two different temperatures. As shown in Figure 1, the H_2 equivalent increased as the SMBH/SBH increased but did not increase any more when approaching the highest possible equivalent (= 4) for higher SMBH/SBH. It is clear that even if the H_2 equivalent is the same, as the amount of SMBH increases, the total weight (SBH + SMBH) also increases, so the H_2 yield decreases. In this study, the maximum overall H_2 yields of 4.7 and 5.1wt% were obtained at 200 and 250°C, respectively.

B. Characterization of solid products

The solid products examined above were further characterized by ^{11}B solid-state NMR. The NMR spectral peaks for SBH and SMBH are generally observed at near 1 and -42 ppm, corresponding to $[B(OH)_4]^-$ and $[BH_4]^-$, respectively. The peaks assigned to both SBH and SMBH were seen in the final products obtained at 150°C, indicating that some SBH were left unreacted. For 200°C, however, the peaks corresponding to SBH disappeared and the same peak profile as SMBH was observed, meaning that the final products are homogeneous with SMBH, therefore, there is no need for post-reaction separation for the regeneration of the spent fuel.

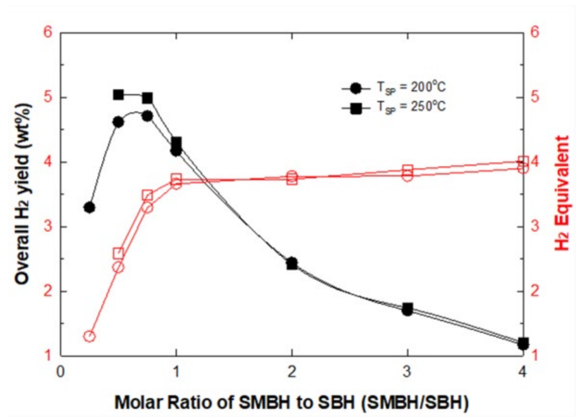

Figure 1: Effect of SMBH/ SBH on H_2 overall yield and equivalent for different temperature

III. CONCLUSIONS

The safety hazards due to self-hydrolysis of SBH are eliminated as the mixture of SBH and SMBH is stable at ambient temperature. In addition, SMBH is a product of the hydrolysis of SBH. Since the final products are homogeneous with SMBH, therefore, there is no need for post-reaction separation for the regeneration of the spent fuel. Using the proposed method, the maximum overall H_2 yields of 4.7 and 5.1wt% were obtained at 200 and 250°C, respectively. With high hydrogen yield and simplification of the regeneration process, this proposed method is promising for hydrogen storage for fuel cell applications.[1]

ACKNOWLEDGEMENTS

This work was supported by the R&D Program (JE230003) of the Korea Institute of Industrial Technology (KITECH).

REFERENCES

1. Hwang, H.T. and Varma, A., "Hydrogen storage for fuel cell vehicles." *Current Opinion in Chemical Engineering*, 5, pp.42-48, 2014

Facile Soft-lithographic Micromolding Approaches for Controlled Fabrication of Micropatterned Opal Hydrogel Materials

Subhash Kalidindi and Hyunmin Yi
Tufts University, Medford, MA 02155 USA

INTRODUCTION

Artificial opal-structured hydrogel materials offer significant potential in a wide range of sensing applications. However, it remains challenging to manufacture such potent materials in a simple, tunable and reliable manner. Existing photolithographic and microfluidic techniques suffer from long opal deposition times, and often involve complex and arduous steps. In this presentation, we report a simple micromolding-based evaporation-polymerization method for the fabrication of synthetic and biopolymeric hydrogel films containing micropatterned opal structures as well as opal microparticles.

RESULTS AND DISCUSSION

Intense and uniform opalescent colors were achieved by a simple evaporative deposition of polystyrene (PS) bead solution in patterned micromolds. The observed colors, diffraction spectra and PS bead sizes measured with dynamic light scattering (DLS) all correlated well with expected values through modified Bragg-Snell equation, confirming reliable assembly as well as simple and robust fabrication scheme.

These micropatterned opal structures were then captured in hydrogel films by simple UV-indued photopolymerization or thermal gelation. The as-prepared films show high tunability as well as responsiveness to various environmental cues such as humidity, pH and ionic strength that are manifested via shifts in color readily observable with bare eyes.

Importantly, a potent aminopolysaccharide chitosan enables multitude of desirable features both for fabrication and the resulting functionality, ranging from stable opal formation, reliable and high yield pattern transfer, chemical functionality, stability in a wide range of extreme conditions, and to spatially selective electroassembly as well as inverse opal fabrication.

Combined with UV-vis reflectance spectroscopy and morphological characterizations, these evidences illustrate the robust, simple and reliable nature of our integrated deposition-polymerization approach for controlled fabrication of optically active and stimuli-responsive functional materials. We thus envision that the results and the facile approach reported here can be extended to many applications including environmental monitoring, medical diagnostics and biosensing applications. In this presentation, our recent progress on a range of biopolymer-mediated fabrication and responsiveness studies will also be highlighted.

ACKNOWLEDGEMENTS

We gratefully acknowledge partial financial support by U.S. National Science Foundation (CBET-1703549).

REFERENCES

1. A Robust Fabrication Technique for Hydrogel Films Containing Micropatterned Opal Structures via Micromolding and an Integrated Evaporative Deposition-Photopolymerization Approach. Maurice Bukenya, Jun Hyuk Lee, Subhash Kalidindi, Michael DeCortin, Lauren Tice, Pil J. Yoo, and Hyunmin Yi, Langmuir, 2021, 37(4) 1456–1464.
2. Robust and Reliable Fabrication of Gelatin Films Containing Micropatterned Opal Structures via Evaporative Deposition and Thermal Gelation. Subhash Kalidindi and Hyunmin Yi, ACS Applied Materials and Interfaces, 2023, 14(51) 57481–57491

Real-time investigation of Nanoparticle Self-assembly mechanisms and its controlling factors

Jaewon Lee[1],
[1] *Department of Mechanical & Aerospace Engineering, University of Missouri, Columbia, MO 65211, USA.*,

Superlattice structures formed by nanoparticle (NP) self-assembly have attracted increasing attention due to their potential as a novel class of nanomaterials with enhanced physicochemical properties tailored by the assembly structure.[1] For instance, rationally designing superlattice patterns with defined separation distances can play an important role in controlling properties such as surface plasmon resonance. However, many key questions remain regarding the correlation between the dynamics of individual NPs and the emerging superlattice patterns. Such self-assemblies directly result from a subtle balance between various forces between NPs over different length scales. Brownian force (F_{Br}) resulting from thermal energy triggers motions of NPs. The van der Waals force (F_{vdW}) between NPs is generally a major attractive force at close separations, whereas the electrostatic force (F_{el}), hydrodynamic force (F_D), and steric hindrance repulsion force (F_{Sh}) are repulsive forces.(Fig 1a)

To gain insights into the self-assembly process, we conducted in situ liquid cell TEM (LCTEM) experiments (Fig.1b and Fig.2) and monitored the silver or gold NP assembly process in real time to reveal the kinetics and the driving sources of assembly process under various experimental conditions, such as solvents and ligands.

To understand kinetic details of the process, the self-assembly of gold NPs are further analyzed by calculating the contributions of various forces involved [3-4]. Our results show that these forces, including F_{Br}, F_{vdW}, F_{el}, and F_D, and their interplay play a key role in NP self-assembly process. The superlattice structure can be controlled *via* solvents or ligands.

These results provide insights into the complex competition between forces at different scales, as well as the detailed coupling between dynamics and energetics of self-assembly. The obtained knowledge of interactions between surface coating materials can be extended to a wide range of ligands with different chain lengths, functionalized groups, or biodegradable polymers that can be applied to the fields of material synthesis, bio-mineralization, bio-sensors, or electronic devices..

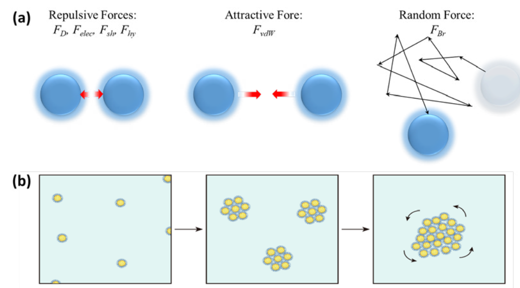

Figure 1 Schematic drawing of (a) particle-particle force interactions and (b) self-assembly process of NPs as a function of time.

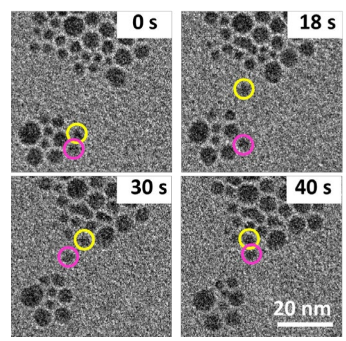

Figure 2 Snapshots of in situ LCTEM images of silver NPs. Yellow and red highlighted particles moved from a small cluster to a large cluster.

REFERENCES

1. Boles, Michael A., Michael Engel, and Dmitri V. Talapin. "Self-assembly of colloidal nanocrystals: from intricate structures to functional materials." *Chemical reviews,* Vol. 116, No. 18, pp 11220-11289, 2016
2. Russel, William Bailey, W. B. Russel, Dudley A. Saville, and William Raymond Schowalter. “Colloidal dispersions”, *Cambridge university press*, 1991.
3. J. N. Israelachvili, in “Intermolecular and surface forces”, Elsevier, Santa Barbara, 2011

Disordered Cathode Materials for High-Energy Lithium-Ion Batteries

Juhyeon Ahn
Lawrence Berkeley National Laboratory

I. SUMMARY

Mn-based transition-metal oxides and oxyfluorides have been considered promising earth-abundant and inexpensive cathode materials. However, these materials often face structural deteriorations that degrade electrochemical cycling performance of lithium-ion batteries. Here I present improved electrochemical performances by unique approaches to changes in the structural and compositional changes of the disordered rocksalt materials. It includes fluorination method, local structural rearrangements, and phase transformations. The resulting cathode materials enhance the Li-diffusion kinetics through reversible structural changes during the charge and discharge process, allowing the stable cycling performances. The study provides the material design principle for next-generation high-energy cathodes.

II. RESEARCH APPROACHES

A. Anion Substitution with Fluorine

The use of a fluoropolymer as an F precursor to synthesize Li transition-metal oxyfluoride materials enables a wide variety of chemical and compositional designs in a rocksalt crystal framework within the $Li_aM_bM'_cO_dY_{2-d}$ system, where M and M' are the redox active and inactive transition metals, respectively (Fig. 1a).

B. Local Structural Rearrangements

By simultaneously increasing Mn and F contents in the disordered rocksalt, the resulting cathode materials experience voltage and capacity evolution over cycling (Fig. 1b). Through advanced characterization analyses, the local structural rearrangements occur along with the Li insertion into the tetrahedral and octahedral sites while the reversible cationic Mn and a small anionic oxygen redox sources participate.

C. Disordered Phase Transformations

With further increasing the Mn content (Li1.1Mn0.8Ti0.1O1.9F0.1), remarkably higher capacity and energy were obtained nearly 320 mAh/g and 900 Wh/kg, respectively. The wide-angle X-ray scattering (WAXS), solid-state nuclear magnetic resonance (NMR), and high-resolution transmission electron microscopy (HRTEM) provide solid evidence of phase transformation occurring in the randomly distributed nanodomain orientations. The disordered cubic rocksalt structure with α phase (Fig. 1c) partially evolves to a more ordered δ and β' phases during the repeated Li insertion/extraction followed by the Mn3+/4+ redox process. The phase transformations between α, δ and β' are reversible, leading to the stable cycling performance.

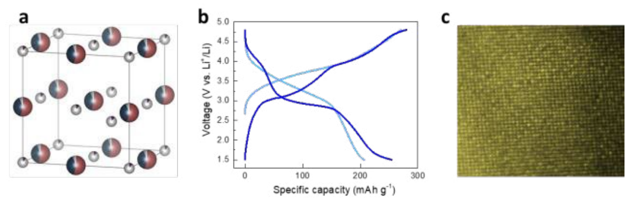

Figure 1: Disordered Rocksalt Cathode Materials. **a**. Crystal structure. b. Voltage profiles of the initial and after numerous cycles. c. STEM-HAADF image obtained from a particle sample.

ACKNOWLEDGEMENTS

This work was supported by the Assistant Secretary for Energy Efficiency and Renewable Energy, Office of Vehicle Technologies of the U.S. Department of Energy under Contract No. DE-AC02-05CH11231.

REFERENCES

1. J. Ahn et al., “Ultrahigh-Capacity Rocksalt Cathodes Enabled by Cycling-Activated Structural Changes,” *Advanced Energy Materials*, 202300221, 2023.
2. J. Ahn et al., “Exceptional Cycling Performance Enabled by Local Structural Rearrangements in Disordered Rocksalt Cathodes,” *Advanced Energy Materials*, Vol. 12, No. 27, 2200426, 2022.
3. J. Ahn et al., “A Fluorination Method for Improving Cation-Disordered Rocksalt Cathode Performance,” *Advanced Energy Materials*, Vol. 10, No. 35, 2001671, 2020.

Spreading and wetting of transiently-crosslinked polymer spheres

Kyujin Ko, Jonathan T. Pham

Chemical and Environmental Engineering
University of Cincinnati
Cincinnati, OH 45221

I. SUMMARY

The interface between coating materials and substrates are critical for a range of applications, including adhesives[1], organic coatings[2], and inkjet printing[3]. For adhesives and coatings, it is important to understand how polymeric materials interact with substrates, including spreading and wetting behavior[4]. This is different than commonly considered water drops. For polymers, crosslinked networks, and non-Newtonian fluids, spreading, wetting, and interfacial behavior have been studied as a function of material properties, such as modulus and chemical bonding, as well as the effects of surface energies of the substrate. Recently, polymeric materials that have transient bonds, characterized by their dynamic reversibility, have become a popular route to control unique viscoelastic properties[5]. However, understanding the interaction between transient polymeric materials and surfaces is an ongoing challenge.

In this study, silicone networks with dynamic bonds are prepared by using an amine group on a polydimethylsiloxane (PDMS) backbone. These networks can associate or dissociate reversibly with an aldehyde group that acts as a crosslinker. The modulus can be controlled by adjusting the amount of crosslinker and duration of curing in the oven. By controlling the material properties, we study the spreading behavior of transient PDMS spheres by tracking changes in shape. An example image of a spreading sphere is shown in Figure 1.

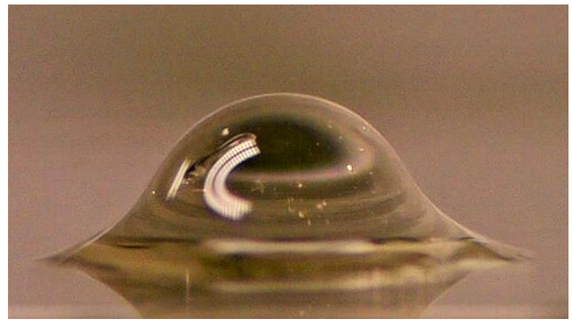

Figure 1: Spreading of polymer sphere on glass substrates

ACKNOWLEDGEMENTS

This work is supported by the National Science Foundation award 2043732.

REFERENCES

1. Zhou, S., Luan, B., and Liu, Y. Recent advances in understanding adhesion of soft materials. Journal of Materials Chemistry B, 9, 17, 3463-3484, 2021
2. Jamil, M., Rafique, M., Rafique, M. S., and Abbas, T. Review of smart coatings: From organic to inorganic, self-healing, and responsive coatings. Journal of Coatings Technology and Research, 17, 4, 871-896, 2020
3. Nakamura, M., and Uchida, K. Recent advances in inkjet printing technologies for functional materials. Applied Physics Reviews, 8, 4, 041303, 2021
4. Cai, Z., Skabeev, A., Morozova, S., and Pham, J.T., Fluid separation and network deformation in wetting of soft and swollen surfaces. Communications Matererials 2, 21 2021
5. Wang, P., Yang, L., Dai, B., Yang, Z., Guo, S., Gao, G., and Zhu, J. A self-healing transparent polydimethylsiloxane elastomer based on imine bonds. European Polymer Journal, Vol. 123 pp. 109382, 2020

Technical Group C-3

Mechanical, Aerospace, and Naval Engineering (MAN)

Practical and Economical Additive Manufacturing for High Temperature Applications

Hoa Nguyen[1], Bibek Poudel[1], Zgiyuan Qu[1], Patrick Kwon[1], Haseung Chung[1]
[1]Michigan State University
East Lansing, Michigan, USA

INTRODUCTION

Heat exchanger intensification through powder processing and enhanced design (HIPPED) is a groundbreaking heat exchanger concept geared towards transforming power generation by enabling very high efficiency closed-loop supercritical CO_2 based power cycles. At Michigan State University (MSU), Haynes 214, a nickel-based superalloy, is being explored as a possible solution to realize this concept by additive manufacturing (AM) technology. We have developed a new patent pending AM process called scalable and expeditious additive manufacturing (SEAM) at MSU, providing an economical solution.

Experimental Setup

Scalable and Expeditious Additive Manufacturing (SEAM)

The SEAM process fabricates the part through multiple steps: (1) premixing the starting metal powder with a photopolymer (2) curing the photopolymer with a digital light projector (DLP) to temporarily bond the metal powder corresponding to the CAD (computer-aided design) model (3) eliminating carbon residue from the photopolymer while initiating direct bonding among the metal powders via diffusion, and (4) consolidating the metal powder to densify the 3D structure [1]. Figure 1 illustrates the overview of SEAM process.

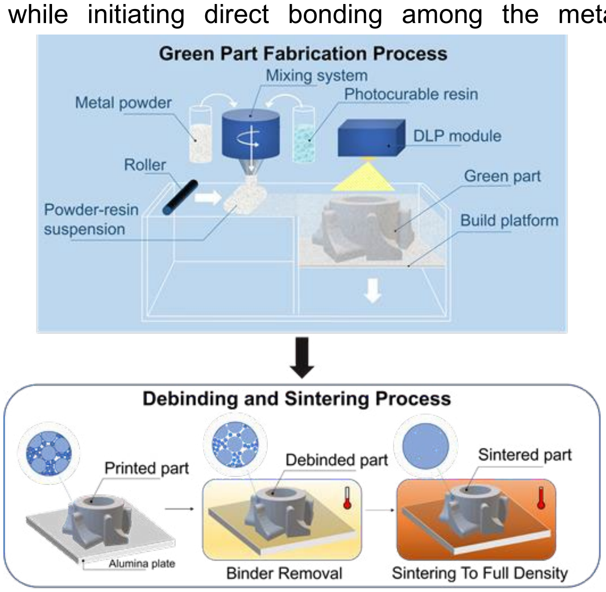

Figure 1. Schematic diagram of the SEAM process

This SEAM process can (1) provide a platform suitable for large-scale printing, (2) expedite printing speed, (3) create fully dense parts with consistent microstructures, and (4) generate reliable and consistent parts.

RESULT

An innovative strategy to attain a complete binder removal and high density as well as dimensional accuracy were developed and employed to achieve final metal parts with relative density above 99.5% and no geometrical distortion.
Also, an internal cost analysis process was carried out on the fabrication of heat exchanger assembly designed by MSU, and the results indicate a 6-9 times total cost reduction by using SEAM process in comparison with selective laser melting (SLM) which is one of widely used AM process, depending on the number of heat exchanger plates per assembly.

ACKNOWLEDGEMENTS

This research was supported by Michigan State University and ARPA-E grant number DE-FOA-0001970 and DE-AR0001476.

REFERENCE

1. Nguyen, H. X., Suen, H., Poudel, B., Kwon, P., and Chung, H., 2020, “Development of an Innovative, High Speed, Large-Scaled, and Affordable Metal Additive Manufacturing Process,” *CIRP Annals*, 69(1), pp. 177–180.

Via Metrology and Inspection for Advanced Electronics Packaging

ChaBum Lee[1], Kuan Lu[1], Heebum Chun[1], Byunggi Kim[2], Masahiro Nomura[2], Jiyong Park[3]

[1]Texas A&M University, College Station, TX, USA, [2]The University of Tokyo, Tokyo, Japan, [3]Korea Institute of Industrial Technology, Incheon, South Korea

I. SUMMARY

This paper presents a via quality inspection method based on analysis of curved-edge diffraction interferogram (CEI) that occurred in via edges. Vias on the wafers made of silicon, silicon carbide, glass, etc. or printed circuit board (PCB) are copper-lined holes to enable a three-dimensional (3D) electrical interconnection between the different layers of the circuitry. The edge diffraction interferograms, being collected through the areal imaging method, are affected by via edge topography, edge geometry and defects. After applying statistical feature extraction methods and wavelet transform to the collected fringe data, corresponding features of various defect modes were further extracted. In summary, both proposed methods enabled characterization and identification of various via edge defect modes and shed light on automatic via edge defects detection and categorization for advanced electronics packaging.

II. CHALLENGES IN VIA INSPECTION

With the advent of high-performance electronic devices used in automotives, airplanes, computers, cellphones, televisions, or tablets, PCB and semiconductor industry are looking for high-throughput, reliable, low-cost manufacturing, and inspection technologies of micro/nanoscale vias on circuitry and wafers to achieve advanced electronics packaging. Conventional via inspection methods such as optical microscopy, scanning electron microscopy (SEM), atomic force microscopy (AFM) and so on are limited to single via characterization due to its small field of view (FOV). As the via size gets smaller and smaller, via parameters such as diameter, roundness, via-to-via distance, heat-affected zone, and via edge roughness should be monitored and controlled.

III. MEASUREMENT PRINCIPLE

The authors have been investigating knife- and curved-edge diffraction techniques for the measurement of motion, edge roughness, metal corrosion, tool wear, photomask defects, wafer defects, and so on [1-4], and established computational models associated with Maxwell's equations and validated those models through experimental verification. The CEI method was applied to via metrology and inspection as seen in

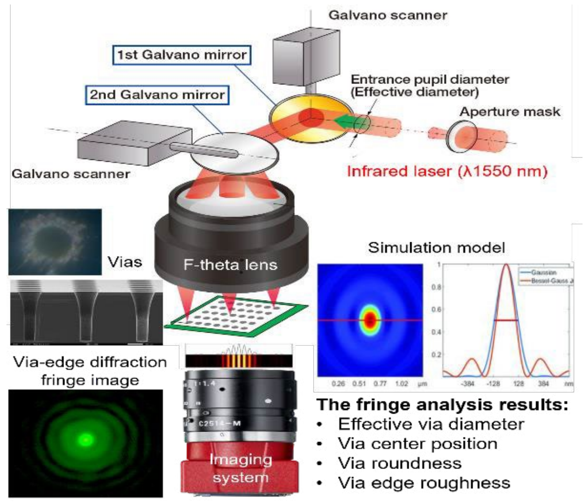

Figure 1: Schematic of the proposed measurement system for via edge metrology

Figure 1. The interferogram obtained by the imaging system was compared with that of the reference-like via. Here the cross-correlation method was employed for quantitative comparison. In this study, micro/nanoscale topographic features on vias with a diameter of 10~100 μm fabricated by laser drilling and chemical etching were inspected and determined their quality in terms of via roundness, center deviation, and via edge roughness by establishing via edge models.

IV. CONCLUSION

The proposed method reveals critical factors that determine the electronic device performance in terms of energy efficiency, life-cycle, and computational functions. The inspection, metrology instrumentation and in-situ analysis techniques will not only benefit the electronics industry with emphasis on quality control but enable their via manufacturing processes under tight control, quality improvement, and reduced scrap rates to enhance environmental sustainability.

ACKNOWLEDGEMENTS

This research was supported by Korea Institute of Industrial Technology (M2302682).

REFERENCES

1. K. Lu, et al, Paper 12496-182, SPIE Advanced Lithography + Patterning, San Jose, CA, 2023 .
2. Z. Wang, et al. Pre. Eng. 77, 104-109 (2022).
3. Z. Wang, et al., Rev. Sci. Instru. 92 125102 (2021).
4. Z. Wang, et al., Appl. Opt. 60(5), 1373-1379 (2021)

Advanced Manufacturing Techniques for Flexible and Wearable Devices

Chi Hwan Lee[1,2,3]
[1]Weldon School of Biomedical Engineering, [2]School of Mechanical Engineering, [3]School of Materials Engineering, Purdue University, West Lafayette, IN 47907 USA

I. INTRODUCTION

Large-scale manufacturing of flexible and wearable devices remains challenging due to the limitations of existing techniques. This study introduces methods that combine wafer-scale transfer printing and programmable dual-regime spray to develop thin film flexible devices and wearable biomedical e-textiles. The wafer-scale transfer printing technique facilitates defect-free separation of high-performance thin-film electronics and enables multiple wafer reuses. Concurrently, the programmable dual-regime spray enables direct custom writing of functional nanoparticles onto various fabrics, achieving submillimeter resolution over a meter scale. The resulting e-textiles preserve their intrinsic properties, including mechanical flexibility, water-vapor permeability, and comfort, even after multiple uses and washes. They also provide a secure fit for different body sizes and shapes, allowing accurate recording of physiological and electrophysiological signals during ambulatory conditions.

II. APPROAH

A. Transfer Printing for Flexible Thin Film Devices

This study presents a complementary transfer printing process composed of crucial steps to produce thin-film electronics. (i) We define different combinations of dissimilar forms and compositions of single-crystalline semiconducting nanomaterials at desired locations on a SiO_2/Si wafer in a single device layout. This is followed by conventional CMOS fabrication processes, resulting in completed electronic circuits on the wafer. (ii) We detach the entire layer of completed thin-film electronics from the SiO_2/Si fabrication wafer without defects, enabling wafer recycling for subsequent fabrication cycles. The separated thin-film electronics can then be attached to any supporting substrates or surfaces. Experimental and computational studies were conducted to understand the transfer printing process's underlying mechanism, ensuring scalability, controllability, and reproducibility in manufacturing. Demonstrations of this method were performed on various representative electronics and nanosensors, such as logic gates, switches, photodetectors, and environmental monitors. These devices exhibit electronic properties comparable to control counterpart devices, highlighting the effectiveness of this approach.

B. Dual-Regime Spray Techniques for E-textiles

This study presents a novel approach utilizing a programmable dual-regime spray to produce custom-designed e-textiles with high spatial resolution (sub-millimeter scale) over a large area (meter scale), surpassing conventional methods. The dual-regime spray consists of two separate airflow modules (i.e., high- and low-speed) mounted on a three-axis computer numerical control (CNC) gantry. This setup allows direct custom spraying of conducting nanoparticles onto arbitrary fabrics with precise control over mass loading and penetration depth, eliminating the need for shadow masks or dedicated vacuum equipment typically required in existing approaches. Pilot field tests were conducted in a remote health-monitoring setting involving large animals, such as horses, demonstrating the scalability and utility of these e-textiles. This approach offers rapid prototyping capabilities for custom e-textiles tailored to diverse clinical needs and opens new possibilities for integrating electronic features onto various surfaces.

III. ILLUSTRATIONS

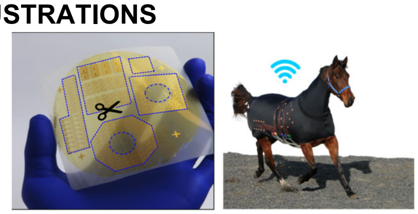

Figure 1: Advanced manufacturing techniques for flexible thin film devices and e-textiles.

ACKNOWLEDGEMENTS

These works were published in *Adv. Mat.*, 34, 9, 2108021 (2022), *ACS AMI*, 13, 20, 24024 (2021), *Nano Lett.*, 19, 81, 5796 (2019), and *PNAS*, 115, 7236 (2018)

A novel approach of mold-free manufacturing for highly sensitive pressure and tactile sensors

Sunghwan Lee[1], Jinwook Baek[1], Yujie Shan[1], Mitesh Mylvaganan[1], Huachao Mao[1], Han Wook Song[2]

[1] School of Engineering Technology, Purdue University, West Lafayette, IN 47907, United States
[2] Center for Mass and Related Quantities, Korea Research Institute of Standards and Science (KRISS), Daejeon, 34113, Republic of Korea

I. SUMMARY

We present a novel manufacturing paradigm that eliminates the reliance on traditional mold-dependent methods for producing pressure and tactile sensors. Conventional manufacturing processes involve intricate and expensive patterning techniques such as mask aligning, photolithography, etching, and transferring patterns onto flexible substrates. In contrast, our mold-free fabrication approach utilizes high-resolution multiscale 3D-printed microstructures as the substrate and employs a gas-phase conformal polymer coating technique to create a mold-free sensing platform.

II. RESULTS AND DISCUSSION

The utilization of state-of-the-art 3D printers enables the fabrication of intricate structures with complex geometries and customized shapes through precise micropatterning. We employ an array of dome and spike structures with controlled spike density as the substrate, ensuring a high surface area for enhanced sensor performance. To achieve uniform coating on the microstructured surface, we utilize oxidative chemical vapor deposition (oCVD) at low temperatures (< ~100 ℃) to deposit a highly conformal and conductive electrode known as poly(3,4-ethylenedioxythiophene) (PEDOT).

The fabricated pressure sensor exhibits sensitive response to a wide range of pressures, with the sensitivity depending on the density of the spikes. It demonstrates high sensitivity and rapid response/recovery time (~36 μs) even at ultra-low pressures below 0.05 kPa. To validate the mechanism behind this exceptional performance, we conducted finite element analysis, which revealed a correlation between the surface structure and the sensor's characteristics.

Our unique findings have significant implications for technologies that require improved sensing capabilities, scalability, and easy adjustment of sensor geometry, all achieved through a cost-effective manufacturing process.

III. ILLUSTRATIONS

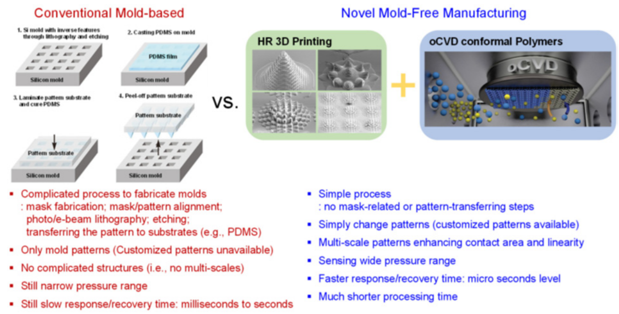

Figure 1: Comparisons of the manufacturing process of pressure/tactile sensors between the conventional mold-based and mold-free manufacturing[1-4]

ACKNOWLEDGEMENTS

This work was partially supported by National Science Foundation, Award number CBET-2207302. S.L. and H.W.S. acknowledge the support from the Improvement of Measurement Standards and Technology for Mechanical Metrology (Grant No. 23011043) by KRISS.

REFERENCES

1. Heydari Gharahcheshmeh, M.; Wan, C. T.-C.; Ashraf Gandomi, Y.; Greco, K. V.; Forner-Cuenca, A.; Chiang, Y.-M.; Brushett, F. R.; Gleason, K. K., Ultrathin Conformal oCVD PEDOT Coatings on Carbon Electrodes Enable Improved Performance of Redox Flow Batteries. *Advanced Materials Interfaces* **2020,** *7* (20), 2000855.
2. Clevenger, M.; Kim, H.; Song Han, W.; No, K.; Lee, S., Binder-free printed PEDOT wearable sensors on everyday fabrics using oxidative chemical vapor deposition. *Science Advances* **2021,** *7* (42), eabj8958.
3. Kim, H.; Zhang, Y.; Rothschild, M.; Roh, K.; Kim, Y.; Jang, H. S.; Min, B.-C.; Lee, S., Hybrid Silicon-Polymer Photodetector Engineered Using Oxidative Chemical Vapor Deposition for High-Performance and Bias-Switchable Multi-Functionality. *Adv. Funct. Mater.* **2022,** *32* (29), 2201641.
4. Mannsfeld, S. C. B.; Tee, B. C. K.; Stoltenberg, R. M.; Chen, C. V. H. H.; Barman, S.; Muir, B. V. O.; Sokolov, A. N.; Reese, C.; Bao, Z., Highly sensitive flexible pressure sensors with microstructured rubber dielectric layers. *Nature Materials* **2010,** *9* (10), 859-864.

Additive Manufacturing of Rubber

Sarath Kamath[1], Jae-Won Choi[1],
[1]Department of Mechanical Engineering, The University of Akron

I. INTRODUCTION

Rubber is a versatile, durable, resistant, and insulating material which has a plethora of applications. However, processing condition requirements such as high pressure and temperature for natural and synthetic rubbers make additive manufacturing (AM) of rubber challenging. The purpose of this study is to investigate whether natural and synthetic rubbers can be used as a 3D printable material. A printable ink was developed using rubber latex, synthetic liquid rubber or blended in varying amounts to increase the ink's total solid content and prevent shrinkage. The formulated ink is made with close relation to any traditional rubber formulation and the ink after printing (green part) undergoes heat treatment to incorporate crosslinking and induce vulcanization in the printed specimens. The rheological properties of the ink were investigated for consistent extrusion and shape retention in the printed parts. The dimensional accuracy, printability, and mechanical properties of the 3D printed specimens were also examined.

II. MATERIALS AND METHODS

The properties of high solid content rubber inks used in the direct print process were evaluated to determine the ideal printing parameters, and the 3D printed specimens were subjected to vulcanization.

Materials: The natural rubber (NR) latex purchased from Liquid Latex Direct (Burton-upon-Stather, UK) and liquid butadiene rubber was obtained from Kuraray Company, Ltd (Tokyo, Japan). TritonX-100 surfactant and stearic acid activator were purchased from Sigma-Aldrich (St. Louis, USA). The vulcanizing agents and accelerators used in this study—sulfur, zinc oxide, tetramethyl thiuram disulfde (TMTD), and Ncyclohexyl-2-benzothioazole sulfenamide (CBTS) — were provided by Akrochem Co. (Akron, USA).

Vulcanization: A conventional rubber vulcanization technique that inserts sulfur crosslinks using heat treatment was adopted in this system by using the same additives as initiators, activators, crosslinking agents and accelerants. The high viscosity of the blended mixture enabled the additives (sulfur, stearic acid, zinc oxide, TMTD and CBTS) to diffuse homogenously. Vulcanization of the material was then achieved by thermal treatment of the sample at 140 °C to 160 °C for 20 minutes.

III. RESULTS

This study shows the viability of utilizing rubber inks for AM and demonstrates the potential for rubber inks using the direct-ink write (DIW) process. AM provides manufacturers the freedom to customize and produce parts on a small scale at a lower cost. The successful 3D printing and processing of the design models demonstrates that the rubber ink in this study can be printed, processed, and used in future applications in the automotive and aerospace industries.

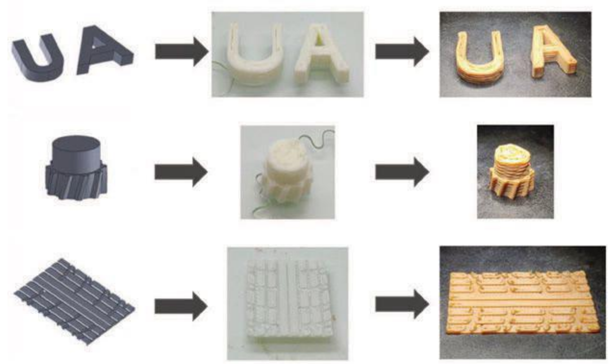

Figure 1: 3D structures fabricated by DIW

ACKNOWLEDGEMENTS

This study was partially supported by research grants from the Center for Tire Research (CenTiRe) at The University of Akron.

REFERENCES

[1] M. Kim and J. W. Choi, “Rubber ink formulations with high solid content for direct-ink write process,” *Addit. Manuf.*, vol. 44, no. March, p. 102023, 2021.
[2] S. S. Kamath, J.W. Choi, “3D printing of synthetic rubber ink via direct ink writing process,” *Rubber world*, vol. 265, no. 2, pp. 40–45, 2021.

Cutting mechanisms of cross-ply carbon fabrics using a drag cutter

Jeremiah Westrum, Dave Kim
School of Engineering and Computer Science, Washington State University, Vancouver, WA, USA.

I. SUMMARY
An experimental study investigates cutting mechanisms of cross-ply woven carbon fabrics. The thrust force decreases with increasing the cutter angle from 15° to 45°. The thrust force increases, and the feed force decreases when the fiber orientation becomes from 0°/90° to 45°/135°. The effect of feed on cutting forces is minimal.

II. INTRODUCTION
Dry carbon fiber fabrics are typically cut to the desired shape and size using computer-controlled cutting machines before the stacking-up process when fabricating carbon fiber reinforced plastics (CFRP) [1]. This study aims to investigate the effect of the cutting conditions and the fiber orientations on cutting forces when cutting cross-ply dry carbon fabrics with a drag cutter.

III. METHODS
The workpiece material is a woven carbon fiber fabric manufactured by Hexcel, a 5 harness satin weaving type. The experimental setup uses a 3-axis CNC milling center to cut the workpiece placed in a vacuum plate (20 inHg) mounted with a 3-axis dynamometer for output cutting force recording. The input variables include 1) fiber orientations: 0°/90° and 45°/135°, 2) feed: 2.54 m/min and 10.16 m/min, and 3) drag cutter angle: 15° and 45°.

III. RESULTS AND DISCUSSION
When the drag cutter is applied to the dry fabric specimen, the thrust force (Fz) rises rapidly due to the cutter's pressing the jig. As the cutting proceeds, the feed force (Fy) increases from 0 N to 1.5 N, cutting with an average force of 1.5 N, and then, after the maximum cutting principal force of 2.4 N is generated immediately before completing.

Fig. 2 shows how average cutting force is affected by fiber orientation, feed speed, and cutter angle when using the drag cutter. All three input parameters have little effect on the feed force and the later force, while the thrust force is influenced highly by the fiber orientation and the cutter angle, which is the angle between the cutter's edge and the feed direction.

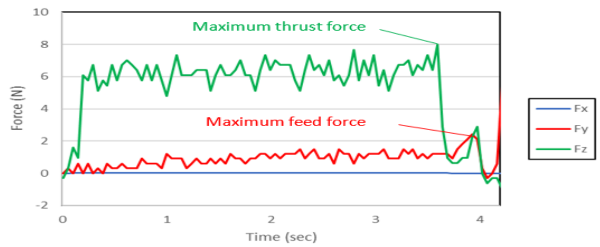

Fig. 1: Cutting forces during the cutting process (45°/135° fabric; 2.54 m/min; 15° cutter angle)

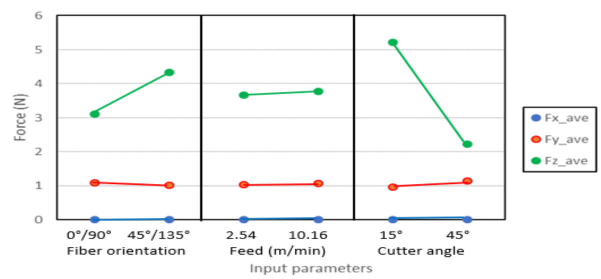

Fig. 2: Cutting force variations

III. CONCLUSION
When using the drag cutter, the cutting forces of the dry woven carbon fabrics depend highly on the cutter angle, which reduces thrust force with the increment. The fiber orientation also affects the cutting forces, and the 45°/135° fabric results in higher thrust force. The feed did not influence the cutting force magnitudes.

ACKNOWLEDGEMENTS
This work was supported by the Joint Center for Aerospace Technology Innovation (JCATI) of the WA State, USA, and the Ministry of Trade, Industry & Energy (MOTIE, Korea) [grant number 20018553, entitled "Development of preform manufacturing work-cell for a high productivity and high-quality RTM (resin transfer molding) process."

REFERENCES
1. Snape, A.E., Turner, J.L., El-Dessouky, H.M. Saleh, M. N., Tew, H., Scaife, R. J., "Stabilising and Trimming 3D Woven Fabrics for Composite Preforming Applications." *Appl Compos Mater* 25, 735–746 (2018).

3D Printed Microchannel-based Blood Plasma Self-separation for Biomedical Applications

Eon Soo Lee[1], Yudong Wang[1], Bharath Babu Nunna[1]
[1]Advanced Energy Systems and Microdevices Laboratory, Department of Mechanical and Industrial Engineering, New Jersey Institute of Technology, Newark, NJ 07102, USA

I. INTRODUCTION

A critical factor in facilitating the widespread implementation of lab-on-a-chip devices for point-of-care applications is the effective extraction of cell-free plasma and precise measurement of biomarkers within blood samples due to the extensive use of blood plasma in disease diagnosis can be attributed to its abundance of biomarkers. In this study, we propose a novel approach that combines the Dean vortex and micro-filtration methods, fabricated through 3-D printing, to create three-dimensional structured microfluidic channels. This innovative method enables on-chip extraction of cell-free plasma.

II. TECHNICAL APPROACH

A. Microchannel Fabricated by 3-D Printing

In this study, we utilized the Photonic Professional GT system (Nanoscribe) to fabricate three-dimensional (3-D) microchannels of varying depths. The objective was to establish a micro-filtration methodology employing a spiral channel design. The photoresist material was crosslinked at a voxel scale of 1 um^3 using an infrared laser, enabling the creation of intricate molds for the microchannel structures, as shown in Figure 1a. Subsequently, the soft lithography method was used to fabricate the Polydimethylsiloxane (PDMS) microchannel.

B. Blood-plasma Separation

To enhance the separation of cell-free plasma, we integrated one hundred 1 × 2 × 30μm (W, H, L) filter sub-channels into the outer trifurcation outlet of the spiral microchannel. This spiral channel design first effectively concentrates red blood cells towards the inner outlet channel, reducing cell concentration in the blood flow before reaching the micro-filters in the outer outlet channel. The efficiency and separation speed were substantially enhanced through the implementation of a cross-flow design and lower cell concentration. This strategic approach effectively mitigated the issue of clogging, leading to notable improvements in the overall performance of the system, as shown in Figure 1b.

III. RESULT AND DISSCUSSION

The integration of micro-filtration into the spiral channel for blood plasma separation achieving an average hematocrit reduction ranging from 99.8% to 100% within a rapid timeframe of 52 seconds. This design exhibits significant potential for integration into widespread Point-of-Care devices.

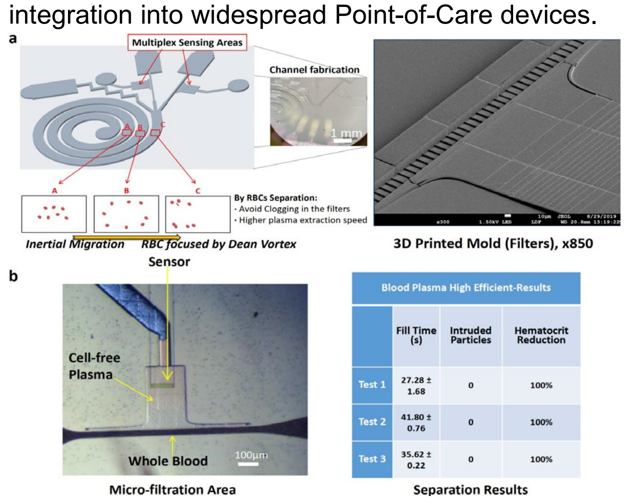

	Fill Time (s)	Intruded Particles	Hematocrit Reduction
Test 1	27.28 ± 1.68	0	100%
Test 2	41.80 ± 0.76	0	100%
Test 3	35.62 ± 0.22	0	100%

Figure 1: (a) Microchannel design (left), 3-D view of the channel(mid), and SEM image of micro-filters (right); (b) Real-time frame of blood-plasma separation in the micro-filtration area (left), High-efficient cell-free plasma separation results (right).

ACKNOWLEDGEMENTS

The authors acknowledge the research support from the New Jersey Institute of Technology (NJIT) and the National Science Foundation (Grant ID: NSF IIP-1643861).

REFERENCES

1. *Ingis, B, and Lee, E.S. "3D Printing for Whole Blood Filters Designed for Simple Integration with a Variety of Sensor Platforms." In 2019 IEEE HI-POCT, pp. 143-146. IEEE, 2019.*
2. *Wang, Y., Nunna, B.B., Talukder, N., Etienne, E.E. and Lee, E.S., 2021. Blood plasma self-separation technologies during the self-driven flow in microfluidic platforms. Bioengineering, 8(7), p.94.*

Sound Recognition Using MTConnect Framework for Real-time Cutting Condition Monitoring of CNC Milling Machine

Eunseob Kim[1,2], Junyi Yuan[1], Michael Fassnacht[2], Martin B.G. Jun[1,2]
[1]School of Mechanical Engineering, Purdue University, West Lafayette, IN47907,
[2]Indiana Next Generation Manufacturing Competitiveness Center (IN-MaC), Purdue University, West Lafayette, IN47906

I. Introduction

Well-experienced operators in the metal cutting industry can tell the cutting conditions by listening to the sound of the machine's operation. Based on their experiences in a context and with sound made by the machine, they determine whether cutting is good. In the previous study, cutting state monitoring and productivity prediction for a tube-cutting machine were performed [1]. This study presents the development and application of sound recognition for real-time cutting condition monitoring of CNC milling machines. To adopt human auditory sensing for manufacturing sound recognition, we utilized the MTConnect framework to make the real-time stream of the sound sensors. For the artificial intelligence (AI) algorithm to implement real-time monitoring, we utilized one-dimensional (1D) convolutional neural network (CNN) model.

II. Proposed method

Figure 1 illustrates the outline of the proposed monitoring method for real-time remote sound recognition of the CNC mill. Raspberry Pi was used for edge computing for the sensors and the AI model. multiple stethoscope-based USB microphones, so-called internal sound sensors, were deployed to the machine. MTConnect was employed to enable sound streams from the sensors so that the AI model predicts cutting conditions in real-time. The end users monitor the cutting conditions using web-based dashboards.

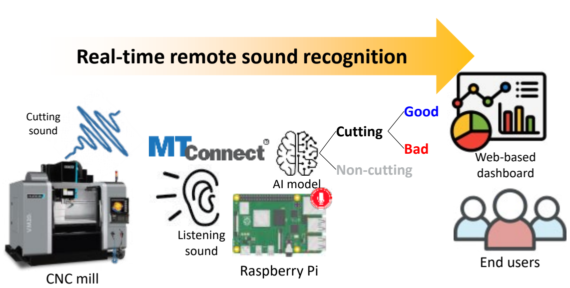

Figure 1: Outline of real-time sound recognition system for CNC mill

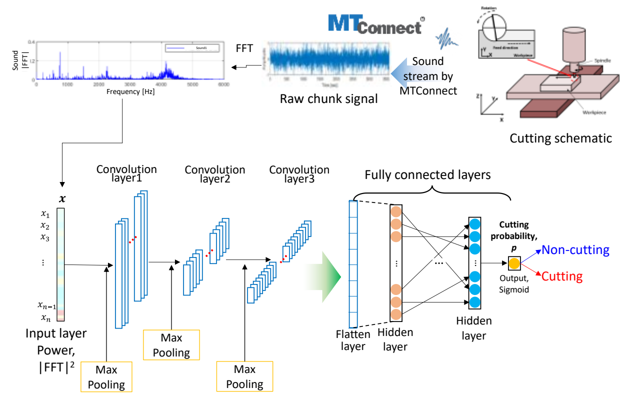

Figure 2: Sound data pipeline and CNN architecture

III. AI model and implementation

Figure 2 showed a real-time sound data pipeline and the 1D CNN architecture. As an input feature of the CNN model, the square magnitude of FFT (fast Fourier transform) was utilized. The feature is fed into the CNN architecture. Three convolutional layers and three hidden layers were adopted in the CNN architecture. The output layer of the CNN model is a binary that has True or False. In Figure 2, True means cutting, and False means non-cutting. The entire system was deployed on Raspberry Pi. A program for AI algorithms was written in Python. For the CNN model, TensorFlow Lite module was used. Sound recognition for cutting condition monitoring was successfully implemented.

ACKNOWLEDGEMENTS

This research was supported by Wabash Heartland Innovation Network (WHIN) and Indiana Next Generation Manufacturing Competitiveness Center (IN-MaC).

REFERENCES

1. E. Kim et al., "Sound Recognition based on Convolutional Neural Network for Real-Time Cutting State Monitoring of Tube Cutting Machine," Int. J. Precis. Eng. Manuf. Smart Tech. Vol1, No. 1, pp. 1-18, 2023

A Study on the Development of Terrain Following Simulator using Digital Terrain Elevation Data(DTED)

MunGyou Yoo[1], Jisu Lee[1], Sangchul Lee[1]

[1]Department of Smart Air Mobility, Korea Aerospace University, Goyang, Gyeonggi-do, Republic of Korea

I. INTRODUCTION

The terrain following(TF) technique is used by aircraft to fly at low altitudes to reduce the probability of being detected by the enemy. A TF simulator recognizes the terrain using DTED and generates and guides the flight path based on the aircraft's performance. In this paper, we develop the TF simulator which consists of a radar simulator, terrain following computer(TFC) simulator, and flight simulator as shown in Fig. 1.

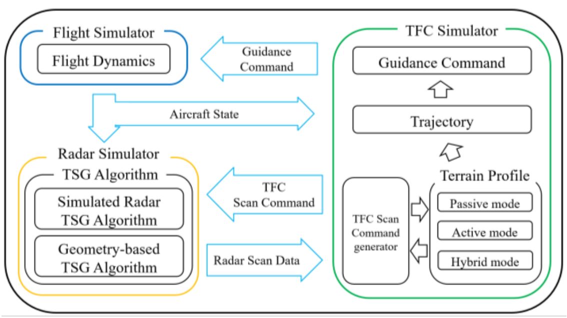

Figure 1: Configuration of Terrain Following Simulator

The radar simulator receives the terrain scan command, generates measurements which are then processed into terrain scan data(TSD) and sends TSD to the TFC. After receiving the TSD, the TFC generates a flight trajectory for the aircraft to follow. The TSD generation algorithm was developed and implemented in the radar simulator, and the phased array radar was simulated to generate TSD with DTED Level 2 database [1]. To develop TF algorithm without actual flight tests, it is essential to develop a TF simulator. Using high-fidelity simulator can partially replace the real flight verification. Therefore, the cost and time required for TF system development can be reduced, and the risks can be minimized.

II. METHOD

The TFC Simulator consists of terrain profile module, trajectory module, and guidance command moule. And three Modes can be selected in TFC Simulator: passive mode, active mode, and hybrid mode. Depending on the selected mode, the corresponding terrain profile, trajectory, and guidance command are generated. The terrain profile module is a module for obtaining the terrain information [2]. The trajectory module generates the flight path by applying morphological dilation operation and circular path [3]. The guidance command module generates vertical accelerations based on the generated TF flight path and communicates with the flight simulator. Based on the requirements of the terrain profile, trajectory, and guidance command modules, unit tests were conducted and the results were shown in fig.2.

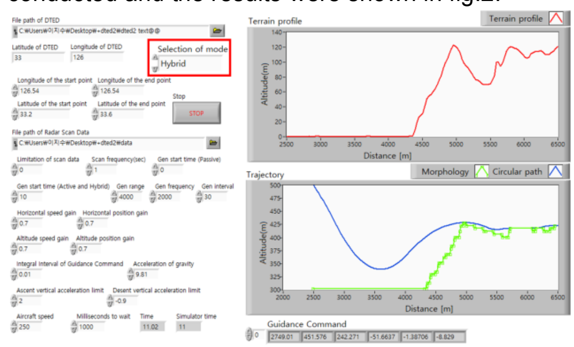

Figure 2: Hybrid mode in TFC Simulator

III. RESULTS

This paper proposes the TF simulator which could be used for the development of TF algorithm without real flight test. The TF simulator consists of the radar simulator, the TFC simulator, and the flight simulator. The simulation results of the TF simulator are presented.

REFERENCES

1. Lee, J. S., Yoo, M. G., Kang, S. H., Cheon, D. I. and Lee, S. C., "Development of Automatic Terrain Following Simulator using a Terrain Scan data Generation Algorithm," In *The Proceedings of the 2022 Asia-Pacific International Symposium on Aerospace Technology*, 2022.
2. Lee, H. J., Hahn, S. H., Lee, S. C., Lee, S. I., and Seo, K. S., "A Study on Terrain Profile Generation for Terrain Following," Journal of the Korean Society for Aeronautical and Space Sciences, Vol. 51, No. 1, 2023, pp. 49~56
3. Hahn, S. H., Lee, H. J., Lee, S. C., Choi W. Y. and Jung, J. H., "A Study on the Terrain-Following Trajectory Generation Method Using Morphology and Circular Path," Journal of the Korean Society for Aeronautical and Space Sciences, Vol. 51, No. 2, 2023, pp. 93~102

Decarbonization Effort in Non-Road Heavy-Duty Equipment

Youngjin Son[1]
[1]Caterpillar Inc.

I. SUMMARY

Climate change is one of the most challenging problems and to keep the planet from warming, most countries have goals to reach net zero by 2050. Caterpillar continued its investments to support this global initiative in various area via its own business in energy and transportation sectors. In this paper, Caterpillar's efforts and solutions in alternative and renewable power generation sources and transportation area will be introduced.

II. ENERGY, FUEL ECONOMY AND EMISSIONS

Caterpillar continues to improve existing power solution using diesel or natural gas fuel with better fuel efficiency and less emissions meeting most countries' emission regulation including US Tier4, EU Stage V, and more to reduce greenhouse gas. These products enable customers to achieve their climate-related goals.

III. PRODUCTS

Caterpillar committed to continue investment in products to enable de-carbonization to save the environment.

A. Lower-carbon intensity fuels

Fuel choice is one-way customers can reduce greenhouse gas emissions. Many Caterpillar products are operating on lower-carbon alternatives to diesel and natural gas today, including biodiesel, renewable diesel, and biogas. For example, HVO can reduce carbon intensity by 45% to 85% versus diesel. Caterpillar engines operating on natural gas blended with up to 80% hydrogen are being demonstrated in power generation projects today. Turbines can operate on up to 100% hydrogen.

B. Hydrogen fuel cell

Caterpillar has a three-year project through a collaboration with Microsoft and Ballard Power Systems to demonstrate a power system incorporating large-format hydrogen fuel cells to produce reliable and sustainable backup power for Microsoft data centers. Hydrogen fuel cell powered locomotive train is being demonstrated.

C. Electrification

D6E XE high-drive dozer, for example, offers up to 35% better fuel efficiency and up to 23% less fuel usage than previous models. The 795 electric drive mining truck with a diesel-electric drivetrain has been paired with a trolley-assist system.

D. Battery-stored power

Worksite power solution for a land-drilling operation that pairs a G3512 Natural Gas Generator with the Cat Energy Storage System with fully integrated controls.

E. Microgrids

Microgrids integrate renewable energy sources.
into electric power systems. These worksite installations are particularly valuable in remote locations where renewable energy sources like solar or hydropower are readily available and electrical grids may deliver inconsistent power.

Figure 1: Hydrogen-Fueled Genset

REFERENCES

1. Caterpillar sustainability report, Caterpillar, Inc., 2021.
2. Industrial decarbonization roadmap, DOE, 2022
3. The U.S. National blueprint for transportation decarbonization, 2023

High performance green composites made with cellulose long filament and vanillin epoxy

Jaehwan Kim[1], Samia Adil[1], Bijender Kumar[1], Yaohui Ci[1]

[1]CRC for Nanocellulose Future Composites, Inha University, Incheon 22212, Republic of Korea

I. INTRODUCTION

Recently, the bio-resource demand for developing high-performance and environmentally friendly composites has been increasing because of net zero emissions and replacing petroleum-based materials [1]. The enticing hierarchical structure of cellulose has made it possible to fabricate bio-based fibers via wet-spinning. Strong and tough cellulose long filament (CLF) has been developed by wet spinning cellulose nanofiber suspension [2]. By developing an ideal biodegradable resin with superb adhesion properties, the NF could promise high-performance and all-green fiber-reinforced polymer composite fabrication. Vanillin is an excellent source to make bio-based composites [3]. In this work, green vanillin epoxy (VE) resin was synthesized from vanillin and utilized for fabricating CLF-reinforced green composites (CFRGC).

II. Methods

A. Nanocellulose filament fabrication

Strong, tough and long filament was made by wet spinning cellulose nanofiber (CNF) suspension followed by coagulation, washing, drying and stretching. 1.6 wt% CNF suspension was wet spun at a spinning speed of 250 cm/min in citric acid solution to get CLF.

B. Resin synthesis and composite fabrication

To prepare CFRGC, firstly, bio-based VE was prepared by the reaction of vanillin and epichlorohydrin (ECH). To prepare the resin, VE (0.12 mol) and 4,4-diamino diphenylmethane (DDM, 0.089 mol) were dissolved together in excess of acetone to get the uniform mixture. After complete dissolving, the acetone was evaporated at 80°C to obtain the viscous epoxy-based resin. Biobased VE-DDM resin was then impregnated with CLFs mats using the vacuum assisted resin transfer molding (VARTM) technique.

III. RESULTS

The proposed all-green composite combines the high mechanical strength and stiffness of wet-spun nanocellulose long filaments with the rigidity of biobased VE resin. The developed composite material is very lightweight, The reinforcement with CLFs improved the flexural strength and flexural modulus of neat biobased VE resin remarkably by 135.1% and 542.8%. The green composite possessed a T_g of 144°C and a water contact angle of 96.4°, demonstrating good thermal stability and hydrophobic properties. Figure 1 shows schematic of CFRGC fabrication process.

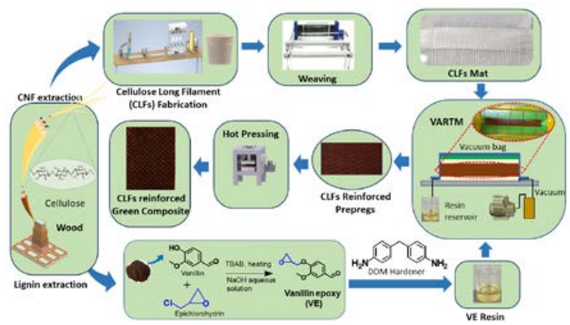

Figure 1: Schematic of CLF-reinforced green composite fabrication.

ACKNOWLEDGEMENTS

NRF of Korea supported this research (NRF-2015R1A3A2066301).

REFERENCES

1. Kumar, B.; Agumba, D.O.; Pham, D.H.; Kim, H. C.; Kim, J. Recent Progress in Bio-Based Eugenol Resins: From Synthetic Strategies to Structural Properties and Coating Applications. J. Appl. Polym. Sci. 2021, 51532.
2. Kim, H.C., Kim D., Lee J.Y., Zhai L., Kim J. Effect of Wet Spinning and Stretching to Enhance Mechanical Properties of Cellulose Nanofiber Filament. Int J Precis Eng Manuf - Green Technol 2019, 6:567–75.
3. Kumar, B.; Agumba, D.O.; Pham, D.H.; Kim, H.C.; Alrobei, H.; Kim, J. Recent Research Progress on Lignin-Derived Resins for Natural Fiber Composite Applications. Polymers 2021, 13:1162.

Morphology Control of Inkjet-Printed Micro-Patterns for Printed Electronics

Jun Young Hwang, Jun Ho Yu, Kwon Yong Shin, Chanwoo Yang, Kwan Hyun Cho, Sang-Ho Lee
Korea Institute of Industrial Technology

SUMMARY
In printed electronics, morphology of the printed micro-patterns has a significant impact on the performance of the device. In particular, the industries of highly integrated electronics and opto-electrical energy devices demand highly fine and highly conductive electric interconnections. On the other hand, for flexible OLED/QLED displays and lighting devices, uniform thickness is essential for micro-pixel printing of electro-emission layers and color conversion layers, as well as for organic layer printing of thin film encapsulation. This presentation introduces several state-of-the-art techniques for control the morphology of the inkjet-printed micro-patterns of photo- and electro-functional materials [1~3].

ACKNOWLEDGEMENTS
This study was conducted with the support of the Ministry of Trade, Industry and Energy (MOTIE, Grant No. 20016124)

REFERENCES
1. I. Sim, S. Park, K.-Y. Shin, C. Yang, H. Kang, J.Y. Hwang, S.-J. Moon, "Inkjet Printing of High Aspect Ratio Silver Lines via Laser-Induced Selective Surface Wetting Technique," *Coating*, Vol. 13, No. 683, pp. 1-11, 2023.
2. S. Sim, S.-H. Lee. K.H. Cho, J.H. Yu, "Feature Size Control by Layer-by-Layer Printing and Non-wettable Patterns for Inkjet Printing of Micro Metal Electrode," *J. Electr. Eng. Technol.*, Vol. 16, pp. 2157-2165, 2021.
3. S.Y. Lee, C. Sakong, S.-H. Choi, B.-K. Ju, K.H. Cho, "Controlling the Surface Modification by CF_4 Plasma Treatment for Inkjet Printed Color Conversion Layer with InP-Based QDs Ink," *Adv. Mater. Interfaces*, Vol. 10, No. 2201851, pp. 1-8, 2023.

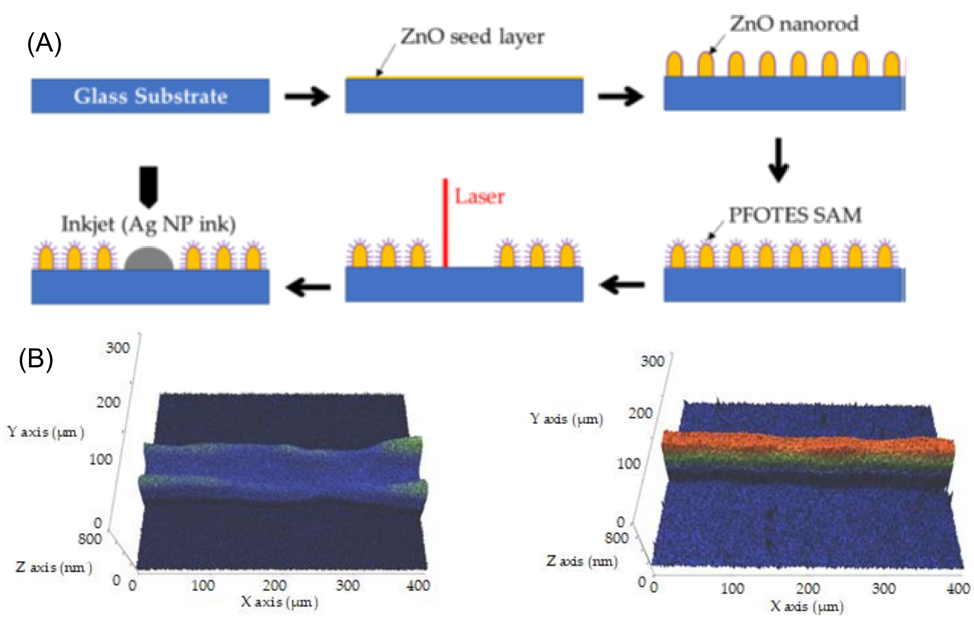

Figure 1: (A) Inkjet printing via laser-induced selective surface wetting technique [1].
(B) 3-D profiles of printed silver lines on bare glass (left) and on the surface with selective wetting technique, where inkjet drop spacing is 5 μm and laser ablation width is 40 μm.

Multifunctional Mechano-Luminescence-Optoelectronic Composites for Non-Invasive and Self-Learning Health Monitoring Wearables

Donghyeon Ryu[1]
[1]Department of Mechanical Engineering, New Mexico Tech; donghyeon.ryu@nmt.edu

I. SUMMARY
This study presents an invention of multifunctional mechano-luminescence-optoelectronic (MLO) composites and up-to-date progresses on an application of the MLO as a self-powered strain sensing component for health monitoring wearables. MLO fibers will be woven into traditional garments to sense physical deformation on human body surface without battery use. The mechanical strain data are processed in machine learning algorithms to create 3D mapping of strains on the body surface for diagnosis and prognosis of health disorders. So, the MLO-based health monitoring wearable system is expected to be self-powered and self-learning to adopt its strain-based health monitoring by feeding the history of end-user's personal data into the machine learning algorithm.

II. Multifunctional mechano-luminescence-optoelectronic composites

A. Materials and Fabrication

The MLO composites (figure 1) are composed of two functional constituents, such as mechano-luminescent (ML) copper-doped zinc sulfide (ZnS:Cu)-based elastomeric composites and mechano-optoelectronic (MO) poly(3-hexylthiophene) (P3HT)-based thin films.

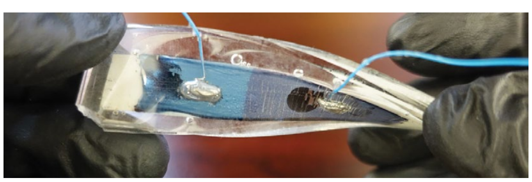

Figure 1: Multifunctional MLO composites prototype

ML elastomeric composites are fabricated by blending the ZnS:Cu micro-particles in polydimethylsiloxane (PDMS) elastomer and mold-casting the ZnS:Cu-PDMS. MO P3HT-based thin film is fabricated by spin-coating the P3HT-based solution on a PDMS substrate. The ML and MO constituents are assembled to prepare the MLO.

B. Coupled mechanical-radiant-electrical energy conversion

The MLO generates direct current (DC) when subjected to external dynamic mechanical stimuli. The ML constituent glows under strain, and the ML light is absorbed by the MO thin film to generate DC (figure 2).

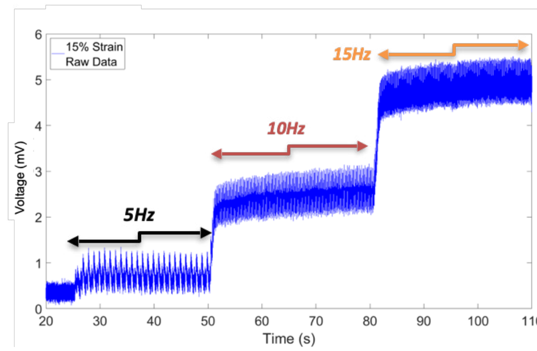

Figure 2: DC voltage from MLO under tensile strain up to 15% strain at varying loading frequencies

C. Self-powered strain sensing

The generated DC from MLO was shown to vary its magnitude with strain and strain rate (figure 3). It is mainly attributed to strain-sensitive ML light intensity as well as optoelectronic properties of the MO thin films.

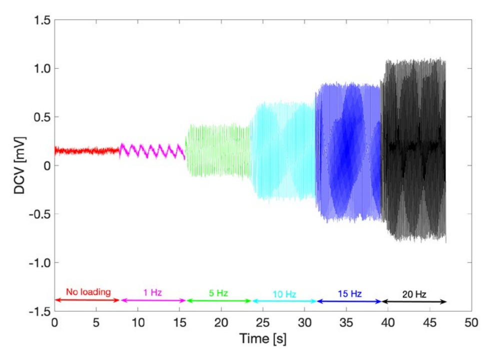

Figure 3: DC voltage v. cyclic loading up to 5% strain with varying frequencies

ACKNOWLEDGEMENTS
Author thanks New Mexico Space Grant Consortium, NASA's Space Grant College and Fellowship Program and NASA EPSCoR CAN (grant #: 80NSSC17M0050) for supporting this study.

Cells function as ternary logic gates to decide their migration direction under combined chemical and fluidic cues

Bumsoo Han[1], Hye-ran Moon[1], Soutick Saha[2], Andrew Mugler[2]
[1]Purdue University, [2]University of Pittsburgh

I. INTRODUCTION

Directed cell migration is ubiquitous in many physiological and pathological processes [1-2]. During these processes, cells sense and process multiple and often heterogeneous cues, including chemical, mechanical, and fluidic ones [3-4]. Even though extensive research has been performed to identify key signaling molecules for various environmental cues [5-6], it is still puzzling how cells decipher simultaneous heterogenous cues and decide on a migration direction. Specifically, how cells respond to integrated chemical and fluidic cues is still not well understood. In the present study, we investigated the cellular signal processing machinery by reverse-engineering directed cell migration to elucidate a biophysical understanding of how cells decipher integrated chemical and fluidic cues to determine migration direction.

II. RESULTS AND DISCUSSIOM

A. The engineered microenvironment with controlled chemical and fluidic cues

We applied pressure-driven flow to the cells using microfluidic platform that were simultaneously exposed to the TGF-β gradient in two scenarios: 1) parallel flow of an additive cue with the TGF-β gradient and 2) counter flow of a competing cue to the TGF-β gradient. Then, we analyzed the complication of the integrated chemical and fluidic cues asking if the non-linear cue profiles fulfill the physical chemical cue-detection limit of the cells. In results, most of cells were located in the area where a relatively shallow gradient is present even for cells not to detect the gradient.

B. Intra-cellular processing of two cues simultaneously

We observed that cells effectively select a cue to follow in processing the mixed chemical and fluidic cues. When cells are capable of sensing both chemical and fluidic cues, cells tend to follow a chemical gradient direction in both the additive combination with the parallel flow and the competing with the counter flow. The cells were biased toward the upstream direction of the fluidic cue, only when the chemical gradient was too shallow for cells to detect it. Most strikingly, the cellular biased response was completely ruled out when the processing capacity is saturated with high background concentration of TGF-β.

C. Cellular signal processing machinery can be modeled as a ternary logic gate

By reverse-engineering the results, we construct a logic gate model to reconstitute the function of the cellular signal processing machinery. The cellular response to the cues of directions (+, 0, or –) presents three variables as outputs of cell migration direction, allowing us to develop a ternary logic system.

III. CONCLUSION

The present study laid a framework for understanding how cells decode chemical and fluidic cues to determine migration direction by proposing a ternary gate circuit.

ACKNOWLEDGEMENTS

This work was partially supported by grants from NIH (HL143403, CA254110, HL 159948, CA274304, and CA023168) and NSF (MCB-2134603, MCB-1936761, and PHY-1945018).

REFERENCES

[1] Luster AD, Alon R, and von Andrian UH (2005). *Nat. Immunol.* 6(12):1182-1190.
[2] Roussos ET, Condeelis JS, and Patsialou A (2011) *Nat. Rev. Cancer* 11(8):573-587.
[3] Shellard A and Mayor R (2020) *Trends Cell Biol.* 30(11):852-868.
[4] Artemenko Y, et al., (2016) *PNAS* 113(47): E7500-E7509.
[5] SenGupta S, Parent CA, and Bear JE (2021) *Nat. Rev. Mol. Cell Biol.* 22(8):529-547.
[6] Swaney KF, Huang C-H, and Devreotes PN (2010) *Annu. Rev. Biophys.* 39(1):265-289.

Development of gamifying robots for improving stroke recovery and cross-disciplinary undergraduate research experience

W. Jong Yoon[1]
[1]University of Washington Bothell, WA

I. SUMMARY

There is currently a need for scientific evidence on how new technologies can be incorporated into clinical practice to improve the functional outcomes of stroke survivors. This paper focuses ongoing example projects developed and conducted by cross-disciplinary undergraduate student teams, as well as how gamifying robots can enhance a physical, interactive element to otherwise tedious rehabilitation activities. These two demonstrated initiatives, which aim to increase engagement for patients with upper motor function deficits and hemispatial neglect (HSN), are set to be tested on human subjects in 2023.

II. METHODS

A. Gizmo 1.0 – for gamifying upper limb motor stroke deficits

Gizmo 1.0 targets to improve engagement for patients with upper motor functional deficits after an ischemic stroke. This robot accomplishes this by guiding patients through physician drawn paths and pausing at specific points along the path for the patients to reach out and trigger the robot's ultrasonic sensor. The collected data can also be used by rehabilitation therapists for improvement tracking and goal setting. We are waiting to soon perform a final human test to be conducted by our consultant clinician. We already received approval of the study from the Institutional Review Board (IRB).

B. Gizmo 2.0 – Towards treating Hemispatial neglect

At the strategic level, this project seeks to assist patients suffering from a stroke in the right parietal lobe, which causes 'spatial/visual neglect' - they lose awareness (attention) of objects to the patient's left side [1]. Two metrics for 'patient attention' have been identified and implemented – face image via a robot-mounted camera and an EEG system. A small robot that responds to brain activity/face tracking and attempts to regain the patient's attention by marching back and forth across the 'edge' of the patient's attention/inattention zones was developed. A facial orientation tracking software has been developed. Regarding the EEG system, which monitors brain function or its proxies, we have collected a variety of data that will be analyzed for attention metrics.

III. CONCLUSION AND FUTURE WORK

Our research aims to provide readily accessible technology (relatively low cost and easy to use and transport, including at home). The developed robots are expected to promote patient compliance by increasing their engagement with therapy as well as the involvement of their supporting community/care-givers because it is fun not only for the patient but also for those around the patient.

With undergraduate students from computer science, engineering, industrial design, and health studies, we offered ourselves as a model of cross-disciplinary scholarship. The proposed study also includes rich educational components. The system's architecture, as currently designed, is also intended to serve as an educational sandbox where students can learn and experiment with new technologies. Three CS undergraduate students completed their capstone project working as a team on this project.

Figure 1: EEG system, Gizmo 2.0, and face tracking software.

ACKNOWLEDGEMENTS

Research reported in this study was supported by the UW Bothell Scholarship, Research, and Creative Practice (SRCP) Seed Grant Program with additional funding from other sources.

REFERENCES

1. http://www.scholarpedia.org/article/Hemineglect

CNN-based Vibration Signal Classification through Image Conversion of Feature Matrix

Tae Hong Min[1], Byeong Keun Choi[1]
[1]Department of Energy & Mechanical Engineering, Gyeongsang National University, Republic of Korea

I. Summary

The purpose of this research is to classify the fault data by acquiring vibration data through the lab-scale gearbox for diagnosing the fault of the rotating machine. Image data are created from the acquired vibration data and utilize them to classify fault data by applying image data to Convolutional Neural Network(CNN) algorithms that show excellent performance in object and image recognition.

II. Research methods

A. Experiment

Vibration data are obtained by attaching three acceleration sensors vertically on the driveshaft Inboard and Outboard and the non-drive shaft Inboard of the bearing housing in the lab-scale gearbox. Vibration data of three single faults(misalignment(M), backlash(B), gear fault(GF)) and three composite faults including normal conditions are obtained, and a total of seven conditions are simulated.

B. Data acquisition and training process

Vibration data are obtained through the fault simulation of lab-scale gearbox and 60 seconds are obtained at a sampling rate of 65,536 Hz for 7 states. For the training of CNN model through data pre-processing for each state, training data is composed through feature matrix calculation and imaging. 2/3 of the image data are used for learning, and 1/3 are used to evaluate the classification performance of the learned CNN model.

C. Data pre-processing

To secure training data, data sampling is performed in units of 1 second, and features are extracted in units of samples. When extracting features, time domains(T), frequency domains(F), entropy domains(E), and capstrum domains(C) are utilized. The feature matrix is computed by features extracted from the sample signal, and standardized, and is imaged by performing an outer product of a vector to represent it in matrix form.

III. Conclusions

Classification performance was evaluated for 30 cases, and Table 1 shows the results of composing only a single domain and the results with the highest classification performance. Figure 1 shows an image of each state for the feature matrix composition model with the highest classification performance.

The results of combining each feature domain to form a feature matrix show higher classification performance than when using only the features of a single domain. In particular, the classification performance of the cepstrum domain was evaluated higher compared to the time, frequency, and entropy domains, and the case of combining these feature domains with each other was shown to be higher.

As a result, the research method presented in this paper classified single and composite fault types as classification performance of 100%, and the vibration signals obtained through lab-scale gearbox confirmed the classification possibility of fault data through the method performed in this research.

Table 1: Classification result(%)

Division	T-T	F-F	E-E	C-C	TC-FE
Single fault (3 cases)	98.3	90.0	91.7	96.7	100
Composite fault (3 cases)	86.7	96.7	80.0	98.3	100

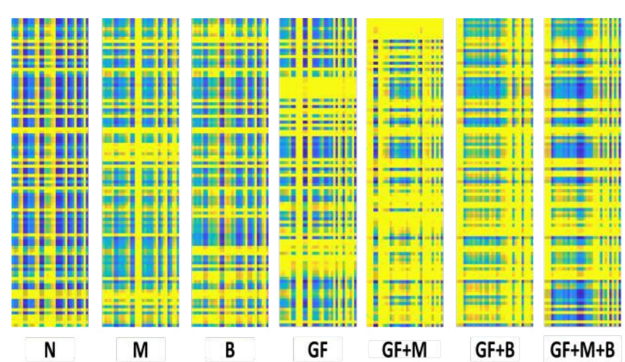

Figure 1: Image composition model of TC-FE

Optimal Design Process of Variable Geometry Turbocharger Turbine Impeller

Jae-Min Kim[1], Jeong-Eui Yun[2], Jung-Bae Kim[3], Gi-Yong Kim[3]
[1]Department of Mechanical·Vehicle Engineering, Kangwon National University, Samcheok-si, Gangwon-do, South Korea,
[2]Graduate School of Disaster Prevention, Kangwon National University, Samcheok-si, Gangwon-do, South Korea
[3]Keyyang Precision Co., Ltd, Gimcheon-si, Gyeongsangbuk-do, South Korea

I. INTRODUCTION

Recently, a variable geometry turbocharger (VGT) has been actively adopted to effectively recycle the energy of low exhaust gas to improve the efficiency of a gasoline engine. In particular, in order to drive the VGT even under low exhaust energy conditions in the low speed and low load section, an optimal design in conjunction with the vane that moves the VGT's turbine impeller in a variable position according to the operating conditions is required. In this study, the optimal design of a turbine impeller operating at the highest efficiency under the most vulnerable operating conditions was performed using computational flow analysis. The optimal design of the turbine impeller first constructs an optimization objective function consisting of three main design variables that determine the shape of the meridional plane and four design variables that determine the torsion of the blade, and then guarantees the minimum flow rate in terms of securing the compressor driving force. It was performed in terms of efficiency maximization as a constraint condition.

II. APPROACH and RESULTS

The upper right of Figure 1 shows the process of optimizing the eight design variables that determine the shape of the turbine impeller using the computational flow analysis results. And the figure on the left shows the optimization process of finding the optimal value after creating a meta-model using the results of computational flow analysis. The middle part of Figure 1 shows the efficiency change before and after the turbine impeller optimization design according to the vane position change, and the lower part shows the gas velocity distribution in the turbine according to the vane position change. From the figure, it is shown that the optimized design of the turbine gives an increase in efficiency from up to 11% to 3% depending on the position of the vanes compared to the conventional model.

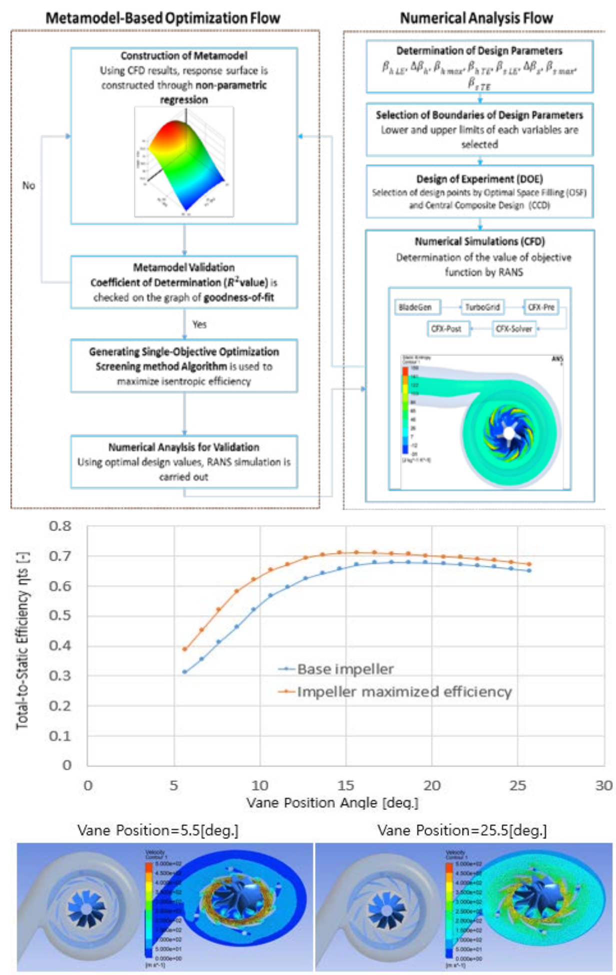

Figure 1: Optimal design process based on meta-model and efficiency comparison result before and after optimal design

ACKNOWLEDGEMENTS

This work was supported by the Development of Variable Geometry Turbocharger for High-efficiency Gasoline Engines [grant number 20018843] as a support project for the Automobile Industry Technology Development (Green Car) of the Ministry of Trade, Industry and Energy.

Thermal Control in Metal Additive Manufacturing

Jihoon Jeong and Jian Cao
Department of Mechanical Engineering, Northwestern University

I. SUMMARY

Laser, powder-blown directed energy deposition (DED) has been recognized for its flexibility in geometry and materials. Typical coaxial alignment of the laser and powder stream supports 5-axis fabrication, and the powder-blown delivery process enables functionally graded materials. Despite being widely used in various industries, such as automotive, aerospace, and medical, challenges remain in ensuring uniformity in the manufactured parts. To address this issue, coaxial monitoring in DED typically involves implementing a beam splitter (or dichroic mirror) within the laser optic train which redirects light emitted or reflected from the melt pool to a sensor (infrared, CCD, pyrometer, etc.).

This research will introduce implementing a coaxial photodiode array in a custom-built DED machine in order to capture melt pool information at fast rates (~100 kHz). The photodiode signals were used to monitor reflected laser light, light emitted/radiated from the melt pool, and relative temperature. Leveraging these signals, a closed-loop control scheme can be implemented to reach a desired melt pool temperature throughout a single part. Various sample geometries will be presented that demonstrate signals obtained with the photodiode array as well as the implementation of the control scheme. In addition, a simulation-guided feedforward-feedback control framework will be discussed to effectively control the melt pool temperature in DED processes.

II. Methods

We conducted a series of experiments using our in-house Additive Rapid Prototyping Instrument (ARPI), which is an open-architecture directed energy deposition (DED) machine. The ARPI system comprises an IPG Photonics 1070 nm continuous-wave fiber laser and a Precitec modular optics head that directs the laser to the deposition point. The laser spot diameter, measured at the nominal standoff distance of 10 mm beyond the powder nozzle, was set at 2.24 mm, following a Gaussian power distribution. ARPI utilizes a coaxial, annular nozzle to deliver powder feedstock, which is metered from a GTV rotating-disk feeder, to the melt pool. For all our experiments, the powder mass flow rate was maintained at 12 g/min. We used spherical, gas atomized Inconel 718 powder with a diameter ranging from 45 to 106 µm as the feedstock in all experiments. The substrates employed were low-carbon steel disks with a nominal diameter of 101.6 mm and a thickness of 12.7 mm.

To effectively monitor the temperature of the melt pool in ARPI, the system incorporates on-axis photodiode-based Planck thermometry (PDPT) [1]. Within the laser processing head, a beam splitter is employed to direct the radiated emission from the melt pool towards the PDPT system. This system consists of two avalanche photodiodes (APDs) equipped with focusing lenses and narrowband filters. The bandpass filters have a width of 10 nm and are centered at 680 nm and 700 nm, respectively. This configuration minimizes the impact of emissivity dependence on wavelength. The voltage outputs from the two APDs are then utilized to calculate the temperature of the melt pool.

To facilitate the acquisition of signals from the APDs, an NI USB-6221 DAQ is employed. A LabView VI (Virtual Instrument) is utilized to process the acquired signals and calculate the melt pool temperature. Additionally, the LabView VI computes the corrected laser power using either feedback-only control or feedforward-feedback control approaches. For the feedback control, the proportional gain (K_p) and integral gain (K_i) are set at 10^{-4} and 10^{-3}, respectively. The feedback controller operates at a frequency of 415 Hz [2].

REFERENCES

1. Jeong, J., Webster, S., Liao, S., Mogonye, J.-E., Ehmann, K., Cao, J., “Cooling Rate Measurement in Directed Energy Deposition using Photodiode-based Planck Thermometry,” *Additive Manufacturing Letters*, Vol. 3, p. 100101, 2022.
2. Liao, S., Jeong, J., Zha, R., Xue, T., Cao, J., “Simulation-guided feedforward-feedback control of melt pool temperature in directed energy deposition,” *CIRP Annals*, in press.

Development of rule-based automatic diagnosis technology for motor pump system diagnosis

Deok Yeong Cheong[1], Byeong Keun Choi[1], Kyung Ho Sun[2], Byeong Chan Jeon[2]
[1]Dept. of Energy Mechanical Engineering, Gyeongsang National Univ.
2Dept. of System Dynamics, Korea Institute of Machinery & Materials (KIMM)

I. INTRODUCTION

Rule-based diagnostic technology is a technology that can diagnose the condition of a facility through a decision tree that models human inductive reasoning based on expert experience and knowledge. Use a decision tree deduced by defining academically established defects and occurrences as classes and attributes, and define rules for facility defects and assessments to determine the status of data for universal application. The rule-based diagnostic technology currently developed uses signals from one-point sensors to perform facility diagnostics, but when performing actual facility diagnostics, various signals obtained from multipoint are analyzed. Therefore, in order to advance the developed rule-based diagnostic technology, it is necessary to develop a diagnostic technology using automation and real multipoint signal information.

II. DEVELOPMENT TECHNOLOGY

A. Decision Tree

In this study, the decision tree consists of a total of 7 types. The seven decision trees were set based on the mechanical parts(component) constituting the BFP and are shown in Figure 1. In addition, there are a total of 21 diagnostic results (Class) for each tree.

B. Signal recognition

Signal recognition technology is an essential technology for automation of Rule-base diagnosis. This is a concept that automatically extracts and applies diagnostic information when only the information of the target facility and the vibration signal are input. In this study, diagnostic information such as Peak, Sideband, Haystacks, Phase, and Beating of FFT Spectrum can be automatically extracted.

III. CONCLUSION

This study is a rule-based diagnostic technology that applies Relative Phase Recognition technology using multipoint signals along with signal processing technology (Peak, Sideband, Haystack) for rule-based diagnostic automation. In order to verify this, various facility conditions (Normal, Bearing fault, Impeller fault,...) were simulated and experimented using the BFP Test rig of the actual scale. Based on the experiment and improved rule-based diagnostic technology, the diagnostic scope and reliability of the existing rule-based diagnostic system were improved, and the diagnostic results of the development technology for the model were verified using experimental data.

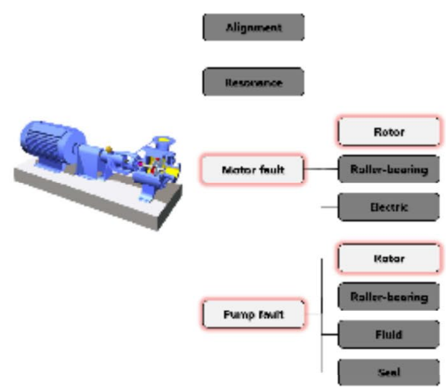

Figure 1: Rule-based diagnosis concept

Table 1: Rotor part decision tree

No.	Attribute	Class
1	Is the 1X amplitude greater than 80% of the set refernce value?	Unbalance
2	Does 3 or more of the Subharmnics(1/2X, 3/2X,...) exceed 20% of the setting reference value?	Rubbing
3	Does one or more of the Subharmnics(1/2X, 3/2X,...) exceed 25% of the setting reference value?	Looseness (Shaft-BRG)

ACKNOWLEDGEMENTS

This research was supported by grant entitled “A study on Rule-based Diagnostics for AI Expert System”(Korea Institute of Machinery & Materials (KIMM), NK244B).

Electrified Personal Tracked Vehicle for Automation

Santiago Ricoy, Dr. Paul Oh
University of Nevada, Las Vegas, University of Nevada, Las Vegas

I. SUMMARY
The personal tracked vehicle prototype was updated to include an all-electric drivetrain for improved performance. Now emissions-free, with improved foot space and increased towing capacity, the electric PTV demonstrates an alternative to traditional all-terrain vehicles in last-mile applications.

II. Project Overview

A. Introduction

The original personal tracked vehicle (PTV) concept, designed as a small form factor all-terrain vehicle, was targeted at providing an accessible and cost-effective transportation solution for disaster scenarios [1]. The initial prototype faced several challenges, including track resistance and drivetrain slippage, along with ICE maintenance. Electric updates remove several of these challenges.

B. Primary Upgrades and Improvements

Under the platform's ethos of easy repairs and replacements, a propulsion system based on electric skateboard motors was chosen. Gearing down the motors via chain drive (10.8:1) was chosen as a prototyping method to allow rapid change of gear ratio for numerous testing scenarios. The new commercially available motors offer a combined output up to 8400W, resulting in a power boost over the original engine at 4500W. The electric drivetrain not only improves the vehicle's performance but also contributes to its environmentally friendly credentials.

C. Performance

The PTV's new drive system now facilitates turning in place, which was not possible with the previous drivetrain. A top speed of 24kph is achieved, outpacing the former 10kph. Protective shields were included over the tracks for safety, while the battery form factor opens the riding platform standing space.

The control system now allows more flexible control via PWM, UART, or CAN communication. As a proof of concept, an Arduino Mega 2560 was employed for initial tests, laying the foundation for simple automation in the future.

Swappable batteries can now be kept on trickle charge indefinitely, keeping them immediately available for deployment in any rapid response scenario. Battery expandability allows greater range, speeds, or torque depending on requirements. The current configuration, a 12S6P 21700 Li-Ion cell battery and 10.8:1 gear ratio, lets the vehicle tow 350lb along with a driver over rough terrain, at up to 30% grade. Range was found at 24km with this capacity.

C. Cost

While the original ICE iteration was quoted at around 1,700USD, the electric platform is estimated to cost nearly 2,000USD for a full build from scratch. The electric PTV demonstrates the potential for further development and refinement.

III. Future work

An updated drive system to improve track alignment could improve reliability, efficiency, and speed. Waypoint finding to a simulated disaster victim that can then ride the vehicle to safety is an upcoming avenue of testing beyond basic performance metrics.

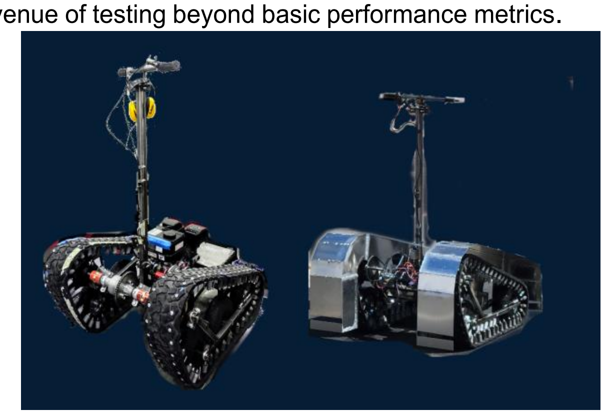

Figure 1: ICE-powered on left, electric with shields on right

ACKNOWLEDGEMENTS
We thank Devan Henriott and Peter Matejic for their help in troubleshooting the prototype.

REFERENCES

[1] S. Ricoy, L. Georgescu, and P. Oh, “Personal tracked vehicle autonomy platform,” in *2018 IEEE International Conference on Consumer Electronics (ICCE)*, Jan. 2018, pp. 1–2. doi: 10.1109/ICCE.2018.8326355.

Optimization of Direct Energy Deposition Additive Manufacturing Process for Al-Mg-Si Alloy and H13 Steel

Jeki Jung[1], Seyed Mohammad Hosseini[1], Chang-Hwan Choi[1,*]

[1]Stevens Institute of Technology, Hoboken, NJ 07030

I. ABSTRACT

Direct energy deposition (DED) conditions in additive manufacturing of AA6063 and H13 were optimized using microstructural analysis. Increasing a laser power at a constant powder feed rate resulted in an increase in the height of the printed layer, while decreasing a scan speed led to an increase in heat input and the formation of pores at the interface between beads. The results contribute to optimize the DED conditions for bi-metal structures using aluminum alloy and steel.

II. INTRODUCTION

DED of multi-materials draws much attention in additive manufacturing [1]. For example, the application of DED of light metals is increasing to secure crash stability and improve fuel efficiency in the automotive industry [2]. A typical example of the multi-material is a combination of aluminum and steel. The process variables in DED process include laser power, scan speed, printing direction, and powder feed rate [3]. In DED of the mixture of Al alloy and steel powders, Fe-rich intermetallic compounds are formed at the interface between Al alloy and steel. This compound is brittle and can cause cracking at the interface. Therefore, the growth of Fe-rich compounds must be controlled by process optimization. We investigate an optimized DED process for AA6063 aluminum alloy and H13 steel.

III. RESULT & DISCUSSION

At a given laser scanning condition, the melting area varies according to the difference in laser absorption of the metals. Increasing a laser power at the same powder feed rate resulted in an increase in the height of the printed layer, while decreasing a scan speed led to an increase in heat input and the formation of pores at the interface between beads. Pores between the beads were formed by high energy density. Compared to the melt pool of AA6063 aluminum alloy, the dilution area of the melt pool of H13/AA6061 showed an irregular shape. Figure 1 shows the optimized manufacturing conditions based on the microstructure analysis and the calculated peak temperature of the melt pool.

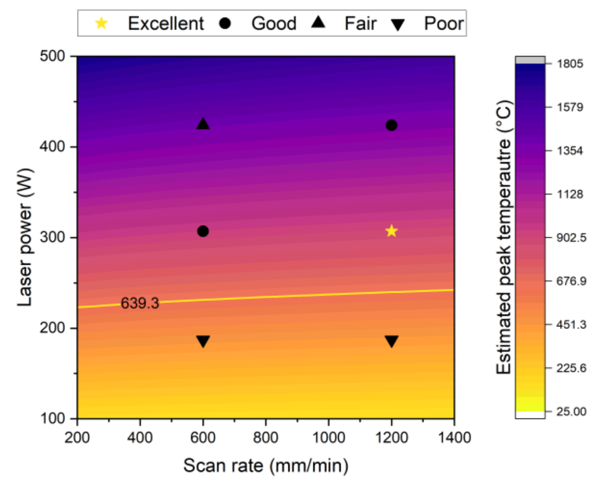

Figure 1: Calculated peak temperature map of melt pool for AA6063 during DED process.

ACKNOWLEDGEMENTS

This work was supported by the Korea Evaluation Institute of Industrial Technology (KEIT) (grant number K-G012000875302).

REFERENCES

1. M. Ghasri-Khouzani, X. Li, A.A. Bogno, Z. Chen, J. Liu, H. Henein, A.J. Qureshi, "Fabrication of aluminum/stainless steel bimetallic composites through a combination of additive manufacturing and vacuum-assisted melt infiltration casting", Journal of Manufacturing Processes, Vol. 69, pp. 320-330, 2021.
2. W. Zhang, J. Xu, "Advanced lightweight materials for Automobiles: A review", Materials & Design, Vol. 221, 110994, 2022.
3. J.-Y. Son, K.-Y. Lee, G.-Y. Shin, C.-H. Choi, D.-S. Shim, "Mechanical and Thermal Properties of the High Thermal Conductivity Steel (HTCS) Additively Manufactured via Powder-Fed Direct Energy Deposition", Micromachines, Vol. 14, No. 4, 872, 2023.

Towards Embodiment of Miniature Humanoid through Virtual Reality.

Akshay Dave[1], **Paul Y. Oh**[2]
[1]University of Nevada, Las Vegas, [2]University of Nevada, Las Vegas

I. ABSTRACT

In the past, multiple miniature humanoids have demonstrated social capabilities and provide human companionship. Ranging from different levels of autonomy, human-robot collaboration was done using robots like Darwin-OP, NAO robot, Moxie and many more. Authors themselves provided an in-depth demonstration of a social robot called Avatar-Darwin [1]. Work presented in the paper became the foundation for converting a deprecated system such as Darwin-OP into a telepresence capable platform. Following this paper will build upon the previous work by first highlighting some upgrades then discussing future work. This will eventually help to achieve higher level of immersive embodiment.

II. System Architecture

A. Hardware

Darwin-Op originally only had 3 DoF arm which was not enough for teleoperation. Authors added 3 more actuators, allowing for a higher level of dexterity and motion. By adding actuators to the wrist and gripper, operators could do tasks like basic grasping and manipulation. To accommodate features like VR control and stereo vision, the onboard computer was changed from Atom Z530 processor to cutting edge Nvidia Jetson.

B. Software

In terms of software upgrades, Avatar-Darwin is fully equipped with the Robot Operating System (ROS); a popular middleware suited for robotics systems. Furthermore, custom ROS modules were created that allowed Avatar-Darwin to be controlled using Unity, a common Virtual Reality(VR) development software. After running a series of tests, it was clear that Visual and auditory latency heavily impacted the immersion factor. To overcome this, a Realtime Video/Audio protocol such as WebRTC was implemented to lower the latency. Operators arm motion were recorded using a VR tracker and then it was translated into robot's joint angle. While maintaining sub 500ms latency.

C. Future Lower Body Design

Following upgrades provided a strong foundation for telepresence systems. An operator could truly immerse themselves and interact with others though Darwin as an intermediary Avatar. Unfortunately, added actuators and computers restricted Avatar-Darwin locomotive capabilities. The robot balance while walking was unstable, and legs did not provide major agility.

For the next phase of research, authors are going to redesign the bottom half of this miniature humanoid and create a more agile walking system. Smart servos used for the Avatar-Darwin provided great level of accuracy and torque, but they are slow. To have a true agile robot, authors will explore creating legs using brushless motors.

III. Result

Following figure shows Avatar-Darwin sitting on a custom desk, an operator is controlling its arm and head through Vr, from a remote locaion.

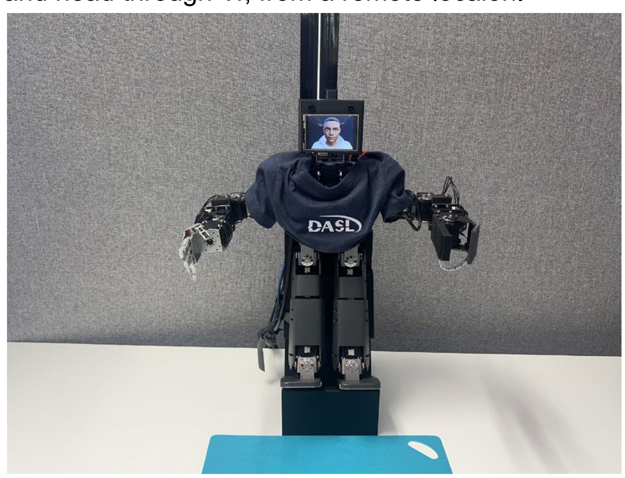

Figure 1: Avatar-Darwin Platform

REFERENCES

1. A. Dave, J. C. Vaz, J. Kim, N. Kosanovic, N. Kassai and P. Y. Oh, "Avatar-Darwin a Social Humanoid with Telepresence Abilities Aimed at Embodied Avatar Systems," 2022 IEEE-RAS 21st International Conference on Humanoid Robots (Humanoids), Ginowan, Japan, 2022, pp. 47-52, doi: 10.1109/Humanoids53995.2022.10000176.

Trajectory Planning for a Cable Driven Parallel Robot

Zahir Abram Castrejon[1], Dr. Paul Oh [2]
[1]University of Nevada Las Vegas, [2]University of Nevada Las Vegas

I. Abstract
Within Cable Driven Parallel Robots, the cable lengths and tension for a given workspace space provide the stability, control, and overall safety of the system. For automation purposes within an industry setting such as warehouse, path planning and maneuvering the end-effector to a desired position takes account of the proper cable lengths and tensions suitable. This paper provides the static analysis of a CDPR with four cables and method for trajectory planning.

II. Introduction
As challenges within inventory management to meet demand-supply cycle, Cable-driven parallel robots (CDPRs) offer a potential solution to the current rise in inventory processes around the world. A CDPR consists of multiple cables attached to an end-effector and motors to actuate each cable attached for the desired trajectory. The advantages offed by CDPRs over Unmanned Aerial Vehicles and Unmanned Ground Vehicles consist of low inertia, modularity, and high operation volumes. Tall double-deep racks within a warehouse environment put workers that operate forklifts and heavy machinery under extreme stress and risk of injury. CDPRs ability to be reconfigured to a warehouse environment with a given cable orientation and static analysis. This paper presents trajectory planning for a CDPR system.

III. Methodology
To automate a four link CDPR within a warehouse, a method to control the end-effector for the desired set of positions must be developed. For the CDPR to move, cable lengths change with rotation of a winch by way of motor actuation. The length of each cable is calculated using the Euclidean distance of the anchor points and the position of the end-effector.

$$l_i = \sqrt{\sum (Anchor_i - Position)^2}$$

For $i = 1,2,3,4$. The Tension of each cable must be analyzed in order to ensure that positive tensions are provided as the end-effector progresses through the desired trajectory. The weight of the end-effector is distributed along the four cables with the assumption of a 20’ x 20’ x 8’ symmetric workspace.
The tension for each cable is taken with the vertical component as $T_i * Cos(\theta_i)$ and for the given cable orientation. Tension for a given cable is shown as $T_i = \frac{Weight}{4Cos(\theta_i)}$

III. Results and Discussion
The criteria needed for the CDPR to safely navigate along a trajectory includes consistent positive tension to avoid instability. Position feedback control can be established using the length of each cable for the corresponding position. To ensure positive tension from the start, a calibration process must be performed. [0,0,0] meters represent the origin at which calibration takes place. From Figure 1, the end-effector approaches the singularity and the edges of the workspace while tensions increase for position [0,1,2.2] meters. Under a static analysis, the tensions reached up to 70.97 N for both cable 1 and cable 2 and 51.48 N for cable 3 and cable 4. Further modifications can be made to justify the cable lengths and limit error accumulated from the elasticity of the cables before a dynamic analysis is performed.

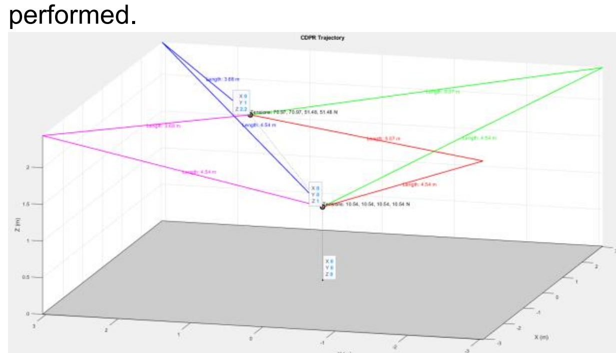

Figure 1: CDPR Trajectory

ACKNOWLEDGEMENTS
Armaun Zargari, Dongbin Kim, &Nicolas Kosanovic.

REFERENCES

1. Zake, Z., Chaumette, F., Pedemonte, N., Caro, S. (2019). Vision-based control and stability analysis of a cable-driven parallel robot. IEEE Robotics and Automation Letters, 4(2), 1029-1036

Crack morphologies during ultra-precision machining of single crystal 8 %mol yttria-stabilized zirconia

Dae Nyoung Kim[1], Sangkee Min[1]
[1]Department of Mechanical Engineering, University of Wisconsin-Madison

I. INTRODUCTION

Ultra-precision machining (UPM) is an emerging method for machining brittle single crystal ceramics to achieve fine or uncracked surfaces. However, compared to conventional macro-scale machining processes, the material behavior in UPM is not yet fully understood. This study aims to investigate the crack morphologies of single crystal 8%mol yttria-stabilized zirconia (YSZ) with respect to fracture systems.

II. EXPERIMENTAL SETUP

The study utilized a 5-axis ultra-precision machine tool with a command resolution of 1 nm, along with a nano-polycrystalline diamond tool featuring a nose radius of 0.5 mm, to carry out ultra-precision cutting on single-crystal 8%mol YSZ. The force in the x, y, and z directions during the machining process was measured using a dynamometer. The cutting was conducted on the (001) plane of YSZ, with four different cutting orientations ranging from an angle of 90° to 150° from the [0 1 0] direction, including angles of 90, 120, 135, and 150 degrees. Each path was set to have a slope of 1/500, and a feed of 5 mm/min was used. [1]

III. RESULTS AND DISCUSSION

The measured force data were converted using the following equation to evaluate the likelihood of fracture occurrence. This parameter was referred to as the cleavage fracture parameter (F- parameter). The variables used in the equations included ψ_i, which respectively represented the angles between the applied force and the normal vector of the cleavage plane. The fracture toughness for the j-th fracture system was represented by $K_{IC,j}$.

$$F_j = \cos^2 \psi_j / (K_{ICj} / min_j K_{ICj}) \qquad \text{Equation 1 [1]}$$

Table 1: Cleavage fracture parameters of each cutting angles

	Cutting angle degree			
Plane	90°	120°	135°	150°
$(01\overline{1})$	**0.997**	**0.875**	**0.724**	0.601
(001)	0.434	0.451	0.645	0.484
(010)	0.345	-	-	-
$(10\overline{1})$	-	0.589	**0.724**	**0.873**
(110)	-	0.393	0.172	0.353

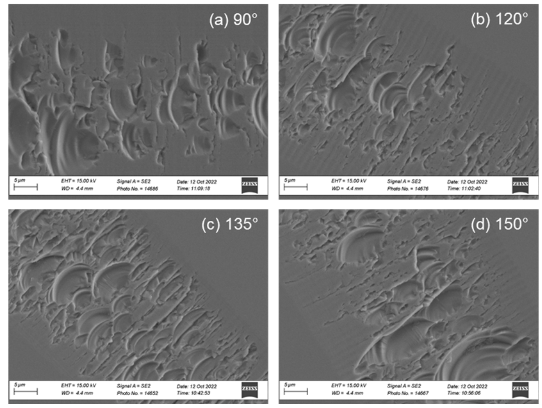

Figure 1: SEM images of machined surfaces

By comparing the results of F- parameters in Table 1 and the crack morphologies shown in Figure 1, the shape of the crack can be explained by the cleavage plane. Specifically, in case of 90°, where the $(01\overline{1})$ and (001) planes are orthogonal to the cutting direction, the lateral crack visible in figure 1 (a) occurs.

However, in cases of 120, 135, 150°, lateral cracks corresponding to the (110) plane can be observed in Figure 1 (b), (c), and (d), even though the F- parameters for these cleavage planes are smaller than those for other planes such as $(01\overline{1})$,$(10\overline{1})$. This suggests that even with a lower likelihood of crack initiation, lateral cracks can still occur during the YSZ machining process.

In every case, the presence of fan-shaped cracks suggests that there may be an interaction between multiple cleavage planes. Further investigation is needed to confirm the exact cleavage planes involved in this phenomenon. Future research will be conducted using surface profiling.

ACKNOWLEDGEMENTS

This material is based on work supported by the NSF under grant No. CMMI-1844821. Authors gratefully acknowledge kind support from the FANUC Corporation, Japan, for the donation of the ROBONANO α-0iB, and A.L.M.T. Corp., Japan, for discounted PCD tools to MIN LAB at UW-Madison.

REFERENCES

1. Kwon, Suk, Bum et al, “Study of material removal behavior on R-plane of sapphire during ultra-precision machining based on modified slip-fracture slip-fracture model,” *Nanotechnology and Precision Engineering*, Vol. 3.3, No. Y, pp.141-155, 2020.

Method for Real-Time Joint Trajectory in Telepresence Avatar Robotics

Baekseok Kim[1], Jean Chagas Vaz[1], Paul Oh[1]
[1]University of Nevada Las Vegas

Abstract - This paper presents a novel controller for Avatar-Hubo, a telepresence robot, enhancing its movement accuracy, responsiveness, and safety, which are crucial for effective telepresence in remote or hazardous locations.

I. INTRODUCTION

While machine learning has made notable strides, as showcased in Chat-GPT, similar advancements in robotics are yet to surpass basic tasks. The 2022 ANA Avatar XPRIZE competition emphasized the goal of telepresence robotics, enabling genuine remote interaction via robots. The competition underscored the need for low-latency systems, something teleconferencing tools have significantly improved. However, motion and haptic systems haven't seen similar progress. This research introduces a new control system for the Avatar-Hubo telepresence robot, leveraging filter fusion for safer, more reliable motion trajectories.

II. METHOD

This research addresses challenges in human-to-robot motion transfer, particularly due to disparities between human and robot arm characteristics [1]. We implemented an operator-specific calibration and the BIO-IK algorithm to mitigate this. Due to the non-real-time nature of transferring joint values from the Virtual Reality Operating System (VROS) to Avatar-Hubo and potential communication delays, we used a real-time lowpass filter and PD controller to ensure smooth, accurate, and low-latency motion. The improved system's speed and accuracy were tested using an operator tracking a moving virtual target in VROS, which Avatar-Hubo then replicated. This process was repeated across 20 trials for both the original and proposed control systems.

III. RESULTS

The performance of control systems is assessed by comparing Avatar-Hubo to its Digital Twin, specifically regarding transient end-effector tracking accuracy. Graphical comparison in Fig. 1 reveals a

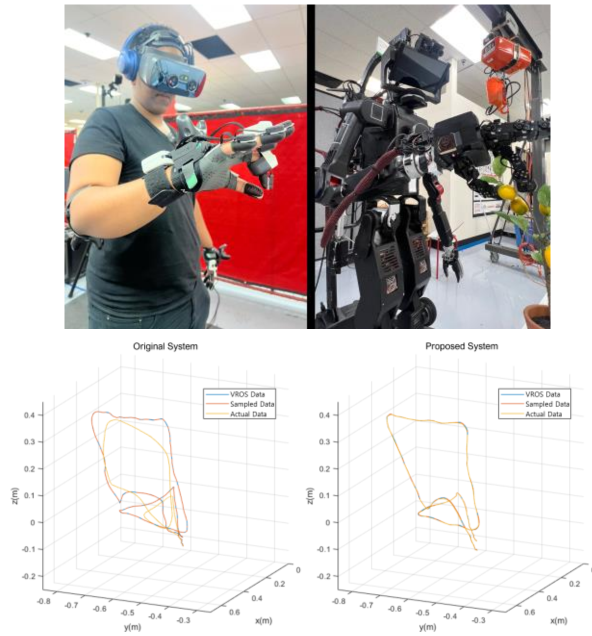

Fig 1 Avatar-Hubo mimics the motions of a human operator in real-time (Up) End-Effector Path during square trajectory VR target tracking trial.(Down)

significant alignment between Avatar-Hubo and its Digital Twin's end-effector paths, exclusive to the proposed system, indicating its improved tracking accuracy.

IV. DISCUSSION&CONCLUSION

The proposed control system for Avatar-Hubo effectively improves motion latency, tracking, and safety. Future enhancements include torque-controlled compliance for safer human-robot interaction. Ultimately, these advancements aim to make telepresence more user-friendly, adaptable, and dependable.

ACKNOWLEDGEMENTS[1]

REFERENCES

1. Dave, Akshay, et al. "Avatar-Darwin a Social Humanoid with Telepresence Abilities Aimed at Embodied Avatar Systems." *2022 IEEE-RAS 21st International Conference on Humanoid Robots (Humanoids)*. IEEE, 2022.

[1] The work in this paper is partially by the Nevada NASA Space Grant AWD-02-00001955, the Nevada NASA EPSCOR AWD-02-00001965, Tesla Robotics in Construction AWD-02-00001843, and the INSPIRE UTC project is provided by the U.S. Department of Transportation, Office of the Assistant Secretary for Research and Technology (USDOT/OST-R) under Grant No. 69A3551747126 through INSPIRE University Transportation Center (http://inspireutc.mst.edu) at Missouri University of Science and Technology.

Contact Guidance of Hs27 Fibroblasts

Chunghwan Kim[1], Michael Robitaille[2], Joseph Christodoulides[2], Yisha Ng[1], Marc Raphael[2], Wonmo Kang[1]
[1]Mechanical Engineering, School for Engineering of Matter, Transport and Energy, Arizona State University, Tempe, AZ 85281, United States
[2]US Naval Research Laboratory, Washington, DC 20375, United States

I. INTRODUCTION

Cellular morphology and mobility have an essential role in several physiological and pathological processes, e.g., fibroblasts migration toward a wound site and regeneration of extracellular matrix. This work investigates the cellular static and dynamic response of Hs27 fibroblasts under a wide range of topographical conditions, which are previously uncharacterized, by using a multiplexed microchip. Our experimental results with a possible mechanistic explanation are important for a fundamental understanding of cell behavior induced by anisotropic environmental features and thus, associated with a development of new bio-platforms/tools, which enables us to interpret biological processes in tissue regeneration and repair by achieving effectively guided cell morphology and migration.

II. RESULTS AND DISCUSSION

The cellular morphology and mobility are strongly influenced by topographical features such as lateral and vertical dimensions, namely, ridge and groove widths, and groove depth ($\mathrm{R_w}, \mathrm{G_w}, \text{and } \mathrm{G_D}$, respectively). However, the effect of the individual dimensions as well as their interactions on cellular function remain unexplored. In this work, we explore the morphology and migration of Hs27 fibroblasts on multiplexed monolithic quartz chips [1] in a wide range of dimensional space well beyond what has been previously studied. First, we perform a static analysis on three different morphological metrics, i.e., cell spread area, aspect ratio and cell alignment degree. Our static analysis shows that groove depth ($\mathrm{G_D}$) as deep as 725 nm causes considerable elongation and alignment of the fibroblasts, while further increase of $\mathrm{G_D}$ to 1000 nm slightly diminishes both measurements (see Figure 1). The regression analysis reveals that the $\mathrm{G_D}$ coupling term (i.e., $\mathrm{G_D} \cdot \mathrm{R_W}$) is also important for the cell elongation and alignment. Secondly, we characterize migration path as well as speed of individual cells, as dynamic measurements of the cell response, on different topographical conditions. Our dynamic analysis

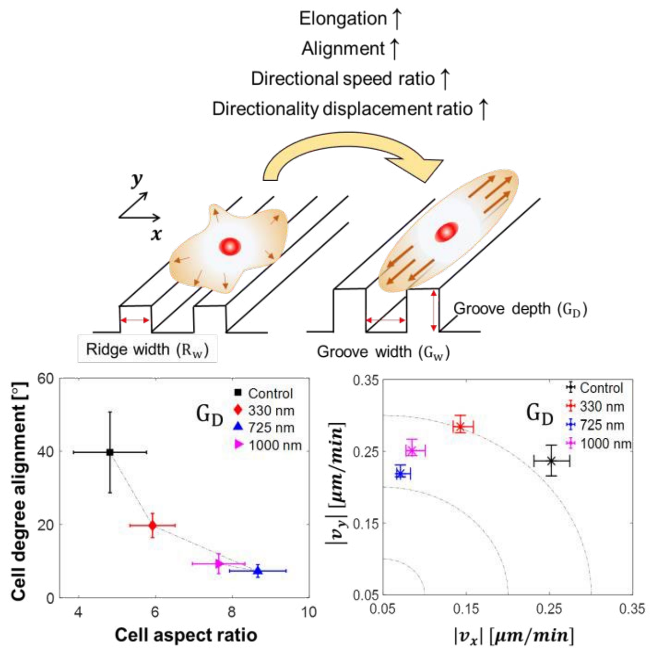

Figure 1. A schematic diagram of our multiplexed microchip with topographical features (i.e., ridge and groove widths (R_w and G_w) and groove depth (G_D)). Summary of the static (bottom right) and dynamic response (bottom left) of Hs27 fibroblasts under different G_Ds. v_x and v_y represents the cell average speed along x and y axis, respectively.

confirms that the effect of $\mathrm{G_D}$ as deep as 725 nm is significant for better guidance of cell migration path along the groove direction (i.e., y direction in Figure 1), while their average speed slightly decreases (see Figure 1). We propose possible scenarios based on well-known models (i.e., focal adhesion model and cell membrane deformation) and *in vitro* conditions to offer mechanistic interpretations of the observed cell response including the $\mathrm{G_D}$-dependent transition.

ACKNOWLEDGEMENTS

This research was funded by the Office of Naval Research (N00014-20-2409).

REFERENCES

1. Robitaille, M.C., et al., “Monolithic quartz platform for cellular contact guidance” *MRS Communications,* 2020. **10**(2): p. 242-251.

AMINATED GRAPHENE-FILLED GLASS FIBER COMPOSITES FOR ENHANCED MECHANICAL PROPERTIES

Ning Bian[1], Ashutosh Shrivastava[2], Gabriel R Morel-Torres[3], Runyu Zhang[1], Samsuddin Mahmood[4], Duck J Yang[2], Hongbing Lu[1]

1 Department of Mechanical Engineering, University of Texas at Dallas, Richardson, TX 75080, United States

2 Department of Chemistry and Biochemistry, University of Texas at Dallas, Richardson, TX 75080, United States

3 Department of Mechanical Engineering, University of Puerto Rico, Mayagüez, PR 00681, United States

4 GrapheneTX Inc., 619 Mogonye Lane, Elgin, TX 78621, United States

I. SUMMARY

Glass fiber/epoxy composites have been used as structural materials for many engineering applications, such as wind blades, infrastructure, and constructions, due to their low density, high strength, easy formability, chemical stability, and corrosion resistance. However, further developments are required in weight-critical applications such as ever-increasing lengths of wind blades. This necessitates a call for low-density structural materials with significantly enhanced mechanical properties and prolonged service life. Most of the failures of glass fiber composites are due to the poor mechanical properties of the polymer matrix. The matrix damage induced at initial cycles triggers early fatigue failure with further cycling for composites [1]. Hence, in this presented work, we premixed the US-patented [2] oxygen-free aminated graphene with the hardener of epoxy, and fabricated glass fiber/epoxy composite plates through vacuum-assisted resin transfer molding. The enhancement of the matrix-dominated properties such as transverse tensile strength, ILSS, and fatigue performance of glass fiber composites are studied.

II. RESULTS AND CONCLUSIONS

The covalent bond formed between the amine group in aminated graphene and epoxy helps increase the transverse tensile strength and ILSS of glass fiber composite by ~11%. Figure 1 shows the fatigue life and damage parameter of AG-glass fiber composites. Both composites successfully survive over 1 million cycles and the endurance limit of 0.02 wt.% AG-epoxy/glass fiber composite is significantly improved over the reference glass fiber/epoxy composite. It is also noteworthy to mention that the fatigue life of glass fiber composite got improved up to 10 times at an even lower fatigue strength level. It is also noteworthy to mention that 0.02 wt% AG-filled glass fiber composite has an extended steady-state degradation than that of baseline glass fiber composite. The slope of the damage parameter curve for baseline glass fiber composite became steep at around 20,000 cycles, while for 0.02 wt% AG glass fiber composite the steady degradation extended to around 60,000 cycles before the slope goes steep. In addition, the slope of the damage parameter curve at the last stage is also smaller than that of the baseline glass fiber composite. With the incorporation of aminated graphene in the polymer matrix, glass fiber composite can absorb more energy in the steady degradation phase, and hence extend the fatigue life of the composite.

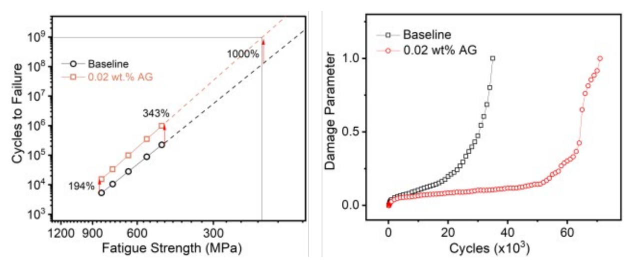

Figure 1: Fatigue life and fatigue degradation of AG-glass fiber composites

ACKNOWLEDGEMENTS

We acknowledge the support of NSF under 2219347 and the support of GrapheneTX Inc.

REFERENCES

1. J. B. Knoll, et al, "The effect of carbon nanoparticles on the fatigue performance of carbon fibre reinforced epoxy," *Composites Part A: Applied Science and Manufacturing*, vol. 67, pp. 233–240 2014.
2. M. A. Wunch, S. F. Mahmood, D. J. Yang, "Facile direct functionalization of pristine graphene nanoparticles". US patent, 2021, US11111150B2.

Path planning problem
for Self-Rechargeable Unmanned Aerial-Ground Vehicle Group

Jaekyung J Lee[1], Sivakumar Rathinam[1]
[1]Mechanical Engineering, Texas A&M University

I. INTRODUCTION

Unmanned vehicles have gained significant popularity in both the research and industrial sectors due to their diverse applications. These vehicles are essential for operations including surveillance, target tracking, reconnaissance, and search and rescue. In this paper, our primary focus is to address the challenges of path planning and scheduling for multi-agent unmanned aerial vehicles (UAVs) with battery constraints, while also considering the presence of unmanned ground vehicles (UGVs) capable of recharging them. During a 72-hour period, the UGV, equipped with two charging pads on top, travels along the predetermined road network, charging the UAVs to ensure they can continue their mission without discharge.

We present simulation results that illustrate the algorithm's runtime and whether visiting areas of interest and continuous charging schedules are met.

II. PROPOSED HEURISTICS

We address this problem in a meta-heuristic approach, especially tabu search. The primary objective is for multiple agents to participate to maximize the overall collected rewards based on time or distance constraints. Typically, it is not feasible to visit all targets. Our approach enables us to identify the feasible path, although this problem falls under the category of NP-hard.

A. Greedy Insertion Heuristic

To begin the procedure, we select the starting and ending points for each UAV. These points are determined by the position of the UGV, which serves as a shared rendezvous point. To find feasible routes, we repeat the following steps:

1. Exchange two points.
2. Move one point.
3. Perform a two-opt clean up.

B. Tabu Search Meta-Heuristic

Tabu search is a popular meta-heuristic technique for optimization problems. It provides a systematic approach to exploring the solution space while avoiding getting stuck in local optima.

III. SIMULATION RESULTS AND CONCLUSIONS

Over a 72-hour period, we applied our algorithms to this problem instance and obtained promising results.

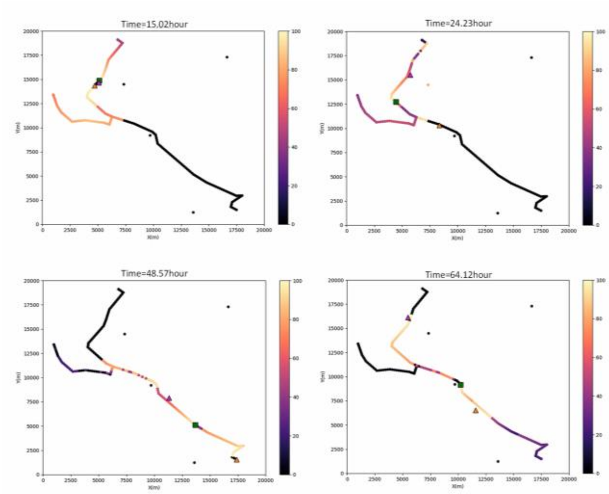

Figure 1: 72 hours simulation results for 2 UAVs and 1 UGV

This study makes a valuable contribution to the field of UAV operations by offering a comprehensive solution to the path planning and scheduling problem. Our approach considers battery constraints and employs a multi-phase strategy, thereby enhancing the overall effectiveness of reconnaissance surveillance systems without human intervention.

ACKNOWLEDGEMENTS

The research is sponsored by the U.S. Army Research Lab.

REFERENCES

1. Chour, Kenny, et al. "An agent-based modeling framework for the multi-UAV rendezvous recharging problem." *Robotics and Autonomous Systems* (2023): 104442.

Waveguided-based Darkfield Microscopy for Wafer Edge Inspection

Heebum Chun[1], ChaBum Lee[1]
[1]J. Mike Walker '66 Department of Mechanical Engineering, Texas A&M University

I. INTRODUCTION

Inspection for defectivity in the semiconductor industry poses significant challenges as semiconductor technology becomes more complex. In particular, wafer edge defects have emerged as a critical factor influencing the yield rate of semiconductor manufacturing because more chips can be produced by saving the near-edge area. Various methods are currently employed for wafer edge defect inspection, including visual inspection, brightfield microscopy, scanning electron microscopy (SEM), atomic force microscopy (AFM), optical coherence tomography (OCT), and others. Although existing methods are useful in certain aspects, they fall short of meeting the requirements for high-resolution, sensitive, and rapid wafer edge defect inspection. To address limitations, this study introduces a novel approach to wafer edge inspection using waveguide-based darkfield microscopy.

II. METHODOLOGY

The methodology employed in this study utilizes waveguide-based darkfield microscopy for wafer edge inspection, aiming to enhance image quality by improving image contrast. Figure 1 schematically illustrates the proposed waveguided darkfield microscopy, where an incident light beam is directed toward the edge of the wafer. As the light beam propagates through the wafer, it is guided by the top and bottom surfaces through total internal reflection within the wafer. This guided light continues to propagate and can be observed at the opposite side edge of the wafer, enabling the capture of wafer edge images with high contrast.

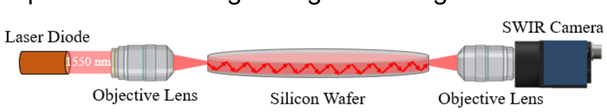

Figure 1: Schematic of waveguided-based darkfield microscopy.

III. EXPERIMENT AND RESULT

Bright and darkfield images were compared by evaluating contrast and intensity, as shown in Figure 2. The contrast, C, was determined by the ratio of the standard deviation to the mean intensity of the region of interest (ROI) [1].

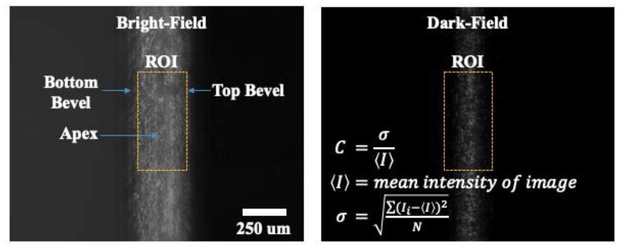

Figure 2: Bright and darkfield wafer edge images.

Figure 3 presents the contrast and intensity comparison for 10 different edge locations. It was observed that the brightfield images exhibited higher intensity compared to the darkfield images. However, the proposed darkfield imaging method demonstrated significantly higher contrast, approximately 4.5 times larger than that of the brightfield images. This indicates that defects can be detected more effectively using the proposed method, which provides sharper images. Consequently, the proposed method holds the potential to contribute to the development of more accurate and efficient inspection techniques for wafer edge inspection.

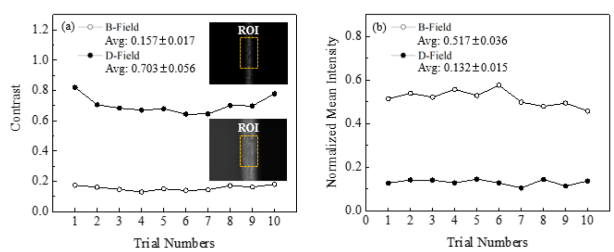

Figure 3: Bright and darkfield a) contrast and b) normalized mean intensity comparison.

ACKNOWLEDGEMENTS

This research has been supported by National Science Foundation (CMMI #212499)

REFERENCES

1. Prabhathan, P., et al. "Intensity and contrast-based surface roughness measurement approaches for rough and shiny surfaces." *Fifth International Conference on Optical and Photonics Engineering*. Vol. 10449, pp.180-185 SPIE, 2017.

Parametric Machine Learning Model for Laser Powder Bed Fusion

Jong Wook Kim[1], and Yongho Sohn[1]
[1]Department of Materials Science and Engineering, University of Central Florida, Orlando FL

I. INTRODUCTION

Laser Power Bed Fusion (LPBF) is one of the most robust techniques for additive manufacturing (AM). In the LPBF process, there are identified factors that can directly affect properties of materials. The flaw formation, for example, is nonlinearly associated with parameters of laser power, scan speed, hatch spacing, and layer thickness. In this study, we provide an introduction to a Bayesian machine learning model that can summarize and predict the nonlinear dynamics of parametric relationships based on both data and theory.

II. ENSEMBLE MODELING APPROACHES

We use an ensemble modeling approach that can tie a mechanistic model based on theory to a machine learning (ML) model with experimental data. A ML approach usually requires a sufficient amount of data to learn for improved predictive accuracy. This can be improved by using a theory-based constitutive equation as a mechanistic model, which can help the ML model learn from the data. Particularly, a Bayesian approach can support ML models to be more explainable by data – it can characterize exponential increase and decay with inputs and outputs related to the parameters.

Constitutive relations can be typically developed to identify regularity of the density and other LPBF related factors (i.e., laser power, etc.) The parametric equations attempt to characterize the change of density values by laser power and other parameters. The nonlinear relationships among the parameters can be represented by a constitutive equation with assumption that the density is proportional to laser power (P) that is divided by a product of three variables including scan speed (s), hatch spacing (h), and slice thickness (t), that is $E = P/hvt$.

$$\rho(E) = a - b \cdot exp\left(-\frac{E}{c}\right) + d \cdot exp\left(-\frac{E}{e}\right)$$

In the equation, there are positive unknown 5 coefficients $a, b, c, d,$ and e. The two exponential equations represent thermally activated processes of melting and solidification.

Estimating parameters from the constitutive equations can be considered an inverse problem because experimental data are used to infer the parameters [e.g., 1]. A Bayesian model is represented by a mathematical model of prior knowledge of parameters and of the data generating process given the parameters. That is, mathematically, a prior density $p(\theta)$ over the sequence of parameters θ express knowledge of parameters before the collected data set.

$$p(\theta|y) = \frac{p(\theta, y)}{p(y)} = \frac{p(y|\theta)p(\theta)}{p(y)} \propto p(y|\theta)p(\theta)$$

A vector of the sequence of parameters, θ, and a prior density distribution of the parameter vector, $p(\theta)$ summarize our information about the parameters before we observe the data. A sampling distribution known as the likelihood function, $p(y|\theta)$, characterizes the distribution of measured data y given parameters θ. The Bayes's rule provides a general solution to the inverse problem, expressing the posterior $p(\theta|y)$ in terms of the prior $p(\theta)$ and likelihood $p(y|\theta)$. The posterior distribution is denoted as $p(\theta|y)$.

III. RESULTS

A mechanistic model consists of a number of unknown deterministic parameters, explaining the LPBF process characteristics. A parametric equation is limited to summarize the materials and their features. Thus, we take an ensemble modeling approach both with a parametric equation and a Bayesian modeling approach from data. As a forward model, the constitutive equations can theoretically summarize the density with regard to the parameters. The Bayesian inverse approach is implemented, using the R and Stan platform, in an attempt to iteratively develop a more feasible computational model deeply based on theory.

IV. CONCLUSIONS AND DISCUSSION

Our approach provides predictive information by inferring a probabilistic surrogate model updated by the data set [e.g., 2]. The Bayesian perspective, proposed in this paper, can be iteratively utilized to find the next optimal parameters set in LPBF, maximizing the expected improvement [e.g., 3]. It is promising to accelerate the process of design, discovery, and fabrication of materials used in LPBF.

REFERENCES

1. Aster, R.C., B. Borchers, and C.H. Thurber, *Parameter estimation and inverse problems*. 2018: Elsevier.
2. Huang, C., et al., *Bayesian optimization of functional output in inverse problems.* Optimization and Engineering, 2021. **22**: p. 2553-2574.
3. Jones, D.R., M. Schonlau, and W.J. Welch, *Efficient global optimization of expensive black-box functions.* Journal of Global Optimization, 1998. **13**(4): p. 455.

Static analysis of a carbon fiber rotor in an axial flux motor

Joon Gyeong Jo[1], Chase Wiley[2], Moble Benedict[1,2]
[1]Department of Mechanical Engineering, Texas A&M University
[2]Department of Aerospace Engineering, Texas A&M University

I. INTRODUCTION

Aligning with the effort to decarbonize the aviation sector, the US Advanced Research Projects Agency -Energy (ARPA-E) introduced the Aviation-class Synergistically Cooled Electric-motors with iNtegrated Drives (ASCEND) program. It aims to invent a lightweight and efficient electric powertrain for aircraft propulsion. More specifically, the new powertrain system must have at least 93 % efficiency with ≥12 kW/kg specific power [1].

After selecting the carbon fiber as a material for the rotor to account for the optimized strength and weight, the static analysis was conducted using both experimental and simulation methods. This was based on the materialistic behavior of carbon fiber that it resembles that of metallic material until a certain amount of load, where the failure occurs [2].

II. METHODS

A. Experimental method

The rotor was mounted on the Universal Testing Machine (UTM) with 40 bolt holes being connected to represent the tensile force of $5{,}750\ N$.

B. Simulation method

The 3D model was created using the SolidWorks software program, which was then imported by Abaqus software for the detailed analysis (FEA) using the Finite Element Method (FEM).

III. RESULTS

Compiling the recorded data on the computer throughout the 5-time tests, the results came out to be consistent, as in **Fig. 1(a)**. When the exerted force reached $5{,}750\ N$, the maximum deflection of the value $0.75\ mm$ was logged.

The simulation results using the Abaqus software, which imported the 3D model made by SolidWorks, showed that the maximum deflection for the static load of $5{,}750\ N$ around the rim of the rotor is $0.854\ mm$. Interpolating and viewing for the experimental measurement point, the deflection came out to be $0.745\ mm$, which matches with the experiment result.

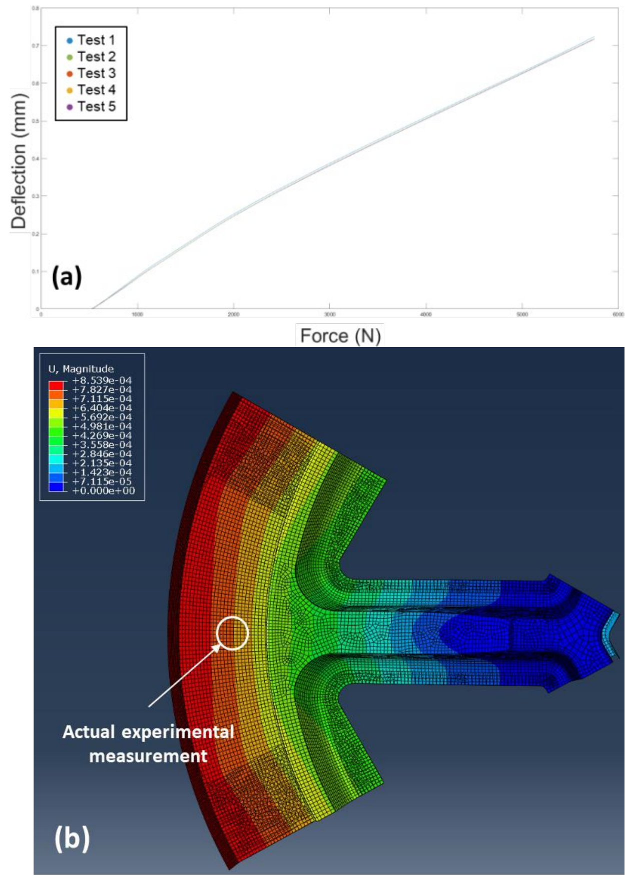

Fig. 1: (a) Experimental deflection plot, **(b)** FEA

ACKNOWLEDGEMENTS

The authors are deeply grateful to ARPA-E for the provision of the project, and all those relevant to ARPA-E for their constant feedback and support.

REFERENCES

1. "DE-FOA-0002238: Aviation-class synergistically cooled electric-motors with integrated drives (ASCEND)", Department of Energy, Advanced Research Projects Agency Energy, Dec. 2019.
2. Zhu, Z. F., Wang, W. W., Harries, K. A., & Zheng, Y. Z. (2018). Uniaxial tensile stress–strain behavior of carbon-fiber grid–reinforced engineered cementitious composites. Journal of Composites for Construction, 22(6), 04018057.

CNN-based condition classification of vibration signal considering fault location

Jeong jun Lee[1], Dong hee Park[2], Byeong keun Choi[1]
[1]Department of Energy & Mechanical Engineering, Gyeongsang National University, Republic of Korea.
, [2] DAVISS Inc, Republic of Korea.

I. SUMMARY

In this paper, the possibility of classifying normal and fault condition were confirmed by generating images considering the fault component and occurrence location of the vibration signal and applying to CNN-based deep learning technology.

II. INTRODUCTION

In this paper, confirmed the possibility of classifying the normal and failure condition of the rotating machine by generating an image considering the frequency component and occurrence location of the vibration signal and applying it to CNN-based deep learning. STFT (Short Time Fourier Transform) was performed for each sensor position to produce an image considering the frequency component of the acquired vibration signal data, and the STFT of attached sensor position was converted to red, green, and blue to express location information. In order to verify this method, the reliability of this thesis was reviewed by confirming the possibility of distinguishing between normal and faulty conditions based on the data obtained from the gearbox test equipment.

III. MODEL & IMAGE PROCESSING

Vibration data were acquired by conducting a fault simulation experiment for the gearbox. The gearbox test rig consists of a motor, gearbox, and load device. It is a gearbox inside of a pinion of a driven shaft that has 25 teeth and gear of non-driven shaft that has 38 teeth. Fig. 1 shows an example of the overall sequence of image conversion including location information for vibration data. The converted image is resynthesized into one image, and it is possible to determine which sensor position the dominant component appeared according to the amplitude color of the combined image. Therefore, it was possible to visualize which facilities have high vibration and predominant frequency components in the image, which means that multipoint diagnosis can be possible with one image. Fig 2 is shown the layers of the CNN model used for training. In the features engineering step, the layer composed of Convolution(COVN), Batched normalization(BN) and Drop out(DO) was used the three times, and max pooling(MP) was performed only at the last step.

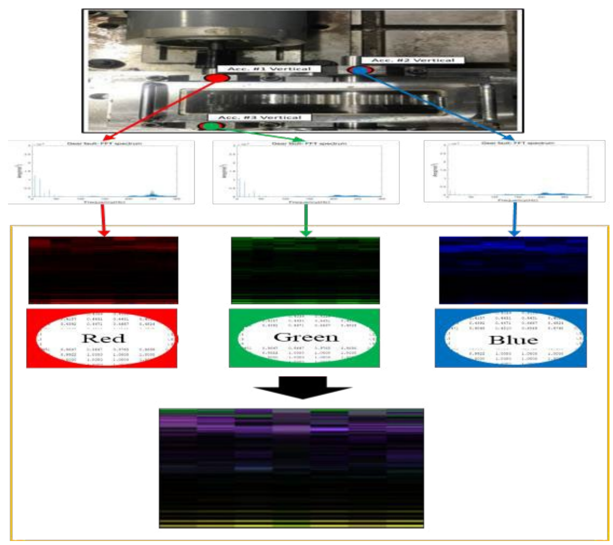

Figure 1: Flow of convert RGB image in STFT

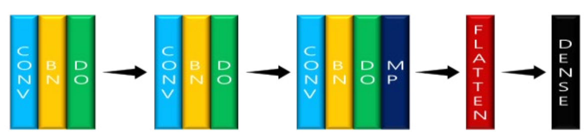

Figure 2: A specific architecture of CNN model

REFERENCES

1. S. Duan et, al., “A Novel Classification Method for Flutter Signals Based on the CNN and STFT,” *International Journal of Aerospace Engineering*, pp. 1-8, 2019
2. Tarun Kumar let, al., “A Theory Based on Conversion of RGB image to Gray Image”, International Journal of Computer Applications Vol. 7, No. 2, 2010.

A Novel Approach to Mosquito Trap: Utilizing 3D Flight Tracking

Soohwan Kim[1], Chris Zuo[1], Alex Cohen[2], Chenyi Fei[2], Jörn Dunkel[2], David Hu[1]

[1]Department of Mechanical Engineering, Georgia Tech, [2]Department of Mathematics, MIT

I. SUMMARY

Mosquitoes are the most dangerous animals on the planet, transmitting diseases such as malaria, dengue virus, and Zika, thus causing millions of deaths every year. The ability to trap and survey intact mosquitoes is important for monitoring their populations and transmissible diseases so the appropriate amount and type of insecticide may be deployed. However, despite a century of mosquito trap design, a trap's efficiency, the proportion captured of those lured to the trap, can be low and highly variable, ranging from <10% to 58%. The goal of this study is to elucidate mosquito behavior in response to suction flows and to use this behavior to design a more efficient trap.

II. METHODS

A. Tracking experiments with mosquitoes

At the CDC, we utilize the capabilities of their environmental chamber along with the Photonic Sentry camera which allows us to measure the 3D flight trajectories of mosquitoes near mosquito traps. We tested different scenarios such as mosquitoes in still air, with visual cues, odor and suction. We will also introduce external wind to simulate outdoor conditions. By analyzing the 3-D tracks, we will measure average velocity, spatial distribution, and swarming behavior. Our hypothesis is that consistent experimental conditions will yield repeatable probability distributions and capture rates, providing insights for trap design enhancements.

B. CFD and agent-based simulations

We simulate velocity and odor concentration fields from the trap using CFD. By building mathematical models of mosquito flight behavior in agent-based simulations, we'll incorporate odor, visual cues, and velocity fields to predict mosquito behavior. By fitting the model to experimental data, we'll infer parameters and functions representing their interactions.

C. Optimizing trap design

Finally, we design and test an inexpensive and efficient mosquito trap based on our findings.

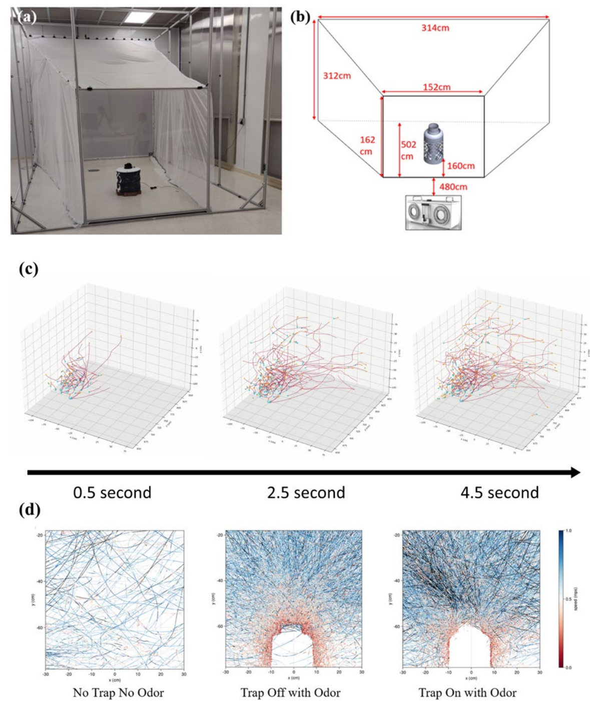

Figure 1: (a) Mosquito trap testing facility combined with the Photonic Sentry tracking system at CDC. (b) The dimensions of the testing chamber. (c) The animated spread of 100 mosquitoes from a single release point. (d) Visualization of flight trajectories near a mosquito trap (BG-Sentinel) for three different conditions (no trap and no odor, trap with odor, and trap with an operating fan).

ACKNOWLEDGEMENTS

We appreciate CDC Atlanta for providing mosquitoes and Photonic Sentry system.

REFERENCES

1. Amos, Brogan A., et al. "Attraction versus capture: efficiency of BG-Sentinel trap under semi-field conditions and characterizing response behaviors for female Aedes aegypti." *Journal of Medical Entomology* 57.3 (2020): 884-892.
2. Cribellier, Antoine, et al. "Flight behaviour of malaria mosquitoes around odour-baited traps: capture and escape dynamics." *Royal Society open science* 5.8 (2018): 180246.

Technical Group C-4

Materials Science and Engineering, Nanotechnology (MSE)

Electrochemistry of Metals with High Oxidation Potential

Choong-Un Kim
Department of Materials Science and Engineering, University of Texas/Arlington

I. SUMMARY

This paper describes an electrochemical mechanism behind the known impossibility of achieving electrodeposition of metals with high oxidation potential like Ti, Al and Nb, and introduces possible processing routes of resolving the mechanism thus enabling conformal deposition of thin films that are essential to various advanced devices yet have been prepared by more expensive and failure prone methods.

I. INTRODUCTION

One of the last frontiers in electrochemistry may be the electrochemical processing of metals or semiconductors with high oxidation potential such as Zr, Ti, Ta, Mb, Mg, Si, and Al. They are materials essential to various advanced applications especially in thin film forms, yet their use involves processes with excessive cost because cheaper routes of achieving conformal deposition like electroplating are not readily available. A few examples of such kind include the deposition of Ti as a diffusion barrier, Nb as a high-T superconductor layer and Zr as a corrosion protection layer. The electrochemical deposition of such elements however hasn't been developed to the full maturity sufficient to produce high quality films without complexity in processing and instrument. Especially lacking is the process possible near at room temperature. Available methods so far rely on catholic reaction either in ionic liquid or molten salt, requiring the plating at elevated temperatures and thus suffering from various limitations.

In theory, all metallic elements should be plateable by the means of electrochemical process. The fact that such method is not readily available for elements with high oxidation potential indicates that there exist mechanism(s) impeding the reduction of metallic ions at cathode surface. Because the exact nature of such mechanism(s) is currently unknown, it is not possible to design a process of enabling electrochemical deposition of elements under desire, motivating investigation detailed in this presentation.

II. Experimental Techniques and Results

Our investigation finds that there are multiple mechanisms behind the impossibility of reducing pure metallic ions by cathodic reaction. The first is found to be related to the high oxidation potential of the elements combined with an abundance of free oxygen (O_2^-) or hydroxide ions ($[OH]^-$) in aqueous solution. As the ions can readily react with oxidizing ions to form complex, the plated layer is a form of oxide or hydroxide. High potential applied to the electrodes cannot make the complex ions to dissociate because of electrolyzation activity of water molecule, that is

$$2H_2O(A) + 2e^- \rightarrow H_2(g) + 2[OH]^- (aq)$$

In order to avoid these problems, the solution needs to be changed from water to less-oxidizing organic solvent. Our exploration with various solvents finds that solvent like dehumidified Methanol can serve a good electrolyte as it consists of far more stable form of ions, $[CH_3O]^-$ and H^+. Fig.1-a shows the optical surface of Cu after plating trial of Nb (representation of metal with high oxidation potential) for 2hrs using Methanol with Nb_5Cl. Greyish surface forms as Nb nucleates but the plating is terminated at this stage because of solution contamination, that is resulted by etching of substrate, Cu in our case. The etching potential is found to develop at the cathode (even with cathodic protection) because of hydrogen induced cathodic polarization. Pre-treating the solution to reduce hydrogen activity is found to enable steady growth of Nb that is pure enough to show a reasonable superconductivity. We believe that the electrochemical deposition of other elements under desire shares the similar challenges that can be resolved by the similar method we developed for the case of Nb plating.

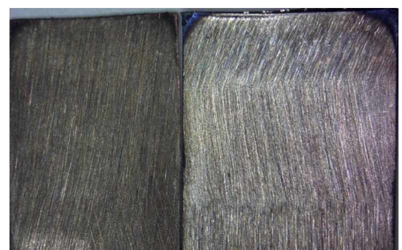

Figs.1 Optical images showing the surface of Cu after a) 2hrs plating in Nb_5Cl-methanol solution, and (b) successful plating with dehydrogenation treatment.

Fabrication of Fe-Ni Invar Alloy using Electrodeposition Technology for FMM Application

Jae-Ho Lee[1], Na-Young Kang[1]
[1]Dept. of MSE, Hongik University, Seoul, Korea

I. SUMMARY

Fe-Ni invar alloy (Fe 64wt%-Ni 36wt%) has very low CTE than any other metals. For this reason, it has been used as fine metal mask (FMM) in RGB patterning of OLED manufacture process. The electrodeposition of invar can be the alternative for fabrication of thin FMM. In this study, the Fe-Ni alloy were electrodeposited varying bath compositions and current density. Also, the effects of ferric ion (Fe^{3+}), produced during electrodeposition on inert anode, on the behavior of deposition were investigated. Finally, the Fe-Ni alloy with 36-40 wt% Ni were obtained.

Keywords: Fe-Ni invar alloy, electrodeposition, anomalous codeposition, current efficiency

II. INTRODUCTION

Fe-Ni alloy with Fe 64 wt%-36 wt% Ni, commercially known as invar, has a low CTE than any other metals. Based on its dimensional stability, Fe-Ni invar has been used as the materials of fine metal mask(FMM), a key component in RGB patterning of organic light-emitting diode (OLED) display, to avoid distortion of patterns during evaporation process at high temperature. Nowadays, commercialized FMM has been produced by wet etching process of invar film with over 20 μm in thickness made by rolling process. However, it is impossible to get higher resolution than QHD with extruded invar thickness. Electrodeposition is considered as one of the methods to make thinner FMM of 15 μm or less, whose resolution is higher than QHD by relatively simple equipment and process, compared to other technologies. However, the properties of electrodeposited Fe-Ni film, such as composition, microstructure, surface morphology, are significantly influenced by various process conditions. In this study, the electrodeposition of Fe-Ni alloy was conducted at various bath composition of ferrous ion (Fe^{2+}) and current density. Also, ferric ion (Fe^{3+}) was added to bath to observe the effect of ferric ion on Fe-Ni electrodeposition behavior. Finally, Fe-Ni films close to invar composition were obtained and the uniformity of deposited was evaluated.

Fe-Ni alloy electrodeposition was conducted in sulfate-chloride bath using dimensionally stabilized anode (DSA) as anode, Ti plate as cathode. The current density was varied from 10 mA/cm^2 to 200 mA/cm^2, and deposition time was adjusted with each current density to maintain total charge of 192 C.

Fig. 1 shows the composition of deposit from 0.35 M Fe^{2+} bath depending on current density. At low current density, the Ni contents is higher than 36 wt% with varying the current density. However, the composition remained almost constant at 36 wt% Ni at over 50 mA/cm^2.

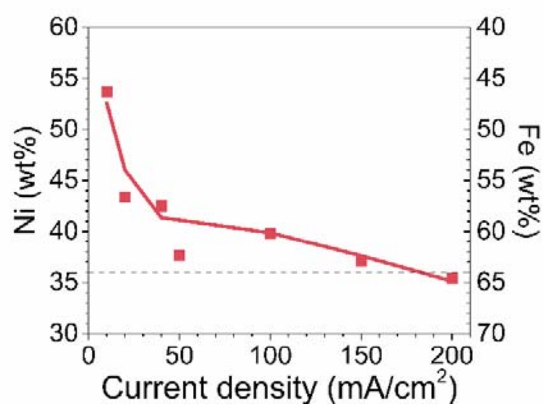

Fig. 1. Composition of deposits at various current density ($[Fe^{2+}]$=0.35 M)

ACKNOWLEDGMENTS

This work was supported by Korea National Research Foundation Nano Material Technology Development Program (2021M3H4A3A02098099)

REFERENCE

[1] E.F. Wassermann, *J. Magn. Magn. Mater.*, **100**, 346 (1991)
[2] C. Kim, O. Kwon, J. Jung, J. Park, D. Kim, K. Jung, *J. Soc. Inf. Disp.*, **28,** 668 (2020)
[3] A. Li, Z. Zhu, Y. Liu, J. Hu, *Mater. Res. Bull.*, **127**, 110845 (2020)

3-Dimensional Integration with High Interconnection Density

Rino Choi
3D Convergence Center, and Materials Science and Engineering at Inha University, Incheon 22212, Korea
(e-mail: rino.choi@inha.ac.kr)

I. Summary

Since the first integrated circuit was introduced, reducing the size of semiconductor devices has been a popular way to increase integration density and improve performance. However, as technology advances and device sizes approach those of molecules, further scaling down becomes more difficult. Recently, advanced applications such as internet of things (IoT), artificial intelligence (AI), and high bandwidth memory (HBM) require various devices to be integrated into smaller areas, with shorter interconnects to reduce power consumption and signal delay. To address these challenges, 3D integration is becoming more popular. This involves stacking device layers or dies vertically, which can reduce signal delay and the size of the chip. Many approaches have been attempted for 3D integration [1], but monolithic 3-dimension (M3D) integration and hybrid bonding (HB) are promising because they can offer high interconnection and input/output (I/O) density. This presentation will summarize the current progress of M3D and HB and discuss challenges and solutions for 3D integration with high interconnect density.

II. Monolithic 3D integration

M3D is a technique for stacking multiple device layers in a sequential integration process. This involves fabricating devices on an active layer formed on top of other device layers and connect upper and lower device layers with front-end vias formed by photolithographic processes. The high via density of M3D integration enables extremely high I/O density, small signal delay, and reduced power consumption. However, to achieve high-performance 3D integration circuits, many novel processes need to be developed. The active layer for upper devices should be formed on the lower layer. Various techniques have been proposed to form the upper active layer, including SOI bonding, laser-induced polycrystallization, and hydrogen implantation-bonding-cleavage. Laser-induced heat treatments need be implemented to fabricate devices on the upper layer, because conventional high thermal budget processes cannot be used to avoid damaging the devices already fabricated underneath. It requires a precise control of laser power and wavelength. Various challenges and difficulties in processes and cost still need to be addressed to fully realize the potential of M3D technology.

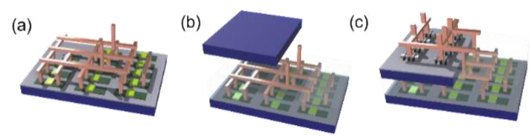

Fig. 1. Process flow of monolithic 3-d (a) lower layer fabrication (b) active layer formation at low temperature (c) upper layer fabrication (stack sequentially)

II. Hybrid bonding

Hybrid bonding (HB) technology has attained attention because it enables high I/O density without thermal budget restriction during device fabrication. HB is a permanent bond of two dies that combines a dielectric bond with embedded metal to form interconnections. Dies to be bonded are parallelly fabricated and completed through conventional BEOL with Cu pads. They are bonded without bumps to achieve finer pitch.

However, issues such as bonding voids, diffusion of copper into SiO_2 regions, and the need for precise bonding alignment and heat management still need to be addressed. Surface treatment and chemical mechanical polishing can improve surface uniformity, and annealing at high temperatures can cause device degradation and misalignment. Advanced alignment technologies and structures that can efficiently dissipate heat are needed.

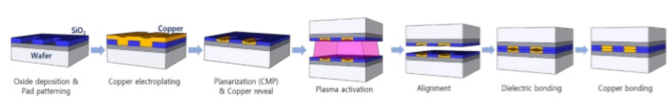

Fig. 2. Process flow of hybrid bonding (a) oxide deposition & pad patterning (b) copper electroplating (c) planarization (CMP) & copper reveal (d) plasma activation (e) alignment (f) dielectric-to-dielectric bonding (g) Cu-to-Cu bonding

REFERENCES

1. E. Beyne, "The 3-D Interconnect Technology Landscape," IEEE Design & Test, vol. 33, no. 3, pp. 8-20, 2016

Electrochemical Stability of Real-Scale Metallic Nanoparticles explored by Machine Learning

Hyuck Mo Lee[1], Kihoon Bang[1,2], Doosun Hong[2], Youngtae Park[1], Donghun Kim[2], Sang Soo Han[2]
[1]Department of Materials Science and Engineering, KAIST
[2]Computational Science Research Center, KIST

SUMMARY
We were able to solve the problem that the construction of Pourbaix diagrams of real-scale nanoparticles (NPs) is not practically possible today due to the extreme density functional theory (DFT) cost issue. As a first step to solving this problem, we developed a bond-type embedded crystal graph convolutional neural network (BE-CGCNN), in which four bonding types were uniquely encoded. BE-CGCNN substantially outperforms the original CGCNN[1] in predicting adsorption energies over a wide range of NP surface coverages. Using BE-CGCNN, we demonstrated the construction of the Pourbaix diagram of Pt NPs up to 6,535 atoms (approximately 4.8 nm in diameter) and the case of 3,871 atoms is shown in Figure 1. Since this diagram is for approximately 3.9 nm Pt, we can now compare the result with the available experimental report. For example, there is a study reporting the measured onset potentials for surface oxide (or fully O-covered phase) generation on Pt NPs, 0.9-1.15 V on 4.0 nm-size NPs from Mom *et al.*[2]. This value is marked on the Pourbaix diagram of Figure 1 and is found near the boundary lines of Pt-(O)1_{ML} in the diagram. Such quantitative agreement well supports that the constructed Pourbaix diagram is highly reliable and that the size dependence is greatly reflected.

Exploring Pt NPs of various sizes and shapes, we find that the machine learning (ML)-based Pourbaix diagrams well reproduce experimental observations, such as an increasing O- to OH-covered phase ratio and a decreasing Pt dissolution area as the NP size increases. By presenting surface Pourbaix diagrams of very large-size NPs, we conclude that BE-CGCNN can serve as a strong tool to enable the stability study of real-scale and arbitrarily shaped NPs in electrochemical environments, which is not possible in the conventional DFT scheme. Currently, our model is limited to specific systems as our data set is only composed of Pt-O or Pt-OH structures. The model will not function well for other adsorbates (e.g., OOH, CO) or for different compositions of NPs (e.g., Pt_3Ni, Pt_3Fe). However, if we precisely prepare a training set for the system we are interested in and follow a similar protocol, the BE-CGCNN model would be effective for the expanded material spaces, which remains as future research.

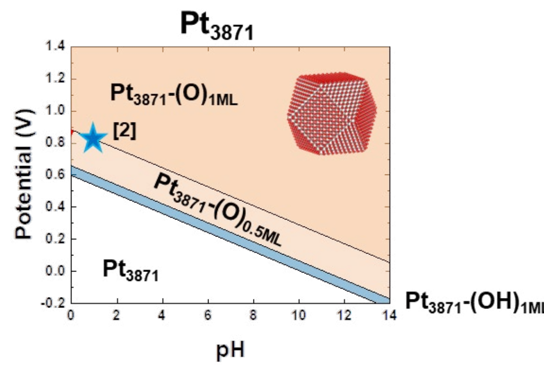

Figure 1: Pourbaix diagram of cuboctahedron $Pt_{3,871}$, which corresponds to 3.9 nm in diameter. The red and gray spheres of the inset atomic model represent oxygen and platinum atoms, respectively. ML is a monolayer.

ACKNOWLEDGEMENTS
This work was supported by the Samsung Research Funding & Incubation Center of Samsung Electronics under Project Number SRFC-MA1801-03.

REFERENCES
1. T. Xie, J. C. Grossman, "Crystal Graph Convolutional Neural Networks for an Accurate and Interpretable Prediction of Material Properties", *PRL* **120**, 145301 (2018).
2. R. Mom, L. Frevel, J-J. Velasco-Vélez, M. Plodinec, A. Knop-Gericke, R. Schlögl, "The Oxidation of Platinum under Wet Conditions Observed by Electrochemical X-ray Photoelectron Spectroscopy", *JACS* **141**, 6537 (2019).

Electrochemical synthesis of single crystalline nanomaterials and applications to interconnect of electronic packaging

Jae Yong Song
Pohang University of Science and Technology

I. SUMMARY

In advanced electronic packaging, the interconnect technology has been developed to keep up with the nano-scaling trend of transistors and high performance in the view of signal integrity and power integrity, e.g. TSV, RDL-interposer, embedded bridge, and more recently, hybrid (direct) bonding of C2C. In the interconnect technology, the main metals are copper and tin, which are generally deposited by electroplating method. Considering the scattering mechanism of carriers, single crystals are more favorable than polycrystalline metals. In this talk, a route of synthesizing single crystalline metallic nanomaterials is introduced and their applicability to interconnecting technology in electronic packaging is discussed.

II. Results

A. Template-assisted electrochemical synthesis of nanomaterials

Sn nanowires are synthesized using AAO nano-templates and their size-dependent properties of melting temperature, lattice parameters, and intrinsic stress are evaluated using DSC and XRD measurements. They show the typical size-dependent properties in the range of 10 to 40 nm in radius. The melting points are affected by their diameters and aspect ratio, the lattice parameter varies depending upon the diameter and their microstructures, such as granular and bamboo structures.

B. Template-free electrochemical synthesis of single crystalline metallic nanomaterials

Single crystalline nanowires such as Ag, Cu, Au, and Ag-Cu alloy are synthesized by electroplating method without templates. It is supposed that they grow due to the filamentary effect in combination with repeated reduction/oxidation processes of precursor metal ions, as depicted in Figure1. This mechanism also enables us to synthesize kinds of metallic alloys. XRD and TEM analyses prove that all the nanomaterials have single crystalline structure with [111]-longitudinal orientation and include several twins.

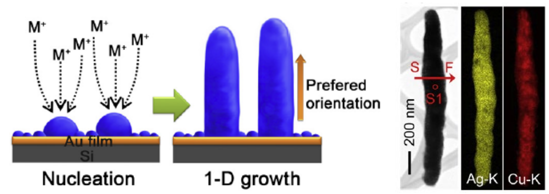

Figure 1: Electrochemical growth mechanism of nanomaterials due to filamentary effect and TEM images of Cu-Ag alloy nanostructure

C. Application to nano-ACF

The vertically grown Ag nanowires are used to fabricate the anisotropic conductive film for the potential application to interconnect technology of electronic packaging, as shown in Figure 2. The nano-ACF is electrically conductive in the thickness-through direction, but insulating in the plane direction.

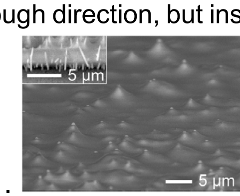

Figure 2: Typical SEM image of nano ACF composed of Ag nanowires embedded polymer matrix film

III. Conclusion

The single crystalline nanomaterials are electrochemically synthesized without templates, which is very low-cost, and expected to be applied to nanoscale interconnect technology in advanced BEOL process, in the view of the lower electrical conductivity of single crystal than that of polycrystal, which is worth being challenged in near future.

ACKNOWLEDGEMENTS

This work was supported by the National Research Foundation of Korea (NRF) funded by Ministry of Science and ICT (RS-2023-00210111)

REFERENCES

1. JY Song et al, J Alloys Comp. 580, 152, 2013; Sensors & Actuators B:Chemical, 273, 804, 2018

Phase-field Simulation of Microstructure Formation in Thin Films

Hwanwook Lee, Jungin Park, and Yongwoo Kwon
Department of Materials Science and Engineering, Hongik University

SUMMARY
We have developed a phase-field model for microstructure formation in thin films. Our model can simulate a wide range of materials including semiconductors, oxides, and metals. Governing equations describe gas transport toward the film surface, formation of amorphous solid at the surface, and crystallization. The various film characteristics such as conformal or nonconformal, amorphous or crystalline, etc can be produced according to the adjustment of model parameters.

Keywords: thin film, microstructure simulation, phase-field method

I. MOTIVATION
The focus of current semiconductor device development is on three-dimensional technology, including gate-all-around (GAA)-FET and 3D NAND. These devices require more precise control of thin film morphology and microstructure. Therefore, the prediction of deposition profile and microstructure will be advantageous.

II. SIMULATION MODEL DEVELOPMENT
We established a phase-field model comprising three partial differential equations on gas transport, solid film formation, and the behavior of grains with different crystalline orientations. They are numerically solved by the finite difference method that was implemented by our own C++ code. Representative simulation examples are demonstrated in Figure 1. Our simulation model is *universal* because it can simulate both amorphous and crystalline films.

ACKNOWLEDGEMENTS
This research was supported by the Nano Material Technology Development Program through the National Research Foundation of Korea (NRF) funded by the Ministry of Science, ICT and Future Planning (NRF-2021M3H4A6A01048300).

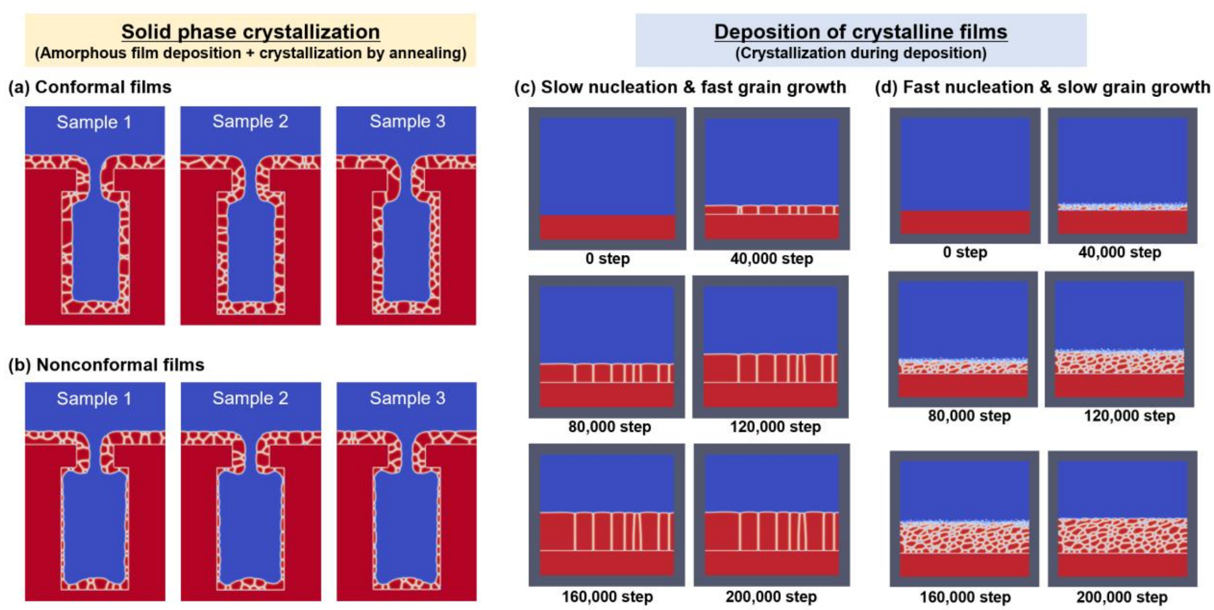

Figure 1. Simulation examples. The left panel shows the simulated microstructures produced by solid-phase crystallization, for example, poly-Si and poly-Ge: (a) Conformal films and (b) nonconformal films. The random nature of nucleation produces different grain configurations for the samples with the same profile of the amorphous film. The right panel shows the simulation of crystalline film deposition such as metals: (c) slow nucleation and fast grain growth and (d) fast nucleation and slow grain growth.

Technology trends of 3D NAND flash memory and pathfinding opportunities

Tae Kyung Kim
Intel

We live in a fast-paced, tech-savvy world thanks to the widespread use of smart devices and cloud services. As we now welcome a new era with machine learning, artificial intelligence, and self-driving cars, demand for easy access to data as well as data storage security has increased. High density NAND flash memory devices are commonly used in personal mobile devices, computers, and cloud servers with non-volatile data storage capability. The semiconductor industry has focused on increasing bit density with high performance by device scaling, structure breakthrough, material innovations and cell array technology. Beyond 2-dimensional scaling, 3D NAND have been developed with 3-dimensional scaling technologies and architectural revolutions. Since the first 3D NAND production with 24-word line layers around 10 years ago, 230+ WL-layer 3D NAND have been announced recently from the major companies in the memory industry. Recent forecasts indicate the introduction of 500+ WL layers in a few years, and the focus will be on pathfinding to build 1000+ WL layers within a decade [1]. Future developments require process engineering, material science, device physics and architectural creativity. High aspect ratio dry etch, conformal atomic layer deposition, wafer stress management, poly silicon grain engineering, 3D metrologies and cell array engineering will be key focus areas in performance and cost scaling [2]. Cell structure competition between CTF (Charge Trap Flash) and FG (Floating Gate) has been an intriguing topic with its own uniqueness in terms of process scaling and device capabilities. Furthermore, wafer bonding technologies are among the latest topics for high performance NAND flash memory. In addition to the process and integration evolution, cell array technologies such as TLC, QLC, PLC and HLC were driven to increase bit density and reliability. In this presentation, we will review how 3D NAND has evolved with device, process, and material technologies. Recent technical/cost challenges and opportunities in forward development will also be reviewed.

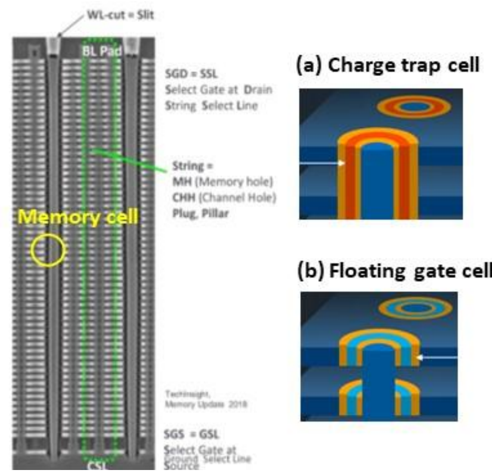

Figure 1: Typical 3D NAND cell structures. (a) Charge trap flash cell with replacement metal gate; (b) Floating gate cell with poly silicon gate.

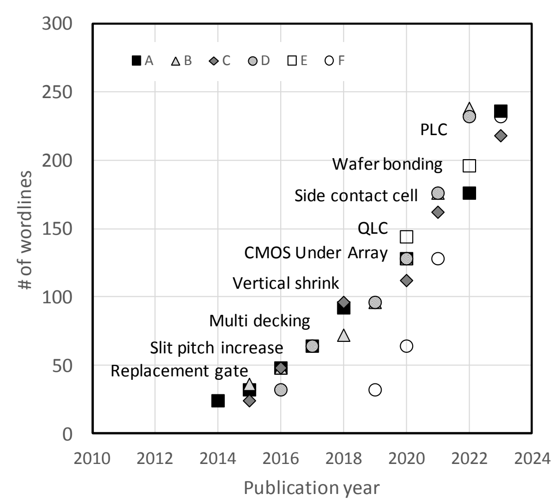

Figure 2: Evolution of 3D NAND: approximate timelines are based on public report, key technologies exhibitions depending on each company's roadmap.

REFERENCES

1. Kinam Kim, "The Smallest Engine Transforming Humanity", *IEEE IEDM*, 2021.
2. Jian Chen, "3D NAND Challenges and Potentials", *IEEE IEDM*, 2019.

Highly-scaled 3D Ferroelectric Transistor Array for Compute-in-Memory

Jang-Sik Lee
Department of Materials Science and Engineering
Department of Semiconductor Engineering
Pohang University of Science and Technology (POSTECH), Pohang 37673, Korea

Hardware-based neural networks (NNs) can provide a significant breakthrough in artificial intelligence applications due to their ability to extract features from unstructured data and learn from them. However, realizing complex NN models remains challenging because different tasks, such as feature extraction and classification, should be performed at different memory elements and arrays. This further increases the required number of memory arrays and chip size. Here, we propose a three-dimensional ferroelectric NAND (3D FeNAND) array for the area-efficient hardware implementation of NNs. Vector-matrix multiplication is successfully demonstrated using the integrated 3D FeNAND arrays, and excellent pattern classification is achieved. By allocating each array of vertical layers in 3D FeNAND as the hidden layer of NN, each layer can be used to perform different tasks, and the classification of color-mixed patterns is achieved. This work provides a practical strategy to realize high-performance and highly efficient NN systems by stacking computation components vertically.

Half-Cycle Interrogation of HfO_2 Atomic Layer Deposition Mechanism Using *in-situ* Reflectance Absorbance Infra-Red Spectroscopy

Jinhyun Kim[1], Siun Song[2], YeEun Hong[2], Dan Le Gardner[1], MinJong Lee[1], Rino Choi[2], Jiyoung Kim[1],

[1]University of Texas at Dallas, Richardson, TX. USA, [2]Inha University, InCheon, Korea

Atomic layer deposition (ALD) characteristics and film properties of $Hf_{0.5}Zr_{0.5}O_2$ (HZO) using anhydrous H_2O_2, O_3, and H_2O as oxidants [1]. It was observed that HZO deposited with H_2O_2 exhibited higher growth per cycle (GPC), lower wet-etch rate, and higher density compared to O_3 and H_2O. Additionally, the HZO capacitor fabricated using anhydrous H_2O_2 showed higher breakdown voltage and lower leakage current compared to the HZO capacitor using O_3 at the same amount of remanent polarization. These superior film properties make H_2O_2 an excellent oxidation reactant candidate for oxide ALD applications. In this study, we investigate the atomic layer deposition (ALD) mechanism of HfO_2 through a half-cycle interrogation approach using in-situ reflectance absorbance infrared spectroscopy (RAIRS). By monitoring the surface reactions and species during the ALD process, we aim to gain insights into the growth mechanism and understand the formation of HfO2 films at the atomic level. The reflecting configuration of the RAIRS system provides a suitable platform for studying the metal-insulator-metal structure fabrication process relevant to HfO2 deposition.[2] Our results shed light on the ligand exchange reactions, reaction site generation, and removal dynamics during the ALD half-cycles, revealing valuable information about the oxide growth process. This work contributes to a comprehensive understanding of HfO_2 ALD with various oxidants. H_2O_2 possesses both strong oxidation power comparable to O_3 and a low dissociation energy of peroxide O-O bonds, which is expected to produce hydroxyl reaction sites and facilitate ligand exchange reactions similar with H_2O. However, commercially available H_2O_2 sources typically have a high concentration of H_2O, making it challenging to distinguish the effects of H_2O_2 from those of H_2O [3]. Therefore, to avoid the influence of H_2O, high-purity anhydrous H_2O_2 was adopted to better understand the growth mechanism, HfO_2/TiN interface formation, and film properties.

HfO_2 was thermally deposited via ALD on a TiN substrate using TDMA-Hf and oxidants at 250 °C. A half-cycle study was performed to acquire differential Fourier transform infrared spectroscopy spectra, providing insights into the growth mechanism with different oxidants. These differential spectra revealed the generation and removal of reaction sites through ligand exchange reactions between the oxidants and TDMA-Hf. Hydroxyl ligand exchange reactions were observed for H_2O, formate reaction sites were generated for O_3, and interestingly, both hydroxyl and formate reaction sites were present for H_2O_2, potentially leading to the formation of a denser film. Furthermore, all oxidants exhibited a similar amount of residual hydroxyl and almost no carbon residue. Notably, while H_2O and H_2O_2 did not experience further Ti-O bonding formation after initial interface formation, O_3 exhibited continuous Ti-O bonding growth, indicating ongoing interface formation during the ALD process.

These results highlight the superior properties of H_2O_2, which generates a minimal HfO_2/TiN interface and denser films, positioning it as an ideal candidate for oxide ALD applications. Moreover, these properties offer significant advantages for scaling down ferroelectric HZO devices to the sub-5 nm regime compared to other oxidants. Further discussion regarding the growth mechanism, oxide growth, and interface formation will be presented in subsequent sections.

ACKNOWLEDGEMENTS

We would like to thank YEST/KEIT for their supports through ISTD Program (No.20010806). This work is partially supported by GRC-LMD program through SRC. This research is also supported by the MOTIE in Korea, under the Human Resource Development Program for Industrial Innovation (Global) (**P0017303**, Smart Manufacturing Global Talent Training Program) supervised by KIAT The ozone generator was provided by TMEIC, and the BRUTE hydrogen peroxide was provided by RASIRC.

REFERENCES

[1] J.H. Kim et al., IEEE, SISC 2021.

[2] S. M. Hwang et al., ECS Trans., 92, 265 (2019).

[3] D. Alvarez Jr. et al., Proc. SPIE 11326, 113260S (2020).

Dopant Control of Ultra-short Channel Gate-All-Around FET for Reliable Threshold Voltage

Rock-Hyun Baek[1], Jinsu Jeong[1]
[1]Pohang University of Science and Technology (POSTECH), Electrical Engineering,
77 Cheongam-Ro, Nam-Gu, Pohang, Gyeongbuk, 37673, Republic of Korea

I. SUMMARY

In this study, threshold voltage (V_{th}) variations caused by undesired Ge and C diffusion into Si channel were investigated in gate-all-around (GAA) nanosheet (NS) FET. Ge and C in the p/n-type source/drain (S/D) epitaxy diffuse laterally into channels. The diffused Ge and C vary channel stress and energy barrier, causing V_{th} variations accordingly. On the other hand, Ge also can be diffused into Si channel vertically by intermixing of Si/SiGe epitaxy stacks. The study is expected to provide comprehensive insight to control Ge and C caused V_{th} variations, which is the critical issue in state-of-the-art logic semiconductor devices.

II. INTRODUCTION

Ultra-nanoscale semiconductor devices are very sensitive to tiny process variations causing significant performance variations. Among them, V_{th} variations are critical problems due to limitation of CMOS supply-voltage scaling. Recently, most studies on process variations of GAAFETs have focused on geometrical variations [1, 2]. However, Ge and C diffusion induced performance variations have not been studied enough although SiGe and SiC are used as S/D in p/nFETs, respectively. Ge and C in S/D diffused into Si channel laterally during thermal process. Furthermore, Ge also can be diffused into Si channel vertically as Si/SiGe epitaxies are stacked. Here, Si and SiGe are inevitably intermixed at their interfaces. As a result, undesired Ge and C diffusion into Si channel causes critical variations of electrical characteristics.

III. RESULTS and DISCUSSION

Schematic and geometric parameters of NSFETs are shown in **Fig. 1** and **Table 1**, respectively**. Fig. 2a** shows the transfer curves of NSFETs with various Ge and C mole fraction of S/D. V_{th} of pFETs ($V_{th,p}$) increases as the Ge mole fraction of S/D (M_{Ge}) increases from 0.3 to 0.5, but decreases when the M_{Ge} is higher than 0.5. Increased M_{Ge} enhances compressive channel stress and Ge diffusion into Si channels. Both retard boron diffusion into channels, and increase $V_{th,p}$. As M_{Ge}> 0.5, E_v of SiGe S/D is much higher than that of Si channels. It decreases energy barrier height (E_{bar}) between the source and channel, resulting in $V_{th,p}$ decrease.

On the other hand, V_{th} of nFETs ($V_{th,n}$) consistently increases as the C mole fraction of S/D (M_C) increases. C atom generally retard phosphorus diffusion, so phosphorus concentration in channels reduces with the high M_C.

Fig. 2b shows transfer curves of NSFETs for different Si/SiGe intermixing. As the Si/SiGe intermixing becomes more severe, Ge inevitably diffuses deeply into channels, and then 'Si' channels gradually become 'SiGe-like' channels. SiGe have higher E_v and E_c than Si which means that NSFETs with SiGe-like channel have lower and higher E_{bar} in p/nFET, respectively. As a result, $V_{th,p}$ decreases and $V_{th,n}$ increases as the Si/SiGe intermixing becomes severe.

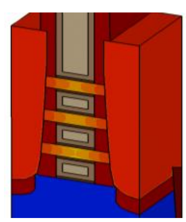

Table 1: Geometry of NSFETs

Parameters	Value [nm]
Contact poly pitch	40
Sheet pitch	56
Gate length	12
NS thickness	5
NS width	40

Figure 1: 3D Schematic of NSFETs.

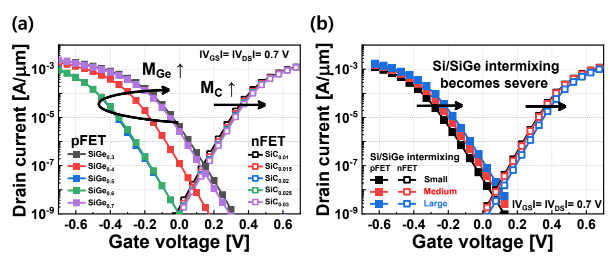

Figure 2: Transfer curves of NSFETs (a) with M_{Ge} and M_C, and (b) with three Si/SiGe intermixing types.

REFERENCES

1. Y.-S. Wu *et al.*, *IEEE Trans. Electron Devices*, Vol. 55, No.11, pp. 3042 – 3047, 2008.
2. J. Jeong *et al.*, *IEEE Access*, Vol. 8, pp35873 - 35881, 2020.

New Device Applications of III-Nitride Wide-Bandgap Semiconductors: Beyond Power Electronics and Visible/UV Photonics

Jae-Hyun Ryou[1]
[1]University of Houston

I. INTRODUCTION

Group-III-nitride (III-N) semiconductor materials have been developed for high-power high-voltage electronics and UV/visible photonics thanks to their wide-bandgap energy and high dielectric strength. However, they possess other excellent properties for new device applications. They are thermally stable, chemically inert, mechanically hard, and radiation hardened, which makes them inherently suitable for extreme-environment applications. They are also biocompatible for selected biomedical applications. III-N materials have spontaneous and piezoelectric polarization. Whereas the piezoelectric coefficients of III-N materials are not as high as those of lead titanate zirconate ($Pb[Zr_xTi_{1-x}]O_3$, PZT), the electromechanical coupling factor and mechanical to electrical energy conversion efficiency of single-crystalline III-N materials are sufficiently high thanks to their low dielectric constants. Finally, single-crystalline III-N thin films are mechanically flexible, enabling applications in flexible electronics and sensing. In this study, we present new device applications based on the wide-bandgap III-N materials utilizing the aforementioned excellent properties.

II. DEVICE APPLICATIONS

A. Mechanical Energy Harvesting

We develop III-N thin-film flexible piezoelectric generator (F-PEG) that can generate an open-circuit voltage of 50 V, a short-circuit current of 15 μA, and a maximum power of 167 μW at a load resistance of 5 MΩ. Applications of the III-N thin-film F-PEG are demonstrated by directly powering electronics such as light-emitting diodes and electric watches, and by charging commercial capacitors and batteries to operate an optical pulse sensor. The III-N thin-film F-PEG shows good durability and a stable output after being subjected to severe buckling tests of over 30,000 cycles.

B. Extreme-Environment Sensing

Extreme environments are often faced in energy, transportation, aerospace, and defense applications and pose a technical challenge in sensing. We develop a piezoelectric sensor based on single-crystalline AlN transducers with high sensitivities of 0.4–0.5 mV/psi up to 900 °C and output voltages from 73.3 mV to 143.2 mV for input gas pressure range of 50 to 200 psi at 800 °C. The operation of the sensor at 900 °C is amongst the highest for pressure sensors and the inherent properties of AlN including chemical and thermal stability and radiation resistance indicate this approach offers a new solution for sensing in extreme environments.

C. Personal Healthcare Monitoring

(1) Pulse sensor: We develop piezoelectric pulse sensors (PPSs) that can detect subtle skin surface deformation caused by arterial pulses for noninvasive continuous pulse waveform monitoring. This biocompatible flexible PPS is sensitive enough to detect pulse waveform with detailed characteristic peaks from most arterial pulse sites when attached to the skin surface without applying external pressure. Useful physiological parameters such as the pulse rate, artery augmentation index, and pulse wave velocity can be drawn from the as-acquired pulse waveforms.

(2) Eye-movement sensor: We also develop a highly sensitive, non-invasive, and skin-attachable sensor made of a stable flexible piezoelectric thin film to overcome the limitations of current computer-vision-based eye-tracking systems and piezoelectric strain sensors. The sensor can detect abnormal eye flickering and conditions caused by fatigue and drowsiness, including overlong closure, hasty eye blinking, and half-closed eyes. The abnormal eyeball motions, which may be the sign of several brain-related diseases, can also be measured, as the sensor generates discernable output voltages from the direction of eyeball movements.

III. CONCLUSION

III-N thin film materials offer new solutions in the applications of energy harvesting, harsh-environment sensing, and personal healthcare systems.

High resolution photolithography for OLED frontplane

Jeong-Hwan Lee
Department of Materials Science and Engineering, Inha University, South Korea

I. SUMMARY

High-resolution OLED displays exceeding 2K pixels per inch (ppi) exhibit significant appeal in the pursuit of next-generation AR/VR displays. Among the prospective solutions to surpass the limitations of the prevailing sheet mask-based evaporation system, photolithographic patterning stands as a prominent contender. Here, we present a compelling lithography technique capable of achieving pixel arrays smaller than 10 μm each, thus showcasing a noteworthy advancement.

II. Results and Discussion

The polymer composed of 1H, 1H, 2H, 2H-perfluorooctyl methacrylate (FOMA), spiropyranyl methacrylate (SPMA), and isononyl methacrylate (IBMA), referred to as FSI, demonstrates excellent solubility in the fluorous solvent HFE-7500. It serves as a highly fluorinated photoresist suitable for application in the photo-patterning process of organic semiconductors for realizing high-resolution displays. However, a critical issue arises during the dry etching process for transferring the photoresist pattern, as it causes damage to the underlying organic film. This problem is attributed to the relatively low remaining thickness and etch resistance of the photoresist.

To address this challenge, we investigated the incorporation of BMOMA as a co-monomer in FSI (referred to as FSIB) to enhance the dissolution contrast. Although the sensitivity to 365 nm UV light improved, no significant enhancement in remaining thickness was observed. As an alternative approach, we used FSIBT by introducing TRIS, which facilitates the formation of SiO_2 *under* O_2 *plasma conditions and thereby improves the etch resistance. FSIBT exhibited excellent solubility in HFE-7500, superior patterning characteristics, and significantly enhanced etch resistance under* O_2 *plasma conditions. These benefits were also observed under alternative etching conditions, such as* O_2/CF_4 *plasma.*

To assess the utility of the developed material, FSIBT polymers were employed to structure the upper layer of the Electron-Transport Layer (ETL) film comprising organic semiconductors. Subsequently, OLED pixel patterning was conducted using this material. The resulting OLED devices displayed minimal damage when compared to reference devices with full evaporation process. Furthermore, they exhibited vivid OLED emission images with less than 10 μm patterned size, *confirming the effectiveness and viability of the proposed lithographic materials for future micro/nano-patterning applications involving various organic materials.*

We anticipate that the imaging materials presented in this study will find extensive practical applications in the implementation of micro/nano-patterning techniques for a wide range of organic materials.

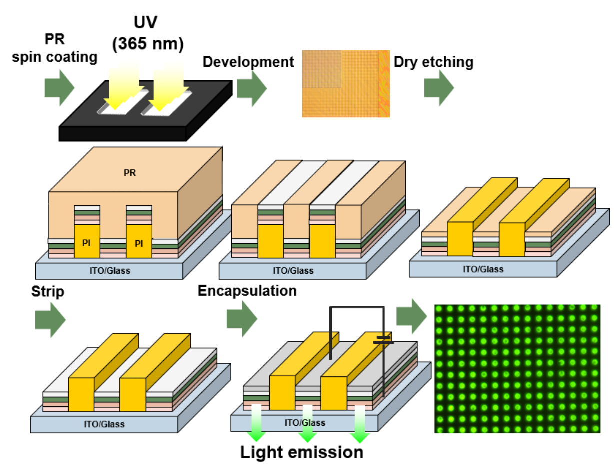

Figure 1: Photolithography process for high resolution OLED displays. The emission image from *10 μm patterned pixels under electrical excitation.*

ACKNOWLEDGEMENT

This work was supported by Korea Institute for Advancement of Technology(KIAT) grant funded by the Korea Government(MOTIE) (P0008458, HRD Program for Industrial Innovation)

Vapor-Phase Infiltration for Microelectronics Applications

Chang-Yong Nam[1]
[1]Center for Functional Nanomaterials, Brookhaven National Laboratory, Upton, NY 11973

Vapor-phase infiltration (VPI) is a material hybridization technique derived from atomic layer deposition (ALD), where “soft” substrates, such as polymer thin films, are infused with inorganic materials in a molecular scale via cyclic exposure of gaseous organometallic precursors and co-reactants. The infusion process is realized by the diffusion of reactants into the organic matrix and subsequent reaction with available reactive moieties. In this talk, I will showcase our efforts on utilizing VPI for two representative microelectronics applications: (a) synthesis of organic-inorganic hybrid extreme ultraviolet (EUV) photoresists that are essential for high-volume manufacturing of extremely downscaled, next-generation logic and memory devices [1]; and (b) hybrid memristors for brain-inspired neuromorphic computing with reduced stochastic variation in switching parameters.[2]

REFERENCES

1. Subramanian et al., *Proc. SPIE* **PC12292**, PC122920L (2022)
2. Subramanian et al., *Adv. Electron. Mater.* **8**, 2200172 (2022)

Charge Transfer Across the Interfaces in Organic Field-Effect Transistors

Hyun Ho Choi[1,2], **Soojin Kim[2]**, **Sang-Yong Nam[1,2]**, **Dong-Jun Kwon[1,2]**, **Se Hyun Kim[3]**
[1]Research Institute of Green Energy Convergence Technology (RIGET), Gyeongsang National University, Jinju 52828, Korea
[2]Department of Materials Engineering and Convergence Technology, Gyeongsang National University, Jinju 52828, Korea
[3]Department of Chemical Engineering, Konkuk University, Seoul 05029, Korea

ABSTRACT

Recent progress in understanding charge carrier transport in organic semiconductors has been greatly facilitated by advances in organic field-effect transistors (OFETs), including synthesizing several high-performance organic semiconductors, and developing device fabrication methods and novel optoelectrical measurement techniques. Smart Carbon Electronics Group is conducting fundamental research centered on unit devices to realize the dream of commercializing organic electronics. In this poster, we focus on charge transfer across the interface between organic semiconductors and gate dielectric in OFETs. First, we discuss the bias-stress effect, which is attributed to the migration and localization of charge carriers into the gate dielectric. In particular, this transfer can be nonlinearly boosted by the coupling of localized states.[1] Next, we discuss the transfer of positive and negative charges across the interface between the organic semiconductor and polymer insulator, which can be significantly propagated by photo illumination, the so-called photoinduced bias-stress effect. The direction of the transverse electric field at the interface determines the sign of the transferred charge, and the field magnitude, light intensity, and absorption coefficient control the transfer rate. We also demonstrate that a photoinduced charge transfer can record rewritable accumulation channels with an optically defined geometry and resolution.[2]

ACKNOWLEDGEMENTS

This research was supported by National Research Foundation (NRF) grant and Korea Institute for Advancement of Technology (KIAT) grant funded by the Korea Government: Grant No. 2020R1A6A1A03038697 and P0017310.

REFERENCES

[1] a) H. H. Choi, W. H. Lee, K. Cho, *Adv. Funct. Mater.* 2012, 22, 4833; b) J. Lee, H. H. Choi, N. Park, H. Min, S. Han, H. Jeong, I. Song, S. H. Kim, H. S. Lee, *J. Phys. Chem. C* 2015, 119, 7670; c) S. Han, S. Kim, H. H. Choi, *in-preparation*.

[2] a) H. H. Choi, H. Najafov, N. Kharlamov, D. V. Kuznetsov, S. I. Didenko, K. Cho, A. L. Briseno, V. Podzorov, *ACS Appl. Mater. Interfaces*, 2017, 9, 34153; b) H. H. Choi, J. Park, S. Huh, S. K. Lee, B. Moon, S. W. Han, C. Hwang, K. Cho, *ACS Photonics* 2018, 5, 329; c) S. Kim, J. Im, S. Han, S. Lee, S. H. Kim, H. H. Choi, *in-preparation.*

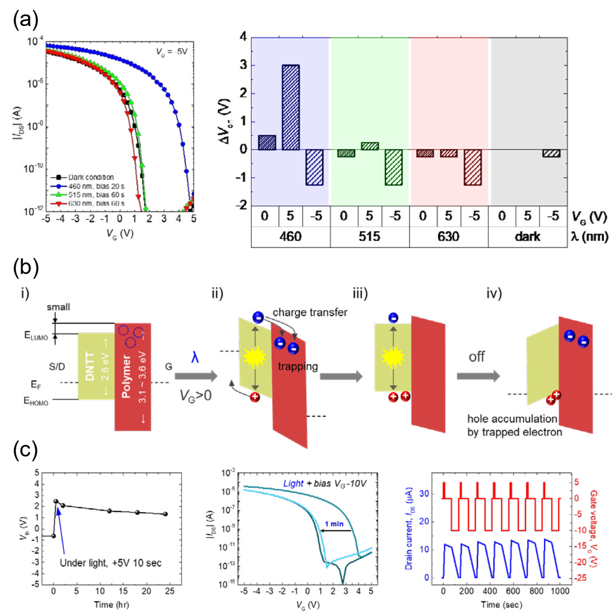

Figure. (a) Transfer characteristics of C8-BTBT field-effect transistors, in which on-set and threshold voltages are programmed by the combination of monochromatic illumination and gate bias. (b) Mechanism of photo- and field-induced charge storage in our device. (c) Results of retention, switching, and cycle tests.

Free-Standing Li4Ti5O12/Carbon Nanotube Electrodes for Flexible Lithium-Ion Batteries

Jun-seok Lee[1], **Sang-Du Yun**[2], **Jeong-Hyeon Yang**[2], **Sun-Chul Huh**[1], **Hyo-Min Jeong**[1], **Tae-Hyun Nam**[3], **Yeon-Ju Ryu**[3] **and Jung-Pil Noh**[1*]

[1]Department of Energy & Mechanical Engineering, Institute of Marine Industry, Gyeongsang National University, Tongyeonghaean-ro 2, Tongyeong 53064, Republic of Korea, [2]Department of Mechanical System Engineering, Gyeongsang National University, Tongyeonghaean-ro 2, Tongyeong 53064, Republic of Korea, [3]Department of Materials Engineering and Convergence Technology, Gyeongsang National University, Jinju-daero 501, Jinju 52828, Republic of Korea

I. Abstract

Lithium-ion batteries (LIBs) have been used in many fields, such as consumer electronics and automotive and grid storage, and its applications continue to expand. Several studies have attempted to improve the performance of LIBs. In particular, the use of high-capacity silicon and tin as anodes has been widely studied. Although anodes composed of silicone and tin have high theoretical capacities, poor electrical conductivity and considerable volume expansion of such anodes deteriorate the LIB performance. Thus, $Li_4Ti_5O_{12}$ (LTO), a zero-strain material, has attracted much attention with high cycle stability and rate capability through improved electrical conductivity. However, LTO has the disadvantages of a low electrical conductivity (10^{-8} to 10^{-13} S cm^{-1}) and moderate Li+ ion diffusion coefficient (10^{-9} to 10^{-16} cm2 s^{-1}). In this study, the flexible and free-standing composite films were fabricated using only LTO and multi-walled carbon nanotube(CNT) with high electrical conductivity and ion diffusivity. The prepared LTO/CNT films showed a higher charge/discharge capacity than the theoretical capacity of the LTO electrode.

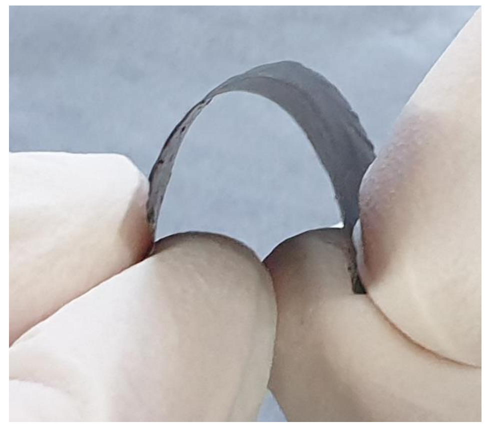

Figure 1: Image of the LTO_CNT film

The Effects of in-situ Atomic Layer Annealing on Thermal Atomic Layer Deposited Silicon Nitride

Si-Un Song[1,2], Dan N. Le[1], Su Min Hwang[1], Jin-Hyun Kim[1], Rino choi[2] and Jiyoung Kim[1]

[1]The University of Texas at Dallas, Richardson, TX, USA.
[2]Inha University, Incheon, Republic of Korea

We demonstrated the deposition of thermal atomic layer deposition (t-ALD) SiN_x over a wide range of deposition temperatures using anhydrous hydrazine (N_2H_4) as the nitrogen precursor in 2021. Within the temperature range of 390-520°C, the GPC (growth per cycle) is approximately 0.049±0.003 nm/cycle, which is higher than SiN_x films grown by ammonia (NH_3). Furthermore, refractive index (R.I.) of SiN_x with hydrazine increases (as high as 1.99) with increase of deposition temperature. Wet etch rate (WER) values are 2.24±0.02 nm/ min for hydrazine, which is still undesirable values, while 7.48±2.6 nm/ min for NH_3.

Herein, we studied the effect of the *in-situ* atomic layer annealing (ALA) process utilizing Ar plasma on thermal ALD silicon nitride (SiN_x) thin films. SiN_x with *in-situ* plasma cycles were carefully investigated and compared to the thermal ALD in aspect of the growth characteristics, wet-etch rate (WER), bonding information, and conformality over different aspect ratio (AR).

When the *in-situ* plasma treatment was introduced in the thermal ALD process, the growth rate of SiN_x was reduced by ~45% compared to the standard process. Despite the decrease in growth rate, the addition of *in-situ* plasma treatment resulted in notable enhancements in the deposited SiN_x thin film properties, such as improved reflective index (RI), lower wet etch rate (WER) and increase in film density. Introduction of ALD/ALA process in deposit SiNx films decreased WER from 12.9 nm/min to 0.69 nm/min (evaluated in diluted HF 200:1).

Ex-situ FTIR was employed to further investigate the effects of *in-situ* atomic layer annealing on embedded $–NH_x$ (x=1,2) bonds within the additional plasma cycles showed a slightly lower $–NH_x$ bond density. Furthermore, the conformality of ALD/ALA SiNx thin films was also evaluated using ~6:1 AR trench structures. The TEM cross-sectional images showed >80% conformality of SiNx thin film could be achieved when incorporating the *in-situ* plasma treatment into the ALD process.

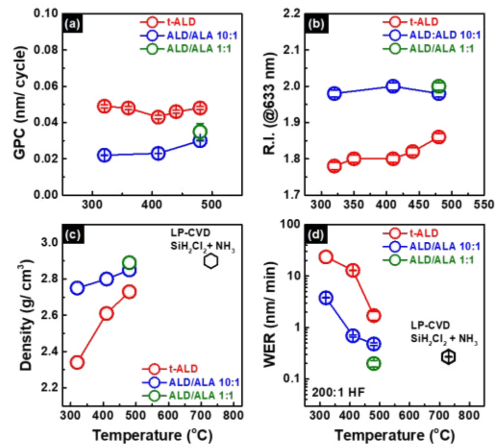

Figure 1: (a) GPC, (b) RI, (c), WER, and (d) density as a function of the deposition temperature of thermal ALD (red), ALD/ALA 10:1 ratio (blue), and ALD/ALA 1:1 ratio (green) of SiN_x thin films. The WER was evaluated in a diluted 200:1 HF solution. The LP-CVD SiN_x sample was prepared using SiH_2Cl_2 and NH_3 at 730°C.

ACKNOWLEDGEMENTS

This research was supported by the MOTIE (Ministry of Trade, Industry, and Energy) in Korea, under the Human Resource Development Program for Industrial Innovation(Global) (P0017303, Smart Manufacturing Global Talent Training Program) supervised by the Korea Institute for Advancement of Technology (KIAT). The authors wish to thank RASIRC Inc. for providing the anhydrous hydrazine.

REFERENCES

1. Dan N. Le, “Thermal Atomic Layer Deposition of Silicon Nitride Using Anhydrous Hydrazine and Ammonia,” *ALD 2021*

Analysis of Separation Behavior of Polyamide Structure-Based RO membrane Using Multi-scale Simulation

Kwang Seop Im[1], Tae Kyung Lee[1], Sang Yong Nam[1,*]

[1] Department of Materials Engineering and Convergence Technology, Green Energy Convergence Research Institute, Gyeongsang National University Jinju, 52828, Republic of Korea

I. SUMMARY

The desalination process using membrane has been gaining significant attention as a promising technology that can address the global water scarcity issue. Reverse osmosis, which is a widely used membrane desalination process, have substantial industrial potential due to their ability to convert abundant seawater into fresh water. To enhance the performance, a fundamental understanding of the reverse osmosis mechanism at atomic and molecular level within the membrane's active layer is crucial. In this study, we theoretically investigated the physical permeation behavior of water molecules and ionic substances within the active layer of the membrane using molecular dynamics simulation.

II. Experimental

2.1. Molecular structure modeling

The molecular structure was modeled using the Materials Studio 2023 program. Based on the polymerization of m-phenylenediamine (MPD) and trimesoyl chloride (TMC) molecules, a polyamide structure was computationally modeled. Using the computationally modeled polyamide structure, the active layer was constructed.

2.2 Simulation

Monte Carlo (MC) calculation was used to determine the thermodynamically stable positions of NaCl ions and water molecules absorbed within the polyamide active layer. The structure system obtained from MC calculations was then utilized for molecular dynamics (MD) simulations. Subsequently, radial distribution function (RDF) analysis was conducted to investigate the adsorption structure between NaCl ions/water molecules and the polyamide active layer. The coordination number of the adsorption structure was analyzed through RDF analysis. Additionally, Density Functional Theory (DFT) calculation was employed to analyze the adsorption energies of Na^+, Cl^-, and water molecules on the functional groups of the polyamide.

III. Results

The reverse osmosis exhibited by NaCl and water molecules in the polyamide active layer was investigated using MD simulations and DFT calculations, demonstrating the contribution of the physical adsorption ability between the polyamide functional groups and NaCl ions. The electron density and adsorption energy analysis using DFT calculations showed that the physical adsorption of NaCl is driven by electrostatic interactions rather than van der Waals interactions. Overall, the multiscale simulation employing MC calculations, MD simulations, and DFT calculations elucidated the atomic/molecular level permeation of water molecules and NaCl ions in the polyamide active layer, and derived conditions for enhancing the separation of NaCl ions.

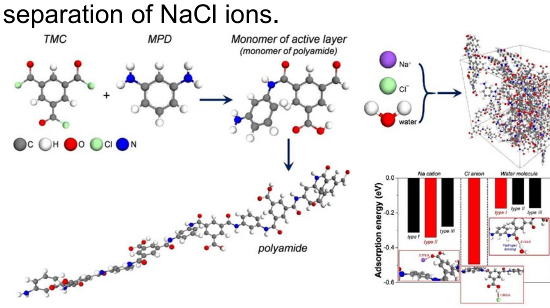

Figure 1. Computerized modeling of membrane active layer based on polyamide structure and adsorption energy of molecules.

ACKNOWLEDGEMENTS

This work was supported by the Technology Innovation Program Development of an hollow fiber membrane composite filter with 1.8 LPM water flow and 95% TDS reduction for direct water purifiers, 20019441 funded By the Ministry of Trade, Industry & Energy(MOTIE, Korea) and Energy(MOTIE, Korea) and this paper was supported by Korea Institute for Advancement of Technology(KIAT) grant funded by the Korea Government(MOTIE) (P0017310, Human Resource Development Program for Industrial Innovation(global))

REFERENCE

1. Malaeb, Lilian, and George M. Ayoub. "Reverse osmosis technology for water treatment: State of the art review." *Desalination*, Vol 267, No. 1 pp 1-8, 2011

Optimal Print Parameter Prediction By Neural Networks For Laser Powder Bed Fusion Additive Manufacturing

Kevin Graydon[1], Yongho Sohn[1]

[1] Advanced Materials Processing and Analysis Center, Department of Materials Science and Engineering, University of Central Florida, Orlando, FL, 32816, USA

I. SUMMARY

A neural network model was developed to determine optimal print parameter windows for novel or previously unprinted aluminum alloys. CALPHAD, ICME, and open-source tools in conjunction with in-house laser powder bed fusion datasets were employed for model creation, testing, and validation.

II. INTRODUCTION

Additive manufacturing by laser powder bed fusion has allowed for increased flexibility in terms of geometric design. However, the print parameters specified to achieve nearly fully dense, net-shaped parts for a given aluminum alloy remain a challenge to determine due to the time and costs associated with performing parametric optimization studies for each material. By way of CALPHAD and ICME tools coupled with Keras neural networks, a link between high-level printer parameters, material-specific thermophysical properties, and resultant relative densities can be established. This link can be harnessed to narrow the experimental printing range thereby reducing development time and costs during alloy design and testing. Additionally, the model can also be used for existing aluminum alloys that have not been previously processed by laser powder bed fusion.

III. RESULTS

Feature analysis was performed, and good predictability was found with the inclusion of material liquidus temperature, latent heat, printer power, and laser scan speed. Figure 1 shows the predicted relative density values for an Al-8wt%Ce-10wt%Mg alloy processed by laser powder bed fusion and printed at 350W over a range of scan speeds with constant hatch spacing and slice thickness [1]. Predictions are in good agreement with experimental values. The shaded region highlights the standard deviations of the determined relative densities of which the predictions mostly fall within.

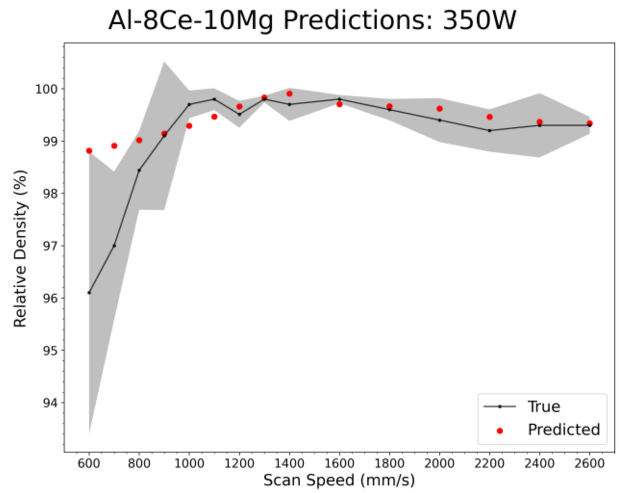

Figure 1. Predicted relative densities for Al-8Ce-10Mg processed by laser powder bed fusion at 350W [1].

ACKNOWLEDGEMENTS

This work has been financially supported by LIFT, a nonprofit, public private partnership operated by American Lightweight Materials Manufacturing Innovation Institute (ALMMII), through its ULIFT program. Authors sincerely appreciate technical and project management guides from LIFT's Dr. David Hicks, Dr. Amberlee Haselhuhn and Mr. Bradley Friend.

REFERENCES

1. Holden Hyer, Abhishek Mehta, Kevin Graydon, Nemanja Kljestan, Marko Knezevic, David Weiss, Brandon McWilliams, Kyu Cho, Yongho Sohn, "High strength aluminum-cerium alloy processed by laser powder bed fusion," *Additive Manufacturing,* Vol. 52, April 2022.

Enhanced ferroelectric polarization of $Hf_{0.5}Zr_{0.5}O_2$ thin films through fast ramp-up annealing process

Seongbin Park[1], Jong Mook Kang[1], Hye Ryeon Park[1], Seojun Lee[2], Jin-Hyun Kim[2], Jiyoung Kim[2,*], and Si Joon Kim[1,*]
[1] Kangwon National University, Chuncheon, Gangwon-do 24341, Republic of Korea
[2] The University of Texas at Dallas, Richardson, Texas 75080, USA
E-mail: jiyoung.kim@utdallas.edu and sijoon.kim@kangwon.ac.kr

SUMMARY

In this study, we investigated the ferroelectric properties of atomic layer deposited $Hf_{0.5}Zr_{0.5}O_2$ (HZO) thin films with various ramp-up annealing times (1 h, 2 h, and 4 h) at 400°C in N_2 ambient. To simultaneously extract the ferroelectric switching polarization and dielectric constant of HZO-based capacitors, the pulse write/read measurements were used. As a result, the fast ramp-up annealing process has a significant impact on improving the ferroelectric properties.

Keywords: Ferroelectric film, $Hf_{0.5}Zr_{0.5}O_2$, atomic layer deposition, ramp-up rate

I. INTRODUCTION

The ferroelectric $Hf_{0.5}Zr_{0.5}O_2$ (HZO) is one of the most promising materials for next-generation memory applications. Previous studies have been reported that the formation of an orthorhombic phase (o-phase) is necessary to obtain ferroelectric properties in HZO thin films [1]. As a crystallization method, a rapid thermal annealing (RTA) process at 400°C or higher has been generally used [1]. In addition, it has been reported that the ramp-up rate of the RTA process affects the formation of the monoclinic phase (m-phase) [2]. However, in this RTA process, it is not easy to analyze the effect of ramp-up rate conditions. Therefore, in this study, the ferroelectric properties of HZO thin films according to various ramp-up annealing times (1-4 h) at 400°C were investigated using a furnace.

II. RESULTS AND DISCSUSSION

The ferroelectric switching polarization (P_{SW}) and the dielectric constant were obtained from the pulse write/read measurements. Detailed measurement methods can be found in our previous study [3]. As the ramp-up rate slows, the P_{SW} and dielectric constant of HZO thin films tends to decrease as shown in Fig. 1. This is associated with the undesired formation of the m-phase. Therefore, the

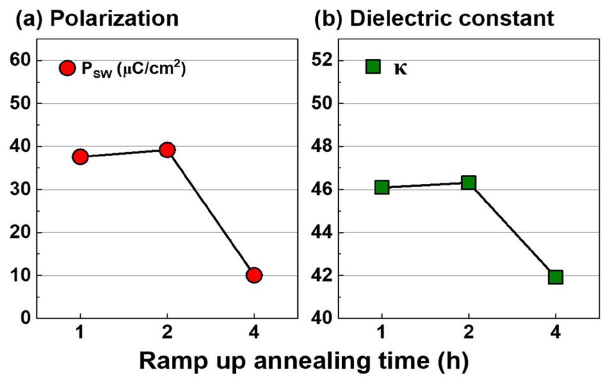

Figure 1: (a) P_{SW} and (b) dielectric constant extracted using pulse write/read measurements.

fast ramping up to 400°C in the annealing proess can be a useful strategy to improve the ferroelectric properties of HZO thin films.

ACKNOWLEDGEMENTS

This work was supported by Korea Institute for Advancement of Technology (KIAT) grant funded by the Korea government (MOTIE) (P0017011 and P0020966, HRD Program for Industrial Innovation).

REFERENCES

1. S. J. Kim, J. Mohan, S. R. Summerfelt, and J. Kim, "Ferroelectric $Hf_{0.5}Zr_{0.5}O_2$ thin films: a review of recent advances," *JOM*, Vol. 71, No. 1, pp. 246-255, 2019.
2. V. K. Narasimhan, M. E. McBriarty, D. Passarello, V. Adinolfi, M. F. Toney, A. Mehta, and K. A. Littau, "In situ characterization of ferroelectric HfO_2 during rapid thermal annealing," *Phys. Status Solidi RRL*, Vol. 15, No. 5, p. 2000598, 2021.
3. S. J. Kim, D. Narayan, J. G. Lee, J. Mohan, J. S. Lee, J. Lee, H. S. Kim, Y. C. Byun, A. T. Lucero, C. D. Young, S. R. Summerfelt, T. San, L. Colombo, and J. Kim, "Large ferroelectric polarization of $TiN/Hf_{0.5}Zr_{0.5}O_2/TiN$ capacitors due to stress-induced crystallization at low thermal budget," *Appl. Phys. Lett*, Vol. 111, No. 24, p. 242901, 2017.

Forming Voltage-Free Memristive Hafnium Oxide Devices for Non-Polar Switching Applications

Ye-eun Hong[1, 2], Minjong Lee[1], Jinhyun Kim[1], Heber Hernandez-Arriaga[1], Rino Choi[2], and Jiyoung Kim[1, *]

[1] The University of Texas at Dallas, Richardson, Texas 75080, USA.
[2] Inha University, 100 Inha-ro, Michuhol-gu, Incheon 22212, Republic of Korea.
*Phone: +1-972-883-5712, Fax: +1- 972-883-5725, E-mail: Jiyoung.kim@utdallas.edu

Resistive memory devices, known as memristors, have been attracted the interests to be a future memory application. Among memristor devices, resistive random-access memory (ReRAM) has been widely studied with its high on/off current ratio and suitability for compute-in-memory applications. However, traditional ReRAM based on a filamentary switching mechanism suffers from reliability issues caused by the electrochemical formation of filaments. Overcoming this challenge is critical for achieving advanced memory behavior[1]. In this regard, C. A. Paz de Araujo et al. reported the universal non-polar switching behavior in carbon-doped transition metal oxide (TMO) films deposited using spin-on fabrication, in which reliable operation and immunity from forming voltage were observed[2].

In this study, we demonstrate the forming voltage-free memristive devices using hafnium oxide (HfO_x) through the conventional low-temperature atomic layer deposition (ALD) techniques. This approach offers high compatibility with 3D structures and the back-end-of-line (BEOL) process. For the ALD process, tetrakis(dimethylamino) Hf (TDMA-Hf) and carbonated hydroperoxide (H_2O_2) were utilized as the Hf and oxygen precursors, respectively. To activate the conductive carbon bond states from hydrocarbon, a rapid thermal annealing process was carried out at 450°C for 1min. By adopting the carbon composited HfO_x films, the switching and memory behaviors were observed without a high forming voltage.

It is noted that the initial reset operation of the demonstrated devices differs from the traditional ReRAM forming process in terms of the magnitude of the switching voltage and current levels. Despite the high resistance states are quite low due to the carbon composition, reliable set and reset voltages are observed at approximately ~1.6V and 0.6V, respectively, with consistent high- and low-resistance states (HRS and LRS) in cycle-to-cycle variation. In addition, the carbon-composited HfO_x devices exhibit intriguing non-polar switching behavior, allowing for programmable transition between HRS and LRS regardless the polarities of the operation voltage. This characteristic enables the devices to operate in both unipolar and bipolar behavior, making them highly compatible for future circuit applications.

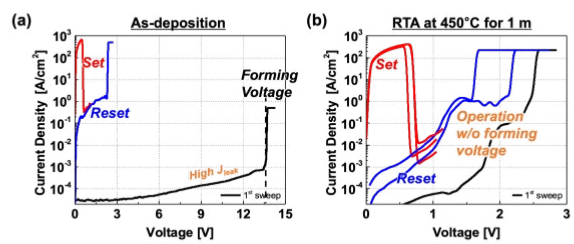

Figure 1. Current density-voltage (J-V) curves of the HfO_2 devices (a) without (b) with annealing process

ACKNOWLEDGEMENTS

This research was supported by the MOTIE (Ministry of Trade, Industry, and Energy) in Korea, under the Human Resource Development Program for Industrial Innovation (Global) (P0017303, Smart Manufacturing Global Talent Training Program) supervised by the Korea Institute for Advancement of Technology (KIAT). The authors wish to thank Dr. Greg Yeric and Dr. Saurabh Suryavanshi in Cerfe Labs for technical supports and valuable discussions.

REFERENCES

1. L. Goux et al, “Coexistence of the bipolar and unipolar resistive-switching modes in NiO cells made by thermal oxidation of Ni layers,” *Appl. Phys.*, 107, 024512, 2010
2. C. A. Paz de Araujo et al., “Universal non-polar switching in carbon-doped transition metal oxides (TMOs) and post TMOs,” *APL Mater.*, 10, 040904, 2022

Characterizing the High Temperature Mechanical Performance and Microstructure of Additively Manufactured Tantalum

Sharon Park[1], Mo-Rigen He[2], Gianna M. Valentino[3], Kevin J. Hemker[1,2]
[1]Department of Materials Science and Engineering, Johns Hopkins University, Baltimore, MD 21218
[2]Department of Mechanical Engineering, Johns Hopkins University, Baltimore, MD 21218
[3]Department of Materials Science and Engineering, University of Maryland, College Park, MD 20742

I. SUMMARY

Advances in additive manufacturing (AM) hold considerable promise in the fabrication and implementation of refractory-based components via near-net-shape processing, but manufacturing refractories with laser-based techniques is not without its challenges. Moreover, the characterization of refractory high temperature properties is rare, much less for those made via AM. Here, we investigate the structure-property relationships for laser-powder bed fusion of tantalum characterized at elevated temperatures. Process optimization studies for AM tantalum [1], conducted at the Johns Hopkins University Applied Physics Laboratory (JHU/APL), led to the determination of optimized laser parameters which were used to fabricate tensile specimens. The elevated temperature mechanical properties showed the typical body-centered cubic behavior of decreasing yield strength with increasing temperature. However, an anomalous strain hardening behavior was observed at 400°C, resulting in a ~9% increase in the tensile strength compared to ambient, while a dramatic increase in ductility was observed at 1000°C. Both unusual behaviors are highlighted in Figure 1. Detailed electron microscopy is underway to understand the non-uniform and highly anisotropic AM microstructure impact on mechanical properties. While higher temperature (>1000°C) tensile testing is the ultimate goal for refractories, oxidation remains a considerable concern. Thus, ongoing efforts are focused on testing refractories using an ultrahigh vacuum (~10^{-7} Torr) environment that is capable of tension testing at temperatures exceeding 2000°C.

II. FIGURE AND TABLE

Mechanical properties, e.g., ultimate tensile strength (UTS) and yield strength (YS) are reported in MPa, Young's modulus (E) in GPa, and elongation (EL) in % strain. These values are included in Table 1.

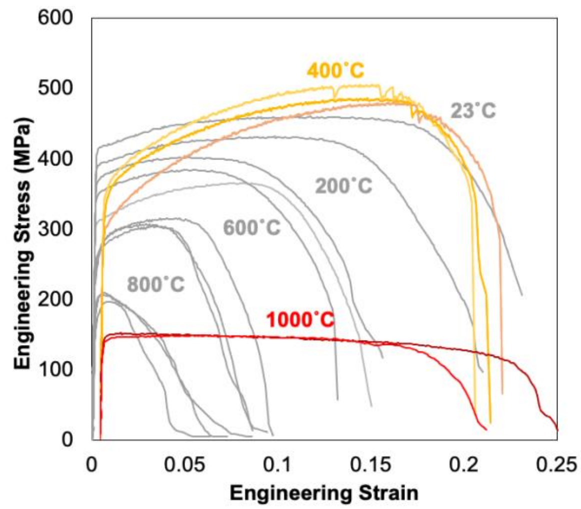

Figure 1: Stress-strain curves for AM tantalum as a function of temperature.

Table 1: Mechanical properties of AM tantalum.

T (°C)	23	200	400	600	800	1000
UTS (MPa)	445 ± 14	383 ± 14	484 ± 11	308 ± 4	204 ± 6	148 ± 3
YS (MPa)	396 ± 17	349 ± 27	331 ± 22	266 ± 3	196 ± 10	141 ± 4
E (GPa)	202 ± 5	165 ± 8	173 ± 3	147 ± 4	97 ± 9	122 ± 39
EL (%)	21 ±1.1	14 ±1.0	21 ±0.6	9 ±0.4	7 ±0.9	23 ± 0.9

ACKNOWLEDGEMENTS

This work was funded by the JHU/APL Research and Exploratory Development Department and student supported by the JHU/APL Graduate Research Fellowship.

REFERENCES

1. G.M. Valentino, et al., "Influence of laser processing parameters on the density-ductility tradeoff in additively manufactured pure tantalum," *Additive Manufacturing Letters*, Vol. 4, 100117, 2023.

Determining Printability of Soft Magnetic Alloys Via Single Track Study

Nicolas Ayers[1], **Yongho Sohn**[1]

[1] Advanced Materials Processing and Analysis Center, Department of Materials Science and Engineering, University of Central Florida, Orlando, FL, USA

Introduction

Magnetic shielding is often required for electronic components operating in a magnetic field. Magnetic shielding ability is dependent on alloy composition and shielding component geometry. The inherent capability of additive manufacturing to print complex, near net shaped components makes it an obvious choice for manufacturing shielding components. Due to limited availability and cost of magnetic shielding alloy powders, initial printability of these alloys was determined by single laser tracks on bulk material.

Experimental Method

Samples of magnetic shielding alloys were sectioned and polished using standard metallographic techniques. A list of tested alloys is presented in Table 1. Samples were then loaded into an SLM 125HL with the top surface of the sample level with the floor of the build chamber. Samples were then exposed to single laser scans. Each melt track was formed from a unique set of laser power and laser scan speed according to an orthogonal text matrix. Melt tracks were analyzed using optical microscopy and ImageJ.

Results and Discussion

Laser melt tracks were characterized by the features observed from the top view and cross-section. Typically observed features are summarized in Figure 1. For one alloy (AISI 1018) tested at constant laser power (200W), melt pool depth followed a power-law decay with increase in scan speed. Melt pool depth decreased from 725μm at 200mm/s to 54μm at 2600mm/s.

For each alloy three regimes were identified from the observed features. An excessive energy regime characterized by solidification cracks and keyhole pores. An insufficient energy regime characterized by unstable melt pools and insufficient melting. An optimal regime or printable window was identified from the sets of parameters that produced samples with stable melt pools, sufficient melting, and a lack of detrimental features.

Conclusion

The single-track study revealed a significantly wide printable window for 4140, 1018, Alloy 50, Alloy 79, and MuMetal.

Future work will be performed to; establish trends between laser power/laser scan speed and melt pool geometry, to quantify track instability using Plateau-Rayleigh analysis, and to quantify the laser-material interaction in terms of laser absorption and solidification phenomenon[1].

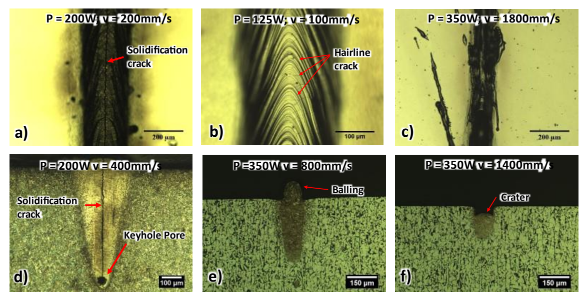

Figure 1: Typically observed detrimental features; solidification cracking (a, d), hairline cracks (b), spattering (c), balling (e), cratering (f).

Table 1: Alloys tested.

Alloy	Composition (wt. %)
1018	0.2%C-0.4%Si-0.9%Mn-Fe(Bal.)
4140	0.43%C-0.35%Si-1.0Mn-1.1Cr-0.25Mo-Fe(Bal.)
Pure Fe (Core Iron)	99.9% Pure
Alloy 79 (Supermalloy)	79%Ni-16%Fe-5%Mo
Alloy 50 (Hypernik)	50%Ni-50%Fe
MuMetal	77%Ni-14%Fe-5%Cu-4%Mo
Pure Ni	99.0% Pure

Acknowledgements

The authors would like to acknowledge the MR-PC division of Philips Healthcare, and Florida High Tech Corridor Council for their financial contributions and guidance throughout this project.

References

1. Yadroitsev, I., et al. "Single track formation in selective laser melting of metal powders." *Journal of Materials Processing Technology* 210.12 (2010): 1624-1631.

Development and evaluation of diaphragm membrane for alkaline water electrolysis

Sang Yong Nam[1,*], Kwang Seop Im[1], Seong Min Han[1]

[1] Department of Materials Engineering and Convergence Technology, Green Energy Convergence Research Institute, Gyeongsang National University Jinju, 52828, Republic of Korea

I. SUMMARY

Alkaline water electrolysis has mainly used asbestos as a diaphragm, but as the use of asbestos is harmful to the human health, it is necessary to develop a new diaphragm. This study focused on the fabrication of diaphragm membranes using $BaTiO_3$ and ZrO_2. The performance is then evaluated and the difference was compared to determine their effectiveness.

II. Experimental

2.1. Material: ZrO_2(Nanostructured & Amorphous Materials, Inc., USA), $BaTiO_3$ (SIGMA ALDRICH), PPS Felt(bowoo, South Korea), N-Methyl-2-pyrrolidone (NMP, SAMCHUN PURE CHEMICAL, 98.0%), Polysulfone (PSf, BASF, Korea)

2.1. Fabrication of diaphragm membrane

A diaphragm membrane was prepared by dissolving 18 wt% of PSf in NMP at 60°C to obtain a polymer solution. $BaTiO_3$ and ZrO_2 were added at 82 wt% and 85wt%, respectively, to prepare slurry solutions. The thickness of the PPS felt was adjusted by hot pressing under various temperature and time conditions. The slurry was then cast onto a PPS felt using the NIPS (non-solvent induced phase separation) method to produce the diaphragm membrane.

2.2. Characterization

The fabricated diaphragm membrane was evaluated for its permeability with KOH solution as well as the porosity. Subsequently, an alkaline resistance test was conducted using a 30% KOH solution. Finally, an IV test was performed to compare the cell performance of alkaline water electrolysis.

III. Results

The result showed that the diaphragm membrane with $BaTiO_3$ and PPS felt which was compressed at a temperature of 150℃ and a pressure of 5 tons had a thickness of 302.56 ㎛ and a porosity of 61.7%. It demonstrated the most outstanding performance with a current density of 0.2 A/cm^2 at a voltage of 2.72 V in the cell test.

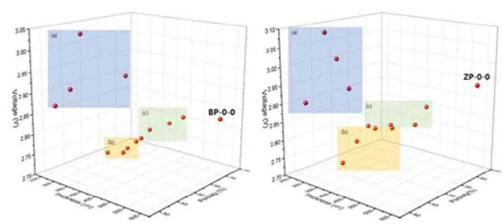

Figure 1: Voltage relation diagram according to thickness and porosity (at 2.0 current density)

ACKNOWLEDGEMENTS

This work was supported by the Technology Innovation Program Development of Membrane Electrode assembly(MEA) for 5kW Scale Waterelectrolysis devises using anion exchange membrane(AEM) for green hydrogen production, 20015599 funded By the Ministry of Trade, Industry & Energy(MOTIE, Korea) and this paper was supported by Korea Institute for Advancement of Technology(KIAT) grant funded by the Korea Government(MOTIE) (P0017310, Human Resource Development Program for Industrial Innovation(global))

REFERENCES

1. K.S. Im, T.Y. Son, H.N. Jeong, D.J. Kwon, S.Y. Nam, "A Research Trend on Diaphragm Membranes Alkaline Water Electrolysis System", *Membr. J.*, Vol. 31,No. 2, pp. 133-144, 2021

2. K.S. Im, T.Y. Son, K.Y. Kim, J. Kim, S.Y. Nam, "Research and Development Trend of Electrolyte Membrane Applicable to water Electrolysis System", *Appl. Chem. Eng.*, Vol 30, No. 4, pp. 389-398, 2019

Manufacturing of Inconel 718 with Enhanced Boron Composition via Selective Laser Melting

Jeongwoo Lee[1], Hernan Aparicio[1], Jianzhi Li[1]
[1]University of Texas Rio Grande Valley

I. INTRODUCTION

The growing interest in renewable energy led researchers to focus on solar energy harvesting. Among three types of solar energy harvesting methods (photovoltaics, solar heating & cooling, and concentrated solar power (CSP)), CSP is considered the most efficient way since it uses molten salt with a high working temperature (550 °C - 720 °C). But such a high temperature creates an extreme working condition (i.e., daily heating and cooling) that applies a cyclic thermal load on the solar absorber tube containing the molten salt. Moreover, molten salt becomes highly corrosive at high temperatures which reduces the lifespan of the containing material. Therefore, there is a high demand for functional materials for solar absorber tubes in the CSP system.

Inconel 718 is a suitable material for solar absorber tube applications because of its high working temperature (500 °C) and high corrosion resistance. Also, Inconel 718, which is a high-nickel alloy, exhibits lower thermal cycle fatigue compared to austenitic stainless steel. However, Inconel 718 has a low absorptivity of ~50% which is far less than the optimal absorptivity of a solar absorber tube, 90 %.

In this study, Inconel 718 was enhanced with boron (B) which exhibits a high absorptance in the visible and near-infrared spectrum. However, boron composition in Inconel 718 should be carefully controlled since a high boron composition (60 ppm – 110 ppm) was reported to create severe thermal cracks and lowers low-cycle fatigue (LCF) lifetime. The maximum limit of boron composition in commercial Inconel 718 is 60 ppm. By utilizing an additive manufacturing technique, selective laser melting (SLM), the boron composition of Inconel 718 was enhanced to 110 ppm, and its mechanical and microstructural properties were analyzed.

II. RESULTS AND DISCUSSIONS

In addition to the target composition (B: 110 ppm), an extreme composition (B: 10,000 ppm) was designed as a comparison. The SLM-printed samples with different boron compositions are shown in Figure 1 (a). The SLM-printed Inconel 718 sample with a high boron composition (B: 110 ppm) was deposited without visual cracks on the outer wall. On the other hand, a severe crack was observed from the SLM-printed Inconel 718 sample with an extremely high boron composition (B: 10,000 ppm). It should be noted that the SLM technique successfully manufactured Inconel 718 with a high boron composition while such a high boron composition was impossible for conventional manufacturing techniques (e.g., vacuum induction melting, vacuum arc remelting). The SEM image (Figure 1 (b)) showed that layers were deposited without defects (i.e., cracks and pores). The microhardness of the SLM-printed Inconel 718 with elevated boron composition was 325.3 HV which is comparable to other SLM-printed pure Inconel 718 samples (Figure 1 (c)).

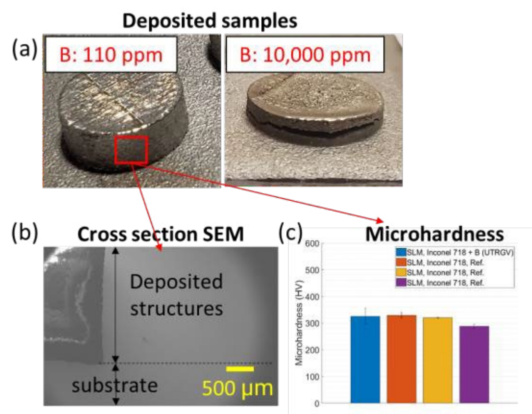

Figure 1 (a) SLM deposited samples with different boron compositions (b) cross section SEM image of B: 110 ppm sample (c) microhardness values of SLM-printed Inconel samples

III. CONCLUSION

The SLM technique successfully enhanced the boron composition of Inconel 718 to 110 ppm without microstructural defects and with acceptable mechanical properties.

ACKNOWLEDGEMENTS

This study is supported by the U.S. Department of Energy's Office of Energy Efficiency and Renewable Energy (EERE).

Evaluation of Interfacial Property and Damage Sensing of Structural Composites Using Electrical Resistance Method

Dong-Jun Kwon[1], Seong-Baek Yang[1], Sang Yong Nam[1*]
[1] Department of Materials Science and Convergence Technology, Research Institute for Green Energy Convergence Technology (RIGET), Gyeongsang National University

I. Introduction

In the composite material industries, "Smart Factory" was also focused to improve manufacturing efficiency [1]. The many publications have been research for automatic manufacturing of composite material parts using additional sensor to monitor resin impregnation in reinforcement [2]. In these monitoring methods, however, it was needed to research on self-sensing to reduce additional cost for monitoring of resin impregnation.

II. Experimental

2.1 Material: T-700 grade CF tow (Toray Inc., Japan) was used for reinforcement with different amounts of sizing agent (50C and 60E type). It was used to determine ER and CF behaviors of CF laminate in impregnation of epoxy resin with different dropping points of epoxy resin droplet. The plain weave laminate of T-700 grade CF was used as the composite reinforcement. Bisphenol-A epoxy (KFR-121, Kukdo Chem., Korea) with amine hardener (KFH-141, Kukdo Chem., Korea) was used for the matrix.

2.2 Measurement of ER of CF in micro and sub-micro scale: The ER behavior of CF was measured with different CF arrays to determine ER behavior with different dropping points of epoxy resin in more detail. Single CF was gathered into CF tow, and attached to slide glass with Scotch PP tape. To imitate the case of epoxy being spread between CF tow, the single CF and CF micro-tow, which was manufactured using three CFs, were arranged to the 1 mm of distance. In the case of epoxy being spread on the CF tow, the micro-tow was used only.

III. Results and Discussion

In figure 1, the ER of CFs shows with different arrangements of CF and initial impregnation points in micro scale. In the case of epoxy resin being impregnated between CF tow, R1, the ER decreased dynamically at initial times by decreasing the contact ER between CF surface. As the impregnation time elapsed, the ER of CFs increased gradually by the impregnation of epoxy resin into CFs. In the case of epoxy being impregnated to the center on tow, R3, however, the ER of CF tow, R3, increased gradually as the epoxy was impregnated into CF tow. It could be predicted that the contact areas among CFs were detached by epoxy impregnation, and the whole ER of CF tow increased by increasing the contact ER.

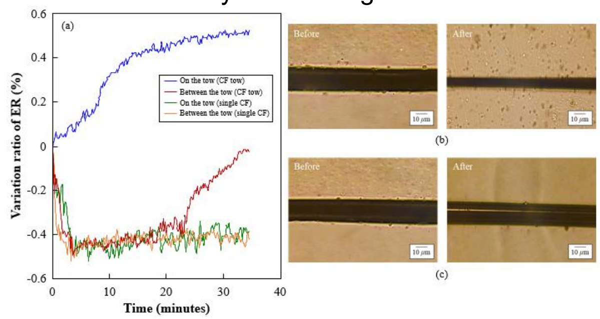

Fig. 1. Interface ER of CFs with different interface between CFs

4. Conclusions

In this paper, the resin flow of CFRP was tried to observe using ER behavior and visualize using ER mapping. To determine effect of the CF array on ER behavior, the ER of CFs were measured, and the CF array was observed with different initial impregnation points of epoxy resin on micro and sub-micro scale. Based on this data, the ER behavior of CF laminate could be determined as the epoxy resin was impregnated in the VARTM process with different vacuum conditions. By using this research, we are praying this research can be contributed to automatize CFRP manufacturing using VARTM process.

ACKNOWLEDGEMENTS

This research was supported by the Korea Institute for Advancement of Technology (KIAT) grant funded by the Korea Government (MOTIE) (P0017310, Human Resource Development Program for Industrial Innovation (global)).

REFERENCES

1. J Zhang et al, "Topology optimization of CFRP hierarchical pyramidal structures fabricated by additive manufacturing," Compos B Eng 224, pp. 109241, 2021.

Fabrication and Electrical Properties of Organic Ferroelectric Gate Transistors

Shihyun Ahn[1], Min Gee Kim[1], Byung Eun Park[1]
[1]University of Seoul

SUMMARY
In this research, organic ferroelectric gate transistor using paper was investigated. Although solution-process was chosen for fabrication, the paper substrate was not affected by solution. Compared to the transistor on rigid substrate, there was not much difference in electrical characteristics.

Keywords: Paper transistor, memory, ferroelectric

I. INTRODUCTION
For flexible and wearable devices, organic materials are now widely investigated. Among the flexible substrate, paper has many advantages including printability, recyclability disposability and eco-friend properties [1-3].
In this research, we fabricated ferroelectric gate insulator using P(VDF-TrFE) gate insulator.

II. EXPERIMENTAL PROCEDURE
Paper with thickness of 0.2 mm was prepared. At the same time, SiO_2/Si substrates were also prepared. Al was deposited by thermal evaporation on both substrates. P(VDF-TrFE) dissolved in methyl ethyl ketone (MEK) of 4 wt% was spin-coated. Then, annealing process was carried out at 140^{o}C for 1 h. On the P(VDF-TrFE) layers, P3HT channel layer was formed by spin-coating method. After second annealing at 120^{o}C for 1 h, Au S/D electrodes were evaporated.

III.RESULTS AND DISCUSSION
Input characteristics of the transistors on paper and rigid substrates were shown in Fig. 1. P-type characteristics of P3HT channel layer is shown. V_G was applied from 20 V to – 20 V. On both substrates, there was not much difference. The obtained memory window was around 16 V on both substrates. Although the on-current is slightly higher in case of the transistors on rigid substrates, on/off ratio was almost same in both cases. It means that paper is able to be used as a substrate of transistors, even with solution-process.

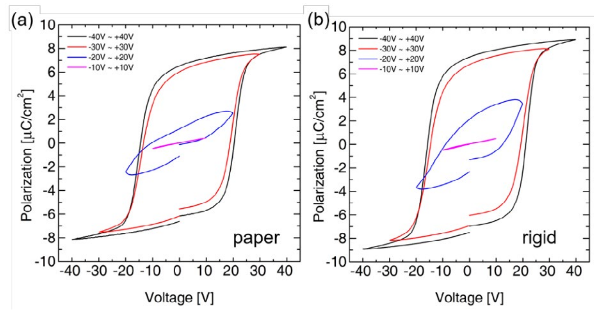

Figure 1: Input characteristics of the transistors on rigid and paper substrates.

ACKNOWLEDGEMENTS

REFERENCES
[1] S. J. Kim, and J. S. Lee, Nano Lett. 10, 2884 (2010).
[2] S. Chung, S. O. Kim, S> K. Kwon, C. Lee, and Y. Hong, IEEE Electr. Dev. Lett. 32, 1134 (2011).
[3] K. Fukuda, Y. Takeda, M. Mizukami, D. Kumaki, and S. Tokito, Sci. Rep. 4, 3947 (2014).

Electrochemical Removal of Nitrate for Ammonia Synthesis and Water Purification

Jeonghoon Lim[1,2], Bryan D. McCloskey[1], Seung Woo Lee[2], Marta C. Hatzell[2]
[1]Lawrence Berkeley National Laboratory, Berkeley, CA 94720, USA
[2]George W.Woodruff School of Mechanical Engineering, Georgia Institute of Technology, Atlanta Ga 30332

I. OVERVIEW & MOTIVATION

Understanding the complexities of nitrogen cycle is critical because when the cycle is not in balance, excess reduced and oxidized nitrogen compounds could result in harmful impacts to life. Electrocatalytic conversion of waste nitrate (NO_3^-) to benign dinitrogen (N_2) and ammonia (NH_3) fuel is an appealing strategy that may easily integrate with renewable energy. The process does not require chemical addition and thus requires operating costs lower than thermal routes. Nearly all nitrogen-based fertilizers rely on ammonia as a feedstock, and thus the demand for this chemical is heavily dependent on the global population and food demand. Over the next three decades, the global population will continue to dictate the market size and value for ammonia, which consequently will have a significant impact on our energy infrastructure.

II. RESEARCH APPROACH

A. Material Synthesis

1. Diverse Pd shape-controlled nanoparticles
2. Controlled Cu surface coverage on Pd nanocubes
3. Atomically ordered structures between Cu and Pd

B. Catalyst Characterization

1. Morphology and element mapping for Pd structure and Cu atoms existence by HRTEM/EDS.
2. Atomic and electronic structure changes in long-term repeated tests by XANES/XAFS.

3. Electrochemical tests and electrolysis for investigating kinetics and ammonia production yields by quantification methods such as colorimetric methods with UV-Vis.

III. RESULTS & DISCUSSION

We successfully synthesized single crystalline facets of Pd and Pd(111) facets could improve the kinetics of the nitrate reactants and Pd(100) facets could enhance the nitrite reduction that lead to a high ammonia yield rate for Pd cuboctahedron. We also introduced Cu secondary atoms onto Pd nanocubes and atomically rearranged structures between Pd and Cu. Both PdCu electrocatalysts exhibited excellent nitrate removal efficiency and nitrogen selectivity with outstanding stability. This work may lead to the paradigm shift in the design of nitrate removal catalysts and could be the candidates for long-term real-life applications.

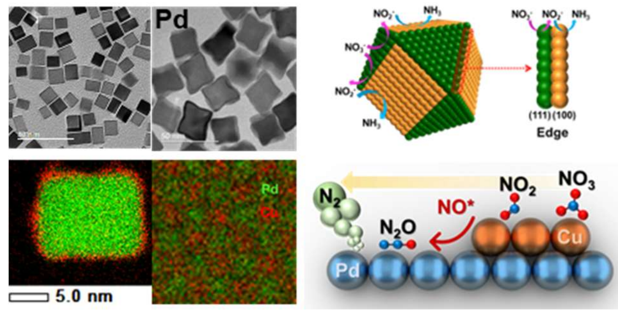

Figure 1: Pd cuboctahedron NPs, Cu deposited on Pd nanocubes, Pd-Cu intermetallic structures

ACKNOWLEDGEMENTS

This material is based upon work supported by the National Science Foundation under Grant No. 1846611 and 1933646. M.C.H. and J.L. were supported by the National Science Foundation through the Center for Advancing Sustainable and Distributed Fertilizer Production (CASFER) under Grant No.EEC-2133576.

REFERENCES

1. **J. Lim**, C. Yu, D. A. Cullen, S. W. Lee*, T. P. Senftle*, and M. C. Hatzell*, PdCu Electrocatalysts for Selective Nitrate and Nitrite Reduction to Nitrogen. ***ACS Catal.*** **2023**, *13*, 87–98.
2. **J. Lim**, C. A. Fernandez, S. W. Lee*, and M. C. Hatzell*, Ammonia and Nitric Acid Demands for Fertilizer Use in 2050. ***ACS Energy Lett.*** **2021**, *6*, 3676-3685.
3. **J. Lim**, C. Y. Liu, J. Park, Y. H. Liu, T. P. Senftle*, S. W. Lee*, and M. C. Hatzell*, Structure Sensitivity of Pd Facets for Enhanced Electrochemical Nitrate Reduction to Ammonia. ***ACS Catal.*** **2021**, *11*, 7568-7577.

The Effect of H-bonding Strength on the Water-responsiveness of *Bacillus subtilis* Cell Walls using Hofmeister Salts

Seungri Kim[1,2], Xi Chen[1,2]
[1]Department of Chemical Engineering, The City College of New York, CUNY,
[2]Nanoscience Initiative, Advanced Science Research Center, CUNY

I. SUMMARY

Water responsive (WR) materials provide opportunities to propel the development of technologies, including soft robotics and green energy harvesting.[1] The cell wall of *Bacillus* (*B.*) *subtills* is a promising WR material that displays a record-high energy density (~72.6 MJ m-3), surpassing conventional actuator materials and all known muscles.[2] Elucidating the fundamentals of WR performance of *B. subtilis* cell walls can suggest design criteria for robust WR actuator materials for energy harvesting. The effects of hydrogen bonding on WR performance were investigated using Hofmeister salts to understand the WR mechanisms and to enhance the WR performance.[3]

II. Investigating the role of H-bonding using Hofmeister salts.

A. Role of H-bonding of nanoconfined liquid in WR

Our previous work highlighted the importance of high-viscous nanoconfined water in determining materials' water-responsiveness, in particular for *B. subtilis* cell walls[3] and high-performing peptide crystals. We set out to investigate the effects of the H-bonding network of nanoconfined liquids on materials' remarkable water-responsiveness, and we also introduce a new, simpler way to tune and improve WR actuation pressure and energy density. In this work, we showed that *B. subtilis* cell walls' WR energy density can be dramatically increased to 101.8 MJ m-3, which is about 4 orders of magnitude greater than that of human muscles and surpasses those of all conventional actuator materials. We conclude that the strength of the H-bonding network dictates WR performance: the H-bonding network of KI-treated cell walls is too weak; cell walls treated by high concentration K_2SO_4 solutions (> 10 mM) give rise to the H-bonding network that is too strong, while slightly enhanced H-bonding network by low concentration K_2SO_4 solutions is favorable for WR actuation. Our findings advance the contemporary understanding of the role of nanoconfined liquids played in materials' WR behavior, and they also provide insight into general mechanisms of high-performance WR actuation.

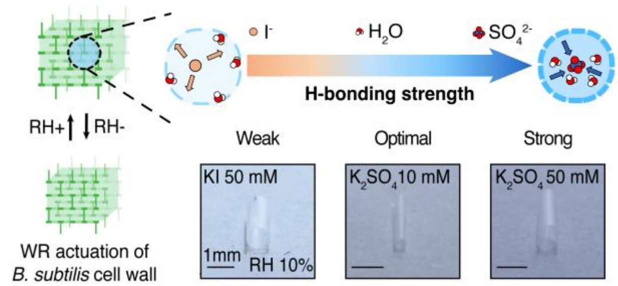

Figure 1: A certain range of H-bonding strength of nanoconfined liquids leads to high-energy water-responsive actuation of *B. subtilis* cell walls.

ACKNOWLEDGEMENTS

This work was supported in part by the Office of Naval Research (ONR) (N47284-00 01) and the Air Force Office of Scientific Research (AFOSR) (FA9550-21-1-0144).

REFERENCES

1. Xi Chen, Davis Goodnight, Zhenghan Gao, Ahmet-Hamdi Cavusoglu, Nina Sabharwal, Michael Delay, Adam Driks, and Ozgur Sahin, "Scaling up nanoscale water-driven energy conversion into evaporation-driven engines and generators.", *Nat. Commun.* **6**, 7346, 2015.
2. Haozhen Wang*, Zhi-Lun Liu*, Jianpei Lao, Sheng Zhang, Rinat Abzalimov, Tong Wang, and Xi Chen. "High energy and power density peptidoglycan muscles through super-viscous nanoconfined water.", *Adv. Sci.* **9,** pp. 2104697, 2022.
3. Roxana Piotrowska, Travis Hesketh, Haozhen Wang, Alan R. G. Martin, Deborah Bowering, Chunqiu Zhang, Chunhua T. Hu, Scott A. McPhee, Tong Wang, Yaewon Park, Pulkit Singla, Thomas McGlone, Alastair Florence, Tell Tuttle, Rein V. Ulijn, and Xi Chen. "Mechanistic insights of evaporation-induced actuation in supramolecular crystals.", *Nat. Mater.* **20,** pp 403-409, 2021

[SEED2023]
Solvent-Free Synthesis and Modification of Membranes for Industrially Relevant Gas Separations

Dennis T. Lee[1], D. Howard Fairbrother[2], J. Anibal Boscoboinik[3], Michael Tsapatsis[1]
[1]Department of Chemical and Biomolecular Engineering & Institute for NanoBioTechnology, Johns Hopkins University, [2]Department of Chemistry, Johns Hopkins University, [3]Center for Functional Nanomaterials, Brookhaven National Laboratory

I. SUMMARY

Metal-organic frameworks (MOFs), comprising over several thousand distinct structures, have garnered significant attention as the rapidly expanding category of porous materials. MOFs generally possess remarkable attributes, including extensive porosity, substantial internal surface area, modular structural characteristics, and facile functionalization.[1]

This poster presentation will focus on various solvent-less approaches developed and demonstrated during my four-year postdoctoral work.[2–4] Such synthetic strategies are particularly fascinating for thin film processing since they can be integrated with solvent-free MOF deposition methods.

As a start, I will introduce a reliable all-vapor-phase processing method to fabricate membrane materials composed of zeolitic imidazolate frameworks (ZIFs), a subclass of MOFs, exhibiting a stable and higher performance in the separation of propylene over propane.

Next, diverse post-synthetic modification (PSM) approaches, which can fine-tune and improve membrane performance in industrially relevant gas separation processes, including propylene/propane separation, purification of hydrogen, and separation of CO_2, will be covered.

Vapor-phase and irradiation-based metal-organic treatment, employed in this work, are facile and practical approaches to tuning the gas separation properties of as-prepared membranes. Moreover, such methods have the potential to be readily applicable to other porous membranes, enabling them to exhibit modified membrane performance for gas pair separations that are crucial but were not achieved using conventional materials modification strategies.

REFERENCES

[1] D. T. Lee, P. Corkery, S. Park, H.-K. Jeong, M. Tsapatsis, *Annu. Rev. Chem. Biomol. Eng.* **2022**, *13*, 529–555.

[2] M. Dorneles de Mello, M. Ahmad, D. T. Lee, P. Dimitrakellis, Y. Miao, W. Zheng, D. Nykypanchuk, D. G. Vlachos, M. Tsapatsis, J. A. Boscoboinik, *ACS Appl. Mater. Interfaces* **2022**, *14*, 19023–19030.

[3] Y. Miao, D. T. Lee, M. Dorneles de Mello, M. K. Abdel-Rahman, P. Corkery, J. A. Boscoboinik, D. H. Fairbrother, M. Tsapatsis, *Chem. Commun.* **2021**, *57*, 5250–5253.

[4] M. Hayashi, D. T. Lee, M. D. de Mello, J. A. Boscoboinik, M. Tsapatsis, *Angew. Chemie Int. Ed.* **2021**, *60*, 9316–9320.

Compositional Redistribution, Phase Transformation, Microstructural Development in SS316L/IN625 Bimetallic Structure Fabricated by Laser Powder Bed Fusion

Asif Mahmud[1], Yongho Sohn[1]
[1]Department of Materials Science and Engineering
University of Central Florida, Orlando, FL, USA

I. SUMMARY
This work reports on the phase constituents, microstructure, nanoscale hardness variation and elemental intermixing in SS316L/IN625 bimetallic structure fabricated by laser powder bed fusion (LPBF). Fully dense and crack free SS316L/IN625 bimetallic structures (cylinders with a diameter of 10 mm, height of 12 mm and support structure 4 mm) were produced using a laser power of 200 W, laser scan speed of 800 mm/s, hatch spacing of 0.12 mm and slice thickness of 0.03 mm. The XRD pattern revealed the dominant presence of austenitic (FCC) ϒ phase. Cross-sectional microstructure near the interface of the SS316L/IN625 bimetallic structure consisted of typical cellular/columnar structure. Intermixing of primary solvents, Ni and Fe was observed for a distance of approximately 200 μm, and their intermixing rate was estimated to be in the order of 10^{-5} m^2/s.

II. LPBF of SS316L/IN625 Bimetallic Structures
Figure 1 presents the macro photographs of SS316L/IN625 bimetallic structures fabricated using in-house SLM 125^{HL} (SLM Solutions Group AG, Lubeck, Germany) system. The SLM 125^{HL} is equipped with a continuous-wave (1070 nm wavelength) 400-W Ytterbium IPG fiber laser with a Gaussian spot size of ~ 70 μm and a maximum build rate of 25 cm^3/h [1]. 15 Cylinders were manufactured on top of an SS316L build plate. Preheating of the build plate was set at 100 °C. The build was performed in an inert Ar atmosphere (ultra-high purity Ar) with an O_2 content lower than 0.15 %.

III. Experimental
X-ray diffraction (XRD) was carried out for phase identification and preferred crystallographic orientation analysis using a PANalytical Empyrean™ diffractometer with Cu target Kα radiation operating at 45 kV and 40 mA. A step size of 0.03° and a counting duration of 90 seconds were employed for a good resolution and statistical significance.

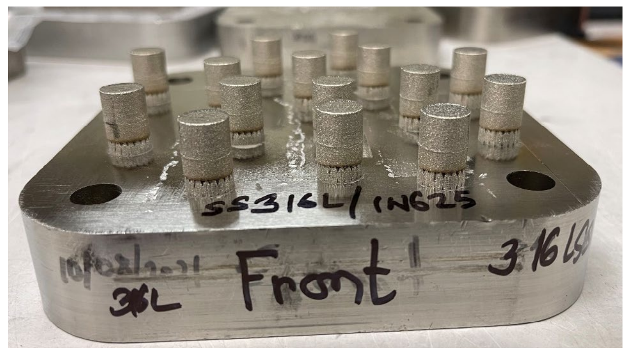

Figure 1: Macrophotograph of the fabricated SS316L/IN625 bimetallic structures. The height and diameter of the cylinders are 12 mm and 10 mm, respectively.

Field emission scanning electron microscope (FE-SEM, Zeiss Ultra-55™) equipped with X-ray energy dispersive spectroscopy (XEDS) was used to examine the surface morphology, cross-sectional phase constituents and microstructure of the interface cross section. A minimum of three concentration profiles, across the interface of SS316L/IN625 were obtained by point-to-point acquisition to study the diffusion profile of the materials and estimate the uncertainties in the intermixing rate. XEDS data were converted to the concentration of various constituent elements in atom percent via standardless analysis.

REFERENCES
1. H. Hyer et al., "Understanding the Laser Powder Bed Fusion of AlSi10Mg Alloy," Metallography, Microstructure, and Analysis, vol. 9, no. 4, pp. 484-502, 2020, Doi: 10.1007/s13632-020-00659-w

Enhancing the performance of tungsten-based alloys through additive manufacturing

Hyeji Im, Wafa Houhamdi, Samuel Price, Ian McCue
Northwestern University, 2220 Campus Drive, Evanston, IL 60208, USA

I. SUMMARY

Additively manufactured W experiences large thermal strain during cooling and passing through its ductile-to-brittle transition. This leads to high number of cracks of additively manufactured W.

We report on fully dense W-based alloys fabricated by laser-powder bed fusion by alloying Ti and Fe. We compared density, microstructure, and mechanical properties of additively manufactured pure W and W-based alloys. The addition of Ti and Fe increased density and reduced formation of pore and crack during additive manufacturing.

II. EXPERIMENTAL

A. L-PBF

Pure W, W-Ti, and W-Ti-Fe were printed and investigated this work. Spherical tungsten powder (Global Tungsten Powders Corp) with the average particle size of 30 um are shown in Fig. 1. W powder was ball-milled for 4 h with Ti powder (-325 mesh, Thermo Fisher Scientific) or Fe powder (-325 mesh, Thermo Fisher Scientific) for fabrication of W-Ti and W-Ti-Fe alloys. Ball-milled powder was printed with Sisma Mysint 100 (Trumpf). It is equipped with a fiber laser of 200W at a wavelength of 1070 nm with a spot diameter of 55 um. Argon was used as an inert gas during the printing process with an oxygen level of 100 ppm. A medium carbon steel (C45) substrate of a 34.5 mm diameter was used.

B. Density measurement

Mass density was density measured using the Archimedes principle.

III. RESULTS

A. Density

A relative density of pure W higher than 92%. The two highest volumetric energy densities (1667 J/mm^3 and 1905 J/mm^3) produced samples with high relative densities. An increase of energy density to 1667 J/mm^3 then to 1905 J/mm^3 leads to lowering the relative density of the printed samples, from 90% to 85% indicating that a higher quality of printed samples can be achieved through a process optimization. On the other hand, the W-Ti-Fe reached relative densities higher than 98%. Pores are still observed after alloying but their density significantly decreased compared to pure W.

B. Microstructure

All pure W and W-based alloy samples have un-melted W powders in microstructure because of high melting point of W. More ductile and less crack occurrence with alloying Ti and Fe to W presents promising features to print more complex parts of plasma fusing materials.

Judging from energy dispersive spectroscopy (EDS) mapping results, Ti and Fe might be melted during printed and fill up gaps between un-melted W powders, improving the relative density of the W-Ti-Fe alloys.

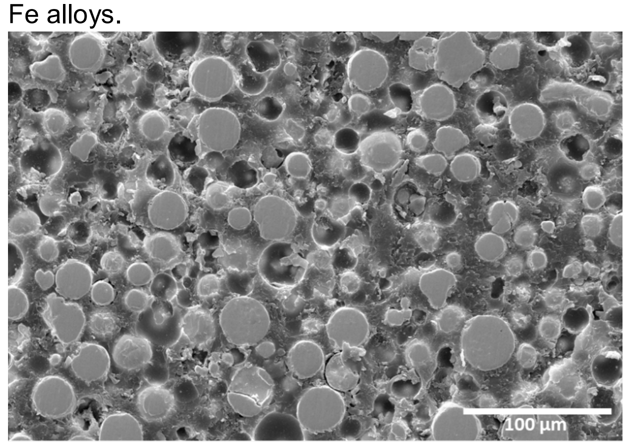

Figure 1: SEM images of W powder (mounted in epoxy).

ACKNOWLEDGEMENTS

This study was supported by the U.S. Department via award DE-SC0017899.

Cross-Point Array of Metal-Ferroelectric-Metal $HfZrO_2$ Capacitors for Compute-in-Memory Applications

Minjong Lee[1,2], **Heber Hernandez-Arriaga**[1], **Jin-Hyun Kim**[1], **Rino Choi**[2], **and Jiyoung Kim**[1,*]
[1]The University of Texas at Dallas, Richardson, TX, USA; [2]Inha University, Incheon, South Korea

Significant progress in electronic technology has leaded the development of high-density and low-power applications, from traditional von-Neumann computing architectures to intriguing compute-in-memory (CIM) configurations. As the use of ferroelectric (FE) materials for CIM application, most research has focused on using FE field-effect-transistor structure to achieve vector-matrix multiplication (VMM) [1], whereas the metal-FE-metal (MFM) structures is rarely studied. In this study, we experimentally demonstrate 2×2 pattern recognition system using a 4×2 cross-point array configuration of $HfZrO_2$ (HZO) MFM capacitors. For the sample preparation, TiN/HZO/TiN stacked MFM capacitors were fabricated by following our previous work.[2] However, the finger shaped TiN top and bottom electrodes (TEs and BEs) were fabricated by the photolithography and Cl-based ICP metal etching, and the 180 nm-thick TiN TEs were deposited to reduce the parasitic resistance along the TE lines.

Because of the polarization-change between up and down states (P_{up} and P_{down}), the HZO MFM capacitors drive the binarized current readout mechanism resulting from two types of charge accumulation whether polarization is changed. To read these accumulated charges, we employed the series connection of low shunt resistor (R_{shunt}) to the devices to measure electrical current signal. This interesting binary memory behavior is also investigated with the device-to-device variation. In the 50×50 μm^2 sized HZO MFM capacitors, the devices exhibit the excellent reproducibility within the obvious separate states. It is worth that HZO MFM capacitors can be regarded as polarization-induced synaptic behavior, which is distinguishable with conventional resistance or capacitance devices. These binarized memory in HZO MFM capacitors is extended from single-device operation to 4×2 cross-point array configuration. Figure 1 shows the schematic and optical microscope image of 4×2 cross-point array of HZO MFM capacitors. For the VMM operation, the number of P_{down} states were initially updated upon one to four devices for write scheme. As a result, the devices enable excellent VMM operations, eligible for CIM applications with binary weights. Based on these characteristics, we assessed a computation capability by experimental demonstration of 2×2 pattern recognition method, following the previous report.[3] Each cell of 2×2 pattern was assigned to TiN TE1–4, in which the white (black) pattern is regarded as P_{down} (P_{up}). The tested patterns are all occurrences in 2×2 patterns (total 16 patterns). As the pattern recognition results, the current readout has the recognition accuracy of 81.3%, which is comparable results with the previous report, thus highlighting the promise of the simple MFM capacitors towards the neuromorphic computing applications.

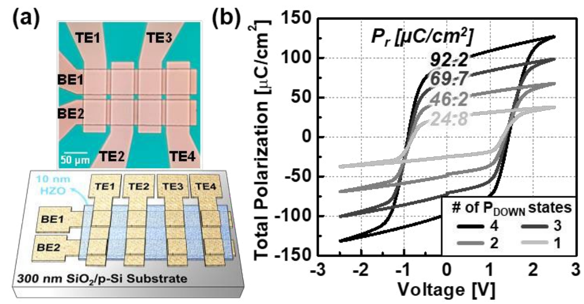

Figure 1: (a) Schematic and optical microscope image of 4×2 cross-point array of HZO capacitors. (b) VMM operation of P–V characteristics in the HZO capacitors with respect to the number of P_{down} states.

ACKNOWLEDGEMENTS

This work is supported by GRC-NMP program (#3001.001) of SRC UT Dallas' Texas Analog Center of Excellence (TxACE). This research is also supported by the MOTIE in Korea, under the Human Resource Development Program for Industrial Innovation (Global) (P0017303, Smart Manufacturing Global Talent Training Program) supervised by KIAT. The ozone generator used in this work was provided by TMEIC.

REFERENCES

[1] K. A. Aabrar et al., IEDM, 442-445 (2021).
[2] S. Kim et al., Appl. Phys. Lett., 115, 182901 (2019).
[3] P. Zhou et al., arXiv:2112.04749v1, Dec. 9th (2021).

High endurance of back-end-of-line compatible ferroelectric $Hf_{0.5}Zr_{0.5}O_2$ thin films through low temperature annealing

Jongmug Kang[1], Seongbin Park[1], Hye Ryeon Park[1], Seojun Lee[2], Jin-Hyun Kim[2], Jiyoung Kim[2,*], and Si Joon Kim[1,*]
[1] Kangwon National University, Chuncheon, Gangwon-do 24341, Republic of Korea
[2] The University of Texas at Dallas, Richardson, Texas 75080, USA
E-mail: jiyoung.kim@utdallas.edu and sijoon.kim@kangwon.ac.kr

SUMMARY

In this study, we investigated the endurance properties of atomic layer deposited $Hf_{0.5}Zr_{0.5}O_2$ (HZO) thin films according to the annealing temperatures. The annealing process of the HZO thin film was performed at various temperatures (300°C, 325°C, 350°C, and 400°C) in nitrogen ambient using a furnace. As a result, the endurance level was improved over 10^9 cycles as the annealing temperature was lowered to 300°C.

Keywords: Ferroelectric film, $Hf_{0.5}Zr_{0.5}O_2$, atomic layer deposition, endurance, low temperature

I. INTRODUCTION

The ferroelectric properties of $Hf_{0.5}Zr_{0.5}O_2$ (HZO) are emerging as a promising material for the development of next-generation non-volatile memory (e.g., ferroelectric random access memory (FRAM)). FRAM has several advantages, such as low-voltage operation, fast switching speed, and CMOS integration [1]. However, in previous reports, the endurance level of HZO thin films was still limited to 10^7~10^8 cycles, making commercialization difficult [2]. It has been reported that internal defects in HZO thin films, such as oxygen vacancies generated during ALD deposition and/or annealing processes, affect endurance properties [3]. From this point of view, this study aimed to improve endurance properties by reducing internal defects by lowering the crystallization temperature of HZO thin films to 300°C.

II. RESULTS AND DISCSUSSION

All HZO thin film-based capacitor devices annealed at various temperatures were measured for endurance properties by applying a switching voltage of 2.5 V. As a result, it was confirmed that the endurance level improved as the annealing temperature decreased (see Fig. 1). Especially, the HZO thin film annealed at 300°C achieved high endurance properties over 10^9 cycles without fatigue. This is associated with the formation of less oxygen vacancies in the HZO thin film and/or the interface between the HZO and TiN electrodes as the annealing temperature decreases.

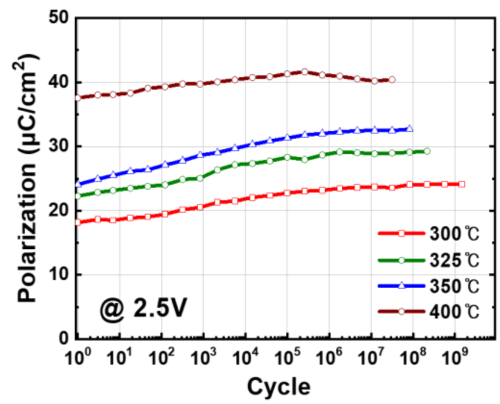

Figure 1: Endurance results of HZO-based capacitors annealed at various temperatures.

ACKNOWLEDGEMENTS

This work was supported by Korea Institute for Advancement of Technology (KIAT) grant funded by the Korea government (MOTIE) (P0017011 and P0020966, HRD Program for Industrial Innovation).

REFERENCES

1. S. J. Kim, J. Mohan, S. R. Summerfelt, and J. Kim, “Ferroelectric $Hf_{0.5}Zr_{0.5}O_2$ thin films: a review of recent advances,” *JOM*, Vol. 71, No. 1, pp. 246-255, 2019.
2. H. J. Kim, Y. An, Y. C. Jung, J. Mohan, J. G. Yoo, Y. I. Kim, H. Hernandez-Arriaga, H. S. Kim, J. Kim, and S. J. Kim, “Low-thermal-budget fluorite-structure ferroelectrics for future electronic device applications,” *Phys. Status Solidi RRL*, Vol. 15, No. 5, p. 2100028, 2021.
3. S. J. Kim, Y. C. Jung, J. Mohan, H. J. Kim, S. M. Rho, M. S. Kim, J. G. Yoo, H. R. Park, H. Hernandez-Arriaga, J. -H. Kim, H. T. Kim, D. H. Choi, J. Jung, S. M. Hwang, H. S. Kim, H. J. Kim, and J. Kim , “Low-thermal-budget (300 °C) ferroelectric TiN/$Hf_{0.5}Zr_{0.5}O_2$/TiN capacitors realized using high-pressure annealing,” *Appl. Phys. Lett.*, Vol. 119, No. 24, p. 242901, 2021.

Computational Design and Analysis of Metal Halide Perovskites: Toward Eco-friendly and Highly Stable Solar Cells

Sang Woo Park, **Ki-Ha Hong**
Department of Materials Science and Engineering, Hanbat National University

I. SUMMARY

Metal Halide Perovskites (MHPs) have garnered significant attention due to their distinctive material properties and remarkable achievements in photovoltaic performance. We have devised theoretical and computational approaches to investigate the fundamental characteristics of MHPs and develop novel materials with reduced toxicity and enhanced stability. This talk highlights the exceptional attributes of MHPs uncovered through our theoretical investigations and elucidates our numerical design methodology, which combines ab initio thermodynamics and machine learning techniques to identify promising lead-free alternatives.

II. INTRODUCTION

Toxicity and instability pose significant challenges to the commercialization of Metal Halide Perovskites (MHPs). To overcome these hurdles and develop environmentally friendly and stable solar cell materials, the exploration of new compounds and compositional engineering strategies is imperative. Among lead-free perovskite alternatives, tin-based halide perovskites have exhibited the most promising behaviors. However, despite this potential, the power conversion efficiency (PCE) of Sn-based solar cells still lags behind, with the best performance remaining below 15%, whereas Pb-based analogs have already achieved efficiencies of 26%. The thermodynamic and chemical stability of Sn perovskites present bottlenecks to further advancements in efficiency. In this study, we have employed computational methods to investigate engineering techniques aimed at addressing the drawbacks of Sn perovskites. In addition to lead and tin, we have explored various metal cations as potential alternatives. To efficiently search for new candidates, we have devised a high-throughput computation and machine learning scheme capable of exploring a vast number of artificial compounds.

III. RESUTS and DISCUSSION

Controlling polymorphism is crucial for achieving stability and efficiency in Sn-perovskite solar cells. In our research, we have conducted investigations into the impact of A- and X-site compositions, as well as additives, on the phase transformation between the black (γ) and yellow (δ) phases of $CsSnI_3$. Through our theoretical methods, we have established a compositional engineering window that effectively prevents the undesired phase transformation from the photoactive black phase to the photoinactive yellow phase, while still maintaining a bandgap below 1.5 eV.

Both tin and lead perovskites suffer from stability issues, as they are prone to decomposition when exposed to humidity and light irradiation. Tri-valent metal halides exhibit improved stability, but their efficiency remains negligible. To overcome these limitations, we have employed high-throughput screening and convolutional neural network schemes to explore an extensive dataset of metal halides and artificial compounds. Our comprehensive analysis of this vast database has revealed that vacancy-ordered tri-valent metal cation halides exhibit the most promising behaviors, providing new avenues for enhanced stability and performance in perovskite solar cells.

III. ILLUSTRATIONS

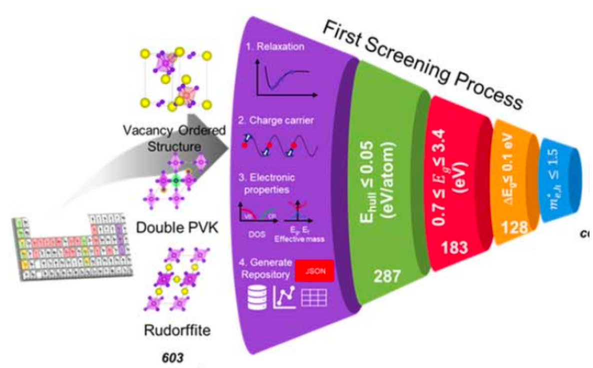

Figure 1. High throughput screening procedure

Effect of Carbon on The Microstructure and Mechanical Properties of Carbon-bearing Steels in Laser Powder Bed Fusion

Thinh Huynh, Yongho Sohn

University of Central Florida

SUMMARY

Novel carbon-bearing steels were successfully gas atomized and used as powder feedstock to explore the feasibility of additively manufactured carbon-bearing steels by LPBF. The effect of carbon on the printability, microstructure, and mechanical properties were examined in the as-printed condition and findings are summarized as follows:

The as-printed low carbon-bearing alloy did not exhibit cracking at any investigated LPBF parameters and density as high as 99.9% was achieved. The as-printed microstructure exhibited some cellular dendrites with 97% martensite and 3% austenite. The lack of cracks and higher fractions of martensite found in the as-printed condition resulted in higher tensile properties compared to the high carbon-bearing alloy.

The high carbon-bearing alloy exhibited cracking at all LPBF parameters and densities higher than 99% were achieved using 200 W and 800 mm/s or 350 W and 1400 mm/s. High cooling rates resulted in an interconnected network of cellular dendrites spanning across an austenitic dominated matrix. The main alloying elements such as Cr, Mo, V, and C were segregated along the cellular boundaries potentially forming nano-scale carbides. At low and moderate energy densities, few lath martensites were found within the prior austenite grains. High energy densities specimens exhibited packets of martensite laths, which correlated to a higher hardness. Furthermore, the repeated heating cycles from the layer-by-layer process produced varying amounts of martensite across the sample height when excessive energy density was used.

The present investigation demonstrated that high carbon-bearing alloys can be sensitive to the volumetric energy density and the extent of in-situ solid-state phase transformation can occur at sufficiently high volumetric energy density. A high carbon concentration can result in an austenitic microstructure and a low carbon concentration can result in a martensitic dominated microstructure under rapid solidification. Grain size refinement through the martensitic transformation may mitigate cracking. By tailoring the carbon concentration, the resulting as-printed microstructure can be fully dense and crack free while offering flexibility in secondary hardening appropriate for the desired application.

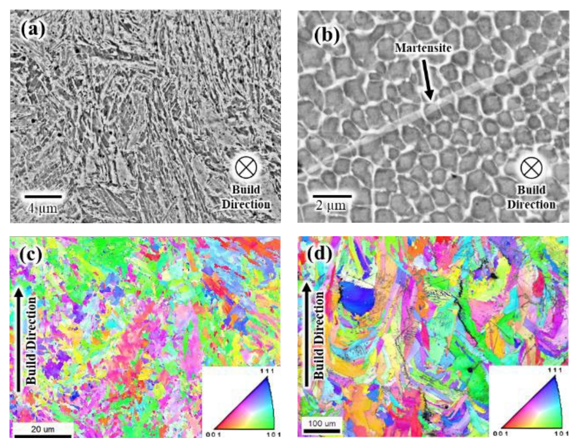

Figure 1: SEM micrographs of (a) low and (b) high carbon bearing steels along with corresponding EBSD maps containing (c) smaller grains and (d) bigger grains.

ACKNOWLEDGEMENTS

Financial support by the DEVCOM Army Research Laboratory (No. W911NF1720172) is acknowledged. The views, opinions, and conclusions made in this document are those of the authors and should not be interpreted as representing the official policies, either expressed or implied, of the DEVOM Army Research Laboratory or the US Government.

Electronic Transport in Pd-PdH_x ($0 \leq x < 0.7$) Film in Ambient Temperature.

Jong-Hee Park[1,2,3], Mary Newberg[1]

[1]Dept. Chem. COD, Glen Ellyn, IL 60435, [2]DePaul University, Chicago, IL 60614,
[3]Argonne National Laboratory Argonne, IL 60439

I. SUMMARY

This study has been investigated the electronic transport behavior in the ambient temperature (T = 20ºC), hydrogen partial pressures, $0 < pH_2$ (atm) < 0.04 corresponding stoichiometry, Pd-PdHx ($0 < x < 0.7$) which incorporated pure metallic Pd, α-Pd, α + β mixture, and β phases in the Pd-H. A palladium film deposited on the slide glass via sputter deposition. Resistance was measured with the 4-probe DC method. The electronic transport behavior from the incorporations of hydrogen as, i) adsorption of H_2 molecule on the Pd surface decreased the conductivity, ii) in α-phase increases the conductivity, iii) β-phases decreasing the conductivity increasing the hydrogen stoichiometry.

The mobility of electronic transport in PdHx as determined 0.052 cm^2/V-s. The electronic transport behavior could be explained as a defect nature in palladium hydride.

Discussion

The 1st H occupation in Pd (FCC) starts from the center of octahedral which is in FCC empty and is excepting least energetic location. The 2nd H is supposed to locate longest distance each other due to the same hydrogen could be repulsive (upon considering both are either in H^+ or H^- ion). From the 2nd H incorporation, hydrogen sub lattice to be constructive, and the thermodynamic concern to be identical after two H association to the x = 0.75 (x in PdH_x). All the 3 coordinating Hs are in H^- ions evidence basis on the electrical conductivity dropping with increasing x value. When the hydrogen stoichiometry $0.75 < x < 1.00$, all the associated hydrogens are equalizing charge and distance between Hs. All the Hs are charge compensating each other between H and H, consequently all hydrogens in the Pd (FCC) are in $1s^1$-$1s^1$ neighboring with $\frac{\sqrt{2}}{2}a$ ($a = \text{lattice parameter}$) and ½ a between Pd-H-Pd.

II. Experimental Data

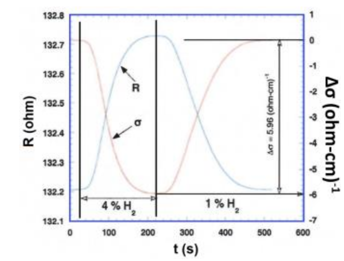

Figure-1.
Monitored electrical resistance (in blue) and calculated conductivity (in red) with switching gases between 1.00% and 4.00% H_2.

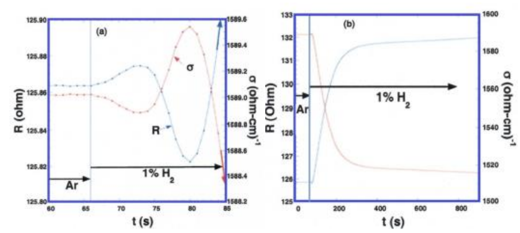

Figure-2.
Resistance (and conductivity) versus time (a) the initial stage and (b) equilibrated in argon gas (Pd) to 1.00%H_2.

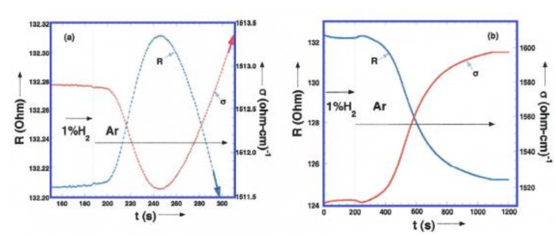

Figure-3. Resistance (and conductivity) versus time (a) the detail for the initial stage and (b) equilibrated in 1.00%H_2 to argon gas (Pd).

ACKNOWLEDGEMENTS
Supported US-DOE, COD stem division.

REFERENCES
1. AFM: R. Nowakowski and P. Grzeszczac, R. Dus, Surface Science **507-510**, 813-818 (2002).

Technical Group C-5

Civil and Environmental Engineering, Architecture (CEA)

Scenario Development Methodology for Automated Vehicle Evaluation

Ilsoo Yun[1], Woori Ko[2]
[1]Ajou University, [2]Ajou University

I. SUMMARY
This study aims to build a test case based on the trajectory of an object to evaluate the safety of automated vehicles (AVs). A test case is a meaningful concrete scenario that can be immediately used to evaluate safety. In this study, a natural driving trajectory was created by analyzing the video with real roads acquired using a drone, and then test cases were developed. In addition, after setting the evaluation index that can consider safety during lane change, the results were analyzed with matlab's simulink simulation.

II. METHODOLOGY OF TEST CASES FOR AV BASED ON REAL TRAJECTORY DATA

A. Analysis of drone video data
The spatial range of the AV driving safety evaluation scenario was set as a ramp section. In this study, drone image data taken in the expressway ramp area was used to simulate the lane change trajectory of the expressway inflow and outflow ramp area.

B. How to generate the AV trajectory
This study develops a driving safety evaluation test type in a situation where the ego cut-in to the front of the target of the adjacent lane in the expressway ramp section. Here, the AV becomes an experiment subject that requires driving safety evaluation, and the target is defined as a surrounding object set for evaluation as shown Figure 1.

C. Create logical scenarios related to lane change on ramp section
A logical scenario sets the type and range of variables related to a specific situation and expresses the specific situation in more detail (Ko et al., 2022). Therefore, the types and ranges of related variables are different for each road section and driving situation. In this study, since the situation as shown in Figure 1 was set, variables related to the cut-in situation of the ego vehicle in the highway ramp section were calculated.

Figure 1: Situation for Evaluation

D. Establishment of safety evaluation index and criteria
The test case extracts the variable combinations of scenarios that have significant results through evaluation. Here, a meaningful result is premised on whether the AV can avoid a collision under the evaluation condition. Therefore, the indicators and standards for evaluating driving safety are different for each specific situation. In this study, the time to steer (TTS) was set as an appropriate safety index because the cut-in situation was modeled. TTS means the time required for steering to avoid a collision with a preceding vehicle.

III. CONCLUSIONS
Experimental values within the selected range are simulated through combination. At this time, the criterion selected as the test case was 0.4s < TTS < 1.0s criterion used as a safety evaluation index through the review of previous studies. As a result, concrete scenarios, which were initially 585 combinations within the range of possible variables, were finally selected as 49 test cases through a valid process.

ACKNOWLEDGEMENTS
This study was supported by the Korea Agency for Infrastructure Technology Advancement (KAIA) grant funded by the Ministry of Land, Infrastructure and Transport (Grant No. 22AMDP-C161752-02).

REFERENCES
1. Ko, W. Park, S. Yun, J. Park, S. Yun, I. “Development of a Framework for Generating Driving Safety Assessment Scenarios for Automated Vehicles”. *Sensors* 2022, 22, 6031

Digital Transformation of Road Management in Korea

Chandle Chae[1], Hanseon Cho[2], Jeehyung Park[3]
[1]Head, Division for Road Transport Policy of Korea Transport Institute,
[2]Cheif Director, Dept. of Road Transport of Korea Transport Institute,
[3]Vice President of Korea Transport Institute

I. INTRODUCTION

Most roads in Korea were built in the 1970s and 1980s and are experiencing rapid deterioration as they have been used for more than 50 years. As a result, road maintenance costs exceed new construction costs, and as a result, the paradigm of road management is shifting from new construction to maintenance.

The core of the maintenance-oriented road policy is to utilize the current road as efficiently as possible, and as a solution, the digital transformation policy of the road management system is being promoted. This study proposed a plan to develop a standard model for evaluating the digital level of the road operating system and use it to derive digital conversion factors and calculate priorities.

II. SURVEY OF CURRENT DIGITAL LEVEL

In this study, the current level of digitization of roads was investigated in order to set the direction of digitization of the road management system. As a result, it was found that 39.1% of the road management work was carried out on a paper document basis, and the use rate of the road management system in the form of software was low at 14.5%. As a result of the survey, it was analyzed that the level of digitization of local governments was lower than that of the central government, and it was determined that digitization of local governments needed to be promoted first.

III. DEVELOPMENT OF DIGITAL LEVEL EVALUATION MODEL

Road work was divided into road planning, road construction, and road operation, and indicators were set to evaluate the digital level. The evaluation index was set as items requiring digitization derived through interviews with road management personnel. The relative weights between the evaluation indicators were calculated through the Analytic Hierarchy Process (AHP), and from the results, the distribution of points for each evaluation index was set as shown in Table 1.

Table 1: Evaluation Model for Road Digital Level

Road Management Task	Evaluation Index	Score
Planning	Mid/long term plan	15
	Road route designation and notification	10
	Feasibility assessment	10
Construction	Design	12
	Road area	9
Management	Road facilities	13
	Road occupancy management	8

IV. MODEL APPLICATION

As a result of applying the digital level evaluation model to Daejeon City and Chuncheon City, Daejeon City scored 36 points and Chuncheon City scored 28.8 points. Since the current digitization of road operation is in its initial stage, it is judged that the score is low, and through the evaluation, it provided a standard for objectively determining which part needs to be digitized first.

REFERENCES

1. Chandle Chae, Jongduk Lee, et al., “Research for Road Digitalization preparing for a New Era of Mobility,” *Annual Research Report of Korea Transport Institute*, 2023.

Facility Management Practice for Public University: A case study on the University of Iowa

Namho Cho[1]
[1]Design Project Manager, The University of Iowa

I. INTRODUCTION

Academic institutions, such as universities and research centers, have complex facilities serving multiple purposes. It is critical to maintain these facilities appropriately to enhance the business structure of universities and support students' education. This study analyzes the facility management (FM) practice used at the University of Iowa (UI) and provides insights for future improvement.

II. FACILITY MANAGEMENT

A. The Environment

Often, the funding provider determines the customer for facility improvement projects, which can complicate FM practices when occupants are not the same as the funders. Understanding the organization's structure is critical to understanding the current FM practices. The UI organization is largely divided into the general education and hospital groups, which manage their properties separately. This study focuses only on the general education FM.

B. The FM for UI

The FM structure includes functions for maintaining the business. Figure 1 shows the structure of FM for the University of Iowa, which consists of four functional groups: (1) Building and Landscape Services (BLS), (2) Design and Construction (D&C), (3) UI Utilities, and (4) FM support. BLS is directly involved in ordinary maintenance practices. If the area managers determine that the issue cannot be resolved with maintenance, the project is issued to D&C. The D&C performs design with third-party professionals and constructs/renovates facilities with contractors. D&C also archives every construction document for future use. UI Utilities oversees utility requirements, and since UI sold its utility function to Engie, construction for utilities is often performed by them. FM support manages sub-functions to operate the entire FM group. Interestingly, Information Technology Services (ITS) is separated and performs its own planning for university internet services.

The FM groups can carry out construction/ renovation projects for customers from different colleges, but they can also be customers for each other. One of the project manager's roles is to coordinate and identify which group should be involved in a project to avoid any conflicts between the departments.

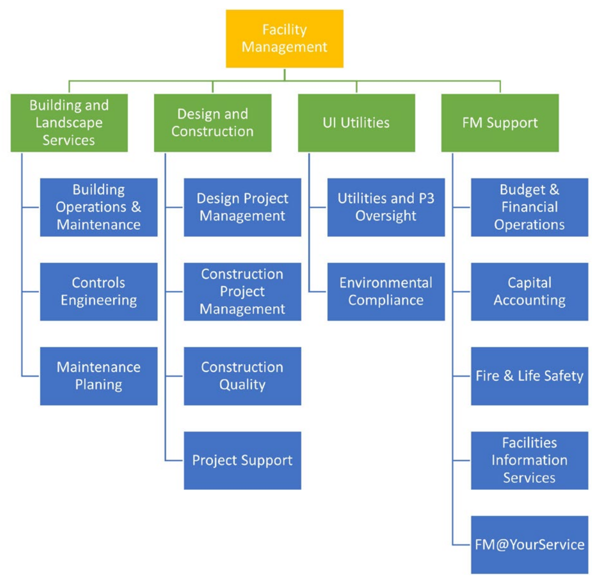

Figure 1: The Structure of FM Dept. for UI

IV. RESULT

Facility management for universities is complex and challenging to track. This paper explains the FM structure used at UI to provide insights into in-field practices. Case studies of multiple institutions can help determine the best FM practices.

REFERENCES

1. The University of Iowa. (2023). *Facility Management*. https://www.facilities.uiowa.edu/ Last access: 03/21/2023

Towards Portable and Accurate Ergonomic Assessment in Construction

JuHyeong Ryu[1]
[1]West Virginia University, Dept. of Industrial & Management Systems Engineering, Morgantown, WV, 26508

I. INTRODUCTION

Construction workers often perform numerous physically demanding tasks and thus are especially prone to work-related musculoskeletal disorders (WMSDs) [1]. For their safety and health, it is essential to mitigate and prevent ergonomic risks by efficiently and accurately estimating biomechanical risks. Traditionally, estimating the whole-body biomechanical loads was a long process requiring a complicated experimental setup and a dedicated space to capture the whole-body motion. However, the Inertial motion capture (IMC) systems—a composite of inertial measurement units (IMUs)—enable whole-body motions collection in any space and eliminate the need for other equipment confined to in-laboratory use. This study developed an ergonomic assessment module applying whole-body inverse dynamics that used an IMC system only to estimate the net moments and forces on all major body joints.

II. METHDOS

The ergonomic assessment tool solves the inverse dynamics of the whole-body model described in Diraneyya et al. [2] to predict the net forces and moments in major body joints, namely lower back compression and shear forces at the L4/L5 disc and moments in shoulders, elbows, hips, knees, and ankles, from motion captured by an IMC system. Additional information required to solve the inverse dynamics problems, including the subject's height and weight, and external loads (e.g., hand loads during manual handling), is manually entered into the module. The subject is also videotaped to visualize the recorded movement alongside the kinematic data. Upon completing the solution process, the module generates the result window, Figure 1. Specifically, it identifies critical moments where the loads on the joints are particularly high and provides a video replay of the at-risk moment, a graph of the joint moment including those critical points, and a colour-code stick figure to represent the risk at various joints in the body.

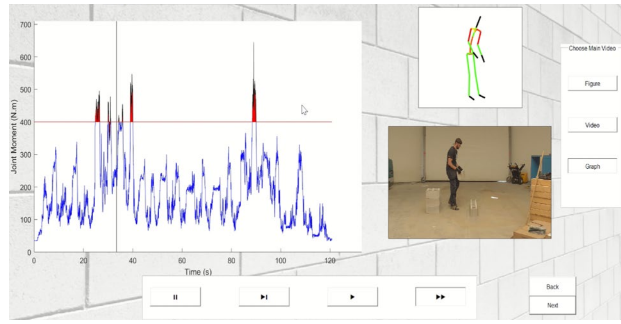

Figure 1: Post-Processing Graphical User Interface of the Ergonomic Assessment Module Report

III. RESULTS AND CONCLUSION

The module was used to analyze ten masons' joint loads experienced during bricklaying. Each participant completed a prebuilt lead wall consisting of 27 standard concrete masonry units (CMUs) with a six-course height—from the 2nd to 6th course, utilizing 45 standard CMUs, weighing 38 lb. The module was validated by comparing its estimations to those obtained from an established static biomechanical analysis software, 3D Static Strength Prediction Program (3DSSPP).

The peak joint loads estimated from the assessment module and 3DSSPP showed excellent correlations for all joints, with intraclass correlation coefficients (ICC) ranging from 0.92 to 0.94. The module allows for a simple estimation of body joint loads, providing a near real-time and portable ergonomic assessment at on-site and training environments. Furthermore, it can improve workplace ergonomics by providing insight into WMSD risks associated with job and workstation design.

REFERENCES

1. J. Ryu, A. Alwasel, C.T. Haas, E. Abdel-Rahman, "Analysis of Relationships Between Body Load and Training, Work Methods, and Work Rate", *J. Construc. Eng. Manag*. 2020.
2. M.M. Diraneyya, J. Ryu, E. Abdel-Rahman, C.T. Haas, "Inertial Motion Capture-Based Whole-Body Inverse Dynamics", *Sensors*. 2021.

Automated Estimation Model for Liquidated Damages in General Provisions of Equipment Purchasing Orders

Eul-Bum Lee[1], **Sea-Eun Park**[1], **So-Won Choi**[1]
[1]Graduate Institute of Ferrous & Energy Materials Technology (GIFT), POSTECH, 77 Cheongam-Ro, Nam-Ku, Pohang, 37673, Korea. Email: dreblee@postech.ac.kr

I. INTRODUCTION

A. Background

Liquidated Damages (LD) in plant projects refer to the monetary damages that the owner may incur in the case of a breach of contract by one of the contracting parties as a consequence of such breach [1]. LD is represented by delay liquidated damages (DLD) and performance liquidated damages (PLD). DLD refers to compensation to the Project Company for losses and damages suffered as a result of late completion of the plant, and PLD compensates the Project Company for losses and damages incurred due to underperformance of the plant. This study aims to develop a model that automatically estimates the LD and the amounts of the General Provision (GP) of equipment purchase contracts in the steel plant. For this, artificial intelligence (AI) technology was applied.

B. Methodology

The LD automatic estimation model using AI technology initially identifies the required variables of the LD clause in the GP and then detects their coordinates. The necessary variables for LD estimation include the contract amount, delivery date, and preliminary acceptance certificate (PAC) issuance date. The variables and date patterns in the document were preprocessed through data normalization. The development process of the LD automatic estimation model is shown in Figure 1.

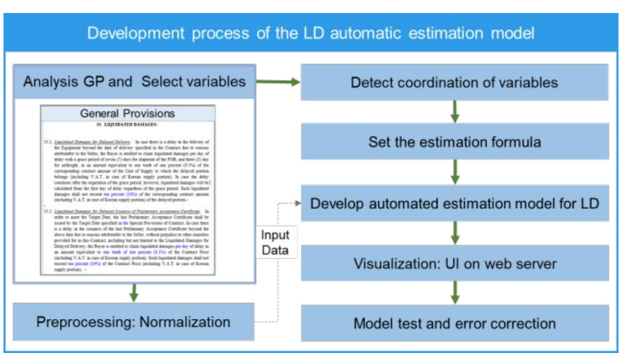

Figure 1: Development process of the LD automatic estimation model

When entering contract documents into the model, the model automatically detects the variables necessary for analysis. The detected variable values are applied as input values for the LD estimation equation set in the model. Then, the resulting LD amount is automatically calculated. The LD estimation model proposed in this study is divided into DLD and PLD. Eventually, the total LD amount, the sum of the DLD and PLD, is estimated. This model was developed using the Python programming language, the main library was PDF-diff, and lxml and PIL were applied for additional support [2]. A web-based prototype system was developed to implement the proposed model. The F1 score was presented as 100% when the value of all variables was inputted accurately. In addition, compared to the manually calculated method by engineers, the LD estimation process was shortened by an average of approximately 18 minutes.

II. RESULT

This study developed a model applying AI technology to automatically estimate LD, a critical contractual risk in plant projects. It confirmed its potential practical applicability in the industry field by developing a web-based prototype system. The proposed LD estimation model can be utilized as an assistive device to reduce the workload of purchasing managers and prevent potential human errors. In addition, it is expected that this study could be expanded into a more comprehensive range of research in contract and risk management.

ACKNOWLEDGEMENTS

The authors acknowledge that this research was sponsored by Pohang Iron & Steel Co., Ltd. (POSCO)

REFERENCES

1. Eggleston, B. *Liquidated damages and extensions of time: In construction contracts;* John Wiley & Sons: 2009.

Virtual Reality Educational Simulation for Construction Management

Suryeon Kim, **H. David Jeong, Zofia Rybkowski, Jinsil Hwaryoung Seo**
Texas A&M University

I. SUMMARY

Educational simulation has recently gained significant popularity and attraction in STEM education. It not only provides educational connotations in a highly immersive environment but also entails entertainment components to keep students engaged during the education process.

The recent emergence of COVID-19 has also raised an urgent need for pedagogical transition for higher education in construction science field, resulting in the physical classroom moving to an online, virtual classroom. This research proposes a new pedagogical approach, virtual reality (VR)-driven educational simulation for construction project management principles and methods and tests its effectiveness.

II. VR-DRIVEN EDUCATIONAL SIMULATION

A. Test Bed – Marshmallow TVD Simulation

The in-person, physical Marshmallow TVD Simulation developed by Munankami (2012) to help students intellectually grasp a simplified, conceptual framework of TVD was selected as a test bed.

B. VR-driven Educational Simulation

The VR-driven Marshmallow TVD Simulation is developed using the Unity™ software to digitalize the physical TVD simulation directly. The software can imitate most physical characteristics such as materials, mass, movement, and reactions to establish real-world scenes in the VR environment. Figure 1 depicts the snapshots of VR-driven Marshmallow TVD Simulation.

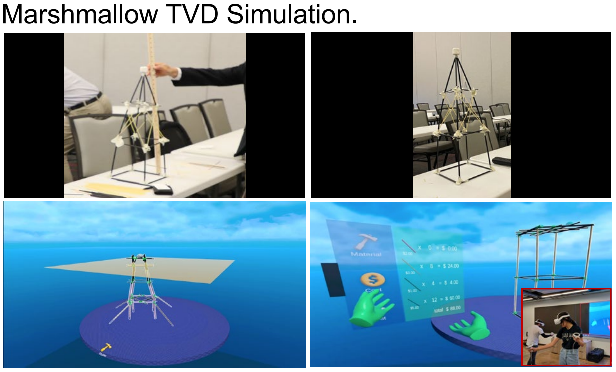

Figure 1: Physical and VR Educational Simulations

III. TESTING AND RESULT

Thirty valid pre- and post-simulation questionnaire surveys were collected from the experiments. A one-way analysis of variance (ANOVA) was conducted to compare the knowledge retention before and after simulation and determine whether statistical evidence shows that the means were significantly different. There was statistical significance in knowledge retention after VR-driven simulation for those five TVD principles: mutual benefit and reward; collaborative decision-making; early involvement of key partners; intensified planning; and appropriate technology (Table 1). The results indicate that VR-driven educational simulation can successfully impart those five TVD principles.

Table 1: Result of ANOVA

TVD Principles	F	p
Mutual benefit and reward	4.397	0.040
Collaborative decision-making	6.621	0.014
Early involvement of key partners	6.222	<.001
Intensified planning	7.331	<.001
Appropriate technology	6.429	.010

IV. CONCLUSION

This research developed a VR-driven educational simulation to teach the basic concept of TVD. Experimental data from participant surveys before and after the simulation investigated the effectiveness of the suggested simulation, and the results showed the potential of VR-driven educational simulation in imparting construction management principles successfully.

The results of this research contribute to creating new knowledge on the quantitative effects of VR-driven educational simulation and the efficacy for future educational simulation designers and developers in the construction industry.

REFERENCE

1. M. Munankami, “Development and Testing of Simulation (Game) to Illustrate Basic Principles of Integrated Project Delivery and Target Value Design: A First Run Study,” MS Thesis, presented to Texas A&M University, College Station, TX.

AI-driven contract risk extraction model

Jeehee Lee[1]
[1]University of Nevada, Las Vegas

I. RESEARCH BACKGROUND

A construction project is a long and expensive endeavor in which the design, on-site conditions, and available resources can change at any point. Consequently, claims and disputes among various stakeholders are inevitable, which leads to cost overruns and schedule delays. To prevent such construction claims and disputes, all participants in construction projects typically make a stipulation regarding their roles and responsibilities by contracting. A construction contract is a mutually agreed upon, dominant, and legally binding governance, and thus contractual relationships and obligations set forth in the contract serve as the basis for important judgments when disputes arise. Therefore, if the risks inherent in the contract are not thoroughly reviewed at the bidding and contracting stage, claims and disputes may arise causing significant financial losses, possibly leading to legal action [1]. This study presents a novel proactive risk assessment model to identify risk-related contract terms in construction contracts. The proposed contract risk extraction model is driven by AI-based natural language processing (NLP) technology and the model discovers and determines risk-related contract terms in an automated manner. The proposed data-driven risk assessment model is expected to reduce the extent of human errors by (1) identifying potential contractual risks that could arise disputes, and (2) supporting to development of appropriate response strategies for the given risks.

II. CONTRACT RISK EXTRACTION MODEL

This study is carried out in the following four steps (Figure 1):

- Risk-related contract terms that are frequently encountered in the owner's modified contract are defined based on real-world construction contracts and previous dispute cases (i.e., legal cases).
- Text data pre-processing is performed 1) to transform unstructured text data (contract documents) to the structured format and 2) to make compound and complex structures of sentences in the contract documents into simple sentences.
- The subject, verb, and object (SVO) part of every sentence in a given contract document is extracted. In addition, additional syntactic rules are developed for extracting SVO tuple in an exceptional sentence structure which contains conditional clauses using the words if or unless.
- Semantic analysis using the contract risk-related lexicon is carried out to recognize the pattern of problematic contract terms based on the types of contract risks defined in the first step.

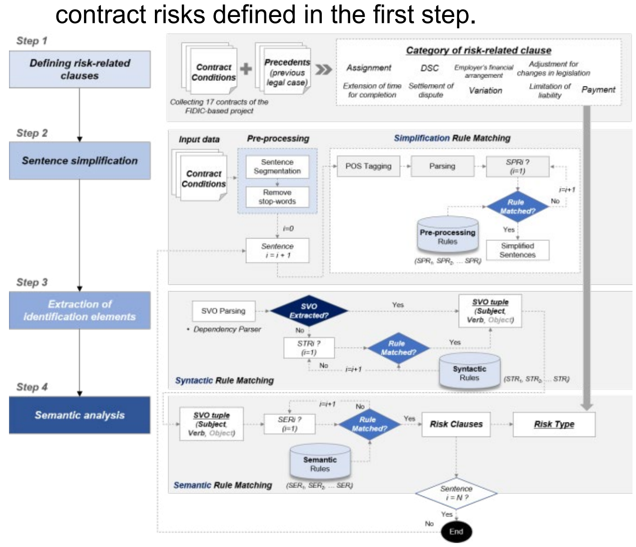

Figure 1 contract risk extraction model development

III. CONCLUSION

The automatic extraction model was designed to automatically extract the intentionally and maliciously modified contract terms and these modified terms are defined as risk-related problematic contract terms. The proposed model is designed to enable contractors to focus on strategizing and making informed decisions with an enhanced understanding of contract risks.

REFERENCES

1. J. Lee, J.-S. Yi, J. Son, Development of Automatic-Extraction Model of Poisonous Clauses in International Construction Contracts Using Rule-Based NLP, Journal of Computing in Civil Engineering. 33 (2019) 04019003.

Using Data to Integrate Equity in Infrastructure Project Selection Process

John McFadden[1], Seri Park[2]
[1]Federal Highway Administration Resource Center Safety and Design Technical Service Team, [2]Associate Professor of Civil Engineering University of Nevada, Reno

I. SUMMARY

On January 20, 2021 President Biden signed Executive Order 13985 "Advancing Racial Equity and Support for Underserved Communities Through the Federal Government" [1]. As a result of this order, the United States (US) Department of Transportation (DOT) indicated that they will undertake a comprehensive approach to advance equity for all and assess to what extent its programs and policies perpetuate systemic barriers to opportunities and benefits for people of color and other underserved groups.

The proposed presentation focusses on how to deploy a data driven process to examine and deliver an equitable distribution of resources on infrastructure investments focused on improving highway safety. A review of how state and local jurisdictions in the US can incorporate equity into their project selection process will be reviewed. Common data driven practices will be examined that include identify data sources (including the US census) and analysis techniques that can help accomplish the US DOT goals stated above.

As examples, two jurisdictions that currently deploy equity-based criteria for roadway infrastructure project selection will be reviewed namely the Delaware Valley Regional Planning Commission (DVRPC, as illustrated in Figures 1 and 2) and the City of Portland, Oregon. These two jurisdictions incorporate equity criteria into the project selection process and this research will explore their approaches. Common census tract variables used to integrate equity in the decision-making process will be identified and documented. The findings of this research could then be used to help communicate best practices for establishing equity-based criteria for project selection for other jurisdictions.

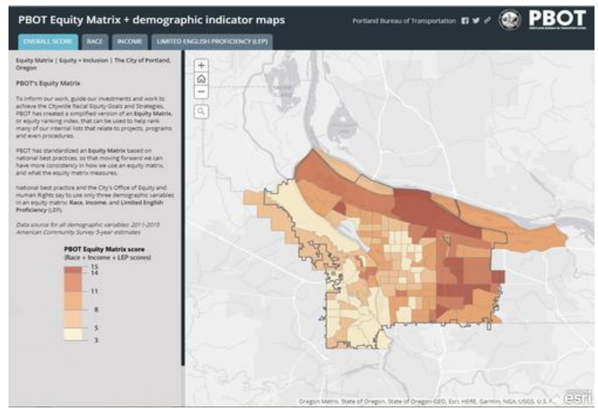

Figure 1: Portland Equity Matrix and Demographic Indicator Map [2]

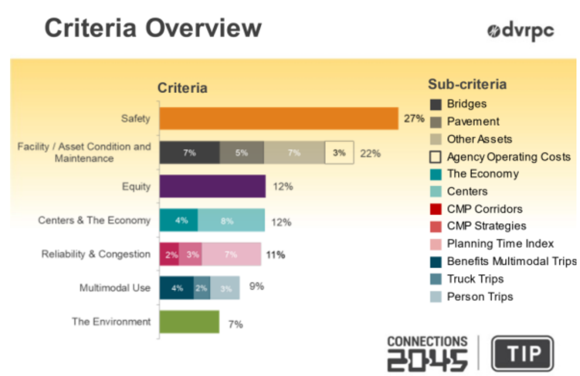

Figure 2: Delaware Valley Regional Planning Commission Project Selection Criteria [2]

REFERENCES

1. Executive Order 13985—*Advancing Racial Equity and Support for Underserved Communities Through the Federal Government*
2. Delaware Valley Planning Commission (DVRPC), Equity Analysis for the Greater Philadelphia Region https://www.dvrpc.org/webmaps/ipd/

Green Infrastructure Design and Runoff Reduction Evaluation for Metro City Level: The Case Study of Suwon City

Jaekyoung Kim[1, 2], Hyereong Yun[2,3], Samuel Park[4], Junsuk Kang[1,2,3,4]
[1]Interdisciplinary Program in Landscape Architecture, Seoul National University, [2]Integrated Major in Smart City Global Convergence, Seoul National University, [3]Department of Landscape Architecture and Rural Systems Engineering, Seoul National University, [4]Research Institute of Agriculture and Life Sciences, Seoul National University

I. SUMMARY

The damages caused by climate change are increasing, and among them, the effects of flooding have a significant impact on cities. In this study, we designed green infrastructure using SWMM 5.2 and evaluated the runoff reduction effect.
When designing an evidence-based green infrastructure for Suwon City, the maximum runoff reduction effect was found to be about 24%.

II. Background and Objectives

Climate change is predicted to worsen, and the global community is making various efforts to achieve carbon neutrality by 2050. The global community is aware of the severity of climate change, and in addition to mitigation, efforts are also being made to focus on adaptation-related measures.

One of the methods for adapting to floods is green infrastructure. Green infrastructure is also referred to as LID (Low Impact Development) and involves managing stormwater in an environmentally friendly way by dispersing it from the initial stage.

According to this background, the objective is set to design green infrastructure and evaluate the reduction in runoff under extreme rainfall conditions.

III. Methods

A. SWMM Modeling

This study used SWMM developed by U.S. EPA. SWMM is a hydrologic simulation software used to model urban stormwater systems. The model can analyze various components such as stormwater runoff, combined and sanitary sewers, and water quality (Kim et al., 2022).

B. Design of Green Infrastructure

Green infrastructure was designed for Suwon City, located in South Korea. A total of six facilities were planned, and the design methodology was applied by referring to the Low Impact Development (LID) Landscape Guideline published by the Ministry of Environment.

C. Time Scenario

Precipitation was applied at 50 mm intervals from 50 mm to 400 mm, and runoff was evaluated. To apply the precipitation scenarios, a method to divide the rainfall into hourly units is required. For this, the Huff equation was used.

IV. Results

The results of this study showed that there was a maximum runoff reduction effect of 10.25% at 400 mm of precipitation and a runoff reduction effect of 24.71% at 50 mm of precipitation.

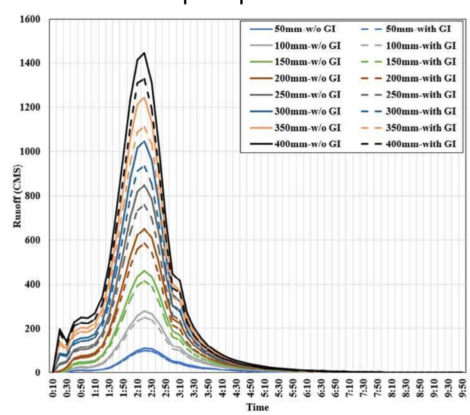

Figure 1: Runoff Reduction Effect of Green Infra

ACKNOWLEDGEMENTS

This work was supported by Korea Environment Industry &Technology Institute (KEITI) through "Climate Change R&D Project for New Climate Regime.", funded by Korea Ministry of Environment (MOE) (2022003570004)

REFERENCES

1. Kim, J., Lee, J., Hwang, S., & Kang, J. (2022). Urban flood adaptation and optimization for net-zero: Case study of Dongjak-gu, Seoul. *Journal of Hydrology: Regional Studies*, *41*, 101110.

Assessing Vulnerability of South Korea to Typhoon Damage Considering Sea Level Rise: A Case Study of Typhoon Maesak Simulation

JINYOUNG KIM[1]

[1]University of Texas at Arlington

I. SUMMARY

This study employed simulations to analyze the evolving patterns of typhoon damage in response to projected low, and high-intensity sea level rise in 2100. Fluid dynamics and wave simulations were conducted using Delft3D-FLOW/WAVE, and the variations in damage pre and post sea level rise were analyzed based on data from Typhoon Maesak in 2020.

II. INTRODUCTION

A. Typhoon Maesak and Modeling

On September 3, 2020, Typhoon Maesak, a very strong typhoon, made landfall in Busan, South Korea, with a central pressure of 950 hPa and a 10-minute average wind speed of 44 m/s. Utilizing the track and wind data from JTWC for Typhoon Maesak, the wind field of the typhoon was generated using the Holland (2010) model for the hydrodynamic/wave simulation.

B. Simulation Details

Numerical models have been employed to study wave and flow dynamics in response to extreme events, such as Tropical storm. This study utilized the Delft3D-FLOW and WAVE models, which combine the hydrodynamic module (Delft3D-FLOW) for solving the Navier-Stokes equations and the wave module (Delft3D-WAVE) for simulating short wave generation and propagation in nearshore areas. The simulation grid consists of two components: a large-scale grid encompassing the entire area of Korea and a detailed grid focusing specifically on the southern region of South Korea. These two grids are interconnected with Domain decomposed boundary in Delft3D model.

C. Sea Level Rise

According to the Projected Sea Level Rise Under Different SSP Scenarios provided by NASA, the projected sea level rise in Busan by 2100 ranged from 0.46 m (Low scenario) to 0.85 m (Very High scenario). Typhoon simulations were conducted to examine the changes in inundation areas under two sea level rise scenarios and a no sea level rise scenario.

III. RESULTS

The maximum wave height due to the typhoon was recorded as 10.52 m in the offshore waters of Busan (Figure 1). In comparison to the scenario without sea level rise, both the Low and Very High scenarios showed areas that were already inundated, and these areas experienced a higher level of flooding during the typhoon's passage.

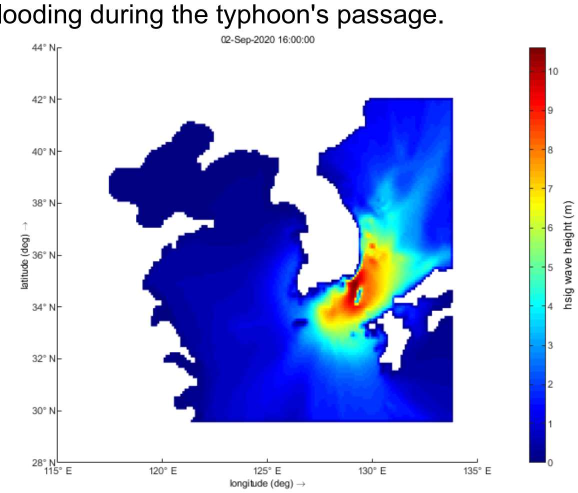

Figure 1: The simulated maximum wave height during the landfall of Typhoon Maesak

However, it should be noted that the model's grid size of 0.02 degrees (approximately 22.2 km) is insufficient to capture detailed inundation patterns. To obtain a more accurate representation of the detailed changes in flooding, a finer grid and high-resolution Digital Elevation Model (DEM) are required.

REFERENCES

Holland, Greg J., James I. Belanger, and Angela Fritz. "A revised model for radial profiles of hurricane winds." Monthly weather review 138.12: 4393-4401, 2010.

Multivariate Frequency Analysis Framework for Hurricane Events and Its Application on Hurricane Ian

Eunsaem Cho[1,2], Ebrahim Ahmadisharaf[1,2*], James Done[3], Chulsang Yoo[4]

[1]Department of Civil and Environmental Engineering, FAMU-FSU College of Engineering, Florida State University, Tallahassee, FL 32310, USA
[2]Resilient Infrastructure and Disaster Response Center, FAMU-FSU College of Engineering, Florida State University, Tallahassee, FL 32310, USA
[3]National Center for Atmospheric Research, 3090 Center Green Drive, Boulder, Colorado 80301, USA
[4]School of Civil, Environmental and Architectural Engineering, College of Engineering, Korea University, Seoul 02841, Korea

I. SUMMARY

This study proposes a framework for evaluating multivariate return periods using event-based frequency analysis techniques. The framework is applied to analyze Hurricane Ian, a recent catastrophic event. Univariate, bivariate, and trivariate frequency analyses are performed using generalized extreme value distribution and copula.

II. Methodology

A. Sampling Annual Maximum Series

Annual maximum series of flood volume, peak discharge, total rainfall depth and maximum wind speed were prepared for the frequency analyses. The annual maximum series were chosen through the block maxima approach.

B. Frequency Analysis Methods

Univariate analyses were conducted using GEV distribution. Bivariate analyses were conducted using copula. Trivariate analyses were conducted using D-vine copula.

III. Data Preparation

53 stream gauges from USGS and 13 weather stations from NOAA were chosen for the frequency analyses. For spatial analyses, we used 30 years of observation. In the case of point-based analyses, 35 years of observation were used.

IV. Results

A. Spatial Pattern of Hurricane Ian's Return Period

Spatial pattern of the return period of Hurricane Ian was generated by averaging the results of bivariate frequency analyses, which are combination of peak discharge & flood volume and total rainfall depth & maximum wind speed (Figure 1).

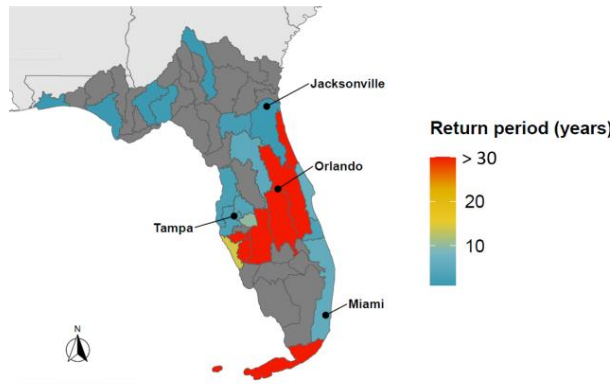

Figure 1: Hurricane Ian's return period map based on the bivariate frequency analyses results.

B. Point-based Return Period of Hurricane Ian

The point-based analyses were conducted using data from Daytona Beach International Airport weather station and Tomoka River Near Holly Hill stream gauge (Table 1).

Table 1. Univariate, bivariate, and trivariate return period of Hurricane Ian

Analysis method	Input variable(s)	Estimated return period (years)	95% confidence interval (years)
Univariate	Q (peak discharge)	60.2	55.7 – 65.0
	V (flood volume)	85.3	82.1 – 88.3
	W (maximum wind speed)	77.3	54.2 – 110.1
	R (total rainfall depth)	39.2	34.1 – 45.0
Bivariate	Q & P	650.3	582.1 – 723.1
	W & R	1592.6	974.5 – 2,593.3
Trivariate	R-centered	439.3	322.4 – 565.2
	Q-centered	1,064.1	905.1 – 1,337.9
	W-centered	1,727.8	904.6 – 3,548.3

ACKNOWLEDGEMENTS

Ebrahim Ahmadisharaf was partially supported through award # 2203180 by the United States National Science Foundation (NSF).

[SEED 2023] Event coincidence of dryness, conflict, and forced migration in Somalia

Woi Sok Oh[1, 2]
[1]High Meadows Environmental Institute, Princeton University, [2]Department of Ecology & Evolutionary Biology, Princeton University

I. INTRODUCTION

Somalia has an increasing number of forced migrations within the country's border mainly due to climate and conflict stresses. The country is infamous for extreme droughts, while it is also successive at the same time. Also, civilians suffer from prolonged armed conflict between the government and al Shabaab, a terror group based in southern Somalia.

Recent researchers worked on how climate, conflict, and forced migration interact [1]. However, the spatial heterogeneity of these interplays has not been fully understood. A country-level study may be too course-grained for capturing the underlying mechanisms of the feedback between climate, conflict, and forced migration. Thus, I conduct an event coincidence analysis to analyze different event coincidence patterns across Somalia.

II. METHODS

A. Data

All data in this study is cleaned up at a weekly scale in 2016–2022. For quantifying migration events, this work uses Protection & Return Monitoring Network data from UNHCR. The data was collected through onsite interviews. If there is any outgoing migration population in week *i*, I define that week *i* have a migration event. I used CHIRPS precipitation data to count dry weeks without any rainfalls. Lastly, I filtered al Shabaab conflict events from ACLED data.

B. Event Coincidence Analysis

This method calculates the temporal coincidence of two or three types of events. For each event of type A in Fig. 1A, you check whether there are any events within the coincidence window (ΔT) with a time lag (τ). If so, the focal event has a coincidence with event type B. After iterating per all events of type A, you calculate the fraction of coincidence. In the mathematical formula, the coincidence rate is:

$$r_p = \frac{1}{N_A}\sum_{i=1}^{N_A} \Theta\left[\sum_{j=1}^{N_B} 1_{[0,\Delta T]}((t_i^A - \tau) - t_j^B)\right].$$

The event coincidence rate of the three event types is calculated in the same way.

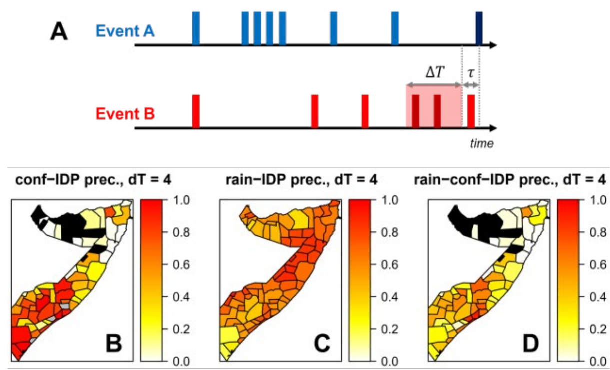

Figure 1: (A) An overview of event coincidence analysis. (B) Conflict-migration coincidence. (C) No rainfall-migration coincidence. (D) No rainfall-conflict-migration coincidence.

III. RESULTS AND DISCUSSION

Fig. 1B-1C exhibits different coincidence patterns in Somalia. For conflict-migration coincidence, the hotspots are located in the south where frequent battles between the government military and al Shabaab take place. Still, Bossaso, a northern port city, shows high coincidence. Coincidence between no rainfall and migration is relatively high across the whole country because most districts are affected by droughts. Central districts have the highest coincidence in this case. No rainfall, armed conflict, and migration coincide in Banadir (Mogadishu) area, the capital of Somalia, and Bossaso. Overall, this study offers valuable insights into building a nexus between climate, conflict, and forced migration.

REFERENCES

1. Abel, Guy J., et al. "Climate, conflict and forced migration." *Global Environmental Change* 54 (2019): 239-249.

Investigating the Relationship between Human Physiological Responses and Indoor Environmental Quality in Commercial Buildings

Joon-Ho Choi[1], Haoyue Dai[1]

[1]Building Science, School of Architecture, University of Southern California

I. SUMMARY

During the COVID-19 pandemic, the significance of Indoor Environmental Quality (IEQ) and its impact on human physiological responses gained attention, particularly for commercial buildings and their influence on occupant health and company performance based on Environmental, Social, and Governance (ESG) criteria. However, existing studies lacked comprehensive experiments to develop predictive models linking human physiological responses with indoor environmental quality. This research investigated the relationship between human physiological responses and IEQ components in two office areas, involving 20 participants. Sensor data collected information on IEQ indicators, and wearable devices recorded human physiological response data. Machine learning techniques were utilized to establish correlations and validate an accurate predictive model. The study aimed to enhance existing IEQ monitoring technologies and ventilation control models while gaining insights into the physiological needs of individual building occupants in relation to their ambient environmental quality.

II. RESEARCH METHODS

The experiments took place at a commercial office building in the downtown Los Angeles, which was divided into five zones to capture various office conditions. Data collection occurred in September and November, with ten volunteers working in the office for a week during regular work hours in each period. Sensors were installed in each office area to collect indoor and outdoor environmental parameters, and volunteers wore smartwatches to capture physiological responses. Paper questionnaires on indoor air quality (IAQ) and thermal comfort were filled out every two hours. Data from the sensors were collected at a 10-minute interval. Statistical software (Minitab) and machine learning (Python) were used for data analysis, aiming to identify relationships between parameters and determine relevant bio-signals.

III. RESULTS AND CONCLUSION

The TLCC (Time Lagged Cross-Correlation) and Granger Causality Test are employed to analyze personal data and identify significant correlations that satisfy two criteria: (1) IEQ indicators leading to bio signals and (2) statistical significance with a p-value of less than 0.05. Any analysis with a p-value greater than 0.05 has been excluded. All participants' data are consolidated into a single dataset for cross-correlation analysis. The findings reveal the three most notable correlations: (1) indoor temperature with EDA (Electrodermal Activity), (2) PM2.5 with EDA, and (3) relative humidity with skin temperature. However, no significant correlation is found between CO2 levels and skin temperature. Figure 1 presents a heatmap of the average coefficients, where negative correlations are depicted in blue and positive correlations in red.

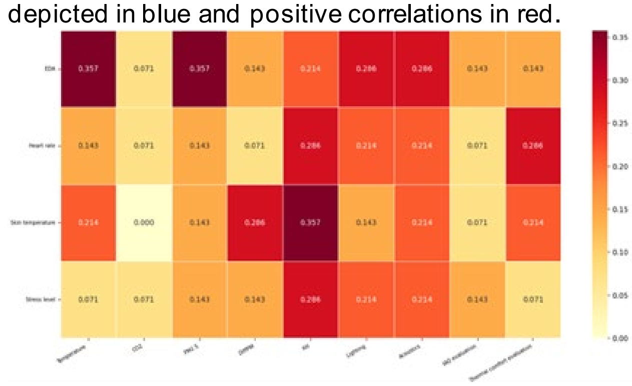

Figure 1: Heatmap showing the percentage of significant correlation cases based on personal data

This study aimed to develop estimation models for an automatic environmental control system based on physiological responses to indoor environmental quality (IEQ) in commercial offices. Significant correlations were found between IEQ indicators and physiological responses, with gender differences observed. Individual-based models outperformed a general model, particularly for individuals with lower BMI. The study highlights the potential of utilizing physiological responses to enhance ventilation control systems.

REFERENCES

Wu, Z., Li, N., & Schiavon, S. (2022). Experimental evaluation of thermal comfort, SBS symptoms and physiological responses in a radiant ceiling cooling environment under temperature step-changes. Building and Environment.

Evaluation of V-COP model for real-time monitoring of EHP performance

Jihyun Seo[1,2], Dong Eun Jung[1,3], Jonghun Kim[1], Haneul Choi[1], Taeyeon Kim[2]
[1] Korea Institute of Energy Research, Korea, [2] Yonsei University, Korea, [3]Korea University, Korea

I. INTRODUCTION

In order to decarbonize buildings, there is a shift towards reducing the use of fossil fuels and transitioning to electricity generated from renewable sources. A crucial technological element in the electrification of buildings is heat pumps, which have approximately 2-5 times higher efficiency compared to conventional heating systems.

However, while the performance of heat pumps is important, the measured coefficient of performance (COP) is typically only calculated in laboratory conditions and not often measured during actual operational stages. This is because it is difficult to satisfy the experimental environment and methods required for COP measurement in real-world settings. Consequently, this study aims to explore the feasibility of creating a data-driven V-COP (Virtual COP) model to facilitate easier on-site measurements and assess its applicability.

II. METHOD

The datasets were obtained using EnergyPlus. An actual office building (3 zones) with an installed Air-to-Air Heat Pump (EHP) was modeled. The cooling capacity of the installed EHP is 23.3 kW, with a power consumption of 4.8 kW, resulting in a rated cooling COP of approximately 4.9. The operational schedule is set from 09:00 to 18:00 on weekdays, with a cooling setpoint temperature of 26℃. To predict the cooling COP, data was extracted at 10-minute intervals for the months of June to August to build the datasets. (The dataset of June and July for training, the dataset of August for test)

In this study, the following steps were conducted using the datasets: 1) Variables that influence the COP were extracted. 2) Correlation analysis was performed among the variables. 3) Variables with a correlation coefficient of less than 0.5 were excluded, prioritizing the remaining variables that are easily measurable in the field as input variables. 4) The selected input variables were used to train and test the V-COP model.

III. RESULTS

In this study, variables that have a high correlation with cooling COP and are easily measurable in the field were selected for practical application. The selected variables were outdoor temperature, cooling power consumption of the heat pump, and supply temperatures for Zone 1, 2, and 3.

Figure 1 represents the rated cooling COP, actual cooling COP, and predicted cooling COP for August. The rated cooling COP was 4.9, and the actual and predicted values show a similar pattern. Comparing the actual and predicted values, the R2 value was found to be 0.9757. The coefficient of variation of the root mean square error (cv(RMSE)) was 25.32%, and the mean bias error (MBE) was 3.34%, both satisfying by ASHRAE Guideline 14.

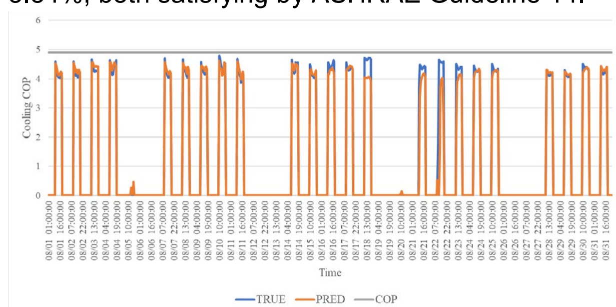

Figure 1: Comparison of true and predicted values

ACKNOWLEDGEMENTS

This research was supported by the Korea Energy Foundation(KEF) grant funded by the Korea government(MOTIE) (C2-5524)

REFERENCES

1. C. Ermel, M. Bianchi, A. Bianchi, P. Schneider, "Thermal storage integrated into air-source heat pumps to leverage building electrification: A systematic literature review," *Applied Thermal Engineering*, Vol. 215, 118975, 2022.
2. J. Son, J. Hong, T. Aum, "A Pilot Study on In-situ Measurement Method for Cooling Performance of Air-source," *Journal of the Architectural Institute of Korea*, Vol. 38, No. 9, pp. 201-207, 2022.

Fast Load Prediction Model of Chiller using Bayesian Optimization

Juwan Ha[1], Byeongmo Seo[1], Seungmin Lee[1], Soolyeon Cho[1]
[1]College of Design, North Carolina State University, Raleigh, NC, 27695, USA

I. INTRODUCTION

Efficient operation of the chiller is crucial for energy savings in cooling. Compared to other components, such as chilled water pumps and fans, chillers consume significantly more energy [1]. Therefore, an accurate prediction model for the chiller's load is necessary for efficient operation.

Existing load prediction models of chiller mainly rely on model-based optimization and grid search methods. However, improving model accuracy using these approaches can be labor-intensive and time-consuming. Thus, this study proposes a fast load prediction modeling method for a chiller using a Bayesian optimization approach.

II. Data Description

The ANN-based chiller's load prediction modeling data is collected from the SC factory. The data spans from June to September 2022, with an hourly interval. Table 1 presents the dataset variables. used for the ANN-based chiller load prediction model. In addition, missing values of sensors were excluded.

III. ANN Modeling

Equation (1) represents the chiller load prediction model. To reflect the characteristics of time in the model, it was classified into hour, day, week, and holiday, and outdoor air temperature and relative humidity, evaporator leaving water temperature, and entering water temperature were selected as input variables of the freezer load prediction model. Also, the actual running capacity variable was selected as an output variable. In addition, Figure 1 compares the actual chiller load data and the ANN prediction data.

$$f_{Chiller,Load} = f_{ANN}(Hour, Day, week, Holiday,\ T_{0A},\ RH_{0A},\ T_{ELWT},\ T_{EEWT}) \quad (1)$$

IV. CONCLUSIONS

Bayesian optimization enables faster and more accurate modeling than traditional grid-based methods due to its sample efficiency in the hyperparameter tuning of ANN models. This paper examines the applicability of Bayesian optimization for fast chiller load prediction model. Three types of acquisition functions (expected improvement, probability of improvement, and lower confidence bound) are explored. In the future, this approach will be applied to modeling other systems such as roof top units (RTUs), ground mounted units (GMUs), and variable refrigerant flow (VRF) systems.

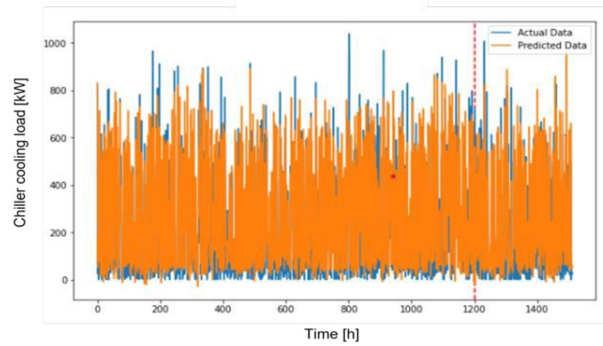

Figure 1. Comparison of actual data and ANN prediction data

Table 1: Time-series dataset variables

Variable Name	Type	Unit
Hour	Numerical	N.A.
Day	Numerical	N.A.
Week	Numerical	N.A.
Holiday	Numerical	N.A.
Outdoor air temperature (T_{0A})	Numerical	°C
Outdoor air relative humidity (RH_{0A})	Numerical	%
Evaporator Leaving water temperature (T_{ELWT})	Numerical	°C
Evaporator Entering water temperature (T_{EEWT})	Numerical	°C
Actual Running Capacity	Numerical	%

REFERENCES

1. Sen Huang et al, "Improved Cooling tower control of legacy chiller plants by optimizing the condenser water set point," *Building and Environment*, Vol. 111, pp. 33-46, 2017.

An Empirical Analysis of Korean Household Appliance Use Patterns: using a national Time Use Survey dataset

Seungmin Lee[1], **Juwan Ha**[1], **Jonghoon Kim**[2], **Soolyeon Cho**[1]
[1]College of Design, North Carolina State University, Raleigh, NC, 27695, USA,
[2]Energy ICT Convergence Research Department, Korea Institute of Energy Research, 152, Gajeong-ro, Yuseong-gu, Daejeon, 34129, South Korea

I. INTRODUCTION

Uncertainty due to occupant behavior in predicting energy usage in residential buildings often leads to a gap between actual and expected energy consumption. In this study, the appliance usage behavior patterns of individual Koreans were investigated through the Korean Time-Use Survey to utilize them as foundational data to overcome such gaps.

II. METHODOLOGY

A. Data preprocessing

This study used 2019 data from the Korean Time-Use Survey, extracting seven appliance codes assumed to be used during specific behaviors. The data was analyzed by dividing it into weekdays and weekends.

B. Clustering analysis

K-means algorithm clustered appliance usage behavior patterns, determining the appropriate number of clusters using the silhouette coefficient. The clustering results are shown in Figure 1 (weekdays).

C. Correlation analysis

Spearman's correlation coefficient was used to identify the main factors affecting appliance usage patterns. A total of 24 variables were analyzed for correlation between clusters.

III. CONCLUSIONS

Correlation analysis revealed negative correlations on weekdays and weekends with household-related variables. The analysis results are shown in Table 1 (weekdays). Higher education and income were associated with the third category, while younger age and fewer elderly members were associated with the first category. On weekends, not working, no economic activity, and unstable employment status were associated with the third category. Lower education level and income were associated with the first category.

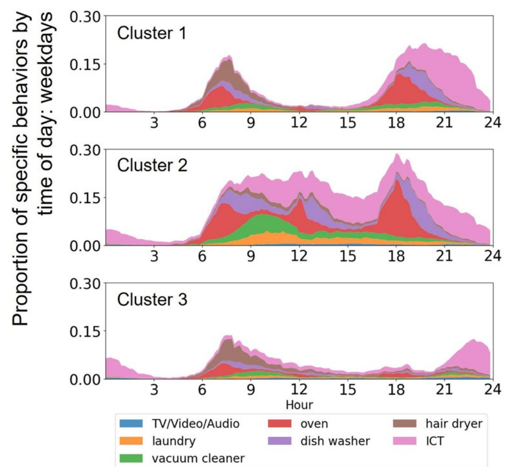

Figure 1: The Proportion of Specific Behaviors Performed during Each Hour (weekdays)

Table 1: Spearman Correlation Analysis Based on Weekday Clustering

Variables	Correlation Coefficient
Educational Level	0.106
Urban Residency	0.066
Marital Status	-0.060
Age	-0.063

ACKNOWLEDGEMENTS

This work is supported by the Korea Agency for Infrastructure Technology Advancement (KAIA) grant funded by the Ministry of Land, Infrastructure and Transport (grant number 22PIYR-C153279-04).

REFERENCES

1. HONG, Tianzhen, et al., “Advances in research and applications of energy-related occupant behavior in buildings,” *Energy and buildings*, Vol. 116, pp. 694-702, 2016

In-situ evaluation of non-destructive insulation performance measurement method of building envelope

Daehwan Shin[1,2], Dong Eun Jung[1,3], Jonghun Kim[1], HakGeun Jeong[1], Sumin Kim[2]
[1] Korea Institute of Energy Research, Korea, [2] Yonsei University, Korea, [3]Korea University, Korea

I. INTRODUCTION

The most well-known non-destructive methods for measuring the thermal insulation performance of building envelopes are the HFM method (Heat Flow Meter Method) based on ISO 9869-1:2014, and the IR method (Infrared Method) based on ISO 9869-2:2018. These two methods were used to evaluate the thermal insulation performance of the walls and windows of the building. The thermal insulation performance of the walls and windows measured using the HFM method showed a significant accuracy, closely resembling the design performance. However, the IR method was found to be suitable only for lightweight structures such as windows. The thermal insulation performance of the walls was additionally measured using formulas from existing literature [1], resulting in similar results to the design performance.

II. METHOD

The insulation performance of the building envelope was measured using the IR method, and its accuracy was evaluated by comparing it with the design value and the HFM method. The target building was a new building completed in 2021, and it was determined that there was no difference between the design value and the current performance. The design values for walls are 0.181 W/m2K and windows are 1.268 W/m2K. The measurement method used the three formulas shown in Table.1.

Table 1: U-Value formula of existing literature

Literature	Equation
ISO 9869-1	$U_{HFM} = \sum_{j=1}^{n} \frac{q_j}{(T_{ij} - T_{ej})}$
ISO 9869-2	$U_{IRT-1} = \frac{Q}{(\theta_{ni} - \theta_{ne}) \times A}$
Albaciti et al, (2010) [1]	$U_{IRT-2} = \frac{\varepsilon \times \sigma \times (\theta_{se}^4 - \theta_e^4) + h_c(\theta_{se} - \theta_e)}{(\theta_i - \theta_e)}$

The HFM method used measurement data during 2023.02.20-27. The IR method used data from 00:00 to 6:00 for a total of 10 days, 2023.02.25-27, 03.04-06, 03.17-20. The HFM method was measured indoors, and the IR method was measured outdoors.

III. RESULTS

In this study, the applicability of the method for measuring the performance of a building in the field was analyzed through non-destructive insulation performance measurement from the outside of the building. Fig.1 shows the results of measuring the U-value of walls and windows through the method presented in the study.

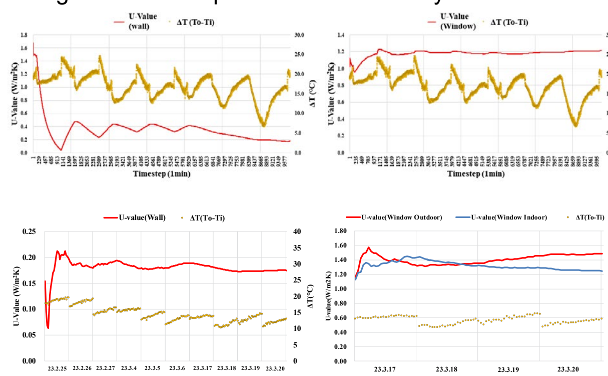

Figure 1: Results of measuring U-Value

The results of U-Value calculated by applying the HFM method showed a difference of about 1.63% compared to the design performance at 0.184 W/m^{2}K for walls and 1.218 W/m^{2}K for windows, showing a difference of about 3.91% compared to the design performance. The results of U-Value calculated by applying the IRT-1 method showed a difference within ± 10% compared to the design performance, with 1.247 W/m^{2}K indoors and 1.398 W/m^{2}K outdoor for windows. However, it was not possible to accurately measure walls. The result of U-Value calculated by applying the IRT-2 method was 0.175 W/m^{2}K for the wall, showing a difference of 3.11% compared to the design performance. However, it was impossible to accurately measure the windows.

ACKNOWLEDGEMENTS

This work is supported by the Korea Agency for Infrastructure Technology Advancement (KAIA) grant funded by the Ministry of Land, Infrastructure and Transport (grant number RS-2019-KA153277).

REFERENCES

1. Albatici, R., & Tonelli, A. M., “Infrared thermovision technique for the assessment of thermal transmittance value of opaque building elements on site”, Energy and Buildings, 42(11), 2177-2183, 2010.

Physics-Informed Neural Network-based Computational Solid Mechanics Model for Problems with Material Heterogeneity

Hye-eun Kong[1], **Pinlei Chen**[2]
[1, 2] Pennsylvania State University

I. SUMMARY

Carbon Fiber Reinforced Polymer composites (CFRP) are used in a broad range of applications from aerospace to marine industries due to their high strength-to-weight, high stiffness-to-weight, and high resistance to corrosion and fatigue. The additive manufacturing process accelerates designing CFRP composite; however, it inevitably produces complicated microstructures, high heterogeneous material phases, and complex interfaces. Modeling this type of structural material is challenging because it is difficult to solve the given partial differential equations (PDEs) either analytically or numerically.

Recently, Physics-Informed Neural Networks (PINNs) have gained popularity as a replacement for numerical methods for the approximation of PDEs, in which physics laws and equations are integrated into neural networks. PINNs can obtain the approximated solution of PDEs by optimizing parameters such as weight and bias; in other words, minimizing physics-based loss function that can be formulated in different ways based on different physics laws.

In this work, we create a PINN-based computational solid mechanics model for linear elastic problems and resolve displacement and stress fields resulting from heterogeneous material. Different loss functions such as the collocation loss function, the energy-based loss function, and the combination of these two are applied and compared in terms of the accuracy of the solution. Also, we are going to integrate the phase-field method into our PINN models and investigate a crack path in the heterogeneous material. The main objective of this work is to design a more accurate and robust PINN model that is specialized for material heterogeneity.

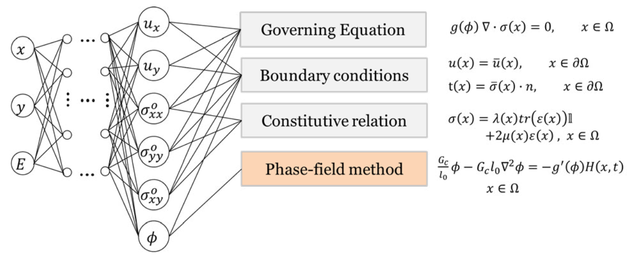

Figure 1: the architecture of the proposed PINN-based computational solid mechanics models

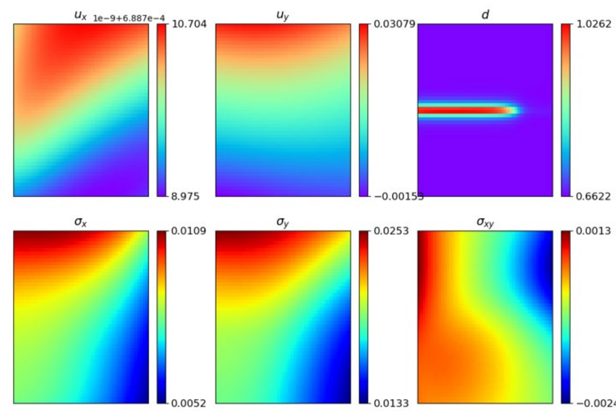

Figure 2: the simulation of the solid mechanics problem where E=0.5, t=0.0275, G_c=4.05e-2, l_0=0.04, ha=1/50, d(0<x<0.5, y=0.5)=1

REFERENCES

1. Bai, J. et al., "An introduction to programming Physics-Informed Neural Network-based computational solid mechanics", DOI: 10.48550/arXiv.2210.09060, 2022
2. Rezaei, S. et al. "A mixed formulation for physics-informed neural networks as a potential solver for engineering problems in heterogeneous domains: Comparison with finite element method", Computer Methods in Applied Mechanics and Engineering, 2022

Field Evaluation Plan of Connected Vehicle Identification System

B. Brian Park[1], **Zeyu Mu**[1], **Kun Yang**[1], **Cong Shen**[1], **Yixin Sun**[1]
[1]Link Lab, University of Virginia

I. SUMMARY

Our recent research has developed an algorithm identifying preceding vehicle connectivity and evaluated its performance in a simulation environment. To assess the feasibility of commercialization and the performance in the real world, this paper presents a field evaluation plan for a connected vehicle identification system, a prototype product to be assembled and tested in the real world. Our prototype system for an ego vehicle consists of a Jetson board, a Wi-Fi dongle, a GPS receiver, and a time-of-flight sensor. The field evaluation will utilize an ego vehicle and 3 additional vehicles (a combination of connected and unconnected vehicles).

II. Research Background and Motivations

Connected automated vehicles are recognized as a promising solution for improving the mobility and safety of urban transportation systems. This is because they can move like a train. For example, fully connected automated vehicles can form a cooperative platoon with as small as 0.6 seconds of time headway between vehicles, compared to human-driven vehicles requiring almost 2 seconds. To form a cooperative platoon, an ego vehicle needs to identify its immediately preceding vehicle's connectivity and establish communication to control its acceleration and braking cooperatively. However, due to privacy concerns, the basic safety messages do not include vehicle-specific information. This will be a challenge in the real-world deployment of cooperative platooning.

As noted, previous research by Park developed a preceding vehicle identification system (PVIS) and evaluated it using a high-resolution simulation based on real-world vehicle trajectory data. To ensure acceptable performance in the real world, it is proposed to develop a prototype system and conduct a field operation test.

III. Prototype System

Our primary goal is to assess the feasibility of commercialization of the prototype. Thus, we must ensure the system is reliable, secure, and applicable in real time. In addition, it has to be commercially viable.

A. Prototype System

While most university-level research prototype systems utilize Raspberry Pi boards, our team decided to use Nvidia's Jetson, which has a similar price range but is more powerful, especially in artificial intelligence and machine learning applications. To enable distance measurements between the ego vehicle and a preceding vehicle, we plan to use an affordable time-of-flight (TOF) sensor. A high-end lidar sensor (e.g., Ouster or Velodyne) will be used to obtain semi-ground truth measurements. The preceding vehicle identification system determines the connectivity of its preceding vehicle by comparing the distance and speed between the ego vehicle and potential preceding vehicles measured by the TOF sensor and GPS devices. In our prototype system, each connected vehicle will have a Jetson device with a Wi-Fi dongle and a GPS receiver, while unconnected vehicles will not have such devices.

IV. Field Evaluation Plan

The team plans to test the GPS receiver, an ad-hoc Wi-Fi communication, and the TOF distance and speed measurements. Once these measurements are collected and validated, the team will conduct field tests at a parking lot and then on real-world roads. We will ensure the safety of drivers/vehicles during the test. The performances will be measured based on (i) an error misidentifying an unconnected preceding vehicle as a connected vehicle (the worst case), (ii) an error misidentifying a connected vehicle as an unconnected vehicle, and (iii) the computation time needed to identify the connected vehicle. The team will pursue commercialization of this technology and prototype system.

ACKNOWLEDGEMENTS

This research is funded by the Commonwealth Cyber Initiative's commercialization funding and partly by the National Science Foundation under Grant No. (CMMI-2009342).

Common Data Requirements for Digital Twin Data Interoperability in Capital Projects

John Oh[1], H.David Jeong[2], Ashrant Aryal[3]
[1,2,3]Texas A&M University

I. SUMMARY

Digital Twin (DT) in the process industry is expected to improve physical assets' functionality through cyber-physical automated data interaction and simulation. Various studies demonstrate that asset lifecycle management would mostly benefit from DT applications. In order to maximize such benefits, careful examination of how data is handed over from Design to Operation & Maintenance (O&M) is necessary. However, current data standards fail to address common data requirements among heterogeneous data sources and formats for the data handover process, which hinders automatic and seamless data exchange. This research proposes a common data requirements definition for interoperable data exchange from Design to O&M.

II. COMMON DATA REQUIREMENT FOR DESIGN-O&M DATA INTEROPERABILITY

A. Current Practice of Design-O&M Data Exchange
The proposed framework is intended to align with the current data exchange practice for prospective industry applications. Engineering, Procurement, and Construction (EPC) firms create the design data and deliver it to the Owner and Operator (O/O) Group for O&M application (Figure 1). Piping & Instrumentation Diagram (P&ID) and 3D models are the major design data used in the design phase, which bears necessary data for the O&M phase.

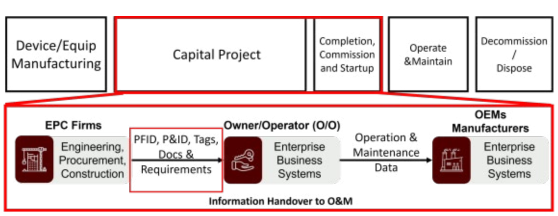

Figure 1: Process Plant Asset Lifecycle and Data Exchange between Project Participants

B. Common Data Requirements from Existing Standards

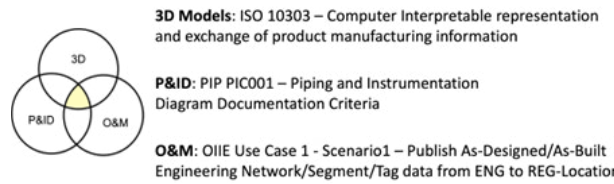

Figure 2: Common Data Requirement from Industry Standard for Design – O&M data

Data requirements for Design and O&M from industry standards were examined to identify common data requirements from the standards (Figure 2). It was intended to identify essential components among heterogeneous data sources and formats. Below is the list of common data requirements.

- Equipment Specification - Plant item category (Identifier, tag, classification)
- Equipment Specification - Plant item property (Engineering properties)
- Plant Breakdown Structure
- Port /Nozzle
    - Connection type, classification
    - Position (coordinate and direction)
- Functional Location (Location-based definition)

III. CONCLUSION
This research has defined common data requirements for interoperable data exchange from Design to O&M with existing standards. This would assist in enhanced standards-based data interoperability between design and O&M data without reinventing an entire data exchange system from the beginning. It would also potentially benefit data exchange within the process plant DT system by bridging different data sources and formats involved in DT data exchange.

REFERENCE
1. H. Lee, "Neutral model-based interfacing of 3D design to support collaborative project management in the process plant industry", *Journal of Computational Design and Engineering*, 2021

Heat Stress Conditions and Awareness of Roofers in South Texas

Min Jae Suh[1], Kenneth Sands II[2], Euijin Yang[1], Pristine Hysten[1]
[1]Sam Houston State University, [2]Auburn University

I. SUMMARY

The numerous construction projects currently underway in South Texas are experiencing serious problems due to the high temperatures in the summer. Especially, roofers are exposed to a direct heat from the sun and an indirect heat from roof materials. This study observed roofer's preparation against heat stress and measured the changes of their core body temperatures.

II. Heat Stress and Roofers

McCann (2000) mentioned roofers have one of highest work-related death rates in a construction project due to fatal falls. Also, heat exhaustion was singled out as another main cause of work-related death because it might be a factor that contribute to fatal falls from a roof. The CRCA (2016) noted heat stress resulted physiological responses such as fogged-up safety glasses, and dizziness. David et al. (2021) found the numbers of deaths caused by heat stress were almost double in the last 10 years compared to the previous decade in Texas and five of the dozen employers who had lost multiple employees due to heat stress in the U.S. were in Texas. This research monitored roofer's preparation against heat stress and measured the changes of roofer's core body temperature at a residential project in South Texas.

III. Case Study: Roofers for Residential Project

A case study is a residential project in Houston metropolitan area, and the project was replacing a roof with asphalt shingles and sidings with hardboards for 2 weeks in August 2022. There were four roofers on a jobsite, and they were all males who were the age from early 20s to late 40s. Two out of four roofers were volunteered to wear a core body temperature for monitoring the changes of their body temperature during the project (Figure 1).

Figure 1: Overview of project, rest station, and wearable core body temperature sensor

IV. Observation Results

A roofing company was a local company, and they had no in-house policy or guideline for heat stress prevention. The roofers had no awareness of heat stress risks on their jobsite, and they prepared what they did at previous projects. The roofers took a few breaks under a shade irregularly and provided sufficient fluids for adequate hydration. At the end of most of the days during this project, their fluid supply was short, and their cooler was empty. Moreover, the range of their core temperature was between 97.9 F° (36.6 C°) and 100.3 F° (38.0 C°) as the below figure. Even if they took a break under a shade, the lowest core body temperature was still higher than researcher's expectation.

Figure 2. The change of core body temperature

The employer needed to build a systematic guideline to provide sufficient fluids and cool down employee's core body temperature. When the guideline was published, a training or education should be offered by the employer to prevent from heat stress risks in construction projects.

ACKNOWLEDGEMENTS

The study is financially supported the Foundation of Roofing Alliance (NRCA).

REFERENCES

McCann M. (2000). Causes of roofer deaths, https://elcosh.org/record/document/1428/d000491.pdf

CRCA (2020). Canadian Roofing Reference Manual, https://roofingcanada.com/docs/canadian-roofing-reference-manual/chapter-1-safety/1-1-general-safety/1-1-5-exposure/.

David, N., Shipley, J., Chavez, S. M., and Ernst, Sara (2021). Texas workers are dying in the summer heat, and companies aren't being held accountable, https://www.texasstandard.org/stories/texas-workers-are-dying-in-the-summer-heat-and-companies-arent-being-held-accountable/.

Fenton-like catalytic ceramic membrane hybrid system for the advanced water treatment

Youngkun Chung[1], Michael S. Wong[1], Seoktae Kang[2,*]
[1]Department of Chemical and Biomolecular Engineering, Rice University,
[2]Department of Civil and Environmental Engineering, Korea Advanced Institute of Science and Technology

I. SUMMARY

The overall goal of this research was to develop a catalytic advanced oxidation processes (AOPs)-ceramic membrane hybrid process for the advanced water treatment. In order to overcome the limitation of heterogeneous Fenton-like reaction catalysts associated with the insufficient generation of hydroxyl radicals (·OH) at near-neutral pH, a novel heterogeneous catalyst was developed and applied in ceramic membrane-based flow system.

II. MATERIALS AND METHODS

Preparation of Fenton-like catalysts

To enhance the Fenton-like reaction at the oxygen vacancies in CeO_2, the Sm doped CeO_2 (SDC) catalysts were synthesized by sol-gel methods [1]. Finally, SDC doped ceramic membrane (SDC@CM) were prepared by pore filling and impregnation coating methods to promote contact between pollutants and generate reactive oxygen species (ROS) inside the confined pores (**Figure 1**).

Performance of H_2O_2-SDC@CM hybrid system

The performance of SDC@CM was tested using 10 mg/L humic acid and selected micropollutants with 10 mM H_2O_2 at pH 7. To evaluate the effect of flux on the removal of CECs, the flux of membranes was controlled from 10 L/m^2/h (LMH) to 300 LMH, which corresponds to a certain contact time between pollutants and H_2O_2 inside pore walls.

III. RESULTS AND DISCUSSION

The activity of heterogeneous Fenton-like catalyst was maximized by adding 20% Sm in CeO_2 (SDC) by promoting the redox cycle of cerium ion. The synergistic effect for enhancing the generation of ·OH was verified using analysis of electron spin resonance and cyclic voltammogram.

The prepared SDC@CM hybrid system showed excellent performance of mineralization with over 80% of total organic carbon (TOC) removal efficiency on selected micropollutants and humic acid at 80 s of contact time (20 LMH of flux) at neutral pH. This is because increased contacts between pollutants and ·OH in the membrane surface and confined pore structures lead to the enhanced conversion of H_2O_2 into ·OH.

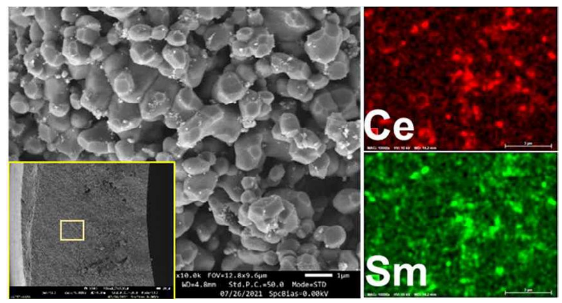

Figure 1: Scanning electron microscopy (SEM)-energy dispersive spectrometry (EDS) images on the cross-section of $SmCeO_2$ ceramic membrane.

IV. CONCLUSION

The H_2O_2-SDC@CM hybrid system was successfully developed by a novel coating method, thus being an effective strategy for enhancing the efficiency of Fenton-like reaction at neutral pH conditions associated with the compact, simple, and continuous system as a mobile advanced water treatment module.

ACKNOWLEDGEMENT

This work was supported by the National Research Foundation of Korea (NRF) (Grant No. NRF-2020R1A2C3012639) funded by the Ministry of Science and ICT (MSIT).

REFERENCE

1. Kyeounghak Kim, Jeong Do Yoo, Siwon Lee, Minseok Bae, Joongmyeon Bae, WooChul Jung, and Jeong Woo Han, “A Simple Descriptor to Rapidly Screen CO Oxidation Activity on Rare-Earth Metal-Doped CeO2: From Experiment to First-Principles”, ACS Applied Materials & Interfaces, Vol. 9, No. 18, pp. 15449-15458, 2017.

Development of Smart Harmful Algal Bloom (HAB) Detection System Using Unmanned Aerial Vehicle (UAV) and Hyperspectral Sensor

Da Yun Kwon[1], Seungkwan Hong[2], Jae Hyeon Ryu[3]
[1, 2] Korea University, [3] University of Idaho

I. INTRODUCTION

The frequency of Harmful Algal Blooms (HABs) is increasing due to rising global temperatures and climate change. HABs not only harm aquatic ecosystems but also decrease the performance of surface water treatment plant operations. As a result, the importance of early detection systems of HABs has been emphasized, and the combination of machine learning and Unmanned Aerial Vehicles (UAVs) has emerged as an intelligent algal bloom monitoring technology (Alayande et al., 2022). In this study, a hyperspectral sensor is mounted on a UAV to obtain image data of HAB. With the hyperspectral image data and the ground truth data, the early HAB detection system is developed.

II. Materials and Methods

A HAB detection model has been developed using images obtained through a hyperspectral sensor and the ground truth data.

A. Study Area

Lake Lowell in Nampa has experienced high concentrations of toxin-producing cyanobacteria in the last few years due to warm temperatures and nutrient inflow. These blue-green algae blooms can be harmful to living being, so that continuous HAB monitoring is required.

B. Sensors

BaySpec OCI-F hyperspectral sensor, which has 120 spectral bands, is mounted on a UAV to collect HAB images. For ground truth data, water samples are collected for lab analysis, and an *Aqua Troll 400* Bundle W/5' cable for Android & iOS is used for in-situ water quality data measurement (pH, dissolved oxygen, temperature, salinity, total dissolved solids, chlorophyll, cyanobacteria (algae) concentration).

C. Software

The software built in software is used to develop the model which can convert the hyperspectral image data to HAB concentrations.

III. Results and Discussion

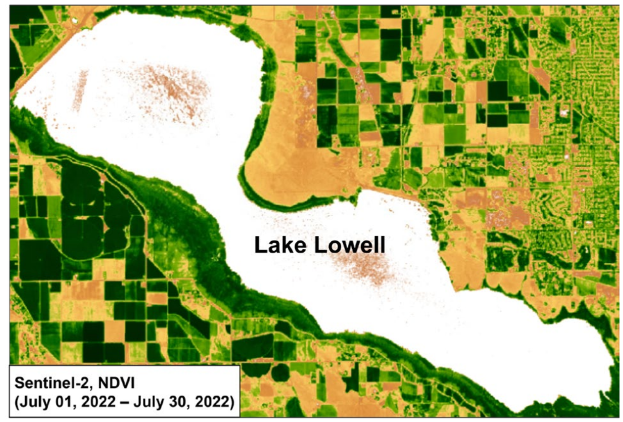

Figure 1: Concentration map of HABs in Lake Lowell, Idaho.

Hyperspectral images enable the measurement of HAB concentrations and other water quality parameters indirectly. The green-blue algae found every summer in Lake Lowell exhibit a high correlation with the near-infrared wavelength region. Figure 1 depicts the concentration map of HABs based on the model developed in this project. By using UAV and hyperspectral sensor, indirect and remote measurement of HAB become possible. For future research, a real-time HAB monitoring system could become possible by utilizing various IoT and communication facilities.

ACKNOWLEDGEMENTS

This work was supported by the National Research Foundation of Korea (NRF) grant funded by the Korea government (MSIT) (Project No. 2022M3J7A1066428).

REFERENCES

1. Abayomi, A. B., Lim, J., Kim, J., Hong, S., Al-Amoudi, A. S., Park, B. (2022), “Fouling Control in SWRO Desalination During Harmful Algal Blooms: A Historical Review and Future Developments,” *Desalination*, Vol. 543, pp. 166094, 2022.

Multiple heavy metal detection in greywater using a novel MoS_2-chitosan-based electrochemical sensor

Jong-Hyun Baik[1] and Woo Hyoung Lee[1,*]

[1]Department of Civil, Environmental, and Construction Engineering, University of Central Florida, USA.

SUMMARY

Heavy metal detection in greywater is becoming important with the increasing practice of water reuse worldwide. Here, we report a novel MoS_2-chitosan-based electrochemical sensor for the rapid and simple electrochemical detection of heavy metal ions (Pb and Cd). The modified sensors showed improved sensitivity with a lower limit of detection (LOD) of Pb^{2+} (1.67 ppb) and Cd^{2+} (3.56 ppb).

Keywords: Electrochemical detection, cadmium (Cd), greywater, heavy metal, lead (Pb), MoS_2 sensor

I. Introduction

As water scarcity and the need for sustainable water management continue to grow, water reuse has become a viable solution to meet water demand in many regions. Greywater, being a potential source for water reuse, requires careful monitoring and treatment to ensure its safety for various applications such as irrigation, toilet flushing, and industrial processes. While conventional analytical methods like ICP-MS are highly accurate and sensitive to heavy metal detection, they often come with certain disadvantages such as high cost, complexity, and the need for specialized equipment and skilled operators. It is urgent to develop a simple and easy detection method for heavy metals in water. The electrochemical method can be an alternative to these conventional methods. The main objective of this study is to develop a novel biopolymer-based electrochemical sensor for rapid and simple heavy metal detection in greywater.

II. Materials and Methods

In this study, chitosan and molybdenum sulfide (MoS_2) was used as a biopolymer and catalytic absorbent, respectively, to improve the sensitivity and stability of electrochemical heavy metal detection at low levels in water. To fabricate the sensor, MoS_2 and chitosan were electrochemically deposited on a carbon screen-printed electrode (SPE) (RRPE1001C, Pine Research Instrumentation, Durham, NC, USA). The MoS_2 solution and biopolymer solution were prepared following the previous studies [1, 2]. The square wave anodic stripping voltammetry technique (SWASV) was used to detect trace concentrations of Pb^{2+} and Cd^{2+} in the concentration range of 0 – 20 ppb. Ag/AgCl electrode was used as a reference electrode. 0.1 M AcB at pH 4.5 was used as a buffer solution for the measurements.

III. Results and Discussions

The XPS and SEM/EDS analysis demonstrated that MoS_2 and chitosan were successfully coated to the carbon SPE surfaces. The experimental setup was as follows: Deposition potential of -1.2 V, deposition time of 300 s, potential step of 0.004 V, amplitude of 0.05 V, and frequency of 20 Hz. Figure 1 shows the electrochemical Pb^{2+} and Cd^{2+} detection in 0.1 M AcB at pH 4.5 using the developed MoS_2-chitosan-modified electrode. (0, 2, 5, 10, and 20 ppb). Compared to the bare carbon SPE, the sensitivity of the MoS_2-chitosan-modified electrode sensor was 1.7 – 1.9 times higher. LOD of Pb^{2+} and Cd^{2+} was 1.67 ppb (SD: 0.58) and 3.56 ppb (SD: 0.08), respectively.

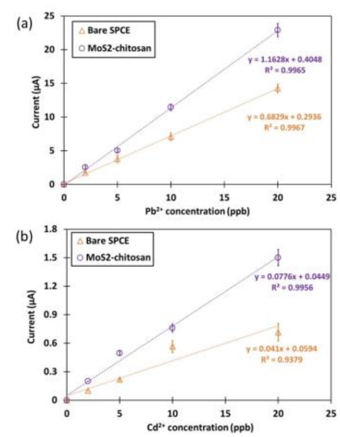

Figure 1: Electrochemical heavy metal detection removal using a MoS_2-chitosan coated SPE sensor.

ACKNOWLEDGEMENTS

This research was supported by Mainstream Engineering Corporation.

REFERENCES

1. Hwang, J.-H., et al., *Recycling urine for bioelectrochemical hydrogen production using a MoS2 nano carbon coated electrode in a microbial electrolysis cell.* Journal of power sources, 2022. **527**: p. 231209.
2. Hwang, J.-H., et al., *A novel Fe-Chitosan-coated carbon electrode sensor for in situ As (III) detection in mining wastewater and soil leachate.* Sensors and Actuators B: Chemical, 2019. **294**: p. 89-97.

Purification of Phosphoric Acid Manufacturing Process Water with Recovery of Critical Materials using MCDI

Jun Kim[1], **Patrick Zhang**[1,2]
[1]Florida Polytechnic University, [2]Florida Industrial and Phosphate Research Institute

I. INTRODUCTION

Every year, the United States consumes more than 20 million tons of phosphate rock mainly for producing fertilizers. Phosphoric acid is also used in everything from food and cosmetics to animal feed and electronics. During the phosphate mining process, the production of highly saline process water with phosphate ion (PO_4^{3-}) is inevitable. Meanwhile, the process water contains an appreciable amount of critical rare earth elements (REEs), such as Y, Dy, Gd, Pr, and Nd[1]. The extraction of REEs has great potential economic benefits when properly recovered from the process water. Membrane capacitive deionization (MCDI) is an ion-selective electrochemical water treatment process for various hazardous contaminants and targeted elements using microporous carbon electrodes and ion-exchange membranes[2]. Kim et al. demonstrated a higher adsorption rate of multi-valent cations and anions, thus MCDI can be further used for resource recovery, especially for trivalent REEs (3+) and phosphate (3-) ions.

II. MATERIALS AND METHODS

A. MCDI reactor

In this study, the membrane capacitive deionization (MCDI) reactor is composed of supercapacitor carbon hydrogel electrodes on titanium substrates, a cation and anion exchange membrane (CEM and AEM) with a spacer in-between. DC 1.2V is applied for electrosorption and reversed voltage (DC -1.2V) is for complete discharge and electrode regeneration.

B. Measurement

A quadrupole inductively coupled plasma - mass spectrometry (ICP-MS, PerkinElmer, NexION 350X) is utilized for the analysis of water samples.

C. Ion-selectivity

The performance of the MCDI is under evaluation in a flow-through cell using binary electrolyte solutions. The total ion adsorption capacity of the electrode remains the same with and without the nanocomposite coating. However, the MCDI reactor demonstrates selectivity towards trivalent cations and anions over the monovalent cations and anions, respectively.

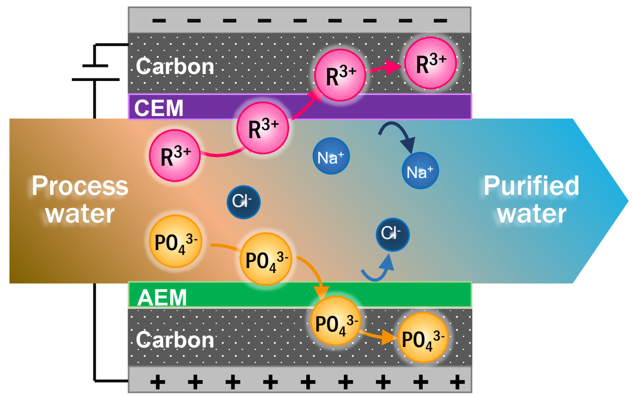

Figure 1: Membrane capacitive deionization process diagram

Table 1: General phosphate process water quality

Parameter	Concentration	Unit
Turbidity	~1.0	NTU
TDS	~40k	mg/L
PO_4^{3-}	~20k	mg/L
SO_4^{2-}	~6k	mg/L
Na^+	~2k	mg/L
REEs	1-2k	mg/L

ACKNOWLEDGEMENTS

This research is part of the Florida Industrial and Phosphate Research (FIPR) Institute projects.

REFERENCES

1. Zhang et al., "The ultimate mineral processing challenge: Recovery of rare earths, phosphorus and uranium from Florida phosphatic clay", Minerals & Metallurgical Processing, 34, 183-188, 2017.
2. Kim et al., "Selective Removal of Calcium Ions from Water Using Target-ion Specific Capacitive Deionization", Water Research, 160, 445-453, 2019.

An Electrical Heating Technique for Environmentally Friendly Winter Maintenance of Transportation Infrastructure

Rajesh Chakraborty[1], Ramita Mohapoo[1], In-Hyouk Song[1], Han-Jin Oh[2], Jung Heum Yeon[1]
[1]Texas State University, [2]Seoul Institute of Technology

I. Introduction

Ensuring drivers' safety has been one of the most critical issues facing our society. According to the nation's icy road accident statistics by the USDOT Federal Highway Administration, the icy road fatality count is 3.6 times the total deaths from all other weather hazards.

Considering the issues with the current winter road maintenance, this study developed an eco-friendly solution to snow and ice removal using an electrical heating technique. This idea will provide a promising solution for enhanced winter road maintenance of roadway/airport runways, improved public safety, and substantial social cost savings.

II. Experimental Program

A. Materials

To formulate an electrically conductive concrete mixture, unsized chopped carbon fibers, multi-walled carbon nanotubes, fiber dispersing agent, conductivity-enhancing agent, air-entraining agent, and high-range water reducer were used at specified mixture proportions in addition to cement, water, and coarse and fine aggregates.

B. Test specimens

A 55 cm wide, 55 cm long, and 25 cm thick concrete slab was cast, of which only the top 5.5 cm was cast with the conductive concrete while the rest 19.5 cm was cast with normal concrete. Four sides of the specimen were insulated with 5 cm-thick foam boards to minimize heat loss. Two #3 rebars were embedded at a distance of 30 cm as electrodes. Thermocouples were installed at various locations to measure the temperature rises. The specimen was treated at -5°C before testing.

C. Equipment and operation scheme

A 4 kW-capacity AC power supply was used to power the slab. The power density of 1,200 W/m^2 was maintained throughout the heating test to heat the slab surface by 20°C in 2 hours of power supply.

III. Results

Figure 1 shows the surface temperature rise in the middle between the electrodes. About 20°C temperature increase in 2 hours was observed. Much more pronounced temperature rises were noted above the electrodes. **Figure 2** illustrates the surface temperature profile measured by an infrared camera at 2 hours of testing.

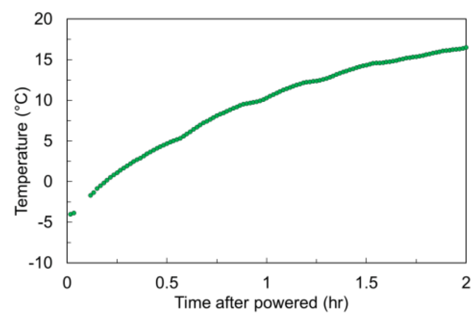

Figure 1: Surface temperature rise in the middle

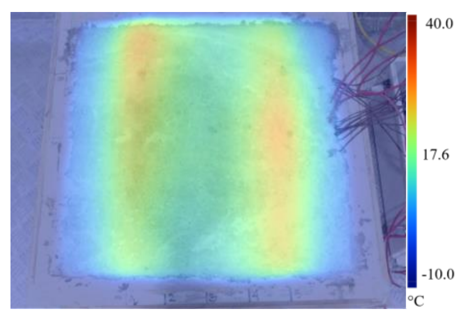

Figure 2: Surface temperature profile by IR camera

ACKNOWLEDGEMENTS

This research was supported by a grant (20014561) of the Regional Customized Disaster-Safety R&D Program, funded by the Ministry of the Interior and Safety, South Korea.

REFERENCES

1. M.U. Salim, F.M. Nishat, T. Oh, D.-Y. Yoo, Y. Song, T. Ozbakkaloglu, and J.H. Yeon, "Electrical Resistivity And Joule Heating Characteristics of Cementitious Composites Incorporating Multi-Walled Carbon Nanotubes And Carbon Fibers," *Materials*, Vol. 15, No. 22, pp. 8055, 2022.

Pathways to a Just Transition: Bridging Regional Inequality of Clean Energy through Hydrogen

Gina Yeonkyeong Park
Department of City and Regional Planning, Cornell University

I. SUMMARY

The United States have regional inequality problem in clean energy development. The Great Plain States have the largest carbon emissions from electricity production, while most disadvantaged communities are located (Figure 1). To enhance energy justice, until the efficient and affordable hydrogen technology is developed in the short run, Liquified Natural Gas (LNG) can be imported and stored at LNG ports with some modification to meet the increasing electricity demand. In the long run, with the great hydrogen potential from dominant renewable resources (e.g., Wind, Solar) in the Great Plain States, green hydrogen can be produced under long-term investment driven by local incentives and subsidies.

II. RESULT

Regional energy disparities in electricity generation can be reduced by implementing two strategies. First, before renewable energy plants become fully operational, hydrogen can be imported, stored underground, and distributed through existing Liquified Natural Gas (LNG) ports (Figure 2) after modification as a short-term strategy. Secondly, in the long run, green hydrogen can be produced in the Great Plain States, which have the greatest geographical potential (Figure 3) for hydrogen production using wind and photovoltaic sources, making it more cost effective and carbon efficient.

III. ILLUSTRATIONS

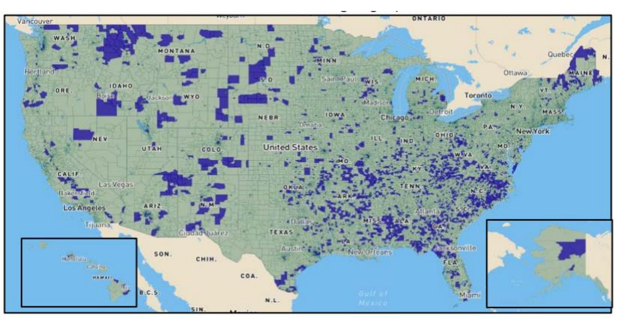

Figure 1: Distribution of Disadvantaged Communities at the Census Tract Level Defined by US Department of Energy (2022)

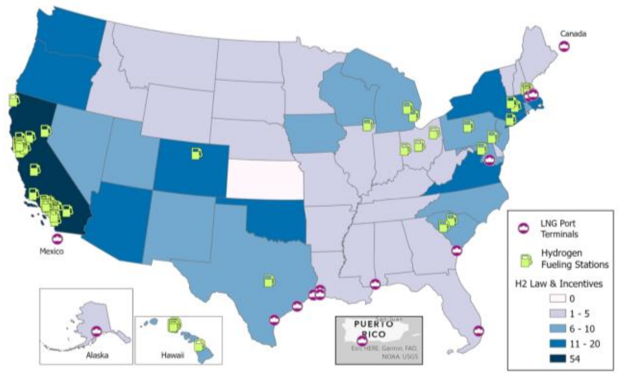

Figure 2: Spatial Distribution of LNG Ports and Hydrogen Charging Stations by Existing Regulation and Incentives

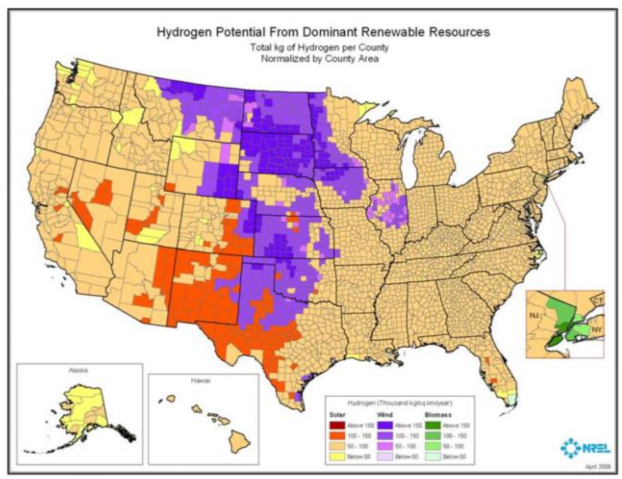

Figure 3: Distribution of Green Hydrogen Potential

ACKNOWLEDGEMENT

This research was sponsored by Cornell Program in Infrastructure Policy (CPIP).

REFERENCES

1. Chen, P. S. L., Fan, H., Enshaei, H., Zhang, W., Shi, W., Abdussamie, N., ... & Yang, Z. (2023). A review on ports' readiness to facilitate international hydrogen trade. *International Journal of Hydrogen Energy*.
2. Vichos, E., Sifakis, N., & Tsoutsos, T. (2022). Challenges of integrating hydrogen energy storage systems into nearly zero-energy ports. *Energy*, *241*, 122878.

[SEED2023] Development of On-site Quality Management System for Asphalt Pavement Using IoT

Dong Hyuk Kim[1]
[1]University of Georgia

I. SUMMARY

Asphalt pavement quality can deteriorate due to problems such as temperature and compaction at the construction site[1]. However, accurate and dense evaluation of temperature and compaction is not possible with existing quality management systems. Therefore, it was developed that the technology to match blueprint information and on-site smart sensing information using IoT(Internet of things) as shown in Figure 1. Table 1 shows the sensors and devices attached to each equipment. The developed technology can precisely link blueprint information and RTK(Real-time kinematic positioning) GNSS(Global navigation satellite system) information to find out precise location information of each equipment. In addition, the smart sensor attached to the equipment can measure the temperature and compaction of the asphalt pavement in real time and transmits the data to the LTE(Long term evolution) module. The transmitted data can be analyzed on the platform and delivered to field supervisors and operators. Currently, this system is being pilot-applied in Korea, and commercialization research is planned in the future.

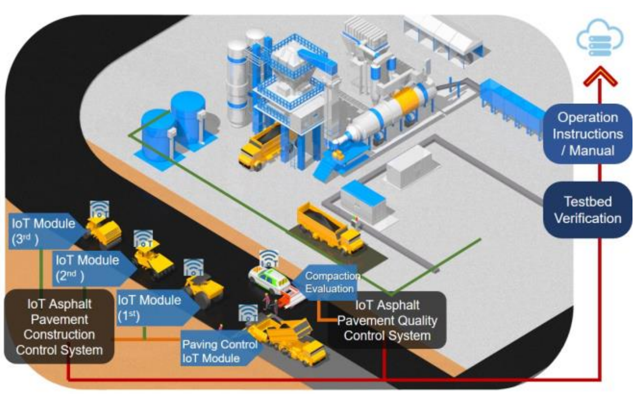

Figure 1: On-site Quality Management System for Asphalt Pavement

Table 1: Sensors and Devices attached to Each Equipment

Equipment	Sensors and Devices
Asphalt Paver	Infrared Camera
	Monitor
	Integrated Board
	RTK GNSS
	LTE Module
	Climate Sensor
	Beacon
Compaction Roller	Accelerometer Sensor
	RTK GNSS
	LTE Module
	Monitor
	Analysis Board
	Infrared Sensor
Compaction Test Equipment	GPR Sensor
	RTK GNSS
	Range Sensor

ACKNOWLEDGEMENTS

This work is supported by the Korea Agency for Infrastructure Technology Advancement (KAIA) grant funded by the Ministry of Land, Infrastructure and Transport Grant RS-2019-KA152690.

REFERENCES

1. Beainy, F., Commuri, S., and Zaman, M., "Quality Assurance of Hot Mix Asphalt Pavements Using the Intelligent Asphalt Compaction Analyzer," *Journal of Construction Engineering and Management*, Vol. 138, No. 2, pp. 178-187, 2012.

Multifunctional Flexible Sensor for Temperature and Strain Detection

Bo Mi Lee[1], Wen Shen[1]
[1]University of Central Florida, Department of Mechanical and Aerospace Engineering,
Functional Materials and Devices Lab

I. SUMMARY
This study presents the development of flexible, multifunctional PEDOT:PSS-based sensors, capable of concurrent mechanical strain and temperature measurement. These sensors were successfully fabricated using the extrusion-based direct ink writing method, promising advancements in sensor technology.

II. Introduction and Background
Flexible sensors, capturing intricate physical and environmental parameters, are growing focus in scientific research and technological development[1]. Traditionally, multifunctional sensing devices have been achieved through the integration of multiple sensors within one architecture. Despite the advances, they suffer from complicated fabrication process, circuit design, and signal processing[2]. In this study, we developed 3D-printed, multifunctional sensors based on PEDOT:PSS composites. These leverage independent piezoresistive and thermoelectric properties for simultaneous mechanical strain and temperature monitoring, thereby streamlining sensor technology.

III. Results and Discussions
A. PEDOT:PSS-based Sensor Fabrication
The fabrication of the PEDOT:PSS-based sensor began with the preparation of a 3D printable ink. First, the PEDOT:PSS aqueous solution was stirred overnight. Then, 5 *wt.*% of dimethyl sulfoxide and 15 *wt.*% of polyethylene oxide (*Mv* = 100,000) were introduced into the solution and magnetically stirred for four hours in a water bath maintained at 43 °C. The PEDOT-PSS ink and silver flake inks were loaded into three separate 3-cc syringe barrels of the BIOX 3D Bioprinter. PEDOT:PSS-based ink was printed on a poly(dimethylsiloxane) film that was fabricated in the lab. Then, silver flake ink was printed on the two ends of the PEDOT:PSS film and annealed on the head bed at 80 °C for 3 hours.

B. Simultaneous strain and temperature sensing capabilities of PEDOT:PSS-based composites
The piezoresistive and thermoelectric properties of the PEDOT:PSS-based composites facilitated strain and temperature sensing, respectively, with no observed crosstalk between the two functions. The PEDOT:PSS sensor was subjected to 3%ε while a temperature difference was applied across the electrodes. A Keithly SourceMeter 2400 was used to apply a voltage sweep from -500 μm to 500 μm, concurrently measuring the resulting current responses. The results are summarized in Figure 1. Uncoupled temperature and strain sensing are facilitated through the independent piezoresistive and thermoelectric effect. The strain and temperature can be determined by measuring the slope change and x-intercept of the I-V curve, respectively.

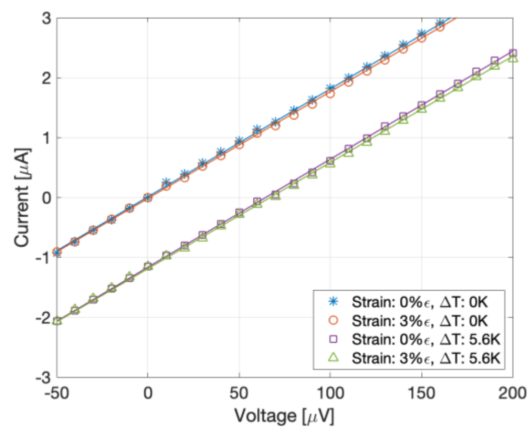

Figure 1: The electrical current responses of PEDOT:PSS sensors as a function of applied voltage

ACKNOWLEDGEMENTS
This research was supported by the College of Engineering & Computer Science, University of Central Florida.

REFERENCES
1. Luo Y. *et al.*, "Technology Roadmap for Flexible Sensors," *ACS Nano*, Vol. 17, No. 6, pp. 5211-5295, 2023.
2. Heikenfeld J. et al., "Wearable sensors: modalities, challenges, and prospects," Lab on a Chip, Vol. 18, pp. 217-248, 2018.

Assessment of Thermal Comfort in Response to Urban Spatial Changes

Seoyoung Lee[1,2], Junseok Hwang[1,2]
[1]Technology Management, Economics and Policy Program, Seoul National University
[2]Integrated Major in Smart City Global Convergence, Seoul National University

I. INTRODUCTION

This research aims to explore the relationship between urban spatial changes and thermal comfort, with a specific focus on assessing the impact of these changes on human well-being. By evaluating the thermal comfort conditions in different urban settings, we can gain insights into the effectiveness of various urban design strategies and interventions in enhancing thermal comfort.

II. METHODOLOGY

A. Finding the most vulnerable area in Seoul

In this paper, high vulnerability areas are identified by utilizing meteorological temperature data to assess the intensity and duration of heat events in different regions.

Through simulations and thermal analysis, we aim to quantify the benefits of changing spatial structure and mitigation strategies in enhancing thermal comfort and reducing the urban heat island effect.

B. Measurement of thermal comfort

For the simulations and analysis of thermal comfort, the software program ENVI-Met is utilized. we examined not only the temperature but also the levels of thermal comfort using the PET (Physiological Equivalent Temperature) and PMV (Predicted Mean Vote) indices.

B-a. The transformation of urban structure

To compare the thermal comfort of urban structures, we employed GIS and programs to create two models: one representing the current urban structure and the other simulating a redevelopment plan. The redevelopment plan includes an increase in floor area ratio (FAR), resulting in the formation of wind corridors, and the expansion of green spaces.

B-b. Application of Mitigation Strategies

To investigate the effectiveness of mitigation strategies, we explored the use of cool pavements and cool roofs. Cool pavements and Cool roofs involve using materials with high solar reflectance to reduce the absorption of solar radiation and minimize heat buildup on paved surfaces.

III. RESULT

Based on the A process, three areas with high vulnerability have been identified: Jamsil, Jangwi, and Jongno.

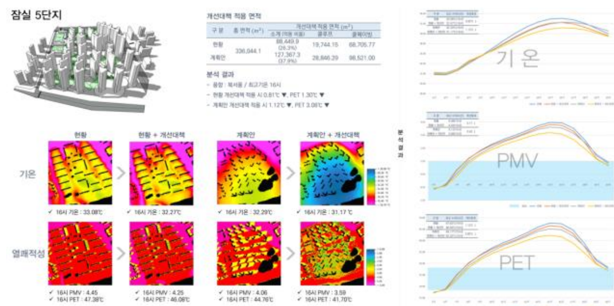

Figure 1: Example results of Jamsil

By altering the urban structure and implementing mitigation factors, the simulation results showed an improvement in thermal comfort in the following areas:

Table 1: PET Improvement

Site	status	Max(℃)	Effect(℃)
Jamsil	Current	47.62	-5.3
	Plan + Mitigation	42.32	
Jangwi	Current	47.97	-6.85
	Plan + Mitigation	41.12	
Jongro	Current	42.70	-1.36
	Plan + Mitigation	41.34	

IV. CONCLUSION

These results indicate that the implemented changes and mitigation measures had a positive impact on the thermal comfort of the respective areas.

ACKNOWLEDGMENTS

This research was supported by the BK21 FOUR (Fostering Outstanding Universities for Research) funded by the Ministry of Education (MOE, Korea) and National Research Foundation of Korea (NRF).

Technical Group C-6

Electrical and Computer Engineering (ECE)

Fabrication of OLED Lighting Auxiliary Electrode by Self-aligned Inkjet Printing Process

Sang-Ho Lee[1], **Sung-min Sim**[1], **Jun Ho Yu**[1], **Kwan Hyun Cho**[1]
[1] Korea Institute of Industrial Technology

I. SUMMARY
This study introduces a self-aligned inkjet printing process to control the reliable line-width with minimizing the shadow area of printed auxiliary electrodes. A silver-insulator bilayer was self-aligned by a hydrophobic bank where the ink did not spread during inkjet printing. The insulator was implemented to fit the line width of the Ag electrode. Also, electro-optical characteristics of 40×40 mm^2 OLED lighting were measured to confirm the effect of the fabricated auxiliary electrodes.

II. INTRODUCTION
Auxiliary electrodes are a key component to reduce voltage drop for uniform luminance of large area organic light emitting diode (OLED) lighting. But, the auxiliary electrode forms a shadow area blocking the light emission by an opaque metal electrode and an insulating layer. The main objective of this paper is to develop an auxiliary electrode printing process to minimize the shadow area due to the auxiliary electrodes after insulator printing. We implemented a self-aligned bilayer inkjet printing (SABP) process to minimize the shadow area. It was possible to fabricate a narrow insulator-cover fitted to the width of the Ag electrodes. Furthermore, OLED lightings without or with auxiliary electrodes were fabricated to verify the effect of the auxiliary electrodes.

III. RESULTS AND DISCUSSION
The auxiliary electrodes were fabricated by Ag and insulator inkjet-printing in the channel formed by a hydrophobic bank. The bank acted as a line width control for the self-alignment of Ag electrodes and insulators. The height and width of three-times printed Ag electrodes were 604 nm and 20.9 nm. The auxiliary electrodes fabricated using the SABP process had the height of 1.09 μm, a width of 21.1μm, and an insulator-covered margin of 200 nm at the edge of the Ag electrodes. The fabricated auxiliary electrodes were employed in an OLED lighting device, and device performance was verified. A 40×40 mm^2 OLED lighting with fabricated auxiliary electrodes emitted red light with no short-circuit problems. The effects of the auxiliary electrodes were analyzed using the J-V-L characteristics measurement results. The OLED lighting with three-times printed Ag electrodes showed improved luminance uniformity of 22%p. At 1000 cd/m^2 luminance, the current efficiency and external quantum efficiency were improved by 1.1 cd/m^2 and 0.9%p, respectively.

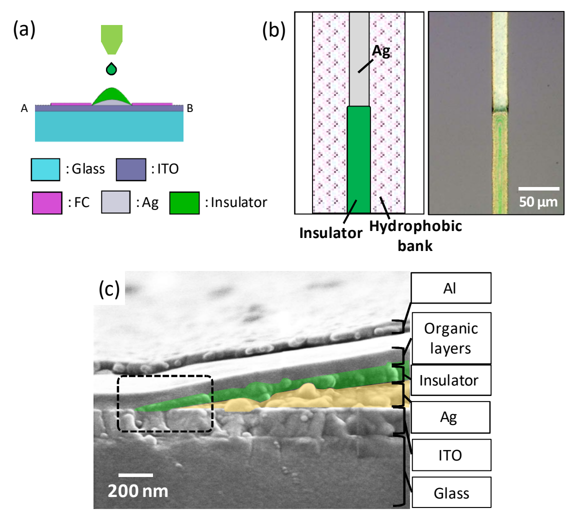

Figure 1: (a) self-aligned bilayer inkjet printing process, (b) printed auxiliary electrode, (c) cross-sectional SEM image of the auxiliary electrode edge

ACKNOWLEDGEMENTS
This work was supported by Materials/Parts Technology Development Program (20017190) funded by the Ministry of Trade, Industry & Energy (MOTIE) of Korea

REFERENCES
1. J.H. Yu, K.-H. Cho, K.-T. Kang, Y.-I. Cho, C.-S. Lee, S.-H. Lee, “Fabrication of Auxiliary Electrodes using Ag Inkjet Printing for OLED Lighting,” SID Symposium Digest of Technical Papers. Vol. 49, pp. 843–846, 2018.

Fully Portable Wireless Soft Stethoscope and Machine Learning for Continuous Real-Time Auscultation and Automated Disease Detection

Sung Hoon Lee[1,2] and Woon-Hong Yeo[2,3,4,*]

[1]School of Electrical and Computer Engineering, College of Engineering, Georgia Institute of Technology, Atlanta, GA 30332, USA.
[2]IEN Center for Human-Centric Interfaces and Engineering at the Institute for Electronics and Nanotechnology, Georgia Institute of Technology, Atlanta, GA 30332, USA.
[3]George W. Woodruff School of Mechanical Engineering, College of Engineering, Georgia Institute of Technology, Atlanta, GA 30332, USA.
[4]Wallace H. Coulter Department of Biomedical Engineering, Parker H. Petit Institute for Bioengineering and Biosciences, Georgia Institute of Technology, Atlanta, GA 30332, USA.
*e-mail: whyeo@gatech.edu

This paper reports a comprehensive study, including soft material engineering, noise-reduction mechanisms, flexible mechanics, signal processing, and algorithm, to realize a fully portable, continuous, real-time auscultation with a soft wearable stethoscope (SWS). <u>For the first time, the soft system demonstrates continuous cardiopulmonary monitoring with multiple human subjects in various daily activities.</u> In this work, the computational mechanics study offers a key design guide for developing a soft wearable system, maintaining mechanical reliability in multiple uses with bending and stretching. Optimizing a system packaging using biocompatible elastomers and soft adhesives allows for skin-friendly, robust adhesion to the body while minimizing motion artifacts due to the stress distribution and conformable lamination. The soft device demonstrates a precise detection of high-quality cardiopulmonary sounds even with the subject's different actions. Compared to commercial digital stethoscopes, the SWS using a wavelet denoising algorithm shows superior performance as validated by the enhanced SNR. Deep-learning integration with the SWS demonstrates a successful application for a clinical study where the stethoscope is used for continuous, wireless auscultation with multiple patients. <u>The results show automatic detection and diagnosis of four different types of lung diseases, such as crackle, wheeze, stridor, and rhonchi, with about 95% accuracy for five classes.</u> Collectively, this paper represents a major shift in how clinicians collect cardiopulmonary sounds for disease diagnosis and health monitoring.

Printed Hybrid Electronics

Donghun Park
3DFlexible Inc.

I. SUMMARY

This talk presents an overview of printed hybrid electronics (PHE), a rapidly growing field that combines printed electronics and conventional electronic components to create hybrid systems. Printed hybrid electronics offer numerous advantages over traditional electronics, such as low-cost production, flexibility, and the ability to integrate with a wide range of substrates and form factors. I will discuss the key components and manufacturing processes involved in printed hybrid electronics, as well as their applications in various industries, including healthcare, automotive, and consumer electronics. The challenges and opportunities facing this emerging technology are also highlighted, along with future directions for research and development. Overall, printed hybrid electronics have the potential to revolutionize the electronics industry by enabling the creation of highly functional, cost-effective, and scalable electronic devices and systems.

II. Rapid Prototyping

Rapid prototyping has emerged as a crucial engineering technology that enables direct production and refinement of parts based on design concepts. Within the field of 3D manufacturing technologies, rapid prototyping has demonstrated its ability to significantly reduce design and production times and costs, particularly for small volume production. It has become an indispensable component of 3D additive manufacturing. Unlike traditional fabrication methods limited to 2D planar structures, 3D manufacturing technologies offer greater design flexibility and material options.

In recent years, there has been a growing interest in utilizing 3D printing technology for the creation of printed electronics. Numerous studies have explored the application of 3D printing in developing conductive traces, capacitors, and RF electronic components such as transmission lines and antennas.

In this discussion, we will present an illustrative example highlighting the agility and cost-effectiveness of rapid prototyping compared to conventional PCB processes for RF electronic devices and sensors. We will explore additive and subtractive manufacturing technologies, which offer the potential to apply this technique across various sensor applications while maintaining high signal integrity without significant increases in noise levels.

III. RF devices and sensors

Incorporating RF devices and sensors into small form factor devices has the potential to enable the creation of complex RF systems in various fields, including robotics and circuits/controllers, as shown in Figure 1 (left). The PHE approach can be readily customized and integrated with other RF passive electronics or bio-sensors. This not only establishes the feasibility of this technique but also allows for the development of innovative RF devices, such as the 3D conical spiral antenna presented in Figure 1 (right), that can be seamlessly integrated with a conformal surface.

Figure 1: (left) Controller circuitry inside a cylinder structure. (right) Conical spiral antenna (3DFlexible)

ACKNOWLEDGEMENTS

We thank Ms. Katie Park, Mr. Joseph Kim, and Dr. Jungyup Woo for their support and suggestions.

Donghun Park's contribution to this publication was not part of their University of Maryland duties or responsibilities.

Self-Rotating Discharge using a Pattered Dielectric Area in Ambient Air and Potential Application in Materials Surface Modification

Choon-Sang Park[1], **GyuTae Bae**[2], **Do-Yeob Kim**[3], **Hyung-Kun Lee**[3], **and Heung-Sik Tae**[2]
[1]Department of Electrical Engineering, Milligan University, USA, [2]School of Electronic and Electrical Engineering, Kyungpook National University, Korea, [3]ICT Creative Research Laboratory, Electronics and Telecommunications Research Institute (ETRI), Korea

I. SUMMARY

In this work, in order to produce the self-rotated plasma regularly and stably in ambient air, we have proposed novel atmospheric pressure (AP) plasma devices with a dielectric pattern, that is, the metal plate surrounded by a dielectric layer. The effects of dielectric on the edge of the electrode on the behavior of self-rotation discharge were examined using a high-speed camera. Furthermore, we exhibit that the proposed AP air plasma reactor can uniformly treat large areas of material surfaces by employing linearly patterned dielectric. In order to confirm the effect of the self-rotating plasma for water treatment, conventional representative plasma treatment methods such as atmospheric pressure plasma jet and pin-to-liquid discharge were also compared.

II. EXPERIMENTAL SETUP

Fig. 1 shows the schematic diagram of the proposed AP air plasma reactor and experimental setup employed in this study. In the plasma reactor, a powered electrode consists of a conductor area of a copper disk with a diameter of 20 mm and a dielectric area coated on the edge of the copper disk. A sinusoidal voltage with a peak voltage of 10 kV and a frequency of 27 kHz was applied to this electrode. Indium tin oxide (ITO) glass was used as the counter electrode in an electrically floating ground state, and the distance between the powered and counter electrodes was fixed at 6 mm.

III. EXPERIMENTAL RESULTS

The self-rotating plasma behaviors in ambient air controlled by the patterned dielectric area at the edges of planar electrodes have been investigated for application in large-area surface treatment. To verify the effect of the dielectric pattern on the movement of plasma, a small area containing the dielectric pattern in the powered electrode was monitored using a high-speed camera.

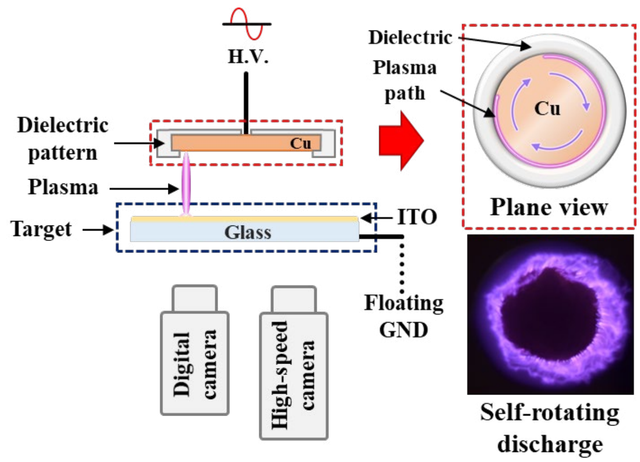

Figure 1: Schematic diagram of the experimental setup and optical images of self-rotating discharge according to the dielectric patterns.

As a result, the plasma was observed to be repeatedly generated at one location instead of moving continuously. Based on the experimental observation, the detailed mechanisms of self-rotating streamer discharge are under study and will be discussed in detail.

Furthermore, we demonstrated that the proposed AP air plasma reactor using linear patterned dielectric could be used to treat large areas uniformly of materials surfaces such as ITO glass, fluorine-doped tin oxide glass, semiconductor, and water surfaces. The detailed characterizations of surface treatment by the proposed self-rotating discharge method using water contact angle, scanning electron microscope, atomic force microscope, UV-vis spectrophotometer, conductivity meter, and hydrogen ion exponent meter are under study and will be discussed in detail.

REFERENCES

1. H.-S. Tae, C.-S. Park, G.T. Bae, H.-K. Lee, D.Y. Kim, “Atmospheric pressure plasma device,” U.S. Patent 11 011 352, May 18, 2021.

Lab on a Smartphone (LOS): a smartphone-integrated optoelectrowetting platform as a portable environmental sensor for on-site water quality monitoring

Sung-Yong Park
Department of Mechanical Engineering, San Diego State University, San Diego, USA

I. SUMMARY

We present a lab-on-a-smartphone (LOS) platform as a portable environmental sensing tool for on-site detection of water quality. The LOS performs multiple laboratory functions on a smartphone and experimentally demonstrated (1) automated on-chip water sample processing using optoelectrowetting (OEW) technology, (2) on-site fluorescent detection of harmful algae cells using a smartphone-integrated fluorescence microscopy, and (3) fecal contamination of water through portable loop-mediated amplification (LAMP) assays.

II. INTRODUCTION

Water is the most important natural resources. A wide variety of species can be found in our water systems, including viruses and bacteria. Some of these aquatic viruses and bacteria can pose immediate threats to human health. Therefore, timely detection and monitoring of harmful pathogens in water systems as well as swift communication on pollution in water systems with a central host are crucial aspects of proper water quality management. However, conventional cell-culturing techniques for water quality detection have proven to be cost-ineffective, labor-intensive, and inefficient.

III. METHODS

To address these issues, a lab-on-a-smartphone (LOS) has been developed as a smartphone-integrated portable biosensor for on-site detection of water quality [1]. The LOS has been designed as a portable platform that mainly incorporates an optoelectrowetting (OEW) device, a transparent heater, and a smartphone. This integrated platform can fully eliminate the need of auxiliary optical and mechanical components (e.g., pumps or tube for reagents delivery, and microscope and CCD camera for fluorescence microscopic analyses) typically required in a conventional lab-on-a-chip (LOC) setup. As shown in Fig. 1, the integrated OEW device performs optical droplet manipulations for on-chip water sample preparations. Secondly, the incorporation of a transparent heater (Fig. 1c) allows the LOS platform to initiate LAMP assays for in-situ analysis of water quality, where isothermal amplification of nucleic acids at 65 °C can be carried out without the need for bulky and costly equipment (e.g., thermal cycler). Furthermore, several features equipped on the smartphone can eliminate the need for other auxiliary equipment and components. Its display screen is utilized as a low-intensity light source to illuminate optical patterns onto the OEW device for light-driven manipulation of water samples. Additionally, the smartphone's built-in camera and image processing app can be used to capture snapshots and perform real-time quantitative analyses (via time dependent RGB color changes) of the target water samples respectively during a LAMP reaction (Fig. 1d).

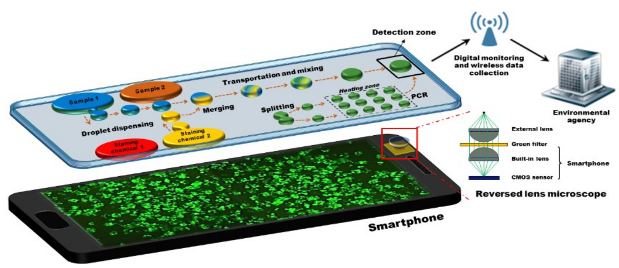

Figure 1: A lab-on-a-smartphone (LOS) platform for on-site water quality management through portable LAMP testing and fluorescence microscopy.

ACKNOWLEDGEMENTS

This work was supported by the NSF CAREER Award (ECCS - 2046134), USA.

REFERENCES

1. S. K. Thio, S. W. Bae, and S.-Y. Park, "Lab on a smartphone (LOS): A smartphone-integrated, plasmonic-enhanced optoelectrowetting (OEW) platform for on-chip water quality monitoring through LAMP assays," *Sensors and Actuators B: Chemical,* vol. 358, p. 131543, 2022

Microfabrication of Hollowed Microneedle Array by Diffraction Lithography

Jun Ying Tan[1], Sanha Kim[2], Keun Ho Lee[2], Jeong Hyun Bae[2], Suk Hee La[2], Do Hyun Jeong[2], Jungkwun 'JK' Kim[1]

[1]University of North Texas USA, [2]Raphas, Inc. South Korea

I. SUMMARY

This paper presents a simple fabrication method for hollow microneedles, which are highly desirable in drug delivery applications. The method involves using diffraction UV lithography and solid-liquid light propagation. The process utilizes the exposure of a liquid photosensitive resin through a photomask pattern with multiple apertures. Hollow microneedles of various heights, ranging from 400 μm to 600 μm, were successfully fabricated within a few minutes of UV exposure. The microneedles exhibited good tip strength, with 0.35 N per single unit. A hollow fluidic test conducted on pig cadaver skin showed promising potential for drug delivery. Furthermore, the batch fabrication process, which allows for multiple microneedles on a single substrate, proved to be compatible with the overall manufacturing process.

II. FABRICATION

The fabrication process of the hollow microneedle array involves two steps: creating a through-hole substrate and fabricating the hollow microneedles. The through-hole substrate is prepared by coating a circular opaque photomask with photosensitive resin, followed by UV exposure and development. The resin is detached from the photomask, completing the substrate. In the next step, another photomask is used to align the substrate, which is coated with photosensitive resin and undergoes UV exposure and development. The substrate, along with the hollow microneedles, is peeled off from the photomask. The sample is then cleaned and dried to obtain the hollow microneedle array.

III. CHARACTERIZATION and RESULT

The hollow microneedle array was characterized, focusing on key parameters: conduit opening size, tip profile, and needle height. The fabrication method provided control over these parameters, determined by the diameters of the outer and inner patterns, offset distance of the inner pattern, UV source intensity, and total UV exposure energy.

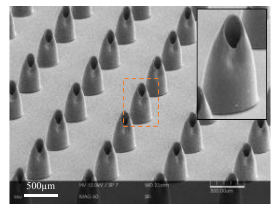

Figure 1. SEM image of the 20x20 hollow microneedles array

Batch manufacturability and reliability were demonstrated by fabricating a 20x20 array of hollow microneedles (Fig. 1). The average height of the microneedles was 515 μm, with an average conduit opening size of 230 μm.

The functionality of the hollow microneedles was assessed through various tests. A liquid ejection test confirmed the presence of a hollow cavity, with the microneedles successfully ejecting blue ink streams. In a skin penetration test using pig cadaver skin, 100% successful insertion was observed with no visible damage or fracture. The force-displacement test showed a peak force of 0.35 N per needle, indicating a suitable penetration force.

In conclusion, a simple and cost-effective fabrication method for hollow microneedles was proposed and demonstrated. The method allowed for the production of various microneedle types by adjusting the photo pattern. The fabricated microneedle arrays exhibited successful insertion into pigskin, sufficient strength, and the potential for batch manufacturing.

ACKNOWLEDGEMENTS

This work has been supported by a grant CNS 2039014, ECCS 2054567, and ECCS 2029086 from the National Science Foundation (NSF) of the United States, as well as 20018023 from Korean Evaluation Institute of Industrial Technology (KEIT).

REFERENCES

1. Tan, Jun Ying et. Al. "Experimental Validation of Diffraction Lithography for Fabrication of Solid Microneedles" Materials 15, no. 24: 8934, 2022.

Automatic Array Calibration System for Wireless Microwave Power Transmitter

Sang-Hwa Yi[1], **Wonseob Lim**[1]
[1] Korea Electrotechnology Research Institute (KERI)

I. INTRODUCTION

Since "Carbon Net Zero" has become a duty for the human race, Space Based Solar Power (SBSP) is receiving serious attention from leading countries. In Korea, two research institutes are preparing for the long-term goal of the SBSP system. KERI developed a 4.8 kW wireless power transmission (WPT) system tracking a moving target 50 m ahead in real-time [1] and proposed the first Korean pilot system for SBSP in collaboration with Korea Aerospace Research Institute (KARI)[2]. The WPT system for SBSP includes a large number of phased array channels, and their rapid and precise calibration is essential. Unlike radar, power receivers exist in a remote place in the WPT system. Using this receiver as a measuring point enables precise calibration of the transmitter. However, as the number of arrays increases, the calibration time is extended because measurement, control, and calculation are required for each channel. In addition, remote calibration of the microwave power transmitter (MPT) array requires signal synchronization between the transmitting and receiving devices.

II. CALIBRATION SYSTEM FOR MPT ARRAY

A system that can automatically calibrate a large MPT array in a short time has been developed. The rotating element electric-field vector (REV) method was used, which measures only the amplitudes of signals at the power-receiving location. A reference signal transmitter (RST) capable of rapid phase rotation was manufactured, and one of four channels of an MPT module was replaced with it. In addition, a calibration signal detector (CSD) was fabricated to measure the synthesized waveform of the reference channel and the under-test channel signal at the receiving position. In order to check the developed system's operation in the laboratory, the signals of the reference and under-test channel of the RST-embedded MPT module were combined by the Wilkinson combiner and input to the CSD. The reference signal's phase was rotated by 10 kHz, and the signal was synthesized as expected and measured well.

The hardware of the proposed long-distance array calibration system was installed in arrayed WPT system (5.8 GHz, 96 ch, 50 W/ch), and the calibration software was integrated with the control program of the WPT system. The entire array was successfully auto-calibrated using the CDS located at 15 m in an anechoic chamber and also done outdoors with the CDS at 50 m. It could be completed within 3 minutes using Ethernet wired communication and 4 minutes using 922 MHz wireless communication. Also, the beam concentration and transmission power increase were confirmed after the calibration.

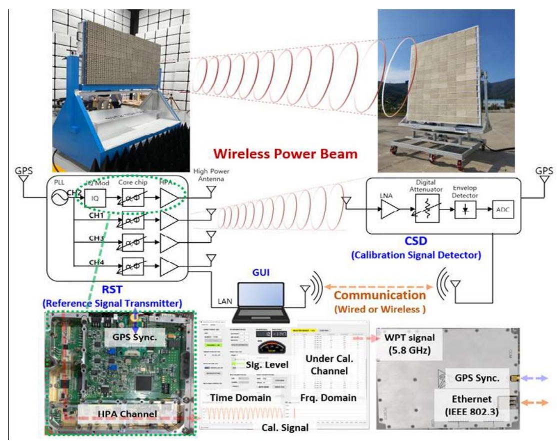

Figure 1: Array calibration system for microwave wireless power transmitter

ACKNOWLEDGEMENTS

This research was supported by KERI Primary research program through the NST funded by the MSIT (No. 23A01075)

REFERENCES

1. S.-H. Yi, et al., "Real-time target tracking energy delivery of active array WPT system," *73rd Int. Astronautical Congress (IAC), Paris, France,* 18-22 Sep. 2022.
2. J.M. Choi, S.-H. Yi, "Proposal of the first Korean Pilot System for Space Based Solar Power (SBSP)," *73rd Int. Astronautical Congress (IAC), Paris, France,* 18-22 Sep. 2022.

5.8 GHz High-power Rectifier using GaN-HEMT diode for wireless Power Transmission Application

Wonseob Lim[1], Sang-Hwa Yi
[1]Korea Electrotechnology Research Institute

I. Introduction

As of late, much attention is paid to wireless power transmission using microwaves, which allows long distance transmission while ensuring the mobility of the receiver through beamforming technology. For microwave wireless power transmission system, it is crucial to design a high-performance receiver that receives and converts high RF to DC power with high efficiency. A GaN-HEMT device has advantages for high-power designs because of their wide energy bandgap, high breakdown voltage, and high current density. In this study, a rectifier was designed to operate at high power in the C-band with GaN-HEMT diodes.

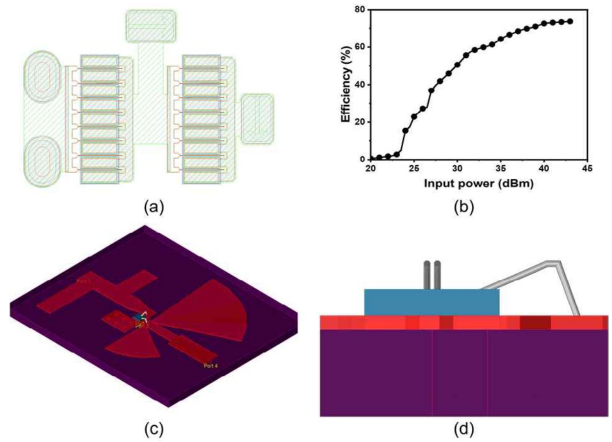

Figure 1: Proposed 5.8 GHz high-power rectifier using GaN-HEMT diodes

II. DESIGN AND SIMULATION

Figure. 1-(a) shows the layout of the GaN-HEMT diode used in the proposed rectifier. The GaN-HEMT diode was designed using NP25-20 process of Winsemiconductor. To use the GaN-HEMT device as a diode, the gate was used as anode and the drain and source tied to each other were used as a cathode. The diode MMIC was designed using two diodes to be implemented as proposed rectifier of voltage doubler structure. Figure 6-(b) and (c) show the diagrams of the proposed rectifier circuit and the bond-wire simulation, respectively. Keysight's ADS harmonic balance circuit simulator and momentum 2.5D EM field simulator were used for the design. The rectifier was optimized at over 40 dBm of input RF power. The input matching circuit was designed to include a third harmonic matching circuit as well as a fundamental frequency matching circuit. The fundamental frequency and third harmonic were matched to be 18+j*19 and open, respectively. For the output matching circuit, a filter was designed to be short-circuited at the fundamental frequency and second harmonic using radial stubs, which can suppress harmonic components and increase the RF to DC conversion efficiency. Figure 6-(d) shows the simulation result of the efficiency of the designed rectifier. The circuit simulation was performed in a range that does not exceed the breakdown voltage of the diode. The designed rectifier exhibited 73% of efficiency and 14.68 W of DC output power at 5.8 GHz with 43 dBm of an input RF power.

III. CONCLUSION

In this paper, GaN-HEMT diodes with a voltage doubler structure were used to design a rectifier that operates at an input power of over 40 dBm in the 5.8 GHz. High efficiency was achieved by matching the third harmonic impedance to be open at the input stage and adopting a harmonic filter at the output stage. The designed rectifier exhibited 73% of efficiency and 14.68 W of DC output power.

ACKNOWLEDGEMENTS

This research was supported by the KERI Primary research program of MSIT/NST (No. 23A01075)

REFERENCES

1. J.-M. Woo *et al.*, "Extendable Array Rectenna for Microwave Wireless Power Transfer System," *IEEE Access*, Vol. 9, pp. 98348-98360, 2021.
2. J. Bae *et al.*, "5.8 GHz high-efficiency RF-DC converter based on common-ground multiple-stack structure," *Sensors*, vol. 19, no. 15, p. 3257, Jul. 2019.

Energy harvesting power management circuits for dual-battery configuration

Kyoungho Lee[1]
[1]KERI

I. INTRODUCTION

Energy harvesting technology that harvests electrical energy from surrounding discarded energy has a specific voltage and current that outputs the most energy depending on the energy harvesting conditions, and the energy harvested by external environmental conditions varies greatly, resulting in unstable power supply [1-2]. Due to an unstable power supply, it is essential to charge and use the battery when configuring a power supply with energy harvesting. Using a battery with a sufficiently large capacity has the advantage of being able to supply power stably, but has the disadvantage of long initial start-up time. This means that it takes a long time to operate LOAD again when the battery is completely discharged due to an accident. Therefore, if the battery is divided into a small-capacity main battery and a large-capacity auxiliary battery in preparation for an emergency, the energy harvesting technology can be used more stably. In this work, a battery dualization connection control circuit that enables fast start-up as well as a stable power supply by applying battery dualization technology was proposed.

II. POWER MANAGEMENT CIRCUITS FOR DUAL-BATTERY CONFIGURATION

The proposed battery dualization connection control circuit serves to properly connect a relatively small capacity CAP and a large capacity BAT. The dual battery configuration quickly supplies power to the load with a relatively small capacity CAP when starting after complete discharge, and charges the large-capacity BAT with the remaining power consumed by the load. And after the BAT is charged up to the load driving voltage, it is used as a power source along with the CAP, and even if the harvester output is cut off like in an accident situation, the load can be driven with the BAT power.

Figure 1 shows the proposed battery dualization connection control circuit. The proposed battery dualization connection control circuit includes comparator 1 which controls SW_1 by sensing the V_CAP voltage, comparator 2 that controls SW_2 by sensing the V_BAT voltage, and VLOAD. It consists of comparator 3 which controls the voltage not to exceed 4V. R1~R4 determines the SW_1 on-off hysteresis, R5~R8 determines the SW_2 on-off hysteresis, and R9~R12 determines the overvoltage protection comparator hysteresis.

III. MEASUREMENT RESULT

It was measured using an in-door PV cell. The large-capacity BAT was not fully charged, but the small-capacity CAP was quickly recharged, so it could be seen that power was supplied stably to the load. It means LOAD can be driven by CAP during BAT start-up time.

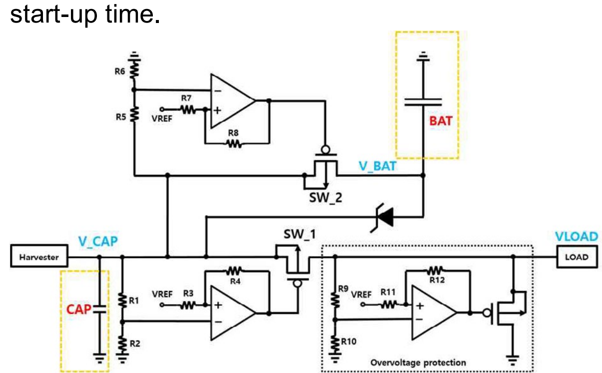

Figure 1: Proposed battery dualization connection control circuits

ACKNOWLEDGEMENTS

This research was supported by the National Research Council of Science & Technology(NST) grant by the Korea government (MSIT) (No. CPS22181-110).

REFERENCES

1. S. Roundy, P. K. Wright and J. M. Rabaey, Energy Scavenging for Wireless Sensor Networks, Norwell, MA: Kluwer Academic, 2003.
2. Merrett G.V., Weddell A.S. Supercapacitor leakage in energy-harvesting sensor nodes: Fact or fiction?; Proceedings of the 2012 Ninth International Conference on Networked Sensing (INSS); Antwerp, Belgium. 11–14 June 2012; pp. 1–5.

An overview of DRAM cell architecture post-Moore's era

Wookyung Sun
Department of Electrical and Computer Engineering, Seoul National University, South Korea

I. Introduction

During the era of Moore's Law, the semiconductor industry attempted to follow the Moore's Law, but currently, the industry is exploring the direction in which DRAM should evolve in the post-Moore's era. And, discussions about 4F2 or 3D DRAM are underway in academia and the semiconductor industry.

In sections II, we review the 4F2 and 3D DRAM architectures that are expected to be the future of DRAM structure.

II. The future of DRAM architecture

To continue scaling down DRAM, advancements in cell transistor structure and process integration are essential [1]. The current structure of DRAM has developed into a structure where capacitors are stacked vertically on top of transistors. However, research and development for future DRAM are currently progressing in two major directions: 1) transitioning to a 4F2 structure of DRAM and 2) transitioning to 3D DRAM [2]. 4F2 DRAM is the most compact cell architecture that can allow an area reduction of 33% with respect to a 6F2 architecutre. VCT(Vertical channel transistor) or VGT (Vertical gate transistor) is considered a promising candidate to enable the 4F2 DRAM structure. In the literature, there are demonstrations of 4F2 cell architecture to further scale down the DRAM cell and a VGT offers superior driving capavility than a conventional saddle transistor [2]. Discussions about 3D DRAM, which stacks gates vertically and aligns capacitors horizontally, are underway in academia and industry. A vertically stacked capacitor can help address the challenges of high aspect-ratio processes without sacrificing cell storage capacitance [1]. However, there are design issues to be addressed, such as the need for individual B/L for each transistor, as well as the challenge of securing transistor performance on deposited materials rather than on single crystal wafers.

III. Conclusion

As DRAM technology has scaled down so far, various research and development for DRAM architecture will continue to be conducted in the future, and scaling down of DRAM cell using methods such as 4F2 or 3D DRAM will persist in the post-Moore's era as well.

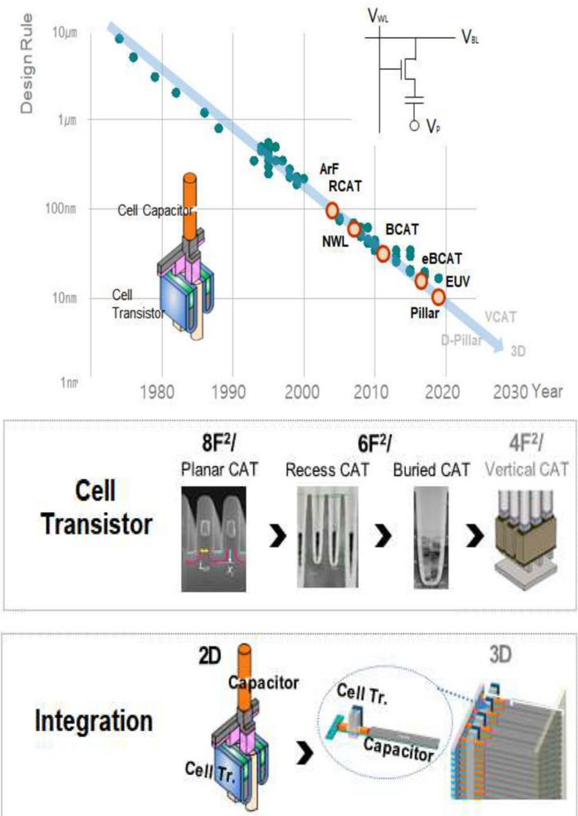

Figure 1: DRAM technology evolution and structure innovations [1]

REFERENCES

1. Kinam Kim, "The Smallest Engine Transforming Humanity: The Past, Present, and Future," *IEEE International Electron Devices Meeting (IEDM)*, pp. 1.1.1-1.1.8, 2021.
2. Alessio Spessot and Hyungrock Oh, "1T-1C Dynamic Random Access Memory Status, Challenges, and Prospects," *IEEE Transactions on Electron Devices*, Vol. 67, No. 4, pp. 1382-1393, 2020.

Plasmon FET for Tailored Photodetection and Bio Sensing

Hossein Shokri Kojori[1], Seongman Cho[1], Sung Jin Kim[2]

[1]Dept. of Electrical and Computer Engineering, University of Miami, Miami, FL, USA

[2]Deptartment of Electrical and Computer Engineering, University of Louisville, Louisville, KY, USA

SUMMARY

We introduce a novel plasmon field effect transistor (FET) that enables direct detection and efficient amplification of plasmon energy. This paper summarizes the details of plasmon FET and recent work on wide-band detection and biological sensing applications.

Keywords: Surface Plasmon, Biosensing, wideband detector, Thin Ffilm Transistor

I. INTRODUCTION

We have developed a hybrid device, plasmon Field Effect Transistor (FET) using metallic nanostructures and a conventional thin film transistor. This device provides a unique optoelectrical property, which can directly convert the plasmonic resonance signal into the current. In this paper, we will discuss the details of underlying physics of the plasmon FET and its optical and electrical properties. Then, we will discuss excellent sensing capability to detect biological markers and its broad band light detection beyond the bandgap of semiconducting materials.

II. DISCUSSION

Figure 1-(a) shows the typical device structure of the plasmon FET. We used N-type InGaZnO (IGZO) thin film and self assembled Au nanoparticles(NPs) on the active channel, and it forms a Schottky junction with the IZGO film. The Au NPs has a strong plasmonic absorption, and the hot electrons generated by this absorption will overcome the Schottky barrier and move to the IZGO channel. The Gate bias will facilitate the collection of the hot electrons. Consequently, it increases the channel conductivity. We use the refractive index change by the attached molecules on the gold surface for biomedical sensing. Small index changes of the functionalized Au NPs by the molecular interaction can be easily converted to the change of the drain current of the plasmon FET (Figure 1-(b)). The distinction between the plasmonic FET platform and conventional LSPR is that the former uses light for excitation, but electronic detection, whereas the latter uses both optical excitation and detection.[1,2] Another application is tailored optical detection using plasmon FET. The gold nanostructures can be designed to have different absorption wavelengths. We used different designs that convert from UV to NIR communication wavelengths. Even though we used a wide bandgap material (ZnO) for the active area, the detection spectrum can be extended to NIR due to the tailored plasmonic absorption of gold nanostructures.[3]

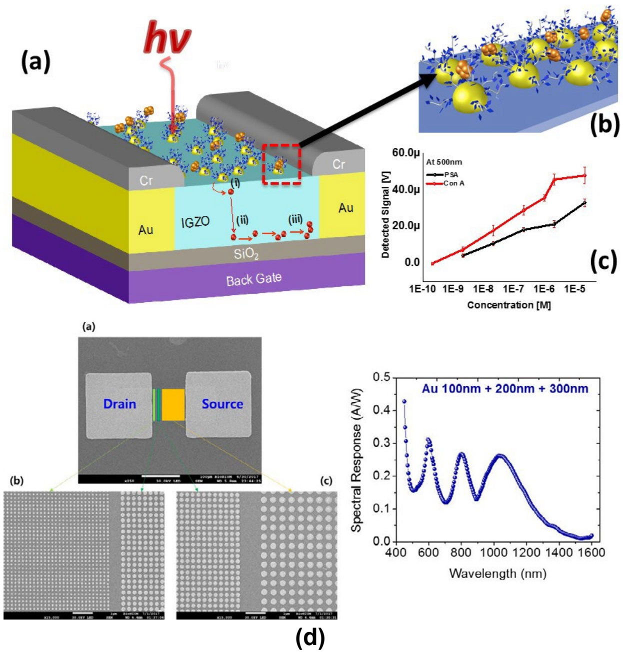

Figure 1 (a) plasmon FET structure and operating principles, (b) illustration of functionalized Au NP for biological sensing, (c) Protein detection response, and (d) Nanostructures on Plasmon FET and its broadband detection spectrum.

ACKNOWLEDGEMENTS

This research was partially supported by NSF (ECCS-1235036 and CBET-1605325).

REFERENCES

1. H. Shokri Kojori, et al., "Monitoring Interfacial Lectin Binding with Nanomolar Sensitivity Using a Plasmon Field Effect Transistor", *Nanoscale*, 8, 17357-17364, 2016
2. H. Shokri Kojori, et al., "Plasmon Field Effect Transistor for Plasmon to Electric Conversion and Amplification", *Nano Letters*, 16, pp. 250-254, 2015
3. Cho, S. et. Al., “Efficient broadband energy detection from the visible to near-infrared using a plasmon FET”, Nanotechnology, vol. 29, pp. 285201, 2018

Innovations in Nanoelectronics: Exploring the Possibilities of 2D Materials

Jeongwon Park[1]
[1]Department of Electrical and Biomedical Engineering, University of Nevada, Reno, NV 89557, USA

I. INTRODUCTION

The rapid development of the nanoelectronic industry over the past decades has relied on transistor scaling to significantly improve transistor performance at a reduced cost [1]. To expand the semiconductor industry, researchers have explored new material systems, designed new transistor structures, demonstrated new functionalities, and developed new applications [1-2]. They have spawned the new era of artificial intelligence (AI), quantum computing, and 5G wireless networks. Semiconductor chips have been getting smaller and smaller every year since the 1960s, with double the number of transistors fitting into the same chip space each year. This follows the predicted trajectory stated in Moore's Law. However, there may be a lower limit for semiconductor downscaling that we are beginning to approach.

II. Future Semiconductors of logic transistors

There are different architectural approaches explored to keep up with the trend, such as Vertical Field Effect Transistors (VFET), Multi-Bridge Chanel FET (MBCFET), 2-Dimensional (2D) channel materials, and Negative Capacitance FET (NCFET), as shown in Fig.1 [3-7]. Developing these new technologies is essential to the continued success of the semiconductor industry and will allow for the continued development of faster, smaller, and more powerful chips. However, the end of Moore's Law is inevitable. The ultimate limit of CMOS scaling was predicted almost immediately after the technology was invented, and several technological and economic factors will eventually prevent further scaling. The several limitations of CMOS technology are associated with the short-channel effect (SCE), switching speed, and power consumption. As the gate length of a transistor decreases, the SCE becomes more pronounced. This effect causes the transistor to lose current, reducing its performance. Several ways, such as tri-gate (FinFET) structures, MBCFET structures, and high-k dielectric materials, mitigate the SCE, but they all have trade-offs [4-7]. New 2D materials (MoS_2, WS_2, BN, etc.) are studied aggressively to realize high energy efficiency and memory/logic functions for system compactness [6]. This talk will introduce various technologies that are based on 2D materials and will be discussed possible applications. In addition, traditional silicon-based high-performance devices will be discussed.

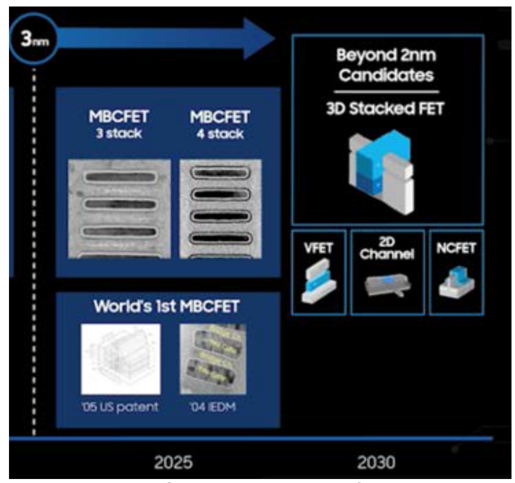

Fig. 1. Future Semiconductors of logic transistors [4-7].

REFERENCES

[1] Shalf, John., *Philosophical Transactions of the Royal Society A* 378, no. 2166 (2020): 20190061.

[2] Taha, Taha Basheer, Azeez A. Barzinjy, Faiq HS Hussain, and Togzhan Nurtayeva*, Circuits and Systems* (2022): 100011.

[3] Datta, Suman, Wriddhi Chakraborty, and Marko Radosavljevic, *Science* 378, no. 6621 (2022): 733-740.

[4] Radosavljevic, Marko, and Jack Kavalieros, *IEEE Spectrum* 59, no. 12 (2022): 32-37.

[5] Sun, Ying, Xiao Yu, Rui Zhang, Bing Chen, and Ran Cheng, *Journal of Semiconductors* 42, no. 2 (2021): 023102.

[6] Das, S., Sebastian, A., Pop, E., McClellan, C.J., Franklin, A.D., Grasser, T., Knobloch, T., Illarionov, Y., Penumatcha, A.V., Appenzeller, J. and Chen, Z.,, *Nature Electronics* 4, no. 11 (2021): 786-799.

[7] Yang, Juchen, In *2022 International Conference on Applied Physics and Computing (ICAPC)*, pp. 198-204. IEEE, 2022.

Region-based conversion of neural activity across sessions

Woohyun Eum
Dept. of Electrical and Computer Engineering
University of Florida
Gainesville, US
woohyun.eum@ufl.edu

Carlton Smith
Dept. of Physics
Yale University
New Haven, US
carlton.smith@yale.edu

Shreya Saxena
Dept. of Electrical and Computer Engineering
University of Florida
Gainesville, US
shreya.saxena@ufl.edu

***Abstract*—A common way to advance our understanding of brain processing is to decode behavior from recorded neural signals. In order to study the neural correlates of learning a task, we would like to decode behavior across the entire timespan of learning, which can take multiple recording sessions across many days. However, decoding across sessions is hindered due to a high amount of session-to-session variability in neural recordings. Here, we propose utilizing multidimensional neural signals from Localized semi-non negative matrix factorization processing (LocaNMF) with high behavioral correlations across sessions, as well as a novel data augmentation method and region-based converter, to optimally align neural recordings. We apply our method to widefield calcium activity across many sessions while a mouse learns a decision-making task. We first decompose each session's neural activity into region-based spatial and temporal components that can reconstruct the data with high variance. Next, we perform data augmentation of the neural data to smooth the variability across trials. Finally, we design a region-based neural converter across sessions that transforms one session's neural signals into another while preserving its dimensionality. We test our approach by decoding the mouse's behavior in the decision-making task, and find that our method outperforms approaches that use purely anatomical information while analyzing neural activity across sessions. By preserving the high dimensionality in the neural data while converting neural activity across sessions, our method can be used towards further analyses of neural data across sessions and the neural correlates of learning.**

***Index Terms*—Brain decoding, Calcium imaging, Decision making, Multi-session decoding**

I. INTRODUCTION

Decision-making provides a rich experimental setting in which to explore the process of transforming a stimulus to a choice [1]–[4]. A two-alternative forced choice (2AFC) task is a common decision-making paradigm in mice, and allows for simultaneously recorded large-scale neural activity in head-fixed animals. However, the process by which an animal learns the 2AFC task has remained relatively under-explored. With the advent of large scale recording technologies that are able to record the neural activity with a high resolution over multiple sessions, we can now try to understand how learning of decision-making takes place across several days or even months. Widefield imaging calcium imaging (WFCI) provides an unprecedented view of neural data across the entire dorsal cortex of the mouse during these tasks. However, the analysis of the resulting neural data across sessions poses several challenges.

Day-to-day noise and small shifts in the recording modality, such as imaging cameras, result in significant session-to-session variability in the recordings. Preprocessing methods include (a) pixel-wise averaging, resulting in one temporal signal per brain region, (b) singular value decomposition (SVD), resulting in components that cannot be directly assigned to any region of the brain, and (c) LocaNMF, resulting in a low dimensional set of temporal components anchored to each brain region. While pixel-wise averaging results in signals that are directly comparable across sessions, these signals do not capture the full extent of information in the brain region. SVD applied to the entire WFCI data makes it impossible to compare signals across sessions since the components may change drastically across sessions. Finally, while LocaNMF provides a lower-dimensional set of signals, it is still difficult to directly align the resulting components from one session to another. Alignment of neural data across sessions has been explored in the past for neural activity ranging from relatively low spatial resolution such as with functional Magnetic Resonance Imaging (fMRI), to single-cell neural recordings [5]–[7]. Here, we extend past methods by proposing a novel method to align WFCI data across sessions, and test out our algorithm on a rich WFCI dataset from 80 sessions across a mouse learning a 2AFC visual and somatosensory task.

In this paper, our main novelties are threefold. First, we present a new data augmentation method to train our models and unify the data across sessions. Second, we design a region-based neural converter to generalize temporal neural signals across sessions while preserving the dimensionality in the neural data across regions. Finally, we introduce a concrete test to evaluate our results: we decode the choice made by the animal using the converted data. Specifically, if we can decode the choice of the animal using the same decoder on converted data as trained on the original dataset, our conversion process can be considered a success. We compare our results with two established ways to align WFCI data across sessions. Using the results of the converter, we show how neural correlates evolve in each brain region during learning.

II. Methods

A schematic overview of our method is shown in Figure 1. First, we preprocessed our data using a data augmentation method to decrease trial-to-trial variability during downstream steps. Subsequently, we designed a region-based neural converter across sessions to optimally align our temporal neural data across sessions. We also implemented two comparison methods for aligning data across sessions: clustering of spatial components, and pixel-wise averaging. These additional methods act as baselines for comparisons with the neural converter, and have been used before for analysis of WFCI [7]. Finally, we decoded the choice of the animal (left vs. right) using the converted neural signals as a measure of the performance of conversion. To quantify this, we calculated the accuracy of each model using the Area under the Receiver Operating Characteristic curve (AUC-ROC).

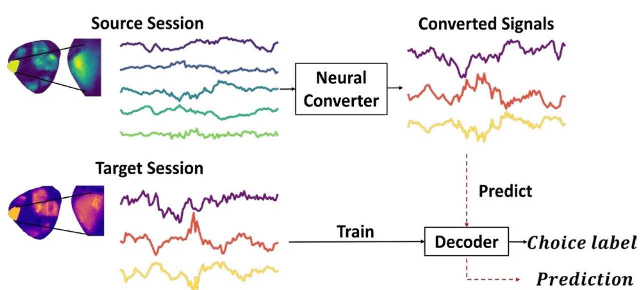

Fig. 1. A schematic overview of our methods: (a) data augmentation, (b) neural conversion of population activity, and (c) evaluation of converter using a choice decoder.

A. Experimental Methods

This experiment was conducted on a head-fixed mouse as it went through learning a visual and tactile delayed 2AFC spatial discrimination task over 80 sessions. The mouse was transgenic, expressing the calcium indicator GCaMP6f in excitatory neurons, and was imaged across multiple sessions using a custom-built widefield macroscope as in [8], to capture the entire dorsal cortex from above. The mouse was trained on two different modalities for the decision-making task: visual and tactile stimuli. The mouse licked the left or right spout to indicate choice after a delay period, and a water reward was provided if the choice direction was the same as the stimulus presentation side. To force the animal to commit to its initial decision, the opposite spout was moved out of reach after one spout was contacted. The mouse was observed over four months during 80 sessions as it performed experiments, and each session contained an average of 371 trials. The detailed experimental details are similar to those in [8].

B. Preprocessing

1) LocaNMF Decomposition: Calcium imaging is helpful for recording large neural populations, but may require downstream processing to recover the neural signals that we can use to understand the behavior. Moreover, it is difficult to segment the data into signals pertaining to each region. Here, we perform temporal denoising, and decompose WFCI videos into temporal and spatial components using Localized semi-Nonnegative Matrix Factorization (LocaNMF) as in [9]. LocaNMF decomposition relies on the following mathematical modeling:

$$\hat{Y}(p,t) = \sum_k a_k(p)c_k(t) \tag{1}$$

Where $\hat{Y}$ is an estimated raw neural recording, a_k is a spatial component, c_k is a temporal component, p is pixel, t is time point, and $k \in [1, K]$, where K is the number of neural components. These spatial and temporal components are divided into different regions, and the temporal activity of any one region can now be represented using the following formula

$$X \sim f(tr, t, k) \tag{2}$$

where X is temporal activity of one brain region, tr is a trial, t is time point, k is the neural component, and f is the distribution of temporal neural activity from each session. We apply LocaNMF to each session's activity separately in order to model session-specific noise. Thus, we obtain 3-9 components per session in each brain region, representing the region's activity during the task. We would like to understand the relationship of the neural activity to the environment, and would thus need to align the neural activity across sessions.

2) Data augmentation: In order to have an adequate number of samples to train downstream models, we propose a data augmentation as in Figure 2. First, we divided entire trials into two groups depending direction of response (Left L or Right R). Second, we sampled a specified number of trials from each group. Third, we averaged over the sampled set and calculate the z-score. We refer to this as an 'augmented' trial. Finally, we assign each augmented trial with the corresponding label (L/R) depending on the group that it was sampled from. The advantage of this method is that we can generate as many augmented trials as we need. For this study, we generate an equal number of Left and Right augmented trials for the conversion and decoding process.

C. Conversion of Neural Activity across Sessions

To study how neural activity evolves during learning, we need to align the neural data across sessions and then relate the resulting neural correlates to behavior. For this goal, we introduce a neural converter that takes as inputs LocaNMF temporal components $\{c_k\}$ in one session, and outputs the temporal components in another session. This procedure is performed for each brain region, and is termed a 'region-based converter' here. We compare this converter to two established methods, spatial clustering and pixel-wise averaging.

1) Region-based Converter: The main task of the neural converter is transforming the source session's neural components to map to the target session's neural components, including the number of components. We designed our neural converter with a linear regression model:

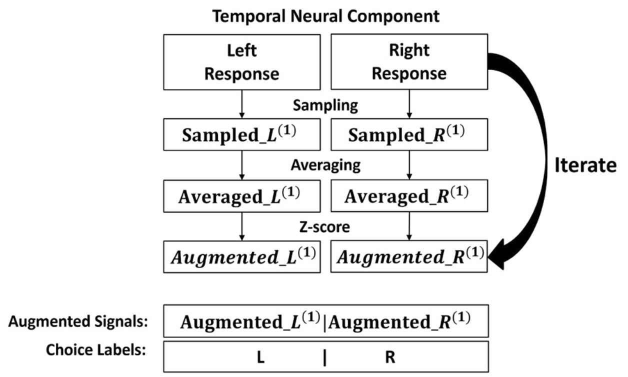

Fig. 2. Schematic for the data augmentation method. We sample trials with replacement according to the direction of response (L/R), and average the set. Next, we construct the labeled data set and iterate the process many times to get an adequate number of training and test samples.

$$\hat{Y}_i = W_{ij} X_j \tag{3}$$

Here, $\hat{Y}_i$ is the estimated target session's neural activity, here session i, with number of temporal components K_i. X_j is the neural signal of the source session, here session j, with number of temporal components K_j. Thus, W_{ij} is of dimension $K_i \times K_j$. Both X_i and Y_j are flattened matrices across times and trials. With our region-based converter, we are successfully able to recast the dimensionality of neural components from the source to the target sessions. After converting, we measured the R^2 score by comparing the estimated signals with the target session's signal to evaluate the performance of the converter.

2) Spatial Clustering: As a comparison to our region-based converter, we consider a method introduced in [7]. We cluster the spatial components resulting from LocaNMF in order to align the components, here using the identity of the neural populations that are activated across sessions. We first downsampled the images by 10% from the original size using 10×10 kernel size in order to reduce the dimensionality and increase the signal-to-noise ratio (SNR) of the high-dimensional spatial components. Next, we applied t-distributed stochastic neighbor embedding (t-SNE) to the downsampled dataset to further reduce the dimensionality of the spatial components. Based on the t-SNE map, we defined associated clusters using OPTICS, while setting a maximum euclidean distance between data points in each cluster. Among multiple clusters, the largest cluster was chosen as a correlated component, and we grouped temporal signals according to this cluster. The process of spatial clustering is shown in Figure 3.

3) Pixel-wise average: Using the brain atlas, here the Allen Atlas, we found pixels corresponding to each brain region. Next, we averaged the temporal signals from all the pixels in a given region, and this forms our one-dimensional pixel-wise average signal that can automatically be compared across sessions.

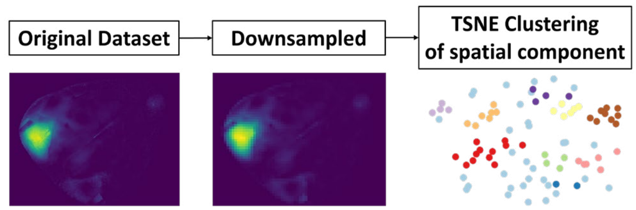

Fig. 3. Schematic and example of the spatial clustering method. To increase the SNR and reduce dimensionality, we downsampled the high-dimensional spatial components. Next, we applied t-SNE to further reduce the dimensionality of the data and to cluster the components. Using the resulting t-SNE map, we grouped the temporal neural components and performed decoding.

Using these two methods, spatial clustering and pixel-wise average, we built baselines for comparing the decoding performance of neural converter.

D. Decoding behavior across sessions

How do we know that our across-session neural converter is performing well? We test the performance of the converter by evaluating the ability of the converted neural data to decode the choice of the animal. We perform the following for data from every brain region separately.

We first train the decoder with the original data in a given session using a logistic regression [10]:

$$L^i = \sum_{j=1}^{T} \sum_{k=1}^{K} \frac{1}{1 + e^{-(\beta_0 + \beta_{jk} Y_{ijk})}} \tag{4}$$

Here, Y_{ijk} is the k^{th} component of the neural activity in the i^{th} trial and j^{th} time point in the trial, L^i is behavior label of i^{th} trial (L / R choice), and $\{\beta_0, \beta_{11}, \beta_{12}, \ldots\}$ are estimated constants.

Next, we convert the session's data from all other sessions, i.e., we consider it as the 'target' session with each other session as the 'source' session. For each estimate of the session's data from other sessions, we then calculate the decoding accuracy while inputting the output of the converter (estimated 'target' session data) into the decoder. See Figure 1 for schematic. We perform this evaluation while considering each session as a target and all other sessions as sources. With the predicted labels, we quantify the decoding accuracy using the Area under the Receiver operating characteristics curve (AUC-ROC score) and calculate a confusion matrix to efficiently view the decoding results.

Since our label is composed of two classes (L/R) with an equal number of trials per class, our chance level is 50%. Therefore, we can validate our decoder by comparing the decoding accuracy with chance level, when it is trained and tested in the same session.

III. Results

To understand how animal learns a decision-making task, we applied our converter - decoder methodology to data from 80 sessions of neural recordings. We evaluated the converter by measuring its decoding accuracy via the AUC-ROC score,

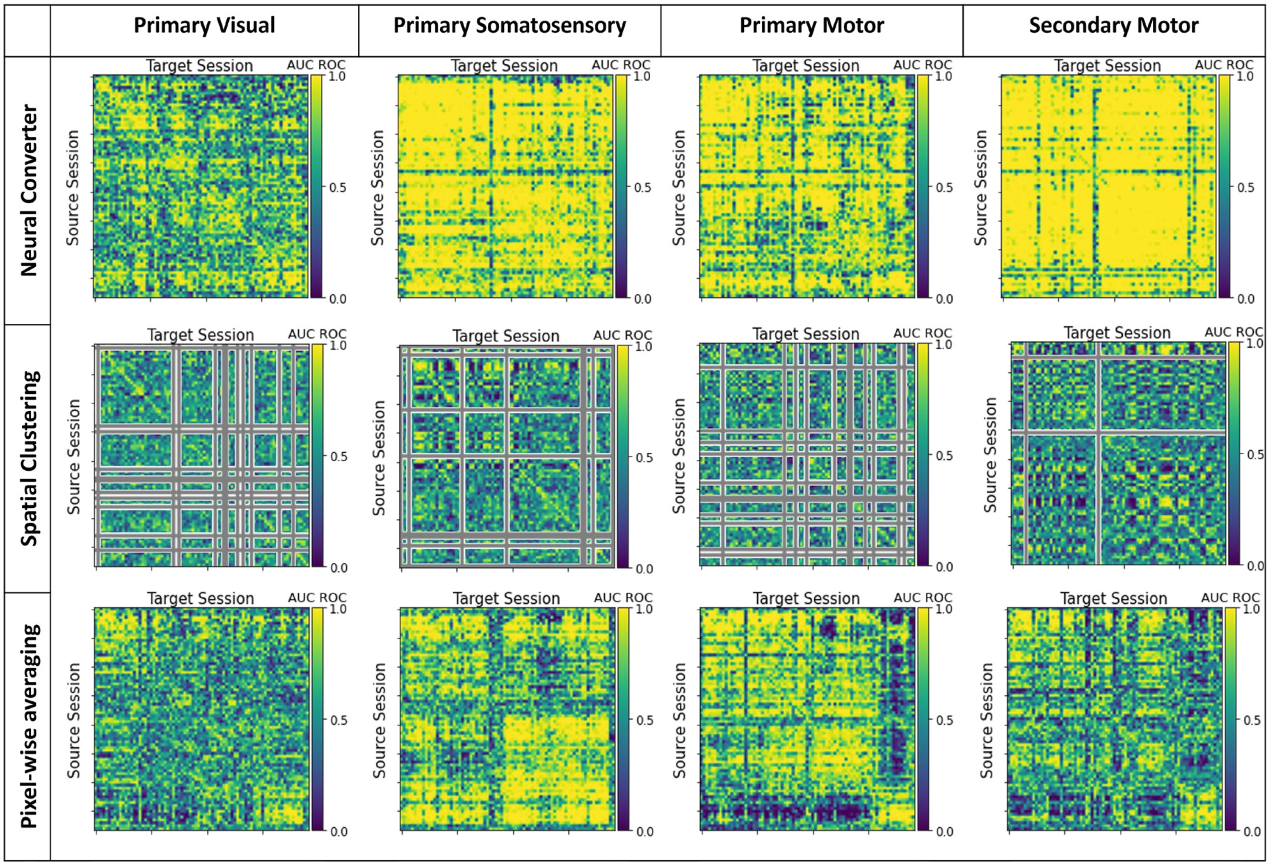

Fig. 4. Decoding accuracy of right side of brain regions: primary visual cortex, primary somatosensory cortex, primary motor cortex, and secondary motor cortex. Accuracy was measured through AUC-ROC score.

while converting the activity of each session to each other session. Moreover, we applied the two baseline methods to show comparisons of our conversion method with other more established methods.

The confusion matrix for the AUC-ROC is shown in Figure 4 for the three types of converter. In this matrix, the x and y axes represent the target and source sessions, respectively. We filled the diagonal points with the 'upper bound' values, which are the decoding scores from equally divided set for train and test in the same session of data. Since we used the same decoder on the converted signals as on the original dataset, each element of the confusion matrix conveys how well the neural signals were aligned between the source and target sessions using the three different conversion methods.

The confusion matrix for our proposed region-based converter attains a very high accuracy on most sessions, and vastly outperforms the baseline methods. The spatial clustering conversion method is not consistently able to convert the signals from each session to each other session. Lastly, the pixel-wise averaging works well, but is not able to achieve a high decoding accuracy. In fact, we note that the pixel-wise average does not always attain a high level of accuracy even while decoding the target session's data itself (diagonal line). Thus, more dimensions from the original data may be necessary in order to achieve a high accuracy, and our proposed region-based converter is able to use all dimensions in the neural data well.

We would have expected a block-diagonal structure in the decoding accuracy to convey that the neural data in neighboring sessions is somewhat stable, but here, the neural data seems to be convertible across all sessions equally well. There does not seem to be a noticeable chronological structure across in the decoding accuracy in any of the conversion methods.

We calculated the confusion matrix for the primary visual cortex, primary somatosensory cortex, primary motor cortex, and secondary motor cortex. Out of these, the primary visual did not convert across sessions as well as the other brain regions. This may be because the visual stimulus enters the brain in a different way than the tactile stimulus, and here we performed the same procedure on trials of all stimulus types.

IV. Conclusion

The study of session-to-session variability relies on the ability to be able to analyze the data from different sessions in the same space, to perform tasks such as decoding. Here, our region-based converter outperformed previously used methods for WFCI neural data. This converter consisted of a data augmentation step and then a linear conversion on extracted region-based data. Our converter is able to act on multi-dimensional data to transform unordered signals from one session to another, and is able to decode the resulting choice of the animal with high accuracy. Future work includes the analysis of learning across the sessions using the learnt converters.

V. Acknowledgments

We thank Anne Churchland for making the Widefield Calcium Imaging data available.

References

[1] Marios G. Philiastides, Roger Ratcliff, and Paul Sajda. Neural representation of task difficulty and decision making during perceptual categorization: A timing diagram. *The Journal of Neuroscience*, 26(35):8965, Aug 2006.

[2] Roger Ratcliff, Marios G. Philiastides, and Paul Sajda. Quality of evidence for perceptual decision making is indexed by trial-to-trial variability of the eeg. *Proceedings of the National Academy of Sciences*, 106(16):6539–6544, Apr 2009.

[3] Marios G. Philiastides and Paul Sajda. Temporal characterization of the neural correlates of perceptual decision making in the human brain. *Cerebral Cortex*, 16(4):509–518, Apr 2006.

[4] Thomas Carlson, David A. Tovar, Arjen Alink, and Nikolaus Kriegeskorte. Representational dynamics of object vision: The first 1000 ms. *Journal of Vision*, 13(10):1–1, Aug 2013.

[5] Juan A. Gallego, Matthew G. Perich, Raeed H. Chowdhury, Sara A. Solla, and Lee E. Miller. Long-term stability of cortical population dynamics underlying consistent behavior. *Nature Neuroscience*, 23(2):260–270, Feb 2020.

[6] Kentaro Yamada, Yoichi Miyawaki, and Yukiyasu Kamitani. Inter-subject neural code converter for visual image representation. *NeuroImage*, 113:289–297, 2015.

[7] Simon Musall, Xiaonan R. Sun, Hemanth Mohan, Xu An, Steven Gluf, Shujing Li, Rhonda Drewes, Emma Cravo, Irene Lenzi, Chaoqun Yin, Björn M. Kampa, and Anne K. Churchland. Pyramidal cell types drive functionally distinct cortical activity patterns during decision-making. *bioRxiv*, 2022.

[8] Simon Musall, Matthew T. Kaufman, Ashley L. Juavinett, Steven Gluf, and Anne K. Churchland. Single-trial neural dynamics are dominated by richly varied movements. *Nature Neuroscience*, 22(10):1677–1686, Oct 2019.

[9] Shreya Saxena, Ian Kinsella, Simon Musall, Sharon H Kim, Jozsef Meszaros, David N Thibodeaux, Carla Kim, John Cunningham, Elizabeth MC Hillman, Anne Churchland, et al. Localized semi-nonnegative matrix factorization (locanmf) of widefield calcium imaging data. *PLoS computational biology*, 16(4):e1007791, 2020.

[10] Christopher M. Bishop. *Pattern Recognition and Machine Learning (Information Science and Statistics)*. Springer-Verlag, Berlin, Heidelberg, 2006.

Effective fetal ECG extraction for non-invasive ambulatory monitoring

Yongkuk Lee* **and Kaylyn Bookers**

Department of Biomedical Engineering, Wichita State University, Wichita, KS, USA

I. INTRODUCTION

Early detection of fetal abnormalities during pregnancy and delivery is critical to reduce fetal mortality, and the most effective way to accomplish it will be ambulatory fetal electrocardiogram (fECG) monitoring. According to the American Heart Association (AHA) and Centers for Disease Control and Prevention (CDC), congenital heart defects (CHDs) are not only the most common birth defects but also the leading cause of birth deaths [1]. Approx. 1% of infants born in the U.S. have a CHD, but the cause of CHDs is unknown in most cases. In addition to CHDs, abnormal cardiac activities of fetus can be an indicator of severe pregnancy complications such as fetal hypoxia and intrauterine growth restriction [2]. Therefore, there is a great interest in accurate long-term fetal heart activity monitoring to provide proper drug and/or surgical therapies in a timely manner to prevent mortality. However, current gold standard techniques such as a Doppler ultrasound and invasive fetal electrocardiogram (I-fECG) are not suitable for the ambulatory fECG monitoring since they are bulk, not portable, and expensive. Furthermore, they require expertise and skills for safe and successful operations. Wearable-based non-invasive fECG monitoring can be safe and easily accepted by users for daily use, but accurate fECG extraction from abdominal ECG (aECG) signals is very challenging. fECG and maternal ECG (mECG) signals often overlap both in time and frequency domain, and the fetal position changes constantly across pregnant women and the gestation age.

II. RESULTS AND DISCUSSION

First, we generated 40 of 10 min-long aECG signals for four different cases (e.g., baseline, fetal movement, normal heart rate change, ectopic beat) with five different levels (0dB to 12dB with 3dB step size) of muscular artifacts and baseline wanders using FECGSYN toolbox, which can help to synthesize aECG signals as mixing stimulated mECG signals, fECG signals, and different types of noises. fECG extraction was performed for those datasets with optimized existing fECG extraction algorithms (e.g., blind source separation, temple subtraction, and Kalman filter), and compared the performance of fECG extraction algorithms using R-peak detection based on Pan-Tompkins algorithm to find the most effective algorithm through all cases.

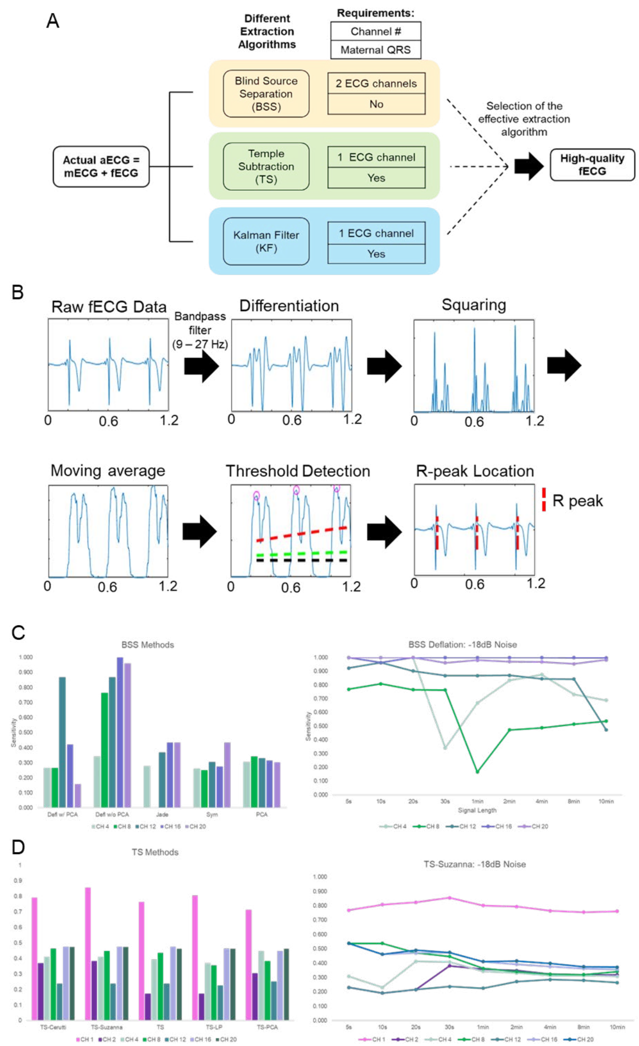

Fig. 1 (A) Overall signal processing. (B) R-peak detection. (C) Performance of BSS extraction. (D) Performance of TS extraction

ACKNOWLEDGEMENTS

This work was supported by NIH (NICHD R15HD107526) and the Kansas INBRE (P20 GM103418).

REFERENCES

1. Centers for Disease Control and Prevention (CDC) Morbidity and Mortality Weekly Report, 2010. **59**(37): p. 1208-11.
2. Bravo-Valenzuela, N.J., et al., Ann. Pediatr. Cardiol., 2018. **11**(2): p. 148-163.

LED Evaluations for Photovoltaic Impedance Spectroscopy

Desmon Simatupang*, Alexander Agrios, John Ayers*, and Sung-Yeul Park***
Department of Electrical and Computer Engineering*
Department of Civil and Environment Engineering**
University of Connecticut, Storrs, USA

I. SUMMARY

Recently, the impedance spectroscopy (IS) of photovoltaic (PV) panel is utilized to identify the dynamic response of PV characteristics including mechanical, thermal, and electrical degradations [1,2]. Light intensity modulation technique is to apply ac ripple on the LED current to provide light perturbation to measure PV IS. The selection of LEDs is one of the key design aspects. This paper presents three LEDs selection: four 100W LEDs, three 70W LEDs, and one 200W LEDs. Single 200W LEDs provide evenly distributed light power. Four 100W LEDs provide the highest PV output power.

II. Light intensity modulation of photovoltaic

A. Overview

Fig. 1 shows the light intensity modulation for photovoltaic. The LED provides modulated light. Then

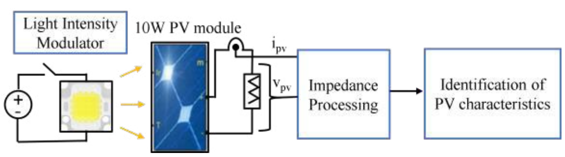

Fig. 1 Light intensity modulation for photovoltaic

the voltage and current of the PV output are measured with respect to frequency perturbation and the impedance is determined in (1). The equivalent circuit parameters can be extracted: series resistance, parallel resistance, and parallel capacitance.

$$Z(\omega) = \frac{V_m \sin(\omega t + \theta)}{I_m \sin(\omega t)} = \frac{V_m}{I_m} \angle\theta \qquad (1)$$

B. LEDs selection

For 10W PV panel, there are three LEDs can be considered: four 100W LEDs, three 70W LEDs, and one 200W LEDs. The performance of the PV panel was measured with three different LEDs selection. Fig. 2 shows three LEDs setup for 10W PV panel. Three LEDs will be evaluated in terms of not only PV performance but also light power distribution.

C. Experimental setup

Fig. 3 shows the experimental setup. It consists of a PV panel, LEDs, power driver, NI-DAQ, and TI control card.

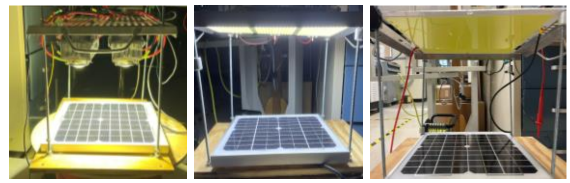

(a) (b) (c)

Fig. 2 Three LEDs for PV light modulation

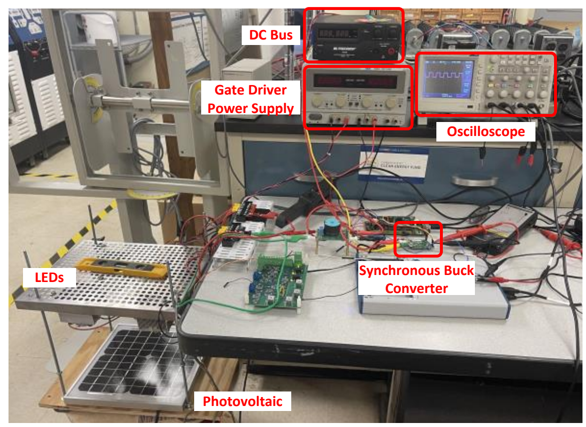

Fig. 3 Experimental setup for light modulation of PV impedance spectroscopy -

D. Experimental results

For 10W PV panel test, four 100W LEDs provide 8.4W PV output, but it has uneven 310mW light power. Single 200W LEDs provide less power output than that of four 100W LEDs. However, it provides more even light distribution.

REFERENCES

[1] S. Osawa, T. Nakano, S. Matsumoto, N. Katayama, Y. Saka and H. Sato, "Fault diagnosis of photovoltaic modules using AC impedance spectroscopy," 2016 IEEE International Conference on Renewable Energy Research and Applications (ICRERA), Birmingham, 2016, pp. 210-215,

[2] Travis Yeow, Jing Sun, Zheng Yao, Jean-Nicolas Jaubert, Kevin P. Musselman, Evaluation of impedance spectroscopy as a tool to characterize degradation mechanisms in silicon photovoltaics, *Solar Energy*, Volume 184, 2019, Pages 52-58.

Evaluation of transient and small-signal stability of Korean power system along the penetration of renewable energy

Jongoh Baek[1], **Dongjoo Kim**[1]
[1]Texas A&M University

I. SUMMARY

Inverter-based renewable energy has asynchronous characteristics and could negatively affect the dynamic stability of the power system if it replaces the existing generator. In order to ensure stable power supply, dynamic stability problems that may occur should be thoroughly analyzed from various perspectives. This paper evaluates the vulnerability of dynamic stability due to the expansion of renewable energy in Korean power systems from the perspective of transient stability and small-signal stability. The evaluation from the transient stability perspective measures the CCT assuming an assumed accident on the 765 kV bus. In addition, the evaluation of the small-signal stability analyzes the inherent vibration characteristics of the system by linearizing the dynamic and static models of Korean power system. The results evaluated from both perspectives indicate the dynamic vulnerability of Korean power system due to the expansion of renewable energy.

II. HOW TO FORMAT THE PAGE

In this chapter, dynamic vulnerabilities were analyzed from the perspective of transient stability and small-signal stability using Korean power system model that gradually increased renewable energy. Renewable energy increases at intervals of 5% up to 50% of the total power generation, and at the same time, existing operating generators were removed in the order of Merit order. The information of the base case used in the simulation is shown in Table 1 below.

Table1. Simulation model

Number of Generator	Number of Load	Number of Shunt
377	1459	584
Total Capacity	Total Load	Total Shunt
107085.2 MW 20537.4 Mvar	105735.7 MW 37077.7 Mvar	-28458.3 Mvar

2.1 Transient stability assessment

To evaluate the transient stability, 10 765 kV bus lines in Korean power system were subjected to three phase grounding accidents The CCTs measured for each bus are shown in Table 2 below.

As the ratio of renewable energy increases, the CCT at each bus tends to decrease. In addition, when the ratio of renewable energy reaches 35%, a bus line that cannot measure CCT appears.

Table 2: Measured CCT

	0%	5%	10%	15%	20%	25%	30%	35%	40%	45%
#1	0.2	0.2	0.19	0.19	0.16	0.14	0.07	0	0.04	0.03
#2	0.31	0.31	0.3	0.3	0.2	0.16	0.07	0	0.05	0.03
#3	0.42	0.42	0.41	0.41	0.38	0.34	0.13	0	0.16	0.37
#4	0.2	0.19	0.19	0.19	0.16	0.13	0.06	0	0.04	0.03
#5	0.63	0.6	0.62	0.56	0.35	0.29	0.1	0.04	0.13	0.38
#6	0.19	0.19	0.2	0.2	0.2	0.21	0.16	0.07	0.18	0.04
#7	0.25	0.24	0.23	0.22	0.18	0.14	0.06	0	0.04	0.03
#8	0.23	0.23	0.23	0.23	0.18	0.14	0.08	0.03	0.07	0.09
#9	0.22	0.22	0.23	0.23	0.23	0.24	0.15	0.06	0.2	0.04
#10	0.16	0.16	0.16	0.17	0.14	0.11	0.07	0.03	0.05	0.07

2.2 Small-signal stability assessment

Among the modes of Korean power system at each stage, the modes with insufficient damping ratio are shown in Table 3. From the time when renewable energy begins to replace 30% of the total power generation, an eigenvalue with a negative damping ratio appears.

Table3: Number of modes with insufficient damping ratio

	0%	5%	10%	15%	20%	25%	30%	35%	40%	45%
0-3%	0	0	0	0	0	0	0	1	0	0
Negative	0	0	0	0	0	0	1	1	2	2
전체	0	0	0	0	0	0	1	2	2	2

Artificial Neural Network(ANN) Based Maximum Power Point Tracking(MPPT) Algorithm for a Photovoltaic Application

Woonki Na, Ph.D(wkna@csufresno.edu)
Electrical and Computer Engineering, California State University, Fresno, CA, USA

I. SUMMARY

In this research, an artificial neural network (ANN) is utilized to improve the efficiency of the maximum power point tracking (MPPT) algorithm in a photovoltaic (PV) application. The data used in this proposed ANN training are obtained from a fuzzy logic controller in the buck converter connected to a PV panel. The use of the combined ANN and the fuzzy logic controller allowed the PV system to operate at its maximum power point in both full and partial irradiation conditions more efficiently compared to conventional algorithms such as perturb and observe (P&O), incremental conductance (IC), and genetic algorithms. The proposed algorithm is tested and validated through MATLAB simulation.

II. ANN MPPT

In recent years, many nations are looking into renewable energy sources to decrease their dependency of fossil fuels. In the future the usage of clean and reliable energy sources such as photovoltaic (PV), and wind will continue to increase. Thus, the main objective of this research is to increase the power efficiency of photovoltaic applications by adapting the proposed ANN based MPPT algorithm[1,2]. The overall system topology is shown in figure 1. The system consisted of a photovoltaic panel, buck/step-down power converter, maximum power point tracking algorithm, pulse width modulation generator, and load.

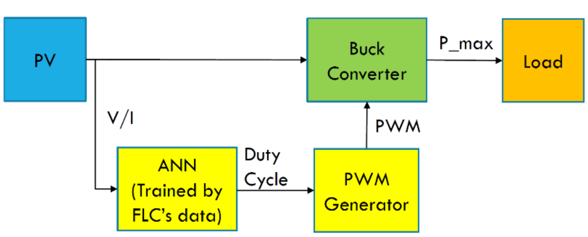

Fig.1 System Configuration

The proposed solution in this research is to combine the fuzzy logic controller MPPT algorithm with the artificial neural network. By using the data, inputs and output, from the fuzzy logic controller to train the artificial neural network algorithm. This approach allows the ANN MPPT algorithm to reduce the error from the fuzzy logic controller. Three different simulations are analyzed. The photovoltaic application with P&O, fuzzy logic controller(FLO), and artificial neural network MPPT algorithm are simulated

	Power Efficiency
P&O	93.20 %
FLC	90.70%
ANN	96.15%

Figure 7: Power Output Efficiency

The simulation's results show that the P&O MPPT algorithm had a slower response compared to the FLC and ANN MPPT algorithm. However, the P&O is more efficient than FLC MPPT algorithm due to FLC's greater error rate.However, when ANN MPPT algorithm is used to reduce the error rate from the FLC, the efficiency of the PV application from this algorithm was most improved.

ACKNOWLEDGEMENTS

This material is based upon 2022 F3 Collaborative R&D challenge: Fresno-Merced Future of Food Innovative Initiative.

REFERENCES

1. B. Subudhi and R. Pradhan, "A Comparative Study on Maximum Power Point Tracking Techniques for Photovoltaic Power Systems," in IEEE Transactions on Sustainable Energy, vol. 4, no. 1, pp. 89-98, Jan. 2013. doi: 10.1109/TSTE.2012.2202294
2. K. Amara et al., "Improved Performance of a PV Solar Panel with Adaptive Neuro Fuzzy Inference System ANFIS based MPPT," 2018 7th International Conference on Renewable Energy Research and Applications (ICRERA), Paris, 2018, pp. 1098-1101.

Fast Recognition of Crop Parts Using 3D Point Clouds and Semantic Segmentation Neural Network

Young-Jae Ryoo[1]
[1]Mokpo National University

I. INTRODUCTION

Due to a decrease in the agricultural population and labor shortage, automation has become necessary. Recognizing crop parts is one of the important technology for automation. We proposed a method to recognize crop parts using 3D point clouds of a plant by applying semantic segmentation neural networks(SSNN). Experiments are conducted to show the proposed method's feasibility.

II. CROP PARTS RECOGNITION SYSTEM

The system consists of five main modules: creating semantic images by SSNN, finding camera poses by ORB-SLAM3, creating semantic point clouds, registering different point clouds by ICP, and recognizing crop parts in the 3D semantic point clouds. The semantic point cloud should be made from many images. It means that many semantic point clouds should be aligned. Therefore, we proposed a method using ORB-SLAM3 to get the camera poses to construct 3D point clouds in the same coordinate system. The ICP algorithm is applied to refine these point cloud poses to reduce the drift accumulated problem.

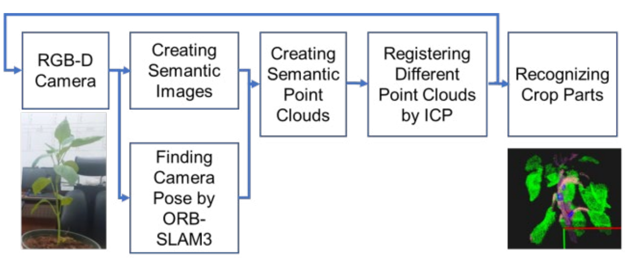

Figure 1: Process of crop parts recognization.

After receiving a start signal, RGB-D images were passed through the SSNN to recognize the crop parts. Then, these results go through the pruning region detection module. On the other hand, RGB-D images were passed through ORB-SLAM3 to detect the camera poses. These are parallel threads. Based on the previous results, semantic point clouds are created at the end of both threads. This process will be repeated until the system gets the stop signal. The ICP algorithm is applied at each loop to align the last semantic point cloud to the new one. When receiving a stop signal, the creation of a 3D semantic point cloud process stops, and the final semantic point cloud is passed through the 3D pruning point detection module to get the final pruning point position.

III. EXPERIMENT

The experiments were set up in the lab with sweet pepper plants. We used the Intel RealSense L515 to capture RGB-D images. The depth and RGB images are aligned before processing by our application. The camera was placed at three different positions for a sweet pepper plant. At each position, the camera was handheld and moved with four different trajectoriesThe camera was stopped at the starting position.

The application was written as ROS nodes under Ubuntu 20.4. There are three nodes. One node wraps ORB-SLAM 3 to provide camera poses. One node was written in Python to predict plant parts by using SSNN and detect pruning regions from RGB-D images. The final node was written in C++, creating a 3D semantic point cloud and recognizing crop parts in 3D space.

ACKNOWLEDGEMENTS

This work was supported by the Korea Institute of Planning and Evaluation for Technology in Food, Agriculture and Forestry(IPET) and Korea Smart Farm R&D Foundation(KosFarm) through the Smart Farm Innovation Technology Development Program, funded by the Ministry of Agriculture, Food and Rural Affairs(MAFRA) and Ministry of Science and ICT(MSIT), Rural Development Administration (RDA)(421032-04 -2-HD060).

REFERENCES

1. Y.J. Ryoo et al., “Fast detection of tomato sucker using semantic segmentation neural networks based on RGB-D Images”, Sensors, 2022, 22, 5140.

Technical Group C-7

Computer and Information Sciences (CIT)

Gated Transformer Networks for Drug Classification using Multi-Dimensional Time-Series Animal Behavioral Data

Sung-Cheol Kim[1]
[1]PsychoGenics

Research on Central Nervous System (CNS) drugs attempts to discover novel chemical compounds targeting the brain to alleviate conditions such as anxiety, depression, chronic pain, psychosis, etc. After careful selection, target drugs are tested on animal subjects, and the reactions are compared to the reference, clinically verified pills. This work leverages a 20-year-old SmartCube platform for recording small rodents in a controlled environment. [1] Deep learning and cloud computing methods were implemented to accelerate the data processing throughput and significantly improve drug discovery accuracy.

This research aims to develop a machine-learning algorithm for drug classification using animal behavior data collected through various sensors in the SmartCube platform. Such an approach has the potential to accelerate drug discovery research by providing a more efficient and reliable way to classify the therapeutic effect of a drug candidate based on its impact on animal behavior.

However, analyzing animal behavior data presents several challenges. The data is complex and multi-dimensional, containing information on various aspects of the subject's behavioral patterns, such as body position, velocity, head orientation, and paw configuration. Moreover, the data is collected over extended sessions, resulting in long time series that are difficult to process and analyze. Finally, the data is prone to noise and variability, making extracting meaningful features and classifying the drugs difficult.

We adopted a Gated Transformer Network (GTN) as a base model to tackle these challenges.[2] The GTN model utilizes double transformer networks to simultaneously learn the temporal and cross-channel correlations in a latent space. However, using the GTN model as in the proposed paper has several technical challenges in the Smartcube platform. For example, the transformer models are easy to become overfitted due to the high model complexity.[3] Furthermore, the session-based long time-series data need a smart augmentation method to overcome the limitations of the GPU memory, breaking the time-series into shorter chunks. Finally, data augmentation techniques are required to reduce the risk of training overfitting issues at the classification level by combining long-term memory.

Despite these challenges, the GTN model shows promising results in drug classification tasks, outperforming the previous feature-based models. GTN has great potential as a tool for drug discovery research, providing a more efficient and reliable way to classify drugs based on animal behavior.

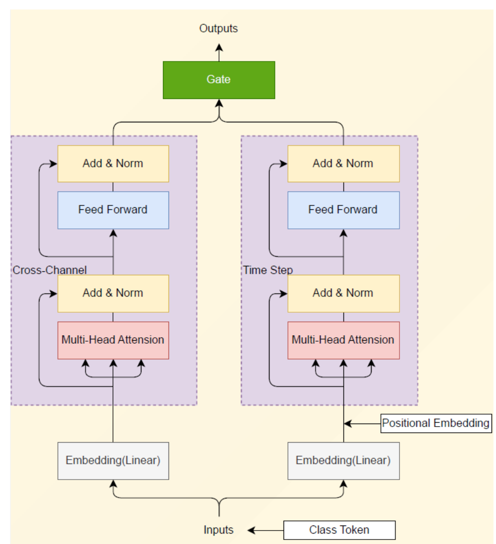

Figure 1: a diagram of the gated transformer network

REFERENCES

1. Vadim Alexandrov et al., "High throughput analysis of behavior for drug discovery", Eur. J. Pharmacol., 2015 mar 5; 750:82-9
2. Minghao Liu et al., "Gated Transformer Networks for Multivariate Time Series Classification," arXiv, 2103.14438, 2021
3. Hassan Ismail Fawaz et al., "Deep Neural Network Ensembles for Time Series Classification", arXiv, 1903.06602, 2019

Cloud-based Integrated Development Environment to Improve Hands-on Activities in a Mobile App Course

Anahita Raeiszadeh, Sam Chung

School of Technology & Computing, City University of Seattle

I. INTRODUCTION

While hands-on activities have dramatically affected the quality of student learning in computer science, there are many challenges with hosting local development environments for technically beginner students such as non-computer science majors or beginners. One of the significant challenges in learning web or mobile development is that those students must spend a lot of time building their computing environment on their local desktops.

Cloud-based Integrated Development Environment (IDE) is emerging. We challenge how we improve hands-on activities in a mobile app course for non-CS background students.

II. RELATED WORK

Mansuri et al. address the advantages, benefits, and applications of cloud computing in education and e-commerce [1]. Krishnan and John offer their curriculum course design experience. They propose that the five components to improve cloud computing education are theoretical, technological, experimentation, laboratory infrastructure, and guest lectures [2]. However, the previous work focuses on the features and benefits of using cloud computing in education and e-commerce. They do not show the cloud-based integrated development environment (IDE) for mobile or web app development.

III. APPROACH - CLOUD-BASED IDE

This paper proposes a cloud-based development environment to improve hands-on activities in a mobile app course. For this purpose, we identify what technical stacks are needed and how they are applied to the course. We started what platforms, engines, and tools are available and why those platforms we need. Also, we explore what languages and frameworks need. Figure 1 shows the cloud-based IDE using GitHub Codespaces and Cloud VSCode. Students have the first hands-on activity to develop the first React Native mobile app.

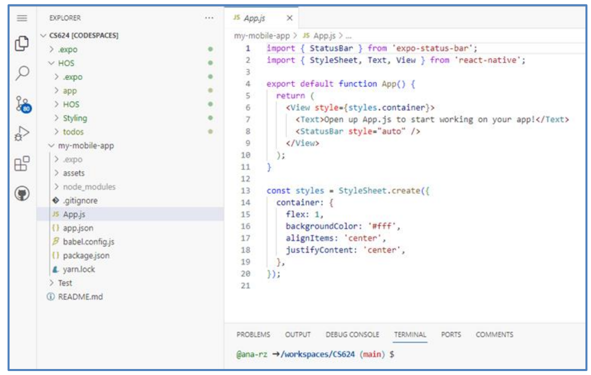

Figure 1: A Cloud-based Development for a Simple React Native Mobile App

We employ platforms like GitHub and GitHub Codespaces, engines like Docker and Node, tools such as VS Code Browser and Expo Go, and languages/frameworks like JavaScript ES6 and React Native. These resources are valuable for version control, cloud-based development, containerization, mobile app testing, web scripting, and software development in the cloud.

IV. CONCLUSIONS

The cloud-based IDE improves hands-on activities in a mobile app course because students do not have to download any software components on their local desktops and configure the software components to develop a mobile app. It significantly simplifies the process of creating a mobile app with React Native, compared to the traditional native approach.

REFERENCES

1. Mansuri, A. M., Verma, M., & Laxkar, P. (2014). Benefit of cloud computing for educational institutions and online marketing. *Information security and computer fraud*, *2*(1), 5-9.
2. Krishnan, R., & John, E. (2013). Design of a curriculum on cloud computing. In *Proceedings of the International Conference on Frontiers in Education: Computer Science and Computer Engineering (FECS)* (p. 1).

Skyscraper Games for Kids: Lessons Learned from a STEM Contest for Kids

Frank J. Lee
Professor of Digital Media, Drexel University, Philadelphia PA 19104

ABSTRACT

In 2015, I received funding from Intel to offer weekend game programming workshops for middle-school girls to get them interested in computer science as a field. However, I was concerned that simply having them only over the weekend may not have the long-term effect that we were hoping for. Hence, I proposed and received additional funding from Intel for a pilot project to greatly scale up our outreach efforts that led to Skyscraper Games for Kids in 2019.

EARLIER EFFORTS

After offering game programming workshops for middle-school girls during the weekends of 2015-16,[1] as a way to encourage their interest in computer science, I became concerned about the persistence of their interest over the long-term. In addition, I was also concerned with the potential self-selection bias that is inherent in the weekend workshop model that we were using. Although we partnered with a local non-profit to gather participants in these workshops, the time commitment on the caregiver, who had to make time during the weekend to bring the child to the workshop, would largely limit the participation to highly motivated parents with most likely high achieving kids. The question for us was how we can diversify our outreach efforts, which centered on getting young girls and boys, especially those who are underrepresented in STEM areas and industries, to view STEM as a potential career choice.

SKYSCRAPER GAMES FOR KIDS

In 2017 I received additional funding from Intel to pilot an idea that sought to correct some of the issues that I previously noted. We proposed a game development contest for kids, where they would create games for the Cira Centre, a 29-story tall skyscraper in Philadelphia, using the tools that we developed to create our game projects for the Cira Centre.[2] First, we put out an open call for middle-school teachers who were interested in participating in our year-long pilot project, where in the Fall term they would learn how to use our tools (See Figure 1) for making games for the Cira Centre and then in the Spring term, teach their students how to use the tools and oversee their students' efforts to make games for the Cira Centre, which was to be showcased in the summer. There were six teachers participating in the project from schools that ranged from an all-girls private school located in the suburb outside of Philadelphia to an urban public school in the heart of west Philadelphia.

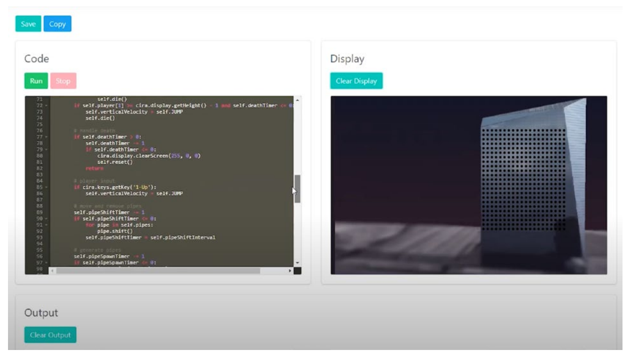

Figure 1: IDE for Skyscraper Games

PUBLIC SHOWCASE

The games by the students were completed and submitted at the end of spring 2018 and we held the public showcase in summer of 2019.[3]

PUBLIC SHOWCASE

The work reported in this paper was supported by the Intel Corporation in 2015 and 2017.

REFERENCES

1. Çakir, N.A., Gass, A.B., Foster, A., Lee, F.J. (2017) “Development of a game-design workshop to promote young girls' interest towards computing through identity exploration,” *Computers & Society.* https://doi.org/10.1016/j.compedu.2017.02.002
2. The New York Times. (2014, April 6) Playing the World's Biggest Tetris Game [Video]. YouTube. https://youtu.be/0atY4mboD4w
3. Mordechai, R. (2019, June 20). Skyscraper Games. TIME for Kids.

Disadvantaged Business Enterprise (DBE) Program Fraud Detection using Natural Language Processing

Jay Jaeshik Shin[1], Young Hoon Kwak[2]
[1]Graduate School of Engineering Practice, Seoul National University
[2]Department of Decision Sciences, The George Washington University

ABSTRACT

This study presents a Natural Language Processing (NLP) model to analyze Disadvantaged Business Enterprise (DBE) fraud patterns using public data. The research utilizes a feature-based supervised learning approach with Named Entity Recognition (NER), applying Bidirectional Long Short-Term Memory – Conditional Random Field (BiLSTM-CRF) for enhanced semantic accuracy. The proposed model will offer insights for DBE fraud investigators, promoting increased vigilance and program integrity.

I. INTRODUCTION

The Disadvantaged Business Enterprise (DBE) program is a government-backed policy that promotes diversity, equity, and inclusion. It is designed such that if a company's representative owns 51% of the company's shares and meets certain racial or disability criteria set by the government, they can apply for a portion of a specific business right. However, there has been a surge in instances of exploiting the benefits of the DBE program by not meeting the minimum required DBE's conditions. Previous studies looked into the attributes of DBE companies by examining the characteristics and information of companies that have received DBE certification [1]. This research proposes a model that can identify trends and characteristics of DBE fraud through data mining of public information listed as DBE Fraud, using Natural Language Processing (NLP).

II. PROPOSED METHODS

Given that the data is provided in textual form, the research plans to employ NLP method called the Named Entity Recognition (NER) technique NER is an information extraction (IE) method of extracting structured data from unstructured documents Among various NER techniques, a feature-based supervised learning approach [3] that applies feature engineering using domain expertise will be used. In terms of architecture, the study will employ Bidirectional Long Short-Term Memory (BiLSTM)-Conditional Random Field (CRF) [4]. BiLSTM has the benefit of providing balanced meaning by reflecting the position of a specific word in forward and backward meanings, while CRF enhances semantic tagging accuracy within the corpus.

III. EXPERIMENTS PLAN

A. Data Mining & Preprocessing: Tokenization
B. Data Split: 80% training, 20% testing data
C. Methodology: NER with BiLSTM-CRF
D. Validation Exact-match evaluation with F-score

IV. CONCLUSION

This study proposes a methodology to analyze the trends and characteristics of DBE fraud using a feature-based supervised learning approach with NER. To achieve greater accuracy, the study will employ a BiLSTM-CRF architecture. The results could be applied in future DBE reviews or fraud investigations, enabling officials to identify trends and proceed with their tasks with enhanced vigilance.

ACKNOWLEDGEMENTS

This research was supported by Korea Institute for Advancement of Technology (KIAT) grant funded by the Korea Government (MOTIE) (P0017304, Human Resource Development Program for Industrial Innovation)

REFERENCES

1. Dang, H. and Shane, J. "A Linear Development Model for Disadvantaged Business Enterprises in Construction Engineering and Management." *Construction Research Congress 2020:*
2. Li, Jing, et al. "A survey on deep learning for named entity recognition." *IEEE TK and Data Engineering* 34.1 (2020): 50-70.
3. Huang, Zhiheng, Wei Xu, and Kai Yu. "Bidirectional LSTM-CRF models for sequence tagging." *arXivpreprint arXiv:1508.01991* (2015)

Enhanced Deep Learning Model for Structural Damage Identification via Random Vibration

Jongyeop Kim[1], Jinki Kim[2], Matthew Sands[3]
[1, 2, 3] Georgia Southern University

I. SUMMARY

Structural health monitoring (SHM) is crucial for ensuring our life safety and extending the service life of systems. Among various means, vibration-based methods are one of the most popular SHM approaches capable of determining information on the health, serviceability, integrity, and possible safety hazards associated with a structure. On the other hand, in practical situations involving civil, mechanical, and aerospace applications, it is generally challenging to control or measure the excitation that induces vibration, as the structural system are often subject to operation, traffic, or wind, all of which are unpredictable and noisy vibration excitations. This study proposes a novel method for identifying structural anomalies by analyzing output-only random vibration signals via an enhanced deep-learning model. A novel method to selectively filter large amplitude response (so-called signal caricature) from random vibration signals is introduced to various deep learning algorithms, including Long Short-Term Memory(LSTM), Gated Recurrent Unit(GRU), and bidirectional LSTM, to identify the structural damage characteristic.

II. EXPERIMENTAL SETUP

A. Data Collection

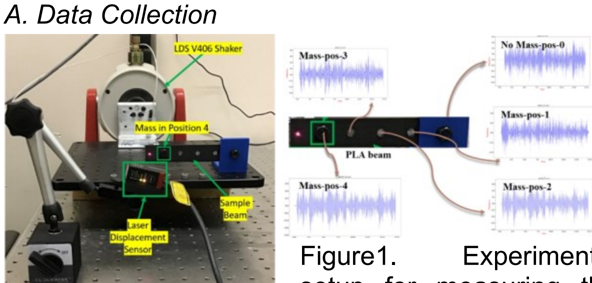

Figure1. Experimental setup for measuring the dynamic response of a cantilever beam gives a random vibration excitation, and the measured signals for damage (additional mass) located at each position. The visualized plot of the signals collected from each point of the sample beam is displayed.

B. A DEEP LEARNING MODEL

def M_Training(x_Train, y_Train)

1. *M^{tr} = Sequential( )*
2. *M^{tr}.add((**Model** (10, return_sequences=True, input_shape=(x_train.shape[1], 1))))*
3. *M^{tr}.add((**Model** (10, return_sequences=False)))*
   M^{tr}.add(Dense(10, activation='tanh'))
4. *M^{tr}.add(Dense(1, activation='hard_sigmoid'))*
5. *M^{tr}.compile(loss='binary_crossentropy', optimizer='adam', metrics=['accuracy'])*
6. *M^{tr}.fit(x_train, y_train, batch_size=500, epochs=100*
7. ***M^{trd}***

III. RESULTS

The results illustrate the signal caricature data set leading to a more accurate and efficient characterization of the structural health state, compared to utilizing the entire time response as an input to the models. Modal properties obtained by traditional vibration analysis support the effectiveness of utilizing the signal caricature with LSTM/GRU models, demonstrating great potential in identifying defects in practical applications. Furthermore, the ensemble's deep learning approach and enhanced model utilizing multiple evaluation mechanisms provided higher damage classification accuracy.

Models	f1-score			TP	FN	FN	TN
	1	0	W*				
GRU	0.6	0.90	0.84	3	2	2	18
Ensemble	0.73	0.92	0.88	4	2	2	18
Enhanced	1	1	1	5	0	0	20

W*: Weighted average

Figure2. Summarize Trend for GRU, Ensemble, and Enhanced model.

REFERENCES

1. Sands, Matthew, et al. " Output-only Structural Damage Detection via Enhanced Random Vibration Analysis using LSTM/GRU model.
   DOI: 10.1109/SERA54885.2022.9806775
2. Sands, Matthew, et al, " A Deep Learning Model for Predicting Damaged Points via Random Vibration Signal Analysis
   DOI: 10.1109/SNPD54884.2022.10051778
3. Ensemble Deep Learning Model for Damage Identification via Output-Only Signal Analysis
   DOI: 10.1109/SNPD54884.2022.10051770

A Comparative Study of PWAs and React Native Mobile Apps

Veerendra Sai Jagatha, Sam Chung
School of Technology & Computing, City University of Seattle

I. MOTIVATION

The rise in demand for mobile apps that offer consistent user experiences on multiple devices has made Progressive Web Apps (PWAs) and React Native apps popular choices. These options provide cross-platform development advantages and native-like user experiences. Native apps, while high-performing and accessible, require separate development for each platform and can be costly to maintain. Therefore, ensuring compatibility with major mobile platforms is vital for the success of an app [1].

II. PROBLEM STATEMENT

This paper compares the performance and user experience of PWAs and React Native mobile apps. By converting a web application to both platforms using, the React framework, the study examines challenges, modifications, and insights to aid developers in choosing the optimal approach for specific use cases. The goal is to empower developers with informed decision-making when selecting between PWAs and React Native mobile apps.

III. RELATED WORK

Comparative studies have been conducted to help developers choose between Progressive Web Apps (PWAs) and React Native. Zohud and Zein conducted a case-study analysis of cross-platform mobile app development, while de Andrade Cardieri and Zaina focused on user experience in mobile web, native, and PWA [1,2]. However, there is currently limited research available that directly compares the PWA and React Native platforms in terms of architecture, performance, and user experience.

IV. APPROACH

This research paper comprehensively analyzes the architecture, performance and user experience of PWAs and React Native apps, focusing on their interface design, to provide valuable insights and inform future development practices. Our methodology involves transforming a web application into both PWA and React Native platforms, allowing for a comparative analysis as shown in Figure 1 based on the established criteria.

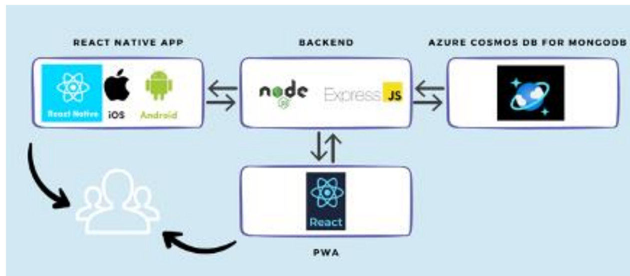

Figure 1: Comparative study of PWAs and React Native Mobile apps

IV. CONCLUSIONS

Conducting a comparative study of PWAs and React Native mobile apps offers an opportunity to gain practical knowledge about two popular cross-platform app development approaches. By exploring both approaches, developers can make better-informed decisions and build efficient, effective apps for their clients or employers. The benefits of this research are to provide developers with valuable insights and guidance to make informed decisions when choosing between PWAs and React Native mobile apps. PWA is suitable when you want to create a web-based application that can be accessed across different devices and platforms, while React Native is a better choice when you require a more native-like mobile app experience with access to device-specific features.

REFERENCES

1. Zohud, T., & Zein, S. (2021). Cross-platform mobile app development in industry: A multiple case-study. *International Journal of Computing*, *20*(1), 46-54.
2. de Andrade Cardieri, G., & Zaina, L. M. (2018). Analyzing user experience in mobile web, native and progressive web applications: a user and HCI specialist perspectives. In *Proceedings of the 17th Brazilian Symposium on Human Factors in Computing Systems* (pp. 1-11).

Integrating Geographic Information Systems and Automatic Identification Systems for Maritime Logistics

EunSu Lee[1], Eun Soo Kim[2] & Sung Woo Lee[2]

[1] New Jersey City University, Jersey City, NJ 07311
[2] Korea Maritime Institute, Busan, Korea 49111

I. Introduction

A Geographic Information System (GIS) is a comprehensive system that includes hardware, software, and operational management. It gathers, stores, and disseminates location data on land and water. This data is then analyzed and presented to users in visualized and tabulated formats, tailored to meet specific business and user requirements [1]. The Automatic Identification System (AIS) is a system for sharing vessel location data agreed upon by the International Maritime Organization (IMO). It was implemented in 2002 to prevent collisions and unexpected behaviors of ships by sharing the location of waterborne vessels. Additionally, it facilitates emergency response, including immediate rescue and search, in the event of an accident [2]. This vessel data is confirmed by communicating with satellites and antenna receivers on the ground, and the information includes dynamic and static data. The data carries vessel specifications, position, speed, and freight. This presentation will cover the collection, storage, processing, analysis, and visualization of AIS information using a GIS system. Participants will gain a thorough understanding of GIS and AIS fundamentals and explore their various applications.

II. Data and Research Framework

A. Automatic Identification Systems (AIS)

Starting from 2005, the Global AIS database mandates the installation of AIS collection devices on all passenger ships and vessels, both international and domestic, with a gross tonnage of 300 or more on international voyages, and cargo ships with a gross tonnage of 500 or more on non-international voyages [1]. The U.S. Coast Guard carries out the collection of AIS vessel traffic information. This data is mainly utilized by the Bureau of Ocean Energy Management (BOEM), the National Oceanic and Atmospheric Administration (NOAA), and the USCG. Additionally, maritime shipping researchers and companies are increasingly using this information. The National AIS (NAIS) is a comprehensive system that includes AIS base stations, data storage, data processing, and network infrastructure for communication purposes. The United States boasts an impressive network of approximately 130 stations that gather this data strategically placed in coastal, freshwater, and offshore areas. Among these, 58 major ports and 11 inland waterways can be found nationwide.

B. ***Integrating GIS and AIS***

When integrating AIS with GIS, communication between the two systems relies on geodata. This can be achieved using table joins or spatial joins. Table joins merge attribute values stored in the shared attributes, while spatial joins recognize locational similarities within an acceptable buffer distance.

III. Discussion and Conclusion

When working with data downloaded from the U.S. government's public data center, it can be helpful to visualize it and filter out unwanted information. To quickly analyze the data, it's best to process it in a table format and use GIS for spatial analysis and visualization If you want to analyze data in a tabular format, you can filter it by specifying the target date, location, and vessel specification to reduce the file size.

References

1. EunSu Lee, “Geographic Information Systems for Intermodal Transportation: Methods, Models, and Application,” (2023). Elsevier: Amsterdam, 1st edition, ISBN: 9780323901291.
2. EunSu Lee, Amit Mokashi, Sang Moon, & Geunsub Kim, “The Maturity of Automatic Identification Systems (AIS) and Its Implications for Innovation,” *Journal of Marine Science and Engineering*, 7(9), 287, 2019.

A Case Study of Next.js's Hybrid Rendering vs. React.js' Client-Side Rendering

Shingo Kise, **Sam Chung**
School of Technology & Computing, City University of Seattle

I. MOTIVATION

Next.js, built on React.js, combines server-side rendering (SSR) and client-side rendering (CSR) to enhance web application performance. This approach achieves a middle ground between server-generated content and client-side interactivity, which leads to improved performance. However, the literature review by the authors did not find any comparisons between the web performance of hybrid rendering (HR) Next.js applications and React.js applications [1, 2].

II. PROBLEM STATEMENT

In this study, we aim to compare the performance of the HR approach in Next.js with the CSR approach in React.js for a web application. Our focus is to evaluate the web performance of the HR method as compared to the CSR method, using Google Chrome Lighthouse performance metrics as a benchmark.

III. RELATED WORK

In Dinku's analysis (2022), identical applications were developed using React.js and Next.js frameworks, and the performance was evaluated based on Google Chrome Lighthouse metrics. Results indicated that React.js outperformed Next.js overall [1]. Lazuardy and Anggraini (2022) discussed the pros and cons of both frameworks, including a web application demonstration [2]. While both studies acknowledged the potential performance improvement through the Next.js' SSR method, neither study specifically highlighted the advantages of the Next.js' HR method in comparison to the React.js' CSR method.

IV. APPROACH

In this paper, we develop identical demo applications using the HR and CSR methods. Figure 1 shows the demo applications side by side. Table 1 provides an overview of the average web performance metrics for both demos across multiple tests.

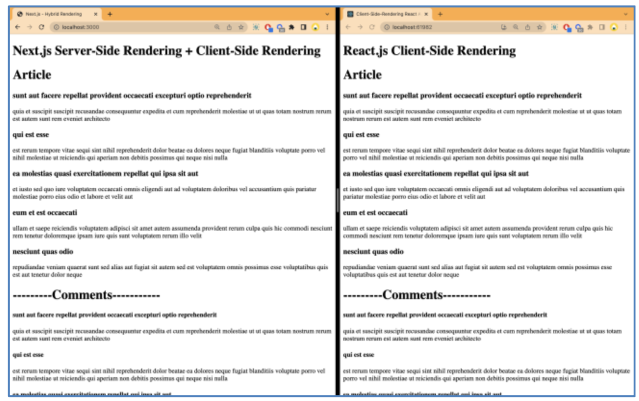

Figure 1: Next.js demo with HR method and React.js demo with CSR method

Google Chrome Lighthouse Metrics	HR	CSR
First Contentful Paint	1.25s	1.3s
Total Blocking Time	170ms	93ms
Speed Index	1.25s	1.33s
Largest Content Paint	1.45s	2.33s
Cumulative Layout Shift	0	0.034

Table 1: Google Chrome Lighthouse web performance comparisons

V. CONCLUSION

The comparison of identical hybrid-rendered and client-side rendered demos demonstrated that the hybrid-rendered demo outperformed according to Google Chrome Lighthouse metrics, except for Total Blocking Time. This finding highlights the HR method of Next.js outperformed the CSR method of React.

REFERENCES

1. Dinku, Z. (2022). React. js vs. Next. js.
2. Lazuardy, M. F. S., & Anggraini, D. (2022). Modern Front End Web Architectures with React. Js and Next. Js. *Research Journal of Advanced Engineering and Science*, *7*(1), 132-141.

Enhanced Real-Time Fingerprinting Attacks on Tor Networks

Donghoon Kim[1], **Doosung Hwang**[2]
[1]Arkansas State University, [2]Dankook University

I. SUMMARY

Website fingerprinting attacks have exposed a vulnerability in Tor network. Previous studies on website fingerprinting attacks have demonstrated some level of effectiveness against the Tor network, bringing the possibility of such attacks closer to reality. For website fingerprinting attacks to be successful in real-world scenarios, the feature vectors used must be enhanced to allow real-time execution. This research examines the feasibility of real-time fingerprinting attacks by utilizing a reduced set of features that have already been proven effective. Our results indicate that it's possible to maintain performance while minimizing the number of features and reducing the training time. This implies that real-time fingerprinting attacks can be executed.

II. APPROACH

Data was collected from a sample of 10 V3 onion services, each consisting of 150 instances. Based on this collected dataset, the study builds upon the feature vectors introduced in two previous works, namely CUMUL [1] and 125 features [2], to generate new feature vectors. These new feature vectors include 81, 90, and 141 features. All feature vectors incorporate common features. Specifically, from a pool of 125 features, 36 features were selected based on their feature importance. Additionally, 4 basic features were extracted from CUMUL, and the remaining features consisted of the number of linear interpolation features from CUMUL. Consequently, the 81-feature vector includes 36 features from the initial 125 features, 4 features from CUMUL, and 41 features from the interpolation features in CUMUL.

III. ANALYSIS

In the experiment, a multi-classification was conducted, with the goal of classifying 10 different V3 onion services using two machine learning models: Random Forest (RF) and XGBoost (XGB). Table I shows that three different sets of features (about 92%) are higher performance than CUMUL (89%). In RF, three different sets of features show 3 times lower training and testing time than CUMUL. Compared among three different sets of features, there is similar results in performance between 91.66% and 92.40%. When using 81 features, both RF and XGB showed a highest performance with RF achieving 92.73% and XGB achieving 92.00%. The main distinctions between the three different sets of features are the time required for training and testing. When using XGBoost, 81 features resulted in the fastest training and testing time, followed by 90 features. The findings suggest that a model with similar performance can be built using fewer features, reducing training time and enabling real-time fingerprinting attacks.

Table 1: Multi classification.

Model	Metrics	Feature vectors			
		81	90	141	CUMUL
RF	Accuracy	0.9273	0.9240	0.9240	0.8847
	Precision	0.9340	0.9300	0.9300	0.8860
	Recall	0.9280	0.9220	0.9240	0.8860
	F1-score	0.9280	0.9220	0.9240	0.8860
	Time (secs)	0.3168	0.2826	0.3444	1.0735
XGB	Accuracy	0.9200	0.9166	0.9166	0.8933
	Precision	0.9200	0.9200	0.9200	0.9000
	Recall	0.9200	0.9200	0.9200	0.8900
	F1-score	0.9200	0.9200	0.9200	0.8900
	Time (secs)	2.4719	2.6353	3.5946	4.8520

IV. CONCLUSION

Onion services have been able to improve user privacy by fully transitioning from V2 to V3. However, our experimental results have shown that our designed features significantly enhance the chances of real-time fingerprinting attacks.

ACKNOWLEDGEMENTS

This material is based upon work supported by the National Science Foundation under Award No. OIA-1946391.

REFERENCES

1. A. Panchenko, F. Lanze, J. Pennekamp, T. Engel, A. Zinnen, M. Henze, and K. Wehrle, "Website fingerprinting at internet scale.," in NDSS, 2016.
2. H. Oh, D. Kim, W.-g. Kim, and D. Hwang, "Performance analysis of tor website fingerprinting over time using tree ensemble models," in 2020 International Conference on Computational Science and Computational Intelligence (CSCI 2020), 2020.

HIERARCHICAL REINFORCEMENT LEARNING ARCHITECHTURE TO DEAL WITH MULTI-HORIZON COMPLEX SYSTEMS

Prasad Nethala[1], Dugan Um[2]

[1]Computing Sciences, [2]College of Engineering-Texas A&M University- Corpus Christi

I. SUMMARY

Agricultural production would need to rise by at least 70% from its current levels. Manual harvesting costs up to 60% of annual operating costs per acre.

Due to conflicting objectives of goal reaching and obstacle avoidance, especially in a dynamic environment, harvesting is a challenging task for any robotic system. Single Agent methods are performing poor in these complex environments.

We proposed a hierarchical reinforcement learning (HRL) algorithm with multiple agents to do multitask objectives for both goal reaching and obstacle avoidance as sub goals. A HRL architecture namely Hierarchical Deep Deterministic Policy Gradient (HDDPG) and Hierarchical Proximal Policy Optimization (HPPO) agent composed of a DDPG/PPO agent at a higher layer and multiple DDPGs / PPO agents at a lower layer as workers. Direct access to the state of the environment enables the manager to understand the changing circumstances and select right worker for right task. Each DDPG will receive selected states from total states and reward from a tailored reward system for each agent. The design specification of HRL enables transfer learning for multiple task execution with minimal learning period in a complex environment.

II. Methodology

A. Hierarchical Reinforcement Learning (HRL)

HRL algorithms have the potential to be useful in applications, particularly those where tasks can be decomposed into a hierarchy of subtasks. HRL agent used as an agent for the mobile robot with 6-DOF manipulator mounted on top of it to collect fruits in a test environment (Farm) and transferred from a simple train environment.

B. Observations

This architecture is demonstrated with the goal of expanding a reinforcement learning scheme towards a generalized AI through flexibility and expandability.

we use a manager and four workers to demonstrate the performance of the Hierarchical Architecture. The proposed HDDPG and HPPO are compared with PPO and DDPG algorithms for performance evaluation. The results show the HRL Architecture models collected more than 70% fruits compared to other algorithms.

III. ILLUSTRATIONS

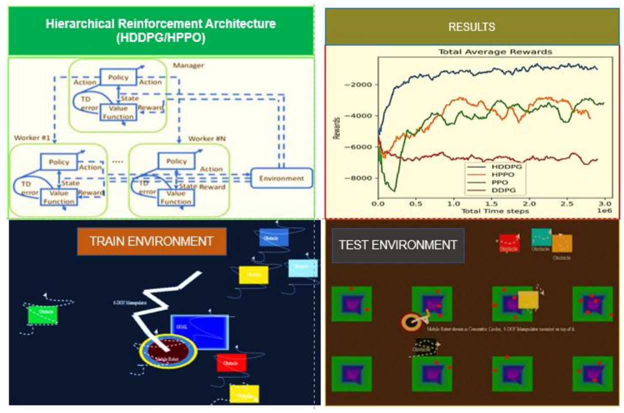

Table 1: Description of the figures above

Fig	Name	Illustrations
1	**HRL Architecture**	HDDPG/HPPO
2	**Average Reward Plot**	HRL outperformed others
3	**Train Environment**	Trained in simple environments.
4	**Test Environment (Farm)**	Tree area shown in green, a circular mobile robot with a 6-DOF manipulator mounted on top of it to collect red dotted fruits by avoiding dynamic obstacles shown in small squares objects.

REFERENCES

1. Um. D, Prasad. N, and Hocheol. S. 2022. "Hierarchical DDPG for Manipulator Motion Planning in Dynamic Environments" AI 3, no. 3: 645-658.

Hippocampus Inspired Cognitive Architecture (HICA) for Few-shot Learning

Deokgun Park
University of Texas at Arlington

I. Introduction

Current embodied agents trained with reinforcement learning (RL) lack rapid adaptability, limiting their applications in real-world missions. Sample inefficiency has been one of fundamental challenges in the current deep learning approach for embodied agents. As a concrete example, imagine a rodent or a human in a new maze environment where there are different elements such as food, water, or beds located randomly in a maze. Within a few trials, they learn to navigate to the right location according to their needs. Current RL agents need millions of training episodes to adapt to a new environment [1]. In biological intelligent agents, there are different components working together to achieve rapid learning in a maze, where a trial-and-error based reinforcement learning is one of those components. In this paper, we propose the Hippocampus Inspired Cognitive Architecture (HICA) for few-shot learning.

II. HICA

HICA explains a learning mechanism in which agents can learn a new behavior policy in a few trials as mammals do in maze navigation or operant conditioning experiments. HICA is composed of two components, a universal learning module and an innate hippocampal program module.

A. Universal Learning Module

A universal learning module type approximates a cortical column in the neocortex gray matter. The working principle is modeled as Modulated Heterarchical Prediction Memory (mHPM) [2]. In mHPM, each module learns to predict a succeeding input vector given the sequence of the input vectors from lower layers and the context vectors from higher layers. The prediction is fed into the lower layers as a context signal (top-down feedback signaling), and into the higher layers as an input signal (bottom-up feedforward signaling). In mHPM, each module updates in a local and distributed way compared to conventional end-to-end learning with backpropagation of the single objective loss. This local structure enables the heterarchical network of modules.

B. Hippocampal Program

Modules modeling organs such as the amygdala, hippocampus, and reward center are pre-programmed to enable instinctive behaviors. The hippocampus plays the role of the simulator. It is an autoregressive prediction model of the top-most level signal with a loop structure of memory, while cortical columns are lower layers that provide detailed information to the simulation with a top-down feedback activation of universal learning module. The simulation becomes the basis for the deliberate planning required for System 2 thinking.

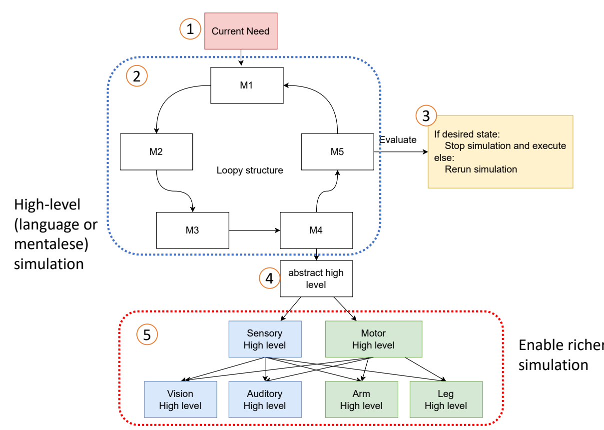

Figure 1: Simulation in HICA. The hippocampal loop structure predicts the next situation in high-level, and it activates lower layers that provide the richer multi-modal simulation with encoded world models.

REFERENCES

1. Pasukonis, Jurgis, Timothy Lillicrap, and Danijar Hafner. "Evaluating Long-Term Memory in 3D Mazes." *arXiv preprint arXiv:2210.13383* (2022).
2. Park, Deokgun, et al. "Hippocampus-Inspired Cognitive Architecture (HICA) for Operant Conditioning." *arXiv preprint arXiv:2212.08626* (2022).

Machine Learning Algorithm: Predicting the Price of Soybean

Soon-Ok Park
Computer Science, College of Arts and Sciences
Governors State University, University Parkway, University Park, IL 60484
E-mail: spark@govst.edu

I. SUMMARY

Machine learning (ML) algorithms are used a wide range of applications. This paper explores various ML algorithms to predict the price of soybean. Long Short-Term Memory (LSTM), Recurrent Neural Networks (RNN) and N-BEATS algorithm are applied to predict the price of soybean.

II. INTRODUCTION

In this paper, we present different machine learning algorithms to predict the price of soybean. As a first step, we download historical data from macrotrends website. In order to get meaning predictions, the dataset should be large enough. Our data is from January 2, 2015 to May 23, 2023.

We divide the original dataset into training data and train our model over a subset of the original dataset.

Table 1: Soybean Prices – Historical Data

Date	Price	Date	Price
1/2/2015	10.07	5/17/2023	13.33
1/5/2015	10.46	5/18/2023	13.33
1/6/2015	10.56	5/19/2023	13.05
1/7/2015	10.57	5/22/2023	13.40
1/8/2015	10.49	5/23/2023	13.22

III. IMPLEMENTATIONS

For splitting train and test data sets, we used the train_test_split function form the sklearn library.

```
from sklearn.model_selection import train_test_split
X_train, X_test, y_train, y_test = train_test_split(timesteps,
prices, test_size=0.2, random_state=42)
```

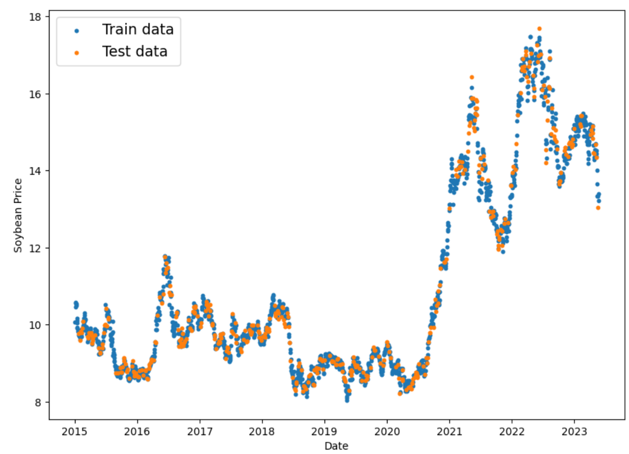

Figure 1: Soybean Price: Plot of Train and Test data

Data analysis with different methods for predicting the price of soybean will be presented.

REFERENCES

Download soybean prices historical data from https://www.macrotrends.net/2531/soybean-prices-historical-chart-data

Niklas Donges, A Guide to Recurrent Neural Networks: Understanding RNN and LSTM Networks Feb, 2023, from https://builtin.com/data-science/recurrent-neural-networks-and-lstm

Science and Engineering Education using Drone

Jounsup Park[1], Taejin Kim[2], Ahreum Ju[3]
[1]California Baptist University, [2,3]City University of Seattle

I. SUMMARY
Drone or unmanned aerial vehicle (UAV) technology is receiving a lot of attention because the range of use of drones is infinite. Building drones requires a variety of advanced technologies. Building a drone gives students easy access to its many advanced technologies. Students can learn about the mechanical, electrical, and computer technologies used in drones and the science behind them.

II. Drone for Science and Engineering Education
Drones can provide a variety of educational opportunities.
(1) Product development: Drones can perform a variety of missions. Students can come up with product ideas for using drones in a variety of situations.
(2) Electrical circuit: Students draw circuit diagrams to connect various electrical components consisting of a drone. Through circuit and PCB design, students will experience first-hand how electrical engineering knowledge can be applied to drone design.
(3) Mechanical design: Case and exterior design can be done using 3D printers. The case design is also essential to meet the specific needs of your drone. Students can experience realizing their ideas through a 3D printer.
(4) System Design: Students can assemble modules and small components on a breadboard or PCB. Students can understand how a product is made by learning the components of a drone, such as the body frame, motors, and propellers. Depending on the purpose of the drone, students can choose different motors and frames to learn which design is optimal. By learning the components of a drone, such as its body frame, motors, and propellers, students can understand how products are built.
(5) Control: Students will engage in challenging missions using custom drones. Students can use drones to move objects to designated areas.
(6) Software: Students can experience how the drone responds by directly coding the software needed to build the drone.

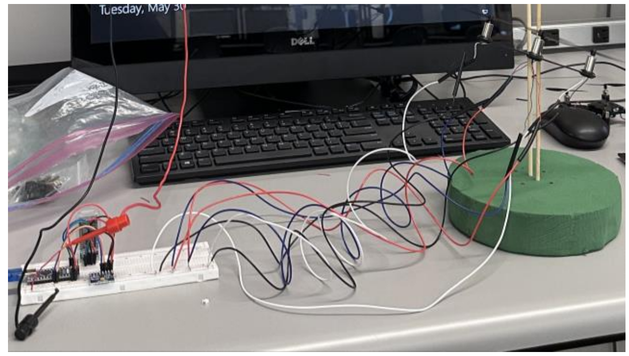

Figure 1. Control circuit design and test kit.

III. Equipment for Drone Education
Equipment for drone education is easily available in online shopping malls. The configuration of the equipment shown in Fig 1 is as follows.
(1) Frame: Frames of various sizes are available, but small and lightweight frames are suitable for training.
(2) Motors and Propellers: There are also various motors and propellers. However, for educational purposes, we have selected the smallest motor and frame.
(3) Bamboo stick and Styrofoam: A drone without a flight controller does not know where it will fly, so a bamboo stick and Styrofoam are used to secure the
(4) Flight controller: The flight controller that operates the drone's propeller was made using an arduino kit. It is configured to control the operation of the drone using arduino nano, gyro sensor, and blue tooth modules.
(5) Power: DC power supply was used to know the power used by the drone.
(6) Software: Open source arduino software Multiwii is used. Since Multiwii [1] expresses the input of the gyro sensor as a GUI, it is very helpful in understanding the operation of the flight controller.

REFERENCES
1. https://www.instructables.com/DIY-Custom-Multicopter-Flight-Controller/.

Analysis of Community Connectivity in Spatial Transcriptomics Data

Kyeong Joo Jung[1], Carter Allen[2], Juan Xie[2], Yuzhou Chang[2] , Subhadeep Paul[3] , Qin Ma[2] , and Dongjun Chung[2,*]

[1]Department of Computer Science and Engineering, The Ohio State University,
[2]Department of Biomedical Informatics, The Ohio State University,
[3]Department of Statistics, The Ohio State University

I. Motivation

The advent of HST technologies has allowed for unprecedented opportunities to characterize spatially distinct cell communities [1]. Existing computational tools do not give the characterization of community connectivity, i.e., the relative similarity of cells within and between communities. This causes missing information about interactive dynamics and spatial heterogeneity of cell sup-populations. In this paper, we present a method that can calculate the community connectivity as well as the sub-populations.

II. Method

BANYAN (**B**ayesian **AN**alysis of communit**Y** connectivity in sp**A**tial single-cell **N**etworks), extension of widely used stochastic block model (SBM) [2], is capable of discerning community connectivity structure and quantifying uncertainty in HST data. HST data turns into similarity networks and quantifies uncertainty in cell spot labels using Bayesian posterior probabilities. We assume for l = 1, 2,

$$A_{ij}^{l}|\mathbf{z},\mathbf{\Theta} \overset{ind}{\sim} \text{Bernoulli}\left(\theta_{z_i,z_j}\right) \text{ for } i < j = 1,\ldots,N,$$

where $\mathbf{z} = (z_1, \ldots, z_N)$, and $\mathbf{\Theta}$ is a K × K connectivity matrix. Model (1) implies that connections among cell spots in the gene expression and spatial layers are governed by a common set of community structure parameters $\mathbf{z}$ and $\mathbf{\Theta}$. Given Model (1) and data A, our inferential objective is to find sub-populations and the cell-cell interaction for *within* and *between* by estimating the parameters $\mathbf{z}$ and $\mathbf{\Theta}$, which is described below using Bayesian approach.

For the latent cell sub-population indicators $z_1, \ldots, z_N$, we assume a conjugate multinomial-Dirichlet prior,

$$z_i \overset{iid}{\sim} \text{Categorical}(\boldsymbol{\pi}), \text{i} = 1, \ldots, \text{N}, \text{for i} < \text{j} = 1, \ldots, \text{N}$$

$$\boldsymbol{\pi} \sim \text{Dirichlet}(\alpha_1, \ldots, \alpha_K), \text{where } \boldsymbol{\pi} = (\pi_1, \ldots, \pi_K)$$

For $\mathbf{\Theta}$, we adopt a conjugate Beta-Bernoulli prior,

$$\theta_{rs} \overset{iid}{\sim} \text{Beta}(\beta_1, \beta_2) \text{ for r<s} = 1, \ldots, \text{K}$$

As a default, we opt for weakly informative priors by setting $\alpha_1 = \alpha_2 = \ldots = \alpha_K = 1$ and $\beta_1 = \beta_2 = 1$[3]. At last, we use the MCMC algorithm to get samples from the posterior distribution and estimate parameters. The banyan package interfaces Seurat workflows, and available at https://github.com/carter-allen/banyan.

III. Application: human melanoma brain metastases

Brain metastases are a common cancer complication which median overall survival is 6 months [4]. Immunotherapy is promising treatment option for brain metastases. Using BANYAN, 4 sub-populations are identified, which corresponds to blood cells, inflammatory immune cells, tumor-inflammatory adjacent cells, and tumor region. In addition, density of cell-cell connectivity decreases as we move from outside to within the tumor. There is relatively high degree of inter-connectivity between blood, immune, and tumor-adjacent sub-populations.

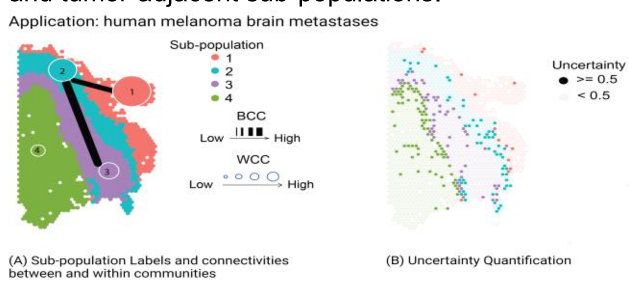

Figure 1: Community structure in melanoma brain metastasis data

REFERENCES

1. Michaela A, Joseph B, and Joakim L. “Spatially resolved transcrip- tomes—next generation tools for tissue exploration.” BioEssays, 42(10):1900221, 2020.
2. Tom S and Krzysztof N. “Estimation and prediction for stochastic block models for graphs with latent block structure.” Journal of classification, 14(1):75–100, 1997.
3. Andrew G, John C, Hal S, David D, Aki V, and Donald R. “Bayesian data analysis.” CRC press, 2013.
4. John S, Rupesh K, Samuel C, Manmeet A, Arjun S, and Eric C. “Current approaches to the management of brain metastases.” Nature reviews Clinical oncology, 17(5):279–299, 2020.

Potential Transformative Impact of Flood Service Drones

Michelle Kim[1], Adan Jun[1],Jae Ryu[2]
[1]KSEA iDrone 2023 Finalist, [2] University of Idaho

I. INTRODUCTION

Climate change and variability continues to lead to more frequent, longer, and higher floods which have deteriorated the situation of city dwellers (Zarin et al., 2023). Undoubtedly, natural disasters, such as floods, negatively impact the world and are difficult to recover from. Many people suffer or potentially die from these inevitable events. However, with the help of technology, people who reside in flooded areas can be aided efficiently.

During the iDrone project, the main objective was to find ways of utilizing drones to benefit society. As a group, we decided on a drone that is able to provide assistance to people who are suffering from floods. Considering multiple parts of the world, we settled on helping Bangladesh because it's the heaviest flooded country.

II. PROJECT OVERVIEW

The flood service drone aims to provide medical and survival supplies to the people, who are exposed to floods, in Bangladesh. Without a doubt, Bangladesh has had one of the worst floods in which a person had to cling to their lives, literally and metaphorically. The unbelievable measures the person had to take, in order to live, made it clear that Bangladesh is in need of assistance.

Therefore, this drone will be installed with GPS sensors, so it can capture the victims' location. By knowing where the victims reside, local rescue teams will have an easier time assisting those people. Also, the drone will operate with a heat sensor which translates body heat into wavelengths so that the human eye can read it (Mayer, 2013). This sensor will allow the drone to detect victims by using the victim's body heat.

Although the process of creating the flood drone could take around a year, the implementation of stations to resupply the drones could take many years. Because Bangladesh faces devastating floods, many restocking stations must be built to help as many victims as possible (Zargar, 2020). In order to create a more effective drone, the medical, engineering, and rescue fields will collaborate with each other to generate a well-structured drone.

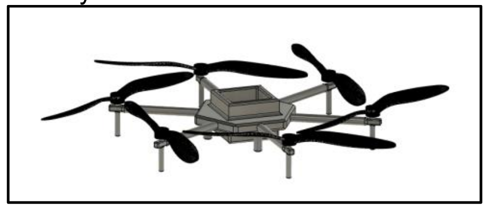

Figure 1: The model of the Flood Service Drone.

III. SUMMARY AND FUTURE WORK

The Flood Service Drone has the potential to assist Bangladesh's people by giving them the necessary materials for survival. Because this drone is specifically built for flood service, we would have to research more about precipitation and climate because the time period and locations of the flood need to be pinpointed.

Furthermore, technology such as Drone Mapping and photogrammetry need to improve so that the drone could easily detect the location of the victims. However, the challenges that the development might face are the math required to find the appropriate stabilization and the optimal size and speed for drones need to be calculated. Also, the advanced sensor package, including high-resolution camera, Global Positioning System (GPS) sensor, and radar sensor should be equipped to accomplish a critical mission during floods.

REFERENCES

1. Mayer, Andre. "How Infrared Cameras Helped End Boston Manhunt Social Sharing." *CBC*, 22 Apr.2013,www.cbc.ca/news/science/how-infrared-cameras-helped-end-boston-manhunt-1.1352618.
2. Zargar, Arshad R. "WORLD Man Rescued After Clinging to Tree for 16 Hours to Escape Flooding That Has Killed 1,000 People." *CBS NEWS*, 17 Aug. 2020, www.cbsnews.com/news/india-floods-bangladesh-deaths-millions-displaced-dramatic-rescue-caught-on-video-today-2020-08-17/.
3. Zarin, S., Bala, S.K., Ryu, J.H. 2023. Assessing urban flooding extent of the Baunia Khal Watershed in Dhaka, Bangladesh. Water 15061183

Conceptualizing Information Drone to Benefit Underserved People

Michael Hsieh[1], Kevin Lee[1], Jae Ryu[2]

[1]KSEA iDrone 2023 Finalist, [2] University of Idaho

I. SUMMARY

An information drone is needed to provide critical information to underserved areas in developing countries. For example, remote regions struggle to access information through traditional means like newspapers. The proposed drone platform can deliver recent news and issue warnings about approaching disasters such as drought, heavy rain, or other climate extremes. We anticipate that the proposed drone platform, therefore, could be a useful alternative to benefit people in developing countries or underdeveloped areas in the United States or around the world.

II. Project Overview

A. Real-world problem and Motivation

Our idea was inspired by seeing the need for modern information, especially for underdeveloped communities and countries around the world. Especially those within the mountainous areas of Korea and scattered communities around countless underdeveloped countries often have poor accessibility to the internet and modern information which is limited due to poor infrastructure, geographical obstacles, and lack of communication facilities. The proposed drone platform, therefore, allows these underserved people to gain access to important information. For example, according to an 2021 ITU estimate, 73% of the population in LDCs - concentrated in rural areas - lack access to the internet [1].

B. Approach

This drone would be used either as a drone chain or drone swarm [2]. The first idea of a drone chain would have small, inexpensive stations that the drones would drop off the delivery or recharge. This drone chain idea would be used for areas that are further away from main stations. The second idea is to send a massive drone swarm which would be used for locations with a high population density, and scattered communities to deliver the packages en masse. The conceptual design of our proposed scheme is illustrated in Figure 1.

III. Summary and Future Work

An information drone was proposed to deliver the early warning of natural disasters for underserved people in developing countries. It appears that a drone chain and drone swarm approach is a feasible solution to provide modern news and critical information to mitigate its impacts. Towards the future, we plan on doing experiments which could test how well the drone performs spreading information in rural areas to volunteers.

This can first be done in underserved areas of the U.S. and gradually work with other developing nations. Doing these experiments will also allow us to determine the costs and effectiveness of this solution.

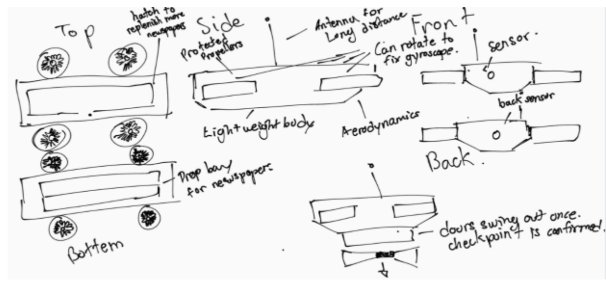

Figure 1: Conceptual Design

Figure 2: Group Photo

REFERENCES

1. ITU, Development Sector *"Measuring digital development,"* 2021

2. H. D. Yoo and S. M. Chankov, "Drone-delivery Using Autonomous Mobility: An Innovative Approach to Future Last-mile Delivery Problems," 2018 IEEE International Conference on Industrial Engineering and Engineering Management (IEEM), pp. 1216-1220, 2018

Resource-Efficient Parameter Tuning in Text-to-Speech Models

Jung Hyuk Lee[1], Chan Gi Hong[1], Midam Kim[2], and Hong Kook Kim[1]

School of EECS, Gwangju Institute of Science and Technology, Gwangju 61005, Korea

School of Business, University of Kansas, Lawrence Kansas 66049, USA

I. INTRODUCTION

Fine-tuning of a text-to-speech (TTS) model has been mainly considered to acquire optimal quality for unseen speakers. The fine-tuning method used in most TTS models trains a lot of data to construct the model and fin-tunes the voice of a specific speaker. However, this process comes with issues associated with the time required to learn all parameters and the storage space required for each model's capacity. In this paper, we present a fine-tuning method using low-rank adaptation (LoRA) [1] and speaker conditioning for Transformer-based TTS models. The TTS model fine-tuned by the proposed method increases the speaker embedding cosine similarity (SECS) by 0.326 over models only fine-tuned with speaker conditioning, while there was a negligible increment of model parameters.

II. PROPOSED METHOD

Figure 1 illustrates how the proposed LoRA-based speaker adaptation is applied to variational inference with adversarial learning for end-to-end TTS (VITS) [2] that is the baseline model in this paper. The VITS model is an end-to-end TTS model that consists of HiFi-GAN-based audio generation which is connected through flow with a Transformer-based text encoder. In the VITS model, text encoder, flow, and HiFi-GAN generator take the speaker conditioning vector which consists of a single convolutional layer. In the experiment, the speaker conditioning layers were set to be trainable while other parameters were inactive. Since LoRA is a technique for transferring the optimization of large-scale models to smaller ones which can update the model weights, we apply LoRA to the Transformer's encoder, specifically on the query and value vectors of self-attention.

III. PERFORMANCE EVALUATION

To evaluate our proposed strategies, we utilized a variant of the voice cloning toolkit (VCTK) dataset, which includes 109 speakers, initially stored at 48 kHz but down-sampled to 22.05 kHz in this work. To measure performance, we used the speaker embedding cosine similarity (SECS), which is a cosine similarity of two speaker embeddings from reference audio and synthesized audio. As shown in Table 1, the full fine-tuning method yielded the highest SECS of 0.703, while applying LoRA and speaker conditioning separately resulted in lower SECS. However, when applying LoRA and speaker conditioning simultaneously, we observed a higher SECS of 0.524, demonstrating the effectiveness of the LoRA-based fine-tuning method. Finally, we compared the number of model parameters depending on the fine-tuning strategy. We observed from the second column of the table that compared to the fine-tuned model by the speaker conditioning only, the proposed method negligibly increased the number of parameters from 3.35 M to 3.37 M, which corresponded to 0.6% increase.

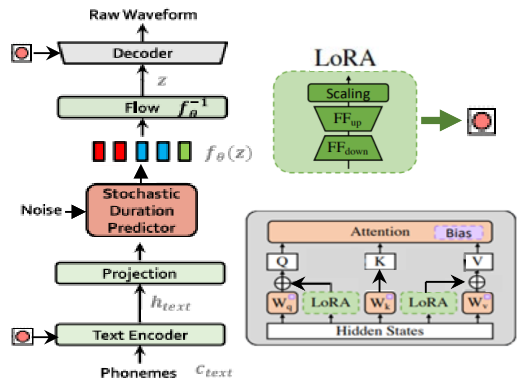

Figure 1: Proposed LoRA-based fine-tuning

Table 1: SECS and Parameter Size according to Fine-Tuning Strategy

Adaptation Method	SECS	Params (M)
LoRA only	0.199	0.018
Speaker conditioning only	0.198	3.35
LoRA + speaker conditioning	**0.524**	**3.37**
Full fine-tuning	0.703	39.70

ACKNOWLEDGEMENTS

This work was supported in part by Institute of Information & communications Technology Planning & evaluation (IITP) grant funded by the Korea government (MSIT) (No.2022-0-00963), and by the GIST-MIT Research Collaboration grant funded by the GIST in 2023.

REFERENCES

1. E. J. Hu, *et al.*, "LoRA: Low-rank adaptation of large language models," in *Proc. International Conference on Learning Representations*, 2022.
2. J. Kim, J. Kong, and J. Son, "Conditional variational autoencoder with adversarial learning for end-to-end text-to-speech," *arXiv preprint*, arXiv:2106.06103, 2021.

Investigating the cause of selection by using an evolutionary model that incorporates amino acid physicochemical properties

Hannah Kim[1], **Sergei L Kosakovsky Pond**[1]
[1]Institute for Genomics and Evolutionary Medicine, Temple University, Philadelphia, PA 19103

I. INTRODUCTION

Physicochemical properties of individual amino acids shape the local environments of the protein structure. These physicochemical constraints directly contribute to the well-recognized differences in exchangeabilities between different residues. However, most codon-based phylogenetic methods ignore differences and treat all changes as equally likely.

II. RESEARCH SIGNIFICANCE

We developed three methods to investigate the cause of selection in protein. PRIME is a codon-based model that directly estimates whether a particular physicochemical property is evolutionarily conserved or altered at a given site in an alignment. PREI is an application of PRIME that imputes the probabilities of evolving a particular codon for a sequence (Figure 1). This method can be used to forecast short-range evolution and detect functionally important sites for sequences that are without prior information. PREV visualization places the numerical estimates from PRIME and PREI back into the context of amino acid location and facilitates the analysis of the important signals.

III. METHODOLOGY

PRIME extends the classic MG94xREV model [1] and uses the distance of physicochemical properties between amino acids to measure the exchangeabilities for each codon position. PREI estimates evolutionary credibility (EC) for each sequence by reconstructing marginal probabilities of observing codon *i* over unobserved ancestral states on the phylogenetic tree that has been conditioned on PRIME parameters. PREV was developed to improve the interpretability of PRIME and PREI output. It has been developed in JavaScript on the Observable platform for fast user accessibility.

IV. RESULTS

PRIME and PREI have been tested not only on simulated datasets, but also on empirical datasets of HIV RT, IAV HA, and SARS-CoV-2 spike. In addition, we have assessed the ability of PRIME to improve positive and negative selection inference in a large collection of mammalian gene alignments.

V. CONCLUSION

We have developed methods that can be used to identify the physicochemical properties of residues that are evolutionarily conserved or changed at site-level resolution. Our methods can be used to refine the interpretation of positive or negative selection signals.

VI. ILLUSTRATIONS

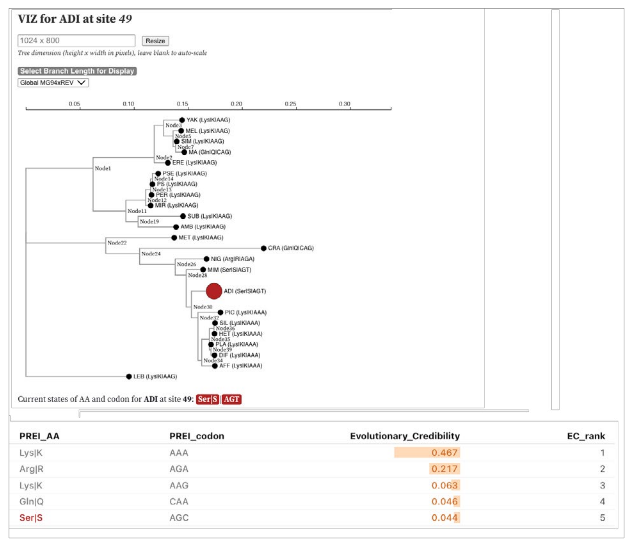

Figure 1: A visualization of PREI output. See https://observablehq.com/collection/@hannahkimincompbio/visualizations-for-prime.

REFERENCES

1. Muse, Spencer V., and Brandon S. Gaut. "A likelihood approach for comparing synonymous and nonsynonymous nucleotide substitution rates, with application to the chloroplast genome." *Molecular biology and evolution* 11.5 (1994): 715-724.

Evaluating Autoencoder Structures for Testing Location Integrity[i]

Chiho Kim[1], Jinpyo Kim[1], Sang-Yoon Chang[2], Jong-Hyun Kim[3], Jinoh Kim[1]
[1]TAMUC, [2]UCCS, [3]ETRI

I. INTRODUCTION

The location of the mobile agents is the crucial information in mobile communications. Location spoofing falsifying the position information would thus be critical, and the mobile network provider should provide an effective tool for resisting such attack attempts. Although there exist a predefined set of location spoofing types [1], there will be a chance of seeing any variation of them in the future. This indicates the need for the capability of detecting previously unseen attack patterns. Autoencoder has been considered for discriminating unusual patterns from known conventions. This study performs a comparison study with different autoencoder structures to see their feasibility for detecting location spoofing attacks using a public vehicular dataset (VeReMi [1]) with the extended feature set defined in [2].

II. AUTOENCODER STRUCTURES

Autoencoders are feed-forward neural networks consisting of the encoder and the decoder, in which the former compresses the input, and the latter reconstructs the compressed representation to the output in a way to minimize the difference between the input and output. While it is possible to organize many different structures for implementing autoencoders, this study considers the following structures popularly applied:

- Plain autoencoder (PAE): This type of autoencoder simply refers to the reconstruction error, the gap between the input and the output.
- Variational autoencoder (VAE): This autoencoder structure relies on a probabilistic model when compressing the input to the hidden representation, which is then restored based on the true posterior distribution and the parametric posterior distribution.
- Convolutional autoencoder (CAE): This autoencoder type utilizes a convolutional neural network for implementing the encoder and the decoder. We implement a CAE under the assumption of one-dimensional input.

III. EXPERIMENTS

We evaluate the three types of autoencoders described above. To determine whether the given location is genuine, we define a threshold (cutoff): if the reconstruction error for the given data instance is less than the predetermined cutoff, then the provided location is genuine; otherwise, the location information is incorrect and falsified. We take the 95th- and 99th-percentile information compiled from the reconstruction error distribution observed in the training phase to set up the cutoff value. From Tables 1 and 2, we can see that using the 99% cutoff performs better than with the 95% cutoff. Overall, VAE outperforms the other autoencoder types, while CAE shows slightly degraded performance.

Table 1: Performance Comparison (Cutoff=95%)

Type	Accuracy	Precision	Recall	F1
PAE	0.984	0.984	0.972	0.997
VAE	0.987	0.978	0.997	0.987
CAE	0.901	0.836	0.999	0.910

Table 2: Performance Comparison (Cutoff=99%)

Type	Accuracy	Precision	Recall	F1
PAE	0.993	1.000	0.987	0.993
VAE	0.996	1.000	0.993	0.996
CAE	0.979	0.961	0.999	0.979

REFERENCES

1. van der Heijden, et al., "VeReMi: A Dataset for Comparable Evaluation of Misbehavior Detection in VANETs." In *SecureComm 2018*.
2. Kim, Chiho, el al., "Reliable Detection of Location Spoofing and Variation Attacks." *IEEE Access* 11 (2023): 10813-10825.

[i] This research was supported by Institute of Information & communications Technology Planning & Evaluation (IITP) grant by the Korean government (MSIT) (No.2021-0-00796, Research on Foundational Technologies for 6G Autonomous Security-by-Design to Guarantee Constant Quality of Security).

Technical Group C-8

Industrial, Manufacturing, and Systems Engineering, Management Sciences, Operations Research (IMS)

The Impact of Misinformation on Health Interventions to Prevent the Spread of Covid-19 in Eastern and Southern Africa

Sang-Heui Lee[1], Stanislas Bigirimana[2]
[1]Pittsburg State University, Pittsburg, KS, USA, [2]Africa University, Mutare, Zimbabwe

I. SUMMARY

Southern Africa and Eastern Africa witnessed a varying degree of information spread about Covid-19 including interpretation and misinterpretation.

This study is providing a framework for the impact of uncensored information about Covid-19 vaccines on the behavior/reaction of people in the area.

II. VARIABLES

A. Misinterpretations (Myths)

1) Vaccines contain chemicals, heavy metals, and “bugs” that will seriously and negatively affect physical and mental health in the medium and long term.
2) Vaccines are targeted at African countries to swipe them away since one drug had a label excluding some regions such as the US, Canada, and the EU.
3) Vaccines will cause genetic defects like down-syndromes or other genetic impacts.
4) Genetic manufacture of vaccines was already forbidden just like genetically modified food (GMOs).

B. Reactions

1) Awareness: this variable will be measured by asking participants about their knowledge of Covid-19 symptoms, modes of transmission, and uptake of preventative or curative measures such as vaccination.
2) Interest: this variable will be measured by asking participants about their level of interest in learning more about Covid-19 symptoms, modes of transmission, and uptake of preventative or curative measures such as vaccination.
3) Decision-making: this variable will be measured by asking participants about their willingness to report symptoms, avoid modes of transmission, and uptake of preventative or curative measures such as vaccination.
4) Action: this variable will be measured by asking participants about their actual identification and reporting of symptoms, avoidance of practices that may lead to Covid-19 transmission and uptake of preventative or curative measures such as vaccination. Table 1 summarizes the processes of assessing the impact.

Table 1: Epistemological processes involved in assessing the impact of social media

INPUT	PROCESS	OUTPUT
Operations	Levels of consciousness	Levels of engagement
Experiencing (perceptual)	Empirical (*pathos*)	Awareness
Understanding (cognitive)	Intellectual (*logos*)	Interest
Judging, Deciding (evaluative)	Reasonable (*ethos*)	Decision
Acting (behavioral and practical)	Responsible (*praxis*)	Action

III. EXPERIMENTS

In step 1, about 500 respondents will take part in the first experiment. Respondents are exposed to fake news on Covid-19. In step 2, half of the respondents are counseled on the importance of Covid-19 and health information. In both steps, the respondents will complete a questionnaire to determine their perception of the impact of misinformation and their behavioral responses.

REFERENCES

1. Kulshrestha, J., Eslami, M., Messias, J., Zafar, M. B., Ghosh, S., Gummadi, K. P., & Karahalios, K. (2017, February). Quantifying search bias: Investigating sources of bias for political searches in social media.

Strategic Capacity Management for Deferred Surgeries

Eojin Han[1], Kartikey Sharma[2], Omid Nohadani[3]
[1]Southern Methodist University, [1]Zuse Institute Berlin, [2]Benefits Science Technologies

I. SUMMARY

The COVID-19 pandemic has necessitated widespread deferrals of elective surgeries. These delays not only increase the cost from potential deterioration of patients' conditions, but also decrease the revenue due to departures. Current policies are ad-hoc and thus not effective to handle various uncertainty to hospital operations. Moreover, its endogeneity renders existing capacity management approaches inapplicable. To this end, we develop an optimization framework based on robust and distributionally robust optimization. We apply our findings to a case of hernia patients in the U.S. and show that the proposed framework can offer sizable improvements over alternative methods.

II. METHOD

A. Uncertainties in Managing Surgical Capacity

Decisions on capacity expansion are typically exposed to two main sources of uncertainty. First, the unknown number of new surgery requests at each time period can be regarded as *demand uncertainty*. The second source is *departure uncertainty*, a group of patients who have been scheduled for surgery but decide to depart the system without receiving the treatment due to various reasons. The impact of these uncertainties renders strategic capacity expansion extremely challenging.

B. Models and Methods

We formulate the strategic capacity expansion problem as a dynamic optimization problem, where the demand and departure uncertainty affect the objective and constraints in a nonlinear fashion. For the robust optimization (RO) approach, we propose the concept of tree of uncertainty products to provide tractable approximations under various decision rules. For the distributionally robust optimization (DRO) approach, we leverage mean and mean-absolute deviation constraints to develop a computationally efficient solution method.

III. THE CASE OF HERNIA SURGERIES

We apply our proposed solutions for hernia patients who are exposed to backlog delays due to unforeseen circumstances from the pandemic. We use the dataset containing all claim records of 15,914 patients to estimate cost parameters and calibrate uncertainties. We then implement our proposed RO and DRO policies along with the ad-hoc deterministic (Det100) policy.

Table 1: Relative Improvement (in percentages) of RO and DRO Policies over Ad-hoc Policies

Departure Level	RO		DRO	
	Mean	CVaR	Mean	CVaR
More Departure	0.49	7.42	5.21	2.56
Less Departure	0.61	1.77	3.41	0.47

Table 1 reports relative improvements in costs of the RO and DRO policies compared to the Det100 policy for different mode of patient departure behavior. Both policies outperform Det100 in average and in conditional value at risk. More specifically, the DRO policy is more effective in improving expectation while the RO policy achieves improved conditional value at risk over the DRO policy. This implies that managers can choose either policies depending on their risk preferences.

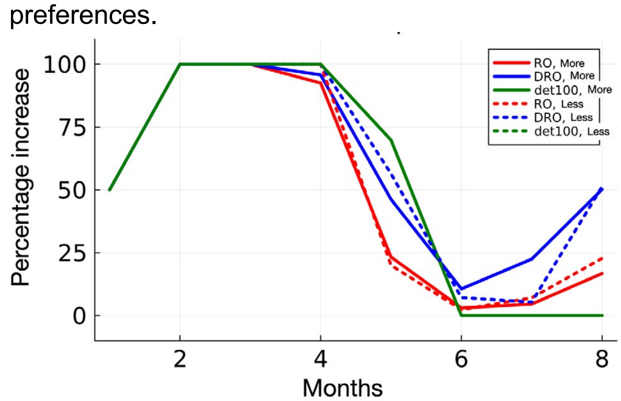

Figure 1: Expanded Capacity over Time (Relative to Initial Capacity), Less vs. More Departure

Figure 1 displays expanded capacities over time, showing that our policies offer faster decrease than the Det100 policy. This is because departing patients are incorporated in our approaches, whereas they are not in the Det100 policy. These cool-downs are also adaptive which are suitable in practice.

Renewable-Battery Hybrid Power Plants in Congested Electricity Markets: Implications for Plant Configuration

James Hyungkwan Kim*, Dev Millstein*, Ryan Wiser*, and Julie Mulvaney-Kemp*
*Lawrence Berkeley National Laboratory, Berkeley, CA, USA

I. SUMMARY
This study investigates the value of coupled wind power and battery hybrid plants ("hybrids") in congested electricity markets, considering geographic constraints. Using a linear optimization program with 2018-2021 market prices, it compares the value of hybrid projects in differently congested areas. Findings indicate that situating a 4-hour battery, sized to 100% of the wind plant capacity, in load centers compared to Variable Renewable Energy (VRE)-rich areas provides additional value. Further, extended energy storage duration reduces battery degradation and enhances value, particularly with capacity contribution incentives. These results underscore the growing significance of wind-battery hybrids in power systems with limited transmission capacity.

II. INTRODUCTION
This study investigates the value of solar and wind hybrid plants in congested electricity markets. These areas, marked by high prices due to limited transmission and high demand, might benefit from hybrid plants, which combine renewable generation and energy storage. Our analysis considers energy and capacity value across different locations, like Load Centers with high demand, and Variable Renewable Energy (VRE) rich areas with substantial renewable generation.

We evaluate the impact of hybrid configurations, particularly focusing on energy storage duration. Additionally, we explore factors affecting energy storage value: battery degradation cost and grid charging capability.

Our findings, detailed in Figure 1, suggest that solar hybrid plants and those located in Load Centers typically yield higher energy and capacity values than wind hybrid plants and those in VRE-rich areas. However, storage duration extension beyond four hours produces smaller-than-expected value increases, and storage value is sensitive to battery degradation cost and grid charging ability.

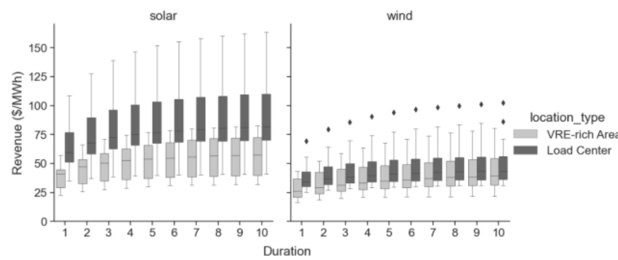

Figure 1: Annual hybrid plant values different location types and by market

Conclusively, hybrid plants can offer significant value in congested electricity markets, but optimal configuration depends on factors like renewable generation type, location, storage duration, battery degradation cost, and grid charging capability, providing valuable insights for stakeholders considering hybrid projects in congested areas.

III. RESULTS and CONCLUSIONS
This research evaluates the value of renewable-battery hybrid plants in congested electricity markets using 2018–2021 data from U.S. independent system operators. We find optimal hybrid configurations differ between high-demand Load Centers and Variable Renewable Energy (VRE) rich areas. Siting a 4-hour battery at Load Centers can increase system value by 48%, although incentives for storage beyond 4 hours are limited. Hybridizing value is sensitive to battery degradation, with lower degradation costs leading to a higher increase in value. Allowing grid charging increases hybrid plant value, with solar hybrids showing significant revenue increase. Wind plants require longer storage to reach capacity credit. Our findings, valuable to energy planners and policymakers, suggest optimizing hybrid configurations for maximum project value in areas with limited transmission capacity. Future studies should address our limitations and explore factors such as battery capacity costs and location diversity's impact on hybrid projects.

Challenges in Managing Workload and Anxiety in Gateway Programming Courses

Hyesung Park, **Kihyun Kim**
[1]Georgia Gwinnett College, [2]Jacksonville State University

I. SUMMARY

The analysis conducted using stepwise regression analysis indicates that anxiety has a negative impact on the grades achieved in programming courses, much like the negative impact of intense pressure on math exam performance.

It was found that creating opportunities for building good learning to workload. Therefore, programming courses must implement pedagogical approaches to ensure successful learning outcomes.

II. INTRODUCTION

US college enrollment has declined significantly over the past decade, with four million fewer students. The NCES reports a decrease in high school graduates enrolling in college, from 70% in 2016 to 63% in 2020. This trend has long-term effects on the economy, including in the IT industry. Though many universities offer computing-related majors, the rigorous curriculum can make it challenging for students to complete on time. Gateway programming courses face declining retention rates while maintaining a rigorous curriculum, which this study aims to address.

III. MANAGING WORKLOAD AND ANXIETY

A. Managing Workload Anxiety and Cognitive Learning

Managing the workload in fundamental programming courses is challenging for experienced and beginner students, causing anxiety. Our study provides learning strategies to alleviate anxiety and promote engagement in gateway programming courses.

The workload can cause work-related stress, depression, and anxiety. Depending on the individual's perspective, anxiety can positively and negatively affect job performance. Some see it as a hindrance, while others view it as a motivator. Studies have shown that anxiety can positively influence healthcare workers (Sun et al., 2022) but can also negatively impact performance, such as in math exams (Chang & Beilock, 2016).

As students juggle academics, work, and personal life, they may experience high anxiety levels (Appadurai, 2020). Educators can use active learning strategies to support them, provide feedback, and encourage reflection. According to the cognitive learning theory, memory, problem-solving, and learning involve mental processes. Cognitive learning entails storing knowledge in long-term memory for retrieval and application (Cooper, 1998). Therefore, introducing complex topics gradually and incrementally can improve student proficiency practically. The theory also explains why information processing capacity can overload if too much information is presented simultaneously.

B. Good Learning Habits

Cognitive learning can be divided into two types: declarative learning and procedural learning. Declarative learning involves acquiring new skills, while procedural learning involves practicing and applying those skills. For example, computing students usually acquire new coding skills by reviewing coding activities, a form of declarative learning. Then, after mastering the necessary skills, students experiment with various coding activities to apply them to different tasks, which is a process of procedural learning.

Reflecting through self-assessment can enhance student learning outcomes (Hsiao et al., 2022), encouraging good learning habits and motivation. Instructors can guide students in building good study habits like regularly reviewing and practicing coding, taking notes in class, and using self-assessment to evaluate their knowledge.

C. Engaged Learning

To succeed in IT courses, it is essential to actively participate. A learning environment that encourages engagement through hands-on activities and project-based learning is flexible and effective in improving skills and promoting independent learning.

D. Peer Learning through Collaboration

The theory of social constructivism highlights the significance of collaborative learning that occurs through interactions among individuals in society. This approach provides insightful viewpoints on the acquisition of knowledge and learning. Additionally, incorporating Pair Programming and self-assessment methods can contribute to developing effective programming courses. Pair programming, when utilized with platforms like GitHub, allows students to collaborate and receive valuable feedback from their peers throughout the semester (Lui & Chan, 2006).

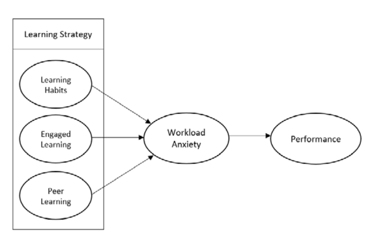

Figure 1: Exploring Learning Strategies, Workload Anxiety, and Performance

References are available upon request.

The Vulnerability of the Blood Supply Chain in the U.S.

Jeong Hoon Choi[1]
[1]Youngstown State University

I. INTRODUCTION

Blood centers have become one of the most profitable enterprises in the United States, since the majority of blood centers have excellent operational efficiency. However, such efficiency in the blood supply chain includes the nonprofit status, which exposes organizations to complexity like a pandemic. Osorio et al. (2015) describe blood supply chain as "the processes of collecting, testing, processing, and distributing blood and blood products from donor to recipient."

The pandemic, particularly its early period caused serious issues with donor and volunteer availability in the United States, potentially causing the nation's blood supply system to fail. In the post-pandemic era, substantial changes in donor recruitment, blood collection, and inventory management are predicted. The blood supply system in the United States may be irreparably transformed now that we are in the post-pandemic age. The epidemic has presented blood operations with a new strategic challenge. This study has two goals. First, this research looks at techniques for monitoring and minimizing the risks of a blood shortage caused by a large drop in donor numbers. Second, this research identifies ordering and collecting methods for accurately matching supply with demand.

II. RESEARCH FRAMEWORK

A. Simulation 1: the strategic partnership to manage the risk of blood shortages

In the first approach, this research examines the option of having a companion to reduce the danger of blood shortages. While the prospect of donor shortages must drive blood center coalitions, the true motivating factor was operating expense.

B. Simulation 2: coordinated effort nationally to create a pooled blood to manage blood shortages

It is well understood that centralized inventory can assist organizations moderate the ups and downs of demand and supply, allowing them to function successfully with smaller safety stock. This is a prominent supply chain management strategy. For example, a third-party logistics company frequently stores electronics inventory for Walmart, Best Buy, and other retailers. This method enables any organization to reduce the amount of safety inventory required while maintaining the same quality of customer service. As a result, in Simulation 2, this study evaluated whether a national coordinated effort to build a pooled blood inventory may assist minimize the risk of donor shortages. Figure 2 shows the results of the simulations. The results showed that the nationally coordinated effort is slightly superior in protecting blood centers from stockouts, resulting in a slightly lower average weekly shortage (for example, 395 units compared to the organization's choice of an 825 unit strategic alliance).

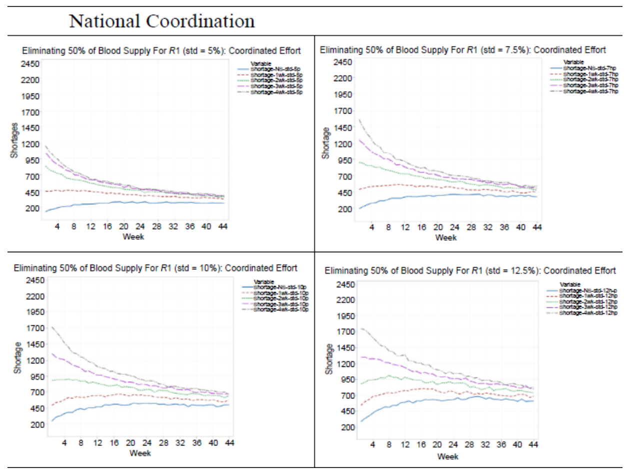

Figure 1: Simulation Results.

III. Discussions

The blood supply chain disruption during the pandemic prompted this study. Such a problem with product scarcity revealed that product scarcity is still an important subject of investigation. This research designed two simulation studies to suggest a nationally coordinated blood supply chain for protecting against national blood shortages.

REFERENCES

1. Osorio, A., Brailsford, S. and Smith, H. A structured review of quantitative models in the blood supply chain: a taxonomic framework for decision-making. *International Journal of Production Research*, Vol. 53 No. 24, pp. 7191–7212. 2015.

Proposal of a Parametric-based Generative Design Tool for Customized Mouse

Eui-Chul Jung[1], Huile Gao[2]
[1]Seoul National University, [2]Seoul National University

I. SUMMARY

The purpose of this research is to develop a customized parameter design tool for an easily graspable mouse using hand feature data. The design tool is developed using Arduino and Grasshopper to make use of hand characteristic data for customized form design system. Combine data such as points, lines, and planes on the palm to generate a mouse suitable for the shape of the hand.

II. INTRODUCTION

Probably everyone has experienced inconvenience caused by using improperly sized products. Finding a product that fits your hand is very difficult. If the product people hold and use every day does not fit in their hand, they will feel more discomfort. The goal of this research is to make use of the hand feature data to propose a generative design tool for a generative design method designed for a mouse.

III. HAND FEATURE GENERATIVE DESIGN

Generative design is an iterative design process and a quick way to explore the possibilities of design [1]. Figure 1 shows the hand data measurement method and form generative logic.

Step 1: Real-time changes of the mouse width and length according to the hand data.

Step 2: Real-time changes with the mouse height as the distance from the palm to the horizontal surface.

Step 3: Real-time changes of the mouse tilt angle as the free tilt of the palm. (Joystick sensor)

Step 4: The bending sensor is used to convert the curvature of the hand into the curvature value of the curve in Grasshopper to control the deformation of the mouse structure line in real-time.

Step 5: Using the joystick to adjust the position of the index finger and middle finger to control the position of the left and right buttons of the mouse.

Step 6: Testing the hand pressure control form structure with the pressure sensor.

The mouse shape created through the six steps is used as an archetype for customized product design.

ACKNOWLEDGEMENTS

This work was supported by the Ministry of Education of the Republic of Korea and the National Research Foundation of Korea (NRF-2021S1A5A2A01070316)

REFERENCES

1. ENGINEERING.com. "Generative Design: The Road to Production". www.engineering.com. Retrieved 2019-12-05.

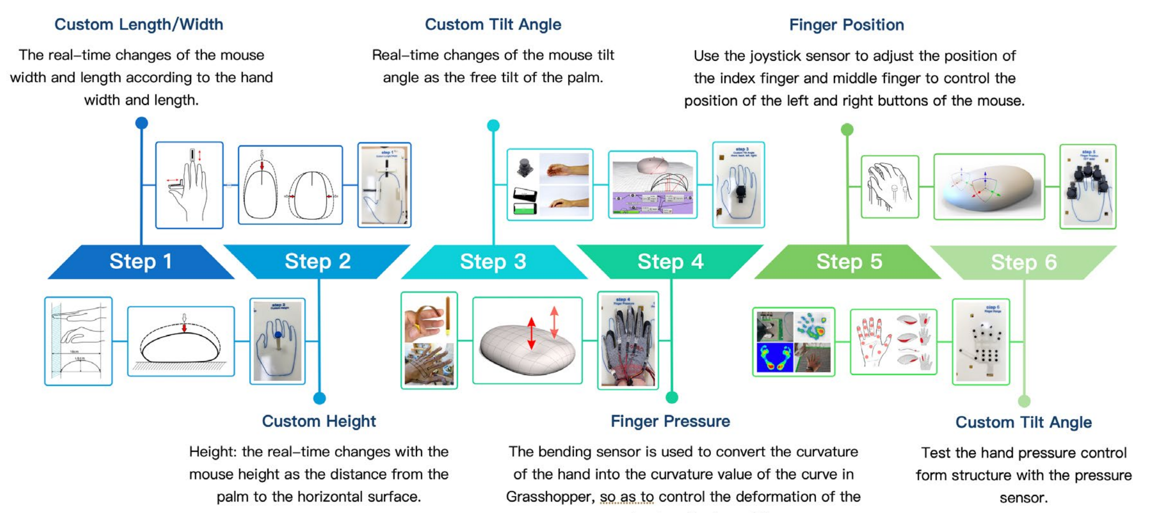

Figure 1: Process of parametric-based generative design tools for mouse shape suitable for hand size

Leveraging Smart Contracts for Secure and Asynchronous Group Key Exchange Without Trusted Third Party

Junggab Son
University of Nevada, Las Vegas

I. INTRODUCTION

Group Key Exchanges (GKEs) are protocols that allow two or more participants to agree on a common secret key (session key) over an insecure communication channel in the network in such a way that one participant cannot derive the session key without the contribution of others. If a GKE protocol ensures that only involved participants can derive the session key, it is said to be *authenticated*. GKE is one of the core components in the security of multi-user systems such as group text message, ad-hoc network applications, Internet of Things (IoT), and so on.

To date, many synchronous GKE schemes have been introduced in the literature. One of the limitations of the synchronous schemes is that they require all the participants to be always online during the execution of the GKE protocol. However, this requirement is difficult to fulfill in the presence of abundance of battery-powered devices that can enter into hibernation mode to prolong their lifetime. Therefore, such resource-constrained devices may not always be online. In addition, these schemes require participants to remember multiple keys and to carry-out all the compute-intensive operations, which can be burdensome for computationally-limited devices such as IoT devices. To address this issue, asynchronous GKE schemes have been proposed in the literature that allow some participants to be offline during the execution of the protocol. These offline participants can come online later at some point and derive the session key. However, such schemes still require participants to carry out all the computations. It is also worth noting that the existing synchronous and asynchronous GKE schemes rely on Trusted Third Parties (TTPs) such as Certificate Authorities (CAs) to allow the participants to authenticate each other and relay messages. Such reliance on TTPs is another significant drawback of the existing GKE schemes. For instance, if a TTP is not available during the execution of a GKE scheme, it can render availability problem for the underlying application and become a single point of failure. Furthermore,

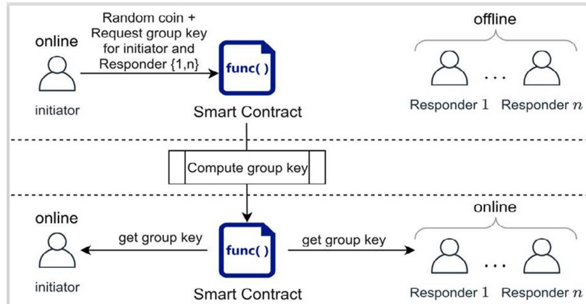

Figure 1. Naive Group Key Exchange Protocol

TTPs are vulnerable to attacks such as rogue certificate and key compromise impersonation that allow attackers to impersonate them.

In addition, a GKE scheme needs to support the following two important security requirements when it is used in a vulnerable environment where devices are more easily compromised than desktop computers, e.g., IoT environment. The first requirement is the Perfect Forward Secrecy (PFS), i.e., the compromise of the long-term identity and key of a participant does not reveal the previously established session keys, and the second requirement is the Post-Compromise Security (PCS), i.e., participants can re-establish the security of a session even after one group member was compromised. A failure to satisfy these additional requirements will result in creating critical vulnerabilities such as cloning attack. Therefore, it is imperative to develop an efficient and robust GKE mechanism to fulfill these requirements.

Our contributions can be summarized as follows:

- We propose an asynchronous GKE protocol that uses blockchain to store the security key-related material and uses smart contracts to reduce the number of operations that the participants must perform. The proposed protocol ensures PFS and PCS and allows the addition and removal of group members.
- We analyze the security of the proposed protocol and show that an attacker cannot obtain the session key from the key materials stored in the blockchain and that our protocol is secure under the standard attacker model.
- We present two implementations of our protocol based on Ethereum. In the first implementation, all key-related materials are stored in the blockchain while for the second implementation, only the key-related materials necessary for the smart contracts are store on the blockchain with the rest kept in a distributed storage.

Safe Drilling Depth for Deep Hole Bone Drilling

JuEun Lee[1], Justin Boetius[2]
[1]Department of Mechanical Engineering, University of the Pacific, Stockton, CA, [2]Abbott Laboratories

I. Introduction

In many surgical procedures, such as neurotologic, orthopaedic, and orthognathic surgeries, bone drilling is performed to insert screws or install prosthetic devices into the bone, which is located at a deeper depth, resulting in having the relatively high ratios of the drilling depth to the drill-bit diameter (approximately 14 to 27) [1].

Recently, Lee et al. [1] observed that a significant increase in force during deep hole bone drilling, which can result in a significant temperature rise in bone, which results in thermal necrosis. Additionally, they reported that the bone drilling behavior at deeper drilling depths showed unpredicted abnormal trends in forces and torque, which can cause other unwanted complications such as drill-bit breakage.

This study aims to investigate the drilling depth where the state of the forces transitions from normal to abnormal state, which is called the transitional drilling depth (TDD) in this study.

II. Materials and Methods

Experimentation was conducted on bovine cortical bones obtained from the mid-diaphysis section of bovine tibia. A CNC milling machine (HAAS VF-HS CNC) was used for the drilling operations. An experimental setup was designed to measure both thrust forces and torques in bone drilling. A dynamometer (Novatech 310) was used to collect the force data during the drilling procedures. The experiments utilized a 2.5 mm drill bit diameter and a hole depth of 36 mm to mimic deep hole bone drilling conditions in surgeries. This study selected three different spindle speeds and feed rates to investigate the effect of the operation conditions, specifically spindle speeds of 1000, 2000, and 3000 rpm, and feed rates of 0.05, 0.075, and 0.1 mm/rev.

III. Results and Discussion

Data for the transitional drilling depth (TDD) were analyzed using a three-way ANOVA performed in MATLAB to test the effects of spindle speed, and feed rate along with interactions.

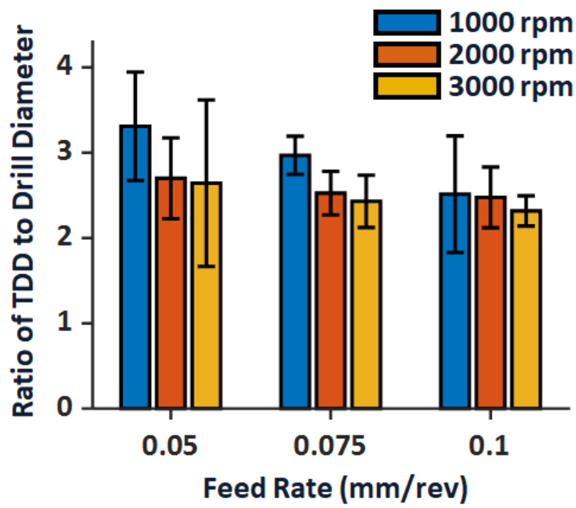

Figure 1: Ratio of Transitional Drilling Depth (TDD) to Drill Diameter observed in Deep Hole Bone Drilling

As shown in Fig. 1, both the spindle speed and feed rate were statistically significant ($p < 0.05$, respectively). A post hoc test of the spindle speed showed statistically significant results for, 1000, 2000, and 3000 rpm while the feed rate significantly differed for 0.05 and 0.075 mm/rev, and 0.05 and 0.1 mm/rev. This can be due to the operation conditions which can influence the chip morphology, resulting in affecting the TDD in deep hole bone drilling. In addition, it has been observed that the chips become more fragmented at higher speeds, and at low cutting speed, the long continuous chips are observed.

ACKNOWLEDGEMENTS

This work was supported by the Eberhardt Award (J Lee).

REFERENCES

1. J.E. Lee, S.Y. Chu, "An Experimental Investigation of Forces on Cortical Bone in Deep-Hole Bone Drilling," ASME *Journal of Engineering and Science in Medical Diagnostics and Therapy*, Vol. 3, pp. 031006-1-7, 2020.

Inventory and firm performance analysis in the pharmaceutical industry

Sam (Sangdo) Choi[1], Jeong Hoon Choi[2]
[1]o9 Solutions, [2]Youngstown State University

I. INTRODUCTION

This study investigates the inventory-firm performance relationship in pharmaceutical enterprises, taking into account both total inventory and its discrete inventory components. Furthermore, this study creates a new taxonomy of pharmaceutical enterprises based on the earnings-turns matrix. For the period 2000-2019, a large panel dataset of firms in the pharmaceutical industry in the United States was compiled. The objective of this research is to investigate the structural characteristics of the pharmaceutical sector prior to the commencement of the Covid-19 pandemic by investigating the relationship between inventory and company performance and developing a taxonomy of pharmaceutical enterprises based on the earns-turns matrix.

II. RESEARCH FRAMEWORK

The results show that inventory turnover ratio is negatively correlated with the financial profitability. We find that the WIPI ratio has shown the increasing trends. It means that most pharmaceutical firms have used internal buffers to avoid interference and assured some degrees of independence in each stage of production. This study also investigates the structural characteristics of the pharmaceutical business by investigating the inventory-firm performance correlation and pharmaceutical company taxonomy based on the earns-turns matrix. Figure 1 shows the different strategic groups of pharmaceutical firms on the earns-turns matrix. In the earns-turns matrix, the results show that strategic categories identified using this taxonomy have varying levels of profitability and inventory turns. Most pharmaceutical companies went from the bottom-right to the top-left area of the earnings-turns matrix, showing that they have prioritized profitability over operational excellence.

III. Discussions

This research explores the structural attributes of the pharmaceutical industry by looking into the inventory-firm performance linkage and the taxonomy of pharmaceutical firms based on the earns-turns matrix. The mapping of strategic groups on the earnings-turns matrix is a valuable tool for graphical depictions of strategic group dynamics in terms of financial and operational performance.

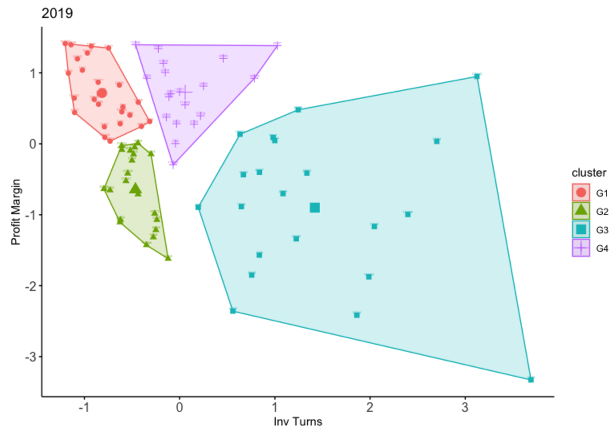

Figure 1: Strategic groups shown on the earns-turns matrix.

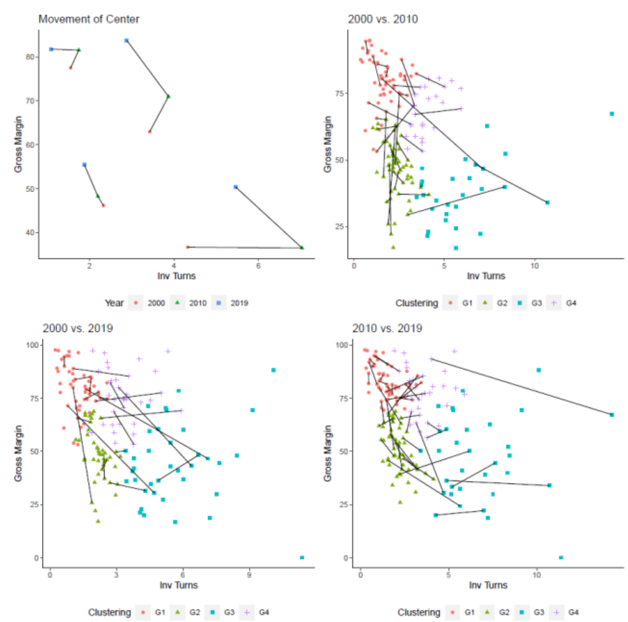

Figure 1: Traces of the centers of pharmaceutical strategic groups over 20-year period

REFERENCES

1. Choi, S. Supply chain performance analysis of Dow Jones Industrial Average indexed firms and top 50 supply chain firms. *Decision Sciences Journal of Innovative Education* 17(1), 33-52. 2019.

Does corporate political advocacy harm your offline business?

Yeohong Yoon[1]
[1]Emory University

Abstract
Politics greatly impacts almost every aspect of our lives, including consumption habits and decision-making. Previous studies have shown that those with strong political beliefs tend to be more consistent in purchasing decisions than those without such convictions. Eco-friendly consumers are more likely to purchase sustainable products than those less concerned (Griskevicius et al., 2010). Similarly, liberals tend to shop from a brand that promotes progressive values, while conservatives might be drawn to those with traditional values (Hydock et al., 2020). For example, customers may opt for Citi Bank over Chase Bank because Citi Bank is seen as being more socially progressive than the other due to its reaction to social issues such as gun control (Jeung, 2022). Likewise, customers' political beliefs can shape their choices when it comes to selecting brands within a particular industry.

In this study, the author will explore how political beliefs affect consumer choice in the retail industry specifically. Using the owner's announcement of political beliefs as an external shock, I address its impact on consumer choices by analyzing foot traffic data in Korea. In January 2022, the owner of the biggest retailer in South Korea became the target of criticism from liberals, and support from conservatives when he criticized the North Korean Communist Party on his SNS. Because of the issue, the stock price of relevant firms decreased by up to 8%, and employees publicly criticized the owner, resulting in an official apology.

It became one of the hottest controversies online, but it is uncertain that the physical stores would have been avoided by customers offline. Firstly, in reality, capturing a boycott behavior could be difficult. It is only possible to boycott if those who criticized were actual customers in the pre-period. That is, they cannot decrease their visits if they have never visited the focal firm. In addition, those who shop offline may be unaffected if actual customers are not active online. On the other hand, there is room for an increase in visits to physical stores. Those who support the idea can easily 'buycott' from the retailer; they can initiate more quantitative impact. Furthermore, with the mere exposure effect, as the media covers the company, there is a possibility that the number of visits increases.

Using the foot-traffic data of the treated stores and competitors, I applied the difference-in-difference approach and observed that the number of visitors did not notably decrease. It shows the possibility that boycotts online did not impact retailers in general. Interestingly, when dividing regions into liberal, neutral, and conservative areas, I found that visits only increased in conservative regions after the shock. Because the trend in the neutral area didn't really change, the author posits the influx of supporters may be the main drivers for the increase in offline store visits rather than the mere exposure effect.

References
1. Griskevicius, V., Tybur, J. M., & Van den Bergh, B. (2010). Going green to be seen: status, reputation, and conspicuous conservation. Journal of Personality and Social Psychology, 98(3), 392.
2. Hydock, C., Paharia, N., & Blair, S. (2020). Should your brand pick a side? How market share determines the impact of corporate political advocacy. Journal of Marketing Research, 57(6), 1135-1151.
3. Jeung, J. (2022) Politically polarized depositors, Working Paper.

Exploring the Impact of the Working Capital in the U.S. Aviation Industry for Profitability and Shareholder Value

Dr. Seock-Jin HONG, Associate Professor
G. Brint Ryan College of Business, University of North Texas

I. SUMMARY

This study examines how working capital impacts profitability, shareholder value, and the relationship between COVID-19 and airline business types in the U.S. airline industry. Working capital is the short-financing indicator crucial for airline management facing economic uncertainty. The cash conversion cycle, the current ratio, the quick ratio, and working capital are explanatory variables. Revenue growth rates, earnings-per-share, and return-on-assets are the explained variables for profitability and shareholder values for the top ten U.S. commercial airlines from 2010 to 2021. This research applied panel data regression using the Hausmann-Taylor panel regression and the General method of moments to avoid heteroskedasticity, endogeneity, and unbiasedness. The authors find that the previous year's activities, days in inventory (DII), days-sales-outstanding (DSO), and COVID-19 as dummy variables impact profitability and shareholder value. DII, DSO, and the days-payable-outstanding of the large airlines are more prominent than those of small airlines. Airlines' business types (full-service, regional, or low-cost carriers) do not significantly impact profitability and shareholder value. The current research contributes to the literature by advancing the aviation industry. The value of this study is the first to explore working capital and its impact on profitability and shareholder with its determinants in the airline service industry, including the Pandemic period.

II. PANEL DATA ANALYSIS

Using airlines' financial data, we applied panel data analysis with ten U.S major airlines from 2010 to 2021. All collected data are strongly balanced, meaning all airlines have data for all years. We first applied the two-stage least squares (2SLS) regression analysis, which uses the explained variable's error terms correlated with the explanatory variables (1) and the instrumental variables (IV) estimator in the context of the classical panel data regression to see how CCC impacted profitability and shareholder value.

$$\Delta Y_{it} = \gamma \Delta Y_{it-1} + \beta_1 \Delta Xk_{it} + (a_i) + \Delta u_{it} \quad (1)$$

where Y_{it} is the dependent variable with i = airlines (i – $1, \dots, n$) and t = time from 2010 to 2021. Xk_{it}, represents k independent variables, and u_{it} is an idiosyncratic error by airlines and time. The unknown intercept for each airline was omitted because of a unique event during the given period, such as merger and acquisition, declared bankruptcy (chapter 11), etc. The model transformed the variables by taking the time average, which is the sum of all values within the sample period of a variable divided by several years. We applied Formula (1) for each airline and time characteristics using the first difference.

III. MANAGERIAL IMPLICATIONS

Working capital captures the attention of top management as corporate goals shift from maximizing profits to securing liquidity (Hogerle et al., 2020). Financial managers should consider the interaction between profitability and short-term financial indicators, especially shortening DSO by coordinating the flow of information, materials, and funds (Losbichler & Mahmoodi, 2012) with their business partners. A decision to adjust payment terms with suppliers may have a consequential impact on their quality of service, impacting inventory levels and, thus, the quality of service to customers (Power & Ball, 2020)

REFERENCES

1. Hogerle, B., Charifzadeh, M., Ferencz, M., and Kostin, K. B. (2020). The development of working capital management and its impact on profitability and shareholder value: Evidence from Germany, *Strategic Management*, *25*(2): 27-39.
2. Losbichler, H., and Mahmoodi, F. (2012). Why working capital should matter to you. *Supply Chain Management Review*,November: 26–33.
3. Power, F., and Ball, C. (2020). *Improving cash and working capital management*. KPMG International.

The Impact of Context and Environment on Driver's Situation Awareness

Sami Park[1], **Yilun Xing**[1], **Kumar Akash**[3], **Xingwei Wu**[3], **Teruhisa Misu**[3], **Linda Ng Boyle**[1, 2]
[1]Dept. of Industrial and Systems Engineering, University of Washington, Seattle, WA,
[2]Dept. of Civil and Environmental Engineering, University of Washington, Seattle, WA,
[3]Honda Research Institute USA, Inc., San Jose, CA

I. INTRODUCTION

This study examines drivers' situational awareness (SA) regarding dynamic road situations. It assesses their ability to identify and anticipate safety situations, considering different road conditions. The study investigates the potential of the proposed Situation Awareness Global Assessment Technique (SAGAT) query method to quantify SA levels and explores factors influencing the accurate perception of objects and trajectories.

II. METHOD

A. Participants and Apparatus

A video-based driving simulation method was employed to collect direct measurements of drivers' situational awareness using the SAGAT. A group of 20 young drivers from the Seattle, Washington area participated in the experiment, which took place in a fixed-base, immersive driving simulator equipped with an actual steering console.

B. Dependent Variable

The participant's SAGAT responses for each object were categorized into four groups:

• Hit. The participant's touch was accurately placed within the labeling boxes in the pause frame, and the selected object type matched the actual object.

• Trajectory-Projection and Delayed Perception. Both categories indicate that touch was out of the labeling boxes in the pause frame but located in one of the estimated boxes on the trajectory.

• Miss. No touch was located in the pause-frame labeling box or the trajectory-frame labeling boxes of an object.

C. Independent Variables

• Object Type. There were three levels for object type: pedestrian, car, and cyclist.

• Size of Object. Area of the labeling box for each object in pixels.

• Visual Image Complexity. This was calculated using the ratio of the compressed and original size.

• Number of Objects. The number of objects in the pause frame for each object type.

• Gender. Female or non-female.

• Roadway Type. Roadway type included three levels: segment, intersection, and roundabouts.

III. RESULTS

The multinomial logit model revealed significant findings at $\alpha = 0.01$. Cyclists were less likely to be perceived and have their trajectories perceived compared to cars and pedestrians. Pedestrians were less likely to be correctly perceived but more likely to have their trajectories perceived compared to cars. Smaller objects had higher perception rates and were more likely to have trajectories projected. Females showed better perception of objects and trajectories compared to non-females. Increased visual complexity improved object perception but decreased trajectory perception. Higher object density increased the likelihood of missing objects in all comparisons.

ACKNOWLEDGEMENTS

This study was made possible by funding from Honda Research Institute.

REFERENCES

1. Xing, Y., Park, S., Akash, K., Wu, X., Misu, T., & Boyle, L. N., "Investigating the impact of context and environment on driver's situation awareness," *Proceedings of the Human Factors and Ergonomics Society Annual Meeting, 66(1), 335–339*, 2022.
2. Park, S., Xing, Y., Akash, K., Misu, T., & Boyle, L. N., "The Impact of Environmental Complexity on Drivers' Situation Awareness," *Proceedings of the 14th International Conference on Automotive User Interfaces and Interactive Vehicular Applications. Association for Computing Machinery, 131–138.*, 2022.

A Drill-Down Demand Analysis of Beef and Hay Consumption in Korea

EunSu Lee[1] & Eun Soo Kim[2]

[1] New Jersey City University, Jersey City, NJ 07311
[2] Korea Maritime Institute, Busan, Korea 49111

I. INTRODUCTION

This study demonstrates to forecast the demand for forage, a nutrient source necessary to produce high-quality beef cattle, using a drill-down technique with time-series predictors. Beef consumption in Korea has been steadily increasing with a 4.72% of CAGR (2010-2021). This consumption is supplied by domestic production and imported beef. High-grade beef, namely 'HanWoo,' is gaining popularity and requires a roughage mix to produce an already high-quality beef even higher. However, most of the forage is imported from abroad due to limited domestic production. Therefore, accurate forecasting of forage demand is essential for future forage supply chain and business analysis to avoid global supply chain disruption. This study utilized the time-series predictors of beef consumption, GDP, population, and the number of cattle.

II. DATA AND METHOD

A. Meat Consumption

A meat consumption dataset is collected from the Korean Census Bureau. It shows a strong correlation with the gross domestic production (GDP) since 2010. The decline in meat consumption in the early 2000s is speculated to be related to the "mad cow disease" scare. The data shows that population growth and meat consumption are correlated but not linear. We need to analyze this relationship in three parts. First, the propensity to consume meat does not increase until 2005, which is an anomaly. Second, population growth and meat consumption trends are linearly related, indicating a strong correlation. Third, despite the country's population growth trend slowing down, meat consumption tends to increase steadily. This means that per capita meat consumption is increasing.

*B. **Cow and Beef Cattle Production***

The early 2000s witnessed a decline in beef cattle, primarily attributed to reduced consumption caused by the mad cow disease epidemic. Additionally, the foot-and-mouth disease epidemic in 2010 and 2017 resulted in the culling of beef and dairy cattle, contributing to a slowdown in the upward trend depicted in the graph. The quantities of beef and dairy cattle can be predicted through time series analysis, considering meat consumption as an explanatory variable. While beef cattle directly impact meat consumption, dairy cattle, primarily used for milk production, indirectly contribute to the meat supply. Hence, these predictions are based on two assumptions. Firstly, livestock farmers determine the number of cattle based on the meat consumption market in the previous year. Secondly, dairy farmers do not raise dairy cattle to supply meat.

*C. **Hay Consumption***

Farmers feed cattle a mixed diet of high-quality hay to ensure high-quality beef and milk production. The forage-to-concentrate ratio depends on the cattle's growth stage. This study uses time series data on hay consumption and the number of cattle explanatory variables to predict hay consumption.

III. Discussion

The pattern of the data shows that population growth slows down. The upward trend will slowly fade if a prediction model uses per capita consumption to predict meat consumption. However, as per capita meat consumption increases, the total meat consumption trend will be upward. Even if meat consumption increases, beef production will be constrained by limited land use and rising production cost. The difference between meat consumption and beef production will likely be filled by imported meat. This study used time series of predictor variables to forecast hay demand. This research contributes to supply chain planning to prepare for supply and demand at the national level.

REFERENCES

1. Lisa Allen & Sun Chol Choi, "Forage Market 2019," *Gain Report: Global Agricultural Information Network*, USDA Foreign Agricultural Service, Washington D.C., KS1926, 8/8/2019.

Prediction and Integrated Control System for the Spread of Hazardous Materials in Industrial Areas

Minho Son[1], Il Ryong Kwon[2]
Podo Inc.

I. SUMMARY

The need for a comprehensive industrial disaster management system is being emphasized, including a paradigm shift towards prevention-focused disaster management due to the increase in safety accidents and the enlargement of them caused by the aging of safety facilities in national industrial parks, and the establishment of a digital safety network. In order to establish an integrated control system for the leakage of hazardous materials based on a digital twin, the inherent district has developed the sensor management and collection system for hazardous materials, integrated with the diffusion model and the hazardous material integrated control system, as well as the technology for tracing the source of hazardous materials using MMF and the UI development. Additionally, they applied digital twin technology, including the development of simulation technology combining material, atmospheric environment, diffusion path, and industrial complex information, and the development of AI algorithms and alarm functions based on simulation results to minimize industrial complex damage.

II. Research Methods and Results

This study developed a technology for predicting the dispersion of hazardous substances using the Multi Model Framework, a hazardous substance dispersion simulation program, and utilizing weather information and predicted wind pathways of buildings provided by the Korea Meteorological Administration. In addition, an inverse tracking technology for identifying the source of hazardous substance leaks was developed. An algorithm for generating citizen evacuation information based on dispersion predictions was also developed for use in disaster response. Various digital twin-based functions were developed, such as a function for visualizing the impact of hazardous substance leaks, estimating the expected location of leaks, providing evacuation routes, and controlling hazardous substance leaks. An API was also developed to integrate with the National Disaster Management System (NDMS).

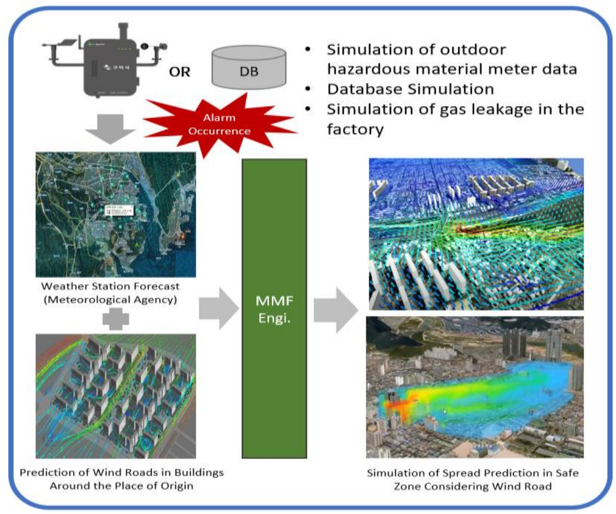

Figure 1 : Prediction Simulation of Hazardous Substances Diffusion

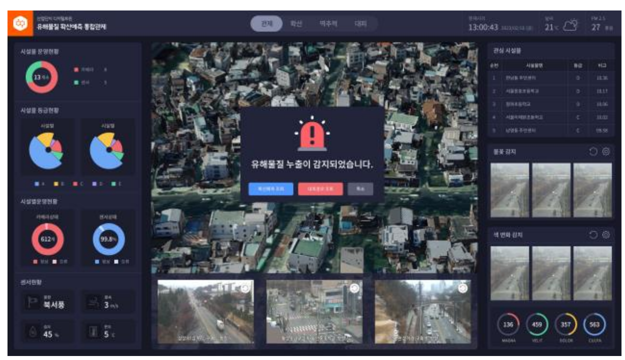

Figure 2 : Hazardous Substances Spread Situation Panel

ACKNOWLEDGEMENTS

The research results are from the development project of a pre-emptive, diffusion prediction, and integrated control system for hazardous material leaks in industrial complexes for the Safety Zone creation of the manufacturing safety innovation technology development project under the Ministry of Trade, Industry and Energy (No. 20022220).

Analysis of the Relationship between Innovation Activities and Profitability in Banking Industry in Korea

Sooyeon Lim[1,2], Junseok Hwang [1,2]

Technology Management, Economics, and Policy Program, Seoul National University1

Integrated Major in Smart City Global Convergence, Seoul National University2

I. SUMMARY

This study analyzed the contents of technology development and innovation occurring inside the banking industry by examining patents applied by all the banks in Korea and analyzed the effect on bank profitability by setting patent activities as innovation proxy variables As a result, a positive (+) relationship in which the registration ratio of the patent is statistically significant to the ROE profitability was additionally confirmed. This study contributed to investigating the content of Fintech and the relationship between patents and profitability in the banking industry from the early 2000s when the overall introduction of IT technology and recent time.

II. Methodology and Result

A. Data

Financial data for 10 years from 2012 to 2021 and 1,308 patents filed by banks in Korea with the Korean Intellectual Property Office were collected. As a result of analyzing the IPC of patents filed by the bank for 10 years, the ratio of G06Q decreased. The concentration on a specific technology occurred in a later period.

B. Methodology

The dependent variable was set ROE, and the independent variable was the value obtained by dividing the number of patent applications and registrations by the number of employees. Panel regression analysis was performed.

C. Result

The quality level of patents showed a positive (+) correlation at the 1% level in model 2, which reflects only the quality level, and a positive (+) correlation at the 10% level in model 3, which reflects both patent activity and quality level. This can be interpreted that the quality level of patents has a positive (+) correlation with ROE profitability (Table 1)

III. ILLUSTRATIONS

Year: 2012–2016 The ratio of an early period	IPC (Frequency)	IPC (Frequency)	Year: 2017–2021 The ratio of a later period
75.90%	G06Q(751)	G06Q(270)	84.90%
4.80%	G06F(48)	G06F(22)	6.90%
2.40%	H04L(24)	G06N(7)	2.20%
1.30%	H04R(13)	H04L(6)	1.90%
1.10%	B60L(11)	G06K(5)	1.60%
1.00%	A61M(10)	G07F(4)	1.30%
1.00%	H04W(10)	G06T(3)	0.90%
Number of patent application	990		318

Figure 1: IPC Frequency Analysis of Bank's Patents

Table 1: ROE, Random effect model analysis

	Model1	Model2	Model3
Patent Quantity	0.13**		-0.11
Patent Quality		0.25***	0.41*
Intercept	21.31***	19.97***	19.06***

(Control variables omitted)

ACKNOWLEDGEMENTS

This research was supported by the BK21 FOUR (Fostering Outstanding Universities for Research) funded by the Ministry of Education (MOE, Korea) and National Research Foundation of Korea(NRF)

REFERENCES

1. Lerner, J., & Tufano, P. "The Consequences of Financial Innovation: A Counterfactual Researc h Agenda" *Annual Review of Financial Economi cs*, Vol. 3, pp 41–85, 2011
2. Noh.M.H, "The Effects of Domestic Banks' BM Patent Activities on Their Profitability Performance", *JBE*, Vol.26, no.1, pp.23-48, 2012

Examining the Transfer of ACC Training to Mental Models After an OTA Update of Advanced Driver Assistance Systems

Jimin Kim[1]
[1]Applied Cognitive Engineering Laboratory, University of Iowa, Iowa City, Iowa, USA

I. INTRODUCTION

As ADAS becomes increasingly complex and requires periotic software updates due to more nuanced ADAS and L3 capabilities, OTA updates will become more common. Such OTA updates provide a more efficient and frequent method to update vehicle software compared to dealer visits. However, one challenge of OTA updates is that they may not provide enough information to vehicle owners about what has changed in the updated system. Some changes may be noticeable, but others may not potentially affect the driver's mental model. Orlovska et al. (2020) note that driving context significantly impacts driver interaction with the ADAS, and any updates should consider contextual differences to prevent unexpected changes in a driver's mental model.

This study aims to investigate the effect of existing mental models on an updated ADAS system. If the drivers possess a correct mental model of the system's capabilities and limitations, it will facilitate the development of a new mental model of an updated system. Also, we examine whether developing a new mental model of the updated system can be expedited by not only current knowledge but also other factors such as system similarity and experience of the system.

II. METHOD

Before the study, participants' general health and susceptibility to motion sickness were checked. They were then given a questionnaire to gather basic demographic information and their experience with Adaptive Cruise Control (ACC). Participants were assigned to one of three conditions, which were: Pedestrian Detection update, Traffic Jam Assist with icon update, and Traffic Jam Assist with both icon and text update. They were then shown a training presentation about the simulator and ACC. The study consisted of three drives: a 10-minute practice drive, a 20-minute study drive 1 with baseline ACC, and a 20-minute study drive 2 with an updated system. Participants answered the Mental Model Assessment questionnaire about ACC between study drive 1 and 2. Participants received the system update notification before study drive 2, depending on their assigned condition. After each drive, they completed a wellness questionnaire before proceeding to the next step. Upon unloading from the simulator, the MMA about Pedestrian Detection and Traffic Jam Assist was administered with a debriefing. For participants in condition 1, they answered the PD MMA first and then TJA MMA. For participants in conditions 2 and 3, the order was reversed.

III. RESULT

The aim of this study was to identify factors that aid the transfer of training during an OTA update. Based on descriptive analysis, most participants had an accurate mental model of ACC, indicating successful training. This implies the potential for transferring an accurate mental model to future updated systems. Results showed a relationship between an individual's pre-existing mental model and their mental model of OTA updated systems, with a stronger relationship for Pedestrian Detection ($r=0.42$, $p<0.05$) than Traffic Jam Assist ($r=0.19$, $p=0.07$). System similarity also facilitated the development of a mental model for the updated system ($t(170)=9.63$, $p<0.01$). Interestingly, experiencing the OTA updated system did not affect participants' mental models of the updated system ($t(95)=-0.3$, $p=0.98$). These findings suggest the need for additional consumer education to aid the understanding of updated systems.

REFERENCES

1. Orlovska, J., Novakazi, F., Lars-Ola, B., Karlsson, M., Wickman, C., & Söderberg, R. (2020). Effects of the driving context on the usage of Automated Driver Assistance Systems (ADAS)-Naturalistic Driving Study for ADAS evaluation. *Transportation research interdisciplinary perspectives*, *4*, 100093.

Technical Group D-1

Social Sciences (Anthropology, Economics, Political Science, Sociology, Public Policy, etc.), Psychology, Digital Arts, STEM Education, and Other Sciences (SSP)

Embodied Learning for Computational Thinking

Kyungbin Kwon
Indiana University – Bloomington

I. SUMMARY

In this study, 40 first and second-grade students engaged in embodied learning activities on a physical mat to explore their understanding of programming symbols and sequences. The study revealed that these activities enhanced the students' conceptual understanding of programming symbols and sequences.

II. Background

A. Computational Thinking Education

CT education for young children is gaining attention due to its positive impact on the development of favorable attitudes towards computer science (CS) and improvement of CT competency. However, the process of how young students learn abstract CT concepts and incorporate CT in their learning is not yet fully understood [1].

B. Embodied Learning for CT

Embodied cognition suggests that thinking is influenced by physical experiences and interactions with the environment [2]. Research indicates that embodied learning activities have a positive impact on CT education.

III. Methods

A. Participants

A total of 47 students participated in the study. Most first graders (n=24) did not have CT education but some second graders (n=23) learned Bee-Bot programming previously.

B. Research Design

This study utilized a repeated measure design without a control group to assess the impact of embodied learning activities on two learning outcomes: 1) cognitive skills related to computational thinking and 2) perceptions of programming or coding. The design controlled for individual variability.

C. AR Learning System for CT

The research team created an AR learning system that utilized virtual objects in cells to represent a virtual world for a student agent to complete missions. The learning objectives were to understand programming symbols by matching bodily movements and symbols, and to solve CT tasks by arranging symbols in certain sequences.

The research team observed and recorded the students' voluntary gestures and movements during the learning sessions. They planned to analyze screen recordings of the AR system, videos of students' movements, and small group interviews to understand how the students interacted with the AR system.

IV. Results

A. CT Concepts

The results of a mixed ANOVA showed that students' overall test scores improved significantly, $F(1, 45) = 29.65$, $p < .001$, $\eta_p^2 = .40$. Regarding the concept of symbols, students showed significant improvement after the learning, $F(1, 45) = 5.10$, $p = .029$, $\eta_p^2 = .10$.

B. Embodied Learning Activities

Overall, the students moved naturally according to the four symbols and the virtual objects were intuitive for them to interact with. Although there were benefits of utilizing AR technology, the findings also suggested some instructional insights to be considered.

ACKNOWLEDGEMENTS

The research has been supported by NSF grant #2048989.

REFERENCES

[1] L. Seiter and B. Foreman, "Modeling the learning progressions of computational thinking of primary grade students," in *ninth annual international ACM conference on International computing education research*, San Diego, San California, USA, 2013, 2493403: ACM, pp. 59-66, doi: 10.1145/2493394.2493403.

[2] A. M. Glenberg, "Embodiment as a unifying perspective for psychology," *WIREs Cognitive Science,* vol. 1, no. 4, pp. 586-596, 2010, doi: 10.1002/wcs.55.

Solar Tree for Science, Technology, Engineering, Art, and Math

Sung Yeul Park
Department of Electrical and Computer Engineering
University of Connecticut, Storrs, USA

I. SUMMARY

Introducing the Solar Tree, which has been developed over the course of two years with the participation of professors and students from the departments of Biology, Materials Engineering, Electrical Engineering, Social Sciences, and Art.

II. Solar Tree Project

A. Project Overview

The University of Connecticut (UCONN) Solar STEAM Tree project started in 2020 and ended in April 2023. It was a project that involved professors, graduate students, and undergraduate students from the natural sciences, social sciences, engineering, and arts colleges [1]. The project focused on creating an artificially made tree that provides solar energy and exploring its social applications. As an author, the contributor worked on the design and installation of the electrical components of the solar tree, with a background in electrical engineering.

B. Collaboration and Communication

As the project was approached from different academic fields, it was a great opportunity to learn how to work together, understand different approaches to decision-making, project management, and collaboration. The contributor would like to share this experience at the UKC conference.

C. Difficulties with the project

How to get started? What to do? When will the work be finished? These were all frustrating and time-consuming questions that came with the vague sense of starting something new. However, during the process of discussing the shape of the tree, defining its functions, and designing each component one by one, it was important to listen to diverse opinions, persuade others of the necessity, and push for consistency in the work. The key was to stay focused on the original purpose of the project and work towards achieving it. Through this process, we learned the value of gaining insight and experience through collaborative work, rather than just personal gain.

III. Solar Tree Design

Fig. 1 shows the solar tree. Nine solar panels (50W, 12V) were installed on the nine branches of the tree, and two batteries (12V, 100Ah Deep cycle AGM) were placed under each bench. The charge controller and LED wiring were installed on the third bench. The total power output is 450 watts, and it is designed to charge mobile phones while sitting on the chair. Additionally, a weather measurement system with a touch screen display was integrated to provide real-time weather information.

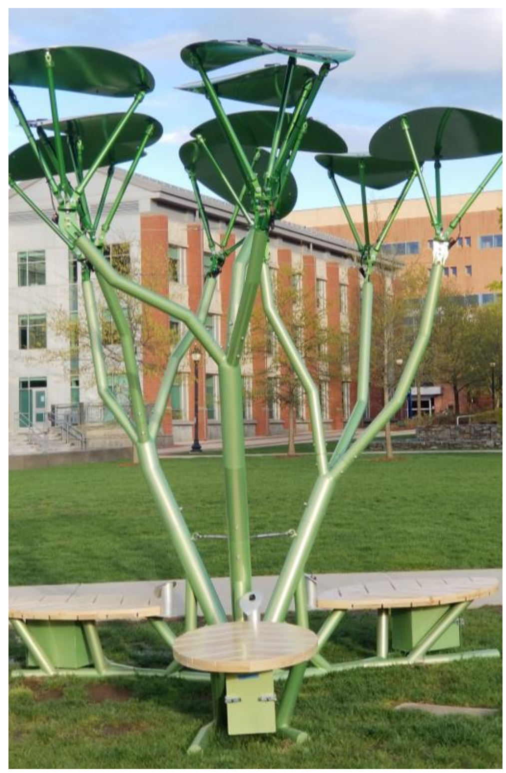

Figure 1: Solar Tree at UCONN

REFERENCES

1. University of Connecticut Solar STEAM Tree website: https://www.energy.uconn.edu/uconns-steam-team-solar-trees-and-the-power-of-community.

Developing AI Chatbot System for Self-Regulated Learning

Hyangeun Ji[1], Insook Han[2]
[1]Temple University, [2]Korea University

I. INTRODUCTION

Compared to the long tradition that self-regulated learning (SRL) studies have had in educational psychology, SRL research in educational technology is relatively new [1]. To better support students' SRL, educational technology researchers have employed various technologies, namely SRL prompts [3]. Recent advances in artificial intelligence (AI) technologies have led educational researchers to increasingly use chatbots in SRL scaffolding. Mobile-based chatbots equipped with advanced AI technologies have the potential to provide adaptive SRL with increased time and space flexibility. However, as an emerging technology in SRL research, our understanding of using chatbots for SRL is still limited. To address this research gap, we developed a mobile-based AI chatbot to support foreign language learners' SRL process and tested its usability.

II. METHODOLOGY

A. Participants and Data Collection

A total of eleven English as a foreign language learners participated in the study, with four learners who enrolled in an intensive English language program at a four-year university in the United States and seven learners who took a general education English course at a university in South Korea. After interacting with the chatbot for four weeks on their mobile phones, learners answered a system usability survey [2].

B. Chatbot Development

We developed the chatbot application, Study Buddy, using Google's Diaglogflow. Study Buddy was used to support Zimmerman's [4] three phases of SRL (i.e., forethought, performance, self-reflection) by providing different SRL prompts and resources at each phase. Study Buddy extracted and classified learners' intentions during the chatbot conversation and assembled dialogues based on predefined rules. These dialogues were intended to trigger planning actions, support self-monitoring, and ask reflective questions. We embedded Study Buddy into the Telegram Messenger app for the participants in the United States and KakaoTalk Messenger app for the participants in South Korea, considering their accessibility and regional popularity.

III. RESULTS AND DISCUSSION

Our findings suggest that chatbots can be effectively integrated into foreign language classrooms to scaffold diverse language learners' SRL skill development at each phase of SRL. Although a small number of learners participated in the study, the learners positively perceived the usability of Study Buddy and valued its flexibility and accessibility. Learners suggested adding chatbot features to send reminder messages and automatically provide the learners' pre-planned goals and strategies and enriching the chatbot response would be helpful. Future chatbot studies can build on our findings by implementing an SRL chatbot for a longer intervention time with suggested improvements and examining how SRL chatbots impacts students' learning performance.

REFERENCES

1. Azevedo, R., & Aleven, V., "Metacognition and learning technologies: An overview of current interdisciplinary research," In *International handbook of metacognition and learning technologies* (pp. 1-16). Springer, 2013.
2. Bangor, A., Kortum, P., Miller, J., "Determining what individual SUS scores mean: Adding an adjective rating scale". *Journal of Usability Studies*, Vol. 4, No. 3, pp. 114-123, 2019.
3. Moos, D. C., "Emerging classroom technology: Using self-regulation principles as a guide for effective implementation," In *Handbook of self-regulation of learning and performance* (pp. 243-253). Routledge, 2017.
4. Zimmerman, B. J., "Attaining self-regulation: A social cognitive perspective," In M. Boekaerts, P. R. Pintrich., M. Zeidner (eds.), *Handbook of self-regulation: Theory, research and applications*, pp. 13–39. Academic Press, 2000.

Unraveling the Effective Teaching and Learning Strategies for Korean College Students in STEM Majors in the COVID-19 Era

Seong Ji Jeong[1]
[1]The Ohio State University

I. Research Background

COVID-19 has changed the teaching-learning delivery setting, accelerating virtual learning and distance education. This left educators to seek effective teaching-learning strategies that guarantee academic outcomes, particularly in STEM majors that rely heavily on hands-on learning (Sedaghatjou et al., 2023). This study aimed to examine the effects of project-based learning (PBL) and flipped learning (FL) strategies for Korean college students in STEM majors before and during COVID-19.

II. Method

A. Data Source and Respondents

This study used the data from the Korean Education and Employment Panel II (KEEP II) Survey. It started in 2016 to track 2nd grade students in high school. For this study, responses from the 4th and 5th waves were used, including college and work life before and during COVID (2019-2020) (n=1,955).

B. Measures

Participation in *Flipped Learning* (FL) and *Project-Based Learning* (PBL) were respectively coded as dummy variables (0 or 1). *The GPA* was calculated as the average of the proportion of earned scores divided by the full scores in two semesters (0~1). Covariates included gender, curriculum satisfaction, STEM majors, college type, and college location.

C. Analysis Method

First, propensity score matching was applied to provide a balanced one-to-one sample of covariates for each model (n=228~806). Second, the regression model was used to examine the FL and PBL effects on GPA in each year, respectively.

III. Result and Conclusion

First, the result showed that FL has a stronger effect on GPA during COVID than pre-COVID. It suggests that using FL can be more effective during COVID, where distance education has become prevalent. Second, the effect of PBL was not significant during the COVID, while it was strongly significant in the pre-COVID. Third, the FL and PBL effects on GPA were significantly moderated by gender, indicating that male students benefit more from the FL strategy during COVID than female students.

Table 1: The effect of FL on GPA

Variables	Pre-COVID (2019)	COVID (2020)
FL *(ref. non-FL)*	0.026+	0.055**
Female *(ref. male)*	0.085***	0.103***
FL x Female	-0.041*	-0.085**
Curriculum satisfaction	0.045***	0.008
Natural science *(ref. engineering)*	0.009	0.039*
Biomedical *(ref. engineering)*	0.003	-0.017
4-year college *(ref. 2-year)*	0.000	0.027
In-Seoul *(ref. Non-in-Seoul)*	-0.002	0.024+
Constant	0.538***	0.699***
Observations	506	228
R-squared	0.162	0.186

Standard errors were not reported due to a lack of space.
*** p<0.001, ** p<0.01, * p<0.05, + <0.1

Table 2: The effect of PBL on GPA

Variables	Pre-COVID (2019)	COVID (2020)
PBL *(ref. non-PBL)*	0.057***	0.009
Female *(ref. male)*	0.091***	0.051**
PBL x Female	-0.038*	-0.012
Curriculum satisfaction	0.038***	0.007
Natural science *(ref. engineering)*	0.012	0.058***
Biomedical *(ref. engineering)*	-0.018	0.008
4-year college *(ref. 2-year)*	-0.011	-0.013
In-Seoul *(ref. Non-in-Seoul)*	0.002	0.033**
Constant	0.559***	0.751***
Observations	806	386
R-squared	0.133	0.108

Standard errors were not reported due to a lack of space.
*** p<0.001, ** p<0.01, * p<0.05, ^ p<0.1

REFERENCES

1. Sedaghatjou M., Hughes J., Liu M., Ferrara F., Howard J., & Mammana M. F. (2023) “Teaching STEM online at the tertiary level during the COVID-19 pandemic,” International Journal of Mathematical Education in Science and Technology, Vol.54, No.3, pp.365-381, 2023.

PROJECT ADAPT – Uncovering the Potential of Arts-Integrated Digital Literacy Professional Development Program in Preservice Teachers' Digital Literacy Development and Learning Engagement

Jewoong Moon, Kathryn O'Harra, Julianne Coleman, Kelley Schoger, Julie Bannerman
The University of Alabama

I. PROJECT SUMMARY

We present the pilot project ADAPT (Assessing the Impacts of Arts-Integrated Digital Literacy Professional Development Program for Preservice Teachers on Digital Literacy Competency and Learning Engagement), funded by the University of Alabama Collaborative Art Research Initiative's (CARI) Joint Pilot for Arts Research (JPAR) grant program. ADAPT explores the intersection of digital literacy and performing arts-integrated learning for pre-service teachers. The project aims to develop four modules focusing on digital literacy competency development, encompassing knowledge construction, innovation/creation, computational thinking, and collaboration. These modules incorporate a variety of activities to engage pre-service teachers in experiential learning environments, where they explore digital literacy lesson design ideas through art-integrated and -infused activities.

In this project, pre-service teachers are guided in designing and implementing transdisciplinary digital literacy lessons that integrate experiential education via performing arts elements, empowering them to enhance their pedagogical skills and create engaging learning experiences for future students. By broadening the perspectives of digital literacy lesson design through multimodal literacy development, ADAPT aims to equip pre-service teachers with the necessary tools and competencies to navigate the evolving educational landscape. Recognizing the increasing role of technology in society, educators must engage learners through diverse modes of communication, fostering creativity, critical thinking, and effective expression.

Implemented in Hyflex settings, ADAPT leverages Microsoft Teams with gamified activity systems to facilitate collaboration and activity design. This platform enables students to collaborate on group projects, generate ideas, and design curriculum-aligned activities through gamified quests, both online and offline. Seamless communication, file sharing, and real-time collaboration support active contributions from both in-person and remote students.

ADAPT adopts an evidence-centered design framework to assess the impact of these guided performing arts integrated activities on pre-service teachers' competency development and their ability to design innovative and inclusive digital literacy lessons. Surveys and feedback from participants will provide valuable insights into the project's effectiveness, informing future instructional practices.

The outcomes of ADAPT will contribute to ongoing discussions on multimodal literacy, digital literacy, the pedagogical value of arts integration, and pre-service teachers' interdisciplinary perspective-taking. It serves as a valuable resource for educators and researchers interested in leveraging performing arts integration to enhance digital literacy and cultivate well-rounded, adaptable, and creative educators.

Exploring Strategic Differences in Debugging Between Two Groups with Different Levels of Computational Thinking Competency: Implications for Teaching Strategies

Eunsung Park[1], Jongpil Cheon[2]
[1]Tennessee Tech University, [2]Texas Tech University

I. SUMMARY
This presentation shares our recent research on students' strategic differences in the debugging process among different competency-level computational thinking (CT) groups in undergraduate CT courses. Our study uncovered both distinct and nuanced differences. In our session, we will discuss the methodological approaches and the implications for teaching strategies for effective debugging.

II. Introduction & Methods

A. Backgrounds
Debugging entails iterative cognitive processes aimed at identifying and rectifying errors to achieve desired outcomes. It is a critical component of CT that presents both challenges and opportunities for enhancing problem-solving skills. By integrating debugging into education, students not only acquire essential technical CT skills but also develop resilience in the face of challenges, thus fostering a valuable learning opportunity. In this study, we focused on investigating the challenging blocks and strategies employed by two groups of students with different CT competencies.

B. Study contexts
This study collected four weekly assignments of 461 coding journals from a total of 123 students (49 male, 74 female) enrolled in online undergraduate-level CT courses over 15 weeks.

C. Methods
We utilized a structural topic model (STM) to discover topics and identify relationships between topics to document metadata (Roberts et al., 2014). This study found group-related challenging blocks and debugging strategies in semester-long CT projects.

III. Conclusion
The findings revealed that low-performing students encountered difficulties with both fundamental blocks (e.g., broadcast, wait) and advanced blocks (e.g., variables, conditions). Furthermore, different strategies were observed among the two groups of students (See Table 1). Given that certain issues and strategies persisted longer than anticipated, it is crucial to prioritize early-stage instruction to effectively address these challenges and teach these concepts (e.g., conditions, data) and practices (e.g., chunking, code review) early this semester.

Table 1: Differences in Debugging Strategies between Group

Low	High
• Seek help • Lack of understanding of the logical flow of codes • Trial and error as continuous strategies • Backward process	• Focus on finding possible cases of errors while playing • Backward & forward process • Testing by a chunk • Logical code review • Edit and run

REFERENCES
1. Roberts, M. E., Stewart, B. M., Tingley, D., Lucas, C., Leder-Luis, J., Gadarian, S. K., ... & Rand, D. G. (2014). Structural topic models for open-ended survey responses. *American Journal of political science, 58*(4), 1064-1082. https://doi.org/10.1111/ajps.12103

Utilizing Artificial Intelligence for Personalized Career Development

Boong Yeol Ryoo
Texas A&M University

SUMMARY

The existing college education primarily focuses on disciplines and poses challenges to offering tailored and personalized education, opening new career fields. This paper presents how students with personal learning interests or careers utilize artificial intelligence to personally define learning objectives, explore relevant knowledge, and structure it to create lesson content in their self-directed learning journey.

Keywords: Engineering Education, Artificial Intelligence, Personalized Learning, ChatGPT

I. INTRODUCTION

Gen Z is showing a growing inclination toward specific career paths in a discipline-centric education environment. In engineering education, teaching critical thinking and problem-solving skills are of utmost importance. Due to limited prior knowledge and lack of practical experience, students often face difficulties in identifying the problem-specific knowledge necessary to solve real-world problems.

The objective of this study was to investigate the potential of utilizing personalized learning with ChatGPT as a means to achieve desired learning outcomes and surpass the constraints associated with traditional discipline-centric education.

II. METHODOLOGY AND APPROACHES

This research focuses on the framework of ChatGPT, an AI model that provides consistent and context-relevant responses even industry knowledge. Often engineering education incorporates practical experience, which hinders students who lack hands-on experience in comprehending essential information, establishing the methodology, and making accurate assessments.

Two groups of students participated in the study: one group consisted of career-change students who held mostly an undergraduate degree in non-engineering, and the other group consisted of undergraduate students who have not yet started upper-level courses.

III. KNOWLEDGE MAPPING

Two things were instructed to perform: (1) determine the foundation knowledge necessary for students to explore a new subject and (2) logically interconnect with the course-specific knowledge mind map to be learned within the new subject.

Several essential and impact factors in personalized career education pathways are: (1) defining a subject and learning objectives, (2) questions and sequence for efficient information gathering, (3) mapping the search results regarding the overall theme, and (4) student engagement.

IV. SUMMARY

Most students demonstrated an ability to identify key information and integrate their prior knowledge into a course-specific knowledge they are going to acquire without significant challenges. Some students faced challenges in knowledge mapping as they grappled with comprehending the findings within a limited timeframe. This concern pertains to their ability to engage effectively in the critical problem-solving process, which involves information processing and making informed judgments.

The accessibility of artificial intelligence and data science techniques enables bridging the two aspects between traditional discipline-centric learning and personalized career-focused learning in specific fields of interest and empowering students to develop their career education pathways.

REFERENCES

1. Junaid Qadir, "Engineering Education in the Era of ChatGPT: Promise and Pitfalls of Generative AI for Education," *2023 IEEE Global Engineering Education Conference (EDUCON)*, Kuwait, Kuwait, 2023, pp. 1-9, doi: 10.1109/EDUCON54358.2023.10125121.
2. Sánchez-Ruiz, Luis M., Santiago Moll-López, Adolfo Nuñez-Pérez, José Antonio Moraño-Fernández, and Erika Vega-Fleitas. "ChatGPT Challenges Blended Learning Methodologies in Engineering Education: A Case Study in Mathematics." *Applied Sciences* 13, no. 10 (2023): 6039.

Enhancing Science Affinities through a Video Project in a Science, Technology, and Society (STS) Learning Approach

Jiyoon Yoon[1], Amanda Olsen[2]
[1]University of Texas Arlington, [2]University of Missouri Columbia

I. SUMMARY

The lack of awareness regarding the interconnectedness of Science, Technology, and Society, coupled with students' aversion to studying science, has contributed to various environmental and social issues. In light of the COVID-19 pandemic, students faced challenges accessing educational resources and demanded new programs to support their scientific learning experiences. This study implemented a science outreach program, utilizing a video project competition based on the Science, Technology, and Society (STS) learning approach, to investigate its impact on 13 randomly selected students ranging from Grades 4 to 11. The video project integrated three foundational theories—identity formation, attitudes toward science, and growth mindset—to enhance students' interest in science and evaluate the program's efficacy. Pre- and post-surveys indicated no statistically significant effects of the STS-based video project on participants with high STEM achievement. Nonetheless, interviews revealed that the study contributed to sustaining and cultivating their enthusiasm for science, fostering learning amid the pandemic by engaging them in the learning process, fostering an understanding of Science and Technology's role in society, and empowering them to make decisions shaping the future of our society.

II. METHOD

A. Purpose of the Study

This case study sought to explore how a student-generated video project using an STS approach could help to retain students (Grades 4-11) in science during the COVID-19 Pandemic. The study focused on 13 individual students and their video projects and analyzed the effects of video production on the student's motivation and affinities for science.

B. Research Questions

1) Does the online video project help students to increase their science identities?
2) Does the online video project improve students' interest in science?
3) Does the online video project promote students' science efficacy?
4) Does the online video project positively develop students' attitudes toward science?

III. RESULTS

Table 1 shows the results of the pre- and post-science affinity test of the 13 future scientists and engineers using paired t-tests.

Table 1: Results of Pre-and Post-tests

Test	N	t	P
Pre(ID)	13	-0.76	0.46
Post(ID)	13		
Pre(Interest)	13	-1.16	0.27
Post (Interest)	13		
Pre(concept)	13	-1.16	0.27
Post(concept)	13		
Pre(Attitude)	13	-0.34	0.74
Post (Attitude)	13		

IV. CONCLUSION

The purpose of the study was to examine the effects of a video project using an STS learning approach on the middle to high school students' science affinities to support and retain these students in science during the COVID-19 Pandemic. This study explored thirteen participants' science identity, interest, self-concept, and attitude. The pre-and post-survey scores showed that this project did not have statistically significant effects on the participants. However, the interview responses that revealed the participants' insights showed that the video project effectively helped to sustain or increase the students' science affinities and their science learning after participating in the video project.

This study aimed to help the students to improve their learning in science by enhancing their affection for science, thus forming their science identities. The video project provided the students at least an opportunity to develop their science motivation, engagement, attitudes, and literacy, thus shaping their scientific integrity and fostering their mindsets.

Virtual Cultural Science Night with Academic Coaching

Jiyoon Yoon
University of Texas Arlington

I. SUMMARY

This study aimed to develop and evaluate a teaching methodology, Cultural Science Night, incorporating students' cultural backgrounds into science education. 17 participating teachers collaborated with culture tellers, creating an online culturally responsive textbook that is composed of culturally responsive science lessons. Academic coaches facilitated synchronous communication and graded teachers' work using diverse rubrics. Open Educational Resources (OER) supported cross-cultural experiences. Data collection included pre- and post-tests, cultural intelligence scales, and a reflective survey. Results showed improved cultural competency and an inclusive learning environment for minority students, demonstrating the effectiveness of the online academic coaching and the online learning tools.

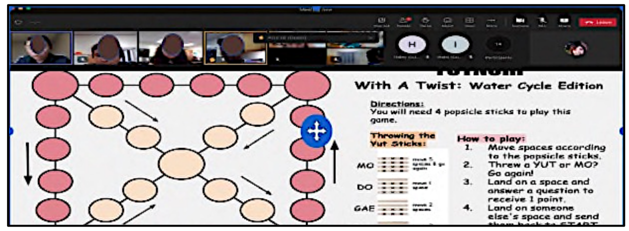

Figure 1. Virtual Cultural Science Night

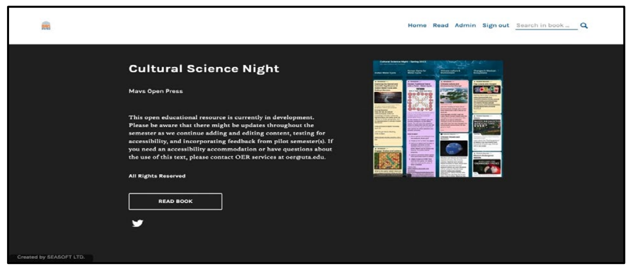

Figure 2. Cultural Science Night Textbook on Pressbook

II. INTRODUCTION

A. Problem

There has been the achievement gap between minority students and their counterparts (Gonzales et al, 2009).

B. Solution

Culturally responsive instructions enable educators to resolve potential cultural differences among students in the classroom and create an equal learning environment for all students, including minority students (Theobald, E. J., et. al., 2020).

III. METHODS

The teachers who were enrolled in an online science method course had a four-day workshop: Day 1) Experiencing other cultures with the cultural professionals, Day 2) Understanding culturally responsive instructions with academic coaching; Day 3) Developing their own culturally responsive science instructions by using OER; Day 4) Performing their instructions to elementary students at the Cultural Science Night. The Cultural Science Night textbook was created by Pressbook.

IV. RESULTS

Pre- and post-survey data analysis with 17 teachers showed no significant improvements in their science affinities and cultural competence. However, interviews revealed enhanced cultural understanding, knowledge acquisition, and increased confidence in teaching diverse students. These positive outcomes were attributed to the academic coaching and the use of Pressbook and OER resources.

V. CONCLUSIONS

The Cultural Science Night, supported by cultural professionals and academic coaching, utilized Pressbook and OER to successfully enhance and sustain teachers' science affinities. It empowered them as culturally responsive instructors, boosting their confidence in teaching and strengthening their cultural competency skills.

ACKNOWLEDGEMENTS

Thanks to the Instructional Connections for their supports.

Synchronous Online Culturally Responsive Academic Tellers and Educational Supporters (SOCRATES) for Online Academic Coaching

Jiyoon Yoon[1], **Kate Koo**[2]
[1]University of Texas Arlington, [2]University of Geogia Athen

I. SUMMARY

This project aims to develop a synchronous online instructional model incorporating academic coaching to facilitate future elementary teachers' learning about diverse cultures and assess its impact on their ability to teach diverse students effectively. Fifty-six participants engaged with culturally responsive academic tellers to explore cultural aspects such as history, art, music, dance, food, clothing, and housing. Collaborating with educational supporters, they developed culturally-responsive science lessons, benefiting from feedback and managing communication threads. Through pre- and post-tests, interactions with tellers and supporters, and final lessons, significant improvements were observed in participants' confidence, multicultural competency, and skills in fostering inclusivity. This online approach, guided by academic coaches, effectively promoted active student engagement in science education.

II. METHOD

A. Purpose of the Study

To close the achievement gap between minority students and their counterparts[1], this study is to develop a comprehensive synchronous online instructional model (Synchronous Online Culturally Responsive Academic Tellers and Educational Supporters: SOCRATES) and assess its effectiveness in improving future teachers' multicultural competency, their ability to create culturally-responsive science lessons, and their confidence in teaching culturally and linguistically diverse (CLD) students.

B. Research Questions

a. To what extent does SOCRATES improve multicultural competency of future teachers?
b. To what extent does SOCRATES enhance future teachers' knowledge and skills in developing culturally-responsive lessons?
c. To what extent does SOCRATES support the confidence of future teachers in teaching CLD students?

III. RESULTS

Table 1 shows the results of the pre- and post-self-efficacy & outcome expectancy test of the 56 future teachers using paired t-tests. Figure 1 illustrates the correlation between teaching efficacy and lesson scores.

Table 1: Results of Pre-and Post-tests

Test	N	t	P
Pre(self)	56	3.26	0.001
Post(self)	56		
Pre(outcome)	56	1.50	0.140
Post (outcome)	56		

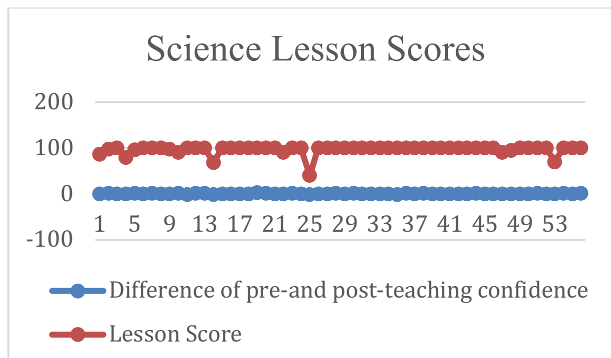

Figure 1. Lesson Plan Scores

IV. CONCLUSION

The study highlights culturally sensitive approaches for educators working with minoritized students. Synchronous online coaches support the educators in understanding students' cultural backgrounds, monitoring progress, and promoting interactive knowledge sharing in virtual learning.

ACKNOWLEDGEMENTS

Thanks to the Instructional Connections for their fund.

REFERENCES

1. Bass, J., Addressing the achievement gap: Implementing diversified classroom instruction in teacher education programs. Journal of Education and Equity, 10(2), 45-62, 2021.

The Anti-Racism Conundrum: Measuring Campus Progress

Katherine S. Cho, Ph.D.[1]
[1]Assistant Professor, Loyola University Chicago

I. SUMMARY

The language of diversity has exponential grown over the past several decades (Ahmed, 2012). While colleges and universities have continued to adopt efforts and creat new initiatives, cycles of activism continue to illuminate how little things have changed (Cho, 2023; Davis et al., 2022). Yet, differing stakeholders within higher education can point to various measures of progress, such as a university implementing a diversity requirement. As a result, educational research must complicate the framing and understanding of institutional progress and its applications to the various constituents within schooling.

II. INSTITUTIONAL RESPONSE FRAMEWORK AND RACIALIZED ORGANIZATIONS

Organizations are not neutral institutions; instead, scholars like Harris (1993) and Ray (2019) have illuminated how the policies, practices, and even organizational culture reflect, embed, and even normalize racism. Educational language like rigor and merit oversimplifies the historic and continued disparities of racist, classist, and gendered policies (Wilder, 2013).

As students, faculty, staff, and administrators engage in campus activism and advocacy towards social justice, educational researchers must be better equipped to merge the framing of progress with organizational theory. Devised by Cho (2018), the Institutional Response Framework (IRF) employs organizational theory with Critical Race Theory. While progress can and has been traditionally viewed through the lens of bridging and buffering (see Honig & Hatch, 2004), Cho places the extent to which demands are met (i.e., bridging) or unmet (i.e., buffering) with dominant coalitions and the lens of power (see Scott & Davis, 2006). In doing so, Cho (2018) positions these demands with the degree to which power is shared within the leading institutional agents (i.e., institutional control) or dispersed in more equitable decision-making (i.e., shared control). As a result, this offers a two-by-two matrix of four responses: schisming, appeasement, co-option, and partnership. Schisming includes how organizations distance themselves from demands via criminalization, silencing, and expressing shock. Appeasement, while offering shared control, can look like the exhaustive committees for which demands will never be concretized. On the other hand, co-option will bridge demands but at the cost of agency. While partnership is considered the gold-star, Cho (2018, 2023) nuances that partnership is not the equivalent to progress *because* of how organizations are not neutral. Organizations engage in partnerships that support racist efforts (that "race Without this nuanced approach, progress remains reduced to cyclical repetitions of the same issues.

III. IRF IMAGE

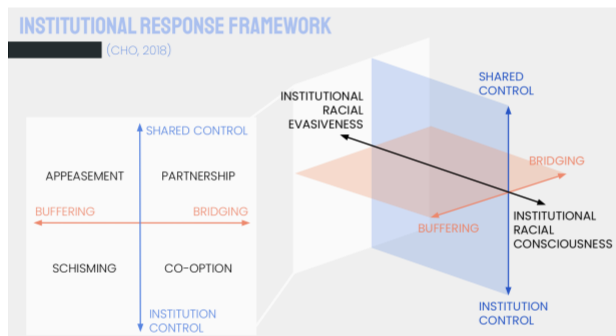

Figure 1: The two-dimensional and three-dimensional illustration of the Institutional Response Framework.

REFERENCES

1. Ahmed, S. (2012). *On being included: Racism and diversity in institutional life.* Duke University Press.
2. Bonilla-Silva, E. (2012). *Racism without racists: Color-blind racism and the persistence of racial equity.* Routledge.
3. Cho, K. S. (2018). The perception of progress: Conceptualizing institutional response to student protests and activism. *NEA Higher Education Journal: Thought and Action, 34*(1), 81-95.
4. Cho, K. S. (2023). Purpose and process: Power, equity, and agenda setting. *New Directions for Student Leadership*, 33-40.
5. Davis III, C. H. F., Morgan, D. L., Cho, K. S. (2023). Activism and social movements in higher education. In M. Bastedo (Ed). *American Higher Education in the Twenty-First Century* (5th Ed.). Johns Hopkins University Press.
6. Honig, M. I. & Hatch, T. C. (2004). Crafting coherence: How schools strategically manage multiple, external demands. *Educational Researcher, 33*(8), 16-30.
7. Ray, V. (2019). A theory of racialized organizations. *American Sociological Review, 84*(1).
8. Scott, W. R. & Davis, G. F. (2007). *Organizations and organizing: Rational, natural and open systems.* Routledge.
9. Wilder, C. S. (2013). *Ebony and ivy: Race, slavery, and the troubled history of America's universities.* Bloomsbury Publishing.

Culturally Responsive Computer Science Learning: Fostering Equity and Engagement for Minoritized High School Students

Jung Won Hur[1], Jay Bhuyan[2]
[1]Auburn University, [2] Tuskegee University

I. SUMMARY

This study aims to investigate the computer science (CS) learning experience of minoritized high school students from low-income families. In light of the prevailing issue of race and gender disparity in STEM fields (Ghazzawi et al, 2021), a CS summer academy was implemented, targeting Black high school students from rural and low-income backgrounds. A total of 31 students enrolled in the program, where they actively learned diverse CS topics, such as software development, mobile and network security. Additionally, they were introduced to Swift Playgrounds and MIT App Inventor, enabling them to develop a mobile app pertinent to their school life and develop collaboration and problem-solving skills. The presentation will highlight the integration of culturally responsive teaching (CRT) strategies as a means to foster interest in CS among Black high school students.

II. Integration of Culturally Responsive Teaching (CRT) into Summer Academy

CRT is an instructional approach that recognizes and appreciates the unique strengths, talents, and cultural backgrounds of diverse learners. Its goal is to enhance students' academic achievement and class engagement by establishing an inclusive and empowering learning environment that connects the curriculum to their cultural experiences and personal lives (Gay, 2000). In this study, CRT was implemented through the following strategies:

- Mentoring and celebration of black accomplishments: Education professors and Black alumni working in the tech industry were invited to provide mentoring sessions. These sessions covered a range of topics, including college preparation, career planning, college financial aid, and resume development.
- Integration of diverse teaching strategies with technology: Students actively participated in culturally enriching activities that incorporated technology. For example, they created and recorded a rap song using Flip, designed app wireframes with Google Slides, and collaborated on group research presentations using Padlet.
- Action research: Students conducted research to identify the mobile app needs of high school students.

III. Data Collection & Impact

Throughout the summer academy, a wide range of data was collected to comprehensively assess the impact of the program. These included pre - individual interviews, pre- and post-surveys, focus group interviews, and artifacts from the students' group projects. The analysis of these data revealed that the incorporation of diverse and engaging cultural activities played a vital role in cultivating students' interest in STEM fields. Figure 1 below illustrates the program's impact by showcasing the positive improvement in students' interest in STEM careers as well as their problem-solving and collaboration skills development.

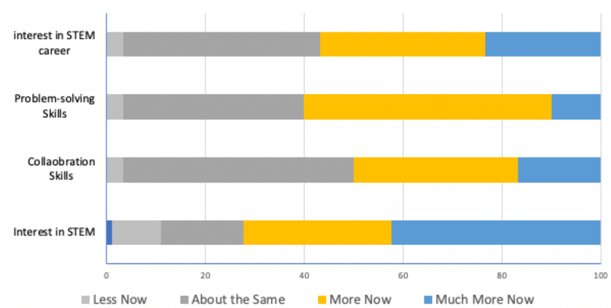

Figure 1: Impact of Summer Academy

ACKNOWLEDGEMENTS

This work was supported by the National Science Foundation under Grant # 2048884.

REFERENCES

1. Gay, G. (2000). Culturally responsive teaching : theory, research, and practice. New York: Teachers College Press.
2. Ghazzawi, D., Pattison, D., & Horn, C. (2021). Persistence of underrepresented minorities in STEM fields: Are summer bridge programs sufficient? Frontiers in Education, 6,630529

What barriers are preventing Asian/Americans from leading Educator Preparation Programs (EPPs)?

Nicholas D. Hartlep[1], Gilbert Park[2]
[1]Berea College, [2]Ball State University

I. SUMMARY
According to Matias, Lewis, and Hope (2022), "Looking at data from the U.S. Integrated Postsecondary Education Data System (IPEDS), we find that the diversity of tenure-track faculty in the USA is not increasing any faster than the diversity of the American public." Does this present reality have any bearing on the future of higher education leadership in terms of diversity? The two panelists of this session believe it does. The Education Field looks at the past and present to forecast what the future holds. One such trend that the field holds in importance is what educators have labeled the demographic imperative, a term used to refer to the racial, cultural, and diversity mismatches between K–12 teachers and their students (see Supplemental Infographic). Because public K–12 schools reflect society, the students who attend them continue to become more diverse, while the teacher workforce remains mostly White and middle-class. Some scholars have labeled the demographic imperative the democratic imperative because diversifying K–12 teachers is so important for society and because it's the right thing to do. Sleeter, Neal, and Kumashiro note, "Addressing the demographic imperative involves not merely encouraging more students of color to become teachers but also removing the institutional barriers that keep them out in the first place." The imperative of K–12 students matching their teachers and removing institutional barriers that prevent this from occurring also exist in higher education. In other words, it's not just K–12 teachers who should mirror their students, but professors should also mirror their students. It is precisely that question—*What barriers are preventing Asian/Americans from leading Educator Preparation Programs (EPPs)?*—that the panelists of this session will address. Scholarship tells us why there currently is a lack of African American K–12 teachers; it is because they were fired by the White power structure. A similar body of scholarship doesn't exist that answers the question: Why are there so few Asian/American EPP leaders in higher education? The two panelists of this session will address their lived experiences as faculty members who work in Educator Preparation Programs in the United States and discuss the implications for Diversity, Equity, Inclusion, and Belonging (DEI+B).

ACKNOWLEDGEMENTS
Dr. Nicholas D. Hartlep would like to thank AACTE for the support in the research for this paper.

REFERENCES

1. Matias, J. N., Lewis, N. A., & Hope, E. C. (2022). US universities are not succeeding in diversifying faculty. *Nature Human Behaviour*. (p. 1)
2. Sleeter, C. E., Neal, L. I., & Kumashiro, K. K. (Eds.). (2015). *Teacher workforce: Preparing and retaining highly effective teachers.* Routledge. (pp. 8–9).

Designing drone-based STEM instruction for formal spaces

Hannah Ziegler[1], Jae Ryu[2]
[1]Vanderbilt University, [2]University of Idaho

I. INTRODUCTION

Amidst the increased integration of emerging technologies such as artificial intelligence (AI), virtual/augmented reality (VR/AR), and autonomous unmanned systems (UAS, or drones) in modern classrooms, drones in particular have become a distinguished hands-on medium for teaching science and engineering practices. However, drone technology is still seldom witnessed in STEM classrooms at the K-12 level.

In recent years, the Idaho Drone League (iDrone) has considerably enhanced secondary youths' STEM identities and interest in post-secondary STEM pathways through hands-on, experiential learning (Ryu et al., 2021). The iDrone program typically serves so-called "tech-savvy" or advanced STEM learners who voluntarily participate in informal workshops. In contrast, this work adopts the iDrone curriculum to design and teach drone-based STEM in a formal classroom serving students consisting of diverse backgrounds, abilities, interest levels, and college/career goals in relation to STEM.

II. PROJECT DESCRIPTION

We worked with approximately 70 students in 9th grade enrolled in a mandatory Earth and Space Science course at a Title I school located in a rural mountain state. In the pre-survey, 70.2% of students disagreed with the following statement: "I identify as being part of the STEM community." 68.7% did not see themselves as a future scientist, mathematician, or engineer. Furthermore, only 25.3% of students noted their regular exposure to STEM in both in-school and out-of-school settings.

In the curricular unit entitled "Drone Climate Project," students designed a drone attachment that addresses issues relevant to climate change that impact the local and/or global community. This not only requires students to understand the societal and environmental impacts of climate change and global warming, but also engage in the engineering design process to examine and solve a personally-relevant problem.

The Drone Climate Project first introduced students to drone mechanics and programming using the iDrone program's drone-building kits, video-based tutorials, and sample Arduino IDE codes. Furthermore, students utilized Tinkercad, a cloud-based, computer-aided design (CAD) software to conceptualize and 3D-print their prototypes. During the final phase of the project, groups collected feedback from peers, teachers, and others in the school community to inform areas for improvement in their designs.

Figure 1: Students during Drone Climate Project

III. RESULTS AND DISCUSSION

The post-project survey revealed a 74% satisfaction rate regarding the provision of hands-on learning, which was ranked the most important STEM learning goal across all students. Additionally, students reported an improved understanding about climate change and technology use. However, the unit did not necessarily enhance students' motivation to enter STEM pipelines.

Overall, our study responds to the dearth of empirical studies that examine the design and implementation of drone-based teaching in K-12 STEM education. Hence, we propose future research that evaluates the pedagogical and design implications of drone-based instruction in formal spaces in relation to other diverse educational settings (e.g., magnet and charter schools, STEM enrichment programs, summer camps, etc.).

REFERENCES

1. Ryu, J., Walters, R., & Ziegler, H. (2021). Interstate Drone League (iDrone National) to promote hands-on remote STEM learning using cloud-based virtual meeting platforms in the global pandemic (COVID-19): IDrone National. *Journal of STEM Education: Innovations and Research*, *22*(4).

Development and dissemination of instructional modules for engineering lab writing

Dave Kim
School of Engineering and Computer Science, Washington State University, Vancouver, WA, USA.

I. SUMMARY
Engineering laboratory report writing instructional modules have been developed for instructors and teaching assistants. In the participating engineering labs across four schools, applications of the developed modules enhanced engineering undergraduates' ability to engage in critical thinking practices, including analysis, interpretation, and evaluation of their lab data/products.

II. INTRODUCTION
Engineering students have declared that hands-on labs were one of the best college experiences while writing lab reports was one of the worst college experiences. Engineering faculty and teaching assistants also consider lab report instructions - assignments, assessments, and feedback - as challenging and time-consuming tasks. Supported by the National Science Foundation Improving Undergraduate STEM Education initiative, researchers from Oregon Institute of Technology, the University of Portland, and Washington State University Vancouver have developed a series of scaffolded laboratory writing modules to support engineering instructors' lab writing instructions.

III. MODULE DEVELOPMENT
The modules were drafted based on the lab report writing outcomes and investigations of student report writing performance at the three participating institutions. Scaffolded learning modules were organized as (1) fundamental topics, (2) intermediate topics, and (3) advanced topics, along with the preface.

Scaffold Level	Module
Preface	Preface / Assignment Design / Assessment Rubric Design
Fundamental	F1: Audiences of Engineering Lab Reports / F2: Lab Report Organization / F3: Lab Report Conventions / F4: Data Analysis 1 – Simple Statistics / F5: Data Presentation
Intermediate	I1: Lab Data as a Primary Source / I2: Conclusion Writing / I3: Data Analysis 2 – Trendlines / I4: Referencing
Advanced	A1: Logical Appeals (Claim-Evidence-Warrant) / A2: Data Analysis 3 – Error / A3: Data Analysis 4 – Propagation of Error

Fig. 1: Engineering lab writing modules structure

The modules have been designed to be compact, straightforward, and user-friendly tools that can assist engineering students in enhancing their abilities in writing engineering laboratory reports. Their primary focus is on effectively organizing and communicating the findings of engineering experiments for the technical audience.

III. MODULE TESTING AND DISSEMINATION
The module webpage has been distributed to instructors who have agreed to test the modules in their lab courses. Those instructors did not participate in any training related to writing; therefore, they relied on only the modules published on the web when updating their lab instructional materials. According to the module testing from six lab courses in one academic year, the engineering students' lab report quality in the participating lab courses was improved from those before using the modules. Notably, student outcomes related to addressing technical audience expectations, illustrating lab data, analyzing lab data, and interpreting lab data were improved. The modules were then refined by the group of engineering faculty, graduate teaching assistants, and writing faculty during the community of practice meeting. The module website is https://labs.wsu.edu/engineering-lab-report-writing/.

III. CONCLUSION
Engineering laboratory report writing instructional modules have been developed for instructors and teaching assistants to improve their writing pedagogies in lab courses.

ACKNOWLEDGEMENTS
This work was supported by the National Science Foundation under DUE # 1915644.

REFERENCES
1. Riley, Charles E., Kim, Dave, Lulay, Ken, & Lynch, John D.. Work in Progress: Supporting Engineering Laboratory Report Writing with Modules Targeted for Instructors. 2022 ASEE Annual Conference Proceedings.

Building Inclusive and Just Pathways to a Clean Energy Economy Through Youth Education of Clean Energy

Hyun Jin Kim[1], Hyunjung Ji[1], Sally Shettles[1], Mark Mueller[1], Amelia Salazar[2], and Laurel Holmes[3]
[1]The University of Alabama, [2]Sam Houston State University, [2]Energy Alabama

I. SUMMARY

The Alabama Energy Transformation Initiative (AETI) explored multiple ways in which energy science and management training can fit into 9th to 12th grade and college education experiences, and investigate student learning outcomes and the program impact. AETI aims to educate underrepresented minority Alabamian students about clean energy practices while providing in-house training for career opportunities. According to the Climate and Economic Justice Screening Tool, many of the Tuscaloosa and Birmingham, AL area communities are disadvantaged in clean energy and energy efficiency, clean transit, and workforce development.

II. INTRODUCTION

While clean energy education can provide tools to students to grow and explore interests in related academic and career pathways, we lack conceptual models and empirical research on how students shape and grow their interests, attitudes, and knowledge of the clean energy economy based on their learning and interactions with mentors and peers. To fill this theoretical and practical gap, we present a research-based practice implemented in Alabama; the Alabama Energy Transformation Initiative (AETI) developed energy science and management training for secondary and higher education and explored its potential to build inclusive and just pathways to a clean energy economy.

II. RESEARCH METHOD

A. Research Design

This research examines to what extent the provision of clean energy education influences both participating student mentors' and mentees' interests in STEM and energy literacy composed of knowledge, attitudes, and behaviors. Pre- and post-program surveys will be conducted with those students taking the energy education sessions (treatment group), with a control group taking the same surveys for a comparative analysis.

B. Sample Characteristics

Our high school mentee student sample is drawn from two majority-minority high schools from Tuscaloosa County and Hale County (located in Black Belt) districts, approximately 60 and 25 students from each school for the program participation. Our sample mostly includes Black, economically disadvantaged students who are suffering from low funding, high student-teacher ratios, and low outcomes in STEM education.

C. Measurement of Energy Literacy

To measure energy literacy of high school students in both treatment and control groups, we use an energy literacy survey developed by the National Energy Foundation (NEF)[1].

III. CONCLUSIONS

Alabama is one example of a state with no environmental education requirement. Not all students have equal access to environmental education, and those from low socio-economic status have the least exposure to the field. AETI is a research-based practice aimed at addressing the gap in understanding how students shape and grow their interests, attitudes, and knowledge of the clean energy economy through learning and interaction with mentors and peers. A full analysis will be conducted after the high school program, and report results regarding the effects of hands-on, real-world, and problem-based energy education on students' perception and disposition towards STEM and energy, as well as the influence of interaction with mentors on students' perception towards scientists/engineers and energy issues.

ACKNOWLEDGEMENTS

This work is funded by the Department of Energy Inclusive Energy Innovation Prize.

REFERENCES

1. E. Richards, G. Swan, & D. Case, "National energy literacy among high school seniors and recent graduates," *National Energy Foundation, Technical White Paper,* 2017.

Thermofluid sciences for elementary school students via flow visualization using smartphones and tablets

Hyun Jin Kim, Shemai'ya Peak, Frances Buntain, Jale Ercan Dursun, Jee Suh, & Celestia Morgan
The University of Alabama

I. SUMMARY
This study examined a promising approach to inspire elementary-level students to pursue a career in STEAM (science, technology, engineering, art, and mathematics) fields through a university-run after-school program at a local majority-minority school located in Tuscaloosa, AL. Pre-service teachers taught basic thermofluid sciences topics such as diffusion, convection, surface tension, viscosity, etc., and helped students conduct the flow visualization with iPads during experiments, including high-speed imaging at up to 120 fps and 720p.

II. INTRODUCTION
Providing STEAM experiences for elementary-age children can improve their perceptions and dispositions toward STEM[1]. Fluid mechanics largely remains a college-level subject matter and has been unrelated to young students. There have been efforts to promote flow visualization in education, but researchers have focused on high school or college programs utilizing advanced techniques such as particle image velocimetry[2].

This study concentrated on using images of phenomena via smartphones or tablets with high-speed cameras to teach fundamental fluid mechanics. The examination also evaluated the potential impact of the after-school program on the participants' learning and outlook on the subjects.

II. RESEARCH METHOD
A. Research Design
The investigation is focused on the problem-based STEAM education approach's effect on elementary students' perception of STEM. Female engineering student mentors' influence on young girls' perception towards STEM disciplines was also studied.

B. Sample Characteristics
Elementary students at the partner school located in Tuscaloosa, AL were invited to register for the afterschool program led by the pre-service teachers from the UA. The demographic breakdown of the partner school according to the National Center for Education Statistics was: 86.7% African American, 10.4% Hispanic, 1.9% Caucasian, and 1.0% Other.

C. Measurement of STEAM Literacy
Surveying was used to gauge students' understanding and perceptions throughout the program. A pre-survey was conducted on the first day of the program to establish a baseline. Drawings were used as an interpretive device for the children to express their preconceptions about engineers.

III. CONCLUSIONS
We designed STEAM classrooms, and analyzed the modified Fluids Perception survey results and the interviews for further development of the STEAM program, and its adoption in elementary education.

The analysis showed an increased percentage of female engineers being depicted with pre-test n = 8 (38.1% out of 30) and post-test n = 9 (42.9% out of 24). Representation of African American scientists saw an increase of 14% from pretest to post-test results. Also, there was a 9.2% decrease in scientists that featured unkempt appearances (such as a mad scientist), in which students started to draw more realistic expectations of what a scientist may look like. As more data is acquired in future studies, we hope to continue seeing a positive trend in underrepresented minorities in STEAM.

ACKNOWLEDGEMENTS
This work was supported by the Joint Pilot for Arts Research Grant administered by the Collaborative Arts Research Initiative at The University of Alabama.

REFERENCES
1. N. DeJarnette, "America's Children: Providing Early Exposure to STEM Initiatives," *Education*, vol. 133, no. Number 1, pp. 77-84, 2012.
2. L. M. Caldwell and A. Minichiello, "Work in Progress: Mobile Instructional Particle Image Velocimetry for STEM Outreach and Undergraduate Fluids Mechanics Education," *ASEE Annual Conf & Expo*, Tampa, FL, 2019.

Utilizing the Medium of Virtual Reality to Teach How To Recycle

Nathan Kassai[1], **Paul Y. Oh**[2]
[1]University of Nevada, Las Vegas, [2]University of Nevada, Las Vegas

I. ABSTRACT

Many students, particularly those in elementary and middle school, struggle with focusing and retaining information presented in their courses. While lecture topics may be interesting to most, the monotony of the presentation often makes it difficult for students to engage with the material. In order to effectively educate and motivate students to improve their engagement, alternative educational mediums must be explored. Virtual and Augmented Reality are examples of such methods that allow students to interact with virtual objects and learn about a wide range of subjects[1], thereby increasing their engagement and enjoyment in any given topic.

II. METHODOLOGY

In order to create the proposed educational platform, a software development environment with a Game Engine must be selected. For this research, Unity was chosen because of its ability to seamlessly integrate with various VR headsets, its Asset Store full of pre-designed 3D models, and its user-friendliness. The educational subject chosen for this project is recycling, as studies have shown that many people lack knowledge on how to properly recycle. The plan is to conduct an evaluation of two methods where half of the participants will be in a control group (learning by reading) while the other half will be in an experimental group (learning in VR simulation). A quiz will be provided after fifteen minutes of either method to determine information retention.

The VR simulation will contain the following: recyclable sorting games, short videos containing important information regarding pollutants, Graphical User Interfaces (GUIs) with buttons that allow a user to transport to various locations (ocean, parks, and streets) and provide trash pollution statistics and facts regarding those locations, short interactive quizzes, and general interactions with the environment (picking up trash from floor, taking trash off of animals, etc). Each VR simulation session is anticipated to last roughly 15 minutes to ensure that users are able to enjoy the experience and digest information provided to them. A screenshot of the platform can be seen in Figure 1.

III. RESULTS

The mean score found for the experimental group was 87%, whereas the mean score for the control group was 72%. Additionally, after the learning session, all participants were asked to complete a survey to provide feedback on their overall enjoyment and their perception of how much they had learned. Both groups reported that they had learned more, but the experimental group not only outperformed the control group in terms of quiz scores, but also reported having a much more enjoyable experience with the interactive learning session and felt that this medium should be utilized in the classroom more often.

Figure 1: Virtual Reality Teaching Environment

REFERENCES

1. Marks, B., Thomas, J. Adoption of virtual reality technology in higher education: An evaluation of five teaching semesters in a purpose-designed laboratory. Educ Inf Technol 27, 1287–1305 (2022). https://doi.org/10.1007/s10639-021-10653-6

A case study of Recreation-based STEM education that improves unplugged coding education using musical activities for kindergarten children

Wonil Chung[1], **Min Jae Park**[2]
[1]Center of SW Education, Kyung Pool National University, [2]Institute of STREAM Academy

I. SUMMARY
This study explores a case of “STREAM”, a new concept that includes recreation to STEM (Science, Technology, Engineering, Art, and Mathematics) to improve STEM education.

In this demonstration case, an unplugged activity is produced as a musical to provide basic SW education for children. The musical, in which concept of AI· SW is included in the content, shows that SW convergence education for children is possible with Recreation-based STEM education.

II. MOTIVATION
While discussing with researchers how to convey concepts in an easy, friendly, and fun way for children who cannot accept artificial intelligence and software knowledge like adults, we have attempted to improve their understanding by producing and providing them with musicals that include music, art, and action.

III. RELATED WORK
The study by Taeho Yoh et al. introduces the concept of STREAM, a new concept, performed by who fifteen college students participated in a recreational activity created by the authors to teach the concept of Blockchain. They present a summary of themes; experiential, fun, instructive, and interactivity[1]. Wonil Chung presents several case study on recreation-based STEM education activities in 2022 KSEA summer conference.[2,3]

IV. APPROACH & OBSERVATION
One artistic director and one researcher work together to create a screenplay suitable for the child's level of understanding, and based on this, one composer, three vocalists, and one director work together to create a musical.

Terms such as Artificial Intelligence, Cloud, Virus, Robot, and Unicorn are included in the content of the performance, and the activities by order, procedure, condition, and repetition following unplugged activities are designed to be expressed by the performers during the play.

More than 50 children and 4 teachers attended each session, and the responses received from the teachers were fun, experiential, instructive, and interactive.

Figure 1: Case of Recreation-based STEM performance by a musical activities.

REFERENCES
1. Taeho Yoh, Jun Kim, Sam Chung, and Wonil Chung. (2021). STREAM: A New Paradigm for STEM Education. Journal of STEM Education, Vol22, 46-51.
2. Wonil Chung, Kyll Joo Chung, and Young Ju Lee. (2022). A Case Study of Play-Based STREAM Activities using air bounce inflatables at a Kidergarten, KSEA poster session.
3. Wonil Chung, Jong Dae Kwon, and Seung Hun Shin.(2022). A Case Study of STREAM Activity Using the Digital Game made with Korean Traditional Play, “Seumnyeguk”for LifelongEducation of Active Digital Seniors, KSEA poster session.

Appendix

UKC 2023 Program

Program at a Glance

<table>
<tr><th>8/1/2023 (Tue)</th><th>8/2/2023 (Wed)</th><th>8/3/2023 (Thu)</th><th>8/4/2023 (Fri)</th><th>8/5/2023 (Sat)</th></tr>
<tr><td colspan="5">Breakfast (7:00 - 8:00 am)</td></tr>
<tr><td rowspan="3"></td><td rowspan="6">SEED</td><td>Opening / Plenary Session
(8:00 - 10:00 am)</td><td>Plenary Session
(8:00 - 10:00 am)</td><td>KSEA Forums, TG Symposiums, IES, FIRE
(8:00 - 10:00 am)</td></tr>
<tr><td colspan="3">Break (10:00 - 10:30 am)</td></tr>
<tr><td>Keynote Symposiums
(10:30 - 12:30 pm)</td><td>Keynote Symposiums
(10:30 - 12:30 pm)</td><td>Closing / Plenary Session
(10:30 - 12:30 pm)</td></tr>
<tr><td rowspan="6">SEED</td><td colspan="3">Lunch (12:30 - 1:30 pm)</td></tr>
<tr><td>Distinguished Forums
(1:30 - 3:30 pm)</td><td>Sponsor Forums
(1:30 - 3:30 pm)</td><td>DSW</td></tr>
<tr><td colspan="3">Break (3:30 - 4:00 pm)</td></tr>
<tr><td rowspan="3">Sponsor Welcome Reception and Banquet (5 pm)

UKC Reception (8 pm)</td><td>TG Symposiums, IES, FIRE, Forum
(4:00 - 6:00 pm)</td><td>TG Symposiums, IES, and FIRE
(4:00 - 6:00 pm)</td><td>DSW</td></tr>
<tr><td>Break
(6:00 - 7:00 pm)</td><td>UKC Poster Session
(6:00 - 9:00 pm)</td><td>Break
(6:00 - 7:00 pm)</td></tr>
<tr><td>UKC Banquet</td><td>Networking Dinner & Poster Session (Continued)</td><td></td></tr>
</table>

Room Information

August 3 _ Thursday _ 2023							
Room/Time	7-8:00 am	8-10:00	10:30-12:30pm	12:30-1:30pm	1:30-3:30pm	4-6:00pm	7-9:00pm
Aviator A	Breakfast			Lunch			
Aviator B							
Foyer	Booth						
Enterprise Ballroom 1		Plenary : Opening	Keynote Symposium (PSE)		CHEY Forum		UKC Banquet
Enterprise Ballroom 2							
Enterprise Ballroom 3							
Enterprise Ballroom 4							
Enterprise Ballroom 5			Keynote Symposium (LSE)				
Enterprise Ballroom 6							
Enterprise Ballroom 7			Keynote Symposium (CSE)			IES	
Enterprise Ballroom 8							
Maverick			Keynote Symposium (WEC)			TGS / B3&C1-BME	
Developers				KWiSE Forum		R&D Leaders Forum	Former P Meeting
Carter					K-Water Forum	TGS / A1-PHY	
Hobby					KHNP Forum	TGS / A3-MAS	
McKee						TGS / C2-CHE	
Vandergriff						TGS / D1-SSP	
Jonsson						TGS / B2-FAN	
Glasscock						TGS / A2-CHM	
Austin			Science Policy Forum		Science Diplomacy	TGS /C8-IMS	
Dallas					Seegene Forum	TGS / B1-MPS	LCP Orientation
Fort Worth					Yuhan Forum	TGS / C4-MSE	
Grapevine					KEIT Forum	TGS / C7-CIT	
Houston					KITECH Forum	TGS / C3-MAN	
San Antonio					KIAT Forum	TGS / C6-ECE	
Lone Star 1						TGS / C5-CEA	
Lone Star 2						TGS / C5-CEA	
Innovation A						FIRE	
Innovation B							
Innovation C							
Innovation D							
Wetzel				Mid-Career Luncheon		University Leaders Forum	

August 4 _ Friday _ 2023							
Room/Time	7-8:00 am	8-10:00	10:30-12:30pm	12:30-1:30pm	1:30-3:30pm	4-6:00pm	7-9:00pm
Aviator A / Aviator B	Breakfast			Lunch	Poster Set-up		Poster
Foyer	Booth						
Enterprise Ballroom 1 / Enterprise Ballroom 2 / Enterprise Ballroom 3 / Enterprise Ballroom 4		Plenary	Keynote Symposium (PSE)				
Enterprise Ballroom 5 / Enterprise Ballroom 6			Keynote Symposium (LSE)				
Enterprise Ballroom 7 / Enterprise Ballroom 8			Keynote Symposium (CSE)			IES	IES Networking Dinner
Maverick			Keynote Symposium (WEC)			TGS / B3&C1-BME	Networking Dinner
Developers						TGS /C5-CEA	Networking Dinner / FP meeting
Wildcatters						TGS /C5-CEA	
Harvesters							
Carter						TGS / A1-PHY	Networking Dinner
Hobby					UNIST Forum	TGS / A3-MAS	
McKee						TGS / C2-CHE	
Vandergriff					KBSI Forum	TGS / D1-SSP	
Jonsson						TGS /B2-FAN	
Glasscock						TGS /A2-CHM	
Austin					SNU Forum	TGS /C8-IMS	
Dallas					KISTEP Forum	TGS /B1-MPS	
Fort Worth					KHIDI Forum	TGS /C4-MSE	
Grapevine					KEIT-SWRI Forum	TGS /C7-CIT	
Houston					KITECH Forum	TGS /C3-MAN	
San Antonio						TGS /C6-ECE	
Lone Star 1					KICT Forum	TGS /C5-CEA	
Lone Star 2						TGS /C5-CEA	
Innovation A / Innovation B / Innovation C / Innovation D						FIRE	
Wetzel				Mid-Career Luncheon			

August 5 _ Saturday _ 2023					
Room/Time	7-8:00 am	8-10:00	10:30-12:30pm	1:30-6:00pm	6:00-12:00am
Aviator A	Breakfast				
Aviator B					
Enterprise Ballroom 1			Plenary : Closing		
Enterprise Ballroom 2					
Enterprise Ballroom 3					
Enterprise Ballroom 4					
Enterprise Ballroom 7		IES / Start-Up Pitch Competition			
Enterprise Ballroom 8					
Developers		KSEA History Forum			
Carter		TGS / A1-PHY			
Dallas		TGS /B1-MPS		LCP Meeting	
Fort Worth				APS Meeting	
Grapevine					
Lone Star 1					Council Meeting
Innovation A		FIRE		DSW	
Innovation B					
Innovation C					
Innovation D					

Plenary Schedule

<table>
<tr><th colspan="3">August 3 _ Thursday _ 2023</th></tr>
<tr><td>8:00–10:00 am</td><td>Opening Ceremony
(Chaired by Dr. Sua Myong, Johns Hopkins U & Tae Joong (TJ) Park, MIT)
• KSEA Introduction Video
• National Anthems (Korea and USA) – Baritone Uram Park
• Introducing Dignitaries & Sponsor Representatives
• Opening Remarks - Yongho Sohn, President, Korean-American Scientists and Engineers Association, KSEA
• Welcoming Remarks
- Tai Sik Lee, President, Korean Federation of Science and Technology Societies, KOFST
• Congratulatory Remarks
- John Cornyn, US Senator for Texas (Video)
- Andy Kim, U.S. Representative, 3rd Congressional District of New Jersey (Video)
- Young Ho Jung, Consul General of the Republic of Korea in Houston
• Award Ceremony
Outstanding Contribution to KSEA Award Presented by MSIT
Scientist of the Year Award Presented by KOFST
Engineer of the Year Award Presented by KOFST
• Plenary Lecture I
Dr. Barry C. Barish, 2017 Nobel Laureate, Professor of Physics Emeritus at Caltech, President’s Distinguished Endowed Chair at Stony Brook University
“Understanding our Universe with Gravitational Waves”
• Group Photo</td><td>Enterprise I-IV</td></tr>
<tr><td>10:00–10:30 am</td><td colspan="2">Break</td></tr>
<tr><td>10:30–12:30 pm</td><td>UKC Keynote Symposium
- Physical Science and Engineering
- Life Science and Engineering
- Computational Science and Engineering
- Workforce of the Future: Education and Careers</td><td>Enterprise I-VIII Maverick</td></tr>
<tr><td>12:30–1:30 pm</td><td>Luncheon</td><td>Aviator A-B</td></tr>
<tr><td>1:30– 3:30 pm</td><td>Distinguished Forums</td><td>Various</td></tr>
<tr><td>3:30 – 4:00 pm</td><td colspan="2">Break</td></tr>
<tr><td>4:00 – 6:00 pm</td><td>Technical Group Symposiums / Forums / FIRE / IES</td><td>Various</td></tr>
<tr><td>6:00 – 7:00 pm</td><td colspan="2">Break</td></tr>
<tr><td>7:00 – 9:00 pm</td><td>UKC Banquet
(MC'd by Dr. Jennifer Cho, Millibatt & Nathan Han, Savills)
• Music Performance: Mariachi Arraigo De America
• Dinner
• Welcome Remarks - Yongho Sohn, President, KSEA
• Congratulatory Remarks
- Tai Sik Lee, President, Korean Federation of Science and Technology Societies, KOFST
• Music Performance
- Guitarist Se-Hwang Kim
- Dance Party: Spjork - The. Mashup. Band</td><td>Enterprise I-IV</td></tr>
</table>

August 4 _ Friday _ 2023		
8:00–10:00 am	**Plenary Session** (Chaired by Dr. Hyojin Kim, NJIT & Dr. Seung Hwan Allen Lee, MIT) • **Research Vision Talks I** - Hyeon Sik Kim, Vice President & CRO (Chief Research Officer) of K-water Research Institute "*K-water & K-water's smart water management*" - Haiyoung Jung, M.D. Ph.D. Chief Deputy Medical Director, SEEGENE Medical Foundation "*Clinical Research Centers in Seegene Medical Foundation*" - Joonyeon Chang , Director-General, Gangneung Institute of Natural Products, Korea Institute of Science and Technology, KIST "*Open R&D Platform for Strategic Technologies*" - Jaeho Yeom, President, TAEJAE University "*The Next Answer for the Future Education*" - Hyeonjun Kim, Vice President for Research, Korea Institute of Civil Engineering and Building Technology, KICT "*About KICT*" • **Plenary Lecture II** **-** Dr. Jin Hyung Lee, Associate Professor of Neurology, Stanford University *"Creating a 'Digital Twin' of the Brain""* • **Research Initiative Talks II** - Jae Young Kim, Executive Vice President for Research Affairs, Seoul National University *"SNU's Transformative Actions: Pioneering the Future"* - Yeol Choi, Dean of International Affairs, Kyungpook National University "*Public research-oriented university*" - Hocheol Shin, Head of KHNP Central Research Institute "*KHNP leads a Global Net-Zero Future*" - Young Hoon Ko, Senior Executive Vice President, R&D Director, Kumho Petrochemical "*Introduction of Kumho Petrochemical*" **KSEA Award Ceremony** • **Award Ceremony** - Graduate Scholarship Award Ceremony - Young Investigator Grant Award - Distinguished Sponsorship Award - Entrepreneur of the Year Award by Maeil Business Newspaper	Enterprise I-IV
10:00–10:30 am	Break	
10:30–12:30 pm	**UKC Keynote Symposium** • Physical Science and Engineering • Life Science and Engineering • Computational Science and Engineering • Workforce of the Future: Education and Careers	Enterprise I-VIII Maverick
12:30–1:30 pm	Luncheon	Aviator A-B
1:30– 3:30 pm	Sponsor Forums	Various
3:30 – 4:00 pm	Break	
4:00 – 6:00 pm	Technical Group Symposiums / FIRE / IES	Various
6:00 – 7:00 pm	Break (Poster Competition)	
7:00 – 9:00 pm	Networking Dinner (Poster Competition)	Various

August 5 _ Saturday _ 2023		
8:00–10:00 am	Forums / Technical Group Symposiums / FIRE / IES	Various
10:00–10:30 am	Break	
10:30–12:30 pm	**Plenary & Closing** (Chaired by Ms. Stella Kim, DSC & Dr. IL Minn, Johns Hopkins) • **Plenary Lecture II** - Youngsuk "YS" Chi, Chairman, Elsevier; Director of Corporate Affairs, RELX *"Navigating Careers in Science, Engineering, and Entrepreneurship in an Ever-Changing World"* • **Award Ceremony** - IES Award - UKC 2023 Paper Award - Appreciation to the KSEA 51st President • UKC 2024 Announcement, Tae (Tom) Hwan Oh, President-Elect of KSEA • Closing Remarks, Yongho Sohn, President of KSEA	Enterprise I-IV
12:30–1:30 pm	Break	
1:30–6:00 pm	• Data Science Workshop (Registration Required)	Innovation

Keynote Symposium

Physical Science and Engineering

Real Solutions to Real Problems Impacting Real People

August 3 _ Thursday _ 10:30am _ Enterprise Ballroom 1-4

Though the rapidly developing robotics and AI technologies are already having a major impact on our everyday lives, often times, we also see many research being conducted without much considerations on how these technologies will impact on our lives and society. AI and robotics can be powerful tools to solve real problems, but also have their own risks and hazards that can bring danger and potentially have a serious negative impact on our society. We would like to see what problems researchers are solving, who is affected by this and how they will impact our society. In this UKC 2023 Keynote Symposium, U.S. and Korean experts in robotics are invited to discuss how the current state of the art and future robotics and AI technologies may impact our everyday lives.

Chair

Dennis Hong

Director, RoMeLa
Robotics & Mechanisms Laboratory

Professor, Mechanical & Aerospace Engineering, UCLA

Do Robots Need to Look Like Human?

In Hollywood, robots are often depicted in the humanoid form. Thus when we think of robots we naturally imagine humanoid robots. For robots to move around in a human environment and to do work using tools made for humans, it is natural to have robots that have the shape and size of a human. We have been developing humanoid robots at RoMeLa (Robotics & Mechanisms Laboratory) for more than a decade for fire fighting and disaster relief applications. However, such robots are still too slow, too unstable, too complex, too expensive, and too unsafe which prevent them to be used in real life situations. Do robots really need to look like human? We revisit this question and present some of the new exciting morphologies as solutions, discuss the creative process, and imagine our future with robots.

Dr. Dennis Hong is a Professor and the Founding Director of RoMeLa (Robotics & Mechanisms Laboratory) of the Mechanical & Aerospace Engineering Department at UCLA. His research focuses on robot locomotion and manipulation, autonomous vehicles and humanoid robots. His work has been featured on numerous national and international media. Washington Post magazine called Dr. Hong "*the Leonardo da Vinci of robots*." Dennis has been named to Popular Science's 8th annual "*Brilliant 10*", "*Forward Under 40*" by the University of Wisconsin-Madison Alumni Association, and also honored as "*Top 40 Under 40*" alumni by Purdue University. Hong's other past awards include the National Science Foundation's CAREER award, the SAE International's Ralph R. Teetor Educational Award, and the ASME Freudenstein / GM Young Investigator Award to name a few. Dr. Hong also actively leads student teams for various international robotics and design competitions winning numerous top prizes including the DARPA Urban Challenge where they won third place and the $500,000 prize, and the RoboCup, the international autonomous robot soccer competition where his team is now a five time World Champions in the Humanoid divisions and brought the Louis Vuitton Cup Best Humanoid Award to the United States for the very first time. Dr. Hong received his B.S. degree in Mechanical Engineering from the University of Wisconsin-Madison (1994), his M.S. and Ph.D. degrees in Mechanical Engineering from Purdue University (1999, 2002).

Paul Oh

Lincy Professor
Unmanned Aerial Systems
University of Nevada, Las Vegas (UNLV)

From Disaster Response to Consumer Robotics

The lines between consumer electronics and consumer robotics are blurry. For example, at the annual Consumer Electronics Show (CES) in Las Vegas, the list of robotics companies exhibits has grown to over 400. Furthermore driverless cars, drones, exo-skeletons, 3D printers and virtual-reality systems are examples of robots that have a consumer focus. This talk highlights observations of this phenomena. This is given in the context of an Age of Acceleration characterized by deep learning, cloud-computing, and artificial intelligence. The talk serves to suggest pathways for roboticists and their design and development endeavors.

Prof. Paul Oh is the founder and director of the Drones and Autonomous Systems Lab (DASL). Prior, he was in Drexel University's Mechanical Engineering Department from 2000-2014. He received mechanical engineering degrees from McGill (B. Eng 1989), Seoul National (M. Sc. 1992), and Columbia (PhD 1999) universities. He is a Fellow of NASA (2002), Naval Research Lab (2003), Boeing (2006) and ASME (2012). He received research (2004 NSF CAREER) and teaching (2005 SAE Ralph Teetor Award for Engineering Education Excellence) awards and authored over 150 publications and 3 books. From 2008-2010, he served as an NSF Program Director managing the robotics research portfolio. He has lead Teams DRC-Hubo, DRC-Hubo@UNLV and Avatar-Hubo for the 2012-2014, 2015, and 2018-2022 DARPA Robotics Challenges Semi-Finals, Finals, and Avatar XPrize respectively. He recently served as General Chair for IEEE IROS 2020 (IEEE Intelligent Robots and Systems) Conference which gathered over 25,000 online attendees.

Joohyung Kim

Associate Professor
Director of KIMLAB
Electrical and Computer Engineering
Mechanical Science and Engineering
University of Illinois Urbana-Champaign

Panelist: Joohyung Kim's research focuses on design and control for humanoid robots, system for motion learning in robot hardware, and safe human-robot interaction. He received BSE and Ph.D. degrees in Electrical Engineering and Computer Science (EECS) from Seoul National University, Korea, in 2001 and 2012. He was with Disney Research as a Research Scientist from 2013 to 2019. Prior to joining Disney, he was a postdoctoral fellow in the Robotics Institute at Carnegie Mellon University for DARPA Robotics Challenge in 2013. From 2009 to 2012, he was a Research Staff Member in Samsung Advanced Institute of Technology, Korea, developing biped walking controllers for humanoid robots.

Daniel Dongyuel Lee

Tisch University Professor
Electrical and Computer Engineering
Cornell Tech

Panelist: Dr. Daniel Dongyuel Lee serves as Head of Global AI for Samsung Research. He received his B.A. in Physics from Harvard University and his Ph.D. in Condensed Matter Physics from the Massachusetts Institute of Technology. He was also a researcher at Bell Labs in the Theoretical Physics and Biological Computation departments. He is a Fellow of the IEEE and AAAI and has received the NSF CAREER award and the Lindback award for distinguished teaching. He was also a fellow of the Hebrew University Institute of Advanced Studies in Jerusalem, an affiliate of the Korea Advanced Institute of Science and Technology and organized the US-Japan National Academy of Engineering Frontiers of Engineering symposium and Neural Information Processing Systems (NeurIPS) conference. His group focuses on understanding general computational principles in biological systems and on applying that knowledge to build autonomous systems.

Mark Yim

Director of the GRASP Lab
Asa Whitney Professor
Mechanical Engineering
University of Pennsylvania

Panelist: Mark Yim established the oldest robotics research laboratory in the country in 1980. His research group focuses on hardware design. They have demonstrated robots ranging from a humanoid displayed at the Philadelphia Museum of Art to transforming robots that can change their shape to the smallest self-powered flying robot in the world. His current research focus includes reconfigurable truss robots that can help in search and rescue operations, swarms of small flying robots that can group into shapes that interact with humans and swarms of microscopic robots that can build structures. His other research interests include product design, robotic performance art, low-cost manipulation, in the search and rescue as well as healthcare applications. Honors include the Lindback Award for Distinguished Teaching (UPenn's highest teaching honor); induction to the National Academy of Inventors in 2018. He has over 50 patents issued (perhaps the most prominent patents are related to the video game vibration control which resulted in over US$100 million in litigation and settlements). He has started three companies, one in robotics, one medical device company and one focusing on thermal storage to reduce carbon impact. Prior to Penn, he spent ten years in industry including positions as Principal Scientist at the Palo Alto Research Center (formerly Xerox PARC) and Virtual Technologies, a virtual reality startup company before that. He received his PhD from Stanford University in Mechanical Engineering.

Physical Science and Engineering

Achieving Carbon Neutrality: Perspectives and Challenges

August 4 _ Friday _ 10:30am _ Enterprise Ballroom 1-4

Climate change driven by greenhouse gas (GHG) emissions is the defining challenge of our time, encompassing not only rising temperatures but also extreme weather events and a range of other impacts. Its effects are global in scope and unprecedented in scale, and they will continue to worsen as global temperatures and GHG emissions increase. Achieving carbon neutrality or net-zero emissions by balancing GHG emissions with removals from the atmosphere is critical to slowing climate change and minimizing its impacts. The keynote symposium will highlight the importance of a scientific understanding of decarbonization technologies, their deployment, and related policy implementation in the timely achievement of carbon neutrality targets. The session will also discuss the technical, economic, and public relations challenges of decarbonization.

Chair

Young-Shin Jun

Professor
Energy, Environmental and Chemical Engineering
Washington University in St. Louis

Dr. Young-Shin Jun received her B.S. and M.S. degrees from Ewha Womans University, holds S.M. and Ph.D. degrees in Environmental Chemistry from Harvard University, MA, and conducted postdoctoral research at the University of California-Berkeley/Lawrence Berkeley National Laboratory, CA. She investigates chemical reactions in energy-related subsurface systems including geologic CO2 sequestration. Further, based on nanoscale interfacial chemistry and solid nucleation, her research group also seeks new techniques and materials for more sustainable energy and the environment. Professor Jun received a 2008 Ralph E. Powe Junior Faculty Enhancement Award, a 2011 U.S. National Science Foundation CAREER award, the 2020 James M. Lee Memorial Award, and the 2022 Jackson Award. She was named a 2015 Kavli Fellow by the U.S. National Academy of Sciences, a 2016 Frontier of Engineering Fellow by the U.S. National Academy of Engineering, a 2018 Fellow of the Royal Society of Chemistry, and a 2019 Fellow of the American Chemical Society (ACS). She serves on ACS's Committee on Science as the Chair of the Science & Technology Subcommittee.

Tae-Hyuk Kwon

Dean, College of Natural Science
Professor, Department of Chemistry
Ulsan National Institute of Science & Technology (UNIST)

Photo/Sono Active Materials for Carbon-Neutral Society

The world is currently confronted with more challenges in the realms of energy, environment, food, and disease than ever before. In the light of these issues, our group has focused on investigating photo/sono active materials for energy recycling, carbon catalysts for environmental and food applications, and photodynamic therapy for treating cancer. To begin, our group has developed a dye-sensitized photo-rechargeable battery that operates wirelessly by harnessing low-intensity indoor light. This advancement holds promise for enhancing energy efficiency in buildings, contributing to a carbon-neutral society, and facilitating the widespread adoption of IoT devices. Additionally, we explore the integration of dye-sensitized solar cells with catalysts in a monolithic device to serve as a power source for hydrogen generation. Furthermore, our group has conducted research on sonocavitation and nebulization synthesis (SNS) utilizing an ultrasonic spray to synthesize frustrated type Lewis acid-base pairs (FLP) doped graphene nanopowder. SNS employs acoustic cavitation, which generates extreme conditions within collapsing bubbles (5000 K and 1000 bar). These unique conditions enable various chemical reactions that are typically inaccessible. We will demonstrate how the utilization of graphitic frustrated Lewis pairs (FLP) as catalysts enables the reduction of CO2 and N2, as well as urea production.

Dr. Tae-Hyuk Kwon earned a B.S. degree in Chemistry from Suwon University and a MS/Ph. D. degree in Chemistry from Seoul National University, Seoul, Korea. Prior to joining the UNIST, he worked as a Postdoctoral Researcher at the University of Melbourne, Melbourne, Australia under the guidance of Prof. Andrew B. Holmes. His current research interests are in the development of dye-sensitized solar cells, focusing on their applications in the field of green energy and biomedicine.

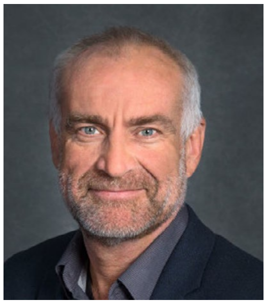

Jens Birkholzer

Senior Scientist and Director
Energy Geosciences
Earth and Environmental Sciences
Lawrence Berkeley National Laboratory (LBNL)

Towards Geologic CO_2 Sequestration at Scale: Geomechanical Impacts, Induced Seismicity Concerns, and Mitigation Measures

After decades of research on carbon capture and geologic sequestration (CCS), the world needs to finally move from pilot and demonstration experiments to industrial-scale implementation. CCS at scale will involve unprecedented fluid injection volumes that can result in large-scale pressure increases in the subsurface and may cause unwanted geomechanical effects, such as generating seismic events and caprock integrity concerns per reactivation of critically stressed faults. This presentation will start with a short description of the current worldwide status of CCS and its role as an important climate-mitigation technology. I will then illustrate basin-scale pressure and geomechanical impacts expected from industrial-scale implementation, based on regional modeling studies of future CCS scenarios. In terms of induced seismicity, I will present lessons learned from two field experiments—one being a controlled-injection fault slip experiment in a clay (caprock) formation which is highlighting the importance of aseismic leakage and its potential coupling to induced seismicity, the other a CO2 demonstration site where micro-seismicity has occurred along pre-existing basement faults—and will finally evaluate brine extraction as a mitigation measure currently tested in a deep reservoir in the southern United States.

Dr. Jens Birkholzer serves as the Director for the Energy Geosciences Division (EGD) in the Earth and Environmental Systems Area (EESA). EGD is a premier organization of ~250 staff and affiliates with expertise in energy geosciences and carbon management. Jens' research is related to evaluating the feasibility and environmental sustainability of a broad portfolio of geo-energy applications, with particular focus on the role of subsurface resources for carbon sequestration and removal. He has over 400 scientific publications, about 170 of which are in peer-reviewed journals. He serves on the Editorial Board of the International Journal of Greenhouse Gas Control (IJGGC), the Energies Journal (Geo-Energy Section), and is also an Editorial Policy Advisor for the Journal of Geomechanics for Energy and the Environment (GETE). Dr. Birkholzer leads the international DECOVALEX Model Comparison Project as its Chairman, is a Fellow of the Geological Society of America, and a Senior Fellow of the California Council on Science and Technology.

Life Science and Engineering

Innovative Discoveries on Regenerative Medicine

August 3 _ Thursday _ 10:30am _ Enterprise Ballroom 5&6

The Regenerative Medicine session will consist of two speakers who have pioneered the field of stem cell-based regenerative therapy. The topics will cover current update on stem-cell based therapy for brain and cardiovascular diseases. Dr. Kwang-Soo Kim from McLean Hospital/Harvard Medical School will present how basic molecular can be translated into novel therapeutic approaches for Parkinson's disease. Prof. Kim's group was the first to apply human iPSC-derived cells to a patient with Parkinson's disease. Dr. Young-sup Yoon from Emory University/Yonsei University will present their development of using human induced pluripotent stem cells, directly reprogrammed cells and engineering technologies for translation of basic discovery to clinical therapy of cardiovascular diseases.

Chair

Youngsup Yoon

Bruce R Logue Professor
Director of Stem Cell Biology
School of Medicine
Emory University

Distinguished Professor
Yonsei University

Cardiovascular Regeneration using Stem Cells, Reprogrammed Cells and Engineering: Bench to Bedside

Ischemic cardiovascular disease is the most common health burden worldwide. The discovery of stem or progenitor cells has provided new hope for many patients with advanced diseases, because cell therapy could alleviate ischemia by forming new vessels. Over the last decade, two new developments have emerged for cell-based therapy for cardiovascular disease: human pluripotent stem cell-derived endothelial cells (ECs) and directly reprogrammed or induced endothelial cells. I will present the recent development on these two types of cells in terms of preclinical development. In addition, we have developed various bioengineering approaches to improve transplanted cell survival and function. We have also been working on simultaneous reprogramming of somatic cells into a tissue-like structure, referred to as reprogrammed cardiovascular tissue (rCVT), which includes ECs, smooth muscle cells, and cardiomyocyte. Implantation of this rCVT onto the infarcted mouse heart reduced regional cardiac strains and improved cardiac function via direct cellular contribution, paracrine effects, and scaffolding effects. These new approaches can serve as a novel platform for cell-based therapy and drug discovery.

Young-sup Yoon, MD, PhD is Bruce R Logue Chair Professor and Director of Stem Cell Biology at Emory University School of Medicine and Distinguished Professor at Yonsei University. His research focuses on cardiovascular regeneration with stem cells, direct reprogramming, and tissue engineering. He is one of the pioneers in using stem cells for cardiac and vascular regeneration. His research has been continuously funded by grants from NIH, Department of Defense, and American Heart Association since 2004. He was elected as prestigious member of American Society for Clinical Investigation as the first Korean. He is Fellow of American Heart Association, a chartered member of NIH study section, and a member of editorial boards of the journals including Circulation Research, Molecular and Cellular Biochemistry (Associate Editor), Frontiers in Drug Discovery (Associate Editor). He also founded a company for the first-in-class clinical trial with human iPSC-derived endothelial cells for cardiovascular regeneration through Karis Bio Inc.

Kwang-Soo Kim

Director
Molecular Neurobiology Laboratory
McLean Hospital

Professor of Psychiatry
Harvard Medical School

Toward a Cure for Parkinson's Disease: From Bench to Bed and From Bed to Bench

Based on our studies of transcriptional regulatory cascade underlying development and maintenance of midbrain dopaminergic (mDA) neurons, we identified the orphan nuclear receptor Nurr1 as a promising therapeutic target of PD. Although Nurr1 was viewed as a ligand-independent, constitutively active transcription factor, we identified both synthetic and endogenous ligands of Nurr1 that prominently regulate Nurr1's function via direct interaction, suggesting that (1) Nurr1 is an "*adopted*" nuclear receptor (thus, "*druggable*") and (2) Nurr1's agonists can be developed as a novel class of mechanism-based, disease-modifying therapeutics for PD. In addition, given that major motor dysfunction of PD is caused by selective degeneration of midbrain dopamine neurons, cell replacement is a promising approach for PD. Thus, we are developing and optimizing human iPSC-based transplantation for autologous, personalized cell therapy and recently treated the first PD patient using the patient's own cells. At the same time, this clinical study revealed new challenges to be addressed. I will discuss how basic molecular studies can be translated into novel therapeutic approaches for PD and vice versa, demonstrating a proof-of-concept of "*bench to bed side*" and "*bed to bench*" approaches.

Kwang-Soo Kim, Ph.D. is a professor and Director of the Molecular Neurobiology Laboratory at McLean Hospital and Harvard Medical School. Based on his >30 years' experiences to investigate the transcriptional regulatory cascade of midbrain dopamine neuronal system, he has been focusing on translating his research to novel therapeutic development of Parkinson's disease (PD). In particular, he is focused on developing a novel neuroprotective drug as well as establishing an efficient platform for personalized autologous cell therapy of PD.

Life Science and Engineering

Innovative Discoveries on Brain Science

August 4 _ Friday _ 10:30am _ Enterprise Ballroom 5&6

Chair

Jin Mo Chung

Professor and Chair
Department of Neuro-biology
University of Texas
Medical Branch

The Brain Science session will consist of three world renowned speakers covering a wide range of brain function spanning from newly discovered brain receptor function, to brain circuit connectivity, to a clinically applicable animal study. Dr. Uhtaek Oh from KIST will talk about the Physiological roles of a newly discovered mechanical sensing receptor in brain function. Dr. Jin Hyung Lee from Stanford University will then discuss how to solve brain circuit function and dysfunction with computational modeling and optogenetic imaging techniques. As an example of an animal study for a disease model, Dr. Jun-Ho La from University of Texas Medical Branch will discuss how chronic pain develops from non-chronic injuries in a sex-dependent manner in mice models of pain.

Co-Chair and Presenter

Uhtaek Oh

Principal Investigator
and Director
Brain Science Institute
Korea Institute of
Science and Technology
(KIST)

Tentonins are mechanically activated channels required for essential functions

Mechanotransduction is a biological process of the conversion of mechanical stimuli into biological responses. Numerous physiological functions such as touch, pressure sensation, hearing, blood pressure sensing, proprioception, and pain require mechanotransduction. Mechanotransduction starts with mechanosensitive (MS) channels in many mechanosensory cells. In the present seminar, we will introduce a novel MS channel gene, Tentonin 3 (TTN3), that elicits MS currents with slow inactivation kinetics distinct from Piezo channels. How TTN3 is different from Piezo1 and 2 will be discussed. A piece of evidence that TTN3 is a bona-fide MS channel, not a regulator of Piezo1 will also be presented. Physiological roles of TTN3 in proprioception, baroreceptor function, and beta-cell functions in pancreas will be summarized.

Dr. Uhtaek Oh is a principal researcher and a former director of the Brain Science Institute of KIST. Before this, Dr. Oh had been a professor of Seoul National University for a long time. His main research field has been ion channels that are essential for numerous physiological functions. This research field requires heavy knowledge on electrophysiology as well as molecular biology. Luckily, Dr. Oh found two important ion channels, Anoctamin 1 and Tentonin 3. As the head of a neuroscience institute, Dr. Oh is also interested in recently developed technology in neuroscience, such as neurotools for studying complex circuits of the brain.

Jin Hyung Lee

Associate Professor
Neurology and Neurological Sciences, Bioengineering, Neurosurgery, and Electrical Engineering (Courtesy)
Stanford University

Solving brain circuit function and dysfunction with computational modeling and optogenetic fMRI

Neurological and psychiatric disorders are dramatically increasing in prevalence due to aging population and social isolation. However, to date, there is no cure for any of the brain disorders. The goal of brain disorder treatments is to restore the brain's function. Therefore, a key challenge is to quantify the brain function underlying behavior. Once the brain function algorithms underlying behaviors of interest can be quantitatively defined, minimizing the normal and diseased brain function difference can be defined as the objective function for the brain disorder treatment. The variables then can be optimized to minimize the objective function. In order to quantify the brain function algorithms underlying behavior, cell type specific whole brain function measurements are necessary. We utilize optogenetics combined with fMRI (ofMRI) to enable such measurements. Through computational modeling of ofMRI data, the functional interactions among different regions of the brain was then quantified. In combination with electrophysiological measurements, we further model brain function at a cellular level. In order to further understand the circuit, pathology relationship, we also utilize brain clearing methods to longitudinally quantify and model pathology. Through these efforts, we aim to enable systematic design of therapeutic interventions necessary for the treatment of brain disorders.

Jin Hyung Lee, PhD is an Associate Professor of Neurology and Neurological Sciences, Bioengineering, Neurosurgery, and Electrical Engineering (Courtesy) at Stanford University. Dr. Lee received her Bachelor's degree from Seoul National University and Masters and Doctoral degree from Stanford University, all in Electrical Engineering. She is a recipient of the 2008 NIH/NIBIB K99/R00 Pathway to Independence Award, 2010 NIH Director's New Innovator Award, 2010 Okawa Foundation Research Grant Award, 2011 NSF CAREER Award, 2012 Alfred P. Sloan Research Fellowship, 2012 Epilepsy Therapy Project award, 2013 Alzheimer's Association New Investigator Award, 2014 IEEE EMBS BRAIN young investigator award, 2017 NIH/NIMH BRAIN grant award, and 2018 Lina 50+ Award Grand Prize, and 2019 NIH Director's Pioneer Award. As an Electrical Engineer by training with Neuroscience research interest, her goal is to analyze, debug, and engineer the brain circuit through innovative technology.

Jun-Ho La

Associate Professor
Department of Neurobiology
University of Texas Medical Branch (UTMB)

Sex differences in pain chronification

Acute injury-induced pain can transition to chronic pain (pain chronification) which predominantly affects women. To understand its mechanisms, we developed a new murine model of pain chronification in which postinjury stimulation of an acute injury area triggers pain chronification without affecting the resolution of the acute injury. Female mice have greater sensitivity and a wider timeframe for postinjury stimulation to trigger pain chronification. The resultant chronic pain state is maintained by ongoing nerve activity at the inciting injury area in females but by reactive spinal microglia in males. In the absence of estrogen, females develop pain chronification that is maintained by none of the two mechanisms. In males, spinal GABAergic disinhibition is critical for normally innocuous peripheral stimulation to activate spinal microglia. Unlike males, females develop pain chronification only when GABAB receptor-mediated spinal inhibition is impaired, which is not dependent on spinal microglia. These results suggest that treatments for pain chronification need the consideration of mechanistic sex differences.

Dr. La received his PhD in veterinary physiology from Seoul National University studying the mechanisms of intestinal dysmotility and visceral pain in a rat model of irritable bowel syndrome. During his postdoctoral training at Gyeongsang National University, he investigated the functional expression of two-pore domain (K2P) channels in dorsal root ganglion (DRG) neurons. As a postdoctoral associate and Research Assistant Professor at the University of Pittsburgh, Dr. La studied long-term changes in DRG neurons in visceral pain conditions. Currently, at UTMB, his research focuses on mechanisms of pain chronification without underlying persistent tissue injury.

Computational Science and Engineering:

Advances in Quantum and High Performance Computing

August 3 _ Thursday _ 10:30am _ Enterprise Ballroom 7&8

High performance computing is at the heart of modern technology, enabling computational sciences, artificial intelligence and information technology. Customized computational resources are deployed in hybrid high performance computing environments to support optimized execution of critical tasks. Quantum computers provide a promise for tackling challenging problems that are intractable using conventional computational capabilities. This symposium will discuss advances in high performance computing, and explore the future trends enabled by quantum computing in hybrid HPC environment.

Chair

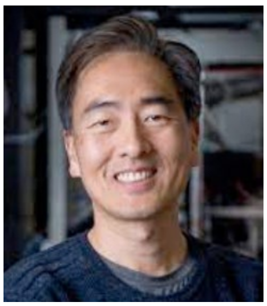

Jungsang Kim

Schiciano Family Distinguished Professor
Electrical and Computer Engineering and Physics
Duke University
Co-Founder and CTO
IonQ

Jungsang Kim is the Schiciano Family Distinguished Professor of Electrical and Computer Engineering and Physics at Duke University, and a Co- Founder and Chief Technology Officer of IonQ, Inc. Kim has pioneered the technology development, system engineering and commercialization of quantum computers based on trapped atomic ions, by leading numerous multi-disciplinary collaborative research initiatives in the US. Prior to Duke University, Kim was a Member of Technical Staff and Technical Manager at Bell Laboratories, leading the development and commercialization of large- scale optical switches and wireless communication systems. He received his Ph.D. degree in Physics from Stanford University (1999) and BS degree in Physics from Seoul National University (1992). He is a Fellow of the American Physical Society and Optica (formerly Optical Society of America).

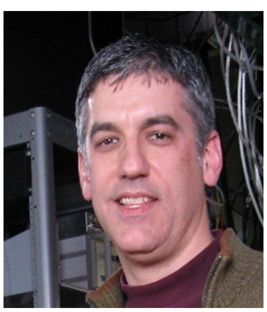

Christopher Monroe

Gilhuly Family Presidential Distinguished Professor
Electrical and Computer Engineering and Physics
Duke University
Co-Founder and Chief Scientist
IonQ, Inc.

Quantum Computers: Applications and Implementations

Quantum computers exploit the bizarre features of quantum physics - uncertainty, entanglement, and measurement - to perform tasks that are impossible using conventional means, such as computing over huge amounts of information, and communicating via teleportation. I will summarize the foundations of quantum computation and the potential exponential scaling quantum computers may hold over conventional computation, along with some examples of quantum speedups based on the parallelism of quantum superposition. I will conclude with a summary of the leading quantum computer architectures, particularly those based on individual atoms, suspended and isolated with electric fields, and individually addressed with laser beams. Ion trap quantum computers have essentially perfect idle qubit/spin coherence properties with fully-connected and reconfigurable entanglement operations. I will present recent results with state-of-the-art ion trap quantum computer systems and simulators, from both the Duke Quantum Center and IonQ, Inc., and summarize the outlook for further scaling of ion trap quantum computers based on a well-defined and modular architecture.

Christopher Monroe is the Gilhuly Family Presidential Distinguished Professor of Electrical and Computer Engineering and Physics at Duke University, and the Co-Founder and Chief Scientist of IonQ, Inc. Monroe has pioneered nearly all aspects of trapped ion quantum computing and simulation, from the demonstration of the first quantum gate, a monolithic semiconductor chip ion trap, and photonic interconnections between separated ion trap systems. He is a key architect of the US National Quantum Initiative, a Fellow of the American Physical Society, Optical Society of America, the UK Institute of Physics, the American Association for the Advancement of Science, and is a member of the National Academy of Sciences.

Jaejin Lee

Dean
Graduate School of
Data Science

Professor
Department of
Computer Science and
Engineering

Seoul National
University

Quantum Computing, Deep Learning, and Accelerated Computing

The deep learning language models, which have recently been in the limelight, require supercomputer-level computing resources that are made up of hundreds or thousands of GPU computer systems when training. Quantum computing is a fundamentally different computing paradigm and is seen as a future option to solve the intractable problems of classical computing using digital computers. However, current quantum computers are still noisy and error-prone, so classical simulation of quantum circuits is essential for the verification of quantum computers and the development of complex quantum algorithms. Classical simulations of large quantum systems mainly use supercomputers because they require exponential memory space and computational complexity depending on the number of qubits. Accelerated computing is a method of mixing a traditional CPU with an accelerator. It is a computing model that reduces computing time by accelerating a specific task in a special processor called an accelerator. Currently, GPUs, FPGAs, and NPUs are mainly used as accelerators. This talk examines the relationship between quantum computing, deep learning, and accelerated computing, and discusses the desirable research direction from the software point of view.

Jaejin Lee is the Dean of Graduate School of Data Science and Professor at the Dept. of Computer Science and Engineering at Seoul National University (SNU). He also serves as the Director of the Center for Optimizing Hyperscale AI Models and Platforms and the Thunder research group at SNU. He received his Ph.D. degree in Computer Science from the University of Illinois at Urbana-Champaign (UIUC) in 1999. He received an MS degree in Computer Science from Stanford University in 1995 and a BS degree in Physics from SNU in 1991. After obtaining the Ph.D. degree, he spent half a year at UIUC as a visiting lecturer and postdoctoral research associate. He was an assistant professor in the Department of Computer Science and Engineering at Michigan State University from January 2000 to August 2002 before joining SNU. He is an IEEE fellow.

Alexander (Lex) Kemper

Associate Professor
Department of Physics
North Carolina State
University

Opportunities for Quantum/Classical Computing

Quantum computing has the potential to help us overcome the barriers that are presented by the end of Moore's law. In the natural sciences, these barriers appear as limitations in computer memory and/or processing speed which prevent scientists from describing the problem fully and forcing them to work on smaller models or with approximate methods. Since nature is fundamentally quantum, it is quite natural to view a quantum computer as a bespoke quantum simulator, where we can examine the open problems in science at a scale not possible with classical computers. In this talk, I will present how this is achieved, discuss some recent advances in the area. In addition, I will discuss the limitations of quantum computing, and where classical computing can play an important role, for both today's quantum hardware and going into the fault-tolerant quantum era.

Lex Kemper is an associate professor in the Department of Physics at North Carolina State University. His work centers at the intersection of quantum computing and condensed matter physics, where his group is studying how near- and future-term quantum computers could be of use in solving outstanding problems in physics. He received his Ph.D in Physics from the University of Florida in 1999, following a BS degree in Physics and Mathematics from the same institution. After obtaining his Ph.D., he spent 2 years at Stanford as a postdoctoral research associate, and 3 years at Lawrence Berkeley National Laboratory as an Alvarez Fellow before joining NC State.

Computational Science and Engineering:

Artificial Intelligence (AI) and Cybersecurity

August 4 _ Friday _ 10:30am _ Enterprise Ballroom 7&8

Chair

Tae (Tom) Oh

Professor- iSchool
Golisano College
of Computing and
Information Sciences
Strategic Initiatives and
Innovation Director
National Technical
Institute of Deaf
Rochester Institute of
Technology (RIT)

The impact of the industrial and digital (information) revolutions has, undoubtedly, been a substantial advancement in our industry, social media, and e-commerce. In addition, AI and cybersecurity have impacted extensive changes and breakthroughs affecting all aspects of our society and life. This results in a richly interconnected organization with decision-making using machine learning and exploiting "*big*" data in a safe and secure environment. Now, consumers can buy goods, and businesses can obtain services from anywhere in the world using the Internet and exploiting the unlimited possibilities using the widespread usage of AI and cybersecurity inventions. The highly selected speakers will share their perspectives on AI and cybersecurity advancements, research, industry, and challenges in this session. Also, they will share the future trends in their area of expertise.

Tae Hyun Hwang

Endowed Chair
Florida
Dept. of Cancer Biology
Mayo Clinic
Comprehensive
Cancer Center

Unraveling Cancer's Complexity: Single-Cell and Spatial Genomics Meet Machine Learning and AI for Personalized Immunotherapies and Cellular Therapies

In this talk, we will delve into how single-cell and spatial genomics, combined with machine learning and AI, can revolutionize biomarker identification and the development of personalized immunotherapies for cancer treatment. By analyzing sequential single-cell CAR-T and PBMC data from CD19 CAR-T cell treated patients, we aim to uncover novel biomarkers and combinatory therapies. Additionally, we will discuss AI-guided biomarker discovery and therapeutic strategies specifically tailored for gastric cancer immunotherapy, ultimately paving the way for more targeted and effective treatments in the rapidly evolving field of oncology.

Dr. Tae Hyun Hwang is a renowned researcher in cancer, holding the prestigious position of Endowed Chair at Mayo Clinic Florida. Focusing on using artificial intelligence (AI) and advanced computing techniques to improve patient outcomes, Dr. Hwang works closely with top healthcare institutions and businesses, including pharmaceutical companies and start-ups, to develop innovative solutions for complex medical challenges. With a strong background in both computer science and medicine, Dr. Hwang's work bridges the gap between these fields, enabling the development of cutting-edge treatments for cancer and heart diseases. In addition to his work at Mayo Clinic, Dr. Hwang has held positions at several prestigious institutions, such as Cleveland Clinic and the University of Texas Southwestern Medical Center. He also leads a team of 20 researchers at the ML and AI Lab, where they work together to advance the use of AI and machine learning in medical research. As a testament to his innovative approach, Dr. Hwang co-founded KURE.AI and KURE.AI Therapeutics, a clinical stage cellular therapy company that develops personalized cell therapy products using AI technology.

Minkyong Kim

Engineering Director
Artificial Intelligence
Machine Learning
Apple

AI Voice Assistants in Industry: Past, Present, and Future.

Voice assistants have become increasingly popular in recent years. These devices use a combination of speech recognition, natural language understanding, and dialogue management to understand and respond to user requests. However, there are still challenges to be addressed before voice assistants can reach their full potential. These challenges include ensuring the safety of generated responses, optimizing for on-device processing, and better understanding how people interact with voice assistants. This talk provides a comprehensive overview of the past and present as well as the challenges and opportunities that voice assistants face in the future.

Minkyong is Engineering Director at Apple, focusing on Siri Voice Assistant. Before joining Apple, she worked as VP at Samsung Electronics in Korea, leading the development of Bixby Voice Assistant for smart appliances. She also worked as the chief coordinating officer for Samsung Global AI Centers. Before that, she worked at IBM T.J. Watson Research Center in New York for ten years focusing on the design and development of IBM Cloud, Messaging Systems, and Stream Processing. She received her Ph.D. in Computer Science and Engineering from the University of Michigan and her M.S. and B.S. in Computer Science and Engineering from Seoul National University. She holds 40+ patents and published 30+ papers at top conferences and journals.

Jeremy Epstein

Program Director
Secure and Trustworthy Cyberspace (SaTC) Lead
Division of Computer and Network Systems (CISE/CNS)
National Science Foundation (NSF)

Cybersecurity Research – Yesterday, Today, and Tomorrow

Cybersecurity and privacy are no longer just technical topics, if they ever were. In the early days, cybersecurity meant encryption, and was closely tied to mathematics. Over the intervening decades, it was mostly confined to computer science. Today, it covers computer science and computer engineering, but also many areas in social sciences, ethics, education, mathematics, statistics, law, policy, business, and even biological sciences. Some even argue that it impacts the arts. The National Science Foundation is undergoing a rethinking of the cybersecurity & privacy field, and how research should be supported and funded for the next decade. Simultaneously, the White House's interagency research coordinating group, Networking and Information Technology Research & Development National Coordinating Office, is working on a rethinking of the Congressionally-mandated Federal Cybersecurity Research Strategy. And in March 2023, the White House Office of the National Cyber Director released the National Cybersecurity Strategy, which includes a section on cybersecurity & privacy research. This talk will bring together these threads of US government activity to describe how government-funded cybersecurity & privacy research will evolve over the next decade, and how they may impact non-governmental research.

Jeremy Epstein leads the National Science Foundation's Secure and Trustworthy Cyberspace (SaTC) program, NSF's flagship multi-disciplinary cybersecurity research effort. Over the past decade, SaTC has sponsored nearly 4000 research projects and almost $1B in spending, and is currently revisiting its mission to focus on the next decade. In addition to leading the SaTC program, Jeremy co-leads the US government's interagency research program for cybersecurity through the Networking and Information Technology Research & Development Cybersecurity & Information Assurance Interagency Working Group (NITRD CSIA IWG), where he is responsible for the National Cybersecurity Research Strategy. His research interests include securing voting and elections. In addition to his work at NSF, he is chair of the Association for Computing Machinery's US Technology Policy Committee (ACM USTPC), a non-partisan scientific expert group providing technical advice on a wide range of computing policy issues. He is also founder and director of the Scholarships for Women Studying Information Security (SWSIS) program.

Workforce of the Future: Education and Careers

Convergence in Education and Workforce Development

August 3 _ Thursday _ 10:30am _ Room Maverick

Chair

Gloria J. Kim

Department of
Engineering Education
University of Florida

Powerful technologies, such as artificial intelligence, automation, robotics, and the internet of things, are disrupting the nature of work and reshaping the landscape of jobs. New forms of learning, skills assessments, and job training are exposing pitfalls of traditional degree-centric requirements in tech hiring. The approach to developing and sustaining talent supply chain must change. This UKC 2023 Keynote Symposium explores convergent perspectives on education and workforce development. Experts and stakeholders are invited to offer insights on how the benefits of emerging technology can be leveraged to equitably impact current and future workforce.

Topical Plenary

Curtis J. Bonk

Professor, School of
Education
Indiana University
2022 American
Educational Research
Association (AERA)
Fellow

Technology Today, Technology Tomorrow: Might Learning Evolutions lead to Learning Revolutions?

Change is inevitable. Technology change is pervasive. Yesterday's technologies wiped entire industries and occupations. Today's technologies are accelerating these changes, and are, in particular, transforming the field of education. Learning is definitely changing. Generative AI has accelerated everything. There is now a pervasive need for innovations in how we teach and how we learn. In response, Professor Bonk will detail a set of 20 "*last*" principles of instruction including (i.e., flexibility, autonomy, meaningful learning, choice, etc.) and he will also highlight new roles for instructors in light of these principles. Next, he will discuss these in light of three megatrends related to learning technology today: (1) the technologies for engagement; (2) the technologies for pervasive access; and (3) the technologies for the personalization and customization of learning. In the third decade of the 21st century, learning has become increasingly flipped, social, collaborative, global, game-like, mobile, modifiable, open, online, visually-based, hands-on, ubiquitous, personal, and much much more. Is this an evolution or a revolution?

Curtis J. Bonk is Professor in the School of Education at Indiana University (IU) teaching psychology and technology courses and Adjunct in the School of Informatics at IU. He is a former software entrepreneur, certified public accountant, corporate controller, and educational psychologist who presently is an educational technologist, award-winning writer, highly published researcher, statewide and national awardee in innovative teaching with technology, and internationally acclaimed presenter. Curt is the author of nearly 400 publications and has given close to 2,000 talks around the world. In 2020, Curt was awarded the IU President's Award for Excellence in Teaching and Learning Technology and in 2021, he received the David H. Jonassen Excellence in Research Award. Recently, the American Educational Research Association named him a 2022 AERA Fellow for his exceptional contributions to, and excellence in, education research, and in 2023 AERA recognized him with the Outstanding International Research Collaboration Award for his joint research with Professor Min Young Doo at Kangwon National University in Korea. Curt co-hosts the weekly award-winning podcast show, Silver Lining for Learning (https://silverliningforlearning.org/). He can be contacted at cjbonk@indiana.edu and his homepage is http://curtbonk.com/.

Wookyung Sun

Visiting Professor
Dept. of Electrical and Computer Engineering
Seoul National University

100,000 by 2026: The COSS Project

The high-tech innovation convergence university project (COSS: Convergence and Open sharing System) is a project that breaks down the boundaries between universities and transcends the walls between departments, enabling any student to pursue education in their desired cutting-edge field irrespective of their major. The goal of this project is to foster 100,000 skilled students in the digital high-tech field by 2026, based on the principles of convergence, openness, and cooperation. The consortium in 13 fields is composed of universities and colleges nationwide. The project is scheduled to run for a period of 6 years, with the government supporting the project cost of 9 million dollars per consortium. In this talk, we will introduce specific details about the COSS project and discuss how the Korean government approaches education to foster future talents in preparation for the Fourth Industrial Revolution.

Dr. Wookyung Sun is currently participating in various human resource development programs related to the next-generation semiconductor industry at Seoul National University in Korea. She worked at HYNIX Semiconductor Inc. research center for ten years, focusing on the cell transistor design and process integration of DRAM. She received her B.S., M.S., and Ph.D. in electronics engineering from Ewha Womans University in Seoul, Korea. Her current research interests include memristor devices for neuromorphic engineering and spiking neural network algorithm modeling.

Junseok Hwang

Professor of Information Science and Technology
Technology Management, Economics, and Policy Program (TEMEP)
Seoul National University

Smart City Education and Training

Prof. Hwang received his Ph. D. in Information Science and Telecommunications from the University of Pittsburgh, a. He began his academic career as an Assistant Professor in the School of Information Studies at Syracuse University. He is the Director of Global R&DB Center, International Technology Professional Program (ITPP), ASEAN Smart City Professional Program, and Transdisciplinary Graduate Program in Smart City Global Convergence (SCGC) at Seoul National University. He has educated and advised more than 200 post graduate government officials, public researchers, academic and industry leaders from about 50 countries as global leaders of ICT innovation and smart city development. Along with the world-wide network of Technology Management, Economics and Policy Program (TEMEP), International Technology Professional Program (ITPP) and Smart City Global Convergence Program (SCGC), he hosts annual International Symposia on Green, Smart, Development and Vision (GSDV) to exhibit transdisciplinary ICT innovation research and practices as a part of global knowledge sharing and collaboration. Currently, he is leading the national funded BK21 program, Smart City Global Convergence (SCGC) Program in SNU as a program director with the dedicated mission of educating international technology specialists and smart city experts from around the globe. His current research focuses on economics of information and networks, management and policy of convergence technologies, social impact study and forecasting of emerging technologies, knowledge and intelligence management. Recent research areas also include smart city technology innovation, sustainability of technology management, appropriate technology for developing economy and community, fourth industrial revolution education, digital transformation.

Charles G. Woychik

Senior Director of Advanced Packaging Platforms
SkyWater Technology

Developing the Talent of the Future through Partnerships

Dr. Charles G. Woychik is Senior Director of Advanced Packaging Platforms at SkyWater Technology in Kissimmee, FL. Prior to joining SkyWater he was the Chief Scientist at i3 Microsystems in St. Petersburg, FL. Other previous positions that he held were: Senior Director of 3D Technologies at Invensas Corporation and Senior Scientist at GE Global Research Center. Most of his career was at IBM Endicott, NY where he held both engineering and managerial positions. His area of expertise is materials and processes for advanced electronics packaging. He holds a Doctorate and Master of Science degree in Materials Science and Engineering from Carnegie-Mellon University. He has a Bachelor of Science degree in Metallurgical Engineering from the University of Wisconsin-Madison. Chuck has presented at numerous conferences and has many publications. He has 123 issued US issued patents to his credit.

Workforce of the Future: Education and Careers

Future Careers in Technology and Entrepreneurship

August 4 _ Friday _ 10:30am _ Room Maverick

The job market, particularly in technology, is constantly evolving with changes such as hybrid remote work, job automation by artificial intelligence, and increasing interests in entrepreneurship and startups. To succeed in the future job market, individuals must stay up to date and adapt to new technologies and the market environment. This keynote symposium targets mid-career and young professionals, as well as the young generation. It will feature speakers discussing future careers in technology and entrepreneurship, how to acquire new job skills, advance in corporate careers, or start a company. The symposium will culminate in a speaker panel session with an open discussion and Q&A.

Chair

Kyeong Ho Yang

Founder & President
Korean-American Innovative Technology Engineers and Entrepreneurs (KITEE)

Kyeong Ho Yang is a technologist and innovator in the fields of video processing, multimedia communication systems, and data science. He has nearly 30 years of R&D experience at companies of various sizes from startups to large R&D labs like Bell Laboratories. He has published over 50 papers in peer-reviewed journals and conferences and holds 40 U.S. patents. He is also an entrepreneur who co-founded multiple technology companies in multimedia communications, mobile apps, and EdTech. Recent years, he has been very actively advising Korean startup CEOs through KITEE that he founded in 2015. He has also led the entrepreneurship activities in the Korean-American Scientists and Engineers Association (KSEA), serving as the founding Chair of the KSEA STEP-UP Conference (2020 and 2021) and Chair of the Innovation & Entrepreneurship Symposium at the US-Korea Conference (Co-Chair in 2019 and 2020, Chair in 2021 and 2022), among others. Through these R&D and entrepreneurship activities, Dr. Yang has successfully established strong relationships with people in various areas including academia, industry, startups, business, and government agencies. He received his B.E., M.S., and Ph.D. degrees, all in Electronics Engineering, from Seoul National University.

Co-Chair

Benjamin Lee

Senior Research Associate
Weill Cornell Medicine

Benjamin C. Lee is a Senior Research Associate in Radiology at Weill Cornell Medicine (WCM). His current research involves developing machine learning algorithms for cardiovascular medical imaging in CT, Echo, ECG, and histopathology data for heart failure, heart transplantation, and coronary plaque characterization. Prior to working at WCM, he was a research scientist in industry for over 10 years at INVIA Medical Imaging Solutions in Michigan researching advanced algorithms for the 4DM nuclear medicine (PET, SPECT) cardiac quantification software. His research interests also include biomedical image segmentation, motion correction, image coregistration, kinetic analysis, and inverse problems. For KSEA, he has also helped lead and organize the Data Science Workshop at UKC for the past 5 years, was the Michigan Chapter President and a TG Councilor and chaired national Young Generation conferences. He received both his Ph.D. and M.S. at the University of Michigan, Ann Arbor in Electrical Engineering and his B.S. from Cornell University.

Stella H. Kim

Chief Marketing Officer
& Global VP
Head of Executive Search
HRCap, Inc.

Future of Work and Career Development

This talk first reviews the evolving job market, particularly in technology, with changes such as hybrid work, job automation, glocalization, and new technologies and vast amounts of information that become available at workplaces. Then, Stella will guide next-gen leaders on how to build greater self-awareness and learning agility to succeed in the future job market. She will also speak on the importance of proactively taking accountability, reskilling and upskilling, and serving as a multigenerational and multicultural bridge. She will finally touch on key topics of professional development, job transitions, and career changes.

Stella H. Kim is a 1.5 generation Korean-American talent executive, modern HR leader, and change agent. Stella is an official Forbes HR Council member and Chief Marketing Officer at HRCap, Inc., the largest Asian-American Executive Search & Total HR Solutions Provider. Formerly, she was a Talent Analytics Specialist and Senior Strategy & Analytics Consultant at IBM. Stella is an expert in identifying capability gaps and unlocking opportunities to empower greater potential in individuals, organizations, and communities. She aids decision making with a data-driven macro-view of the labor economy while driving deep empathy with a social-organizational micro-approach. Stella holds a Bachelor's degree in Economics from Princeton University and a Master's degree in Social-Organizational Psychology from Columbia University.

Chang Kim

Former CEO and
Founder of Tapas Media

Career as an Entrepreneur and Careers at Startups

This talk explores the world of entrepreneurship and sheds light on the journey of founding and exiting a startup. Chang Kim ("CK"), the founder of Tapas Media, will share his experience as an entrepreneur with the audience, discussing the challenges and rewards of starting your own business, and the skills and experience you need to be successful. CK will also talk about the diverse roles and responsibilities available at startups and the opportunities for growth and development that these companies can offer. Join us to gain practical knowledge and a deeper understanding of the entrepreneurial landscape.

Chang Kim ("CK") is a 2x founder and angel investor/adviser for 50+ companies. CK is the original founder and former CEO of Tapas Media, a mobile storytelling platform and community for original IP creators in the US. In 2021, Tapas Media was acquired by Korea's Kakao Entertainment at a $510M valuation. Prior to this, he was a product manager at Google, running Blogger. He joined Google when it acquired TNC, a leading blogging software company in Asia that he co-founded. Before TNC, CK was at Samsung, in charge of Samsung's mobile content strategies. He has a B.S. degree in Physics from the University of Michigan and also studied at Seoul National University.

Anna Ji-Hyun Lee

Director
Prellis Biologics

Panelist: Anna Lee is the Director of Antibody Screening at Prellis Biologics. She joins Prellis with extensive experience in platform development for antibody discovery, having worked for several leading biotech and pharmaceutical companies such as the U.S. Military HIV Research Program, Regeneron, Bristol-Myers Squibb, and IGM Biosciences. She holds an undergraduate degree from the University of Virginia, where she pursued studies in Chemistry and Bioethics, and Master's degrees in Chemistry and Bioinformatics from Villanova and Johns Hopkins University.

Technical Symposium

Technical Symposium Group

Technical Group A-1	**Physics (PHY)**	Chair: Harold D. Kim (Georgia Institute of Technology) Co-Chairs: Yoonseok Lee (University of Florida), Soonwon Choi (Massachusetts Institute of Technology)
Technical Group A-2	**Chemistry (CHM)**	Chair: Jiwoong Park (University of Chicago), Co-chairs: Dong Hee Son (Texas A&M University), Hoi Sung Chung (National Institutes of Health)
Technical Group A-3	**Math/Applied Math/Statistics (MAS)**	Chair: Young-Ju Lee (Texas State University), Co-Chairs: Seungil Kim (Kyung Hee University), Jangwoon Lee (University of Mary Washington)
Technical Group B-1	**Medical and Pharmaceutical Science (MPS)**	Chair: Tae-Hyung Kim (University of New Mexico) Co-Chairs: Jiyoung Lee (George Washington University), Hun-Goo Lee (Massachusetts General Hospital/Harvard Medical School)
Technical Group B-2	**Food, Agriculture, Ecology and Nutrition (FAN)**	Chair:Yoo Kim (Oklahoma State University) Co- Chairs: Sungeun Cho (Auburn University), Kee Hong Kim (Purdue University)
Technical Group B-3 / C-1	**Biological and Biomedical Sciences (Biology, Molecular Biology, Cognitive Science, Botany, Zoology, Biomechanics, etc.)/Bioengineering and Biomedical Engineering (BME)**	Chair: Hyunjoon Kong (University of Illinois at Urbana-Champaign) Co-Chairs: Deok Ho Kim (Johns Hopkins University), Young Bin Choy (Seoul National University)
Technical Group C-2	**Chemical, Textile, Energy, and Nuclear Engineering (CHE)**	Chair: Hyun-Tae Hwang (University of Kentucky) Co-Chair: Jaewon Lee (University of Missouri)
Technical Group C-3	**Mechanical, Aerospace and Naval Engineering (MAN)**	Chair: Eon Soo Lee (New Jersey Institute of Technology) Co-Chairs: Martin Byung-Guk Jun (Purdue University), W. Jong Yoon (University of Washington, Bothell)
Technical Group C-4	**Materials Science and Engineering, Nanotechnology (MSE)**	Chair: Jiyoung Kim (University of Texas at Dallas) Co-Chairs: Chang-Yong Nam (Brookhaven National Laboratory), Jang-Sik Lee (POSTECH)
Technical Group C-5	**Civil and Environmental Engineering, Architecture (CEA)**	Chair: Youngguk Seo (Kennesaw State University) Co-Chair: Jung Heum Yeon (Texas State University)
Technical Group C-6	**Electrical and Computer Engineering (ECE)**	Chairs: Jin W Choi (Michigan Technological University) Co-Chairs: Wookyung Sun (Seoul National University), Jeongwon Park (University of Nevada at Reno), Jungkwun Kim (University of North Texas)
Technical Group C-7	**Computer and Information Sciences (CIT)**	Chair: Ohbong J. Kwon (New York City College of Technology) Co-Chairs: Hoyoung Hwang (Hansung University), Donghoon Kim (Arkansas State University)
Technical Group C-8	**Industrial, Manufacturing, and Systems Engineering, Management Sciences, Operations Research (IMS)**	Chair: Jeong Hoon Choi (Youngstown State University) Co-Chairs: Tai-Woo Chang (Kyonggi University), Hyesung Park (Georgia Gwinnett College)
Technical Group D-1	**Social Sciences (Anthropology, Economics, Political Science, Sociology, Public Policy, etc.), Psychology, Digital Arts, STEM Education, and Other Sciences (SSP)**	Chair: Jongpil Cheon (Texas Tech University) Co-Chairs: Nicholas D. Hartlep (Berea College), Kyungbin Kwon (Indiana University – Bloomington), Gilbert Park (Ball state University)

Innovation and Entrepreneurship Symposium (IES) Group

Chair: IL Minn (Johns Hopkins University)

FIRE (Fostering Innovation in Rising Experts) Symposium

Chair: TJ (Tae Joong) Park (MIT)

Physics (PHY)
Technical Group A-1

Quantum science is rapidly gaining popularity in physics as well as among the general public. To address the rising interest in the subject, the Physics Symposium will feature special focus sessions on topics such as the history of quantum mechanics, its foundations, and the latest developments in the experimental and theoretical study of quantum systems. The symposium will also include a session devoted to promoting the work of junior physicists who have made significant contributions to their fields.

Chair

Harold D. Kim

Georgia Institute of Technology

Co-chairs

Chueng Ji

North Carolina State University

Soonwon Choi

Massachusetts Institute of Technology

Tech Group A-1
PHY

@ Carter

Aug 3 _ Thursday _ 4:00 – 6:00pm

PHY Session I: Quantum Mechanics and Beyond
Chair: Harold Kim (Georgia Tech), Soonwon Choi (MIT)

Time	Title and Speaker
4:00	**Spin Correlations and Bell's Inequality** // Chueng Ji (North Carolina State University)
4:24	**From Quantum Physics to Quantum Computing** // Alexander Kemper (North Carolina State University)
4:48	**DAMSA: A Novel Experiment Concept to Probe Dark Sector Particles** // Wooyoung Jang (University of Texas at Arlington)
5:12	**Investigation of Self-Assembled Water Chains in Biomolecular Interactions** // Byung Kim (Boise State University)

Tech Group A-1
PHY

@ Carter

Aug 4 _ Friday _ 4:00 – 6:00pm

PHY Session II: Quantum Materials
Chair: Chueng Ji (North Carolina State University), Harold Kim (Georgia Tech)

Time	Title and Speaker
4:00	**Manipulation of Quantum Materials** // Na Hyun Jo (University of Michigan)

Time	Title and Speaker
4:24	**Tunneling Andreev Reflection: Direct Access to the Superconductivity in the Atomic Resolution** // Wonhee Ko (University of Tennessee, Knoxville)
4:48	**Quantum Geometry for the Optical Properties of Crystals** Invited // Junyeong Ahn (Harvard University)
5:12	**Quantum Phases and Transitions under Decoherence: Many Body Physics of Information** // Jong Yeon Lee (Kavli Institute of Theoretical Physics)
5:36	**Toolbox for Analog Quantum Simulations** // Soonwon Choi (MIT)

Tech Group A-1
PHY

@ Aviator A

Aug 4 _ Friday _ 6:00 – 9:00pm

PHY Poster Session
Chair: Harold Kim (Georgia Tech), Chueng Ji (North Carolina State University), Soonwon Choi (MIT)

PHY P1	**Launching Multiple Modes in Hyperbolic vdW Heterostructures** // Byung-Il Noh (Auburn University)

Tech Group A-1
PHY

@ Carter

Aug 5 _ Saturday _ 8:00 – 10:00am

PHY Session III: Frontiers of Quantum Information Science and Technology
Chair: Soonwon Choi (MIT), Chueng Ji (North Carolina State University)

Time	Title and Speaker
8:00	**Research and Development of the Multi-qubit Superconducting Quantum Processor in SKKU** // Yonuk Chong (SungKyunKwan University)
8:20	**Magnetic-field-resilient Niobium Cavity Electromechanical System and its Optomechanical Frequency Comb Generation** // Junho Suh (Pohang University of Science and Technology)
8:40	**Deterministic Generation of Multidimensional Photonic Cluster States with a Single Quantum Emitter** Invited // Gihwan Kim (California Institute of Technology)
9:00	**Towards a Practical Quantum Advantage with a High-fidelity Rydberg Quantum Simulator** // Joonhee Choi (Stanford University)
9:20	**Scalable Fault-tolerant Quantum Error Correction with Linear Array of Emitters** // Isaac Kim (UC Davis)
9:40	**Fault-tolerant Quantum Computing with Bosonic Qubits** // Kyungjoo Noh (Amazon Web Services)

Chemistry (CHM)
Technical Group A-2

Chemistry has been crucial to understanding material's properties on the molecular level, and its impacts have been broadened to various applications of energy, new materials, biology, healthcare, and engineering. Thus, interdisciplinary research is becoming increasingly critical in addressing complex problems. This year's Chemistry Technical Group will organize symposia focused on the following research areas: (1) design and characterization of new materials and energy, and (2) molecular approaches for biology and healthcare. Leading researchers working at the forefront of these topics will be invited to discuss the structures and functions of molecular systems and noble experimental, theoretical, and computational techniques. Researchers, postdocs, and students working in academia, industry, and government laboratories are strongly encouraged to participate in scientific discussions and network building.

Chair

Jiwoong Park

University of Chicago

Co-chairs

Dong Hee Son

Texas A&M University

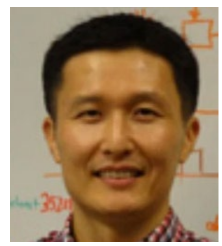

Hoi Sung Chung

National Institutes of Health

Tech Group A-2
CHM

@ Glasscock

Aug 3 _ Thursday _ 4:00 – 6:00pm

CHM Session I: Chemical Approaches for Biomedicine
Chair: Hoi Sung Chung (NIH), Dong Hee Son (Texas A&M University)

Time	Title and Speaker
4:00	**Towards Single Virus Genomics** Invited // Hee-Sun Han (University of Illinois, Urbana-Champagne)
4:20	**Nanotechnology Approaches for Real-time Neurotransmitter Detection in Stem Cell-Derived Neural Interfaces** Invited // Kibum Lee (Rutgers, The State University of New Jersey)
4:40	**Precision tumor cell death through targeting cancer-specific InDel mutations with CRISPR-Cas9** Invited // Taejoon Kwon (Ulsan National Institute of Science and Technology)
5:00	**Structure and mechanisms of DNA damage recognition and initiation in Nucleotide Excision Repair** Invited // Jung-Hyun Min (Baylor University)
5:20	**Transcription-Induced Active Forces Suppress Chromatin Motion by Inducing a Transient Disorder-To-Order Transition** Invited // Sucheol Shin (University of Texas at Austin)
5:40	**Single-molecule characterization of the early phase of amyloid-beta aggregation** Invited // Hoi Sung Chung (NIH)

Tech Group A-2
CHM

@ Glasscock

Aug 4 _ Friday _ 4:00 – 6:00pm

CHM Session II: Chemical Approached for Designed Materials
Chair: Jiwoong Park (U. Chicago), Young Jong Lee (NIST)

Time	Title and Speaker
4:00	**Silver Chalcogenide Infrared Colloidal Quantum Dots** Invited // Kwang Seob Jeong (Korea University)
4:20	**Nature-inspired synthetic polymers for customized biomedical applications** Invited // Soon Mi Lim (Texas A&M University)
4:40	**Photoemission of Upconverted Hot electrons from Doped Quantum Dots Effect of Charge and Ligand** Invited // Dong Hee Son (Texas A&M University)
4:55	**Infrared Sees Proteins in Water, Sensitively** Invited // Young Jong Lee (NIST)
5:10	**Introduction advanced environmental risk assessment for pesticide residues in environmental and AISS** // Hyosub Lee (Residual Agrochemical Assessment Division)
5:25	**New 2D with atomically thin crystals** Invited // Jiwoong Park (University of Chicago)
5:40	**Short oral presentations (each 7 min)** • **Vapor-Phase Anisotropic Polymer Particle Synthesis through Condensed Droplet Polymerization** // Kwang-Won Park (Cornell University) • **Iron-Gold Contacts: An Effective Linker for Ferrocene-Based Single-Molecule Electronics** // Woojung Lee (Columbia University) • **Generalized understanding of double layer for concentrated aqueous electrolytes and ionic liquids** // Suehyun Park (Georgia Institute of Technology)

Tech Group A-2
CHM

@ Aviator A

Aug 4 _ Friday _ 6:00 – 9:00pm

CHM Poster Session
Chair: Jiwoong Park (U. Chicago), Dong Hee Son (Texas A&M University), Hoi Sung Chung (NIH)

Time	Title and Speaker
CHM P1	**Vapor-Phase Anisotropic Polymer Particle Synthesis through Condensed Droplet Polymerization** // Kwang-Won Park (Cornell University)
CHM P2	**Iron-Gold Contacts: An Effective Linker for Ferrocene-Based Single-Molecule Electronics** // Woojung Lee (Columbia University)
CHM P3	**Generalized understanding of double layer for concentrated aqueous electrolytes and ionic liquids** // Suehyun Park (Georgia Institute of Technology)

Mathematics, Applied Math and Statistics (MAS)
Technical Group A-3

The MAS (mathematics, applied math, and statistics) symposium invites enthusiastic researchers, scientists, and engineers to discuss the latest scientific and technical approaches. The symposium covers various aspects of all areas in mathematics, applied math and statistics including, but not limited to, classical theories in mathematics and statistics and practical applications inspired by real-world situations. The UKC 2023 MAS provides an opportunity for scientists and engineers to share their experiences and ideas on how different challenges we face can be turned into opportunities.

Chair

Young- Ju Lee
Texas State University

Co-chairs

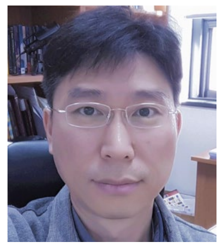

Seungil Kim
Kyung Hee University

Jangwoon Lee
University of Mary Washington

Tech Group A-3
MAS

@ Hobby

Aug 3 _ Thursday _ 4:00 – 6:00pm

MAS Session I: Mathematical Theory and its Applications I
Chair: Seungil Kim (Kyunghee University)

Time	Title and Speaker
4:00	**GMsHDG method for nonlinear porous media** Invited // Minam Moon (Korea Military Academy)
4:20	**An efficient K-way constrained normalized cut and its connection to algebraic multigrid method** // Youngju Lee (Texas State University)
4:40	**The moduli space of holomorphic chains of rank one over a compact Riemann surface** // JingHyung To (Indiana University at Bloomington)
5:00	**Inference about differences in predictive skill between infectious disease forecasting models** // Dongah Kim (University of Massachusetts at Amherst)
5:20	**Exploring dynamics of HIV infections: an analysis of the Susceptible-Infected-Virus model in deterministic and stochastic forms** // Jangwoon Lee (University of Mary Washington)

Tech Group A-3
MAS

@ Hobby

Aug 4 _ Friday _ 4:00 – 6:00pm

MAS Session II: Mathematical Theory and its Applications II
Chair: Youngju Lee (Texas State University), Jangwoon Lee (University of Mary Washington)

Time	Title and Speaker
4:00	**Rigidity of steady solutions to the Navier-Stokes equations in high dimensions** Invited // Jeaheang Bang (University of Texas at San Antonio)
4:20	**Reconstruction of the shape and boundary condition in inverse scattering for an obstacle with partial generalized impedance boundary** // Heejin Lee (Purdue University)
5:00	**Bayesian clustering factor models** // Hwasoo Shin (Virginia Tech)
5:20	**Optimal rational approximation for the fractional diffusion problem** // Seungil Kim (Kyunghee University)
5:40	**Recent development of Bayesian joint modeling for medical sciences** // Seongho Song (University of Cincinnati)

Medical Science, Pharmaceutical Science, Veterinary Medicine, Physical Education (MPS) Technical Group B-1

This year, B-1 (previously MPS) will bring together life sciences and healthcare, and academic professionals on one stage to deliberate on cross-cutting-edge science. The world is changing to have a smart decision among the increased complexities of knowledge. We will deep dive into major three therapeutic areas such as oncology, immunology (including immuno-oncology), and neurology to focus on research and development. All speakers and poster presenters are from across the U.S. and Korea that can share their innovative research and solutions to each therapeutic issue.

Chair

Tae-Hyung Kim

University of New Mexico

Co-chairs

Jiyoung Lee

George Washington University

Hun-Goo Lee

Massachusetts General Hospital Harvard Medical School

Tech Group B-1
MPS

@ Dallas

Aug 3 _ Thursday _ 4:00 – 6:00pm

MPS Session I: Cancer and Metabolism
Chair: Jiyoung Lee (George Washington University)

Time	Title and Speaker
4:00	**Herbal Extracts from Lycii Radicis Cortex and Achyranthes Japonica Prevent Multiple Myeloma Progression** // Donghoon Yoon (University of Arkansas for Medical Sciences)
4:25	**High extracellular glucose promotes cell motility by modulating cell deformability and contractility via cAMP-RhoA-ROCK axis in human breast cancer cellsa** // Tae-Hyung Kim (University of New Mexico)
4:50	**Dysregulated 24-dehydrocholesterol reductase (DHCR24) in Head and Neck Squamous Cell Carcinoma** // Jiyoung Lee (George Washington University)
5:15	**Metabolic Vulnerabilities of Squamous Cell Carcinomas** Invited // Jungwhan Kim (University of Oklahoma Health Science Center)
5:45	**Poster Presentation Flash Talks (3 min each)** • **Expression and Characterization of MYO7A Isoforms Localized to the Stereocilia Upper Tip-link Density** // Jinho Park (University of Florida) • **Slow Myosin Binding Protein-C and Congenital Muscle Disease** // Taejeong Song (University of Cincinnati Medical School)

Tech Group B-1
MPS

@ Dallas

Aug 4 _ Friday _ 4:00 – 6:00pm

MPS Session II: Neurobiology, Immunology, and Beyond
Chair: Hungoo Lee (MGH/Harvard)

Time	Title and Speaker
4:00	**Poster Presentation Flash Talks (3 min each)** • **Augmented Reality Glasses for Enhancing Coaching Abilities of Exercise Instructors** // Jeeyoung Hong (Kongju National University) • **Associations between Binge Eating Severity and Factors from Social Comparison among Korean American women** // Bo Ra Kim (University of Texas at Austin) • **Sigma Anti-Bonding Calcium Carbonate (SAC) cream enhances the wound-healing process in C57/BL6 mouse** // Yeonju Kang (University of Arkansas) • **Sigma Anti-Bonding Calcium Carbonate (SAC) and Biofilm Promote Wound Healing in B6.Cg-Lepob/J (ob/ob) Mouse** // Hyejeong Jeong (University of Arkansas)
4:30	**Sex difference in the profile of extracellular bioactive lipids of conjunctival epithelial cells during allergic inflammation** // Changrim Lee (Harvard Medical School)
5:00	**Modulating the Host's Immune Response for Preventing Peri-implantitis in Mice** // Yejin Ki (University of Pittsburgh School of Dental Medicine)
5:30	**Ets-1 as a Negative Regulator of Peripherally Induced Regulatory T Cells and its implications in autoimmune diseases** // Choong-Gu Lee (Korea Institute of Science and Technology (KIST)
6:00	**Removing the root cause of Fragile X syndrome by Inducing the contraction of CGG repeats and FMR1 restoration** // Hungoo Lee (MGH/Harvard)

Tech Group B-1
MPS

@ Aviator A

Aug 4 _ Friday _ 6:00 – 9:00pm

MPS Poster Session
Chair: Tae-Hyung Kim (University of New Mexico)

Time	Title and Speaker
MPS P1	**Augmented Reality Glasses for Enhancing Coaching Abilities of Exercise Instructors** // Jeeyoung Hong (Kongju National University)
MPS P2	**Associations between Binge Eating Severity and Factors from Social Comparison among Korean American women** // Bo Ra Kim (The University of Texas at Austin School of Nursing)
MPS P3	**Slow Myosin Binding Protein-C and Congenital Muscle Disease** // Taejeong Song (University of Cincinnati Medical School)

Tech Group B-1
MPS

@ Aviator A

Aug 4 _ Friday _ 6:00 – 9:00pm

MPS Poster Session
Chair: Tae-Hyung Kim (University of New Mexico)

Time	Title and Speaker
MPS P4	**Expression and Characterization of MYO7A Isoforms Localized to the Stereocilia Upper Tip-link Density** // Jinho Park (University of Florida)
MPS P5	**Sex Differences in Amino Acid Kinetics in Older Adults with Chronic Morbidities** // Chloe Kang (Texas A&M University Center for Translational Research in Aging & Longevity)
MPS P6	**Sigma Anti-Bonding Calcium Carbonate (SAC) cream enhances the wound-healing process in C57/BL6 mouse** // Yeonju Kang (University of Arkansas for Medical Sciences)
MPS P7	**Development of Humanized Diffuse large B-cell Lymphoma Mouse Models** // Hyejeong Jeong (University of Arkansas for Medical Sciences)
MPS P8	**Multiple Sclerosis Research Across the African Continent: A Systematic Review** // Soonmyung Hwang (Icahn School of Medicine at Mount Sinai)

Tech Group B-1
MPS

@ Dallas

Aug 5 _ Saturday _ 8:00 – 10:00am

MPS Session III: Public Health and Technology
Chair: Soojin Yoo (University of Texas Rio Grande Valley), Co-Chair: Jiyoung Lee (George Washington University)

Time	Title and Speaker
8:00	**Multi-Omics Profiling for Evaluating Carcinogenic Exposure and Health Effects in Firefighters during Emergency Fires** Invited // Jooyeon Hwang (University of Texas Health Sciences Center at Houston)
8:25	**Bridging the Gap: A Community Approach to Addressing Health Disparities in North Nashville through Food Access Community Mapping** // Wansoo Im (Meharry Medical College)
8:50	**Differential Moderating Roles of the Salience Network and Central Executive Network in Internalizing Psychopathology and Fluctuating Negative Affect** // Ha Jeong Park (Texas A&M University Department of Psychological and Brain Sciences)
9:15	**Clinical and Environmental Effects of Healthy Home Interventions** // Insung Kang (Illinois Institute of Technology)
9:40	**Mutations in the UBIAD1 gene, the vitamin K2 synthesizing enzyme, cause Schnyder Corneal Dystrophy (SCD) by inhibiting ER-associated degradation of HMG CoA reductase** // Dong-Jae Jun (UT Southwestern Medical Center)

Agriculture, Ecology, Food, Nutrition (FAN)
Technical Group B-2

Agriculture, Ecology, Food, and Nutrition Symposium will provide professional opportunities for leading and rising scientists and engineers to learn latest scientific, technical advances in various fields of agriculture, ecology, food and nutrition in US and Korea. The symposium covers all areas related to the UKC 2023's topic, '*Discovery, Innovation and dissemination for transformative impact*'. Areas include:

1. Agricultures including agronomy, entomology, crop, soil science, & environmental science, horticulture, plant science, plant pathology, animal sciences, agricultural biotechnology & engineering, agricultural economics & agribusiness, and other agricultural areas
2. Ecology including physiological ecology & behavioral ecology, population ecology, community ecology, ecosystem, landscape, human ecology, and other ecological areas
3. Food science including functional food, food processing, food quality, safety and regulation, food nanotechnology, food microbiology, food chemistry, food engineering, sensory science, and other emerging food technologies
4. Nutrition including dietetics, nutrient metabolism and physiology, precision nutrition, nutritional management in human diseases including obesity, diabetes, cancer, and stroke, muscle and protein metabolism, gene and diet interactions, international nutrition, nutrition and intestinal microbiome.

Chair

Yoo Kim

Oklahoma State University

Co-chairs

Sungeun Cho

Auburn University

Kee Hong Kim

Purdue University

Tech Group B-2
FAN

@ Jonsson

Aug 3 _ Thursday _ 4:00 – 6:00pm

FAN Session I: Food Science and Technology
Chair: Sungeun Cho (Auburn University), Yoo Kim (Oklahoma State University)

Time	Title and Speaker
4:00	**Metabolomics in food and agricultural science** Invited // Joonhyuk Suh (University of Georgia)
4:20	**New antioxidants for frying oil developed in NCAUR, ARS, USDA** // Hong-sik Hwang (USDA, ARS, NCAUR)
4:40	**R&D Direction for Plant-based Meat and Cultivated Meat: Critical Variables for Consumer's Sensory Acceptance** // Jung Han (Eat Just)
5:00	**Comparative Study of the Susceptibility to Blue Light Inactivation of Foodborne Pathogens and Spoilage Bacteria** // Minji Hur (University of Georgia)

Tech Group B-2
FAN

@ Jonsson

Aug 3 _ Thursday _ 4:00 – 6:00pm

FAN Session I: Food Science and Technology
Chair: Sungeun Cho (Auburn University), Yoo Kim (Oklahoma State University)

Time	Title and Speaker
5:20	**Pathway-based metabolomics reveals the biosynthesis of key flavor compounds in apple** // Min Jeong Kang (University of Georgia)
5:40	**Influence of stunning methods on sensory characteristics of chicken breast meat using electronic senses** // Sungeun Cho (Auburn University)

Tech Group B-2
FAN

@ Jonsson

Aug 4 _ Friday _ 4:00 – 6:00pm

FAN Session II: Nutrigenomics
Chair: Kee Hong Kim (Purdue University), Yoo Kim (Oklahoma State University)

Time	Title and Speaker
4:00	**Advancing Sustainable Food Production Through Synthetic Biology** // Eun Joong Oh (Purdue University)
4:30	**Dietary Curcumin Attenuates Hepatic Cellular Senescence by Suppressing MAPK/NF-κB Signaling Pathway in Aged Mice** // Da-Yeon Lee (Oklahoma State University)
4:50	**Systems Genetic Analysis of Atherosclerosis and Gut Microbiota in a Diet-induced Hyperlipidemic Diversity Outbred F1 Mouse Population** // Myungsuk Kim (Korea Institute of Science and Technology)
5:15	**New insights into the role of piceatannol in cancer-associated cachexia** // Kee-Hong Kim (Purdue University)
5:40	**Protective Effects of Dietary Curcumin on Type 3 Diabetes** // Yoo Kim (Oklahoma State University)

Tech Group B-2
FAN

@ Aviator A

Aug 4 _ Friday _ 6:00 – 9:00pm

FAN Poster Session
Chair: Keehong Kim (Purdue University), Yoo Kim (Oklahoma State University)

Time	Title and Speaker
FAN P1	**Development of a method for risk assessment of organic pollutant exposure using monitoring data in the agricultural sector** // Sangik Suh (Geongsang National University)
FAN P2	**Autonomous Stand Counting in Field Pea using Aerial Imagery** // Jeong-Hwa Kim (North Dakota State University)
FAN P3	**Effects of Berry Volatile Extracts on LPS-induced Intestinal Inflammaation in a Caco-2/RAW264.7 Co-culture Model** // Sun-Ok Lee (University of Arkansas)
FAN P4	**System Dynamics Model for Autonomous and Controlled Environment Potato Production System** // Jae Hyeon Ryu (University of Idaho)

Biological and Biomedical Sciences (Biology, Molecular Biology, Cognitive Science, Botany, Zoology, Biomechanics, etc.) / Bioengineering and Biomedical Engineering (BME) Technical Group B-3 / C-1

As in any other major industry, problem solving in modern medicine increasingly requires a true convergence of many scientific and engineering fields. While some of the last frontiers of biomedicine, such as neuroscience and regenerative medicine, critically demands new ideas and tools from other disciplines, paradigm-shifting technological innovations in information science, nanotechnology, and robotics could open new opportunities in healthcare. At the same time, a new generation of engineers, "*fluent*" in many different languages of science, are creating entirely new fields to view the old questions with a fresh look. In the BME symposium, we strive to provide a stimulating forum for all researchers willing to go beyond the "*comfort zone*" to explore new opportunities in biomedical engineering.

Chair

Hyunjoon Kong

University of Illinois at Urbana-Champaign

Co-chairs

Deok Ho Kim

Johns Hopkins University

Young Bin Choy

Seoul National University

Tech Group B-3/C-1 BME

@ Maverick

Aug 3 _ Thursday _ 4:00 – 6:00pm

BME Session I: AI & Big Data Applications in Biomedicine
Chair: YoungBin Choy (Seoul National University), Co-Chair: Juhun Lee (University of Pittsburgh)

Time	Title and Speaker
4:00	**Progress and Trends in Artificial Intelligence for Colonoscopy** Invited // Dongheon Lee (Chungnam National University)
4:17	**Multimodal Interfaces for Immersive Virtual Reality** // Jinryong Kim (University of Texas at Dallas)
4:34	**Image-based Deep Survival Learning Model for Risk Stratification of Cardiovascular Disease using Retinal Fundus Image** // Jooyoung Chang (R&D, XAIMED)
4:51	**Machine Learning of Colors for mHealth Applications** // Young L. Kim (Purdue University)
5:08	**Assessing the generalization of graph neural networks** // Kijung Yoon (Hanyang University)

Tech Group
B-3/C-1 BME

@ Maverick

Aug 3 _ Thursday _ 4:00 – 6:00pm

BME Session I: AI & Big Data Applications in Biomedicine
Chair: YoungBin Choy (Seoul National University), Co-Chair: Juhun Lee (University of Pittsburgh)

Time	Title and Speaker
5:25	**Isotropic cellular resolution across centimeter field of view using subvoxel axially sweeping light sheet microscopy (SV-ASLSM)** // Juhyun lee (University of Texas at Arlington)
5:43	**Analysis of GAN Artifacts in Breast Screening Mammogram Simulation** // Juhun Lee (University of Pittsburgh)

Tech Group
B-3/C-1 BME

@ Maverick

Aug 4 _ Friday _ 4:00 – 6:00pm

BME Session II: Biomedical Devices and Materials for Biosensing, Diagnostics, and Therapeutics
Chair: Youngjae Chun (University of Pittsburgh), Co-Chair: Jaeseok Yu (DGIST)

Time	Title and Speaker
4:00	**Ultra-sensitive Silicon Photonic Opto-mechanical Ultrasound Sensor for Biomedical Photoacoustic Imaging: Proof-of-concept study** Invited // Jaeseok Yu (DGIST)
4:20	**Smart Contact Lenses for Glaucoma Care** // Chi Hwan Lee (Purdue University)
4:40	**Microbead-based Biomaterials for Cellular Immunotherapy** // Kyung-Ho Roh (University of Alabama, Huntsville)
5:00	**In vivo evaluation of fractal microelectrodes for Vagus nerve stimulation** // Hugh Lee (Purdue University)
5:20	**Advanced Cell and Gene Therapies For Effective CNS Repair Using Bionanomaterials** // Ki-Bum Lee (Rutgers University)
5:40	**Development of Novel Ultra-low Profile Coronary Stents to Treat Potential In-Stent Restenosis** // Youngjae Chun (University of Pittsburgh)

Tech Group
B-3/C-1 BME

@ Aviator A

Aug 4 _ Friday _ 6:00 – 9:00pm

BME Session III: Biomedical Engineering Poster Session
Chair: Chi Hwan Lee (Purdue University), Co-Chair: Kyung Ho Roh (University of Alabama, Huntsville)

Time	Title and Speaker
BME P1	**A Homozygous IER3IP1 Mutation Causes Secretory Protein Trafficking Defects in Neural Progenitor Cells** // Lucie Yeongran Ahn (Case Western Reserve University)

Tech Group
B-3/C-1 BME

@ Aviator A

Aug 4 _ Friday _ 6:00 – 9:00pm

BME Session III: Biomedical Engineering Poster Session
Chair: Chi Hwan Lee (Purdue University), Co-Chair: Kyung Ho Roh (University of Alabama, Huntsville)

Time	Title and Speaker
BME P2	**Osteoporosis Drug Testing on Demineralized Bone Paper** // Yongkuk Park (University of Massachusetts Amherst)
BME P3	**Spatial Phenotyping of the Glioblastoma Tumor Microenvironment** // Jungmin Nam (Yale University)
BME P4	**Production of animal stealth red cells by cell surface modulation** // Hyung Kyu Kim (Kyungpook National University)
BME P5	**A Pillar and Perfusion Plate Platform for Robust Human Organoid Culture and Analysis** // Soo-Yeon Kang (University of North Texas)
BME P6	**Studying depressive disorders with a 3D neurosphere model on a micropillar chip** // NaYoung Choi (Inje University)
BME P7	**Estimation of Musculotendon Stiffness and Slack Length Using an Optimization Algorithm** // Hwan Choi (University of Central Florida)
BME P8	**Frequency Analysis on Tissue Perfusion using a Laser Speckle Contrast Imaging in vivo** // Yungjun Yoo (Optosurgical, LLC)
BME P9	**Fundamental Issues in Cognitive Workload Classification** // Junho Park (Texas A&M University)
BME P10	**Integrated Edge-AI Based Closed-loop Stimulation System for Gait Rehabilitation after Spinal Cord Injury** // Ahnsei Shon (Texas A&M University)
BME P11	**Characterization of Decellularized Plant Leaf Biomaterials for Tissue Engineering** // Chanul Kim (University of Wisconsin–Madison)
BME P12	**Development of Nanoparticle Inducing Device Through ML** // Gawon Lim (University of Illinois, Urbana-Champaign)
BME P13	**Modulating the corticospinal excitability using various non-invasive brain stimulation techniques** // Hakjoo Kim (Texas A&M University)
BME P14	**Organic Synthesis Reactions on Digital Microfluidic Device** // Hyejin Moon (University of Texas at Arlington)
BME P15	**Trans-Golgi protein TVP23B regulates host-microbe interactions via Paneth cell homeostasis and Goblet cell glycosylation** // Ran Song (University of Texas Southwestern Medical Center)
BME P16	**Effects of collagen fiber alignments in regulating osteoblasts and mineralization** // Hyejin Yoon (University of Massachusetts, Amherst)

Tech Group
B-3/C-1 BME

@ Aviator A

Aug 4 _ Friday _ 6:00 – 9:00pm

BME Session III: Biomedical Engineering Poster Session

Chair: Chi Hwan Lee (Purdue University), Co-Chair: Kyung Ho Roh (University of Alabama, Huntsville)

Time	Title and Speaker
BME P17	**Blood compatibility assessment of biomaterial surface chemistries to mitigate intrinsic coagulation pathway activation** // Kyung-Hoon Kim (University of Washington)
BME P18	[SEED2023] **Ectopic high endothelial venule-targeted nanodelivery for type 1 diabetes** // Sungwook Jung (Harvard Medical School)
BME P19	[SEED2023] **A Microengineered Organoid-on-a-Chip Model of Alveolar Development in the Human Lung Sunghee** // Estelle Park (University of Pennsylvania)
BME P20	**Injectable Lignin Composites to Improve Neovascularization and Healing of Diabetic Wounds** // Jangwook P. Jung (Louisiana State University)
BME P21	**Sex difference in the profile of extracellular bioactive lipids of conjunctival epithelial cells during allergic inflammation** // Changrim Lee (Harvard Medical School)
BME P22	**Creating a Therapeutic Application Plan through Research on Rare Genetic Disorders** // Bokyeong Song (Sookmyung Women's University)
BME P23	**The Intervention of the Beta Amyloid Protein Dysfunction by Carbon Nanodots in Alzheimer's Disease** // John Bang (North Carolina Central University)
BME P24	**Particulate Matter (PM) induced Beta Amyloid (BA) Protein Aggregation** // Kevin Omar (North Carolina Central University)
BME P25	**Polystyrene Microplastics and their GI Transmembrane Passage Capacity in Zebrafish Embryos** // Majemite Iyangbe (North Carolina Central University)
BME P26	**Analysis of Clock-Controlled Genes (CCGs) in Human Intestinal Enteroids** // Suengwon Lee (University of Cincinnati)
BME P27	**Toward Hyperplexed Immunohistochemistry using Hydrogel Staining, Chiral Nanoparticles, and Nanobodies** // Kyung-Hak Choi (Noul Co., Ltd)
BME P28	**An AI-embedded and Fully Automated Device for Malaria Detection at Remote Setting** // Kyung-Hak Choi (Noul Co., Ltd.)
BME P29	**Structural and biochemical characterization of the thiol methyltransferase 1A and 1B** // Taeyoon Jung (University of Washington)
BME P30	**Numerical and Computational Analysis of Vascular Phantom Model for Sensor Design Validation** // Youngjae Chun (University of Pittsburgh)

Tech Group
B-3/C-1 BME

@ Aviator A

Aug 4 _ Friday _ 6:00 – 9:00pm

BME Session III: Biomedical Engineering Poster Session
Chair: Chi Hwan Lee (Purdue University), Co-Chair: Kyung Ho Roh (University of Alabama, Huntsville)

Time	Title and Speaker
BME P31	**Scalable manufacturing of skin-conformal, stretchable electrodes via screen-printing** // Jong-Hoon Kim (Washington State University)
BME P32	**Multi-responsive injectable ECM-based embolic delivering therapeutic agents for treating cerebral saccular aneurysms** // Seungil Kim (University of Pittsburgh)
BME P33	**Co-transcriptional folding of nascent RNA in the presence of RNA-binding** // Sunghyun Cho (Johns Hopkins University)
BME P34	**Towards Robotic Knee Prosthesis Personalization: Impedance Control With PCA-Based Tuning Methodology** // Woolim Hong (North Carolina State University)
BME P35	**Skin-interfaced wireless device for fetal and maternal monitoring to minimize unnecessary C-section** // Hyoyoung Jeong (University of California Davis)
BME P36	**Genome-wide epigenetic editing of human microsatellite repeats using engineered zinc finger transcription factors** // Y. Esther Tak (Harvard Medical School)
BME P37	**Intelligent Upper-limb Exoskeleton using Deep Learning to predict Human Intention for Sensory-Feedback Augmentation** // Kangkyu Kwon (Georgia Institute of Technology)
BME P38	**[SEED2023] Engineered Helicase Replaces Thermocycler in DNA Amplification While Retaining Desired PCR Characteristics** // Jimin Kang (Johns Hopkins University)
BME P39	**Noninvasive estimation of intracranial pressure via diffuse correlation spectroscopy** // John Sunwoo (Massachusetts General Hospital, Harvard Medical School)

Chemical, Textile, Energy, and Nuclear Engineering (CHE)
Technical Group C-2

This symposium provides a forum for leading experts and young researchers to present and discuss cutting-edge research advances in the broad areas of chemical engineering and related fields. Topics of interest include various aspects of such areas including (but not limited to) advanced nanomaterials/biomaterials, nanoscience/nanotechnology, and complex processes for energy, health, and environmental problems. Both experimental and computational approaches as well as synergistic methods to address grand challenges in aforementioned topics are welcome.

Chair

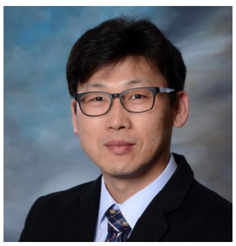

Hyun-Tae Hwang

University of Kentucky

Co-chair

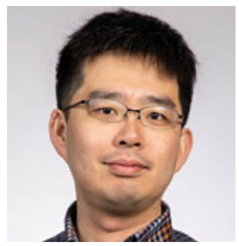

Jaewon Lee

University of Missouri

Tech Group C-2
CHE

@ McKee

Aug 3 _ Thursday _ 4:00 – 6:00pm

CHE Session I: Chemical, Textile, Energy, and Nuclear Engineering
Chair: Hyun-Tae Hwang (University of Kentucky), Jaewon Lee (University of Missouri-Columbia)

Time	Title and Speaker
4:00	**Next-Generation Hybrid Models: Combining Attention Mechanisms and LSTM for Improved Predictions and Process Control in the Chemical Industry** Invited // Joseph Kwon (Texas A&M University)
4:30	**CO_2 EOR and Carbon Capture Utilization and Storage (CCUS): Field-Scale Application of Mobility-Control CO_2 Foams** // Seung Ihl Kam (Louisiana State University)
5:00	**Valorization of Nutrients in Surface Waters Through the Sustainable Biomass Production of the Attached Algae Flow-way for Biofuels** // Sungwhan Kim (Sandia National Laboratories)
5:30	**Solid-State Hydrolysis of Sodium Borohydride for Hydrogen Generation** // Hyun-Tae Hwang (University of Kentucky)

Tech Group C-2
CHE

@ McKee

Aug 4 _ Friday _ 4:00 – 6:00pm

CHE Session II: Chemical, Textile, Energy, and Nuclear Engineering
Chair: Hyun-Tae Hwang (University of Kentucky), Jaewon Lee (University of Missouri-Columbia)

Time	Title and Speaker
4:00	**Facile Soft-lithographic Micromolding Approaches for Controlled Fabrication of Micropatterned Opal Hydrogel Materials** Invited // Hyunmin Yi (Tufts University)
4:30	**Real-time investigation of Nanoparticle Self-assembly mechanisms and its controlling factors** // Jaewon Lee (University of Missouri-Columbia)
5:00	**Disordered Cathode Materials for High-Energy Lithium-Ion Batteries** // Juhyeon Ahn (Lawrence Berkeley National Laboratory)

Tech Group C-2
CHE

@ Aviator A

Aug 4 _ Friday _ 6:00 – 9:00pm

CHEPoster Session
Chair: Hyun-Tae Hwang (University of Kentucky), Jaewon Lee (University of Missouri-Columbia)

Time	Title and Speaker
CHE P1	**Spreading and wetting of transiently-crosslinked polymer spheres** // Kyujin Ko (University of Cincinnati)

Mechanical, Aerospace, and Naval Engineering (MAN)
Technical Group C-3

The Mechanical, Aerospace, and Naval Engineering (MAN) Symposium covers a wide variety of related areas including energy, manufacturing, mechanics, control, robotics, materials and so on. Experimental, theoretical, and computational studies are all welcome to the MAN symposium. The MAN symposium facilitates communication and collaboration on cutting-edge research in mechanical, aerospace, and naval engineering.

Chair

Eon Soo Lee

New Jersey Institute of Technology

Co-chairs

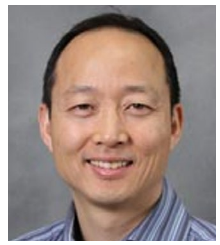

Martin Byung-Guk Jun

Purdue University

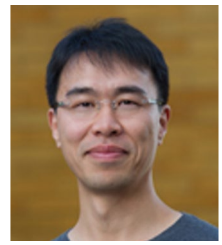

W. Jong Yoon

University of Washington Bothell

Tech Group C-3
MAN

@ Houston

Aug 3 _ Thursday _ 4:00 – 6:00pm

MAN Session I: MAKER-Manufacturing Alliance of Korean Engineers and Researchers
Chair: Martin Jun (Purdue University), Eon Soo Lee (New Jersey Institute of Technology)

Time	Title and Speaker
4:00	**Practical and Economical Additive Manufacturing for High Temperature Applications** Invited // Haseung Chung (Michigan State University)
4:20	**Via Metrology and Inspection for Advanced Electronics Packaging** // Chabum Lee (Texas A&M University)
4:35	**Advanced Manufacturing Techniques for Flexible and Wearable Devices** // Chi Hwan Lee (Purdue University)
4:50	**A Novel Approach of Mold-free Manufacturing for Highly Sensitive Pressure and Tactile Sensors** // Sunghwan Lee (Purdue University)
5:05	**Additive Manufacturing of Rubber** // Jae-Won Choi (University of Akron)
5:20	**Cutting Mechanisms of Cross-ply Carbon Fabrics using a Drag Cutter** // Dae-Wook (Dave) Kim (Washington State University)
5:35	**3D Printed Microchannel-based Blood Plasma Self-separation for Biomedical Applications** // Eon Soo Lee (New Jersey Institute of Technology)
5:50	**Sound Recognition Using MT Connect Framework for Real-time Cutting Condition Monitoring of CNC Milling Machine** // Martin Byung-Guk Jun (Purdue University)

Tech Group C-3
MAN

@ Houston

Aug 4 _ Friday _ 4:00 – 6:00pm

MAN Session II: Future Technologies in Materials and Engineering
Chair: Woon Jong Yoon (University of Washington Bothell), Eon Soo Lee (New Jersey Institute of Technology)

Time	Title and Speaker
4:00	**A Study on the Development of Terrain Following Simulator using Digital Terrain Elevation Data (DTED)** Invited // Sangchul Lee (Korea Aerospace University)
4:20	**Decarbonization Effort in Non-Road Heavy-Duty Equipment** // Youngjin Son (Caterpillar Inc.)
4:35	**High Performance Green Composites Made with Cellulose Long Filament and Vanillin Epoxy** // Jaehwan Kim (Inha University)
4:50	**Morphology Control of Inkjet-Printed Micro-Patterns for Printed Electronics** // Jun Young Hwang (Korea Institute of Industrial Technology)
5:05	**Multifunctional Mechano-Luminescence-Optoelectronic Composites for Non-Invasive and Self-Learning Health Monitoring Wearables** // Donghyeon Ryu (New Mexico Tech)
5:20	**Cells Function as Ternary Logic Gates to Decide Their Migration Direction Under Combined Chemical and Fluidic Cues** // Bumsoo Han (Purdue University)
5:35	**Development of Gamifying Robots for Improving Stroke Recovery and Cross-disciplinary Undergraduate Research Experience** // Woon Jong Yoon (University of Washington Bothell)

Tech Group C-3
MAN

@ Aviator A

Aug 4 _ Friday _ 6:00 – 9:00pm

MAN Poster Session
Chair: Martin Jun (Purdue University), Woon Jong Yoon (University of Washington Bothell)

Time	Title and Speaker
MAN P1	**CNN-based Vibration Signal Classification through Image Conversion of Feature Matrix** // Tae Hong Min (Gyeongsang National University)
MAN P2	**Optimal Design Process of Variable Geometry Turbocharger Turbine Impeller** // Jeong-Eui Yun (Kangwon National University)
MAN P3	**Thermal Control in Metal Additive Manufacturing** // Jihoon Jeong (Northwestern University)
MAN P4	**Development of Rule-based Automatic Diagnosis Technology for Motor Pump System Diagnosis** // DeokYeong Cheong (Gyeongsang National University)

Tech Group C-3
MAN

@ Aviator A

Aug 4 _ Friday _ 6:00 – 9:00pm

MAN Poster Session

Chair: Martin Jun (Purdue University), Woon Jong Yoon (University of Washington Bothell)

Time	Title and Speaker
MAN P5	**Electrified Personal Tracked Vehicle for Automation** // Santiago Ricoy (University of Nevada, Las Vegas)
MAN P6	**Optimization of Direct Energy Deposition Additive Manufacturing Process for Al-Mg-Si Alloy and H13 Steel** // Jeki Jung (Stevens Institute of Technology)
MAN P7	**Towards Embodiment of Miniature Humanoid through Virtual Reality** // Akshay Dave (University of Nevada, Las Vegas)
MAN P8	**Trajectory Planning for a Cable Driven Parallel Robot** // Zahir Castrejon (University of Nevada, Las Vegas)
MAN P9	**Crack Morphologies during Ultra-Precision Machining of Single Crystal 8 %mol Yttria-stabilized Zirconia** // Dae Nyoung Kim (University of Wisconsin - Madison)
MAN P10	**Method for Real-Time Joint Trajectory in Telepresence Avatar Robotics** // Baekseok Kim (University of Nevada, Las Vegas)
MAN P11	**Contact Guidance of Hs27 Fibroblasts** // Chunghwan Kim (Arizona State University)
MAN P12	**Animated Graphene-filled Glass Fiber Composites for Enhanced Mechanical Properties** // Ning Bian (University of Texas at Dallas)
MAN P13	**Path planning problem for Self-Rechargeable Unmanned Aerial-Ground Vehicle Group** // Jackie Lee (Texas A&M University)
MAN P14	**Waveguided-based Darkfield Microscopy for Wafer Edge Inspection** // Heebum Chun (Texas A&M University)
MAN P15	**Parametric Machine Learning Model for Laser Powder Bed Fusion** //Jong Kim (University of Central Florida)
MAN P16	**Static Analysis of a Carbon Fiber Rotor in an Axial Flux motor** // Joon Jo (Texas A&M University)
MAN P17	**CNN-based Condition Classification of Vibration Signal Considering Fault Location** // Jeongjun Lee (Gyeongsang National University)
MAN P18	**A Novel Approach to Mosquito Trap: Utilizing 3D Flight Tracking Technology** // Soohwan Kim (Georgia Institute of Technology)

Materials Science and Engineering, Nanotechnology (MSE)
Technical Group C-4

Materials innovation is at the heart of addressing critical societal challenges related with energy, environment, and sustainability. Materials Science and Engineering (MSE) symposium will bring together scientists and engineers working at the forefront of materials science and technologies, providing opportunities for gaining new perspectives and networking for future collaborations. The topics to be covered by the symposium include but are not limited to: Electronic materials; functional materials; and nanomaterials towards advanced applications such as micro/nanoelectronics, energy conversion/storage, and additive manufacturing to name a few. Also to be discussed are novel materials design, synthesis, processing, and characterization.

Chair

Jiyoung Kim

University of Texas
at Dallas

Co-chairs

Chang-Yong Nam

Brookhaven
National Laboratory

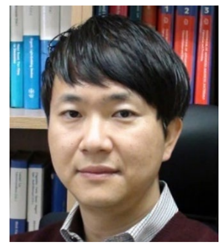

Jang-Sik Lee

Pohang University
of Science and
Technology(POSTECH)

Tech Group C-4
MSE

@ Fort Worth

Aug 3 _ Thursday _ 4:00 – 6:00pm

MSE Session I: Material Synthesis—Electrochemistry and Microelectronics Applications
Chair: Jiyoung Kim (University of Texas at Dallas), Chang-Yong Nam (Brookhaven National Laboratory)

Time	Title and Speaker
4:00	**Electrochemistry of Metals with High Oxidation Potential** Invited // Choong-Un Kim (University of Texas at Arlington)
4:20	**Fabrication of Fe-Ni Invar Alloy using Electrodeposition Technology for FMM Application** Invited // Jae-Ho Lee (Hongik University)
4:40	**3-Dimensional Integration with High Interconnection Density** Invited // Rino Choi (Inha University)
5:00	**Electrochemical Stability of Real-Scale Metallic Nanoparticles explored by Machine Learning** Invited // Hyuck Mo Lee (Korea Advanced Institute of Science and Technology)
5:20	**Electrochemical synthesis of single crystalline nanomaterials and applications to interconnect of electronic packaging** Invited // Jae Yong Song (Pohang University of Science and Technology)
5:40	**Phase-field Simulation of Microstructure Formation in Thin Films** Invited // Yongwoo Kwon (Hongik University)

Tech Group C-4
MSE

@ Fort Worth

Aug 4 _ Friday _ 4:00 – 6:00pm

MSE Session II: Next-Generation Electronic Devices and Materials
Chair: Jang-Sik Lee (Pohang University of Science and Technology), Chang-Yong Nam (Brookhaven National Laboratory)

Time	Title and Speaker
4:00	**Technology Trends of 3D NAND Flash Memory and Pathfinding Opportunities** Invited // Tae Kyung Kim (Samsung Electronics)
4:20	**Highly-Scaled 3D Ferroelectric Transistor Array for Compute-in-Memory** Invited // Jang-Sik Lee (Pohang University of Science and Technology)
4:40	**Half-Cycle Interrogation of HfO2 Atomic Layer Deposition Mechanism Using in-situ Reflectance Absorbance Infra-Red Spectroscopy** Invited // Jiyoung Kim (University of Texas at Dallas)
5:00	**Dopant Control of Ultra-short Channel Gate-All-Around FET for Reliable Threshold Voltage** Invited // Rock Hyun Baek (Pohang University of Science and Technology)
5:20	**New Device Applications of III-Nitride Wide-Bandgap Semiconductors: Beyond Power Electronics and Visible/UV Photonics** Invited // Jae-Hyun Ryou (University of Houston)
5:40	**High Resolution Photolithography for OLED Frontplane** Invited // Jeong-Hwan Lee (Inha University)
6:00	**Vapor-Phase Infiltration for Microelectronics Applications** Invited // Chang-Yong Nam (Brookhaven National Laboratory)

Tech Group C-4
MSE

@ Aviator A

Aug 4 _ Friday _ 6:00 – 9:00pm

MSE Poster Session
Chair: Jiyoung Kim (University of Texas at Dallas), Chang-Yong Nam (Brookhaven National Laboratory), Jang-Sik Lee (Pohang University of Science and Technology)

Time	Title and Speaker
MSE P1	**Charge Transfer Across the Interfaces in Organic Field-Effect Transistors** // Hyun Ho Choi (Gyeongsang National University)
MSE P2	**Free-Standing $Li_4Ti_5O_{12}$/Carbon Nanotube Electrodes for Flexible Lithium-Ion Batteries** // Jun seok Lee (Gyeongsang National University)
MSE P3	**The Effects of in-situ Atomic Layer Annealing on Thermal Atomic Layer Deposited Silicon Nitride** // Siun Song (The University of Texas at Dallas)
MSE P4	**Analysis of Separation Behavior of Polyamide Structure-Based RO membrane Using Multi-scale Simulation** // Kwangseop Im (Gyeongsang National University)

Aug 4 _ Friday _ 6:00 – 9:00pm

MSE Poster Session

Chair: Jiyoung Kim (University of Texas at Dallas), Chang-Yong Nam (Brookhaven National Laboratory), Jang-Sik Lee (Pohang University of Science and Technology)

Time	Title and Speaker
MSE P5	**Optimal Print Parameter Prediction By Neural Networks For Laser Powder Bed Fusion Additive Manufacturing** // Kevin Graydon (University of Central Florida)
MSE P6	**Enhanced ferroelectric polarization of $Hf_{0.5}Zr_{0.5}O_2$ thin films through fast ramp-up annealing process** // Seongbin Park (Kangwon National University)
MSE P7	**Forming Voltage-Free Memristive Hafnium Oxide Devices for Non-Polar Switching Applications** // Yeeun Hong (University of Texas at Dallas)
MSE P8	**Characterizing the High Temperature Mechanical Performance and Microstructure of Additively Manufactured Tantalum** // Sharon Park (Johns Hopkins University)
MSE P9	**Determining Printability of Soft Magnetic Alloys Via Single Track Study** // Nicolas Ayers (University of Central Florida)
MSE P10	**Development and evaluation of diaphragm membrane for alkaline water electrolysis** // Sang Yong Nam (Gyeongsang National University)
MSE P11	**Manufacturing of Inconel 718 with Enhanced Boron Composition via Selective Laser Melting** // Jeongwoo Lee (University of Texas Rio Grande Valley)
MSE P12	**Evaluation of Interfacial Property and Damage Sensing of Structural Composites Using Electrical Resistance Method** // Dong-Jun Kwon (Gyeongsang National University)
MSE P13	**Fabrication and Electrical Properties of Organic Ferroelectric Gate Transistors** // Byung Eun Park (University of Seoul)
MSE P14	**Electrochemical Removal of Nitrate for Ammonia Synthesis and Water** // Jeonghoon Lim (Lawrence Berkeley National Laboratory)
MSE P15	**The Effect of H-bonding Strength on the Water-responsiveness of Bacillus subtilis Cell Walls using Hofmeister Salts** // Seungri Kim (City College of New York)
MSE P16	[SEED2023] **Solvent-Free Synthesis and Modification of Membranes for Industrially Relevant Gas Separations** // Dennis Lee (Johns Hopkins University)
MSE P17	**Compositional Redistribution, Phase Transformation, Microstructural Development in SS316L/IN625 Bimetallic Structure Fabricated by Laser Powder Bed Fusion** // Asif Mahmud (University of Central Florida)

Tech Group C-4
MSE

@ Aviator A

Aug 4 _ Friday _ 6:00 – 9:00pm

MSE Poster Session

Chair: Jiyoung Kim (University of Texas at Dallas), Chang-Yong Nam (Brookhaven National Laboratory), Jang-Sik Lee (Pohang University of Science and Technology)

Time	Title and Speaker
MSE P18	**Enhancing the performance of tungsten-based alloys through additive manufacturing** // Hyeji Im (Northwestern university)
MSE P19	**Cross-Point Array of Metal-Ferroelectric-Metal $HfZrO_2$ Capacitors for Compute-in-Memory Applications** // Minjong Lee (University of Texas at Dallas)
MSE P20	**High endurance of back-end-of-line compatible ferroelectric $Hf_{0.5}Zr_{0.5}O_2$ thin films through low temperature annealing** // Jong Mook Kang (Kangwon National University)
MSE P21	**Computational Design and Analysis of Metal Halide Perovskites: Toward Eco-friendly and Highly Stable Solar Cells** // Ki-Ha Hong (Hanbat National University)
MSE P22	**Effect of Carbon on The Microstructure and Mechanical Properties of Carbon-bearing Steels in Laser Powder Bed Fusion** // Thinh Huynh (University of Central Florida)
MSE P23	**Electronic Transport in Pd-PdHx $_{(0 \le x < 0.7)}$ Film in Ambient Temperature** // Jong-Hee Park (DePaul University)

Civil and Environmental Engineering, Architecture (CEA)
Technical Group C-5

The Civil, Environmental, and Architecture (CEA) Engineering Symposium covers diverse engineering and scientific themes every year. At the 36th annual UKC conference, the CEA symposium presents recent advancements in assessing and promoting the resilience of buildings, transportation infrastructure, and the environment. All participants will share and learn new paradigms and perspectives brought by the unprecedented events and many short-lived trends via three technical sessions: toward the sustainable environment; more resiliency for the built infrastructure; and into the future materials and field practices.

Chair

Youngguk Seo

Kennesaw State University

Co-chair

Jung Heum Yeon

Texas State University

Tech Group C-5
CEA

@ Lone Star1

Aug 3 _ Thursday _ 4:00 – 6:00pm

Transport Institute (KOTI) Session: Korea Highway Management Technology and Policy
Chair: Brian Park (University of Virginia)

Time	Title and Speaker
4:00	**Vice President's Welcome Remarks** // Jeehyung Park (KOTI)
4:05	**Scenario Development Methodology for Automated Vehicle Evaluation** Invited // Ilsoo Yun (Ajou University)
4:25	**Digital Transformation of Road Management in Korea** // Chandle Chae (Road Transport Policy of Korea Transport Institute)
4:50	**Introduction of Panelists** // Jeehyung Park (KOTI), Mihyeon Jeon (Atkins), Hanseon Cho (KOTI)
5:10	**Panel Discussion and Q&A**
5:50	**Wrap-up and Group Photo**

Tech Group C-5
CEA

@ Lone Star2

Aug 3 _ Thursday _ 4:00 – 6:00pm

CEA Session I: Innovative Ideas in Construction
Chair: John McFadden (FHWA), Co-Chair: Namho Cho (University of Iowa)

Time	Title and Speaker
4:00	**Facility Management Practice for Public University: A case study on the University of Iowa** // Namho Cho (University of Iowa)
4:20	**Towards Portable and Accurate Ergonomic Assessment in Construction** // Ju Hyeong Ryu (West Virginia University)
4:40	**Automated Estimation Model for Liquidated Damages in General Provisions of Equipment Purchasing Orders** // Sea-eun Park (POSTECH)
5:00	**[SEED2023] Virtual Reality Educational Simulation for Construction Management** // Suryeon Kim (Texas A&M University)
5:20	**AI-driven contract risk extraction model** // Jeehee Lee (University of Nevada, Las Vegas)
5:40	**Using Data to Integrate Equity in Infrastructure Project Selection Process** // John McFadden (FHWA)

Tech Group C-5
CEA

@ Lone Star1

Aug 4 _ Friday _ 4:00 – 6:00pm

CEA Session II: Natural Disasters: Predictions and Post-damage Assessments
Chair: Min Jae Suh (Sam Houston State University)

Time	Title and Speaker
4:00	**Green Infrastructure Design and Runoff Reduction Evaluation for Metro City Level: The Case Study of Suwon City** // Junsuk Kang (Seoul National University)
4:20	**Assessing Vulnerability of South Korea to Typhoon Damage Considering Sea Level Rise: A Case Study of Typhoon Maesak Simulation** // Jin young Kim (University of Texas at Arlington)
4:40	**Multivariate Frequency Analysis Framework for Hurricane Events and Its Application on Hurricane Ian** // Eunsaem Cho (Florida State University)
5:00	**Event coincidence of dryness, conflict, and forced migration in Somalia** // Woi Sok Oh (Princeton University)

Tech Group C-5
CEA

@ Lone Star2

Aug 4 _ Friday _ 4:00 – 6:00pm

CEA Session III: Towards Sustainable and Smart Buildings
Chair: Eul-Bum Lee (GIFT)

Time	Title and Speaker
4:00	**Investigating the Relationship between Human Physiological Responses and Indoor Environmental Quality in Commercial Buildings** // Joon-Ho Choi (University of Southern California)
4:20	**Evaluation of V-COP model for real-time monitoring of EHP performance** // Jihyun Seo (Korea Institute of Energy Research)
4:40	**Fast Load Prediction Model of Chiller using Bayesian Optimization** // Juwan Ha (NC State University)
5:00	**An Empirical Analysis of Korean Household Appliance Use Patterns: using a national Time Use Survey dataset** // Seungmin Lee (NC State University)
5:20	**In-situ evaluation of non-destructive insulation performance measurement method of building envelope** // Daehwan Shin (Korea Institute of Energy Research, KIER)

Tech Group C-5
CEA

@ Wildcatters

Aug 4 _ Friday _ 4:00 – 6:00pm

CEA Session IV: Future Mobility
Chair: Mihyeon Jeon (Atkins), Co-Chair: Brian Park (University of Virginia)

Time	Title and Speaker
4:00	**Physics-Informed Neural Network-based Computational Solid Mechanics Model for Problems with Material Heterogeneity** // Hyeeun Kong (Penn State University)
4:30	**Field Evaluation Plan of Connected Vehicle Identification System** // Byungkyu Brian Park (University of Virginia)
5:00	**Common Data Requirements for Digital Twin Data Interoperability in Capital Projects** // John Oh (Texas A&M University)

Tech Group C-5
CEA

@ Aviator A

Aug 4 _ Friday _ 6:00 – 9:00pm

CEA Poster Session
Chair: Jun Kim (Florida Polytechnic University)

Time	Title and Speaker
CEA P1	**Heat Stress Conditions and Awareness of Roofers in South Texas** // Min Jae Suh (Sam Houston State University)
CEA P2	**Fenton-like catalytic ceramic membrane hybrid system for the advanced water treatment** // Youngkun Chung (Rice University)
CEA P3	**Development of Smart Harmful Algal Bloom (HAB) Detection System Using Unmanned Aerial Vehicle (UAV) and Hyperspectral Sensor** // Da Yun Kwon (Korea University)
CEA P4	**Multiple heavy metal detection in greywater using a novel MoS2-chitosan-based electrochemical sensor** // Woo Hyoung Lee (University of Central Florida)
CEA P5	**Purification of Phosphoric Acid Manufacturing Process Water with Recovery of Critical Materials using MCDI** // Jun Kim (Florida Polytechnic University)
CEA P6	**An Electrical Heating Technique for Environmentally Friendly Winter Maintenance of Transportation Infrastructure** // Jung Heum Yeon (Texas State University)
CEA P7	**Pathway to a Just Transition: Bridging Regional Inequality of Clean Energy Through Hydrogen** // Gina Park (Cornell University)
CEA P8	[SEED2023] **Development of On-site Quality Management System for Asphalt Pavement Using IoT**// Dong Hyuk Kim (University of Georgia)
CEA P9	[SEED2023] **Multifunctional Flexible Sensor for Temperature and Strain Detection** // Bo Mi Lee (University of Central Florida)
CEA P10	**Assessment of Thermal Comfort in Response to Urban Spatial Changes** // Seoyoung Lee (Seoul National University)

Electrical and Computer Engineering (ECE)
Technical Group C-6

The Electrical and Computer Engineering Symposium is designed to provide emerging technologies and diverse developments in a wide range of disciplines of Electrical and Computer Engineering. With the global success of smart devices and the increasing importance of intelligent systems, this symposium provides a platform to introduce the latest innovations as well as showcase applications enabled by these technologies. This symposium brings together scientists and engineers from the US and Korea, promoting the opportunity for technical information exchange and research collaboration between these two vibrant communities.

- ECE symposium will cover
  i) electronic and photonic devices
  ii) integrated circuits, intelligent systems, control, and networks
  iii) emerging applications in healthcare, artificial intelligence, and robotics
  iv) energy, power, and other areas of smart devices and systems

Chair

Jin W Choi

Michigan Technological University

Co-chairs

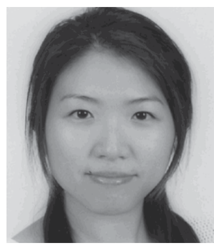

Wookyung Sun

Seoul National University

Jeongwon Park

University of Nevada at Reno

Jungkwun Kim

University of North Texas

Tech Group C-6
ECE

@ San Antonio

Aug 3 _ Thursday _ 4:00 – 6:00pm

ECE Session I: Advancements in Emerging Technologies

Chairs: Jin W Choi(Michigan Technological University), Wookyung Sun(Seoul National University), Jeongwon Park(University of Nevada at Reno), Jungkwun Kim (University of North Texas)

Time	Title and Speaker
4:00	**Fabrication of OLED Lighting Auxiliary Electrode by Self-aligned Inkjet Printing Process** // Sang-Ho Lee (Korea Institute of Industrial Technology)
4:20	**Fully Portable Wireless Soft Stethoscope and Machine Learning for Continuous Real-Time Auscultation and Automated Disease Detection** Invited // W. Hong Yeo (Georgia Tech)
4:40	**Printed Hybrid Electronics** // Donghun Park (3DFlexible Inc.)
5:00	**Self-Rotating Discharge using a Pattered Dielectric Area in Ambient Air and Potential Application in Materials Surface Modification** Invited // Choonsang Park (Milligan University)

Tech Group C-6
ECE

@ San Antonio

Aug 3 _ Thursday _ 4:00 – 6:00pm

ECE Session I: Advancements in Emerging Technologies
Chairs: Jin W Choi(Michigan Technological University), Wookyung Sun(Seoul National University), Jeongwon Park(University of Nevada at Reno), Jungkwun Kim (University of North Texas)

Time	Title and Speaker
5:20	**Lab on a Smartphone (LOS): a smartphone-integrated optoelectrowetting platform as a portable environmental sensor for on-site water quality monitoring** // Sean Park (San Diego State University)
5:40	**Microfabrication of Hollowed Microneedle Array by Diffraction Lithography** // Jungkwun Kim (University of North Texas)

Tech Group C-6
ECE

@ San Antonio

Aug 4 _ Friday _ 4:00 – 6:00pm

ECE Session II: Innovations in Semiconductor and Wireless Technologies
Chairs: Jin W Choi(Michigan Technological University), Wookyung Sun(Seoul National University), Jeongwon Park(University of Nevada at Reno), Jungkwun Kim (University of North Texas)

Time	Title and Speaker
4:00	**Automatic Array Calibration System for Wireless Microwave Power Transmitter** Invited // Sang-Hwa Yi (Korea Electrotechnology Research Institute)
4:20	**5.8 GHz High-power Rectifier using GaN-HEMT diode for wireless Power Transmission Application** Invited // Wonseob Lim (Korea Electrotechnology Research Institute)
4:40	**Energy harvesting power management circuits for dual-battery configuration** Invited // Kyoungho Lee (Korea Electrotechnology Research Institute)
5:00	**An overview of DRAM cell architecture post-Moore law era** // Wookyung Sun (Seoul National University)
5:20	**Plasmon FET for Tailored Photodetection and Bio Sensing** // Sung Jin Kim (University of Louisville)
5:40	**Innovations in Nanoelectronics: Exploring the Possibilities of 2D Materials** // Jeongwon Park (University of Nevada Reno)

Tech Group C-6
ECE

@ Aviator A

Aug 4 _ Friday _ 6:00 – 9:00pm

ECE Poster Session

Chairs: Jin W Choi(Michigan Technological University), Wookyung Sun(Seoul National University), Jeongwon Park(University of Nevada at Reno), Jungkwun Kim (University of North Texas)

Time	Title and Speaker
ECE P1	**Region-based conversion of neural activity across sessions** // Woohyun Eum (University of Florida)
ECE P2	**Effective fetal ECG extraction for non-invasive ambulatory monitoring** // Yongkuk Lee (Wichita State University)
ECE P3	**LED Evaluations for Photovoltaic Impedance Spectroscopy** // Sung Yeul Park (University of Connecticut)
ECE P4	**Evaluation of transient and small-signal stability of Korean power system along the penetration of renewable energy** // Jongoh Baek (Texas A&M University)
ECE P5	**Artificial Neural Network(ANN) Based Maximum Power Point Tracking(MPPT) Algorithm for a Photovoltaic Application** // Woonki Na (California State University, Fresno)
ECE P6	**Fast Recognition of Crop Parts Using 3D Point Clouds and Semantic Segmentation Neural Network** // Young Jae Ryoo (Mokpo National University)

Computer and Information Sciences (CIT)
Technical Group C-7

The Computer Sciences and Information Technologies (CIT) symposium encompasses diverse areas of research and development in CS/IT fields as well as the arts and social sciences. The symposium also provides variety of opportunities to emerge entertainment and other technology related areas such as connected vehicles, smart city and bio-medical. The symposium also provided a unique venue for CS/IT researchers and engineers from both academia and industry in the US and Korea. The topics include artificial intelligent, machine learning, data science, connected vehicles, augmented reality/virtual reality, art technology, software engineering, human computer interaction, big data and data analytics, Internet of Things (IoT), cybersecurity, robotics and computer educations. The CIT Symposium consists of regular sessions and poster session.

Chair

Ohbong J. Kwon

New York City College of Technology

Co-chairs

Hoyoung Hwang

Hansung University

Donghoon Kim

Arkansas State University

Tech Group C-7 CIT

@ Grapevine

Aug 3 _ Thursday _ 4:00 – 6:00pm

CIT Session I: Artificial Intelligence (AI) and Machine Learning (ML)
Chair: Ohbong Kwon(New York City College of Technology), Co-Chair: Hoyoung Hwang (Hansung University)

Time	Title and Speaker
4:00	**Gated Transformer Networks for Drug Classification using MultiDimensional Time-Series Animal Behavioral Data** Invited // Sung-Cheol Kim (PsychoGenics)
4:20	**Cloud-based Integrated Development Environment to Improve Hands-on Activities in a Mobile App Course** // Sam Chung (City University of Seattle)
4:40	**Skyscraper Games for Kids: Lessons Learned from a STEM Contest for Kids** // Frank Lee (Drexel University)
5:00	**Disadvantaged Business Enterprise (DBE) Program Fraud Detection using Natural Language Processing** // Jay Jaeshik Shin (Seoul National University)
5:20	**Enhanced Deep Learning Model for Structural Damage Identification via Random Vibration** // Jongyeop Kim (Georgia Southern University)
5:40	**A Comparative Study of PWAs and React Native Mobile Apps** // Sam Chung (City University of Seattle)

Tech Group C-7
CIT

@ Grapevine

Aug 4 _ Friday _ 4:00 – 6:00pm

CIT Session II: Security
Chair: Ohbong Kwon (New York City College of Technology), Co-Chair: Donghoon Kim (Arkansas State University)

Time	Title and Speaker
4:00	**Integrating Geographic Information Systems and Automatic Identification Systems for Maritime Logistics** Invited // EunSu Lee (New Jersey City University)
4:20	**A Case Study of Next.js's Hybrid Rendering vs. React.js' Client-Side Rendering** // Shingo Kise (City University of Seattle)
4:40	**Enhanced Real-Time Fingerprinting Attacks on Tor Networks** // Donghoon Kim (Arkansas State University)
5:00	**Hierarchical Reinforcement Learning Architecture to Deal With Multi-Horizon Complex Systems** // Prasad Nethala (Texas A&M University-Corpus Christi)
5:20	**Hippocampus Inspired Cognitive Architecture (HICA) for Few-shot Learning** // Deokgun Park (University of Texas at Arlington)
5:40	**Machine Learning Algorithm: Predicting the Price of Soybean** // Soon-Ok Park (Governors State University)

Tech Group C-7
CIT

@ Aviator A

Aug 4 _ Friday _ 6:00 – 9:00pm

CIT Poster Session
Chair: Ohbong Kwon (New York City College of Technology), Co-Chair: Jeongkyu Lee (Northeastern University)

Time	Title and Speaker
CIT P1	**Science and Engineering Education using Drone** // Jounsup Park (California Baptist University)
CIT P2	**Analysis of Community Connectivity in Spatial Transcriptomics Data** // Kyeong Joo Jung (The Ohio State University)
CIT P3	**Potential Transformative Impact of Flood Service Drones** // Jae Hyeon Ryu (University of Idaho)
CIT P4	**Conceptualizing Information Drone to Benefit Underserved People** // Jae Hyeon Ryu (University of Idaho)
CIT P5	**Resource-Efficient Parameter Tuning in Text-to-Speech Models** // Chan Gi Hong (Gwangju Institute of Science and Technology)
CIT P6	**Investigating the cause of selection by using an evolutionary model that incorporates amino acid physicochemical properties** // Hannah Kim (Temple University)
CIT P7	**Evaluating Autoencoder Structures for Testing Location Integrity** // Jinpyo Kim (Texas A&M University-Commerce)

Industrial, Manufacturing, and Systems Engineering, Management Sciences, Operations Research (IMS)
Technical Group C-8

The Industrial Engineering and Management Science (IMS) Symposium aims to discuss recent theoretical advancements and practical developments in the areas of industrial and systems engineering, management science, and supply chain management. The symposium would disseminate, to all branches of academy and industry across the U.S. and Korea, the most relevant theoretical research as well as applications. Topics include, but are not limited to: Intelligent Systems, Internet of Things (IoT), Supply Chain Risk Management, Service Science, Revenue Management, Finance Technology, Artificial Intelligence and Big Data Analytics, Optimization, Network Science, Transportation Science & Logistics, System Simulation, Modeling & Decision Analysis, Quality & Reliability Engineering, Engineering Economic Analysis, and Ergonomics & Human Factors.

Chair

Jeong Hoon Choi

Youngstown State University

Co-chairs

Tai-Woo Chang

Kyonggi University

Hyesung Park

Georgia Gwinnett College

Tech Group C-8
IMS

@ Austin

Aug 3 _ Thursday _ 4:00 – 6:00pm

IMS Session I: Health Care and Sustainability
Chair: Hyesung Park (Georgia Gwinnett College)

Time	Title and Speaker
4:00	**The Impact of Misinformation on Health Interventions to Prevent the Spread of Covid-19 in Eastern and Southern Africa** Invited // Sang-Heui Lee (Pittsburg State University)
4:20	**Strategic Capacity Management for Deferred Surgeries** // Eojin Han (Southern Methodist University)
4:40	**Renewable-Battery Hybrid Power Plants in Congested Electricity Markets: Implications for Plant Configuration** // Hyungkwan Kim (Lawrence Berkeley National Laboratory)
5:00	**Challenges in Managing Workload and Anxiety in Gateway Programming Courses** // Hyesung Park (Georgia Gwinnett College)
5:20	**The Vulnerability of the Blood Supply Chain in the U.S.** // Jeong Hoon Choi (Youngstown State University)
5:40	**Proposal of a Parametric-based Generative Design Tool for Customized Mouse** // Eui-Chul Jung (Seoul National University)

Tech Group C-8
IMS

@ Austin

Aug 4 _ Friday _ 4:00 – 6:00pm

IMS Session II: Industrial Engineering & Management Science Applications
Chair: Jeong Hoon Choi (Youngstown State University)

Time	Title and Speaker
4:00	**Leveraging Smart Contracts for Secure and Asynchronous Group Key Exchange Without Trusted Third Party** Invited // Junggab Son (University of Nevada, Las Vegas)
4:20	**Safe Drilling Depth for Deep Hole Bone Drilling** // JuEun Lee (University of the Pacific)
4:40	**Inventory and firm performance analysis in the pharmaceutical industry** // Sangdo Choi (o9 Solutions, Inc.)
5:00	**Does corporate political advocacy harm your offline business?** // Yeohong Yoon (Emory University)
5:20	**Exploring the impact of the working capital in the U.S. aviation industry for profitability and shareholder value** // Seock-Jin Hong (University of North Texas)
5:35	**The Impact of Context and Environment on Driver's Situation Awareness** // Sami Park (University of Washington)
5:50	**A Drill-Down Demand Analysis of Beef and Hay Consumption in Korea**// Eunsu Lee (New Jersey City University)

Tech Group C-8
IMS

@ Aviator A

Aug 4 _ Friday _ 6:00 – 9:00pm

IMS Poster Session
Chair: Tai-Woo Chang (Kyonggi University), Jeong Hoon Choi (Youngstown State University)

Time	Title and Speaker
IMS P1	**Prediction and Integrated Control System for the Spread of Hazardous Materials in Industrial Areas** // Minho Son (Podo Institute of Technology)
IMS P2	**Analysis of the Relationship between Innovation Activities and Profitability in Banking Industry in Korea** // Sooyeon Lim (Seoul National University)
IMS P3	**Examining the transfer of ACC training to mental models after an OTA update of Advanced Driver Assistance Systems** // Jimin Kim (University of Iowa)

Social Sciences (Anthropology, Economics, Political Science, Sociology, Public Policy, etc.), Psychology, Digital Arts, STEM Education, and Other Sciences (SSP)
Technical Group D-1

The Education Research, STEM and Social Sciences Symposium is organized by KAERA (Korean-American Educational Researchers Association) to invite leading experts and young researchers in emerging technology and DEI (Diversity, Equity, and Inclusion) in Education.

The first session focuses on the integration of advanced technologies into education. These advances brought changes in the way we learn and teach thereby significantly transforming the educational landscape. With this in mind, it will cover a wide range of topics, including but not limited to the ethical implications of AI technology in education, immersive learning experiences through AR or VR, online or flipped learning, gamification, as well as various pedagogies and teaching models.

The second session explores the topic of Diversity, Equity, and Inclusion in STEM education with a focus on Belonging for Koreans and Korean Americans. This session will bring together a group of teacher educators who are doing innovative work in DEI + Belonging. The presentations will focus on issues of DEI+B within the field of STEM teacher education. Topics will include anti-racist pedagogy, cultivating a sense of belonging in the classroom, and unpacking the differences between equity and equality to promote safe learning and teaching environments.

Chair

Jongpil Cheon

Texas Tech University

Co-chairs

Nicholas D. Hartlep

Berea College

Kyungbin Kwon

Indiana University Bloomington

Gilbert Park

Ball state University

Tech Group D-1
SSP

@ Vandergriff

Aug 3 _ Thursday _ 4:00 – 6:00pm

SSP Session I: Education and Social Science (Integration of Advanced Technology)
Chair: Jongpil Cheon (Texas Tech University), Kyungbin Kwon (Indiana University - Bloomington)

Time	Title and Speaker
4:00	**Embodied Learning for Computational Thinking** // Kyungbin Kwon (Indiana University – Bloomington)
4:15	**Solar Tree for Science, Technology, Engineering, Art, and Math** // Sung Yeul Park (University of Connecticut)
4:30	**Developing AI Chatbot System for Self-Regulated Learning** // Hyangeun Ji (Temple University), Insook Han (Korea University)
4:45	**Unraveling the Effective Teaching and Learning Strategies for Korean College Students in STEM Majors in the COVID-19 Era** // Seong Ji Jeong (The Ohio State University)
5:00	**PROJECT ADAPT – Uncovering the Potential of Arts-Integrated Digital Literacy Professional Development Program in Preservice Teachers' Digital Literacy Development and Learning Engagement** // Jewoong Moon, Kathryn O'Harra, Julianne Coleman, Kelley Schoger, Julie Bannerman (The University of Alabama)
5:15	**Exploring Strategic Differences in Debugging Between Two Groups with Different Levels of Computational Thinking Competency: Implications for Teaching Strategies** // Eunsung Park (Tennessee Tech University), Jongpil Cheon (Texas Tech University)
5:30	**Utilizing Artificial Intelligence for Personalized Career Development** // Boong Yeol Ryoo (Texas A&M University)
5:45	**Enhancing Science Affinities through a Video Project in a Science, Technology, and Society (STS) Learning Approach** // Jiyoon Yoon (University of Texas Arlington), Amanda Olsen (University of Missouri Columbia)

Tech Group D-1
SSP

@ Vandergriff

Aug 4 _ Friday _ 4:00 – 6:00pm

SSP Session II: Education and Social Science (Diversity, Equity, and Inclusion)
Chair: Nicholas D. Hartlep (Berea College), Gilbert Park (Ball State University)

Time	Title and Speaker
4:00	**Virtual Cultural Science Night with Academic Coaching** // Jiyoon Yoon (University of Texas Arlington)
4:20	**Synchronous Online Culturally Responsive Academic Tellers and Educational Supporters (SOCRATES) for Online Academic Coaching** // Jiyoon Yoon (University of Texas Arlington), Kate Koo (University of Georgia)
4:40	**The Anti-Racism Conundrum: Measuring Campus Progress** // Katherine S. Cho (Loyola University Chicago)

Tech Group D-1
SSP

@ Vandergriff

Aug 4 _ Friday _ 4:00 – 6:00pm

SSP Session II: Education and Social Science (Diversity, Equity, and Inclusion)
Chairs: Nicholas D. Hartlep (Berea College), Gilbert Park (Ball State University)

Time	Title and Speaker
5:00	**Culturally Responsive Computer Science Learning: Fostering Equity and Engagement for Minoritized High School Students** // Jung Won Hur (Auburn University), Jay Bhuyan (Tuskegee University)
5:20	**What Barriers Are Preventing Asian/Americans from Leading Educator Preparation Programs (EPPs)?** // Nicholas D. Hartlep (Berea College), Gilbert Park (Ball State University)

Tech Group D-1
SSP

@ Aviator A

Aug 4 _ Friday _ 6:00 – 9:00pm

SSP Poster Session
Chairs: Jongpil Cheon (Texas Tech University), Kyungbin Kwon (Indiana University - Bloomington), Nicholas D. Hartlep (Berea College), Gilbert Park (Ball State University)

Time	Title and Speaker
SSP P1	**Designing Drone-based STEM Instruction for Formal Spaces** // Hannah Ziegler (Vanderbilt University), Jae Ryu (University of Idaho)
SSP P2	**Development and Dissemination of Instructional Modules for Engineering Lab Writing** // Dave Kim (Washington State University)
SSP P3	**Building Inclusive and Just Pathways to a Clean Energy Economy Through Youth Education of Clean Energy** // Hyun Jin Kim, Hyunjung Ji, Sally Shettles, Mark Mueller (The University of Alabama), Amelia Salazar (Sam Houston State University), Laurel Holmes (Energy Alabama)
SSP P4	**Thermofluid Sciences for Elementary School Students via Flow Visualization Using Smartphones and Tablets** // Hyun Jin Kim, Shemai'ya Peak, Frances Buntain, Jale Ercan Dursun, Jee Suh, Celestia Morgan (The University of Alabama)
SSP P5	**Utilizing the Medium of Virtual Reality to Teach How To Recycle** // Nathan Kassai, Paul Y. Oh (University of Nevada, Las Vegas)
SSP P6	**A Case Study of Recreation-based STEM Education that Improves Unplugged Coding Education Using Musical Activities for Kindergarten Children** // Wonil Chung (Kyung Pook National University), Min Jae Park (Institute of STREAM Academy)

IES
(Innovation and Entrepreneurship Symposium)

Innovation and Entrepreneurship Symposium (IES)

The Korean-American Scientists and Engineers Association (KSEA) is delighted to present the 5th Innovation and Entrepreneurship Symposium (IES), taking place on August 3-5, 2023 at the Hyatt Regency DFW in Dallas, TX. This symposium is designed to facilitate networking opportunities for entrepreneurial communities from both the US and Korea. The IES Demo session will provide a platform for participating startups to showcase their companies to UKC attendees and an opportunity for advancing to the Startup Pitch Competition (SPC), a highlight of the symposium, offering the chance to pitch their companies to potential investors and industry professionals while competing for a cash prize. The Idea Pitch Competition (IPC) invites early-stage startups and future entrepreneurs to present their ideas and receive feedback from the participating investors. The IPC provides great opportunities to meet future collaborators and seed investors and to compete for cash awards. Throughout the symposium, attendees will have the chance to participate in various networking events with investors, successful entrepreneurs, funding agencies, and experts in law and finance. We extend a warm invitation to all entrepreneurial-minded professionals to attend the IES and explore the growing cross-border business opportunities between the US and Korea.

Organizing Committee

Chair

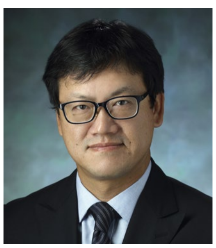

IL Minn

Johns Hopkins University

Co-Chairs

Kwangrog Kim

Fundraising
Primer Sazze

Taegon Lee

Next Generation & SPC

Jungeun Kim

Korea Demo & Fundraising
Quotalab

- **Workshop Committee**: Jangwon Kim (Amazon Health), IL Minn (Johns Hopkins University)
- **Startup Demo, SPC, and IPC Committee**: Kwangrog Kim, Jungeun Kim (Quotalab), Taegon Lee (DoD), Jihee Jung, Nathan Byun
- **Public Relation Director**: Kevin Kim (Brave Turtles)
- **Next Generation Director:** Taegon Lee (DoD)
- **Local Arrangement & Publication Director:** Nathan Byun (Honeywell Robotics)
- **IT Director:** Stella RH Kim
- **General Director:** Taegon Lee (DoD)
- **Advisors:** Jun-Seok Oh (Western Michigan University), Kyungho Yang (KITEE), Jeho Park (Claremont McKenna College)

Program Overview

Time in the US Central Daylight Time, CDT

August 3 _ Thursday _ 4:00 - 6:00pm

Time	Content	Title and Speaker
4:00-5:00 pm	IES Opening Session	Moderator: Jennifer Cho. PhD • Opening Remarks - IL Minn, PhD, IES 2023 Chair • Congratulatory Remarks – Yongho Sohn PhD, KSEA President • IES Keynote: *“The role and prospects of tech start-ups in the era of global tech wars* (tentative)” - Donghoon Lee, CEO, SK Biopharmaceuticals
5:00-6:00 pm	AI and Entrepreneurship	Panel Discussion: The impact of generative AI Moderator: Jangwon Kim, PhD, Sr. Applied Scientist, Amazon Panelists: John Lee: Head of AI Engineering, Software Engineering Institute, CMU Chang Kim: Former Co-founder & CEO, Tapas Media

August 4 _ Friday _ 4:00 - 11:00pm

Time	Content	Title and Speaker
4:00-6:00 pm	IES Startup Pitch Session	• Moderator: TBD 20invited startups will present SPC judges will select 10 finalist
6:30-8:30 pm	IES Networking Dinner	
8:30-11:00 pm	IES Networking Gathering	

August 5 _ Saturday _ 8:00 - 3:30pm

Time	Content	Title and Speaker
8:00-10:00 am	Startup Pitch Competition 1	• Moderator: TBD
10:30-12:30 pm	UKC Closing and Award Ceremony	
1:00-3:30 pm	SPC Networking Lunch	

Call for Participation: Startup Pitch Competition and Idea Pitch Competition at UKC 2023

The Korean-American Scientists and Engineers Association (KSEA) host 5th Startup Pitch Competition and Idea Pitch Competition on August 4 and 5, during the UKC 2023 that is held at the Hyatt Regency DFW, Dallas TX. The competition aims to provide promising early-stage companies from the US and Korea with the platform to pitch their innovative solutions, ideas, and technologies to a captivated audience of industry professionals and acclaimed Investors, especially promoting US-Korea cross-border startups that would maximize the synergy between the two countries. This year features two categories of competition, the Startup Pitch Competition (SPC) for early-stage startups and the Idea Pitch Competition (IPC) for future startups. Of the many that apply, about 20 applicants will be invited for the IES DEMO session to present a short pitch on August 4. 10 finalists will be selected by SPC judges and invited to SPC on August 5 to compete for various types of rewards including cash awards.

Selected Benefits to Invited Companies

- 1:1 meeting with a matched venture capitalist
- Booth presentation during the entire IES and UKC 2023 periods to those who are invited - investors, technologists, industry veterans, UKC 2023 participants
- Networking events with investors and potential partners
- Scale-up opportunities through partnership with KSEA and its affiliated professional societies

How To Apply

Interested? We'd love to see you pitch! We request all applicants to submit a short video (video link) that gives us a sense of who you are and how your solution would be propelling the future of the world. Video submissions should cover the following points in less than 5 minutes:

- Your startup's value proposition
- Problem(s) your product and/or service is solving
- Why your startup is a good fit for the KSEA StartUp Pitch Competition

Eligibility

Eligible startups must meet the following criteria as of June 15, 2023:

- Have not received more than US$7.0 million in diluted funding
  (Category 1 - Idea: US$200K, Category 2 – Startup & W-Startup: US$7.0M)
- Are less than 7 years old

Timeline (11:59 PM in US Eastern time)

Application due	July 7th, 2023
Invitee notification	July 8th, 2023
Idea Pitch competition	August 4th, 2023
Startup Demo	August 4th, 2023
Startup Pitch competition	August 5th, 2023
Winners announcement	August 5th, 2023

How to Win

- Competition Finalists are expected to prepare a presentation showcasing the company's innovative solution, idea, and/or technology. Finalists will pitch in English or Korean.
- Each pitch will be timed to 5 minutes. At the end of the pitch, the panel of judges will be given additional 3 minutes for Q&A (up to three questions).
- Finalists will be assessed by a dedicated panel of judges consisting of acclaimed investors and industry professionals, and the results will be announced at the Award Ceremony & Closing Session on the same day.

Submission should be made at **https://bit.ly/KSEA2023SPC**

Questions may be sent to **spc.ksea@gmail.com**.

Many venture capitalists from USA and Korea accepted to judge or sponsor the competition.

Registration:
UKC.KSEA.ORG/UKC2023

INNOVATION AND ENTREPRENEURSHIP SYMPOSIUM & STARTUP PITCH COMPETITION

AUGUST 3-5, 2023
HYATT REGENCY DFW (DALLAS, TX)

SYMPOSIUM PROGRAM

- Keynote Speech
  Dong Hoon Lee
  CEO, SK Biopharmaceuticals
- General AI & Entrepreneurship
- 1-on-1 Coaching with VCs, Lawyers, Successful Entrepreneurs

IES NETWOKRING EVENTS

- IES Networking Dinner and More
  August 4
- SPC Networking Lunch
  August 5

IES Home:
HTTP://IES.KSEA.ORG/

STARTUP DEMO

August 3 and 4

STARTUP PITCH COMPETITION

Interested? Submit a video of 5 minutes or shorter that gives us a sense of who you are and how your solution would be propelling the future of the world. Submit it at ***https://bit.ly/KSEA2023SPC.***

Application Due	July 7
Invitee Notification	July 8
Idea Pitch Competition	August 4
Startup Demo	August 4
Startup Pitch Competiton	August 5
Winners Announcement	August 5

SUPPORTERS OF IES 2023

SK biopharmaceuticals
KIC Korea Innovation Center Washington DC
PRIMER SAZZE
Uiflow
B.J. KANG LAW, PC ATTORNEYS AT LAW
KDB Silicon Valley Venture Capital
KITEE Innovation to Business
Small/Medium Enterprise Committee

FIRE
(Fostering Innovation in Rising Experts) Symposium

FIRE Symposium

FIRE
Fostering Innovation in Rising Experts
Symposium

UKC FIRE 2023

FIRE is a symposium at UKC comprised of 100 young professionals, graduate/undergraduate students, postdocs, and junior faculty. FIRE gathers the next generation of leaders in industry and academia from North America for knowledge dissemination via two main pathways.

1. Sharing professional development lessons learned (non-technical) such as:
   - Getting promoted/a raise
   - Acing interviews/Building strong resumes
   - Enhancing productivity with AI tools
   - Transitioning fields & unique career paths
   - Choosing between industry and academia
   - Becoming an empowering leader
   - Navigating the U.S. as a Korean/-American
   - Overcoming impostor syndrome
   - Personal Branding & Self-Advocacy

2. Networking within and outside their fields of interest to encourage broad awareness of cutting edge science and engineering fields, interdisciplinary collaborations, and skills cultivation applicable across careers in industry, academia, and government.

Organizing Committee

Chair

TJ Park

PhD Candidate
MIT

Vice-Chair

James Han

Postdoctoral Scientist
Harvard

Vice-Chair

DK Kim

Project Lead
Data Analytics
Zurich

Programs & Networking

Amy Jang

Pediatric Pharmacist
Boston Children's

Programs & Networking

Kate Kyuri Kim

MSc Candidate
University Toronto

Seunghwan Allen Lee

Postdoctoral Associate
MIT

Logistics & Communications

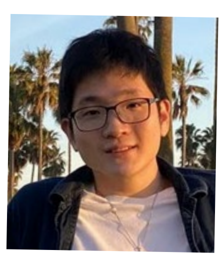

Andy Kim

Medical Scribe
Kaiser Permanente

Tommy Cho

BS Candidate
Rutgers University

Introductory Networking and Career Flash Talk

August 3_Thursday _ 4:00pm _ Innovation Ballroom

Coordinators: TJ Park, James Han, DK Kim, Kate Kim, Amy Jang

Time	Title and Speaker
4:00 pm	**Welcoming Remarks & Introductory Networking (Icebreaker)** // TJ Park, James Han, DK Kim, Kate Kim
4:45 pm	**Importance of Acquiring and Being Aware of Intellectual Properties in academic research** // Chanwook Park (PhD Candidate, Northwestern University)
4:52 pm	**A Nuclear Engineer who Dreams the World Peace** // Jihye Jeon (PhD Candidate, Princeton University)
4:59 pm	**My journey as a female engineer** // Inhwa Son (MS Candidate, University of San Francisco)
5:06 pm	**Thriving through Rejections** // Inyoung Cheong (PhD Candidate, University of Washington)
5:13 pm	**Teaching is everywhere and so are the teachers** // Seoyeon (Shawna) Kim (MSc Candidate, Queen's University)
5:20 pm	**"*Gap*" Year: Learning to Prioritize Yourself** // Hyoungjin (Harry) Park (BS Candidate, University of Southern California)
5:27 pm	**Shamelessness – My Superpower** // Jenny Namkoong (Interventional Cardiology Fellow, University of Manitoba)
5:34 pm	**Maximizing your time outside of work** // Veronica JungYeon Kim (Software Engineer, Weights & Biases)

Panel Discussion: Perspectives on Academic Careers

August 4_ Friday _ 4:00pm _ Innovation Ballroom A

Moderator: Allen (Seunghwan) Lee

Time	Title and Speaker
4:00 pm	**How do you define a successful researcher?** // Jongbok Lee (Assistant Professor, University of Calgary)
4:05 pm	**Succeeding in the Academic Job Market** // Soowon Chang (Assistant Professor, Purdue University)
4:10 pm	**Transitioning from research institution to teaching institution** // Bo Park (Assistant Professor, California State University, Fullerton)
4:15 pm	**How to Engage Students in Class: Improving Comprehension Through Practical Examples** // Daewa Kim (Assistant Professor, University of Delaware)
4:20 pm	**Open Dialogue on Academic Career Trajectories and Motivations**

Panel Discussion: Industry Careers and Interdisciplinary Opportunities

August 4 _ Friday _ 4:00pm _ Innovation Ballroom C&D

Moderator: Jonathan Young Kim

Time	Title and Speaker
4:00 pm	**Betting on yourself - making a change to a different industry or role** // John Lee (Associate Researcher, SEI)
4:05 pm	**Proactive Pathways: Navigating Success as a Korean American in the American Workplace** // Simon Park (Software Engineer, Uber)
4:10 pm	**Job interview strategies I've learned** // Edward Hong (Semiconductor Engineer, TikTok)
4:15 pm	**Hollywood in the Metaverse** // Youngmin Kim (CEO, iXR Studios | Visiting Professor, Sogang University)
4:20 pm	**Open Dialogue on Tech Career Trajectories and Future Pathways**

Presentations and schedule are subject to change.

Panel Discussion: Rewarding Careers in Healthcare and Lessons Learned

August 4 _ Friday _ 4:00pm _ Innovation Ballroom B

Moderator: James Han

Time	Title and Speaker
4:00 pm	**Informational Talk** // Kevin Riutzel (Physician, Kheir Clinic)
4:05 pm	**Lessons During the Unprecedented COVID-19 Pandemic Applicable to Precedented Times** // Jina Lim (Attending Physician, Massachusetts General Hospital / Instructor in Medicine, Harvard Medical School)
4:10 pm	**Dentist Scientist Training Program: full-ride dental school programs and career paths in dental academia** // Seung Jin Jang (DMD PhD Candidate, University of Florida)
4:15 pm	**Pharmaceutical Industry Career: Medical Affairs** // Clara Kim (Senior Manager in Medical Information Rare Tumors, Astellas Pharma US)
4:20 pm	**Open Dialogue on Future Outlook in Healthcare**

Focus Group Talks

August 4 _ Friday _ 5:00pm _ Innovation Ballroom C&D

Moderator: Kate Kim

Topic	Time	Title and Speaker
Career & Personal Development (Table 1)	5:00 - 5:20 pm	**Permission to publish denied** // Chang Hyeon Lim (Data Scientist, Dow Chemical)
	5:20 - 5:40 pm	**Permission to publish denied** // Jeong-wan Park (Postdoc, Argonne National Laboratory)
	5:40 - 6:00 pm	**Life of being Alien in USA** // Gyeonghye Yun (BS Candidate, University of Washington)
Career & Personal Development (Table 2)	5:00 - 5:20 pm	**Keeping my passions with career realities** // JeongYong (Jaylen) Park (PhD Candidate, Texas A&M University)
	5:20 - 5:40 pm	**How to find meaningful connections between my skills and dreams?** // MinYoung Yoo (PhD Candidate, Simon Fraser University)
	5:40 - 6:00 pm	**What more can I do?** // Nathaniel Chung (PharmD Candidate, Northeastern University)
Industry & Academic Career Development (Table 3)	5:00 - 5:20 pm	**Lessons learned from a manufacturing start-up, from different culture.** // Yoonseok Oh (Process engineer, SK Battery)
	5:20 - 5:40 pm	**Applying to the Job You Deserve: Internal vs External** // Jonathan Young Kim (Lead Software Engineer, Capital One)
	5:40 - 6:00 pm	**My journey to achieve a four-year Ph.D. completion in a new field** // Wonjae Yoo (Instructional Assistant Professor, Texas A&M University)
Cultural Challenges & Academic Career Development (Table 4)	5:00 - 5:20 pm	**It's OK not to be OK: How Grad School Became my Therapy** // Eugene Kim (MS Candidate, Georgia Institute of Technology)
	5:20 - 5:40 pm	**Understanding American individualism for networking** // Changkee Hong (PhD Candidate, University of Central Florida)
	5:40 - 6:00 pm	**Few lessons learned as a Korean immigrant to non-traditional graduate student** // Min Kyu Lee (MS Candidate, UCLA / Clinical Research Coordinator, California Vascular Research Foundation)

Presentations and schedule are subject to change.

Focus Group Talks (Continued)

August 4 _ Friday _ 5:00pm _ Innovation Ballroom C&D

Moderator: Kate Kim

Topic	Time	Title and Speaker
Healthcare, Tech & Industry Career Development (Table 5)	5:00 - 5:20 pm	**Confidence Built as a Dentist** // Alex Kang (DMD Candidate, Dental College of Georgia)
	5:20 - 5:40 pm	**Navigating the biotech world without a PhD** // Anna Lee (Director, Prellis Biologics)
	5:40 - 6:00 pm	**Paving the Cowpath: The Career Path of Digital Health Informaticist** // Jaehoon Lee (Lead Digital Health Informaticist, MITRE Corporation)
Interviews, Tech & Personal Development (Table 6)	5:00 - 5:20 pm	**Cultivating Interview Success: 10 Essential Tips for Young Students Embarking on Their Journey** // Dahye Kim (PharmD Candidate, University of North Carolina)
	5:20 - 5:40 pm	**Importance of Design Verification in Engineering** // Sangwoo Park (Silicon Design Engineer 2, AMD)
	5:40 - 6:00 pm	**Searching for Motivation in Work** // Seo Yeon Lee (Clinical Research Assistant, BIDMC)
Resumes & Personal Development (Table 7)	5:00 - 5:20 pm	**The reason why I quit my job after 8 years to study abroad** // Eunmi Jeong (PhD Candidate, University of Wisconsin-Madison)
	5:20 - 5:40 pm	**How to use ChatGPT to fine-tune your resume** // Hye Rin Choi (Data Engineer, Canadian Government)
	5:40 - 6:00 pm	**How to conduct research in unfamiliar research territory** // Dong Seok Lee (PhD Candidate, University of Texas at Austin)
Skills & Personal Development (Table 8)	5:00 - 5:20 pm	**Importance of Self-Advocacy in the Workplace** // Brian Shanahan (Engineer, Primera)
	5:20 - 5:40 pm	**The necessity of sabbaticals** // Jay Han (Engineering Manager, Qualtrics)
	5:40 - 6:00 pm	**Shape the World You Want to Live in** // Namhyeon Cho (Senior Project Engineer, Barton Marlow)
Mental Health, Startups &Industry Career Development (Table 9)	5:00 - 5:20 pm	**Use Imposter Syndrome to Your Advantage** // Yoona Park (Machine Learning Engineer, Apple)
	5:20 - 5:40 pm	**Why I Challenge Everyday: Lessons Learned from Leadership, Collaboration to Entrepreneurship** // Yewon Hong (BS Candidate, UC San Diego)
	5:40 - 6:00 pm	**Bridging the Gap: Merging Art and Technology - Lessons Learned in Professional Development** // Choux Kim (BS Candidate, GeorgiaTech)
Tech, Art, and Startups (Table 10)	5:00 - 5:20 pm	**Permission to publish denied** // Crystal Shin (Assistant Professor, Baylor College of Medicine)
	5:20 - 5:40 pm	**Into the Woods of Free and Open Source Software (FOSS)** // Andrew Jemin Choi (Software Engineer, Algorand)

Presentations and schedule are subject to change.

Poster Exhibition

August 4 _ Friday _ 6:00 - 9:00pm _ Aviators

Coordinators: Amy Jang, Kate Kim

Slot	Title and Speaker
FIRE1	**From Food Science to Nutritional Sciences: A Journey Starting from Scratch //** Da-Yeon Lee (PhD Candidate, Oklahoma State University)
FIRE2	**Between Cybersecurity and Aging** // Donghyun Lee (BS Candidate, Seoul National University/Georgia Tech)
FIRE3	**User Needs and Technology //** Emily Han (BA Candidate, Rutgers University)
FIRE4	**Do what you love, consider the most important values, and keep getting new good stimuli in your life. //** Hojoong Kim (Postdoc, Georgia Institute of Technology)
FIRE5	**Unveiling Passions and Pioneering Paths //** Hyukin Moon (BS Candidate, UC San Diego)
FIRE6	**How I chose my major and advisor/lab //** Inah Gu (PhD Candidate, University of Arkansas)
FIRE7	**Embracing Transformation: From Industrial and Labor Relations to Consumer Finance and Data Science at Meta //** Jonathan Kim (Data Scientist, Meta)
FIRE8	**Navigating Career Paths: MD, PhD, and MD/PhD //** Matthew Jeon (Staff Research Associate, University of California, San Francisco)
FIRE9	**How to navigate through your undergraduate life as an asian/international student. //** Min Joo Kim (BS Candidate, Vanderbilt University)
FIRE10	**Promoting Effective Collaboration: Key Strategies for Success in Research Environments //** Myeongsoo Kim (PhD Candidate, Georgia Institute of Technology)
FIRE11	**From Workforce to Academia: Transformative Lessons in Professional Development //** Rachel Chun (PharmD Candidate, UNC Chapel Hill)
FIRE12	**Baby Steps! //** Riky bae (BS Candidate, Rutgers University)
FIRE13	**Pursuing the Path of an Engineering Entrepreneur: Why I Chose to Follow My Passion. //** Saeyeong Jeon (PhD Candidate, University of Florida)
FIRE14	**Navigating Uncertainties in the Journey Towards a Ph.D. //** Sungyun Yang (PhD Candidate, MIT)
FIRE15	**Permission to publish denied //** Uijeong Jo (PharmD Candidate, UNC Chapel Hill)
FIRE16	**Designing Tomorrow: The Intersection of Creativity and Healthcare //** Venessa Mak (BS Candidate, UTMB)
FIRE17	**Computer Science and Learning Science //** Yongwan Cho (BS Candidate, Kalamazoo college)

DSW
(Data Science Workshop)

Data Science Workshop

Machine Learning on Biomedical Data

Open to all non-biomedical and biomedical backgrounds with some programming experience.
Prior Online Workshop Registration and Fee Required

August 5 _ Saturday _ 1:30-6:00pm _ Innovation Ballroom C&D

Summary

This year's **Data Science Workshop** (DSW) at UKC aims:

- To provide a deeper hands-on experience with a crash course on data analysis, machine learning, and deep learning,
- For those with some prior programming but no data science experience to those looking to expand their knowledge, and
- For those without any biomedical background, as the techniques learned are domain and data agnostic.

Program

The data science workshop will be a **team-based mini-project** from start to finish of a **data science problem** using **real-world biomedical data**. Participants will begin with data cleaning, build a machine learning model, and end with presenting their own trained model. Instructors will assist teams of 2-3 participants on each mini-task to achieve the final goal of training a machine learning model and presenting it. Participants should have some programming experience with Python preferred. The computing environment will be Google Colab and the dataset will be announced at the workshop. The program schedule tentatively includes:

1. **Data Analysis of Tabular Biomedical Data (1:30-3:45pm)**

- Introduction to data science basics and machine learning concepts (e.g. definition of AI vs machine learning vs deep learning, supervised vs unsupervised, accuracy vs interpretability)
- Hands-on review of data handling and machine learning models (e.g. logistic regression, random forests, gradient boosting, artificial neural networks) on real-world biomedical tabular data (such as breast cancer histopathology or cardiac ultrasound measurement data)

2. **Machine Learning Modeling and Project Presentations (4:00-6:00pm)**

- Hands-on model building with code from templates and scratch using Python
- Team presentations of model building and performance results
- Bonus demonstration of deep learning models such as biomedical image classification using convolutional neural networks

Any questions may be addressed to the organizers at **dsw.ukc@gmail.com.**

Organizers / Instructors

Benjamin Lee (Chair) Senior Research Associate at Weill Cornell Medicine

Benjamin Lee is a researcher developing machine learning algorithms for cardiovascular medical imaging in CT, Echo, ECG, and histopathology data for heart failure, heart transplantation, and coronary plaque characterization. Ben received his Ph.D. at the University of Michigan in Electrical Engineering specializing in image processing and image reconstruction and his B.S. from Cornell University. He is currently based in New York City.

June Park (Co-Chair) Data Engineer at Daugherty Business Solutions

June Park is a Data Engineer at a solutions-based consulting company, Daugherty Business Solutions, building and maintaining data pipeline solutions for clients. She was previously a backend software engineer at Groundspeed Analytics, an insurtech startup. June received M.S. in Information at the University of Michigan and B.S. in Computational Media at Georgia Tech. She is currently based in Dallas, Texas.

Karl Kwon (Organizer) Engineering Lead at MITRE

Karl Kwon has worked on various projects, including the development of data visualization, the implementation of machine learning models, and the design of software systems. He holds a Ph.D. in Computer Science from the University of Houston, where he invented and developed a powerful data visualization called ScholarPlot. He earned his MS in computer science and his BS in software engineering. Karl Kwon is currently located in the NYC area.

DK Kim (Organizer) Project Lead & Senior Data Analytics Consultant at Zurich North America

DK Kim worked as a data analyst in the healthcare sector prior to completing a Data Science coding bootcamp. Since then, he has worked in marketing, energy, and finance, and is currently working for an insurance company. DK received his BS in Industrial Engineering with minors in Statistics and Mechanical Engineering from Texas Tech. He is currently pursuing his MS in CS part-time from Georgia Tech. DK is currently located in Chicago, IL.

Distinguished Forum

Seegene Medical Foundation (SMF) Distinguished Forum

Leading the Global Healthcare Market with Digital Healthcare

August 3 _ Thursday _ 1:30 _ Room Dallas

Chair	Co-Chair	Presenters				
						
Min-Cheol Lee	**Sung Yun Jung**	**Tae Hyun Hwang**	**Haiyoung Jung**	**Jongmun Choi**	**Youngjin Park**	**Suk Min Ha**
Vice Director Pathology Center Seegene Medical Foundation (SMF)	Associate Professor Baylor College of Medicine	Chair professor Mayo Clinic	Chief Deputy Medical Director	Lab director NGS Research Center	Senior AI researcher	AI Researcher

Seegene Medical Foundation (SMF) is a large independent reference laboratory in South Korea. The testing center headquarters is located in Seoul, and there are four regional centers. SMF provides over 4,500 testing services, including routine laboratory tests, molecular tests, pathological diagnosis, and clinical research, to clinics and hospitals nationwide. SMF performs approximately 400,000 tests daily. SMF operates the largest molecular diagnostic test center in South Korea. Its systems are capable of performing 400,000 automated COVID-19 tests per day. SMF has tested over 63 million people for COVID-19 since 2020, making it the largest testing center in Korea. SMF played a pivotal role in Korea's successful quarantine program. SMF is exploring diagnostic values through several research institutes, including the Immune Research Institute, the R&D Center for Clinical Mass Spectrometry, the Molecular Diagnostic Research Center and AI Research Center. SMF has a grand vision to be the leader in digital healthcare by leveraging big diagnostic data populated from its in vitro diagnostics services. SMF is promoting overseas expansion specifically in the United States, Europe, Southeast Asia, and Central Asia. In particular, SMF plans to diagnose and prevent diseases through IT-based digital healthcare services, and even provide treatment services.

At this forum, SMF will introduce an Open Healthcare business model for overseas expansion. SMF will also introduce the results of disease diagnosis development research using big data and artificial intelligence. Additionally, we are honored to have Professor Tae Hyun Hwang deliver a special lecture. SMF looks forward to your participation and hopes that we will be able to discuss research and build a collaborative relationship.

Time	Title and Speaker
1:30 -1:35 pm	**Welcoming Remarks** Sung Yun Jung
1:30 -1:40 pm	**Introduction to Seegene Medical Foundation** // Min-Cheol Lee, SMF
1:40 -2:10 pm	**Redefining Boundaries: Harnessing AI to Illuminate Novel Blood-Based Diagnostic, Prognostic, Predictive Biomarkers and Therapeutic Targets for Immuno and Cellular Therapy** // Tae Hyun Hwang, Florida Dept. of Cancer, Mayo Clinic
2:10-2:30 pm	**Introduction to Open Healthcare Business as a referral laboratory service and total health care platform** // Haiyoung Jung, SMF
2:30 -2:50 pm	**How to gain insights in the interpretation of clinical genomics using visualization of genetic big data?** // Jongmun, Choi, SMF
2:50 -3:05 pm	**A Sustainable and Workable Deep Leaning-based Clinical Assistant Diagnosis System for Digital Pathology** // Youngjin Park, SMF
3:05 -3:20 pm	**Multi-Organ Cell Segmentation with Watershed algorithm to automatically calculate Tumor Cellularity** // Suk Min Ha, SMF
3:20 -3:30 pm	**Open Discussion, Concluding Remarks and Photo**

* Please note that presentation time and speakers are subject to change depending on session circumstances.

CHEY Distinguished Forum

Forum on Space Exploration and Discovery CHEY Institute for Advanced Studies

August 3 _ Thursday _ 1:30pm _ Enterprise Ballroom

Chair

Young-Kee Kim

Louis Block Distinguished Service Prof. University of Chicago

Co-Chair

In Kook Park

President Chey Institute for Advanced Studies

Presenters

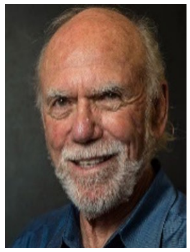

Barry Barish

Nobel Laureate Caltech, UC Riverside

Daniel Scheeres

Distinguished Prof. University of Colorado Boulder

Hyochoong Bang

Professor KAIST

The Chey Institute for Advanced Studies is delighted to present the forum "*Beyond Earth: Space Exploration and Discovery*." This forum aims to illuminate the latest advancements in space science and technology. Distinguished speakers, including Nobel laureate Barry Barish, renowned for his groundbreaking work on the discovery of gravitational waves, Daniel Scheeres, an esteemed expert in celestial mechanics from the University of Colorado Boulder, and Hyochoong Bang, a leading researcher in aerospace engineering at KAIST, will share their expertise. By exploring new frontiers, we anticipate fostering collaboration, exchanging knowledge, and inspiring further advancements in our understanding of the universe.

Time	Title and Speaker
1:30 - 1:35 pm	**Opening** // Young-Kee Kim, University of Chicago
1:35 - 1:45 pm	**Welcoming Remarks** // In Kook Park, CIAS
1:50 - 2:10 pm	**Presentation 1** // Barry Barish, Caltech and UC Riverside
2:10 - 2:35 pm	**Presentation 2** // Daniel Scheeres, University of Colorado Boulder
2:35 - 3:00 pm	**Presentation 3** // Hyochoong Bang, KAIST
3:00 - 3:30 pm	**Open Discussion and Photo** // All Panels

KEIT Distinguished Forum

Forum on Global Technology Strategy

August 3 _ Thursday _ 1:30pm _ Room Grapevine

Chair

Jeongwon Park

Professor
University of
Nevada Reno

Co-Chair

Sunghwan Park

KEIT US

Korea Evaluation Institute of Industrial Technology (KEIT) is the leading organization contributing the growth of manufacturing industry through development, application & commercialization of manufacturing technologies and supports for Small and Medium Enterprises (SMEs) in Korea. Its roles include planning, assessing and management of national industrial research and development programs under the Ministry of Trade, Industry and Energy (MOTIE). Since 2014, KEIT along with MOTIE has organized the KEIT Research Strategy Forum (KEIT Forum). By promoting the participation of Korean-American scientists and engineers in planning of Korea national R&D projects, we hope to improve the productivity and global cooperation in its R&D programs. To better identify and promote creative and innovative ideas for its national R&D projects planning, the major industry and technology trends will be discussed with Korean-American scientists and engineers in various areas and Korean government organization including KEIT. This year's KEIT Forum topics includes presentation of MOTIE's R&D roadmap and KEIT's policies and programs for promoting the emerging industries with focus on four industrial technology areas such as Biomedical, Materials, Batteries, and Autonomous vehicles.

Time	Title and Speaker
1:30 - 1:40 pm	**Greetings & Welcoming Remarks** // Sunghwan Park, KEIT US
1:40 - 2:00 pm	**KEIT Global R&D projects** // Chanhyuk Jung
2:00 - 2:10 pm	**Presentation of Cooperation with SWRI** // Sunghwan Park, KEIT US
2:10 - 2:40 pm	**Technical Presentations** // 4 PDs (Program Directors)
2:40 - 2:50 pm	**Case Study – Int'l R&D projects** // Youhuyn Jang, KHNP
2:50 - 3:00 pm	**Concluding Remarks and Photo** // Sunghwan Park, KEIT US

KEIT Global Technology Strategy Breakout Session (4:00 - 6:00pm)

- Wildcatter, Harvester, Ladybird, McCombs

KHNP (Korea Hydro & Nuclear Power) Distinguished Forum

Forum on Carbon Zero with Nuclear Energy

August 3 _ Thursday _ 1:30pm _ Room Hobby

Chair

Hyungook Kang

Professor
Rensselaer Polytechnic Institute

Co-Chair

Hocheol Shin

Head
KHNP CRI

Presenters

Deokwoo Nam

Senior Researcher
KHNP CRI

Jiyong Oh

General Manager
KHNP CRI

You Hyun Jang

General Manager
KHNP

Howard H. Chung

Professor
Univ. of Chicago- ANL

This forum focuses on achieving carbon neutrality through the utilization of nuclear energy, specifically emphasizing the role of small modular reactors. Currently, KHNP is developing an innovative SMR (i-SMR) and integrated the i-SMR to a platform of a zero-carbon city model, so call i- SMR Smart Net Zero City (SSNC). The SSNC model uses i-SMR for multi-purpose energy source such as electricity generation, hydrogen generation, district heat, desalination and so on. Through this forum, KHNP introduces the i-SMR design and SSNC digital model development status and shares the valuable insights with UKC members about the effective and optimized development strategies regarding i-SMR and SSNC.

Time	Title and Speaker
1:30 - 1:40 pm	**Welcoming Remarks** // Hyungook Kang, RPI & Ho Cheol Shin, KHNP CRI
1:40 - 1:50 pm	**Introduction of KHNP** // Deokwoo Nam, KHNP CRI
1:50 - 2:10 pm	**Nuclear Energy in the Age of Green Technology** // Hyungook Kang, RPI
2:10 - 2:30 pm	**Ocean Nuclear System for Propulsion and Electricity Generation** // Howard H.Chung, Univ. of Chicago- ANL
2:30 - 2:50 pm	**Safety enhancement and optimal design plan for SMR** // Jiyong Oh, KHNP CRI
2:50 - 3:10 pm	**i-SMR Smart Net-Zero City Business to lead global carbon neutrality** // You Hyun Jang, KHNP
3:10 - 3:40 pm	**Open Discussion** // Jiyong Oh, KHNP CRI
3:40 - 3:50 pm	**Concluding Remarks and Photo** // Hyungook Kang, RPI & Ho Cheol Shin, KHNP CRI

KIAT K-TAG Distinguished Forum

USA Annual General Meeting on Promotion of KOREA-US Technical Cooperation

August 3 _ Thursday _ 2:00pm _ San Antonio

Chair

Byung Joo Min

President
KIAT

Co-Chairs

Jong Y Park

Moffitt Cancer Center

Dong Hoon Yoon

University of Arkansas

The Korea Institute for Advancement of Technology (KIAT) is a comprehensive technology support organization committed to promoting industrial technology growth in Korea. Korea-Technology Advisory Group (K-TAG) USA launched by KIAT in July 2014, consists of Korean science and engineering experts in USA. Main activities of K-TAG are 1) to assist Korean Small and Medium-sized Enterprises (SMEs) in finding USA Innovative partners, 2) to provide advice as well as information related to Korea-USA R&D cooperation and 3) to develop and participate in Korea-USA joint R&D projects. In the UKC 2023, the members of K-TAG USA in various technical areas will get together to 1) seek research collaborations, 2) present/propose innovative research projects and 3) discuss R&D program planning with delegates of KIAT in this forum.

Presenters

Cheon Kyo Park

KIAT

Eunjung Kim

KIAT

Jinha Kim

KIAT

Tom Oh

Rochester Institute of Technology

Sunkyu Park

North Carolina State University

Byung-Guk Jun

Purdue University

Woo Hyoung Lee

University of Central Florida

Jungkwun Kim

University of North Texas

Deok-Ho Kim

Johns Hopkins University

Time	Title and Speaker
2:00 - 2:10 pm	**Welcoming Remarks //** Byung Joo Min (KIAT, President), Youngjin Jang (Vice Minister, MOTIE)
2:10 - 2:20 pm	**K-TAG USA Awards**
2:20 - 3:00 pm	**Collaborative R&D Policy of Korea and Revitalization Korea-US Industrial Cooperation** // Jinha Kim (KIAT, Director), TBC (KEIT)
3:00- 3:50 pm	**Open Discussion //** Vice Minister (MOTIE), President (KIAT), All participants
3:50 - 4:00 pm	**Concluding Remarks and Photo**

* Please note that presentation time and speakers are subject to change depending on session circumstances.

KITECH Distinguished Forum

Forum on Additive Manufacturing

August 3 _ Thursday _ 1:30 _ Room Houston

Chair	Co-Chair	Presenters		
		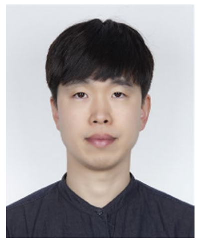		
Kwang Jin Lee Director KITECH USA	**Haseung Chung** Michigan State University	**Cheol Woo Ha** KITECH	**Durim Eo** KITECH	**Holden Hyer** ORNL

Additive manufacturing, commonly known as 3D printing, is progressing rapidly to revolutionize the advanced manufacturing landscape by providing new ways to design component with on-demand and on-site capability. KITECH Distinguished Forum highlights state-of-the-art status on additive manufacturing for various applications including multi-functional (e.g., structure with sensors embedded) and seeks collaborative environment to advance fundamental knowledge in additive manufacturing science.

Time	Title and Speaker
1:30 - 1:50 pm	**Introduction to KITECH** // Kwang Jin Lee, KITECH
1:50 - 2:20 pm	**Recent research on various 3D printing processes using photocuring materials in KITECH** // Cheol Woo Ha, KITECH
2:20 - 2:50 pm	**Challenges and advances in current dissimilar metal additive manufacturing** // Du Rim Eo, KITECH
2:50 - 3:20 pm	**Challenges and Advantages in Additive Manufacturing of High Temperature Strength Resistant Alloys** // Holden Hyer, Oak Ridge National Laboratory
3:20 - 3:30 pm	**Concluding Remarks and Photo** // Haseung Chung, Michican State University

K-Water Distinguished Forum

Forum on Ultra High Purity Water

August 3 _ Thursday _ 1:30pm _ Room Carter

Chair

Hyeon Sik Kim

Vice President & CRO(Chief Research officer) of K-water Research Institute

Co-Chair

Soyoon Kum

Assistant Professor at Angelo State University

Presenters

Jae Hong Kim

Professor Yale University

Young-Shin Jun

Professor Washington University in St. Louis

Kyung Hyuk Lee

Head Researcher of K-water Research Institute

Suk Tae Kang

Professor of KAIST

Jong Chan Yi

Senior Researcher of K-water

Ultrapure water is used for advanced industry such as semiconductor, LCD, Solar panel manufacture. In order to produce UPW (Ultrapure water), water treatment plant for UPW is complicated and require high operation technology. Thus, UPW production is recognized as not only leading-edge technology in the water industry but high value-added industrial water. The Korean government has recently declared to promote Semiconductor industry for national security as well as economic growth. As one of the main infrastructures, key technologies and strategies to promote UPW technology will be discussed.

Time	Title and Speaker
1:30 - 1:40 pm	**Welcoming Remarks** // Hyeon Sik Kim, Chief Research officer of K-Water
1:40 - 2:00 pm	**Membrane-Confined Heterogeneous Advanced Oxidation** // Jae Hong Kim, Professor Yale University
2:00 - 2:20 pm	**Photothermal Membranes for an Environmentally Sustainable and Resilient Clean Water Supply** // Young-Shin Jun, Professor Washington University in St. Louis
2:20 - 2:40 pm	**Promotion of Ultrapure water Technology for Semiconductor Industry in Korea** // Kyung Hyuk Lee, Head Researcher of K-water Research Institute
2:40 - 3:00 pm	**Occurrence and removal of urea during the wastewater reuse for ultra-pure water production** // Suk Tae Kang, Professor of KAIST
3:00 - 3:20 pm	**Advanced analytics techniques for semiconductor industries ultrapure water** // Jong Chan Yi, Senior Researcher of K-water
3:20 - 3:30 pm	**Q&A**

Yuhan Distinguished Forum

Cutting-Edge Research in Oncology

August 3 _ Thursday _ 1:30pm _ Fort Worth

Chair

Jayoung Kim

UCLA

Presenters

Kwon-Sik Park

University of Virginia School of Medicine

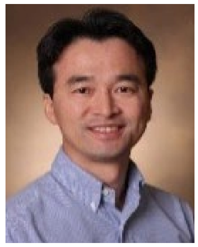

Serkin Park

Korea University College of Medicine

Ju-Seog Lee

UT MD Anderson Cancer Center

Seungwon Chung

Abbvie

Yuhan Corporation is a South Korea-based pharmaceutical company founded in 1926 by Dr. Il-han New, an independence activist, educator and innovative entrepreneur. Yuhan has achieved five out-licensing deals during the past five years, resulting in a total deal size of $3.54 billion. This forum aims to shed light on cutting-edge discoveries and innovative strategies against cancer. Prof. Kwon-Sik Park will discuss the discovery of cancer vulnerabilities by synthesizing human and mouse model data. Prof. Serkin Park will shed light on the biological mechanisms of cancer bone metastasis and present novel diagnosis and treatment strategies. Prof. Ju-Seog Lee will discuss the identification of novel therapeutic targets and the development of targeting approaches, specifically focusing on antisense oligo drugs and metabolic inhibitors. And Seungwon Chung will be sharing insights on the medicinal chemistry efforts in the pharmaceutical company. By bringing together researchers and experts in the field, this forum seeks to accelerate active discussions and collaborations with esteemed academic researchers.

Time	Title and Speaker
1:30 - 1:40 pm	**Welcoming Remarks** // Taejin Yoon, Yuhan Corporation
1:40 - 2:00 pm	**Keynote Talk**
2:00 - 2:20 pm	**Discovery of cancer vulnerability by a synthesis of human and mouse model data** // Kwon-Sik Park, University of Virginia School of Medicine
2:20- 2:40 pm	**Osteoblast-lineage cells as a therapeutic target for breast cancer bone metastasis** // Serkin Park, Korea University College of Medicine
2:40 - 3:00 pm	**Identify novel therapeutic targets and development targeting approaches (antisense oligo drugs and metabolic inhibitors)** // Ju-Seog Lee, UT MD Anderson Cancer Center
3:00 - 3:20 pm	**Medicinal Chemistry effort in pharmaceutical company** // Seungwon Chung, Abbvie
3:20 - 3:30 pm	**Concluding Remarks/ Photo session**

KWiSE Distinguished Forum

KWiSE-WISET Women in STEM Forum in collaboration with KOFWST-KWSE

August 3 _ Thursday _1:00pm _ Developers

Chair

Mihyeon Jeon

Atkins

Co-Chairs

Aree Moon

WISET

Myongsook Oh

KOFWST

Seong Jin Ju

KWSE

Special Guest

Byung-Joo Min

KIAT

Founded in 2004, KWiSE (Korean-American Women in Science and Engineering) is a non-profit organization to promote career development and networking of Korean-American women professionals in the science and engineering fields. Involving all key organizations working for Korean American women in the STEM field in both US and Korea, the main objective of this forum is to exchange ideas on career development, leadership, and empowerment of women in STEM and to discuss potential policies and strategies that are needed to expedite this process. After an opening session by KWiSE and WISET, KWiSE-KWSE Session will discuss the current and planned global collaborations in women in STEM and future directions. Speakers will share examples of various on-going successful global collaborations, including Korea-US and Korea-UK. Based on these examples, we will discuss how women scientists and engineers can further strengthen existing collaboration and foster new collaborations. The KWiSE-KOFWST Session will discuss future directions and vision of organizations working for women in STEM. Vision and path forward of the two organizations (KOFWST and KWiSE) will be shared, then a panel discussion will follow on how to empower women scientists and engineers. This forum is designed to be an interactive and engaging event to foster networking and mentoring among the attendees. The forum will provide an excellent opportunity for the participants to learn from the women leaders in the STEM fields and get inspired to become a future leader in STEM.

Presenters

Jinah Park

KAIST (KWSE)

Young-Sil Kwak

KASI (KWSE)

Minchul Song

ADD (KWSE)

Hee-Kyung Ahn

The Sainsbury Laboratory

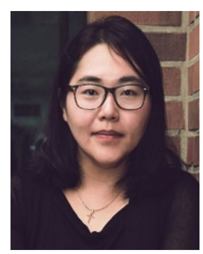

Sungsil Moon

CDC (KWiSE)

Oh Nam Kwon

Seoul National University (KOFWST)

Ran Baik

Honam University (KOFWST)

Eun-Suk Seo

University of Maryland (KWiSE)

Bo Young Park

California State University Fullerton (KWiSE)

Yongho Sohn

University of Central Florida (KSEA)

<table>
<tr><th>Time</th><th colspan="2">Title and Speaker</th></tr>
<tr><td>1:00 - 1:05 pm</td><td colspan="2">Opening by KWiSE President // Mihyeon Jeon, Atkins, KWiSE</td></tr>
<tr><td>1:05 - 1:15 pm</td><td colspan="2">Welcoming Remarks and WISET Lecture by WISET President // Aree Moon, WISET</td></tr>
<tr><td>1:15 - 1:20 pm</td><td colspan="2">Welcoming Remarks from KIAT President // Byung-Joo Min, KIAT</td></tr>
<tr><td>1:20 - 1:30 pm</td><td rowspan="6">KWiSE – KWSE Session: Global Collaborations in Women in STEM</td><td>International Cooperation Activities of KWSE // Seong Jin Ju, KWSE</td></tr>
<tr><td>1: 30 - 1:40 pm</td><td>International Cooperation in Space Science: Focus on Korea-US Cooperation // Young-Sil Kwak, KASI, KWSE</td></tr>
<tr><td>1:40 - 1:50 pm</td><td>Medical Image Computing and Computer-Assisted Intervention – Bringing it to Korea // Jinah Park, KAIST, KWSE</td></tr>
<tr><td>1:50 - 2:00 pm</td><td>Current Status of Korea-US International Cooperation
// Minchul Song, ADD, KWSE</td></tr>
<tr><td>2:00 - 2:15 pm</td><td>Thriving as Women in STEM: Stronger Together
// Heekyung Ahn, The Sainsbury Laboratory, UK</td></tr>
<tr><td>2:15 - 2:30 pm</td><td>Korea-US Collaboration Examples: Examples of US Government Agencies // Sungsil Moon, CDC, KWiSE</td></tr>
<tr><td>2:30 - 2:45 pm</td><td colspan="2">Group Photo Time, Coffe Break</td></tr>
<tr><td>2:45 - 3:00 pm</td><td rowspan="4">KWiSE – KOFWST Session: Future Directions and Vision of Women in STEM</td><td>20 Years of Leadership and Future Vision of KOFWST
// Myongsook Oh, KOFWST</td></tr>
<tr><td>3:00 - 3:10 pm</td><td>What’s Ahead for KWiSE: Vision and Path Forward
// Mihyeon Jeon, Atkins, KWiSE</td></tr>
<tr><td>3:10 - 3:25 pm</td><td>Fostering DE&I and Allyship
// Oh Nam Kwon, Seoul National University, KOFWST</td></tr>
<tr><td>3:25 - 3:55 pm</td><td>Panel Discussion Q&A // Ran Baik, Honam University, KOFWST; Eun-Suk Seo, University of Maryland, KWiSE; Bo Young Park, California State University Fullerton, KWiSE</td></tr>
<tr><td>3:55 - 4:00 pm</td><td colspan="2">Congratulatory Remarks // Yongho Sohn, University of Central Florida, KSEA President
Concluding Remarks and Group Photo Session // Mihyeon Jeon, Atkins, KWiSE</td></tr>
</table>

Sponsor Forum

KBSI Sponsor Forum

Multipurpose Synchrotron Radiation (4GSR):
Current States and Future Prospects at the Korea Basic Science Institute (KBSI)

August 4 _ Friday _ 1:30pm _ Room Vandergriff

Chair

Young-Kee Kim

University of Chicago

Co-Chairs

Sung Kwang Yang

President
KBSI

Hyoung Joong Yun

KBSI

Presenters

Jaehoon Yu

UT Arlington

To promote the collaborative development and utilization of the synchrotron facility, we would like to introduce the recent progress of the new multipurpose synchrotron (4GSR) project and x-ray science programs in Korea. We also invite speakers of accelerator and x-ray science in US society to find a way for future collaboration.

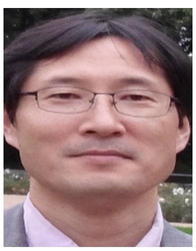

Jae Hun Park

Pohang Accelerator Lab

Seung Hwan Kim

POSTECH

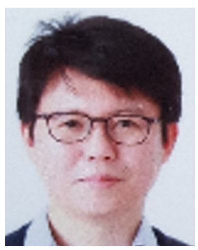

Kyung Tae Ko

KBSI

Won Suk Cha

Argonne National Lab

Time	Title and Speaker
1:30 - 1:35 pm	**Opening Remarks** // Hyoung Joong Yun, Korea Basic Science Institute
1:35 - 1:40 pm	**Welcoming Remarks** // Sung Kwang Yang, Korea Basic Science Institute
1:40 - 1:45 pm	**Introduction Remarks** // Young-Kee Kim, University of Chicago
1:45 - 2:00 pm	**Technical Presentation 1** // Jaehoon Yu, University of Texas, Arlington
2:00 - 2:15 pm	**Technical Presentation 2** // Jae Hun Park, Pohang Accelerator Laboratory
2:15 - 2:30 pm	**Technical Presentation 3** // Kyung Tae Ko, Korea Basic Science Institute
2:30 - 2:45 pm	**Technical Presentation 4** // Won Suk Cha, Argonne National Laboratory
2:45 - 3:25 pm	**Open Discussion** // All participants, Seung Hwan Kim, POSTECH
3:25 - 3:30 pm	**Concluding Remarks and Photo** // Sung Kwang Yang, Korea Basic Science Institute

* Please note that presentation time and speakers are subject to change depending on session circumstances.

KEIT-SWRI Sponsor Forum

Forum on Future Mobility R&D

August 4 _ Friday _ 1:30pm _ Grapevine

Chair

Sunghwan Park

Director of KEIT US

Co-Chair

Terry Alger

SWRI

Korea Evaluation Institute of Industrial Technology (hereafter as ‘KEIT’) signed MoU with South West Research Institute (hereafter as ‘SWRI’) on April 2023 for cooperation in industrial R&D. Since each party agreed to support the cooperative work between the two countries and academic exchange, both parties decided to hold the KEIT-SWRI Academic Forum on Future Mobility R&D in UKC 2023.

Time	Title and Speaker
1:30 - 1:35 pm	**Opening Remarks** // Sunghwan Park and Dr. Terry Alger
1:35 - 1:40 pm	**Welcoming Remarks** // Youngjin Jang, Vice Minister of MOTIE
1:40 - 1:45 pm	**Welcoming Remarks** // Yong Weon Seo, Vice President of KEIT
1:45 - 2:15 pm	**Presentation on Mobility** // KATECH & SWRI
2:15 - 2:45 pm	**Presentation on Batteries** // KETI & SWRI
2:45 - 2:55 pm	**Open Discussion**
2:55 - 3:00 pm	**Concluding Remarks and Photo**

KHIDI Sponsor Forum

Career Development through Research Opportunities in US

August 4 _ Friday _ 1:30pm _ Room Fort Worth

Chair

Soondo Cha

President of KHIDI

Co-Chair

Youngmi Ji

NIH

Presenters

Sanghun Shin

KHIDI

Hoi Sung Chung

NIH

Young-Sup Yoon

Emory university

Jun-Ho La

UTMB

This forum sponsored by Korea Health Industry Development Institute (KHIDI) aims to provide a platform for Korean researchers who wish to gain training experience in the US where researchers with training experience in the US can share their experiences and opportunities. The purpose is to gather opinions presented in this forum and incorporate them into future implementation of the personnel exchange program conducted by KHIDI.

Time	Title and Speaker
1:30 - 1:40 pm	**Welcoming remarks and KHIDI introduction** // Soondo Cha, KHIDI
1:40 - 1:50 pm	**Introduction to KHIDI and KVSTA program** // Sanghun Shin, KHIDI
1:50 - 2:15 pm	**Introduction to research Opportunities at NIH** // Hoi Sung Chung, NIH
2:15 - 2:40 pm	**Post-doc experience sharing - I** // Young-Sup Yoon, Emory University
2:40 - 3:05 pm	**Post-doc experience sharing - II** // Jun-Ho La, UTMB
3:05 - 3:30 pm	**Q & A** // Youngmi Ji, NIH

KICT Sponsor Forum

AI-based Innovative Technology for Advanced Urban Infrastructure Management:
Focusing on Autonomous Driving and Flash Flood

August 4 _ Friday _ 1:30pm _ Room Lone Star I

Chair

Seung-Ki Ryu

Director
KICT

Co-Chair

Sung-Hee (Sonny) Kim

University of Georgia

Korea Institute of Civil Engineering and Building Technology (KICT) is Korea's only government-funded research institute in the area of construction technology. Drawing on the unrivaled R&D capacities we have accumulated over upwards of 40 years, we are an institution dedicated to our social roles and responsibilities as a body for research. In this context, this forum serves as a platform to foster discussion about AI-based innovative technology for infrastructure management by presenting studies and projects from the U.S. and Korea.

Presenters

Jaehong Park

Senior Researcher
KICT

AdamKasliszewks

Project Delivery
Director, CAVNUE

Hyung-Jun Kim

Senior Researcher
KICT

Jaehak Jeong

Professor
Texas A&M University

Dong Sop Rhee

Research Fellow
KICT

Time	Title and Speaker
1:30 - 1:35 pm	**Welcome Remarks** // Hyeonjun Kim, Vice President for Research of KICT
1:35 -1:45 pm	**KICT's Research Activities** // Kang-Suk Kim, Head of Research Policy Division, KICT
1:45 - 2:00 pm	**Innovative Highway Design and Management for Autonomous Driving Environment** // Jaehong Park, Senior Researcher, KICT
2:00 - 2:15 pm	**The Future of Roads** // Adam Kasliszewks, Project Delivery Director, CAVNUE
2:15 - 2:30 pm	**Development of AI Flood Analysis and Forecasting Method based on Intelligent Information Technology** // Hyung-Jun Kim, Senior Researcher, KICT
2:30 - 2:45 pm	**Hydrologic Assessment of Urban Green Infrastructure** // Jaehak Jeong, Professor, Texas A&M University
2:45 - 3:00 pm	**Development of Technology to Reduce Urban Flood Damage through Simulated Inundation on the Environmental Facility** // Dong Sop Rhee, Research Fellow, KICT
3:00 - 3:20 pm	**Panel Discussion** // Chairs and Speakers
3:20 - 3:30 pm	**Concluding Remarks and Group Photo** // All

KISTEP Sponsor Forum

R&D Directions and Policies for Dual-Use Technology

August 4 _ Friday _ 1:30pm _ Room Dallas

Chair

Byung-Seon Jeong

KISTEP

Co-Chair

Tom Oh

Rochester Institute of Technology

Presenters

Seung-Hyuk Lim

KISTEP

Kyung-Shick Choi

Boston University

Brian Shipley

US Navy

Lae Hyunk Kim

KIST

KISTEP Forum on "*R&D Directions and Policies for Dual-Use Technology*" will seek efficient application and linkage of dual-use technology between civil and defense science and technology including commercialization. The forum will find ways to promote cooperation between Republic of Korea and the United States to learn and merge directions and policies through comparison and analysis.

Time	Title and Speaker
1:30 - 1:35 pm	**Welcome Remarks** // Young Chang Joo, Vice Minister for S&T and Innovation, MSIT
1:35 - 1:45 pm	**Welcome Remarks / Introduction to KISTEP** // Byung-Seon Jeong, KISTEP
1:45 - 2:10 pm	**The importance of effectively applying and linking dual-use technologies** // Seung-Hyuk Lim, KISTEP
2:10 - 2:35 pm	**Navigating the Nexus of Data Protection and Information Sharing in Government Cybersecurity** // Kyung-Shick Choi, Boston University
2:35 - 3:00 pm	**Overview of US NAVY SBIR/STTR programs** // Brian Shipley, US Navy
3:00 - 3:25 pm	**S. Korea-US cooperation on Defense R&D** // Lae Hyunk Kim, KIST
3:25 - 3:30 pm	**Closing Remarks and Photo** // All participants

* 10 minutes of presentation (+10 minutes of consecutive interpretation) followed by 5 minutes of Q&A

KITECH Sponsor Forum

Forum on Rare Metals: Eco-Friendly Processing Technology and Applications

August 4 _ Friday _ 1:30pm _ Room Houston

Chair

Kwang Jin Lee

Director of KITECH USA

Co-Chair

Yang-Ki Hong

University of Alabama

Presenters

Kyoung Tae Park

KITECH

Jun Hee Han

KITECH

Lee Seung Kang

ORNL

KITECH Forum focuses on analyzing the current state of the rare metal industry in Korea and highlight the role of the Korea Institute for Rare Metals (KIRAM) at the Korea Institute of Industrial Technology (KITECH). Furthermore, we introduce the infrastructure development projects and research and development (R&D) cases of KIRAM especially on the topic of eco-friendly processing technology and applications, and discuss strategies for enhancing the competitiveness of the Korean rare metal industry and stabilizing the supply chain in the rapidly changing global value chain (GVC) environment.

Time	Title and Speaker
1:30 - 1:40 pm	**Welcome and Introduction to KITECH KIRAM** // Kwang Jin Lee, KITECH
1:40 - 2:05 pm	**Introduction to rare metal industries in Korea** // Kyoung Tae Park, KITECH
2:05 - 2:30 pm	**Overview of research activities in KIRAM** // Jun Hee Han, KITECH
2:30 - 2:55 pm	**Target technology for rare metals processing** // Lee Seung Kang, KITECH
2:55 - 3:20 pm	**Design of magnetic materials and permanent magnet synchronous motors for electric vehicles** // Yang-Ki Hong, University of Alabama
3:20 - 3:30 pm	**Concluding Remarks and Photo** // Chair and Co-Chair

Seoul National University (SNU) Sponsor Forum

Forum on Transformative Actions: Pioneering the Future

August 4 _ Friday _ 1:30pm _ Room Austin

Chair

Jae Young Kim

Executive Vice President for Research Affairs
Seoul National University

Co-Chair

Jaejun Yu

Dean
College of Natural Sciences
Seoul National University

Presenters

Jaejin Lee

Dean
Graduate School of Data Science,
Seoul National University

Junseok Hwang

Director
Global R&DB Center
Seoul National University

Junsuk Kang

Director
Specialized Graduate School of Intelligent Eco-Science
Seoul National University

Seoul National University, a prestigious educational institution renowned for its academic excellence, has consistently pushed boundaries and fostered innovation across various disciplines. This forum serves as a platform to explore and celebrate the transformative actions taken by SNU in paving the way for a brighter and more progressive future.

This forum aims to shed light on the diverse initiatives that have been instrumental in shaping SNU's transformative actions. From groundbreaking research projects and interdisciplinary collaborations to community engagement and sustainability efforts, SNU has left an indelible mark on society.

This forum provides an open and inclusive space for meaningful conversations. Together, let us explore the diverse facets of SNU's transformative actions and their profound impact on the future.

Time	Title and Speaker
1:30 - 1:35 pm	**Welcoming Remarks** // Jae Young Kim, SNU
1:35 - 2:00 pm	**SNU College of Natural Sciences: Driving Innovation and Discovery** // Jaejun Yu, SNU
2:00 - 2:25 pm	**SNU Graduate School of Data Science** // Jaejin Lee, SNU
2:25 - 2:50 pm	**Global Vision for Smart City & Future University** // Junseok Hwang, SNU
2:50 - 3:15 pm	**SNU Specialized Graduate School of Intelligent Eco-Science** // Junsuk Kang, SNU
3:15 - 3:25 pm	**Open Discussion**
3:25 - 3:30 pm	**Concluding Remarks and Photo**

UNIST Sponsor Forum

The Path to Carbon Neutrality: Electrification, Decarbonization, and CO_2 Capture

August 4 _ Friday _1:30pm _ Room Hobby

Chair

Tae-Hyuk Kwon

Dean of College of Natural Science
UNIST

Co-Chair

Jungki Ryu

Associate Professor
UNIST

Presenters

Dong Suk Kim

Professor
UNIST

Tae Seok Moon

Associate Professor
Washington University in St. Louis

Sunkyu Park

Professor
North Carolina State University

Wonyoung Choe

Professor
UNIST

This symposium brings together leading experts to explore innovative approaches for achieving carbon neutrality. Topics include efficient perovskite solar cells, cutting-edge CO_2 capture technologies, electrochemical synthesis of chemicals, production of sustainable fuels from biomass, and synthetic biology for plastics upcycling. Participants will engage in discussions and presentations highlighting breakthrough research and advancements in these areas. The symposium aims to accelerate the global transition towards a sustainable and carbon-neutral future by fostering collaboration and knowledge exchange. By delving into these diverse fields, attendees will uncover transformative solutions, paving the way for renewable energy, effective carbon capture, sustainable chemical production, biomass utilization, and waste upcycling. Together, they strive to create a cleaner and greener world for generations to come.

Time	Title and Speaker
1:30 - 1:35 pm	**Welcoming Remarks** // Tae-Hyuk Kwon, UNIST
1:35 - 1:55 pm	**Major Innovative Trends in Perovskite Solar Cells** // Dong Suk Kim, UNIST
1:55 - 2:15 pm	**Beyond Catalysts: Exploring Systematic Approaches and Alternative Electron Sources in Electrolysis** // Jungki Ryu, UNIST
2:15 - 2:35 pm	**Sustainable Aviation Fuel Production from Waste Streams in Pulp and Paper Industry** // Sunkyu Park, North Carolina State University
2:35 - 2:55 pm	**Engineering Novel Microbes for Upcycling Waste Plastic and Solving the Climate Crisis** // Tae Seok Moon, Washington University in St. Louis
2:55 - 3:15 pm	**Metal-Organic Materials for Carbon Neutrality Applications** // Wonyoung Choe, UNIST
3:15 - 3:30 pm	**Panel Discussion** // Presenters/Panel Participants
3:30 pm	**Concluding Remarks and Photo** // Tae-Hyuk Kwon, UNIST

KSEA Forum

KSEA Science Policy Forum (closed session, invited only)

August 3 _ Thursday _ 10:30am _ Room Austin

Chair

Seunghwan Kim

POSTECH

Moderator

Jaehoon Yu

University of Texas, Arlington

The Science Policy Forum (SPF) will bring together key scientists and law makers in the U.S. and Korea to strengthen their network and collaboration on science and technology policy. In particular, scientists and policy makers can share ideas and best strategies for cooperation on frontier technologies of mutual interests and emerging technologies in the era of global technology supremacy. Policies of bilateral cooperation on science and technology can be discussed such that they could further enhance stronger global collaboration between scientists and policy makers between Korea and the United States.

Time	Title and Speaker
10:30 - 10:40 am	**Welcoming Remarks** // Presidents of KSEA & KOFST
10:40 - 10:50 am	**Theme Introduction** // Jaehoon Yu (University Texas, Arlington)
10:50 - 11:10 am	**U.S. Space Technology and policy** // Eunsuk Seo (University of Maryland)
11:10 - 11:30 am	***TBD** // Korean Leaders in Science & Technology
11:30 - 12:20 pm	**Speeches and Moderated Free Form Discussions** // Invited Participants
12:20 - 12:30 pm	**Concluding Remarks and Photo**

*To be confirmed

KSEA Science Diplomacy Forum

August 3 _ Thursday _ 1:30pm _ Room Austin

Chair

Jaehoon Yu

University of Texas, Arlington

Moderator

Seunghwan Kim

POSTECH

Recently, a compounded wave of global crises involving technology war and security has been affecting the scientific community as well as our society, countries, and world at all levels. As we are heading into more complex, uncertain, and conflict-prone future, it calls for proactive involvements and viable contributions from a global network of science and technology communities in addressing global challenges to our common future.

In this session, we discuss some of the key lessons learned from our experience on global agenda involving science and technology and share our thoughts on the newly found impact and the role of a global cooperation by scientific communities for a sustainable future for all. We discuss how a diverse non-government and government actors can and should work together on science and diplomacy to navigate the complexities of current and future global challenges to human survival and prosperity.

In particular, the Science Diplomacy Forum will serve as a town meeting platform for strengthening science and technology collaboration between South Korea and the United States with partners around the world and exploring the role of scientific organizations and institutions, for example, KSEA and KOFST, in promoting dialogues and bridging the growing networks between scientific and diplomatic communities to better cope with common challenges together.

Time	Title and Speaker
1:30 - 1:40 pm	**Welcoming Remarks** // Presidents of KSEA & KOFST
1:40 - 1:50 pm	**Theme Introduction** // Seunghwan Kim (POSTECH)
1:50 - 2:10 pm	**Keynote Presentation** // Eunsuk Seo (University of Maryland)
2:10 - 2:35 pm	**Presentations** // Sung-Kwang Yang (Korea Basic Science Institute, KBSI), Jeongwook Eom (KOFST)
2:35 - 3:25 pm	**Open Discussions** // Jinwon Kang(KISTEP), KSEA leaders* + CEO Myonghoon Chong*
3:25 - 3:30 pm	**Concluding Remarks and Photo**

*To be confirmed

KSEA R&D Leadership Forum

Roundtable Discussion on R&D Culture and Collaboration

August 3 _ Thursday _ 4:00pm _ Room Developers

Research institutes operated for/by government and private sectors have well-defined and focused missions for technological development and/or scientific knowledge that rely on strong foundational expertise, culture, and capability. Increasingly complex and interdisciplinary requirements for substantial and meaningful outcomes warrant an expansive network of R&D expertise, inclusive activities, and efficient administration. This roundtable discussion will examine the mission, capability, and accomplishment of various research institutes, explore the potential roles of complimentary resources to enhance the mission-critical and mission-supporting R&D activities, and discuss cultural understanding and potential mechanisms needed to further promote US-Korea interactions in R&D.

Chair

Tae (Tom) Oh

Professor
Rochester
Institute of
Technology

Presenters

Rebecca Lynn Spyke Keiser

Chief of Research Security
Strategy and Policy
National Science
Foundation

Jeremy Epstein

Program Director
Secure and
Trustworthy
Cyberspace (SaTC)
Lead Division of
Computer
and Network Systems
(CISE/CNS)
National Science
Foundation (NSF)

R&D Leaders from Korea

Kwang Bok Lee

President
KUSCO / NRF

Soondo Cha

President
KHIDI

Byung-Seon Jeong

President
KISTEP

Sanghoon Lee

Director
KFRI

Joonyeon Chang

Director-General
KIST

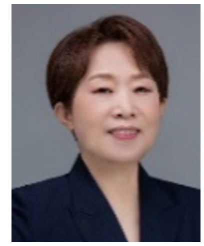

Byung Joo Min

President
KIAT

Sung Kwang Yang

President
KBSI

Young Min Choi

Vice President
KRICT

Jaehyung Kim

CTOof Hanwha
Solutions

Young-Deuk Park

President
KASI

Seungki Park

President
KAIA

Time	Title and Speaker
4:00 - 4:05 pm	**Welcome Remarks** // Tae (Tom) Oh, Professor Rochester Institute of Technology
4:05 - 5:00 pm	**Introduction from the R&D Leaders: Mission, Capability and Accomplishments** // All R&D Leaders
5:00 - 5:10 pm	**National Science Foundation** // Jeremy Epstein, Program Director Secure and Trustworthy Cyberspace (SaTC)
5:10 - 5:20 pm	**National Science Foundation** // Rebecca Lynn Spyke Keiser, Chief of Research Security Strategy and Policy , National Science Foundation
5:20 - 5:50 pm	**Roundtable Discussion** // All R&D Leaders
5:50 - 6:00 pm	**Closing Remarks and Photo** // Tae (Tom) Oh and all participants

- KAIA - Korea Agency for Infrastructure Technology Advancement
- KASI - Korea Astronomy and Space Science Institute
- KBSI - Korea Basic Science Institute
- KFRI - Korea Food Research Institute
- KHIDI - Korea Health Industry Development Institute
- KIAT - Korea Institute for Advancement of Technology
- KIST - Korea Institute of Science and Technology
- KRICT - Korea Research Institute of Chemical Technology
- KUSCO - Korea-US Science Cooperation Center

KSEA University Leadership Forum

August 3 _ Thursday _ 4:00pm _ Room Wetzel

Chair Co-Chair Presenters

김영기

University of Chicago

정병선

한국과학기술기획평가원 원장

권순기

경상국립대학교 총장

홍원화

경북대학교 총장

이용훈

UNIST 총장

김재관

GIST 대외협력처장

염재호

태재대학교 총장

김재영

서울대학교 연구부총장

최기주

아주대학교 총장

장윤금

숙명여자대학교 총장

윤의준

KENTECH 총장

Local cities in Korea are having a hard time due to population decline and urban concentration. Local issues do not simply end as local issues, they are issues of Seoul and of Korea as a whole. Korea is currently aiming to foster regionally specialized projects as one of the measures for local issues. Under this goal, the first session will focus on how local governments, universities, government-funded research institutes, and companies can create a healthy ecosystem that can create synergies with each other. Korea aims at sports as a specialized project in the current situation of local issues, and under this goal, the second session will focus on how local governments, universities, government agencies, and companies can stick together the soil in how to visit the site.

Time	Title and Speaker
4:00 - 4:05 pm	**Welcome Remarks //** 김영기 University of Chicago, 정병선 한국과학기술기획평가원 원장
4:05 - 4:10 pm	**Sponsor Introduction**
4:10 - 5:00 pm (25' remarks + 25' discussion)	**한국은 현재 지방 문제의 한 방안으로서 지역 특화사업 육성을 목표하고 있는데, 이런 목표 하에서 지방 자치단체, 대학, 정부 출연 연구소, 기업들이 어떻게 서로 시너지를 낼 수 있는 건강한 생태계를 만들어 낼 것인가?** • 경상국립대학교 권순기 총장 (Moderator) • 경북대학교 홍원화 총장 • UNIST 이용훈 총장 • 광주과기원 김재관 대외협력처장
5:00 - 5:50 pm (25' remarks + 25' discussion)	**지역의 연구 인력 문제, 지역 소멸 문제는 Globalization에서 일부 해답을 찾을 수가 있는데, Globalization을 추구함에 있어서 도시, 대학, 연구소, 기업들에게는 어떤 전략이 필요한가? Globalization의 관점에서 도시와 대학과의 관계는 어떻게 발전 시킬 것인가?** • 태재대학교 염재호 총장 (Moderator) • 서울대학교 김재영 연구부총장 • 아주대학교 최기주 총장 • 숙명여자대학교 장윤금 총장 • KENTECH 윤의준 총장
5:50 - 6:00 pm	**Concluding Remarks and Photo**

KSEA History Committee Forum

Reflection of KSEA History in 120 Years of Korean Immigration to the United States

August 5 _ Saturday _ 8:00am _ Developers

Chair

Chueng-Ryong Ji

North Carolina State University

Co-Chair

Soolyeon Cho

North Carolina State University

The influence from the historical background appears indispensable in understanding the first generation of Korean-American, in particular, the inherited volunteerism that manifested in founding the KSEA a half century ago. In this forum, the KSEA history will be reflected in broader perspectives of Korean immigration to US for the last 120 years.

Time	Title and Speaker
8:00 - 8:15 am	**Welcoming Remarks and Group Photo** // Yongho Sohn, KSEA President and all participants
8:15 - 9:30 am	**Forebears of Korean Immigration** // Chueng-Ryong Ji
	Early History of Korean Students in US // Kang-Wook Lee
	What is history? // Sung-Kwon Kang
	Early Years of KSEA // Chan-Mo Park
	Academic Contributions // K. Wayne Lee
	Entrepreneurship Development, KSEA Demography // Myung Jong Lee
	Demography of Women Scientists and Engineers // Eun-Suk Seo
	ESTEEM Video Project and the 120 Years Anniversary Book // Jahae Yun
	Video Remarks from the family of the Late Professor Shoon Kyung Kim // Matt Kim and Mrs. Jeung Hi Kim
	Video Presentation of Young Generation Perspectives // Jonathan Kim and YGs
9:30 - 9:55 am	**KSEA and Collaboration Opportunities with Korean Societies including Korean American Association and Community Center (KAACC)** // Casey Youn (KAACCH President), Sam Sangsoo Ryu (ExxonMobil Shipyard Program Manager)
9:55 - 10:00 am	**Concluding Remarks** // Chueng-Ryong Ji and Soolyeon Cho

Scholarship Winners

2023 KSEA - KUSCO Graduate Scholarship Winners

Bo Ra Kim
University of
Texas at Austin

Chunghwan Kim
Arizona State University

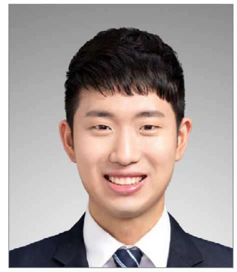

David Ha Eun Kang
MIT

Woojung Lee
Columbia University

Jaehoan Kim
Texas A&M University

Ji-young Lee
Touro College of
Pharmacy

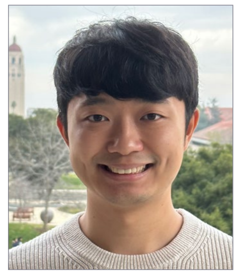

Jinwon Oh
Stanford University

Kyeong Joo Jung
Ohio State University

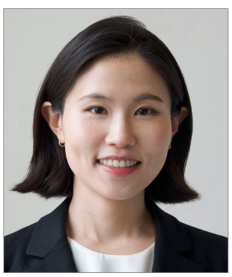

Lucie Ahn
Case Western
Reserve University

Minchae Chloe Kang
Texas A&M University

Saeyeong Jeon
University of Florida

Sanghyun Jeon
UIUC

Serin Lee
MIT

Seungri Kim
The City College
of New York

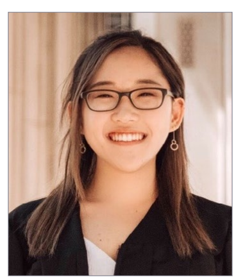

Seungweon Park
Vanderbilt University
School of Medicine

Soohwan Kim
Georgia Institute of
Technology

Soonmyung Hwang
Icahn School of Medicine
at Mount Sinai

Taeyoon Jung
University of Washington

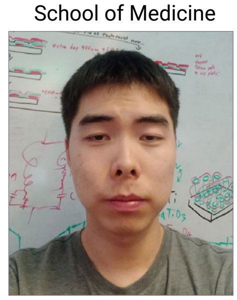

Ilhan Bok
University of
Wisconsin-Madison

Yejin Ki
University of Pittsburgh
School of Dental Medicine

UKC 2023 Sponsors

Co-Organizations

KOFST
Korean Federation of Science & Technology Societies

KUSCO NRF
KOREA-U.S. SCIENCE COOPERATION CENTER
National Research Foundation of Korea

Platinum Sponsor

재단법인 씨젠의료재단
Seegene Medical Foundation

UKC 2023 Sponsors

Gold Sponsors

- CHEY — CHEY INSTITUTE FOR ADVANCED STUDIES
- KEIT — Korea Planning & Evaluation Institute of Industrial Technology
- 한국수력원자력주식회사 — KOREA HYDRO & NUCLEAR POWER CO., LTD
- KITECH — 한국생산기술연구원
- KIAT — Korea Institute for Advancement of Technology
- YUHAN
- K water

Silver Sponsors

- 한양대학교 — HANYANG UNIVERSITY
- KBSI — 한국기초과학지원연구원 — KOREA BASIC SCIENCE INSTITUTE
- KHIDI — 한국보건산업진흥원 — Korea Health Industry Development Institute
- KICT — 한국건설기술연구원
- KIST — Korea Institute of Science and Technology
- KISTEP — 한국과학기술기획평가원 — Korea Institute of S&T Evaluation and Planning
- KNU — 경북대학교 — KYUNGPOOK NATIONAL UNIVERSITY
- beyond the best — KUMHO PETROCHEMICAL
- 서 울 대 학 교 — SEOUL NATIONAL UNIVERSITY
- UCF — UNIVERSITY OF CENTRAL FLORIDA
- TAEJAE UNIVERSITY
- UNIST — 울산과학기술원 — ULSAN NATIONAL INSTITUTE OF SCIENCE AND TECHNOLOGY

UKC 2023 Sponsors

Bronze Sponsors

UKC 2023 Sponsors

General Sponsors

Friends of KSEA

Media Partner

KUSCO
KOREA-U.S. SCIENCE COOPERATION CENTER

The Korea-U.S. Science Cooperation Center (KUSCO) is a non-profit organization established in Vienna, Virginia, founded in 1997, to accomplish two major missions: to enhance cooperative efforts in S&T between Korea and the U.S. and to support Korean - American scientists & engineers in the United States.

VISION & MISSION

The vision of KUSCO is *"Advancement of the S&T collaborations between Korea and the U.S."*
To realize its vision, KUSCO pursues the mission of becoming a premium center for S&T cooperation and Exchanges by pursuing three goals as follows:

- To strengthen S&T cooperation portfolio between Korea and the U.S.
- To broaden global exchange programs
- To support and leverage Korean-American scientists and engineers

MAJOR ACTIVITIES

- Enhance scientific and technological development of both Korea and the U.S.
- Support mutual cooperation and initiate joint programs with U.S. and Korean scientific and engineering societies, academic universities, and other institutions
- Assess significant trends in scientific research and technological developments affecting Korea and the U.S.
- Assist young Korean-American and other scientists in developing and maintaining networks addressing matters of scientific and technical interest to the two countries


CHEY 최종현학술원
CHEY INSTITUTE FOR ADVANCED STUDIES
Scientific Innovation
Geopolitical Risk
Scientific Innovation & Geopolitical Risk
The Chey Institute for Advanced Studies is a non-partisan think tank with the aim to explore the geopolitical dynamics and avenues of scientific innovation in Northeast Asia and beyond. It was established in October 2018 to commemorate the 20th anniversary of the passing of Chairman Chey Jong-hyon, former Chairman of SK group.


Keit 한국산업기술평가관리원
Korea Evaluation Institute of Industrial Technology
R & D
D
연구개발에서 사업화까지
한국산업기술평가관리원이
기업의 성장 속도에
힘이 되겠습니다
때로는 과감하게,
때로는 신중하게,
기업들이 안전하게 성공하도록
기술 개발에 모든 과정마다
든든한 조력자가 되어드립니다
KEIT와 함께
기업의 성장과 국민의 행복에
끝까지 완주하세요
기술주도 혁신성장,
기술기반 산업강국을
향해 나아갑니다
첨단산업 성장기반
기술확보
• 미래전략산업 초격차 기술 확보
• 4차 산업혁명 선도기술 기반 강화
• 생명·안전·재난 대응 유망기술 확보
주력산업의
기술고도화 촉진
• 제조업 고부가가치화 촉진
• 차세대 모빌리티 혁명 기술 리드
• 공급망 선도기술 확보
R&D 혁신 생태계
강화
• 도전적·혁신적 R&D 강화
• 혁신기업의 성장잠재력 확충
• 성과중심 R&D 시스템 강화
성과중심 경영시스템
정착
• 기관운영의 효율성 제고
• 경영혁신 기반 강화
• ESG 경영체제 확립

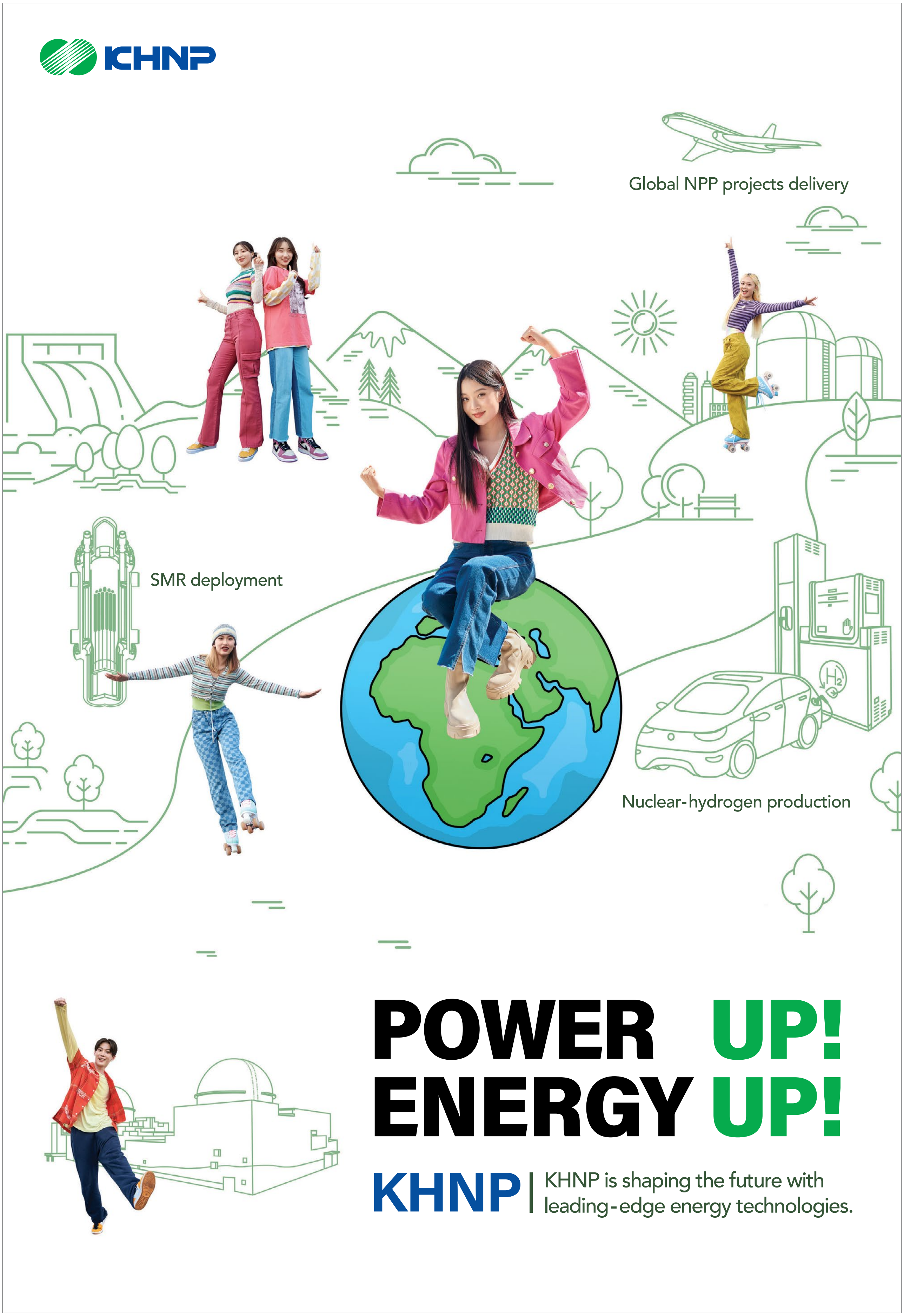
KHNP
Global NPP projects delivery
SMR deployment
Nuclear-hydrogen production
POWER UP!
ENERGY UP!
KHNP | KHNP is shaping the future with leading-edge energy technologies.


KIAT, the innovative growth platform leading future of industrial transformation
KIAT supports specialized human resources, research equipment, R&D funding, commercialization, and international cooperation to execute projects of industrial technology innvation and policy development. Especially, we promote open innovation through international joint R&D and also contribute to industrial development in developing countries through industrial energy ODA.
KIAT will help companies improve their competitiveness in the era of industrial transformation, foster industrial innovation talent that responds to technological paradigm shifts and secure stable global supply chain.
KIAT
Korea Institute for Advancement of Technology

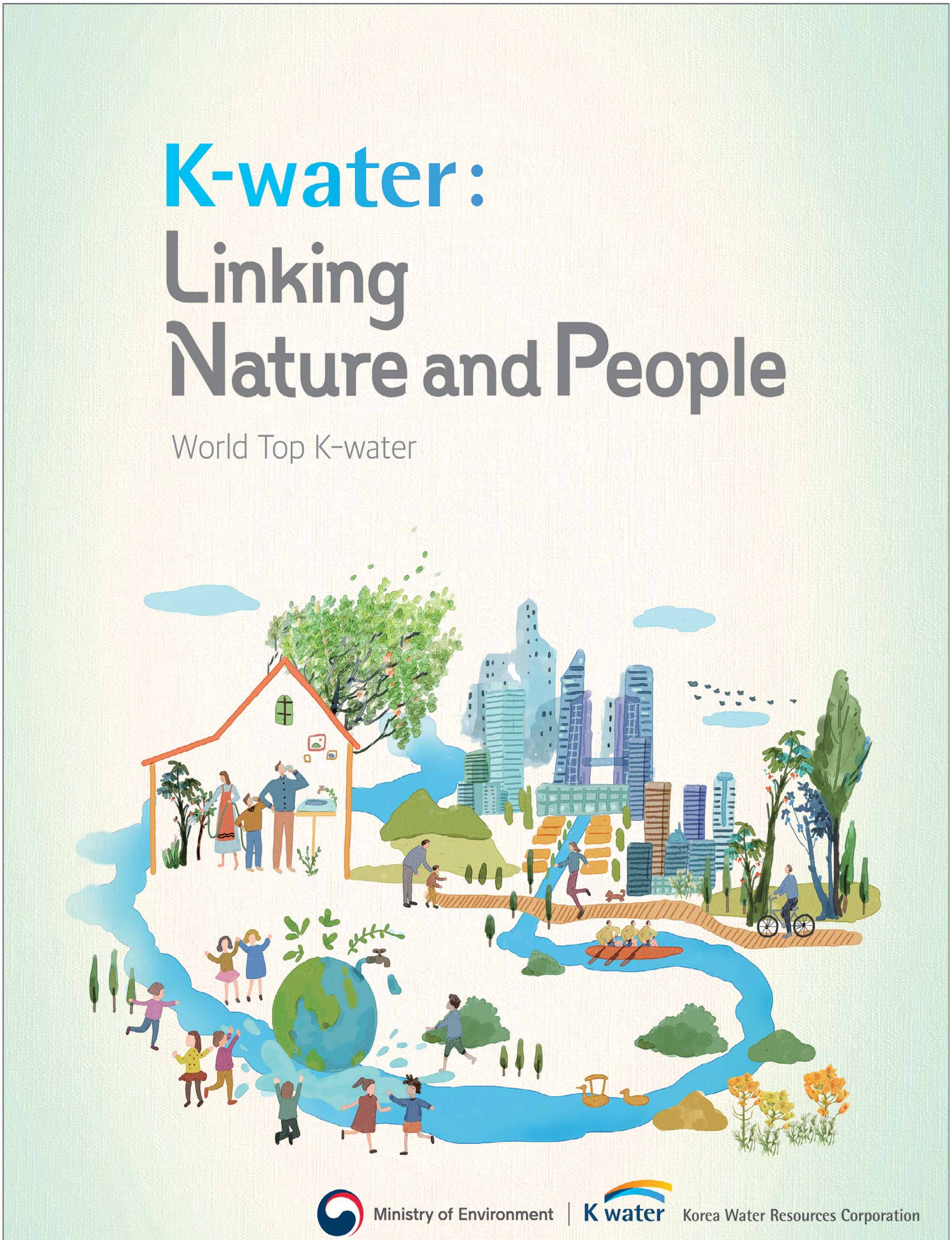
K-water :
Linking
Nature and People
World Top K-water
Ministry of Environment
K water
Korea Water Resources Corporation

KOREA BASIC SCIENCE INSTITUTE

KBSI seeks to implement customer value management(CVM) and quality management system with a set of state-of-the-art research equipment and quality workforce. Utilizing these resources, we will become a leading national institute for co-utilization of research equipment and research support.

Securement of competitiveness in analytical services

·Accumulating know-how in analytical management; developing analytical technologies; enhancing analytical performance and quality management system; and improving the operation system

Research support for joint research involving industrial, academic, and research institutes

·Establishing open research infrastructure for convergence and cooperation Nationwide research support network

National research support network

·Establishing research infrastructure for open research convergence and cooperation

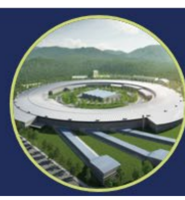

Reaching for the Stars,
the Choice of Visionarie
Kyungpook National University
Selected for the local government university cooperation-based Regional Innovation System (RIS)
Selected for the Leaders in Industry-university Cooperation 3.0 (LINC 3.0)
Ranked 13th in the world and 1st among Korean universities in the 2022 THE University Impact Rankings
KNU KYUNGPOOK NATIONAL UNIVERSITY

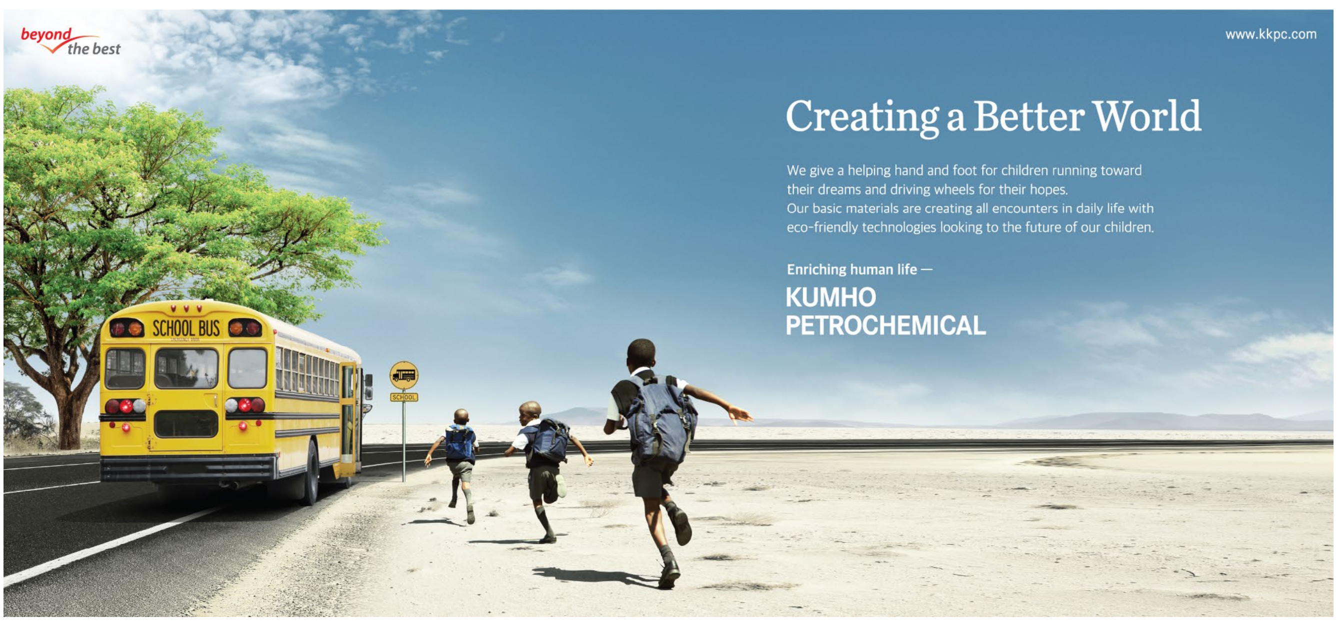

beyond the best
www.kkpc.com
Creating a Better World
We give a helping hand and foot for children running toward their dreams and driving wheels for their hopes.
Our basic materials are creating all encounters in daily life with eco-friendly technologies looking to the future of our children.
Enriching human life —
KUMHO PETROCHEMICAL
SCHOOL BUS


Excelling at "Things that Must Be Done"
기술혁신의 속도가 사람을 압도하는 시대,
우리는 이 시대가 요구하는 변화를 이끌어내야 합니다.
인류를 위해 '해야 할 일'을 잘하는 대학
UNIST가 과학기술로 미래를 선도합니다
울산과학기술원
ULSAN NATIONAL INSTITUTE OF SCIENCE AND TECHNOLOGY
www.unist.ac.kr
+82 52-217-0114

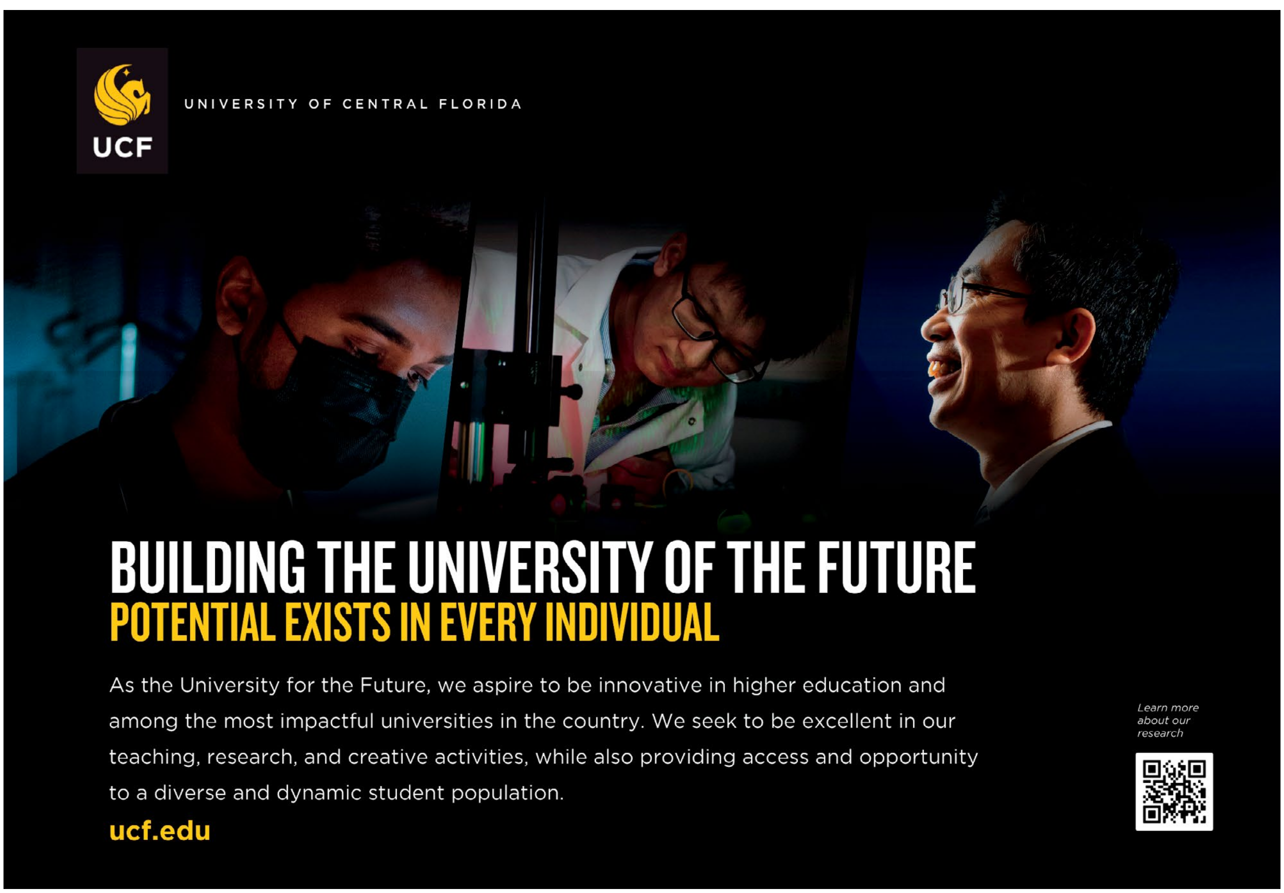
UCF
UNIVERSITY OF CENTRAL FLORIDA
BUILDING THE UNIVERSITY OF THE FUTURE
POTENTIAL EXISTS IN EVERY INDIVIDUAL
As the University for the Future, we aspire to be innovative in higher education and among the most impactful universities in the country. We seek to be excellent in our teaching, research, and creative activities, while also providing access and opportunity to a diverse and dynamic student population.
ucf.edu
Learn more about our research


Sustainable solutions
to advance the world
인류의 더 나은 삶과 지속가능한 미래.
우리는 기후 변화에 대응하는 글로벌 선도 기업으로
스마트한 친환경 에너지 솔루션과
고객 관점의 제품, 서비스를 통해
새로운 기회를 창출하며 인류의 행복한 삶에 기여합니다.
지속가능한 미래를 앞당기는 솔루션.
한화솔루션이 새로운 세상을 열어갑니다.
한화솔루션


70th anniversary
in 2024
인하대학교
INHA UNIVERSITY
새로운 혁신의 출발점에 서다
1960년, 미지의 세계를 향해
로켓을 발사한 인하대의 도전을 기억합니다.
누구도 꿈꾸지 못했던 도전에 성공한 인하대학교는
지금도 새로운 미래를 준비하며
첨단분야 학과를 신설하고 융합 교육을 통해
4차 산업혁명을 이끌어갈
미래 인재를 양성하고 있습니다.
Inspiring the Future,
Innovating Together
인하, 더 높아진 가능성 위에서
시작하다
DEPARTURE
INHA University, Where Excellence Meets Opportunity


KAIST
QAIST New Culture Strategy
for the Next 50 Years of KAIST
Question
Creative Talent
Education
Talents who ask questions
• Education program innovation
• Education method innovation
• Leadership building
• 1 lab 1 book
Advanced Research
Post AI Research
Research
Question-defining Research
• What, not How
• Creative/challenging research
• Affective AI, Brain research
• 1 lab 1 first research
Internationalization
Global Talent
Globalization
World Bridge KAIST
• Campus globalization
• Joint international research
• Spreading the KAIST Model
• 1 lab 1 foreigner
Start-up
Financial Independence
Technology Commercialization
Global Value Creation
• Startup support
• Field/overseas training
• Create funds through tech commercialization
• 1 lab 1 venture
Trust
Shared Vision
Value of Trust
Building Trust
• Nurture trustful talent
• Transparent fund operation
• Innovation for trustful management
• 1 lab 1 volunteer service
Korea Advanced Institute of Science & Technology


KENTECH
Korea Institute of Energy Technology
에너지 혁신의 무한한 상상력
We( )Energy
에너지 AI
에너지 신소재
차세대 그리드
수소 에너지
환경·기후기술
미래 에너지 산업을 주도할
차세대 기술을 연구하고 에너지 리더를 양성하는
세계 유일의 에너지 특화 대학입니다.

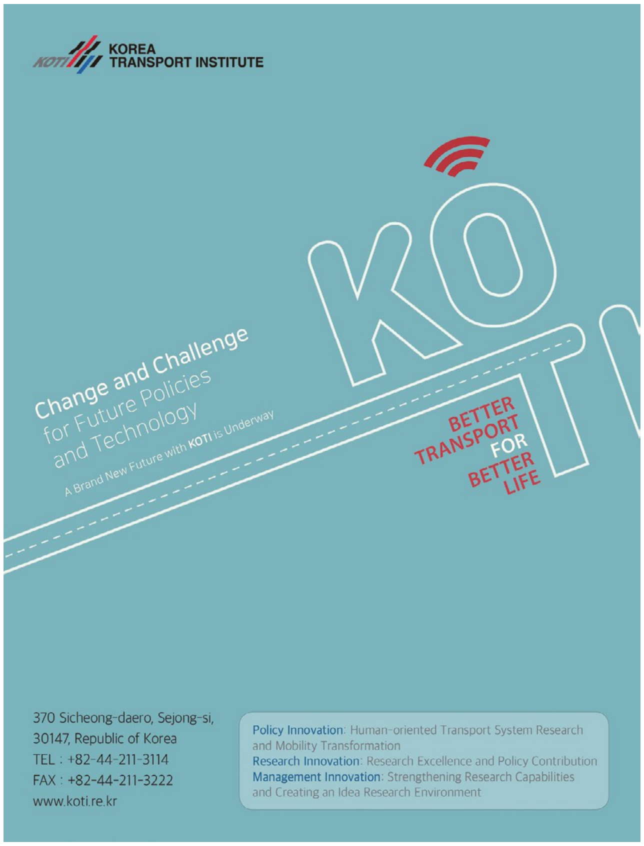

KOREA
TRANSPORT INSTITUTE
Change and Challenge
for Future Policies
and Technology
A Brand New Future with KOTI is Underway
BETTER
TRANSPORT
FOR
BETTER
LIFE
370 Sicheong-daero, Sejong-si,
30147, Republic of Korea
TEL : +82-44-211-3114
FAX : +82-44-211-3222
www.koti.re.kr
Policy Innovation: Human-oriented Transport System Research and Mobility Transformation
Research Innovation: Research Excellence and Policy Contribution
Management Innovation: Strengthening Research Capabilities and Creating an Idea Research Environment

Chemistry for US,
Chemistry for EARTH
KRICT
Towards a
Sustainable Society
Chemistry is part of life, and omnipresent in the world around us.
Chemistry creates a healthy and abundant future.
Environment-friendly chemical technology
Cutting-edge chemical materials
New drug biotechnology
Convergent new technology
Chemical platform technology
KRICT 한국화학연구원
www.krict.re.kr / international@krict.re.kr

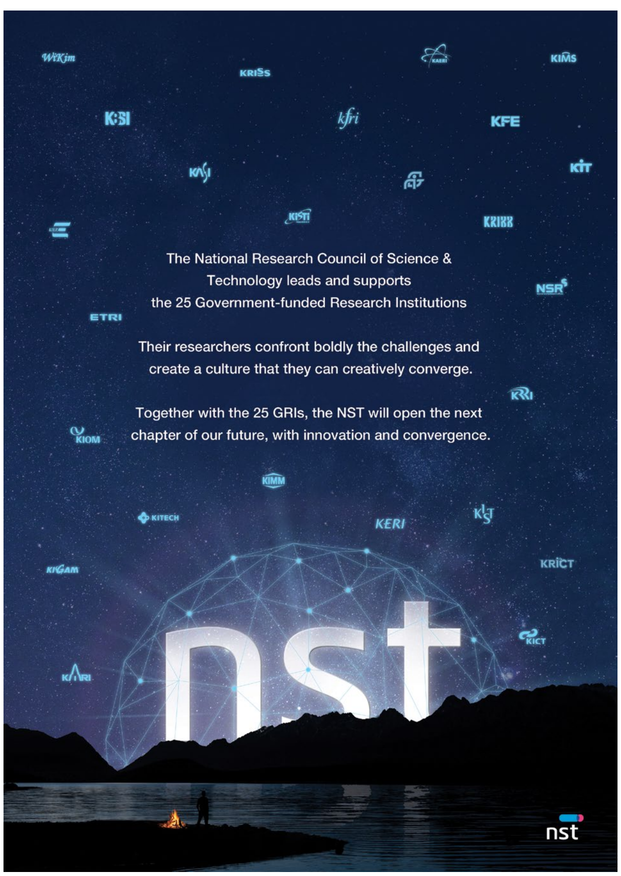

The National Research Council of Science &
Technology leads and supports
the 25 Government-funded Research Institutions
Their researchers confront boldly the challenges and
create a culture that they can creatively converge.
Together with the 25 GRIs, the NST will open the next
chapter of our future, with innovation and convergence.
nst

지구를 위한 그린플루언서 SK innovation
2030 부산세계박람회 유치
SK도 함께 노력하겠습니다
더 나은 지구와 인류의 미래를 위한 행동,
World EXPO 2030 BUSAN의 시작!
WAVE
SK innovation
Net Zero
Carbon to Green
Green Innovation
모두가 꿈꾸는 넷제로 세상,
SK이노베이션이 만들어 갑니다
Hi SK이노베이션의 그린픽쳐
SK innovation SK energy SK geo centric SK on SK enmove SK incheon petrochem SK trading international SK ie technology SK earthon

SOOKMYUNG WOMEN'S UNIVERSITY
숙명여자대학교
The World's Best Digital Humanity University
Digital Convergence Innovation
Startup Incubator Innovation
ESG Practice Innovation
HOMEPAGE
YOUTUBE
INSTAGRAM

RIGET
Research Institute for Green Energy Convergence Technology
HOMEPAGE
YOUTUBE
동남권 첨단소재산업 발전을 위한
글로벌 E4인력양성 사업
"첨단소재 산업 글로벌 인재 지역 안착 프로젝트"
< 그린에너지융합연구소장 남상용 교수 >
BK 21 Four Project
People in GNU IAM Pioneer
Energy
Extreme
Electronics
Emerging
2030 전문화된 자립연구소
2026 성장체제 연구소
2023특성화 연구소
2020 그린에너지융합연구소
1
2
3
4
GNU
경상국립대학교
중점연구소
2030로드맵

HOMEPAGE
YOUTUBE
FACEBOOK
Leading Global
Brain Research
KBRI
Korea Brain Research Institute
한국뇌연구원
Korea Brain Research Institute

KERI
The Electrified World's Hub
As the only government-funded electrotechnology research institute in Korea, KERI has conducted a wide range of activities including R&D, Testing & Certifications related to electricity.
In a new era founded on a cutting-edge electrotechnology, KERI is the core.
Power Grid
Smart Grid
Research
Industry Applications Research
Electrical Apparatus Research
Electrical Materials Research
Electro-Medical Equipment Research
Power Semiconductor Research
Testing & Certification Services
KERI KOREA ELECTROTECHNOLOGY RESEARCH INSTITUTE

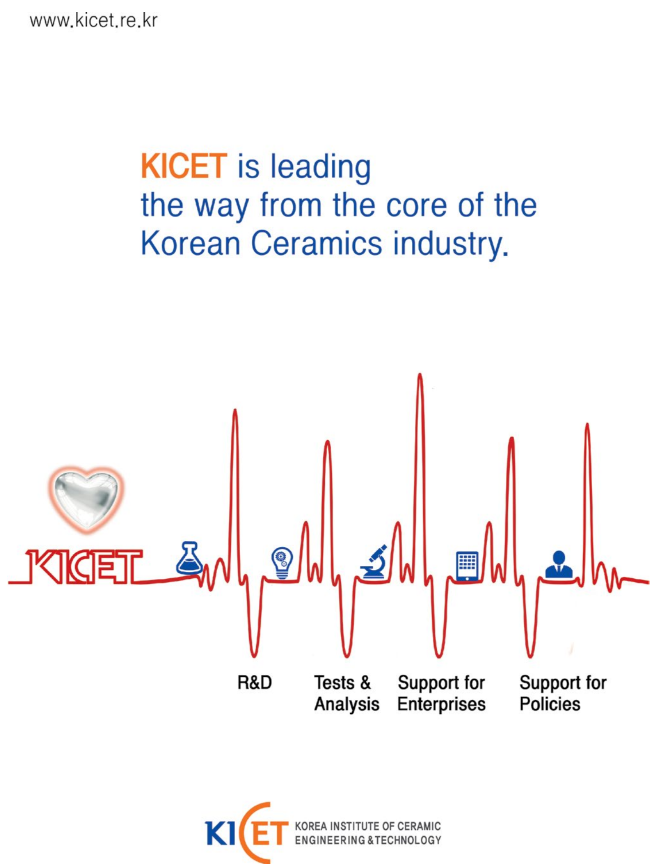

www.kicet.re.kr
KICET is leading the way from the core of the Korean Ceramics industry.
KICET
R&D
Tests & Analysis
Support for Enterprises
Support for Policies
KICET KOREA INSTITUTE OF CERAMIC ENGINEERING & TECHNOLOGY

Happiness and Wellness of Public in the Ocean
Ocean Science and Technology Contributing to Humanity
The Korea Institute of Ocean Science & Technology (KIOST) is being shaped into the world's best marine science and technology research institute through specialized research and is an organization in which the convergence of different fields is possible. We are contributing to the happiness of citizens and development of humanity with a sincere and responsible attitude.
KIOST
KIOST KOREA INSTITUTE OF OCEAN SCIENCE & TECHNOLOGY

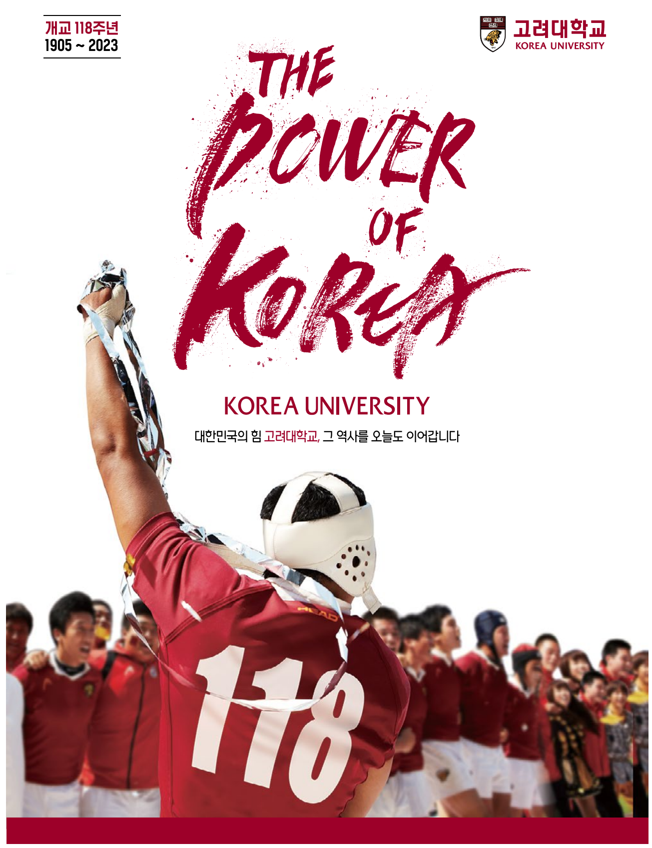

개교 118주년
1905 ~ 2023
고려대학교 KOREA UNIVERSITY
THE POWER OF KOREA
KOREA UNIVERSITY
대한민국의 힘 고려대학교, 그 역사를 오늘도 이어갑니다
118

KOSEN
전세계 한인과학기술자들의
지식 공동체 KOSEN
The Global Network of Korean Scientists&Engineers
kosen.kr
70여개국 17만명
연구자들을 만나보세요!
회원가입 바로가기 ▶
과학기술정보통신부
KISTI 한국과학기술정보연구원

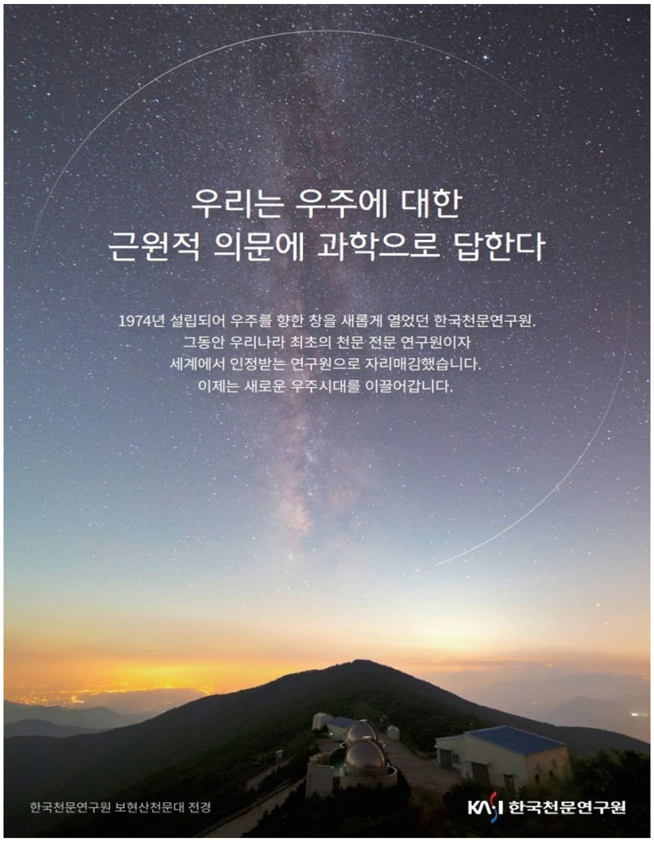

우리는 우주에 대한
근원적 의문에 과학으로 답한다
1974년 설립되어 우주를 향한 창을 새롭게 열었던 한국천문연구원.
그동안 우리나라 최초의 천문 전문 연구원이자
세계에서 인정받는 연구원으로 자리매김했습니다.
이제는 새로운 우주시대를 이끌어갑니다.
한국천문연구원 보현산천문대 전경
KASI 한국천문연구원

NEXTRON
NEXTRON
MICRO PROBE SYSTEM

WISET 한국여성과학기술인육성재단
Korea Foundation for Women In Science, Engineering and Technology
DIVERSITY & INCLUSION IN STEM
Mission & Vision
MISSION
To empower women in STEM to demonstrate their strength and contribute to social value
VISION
The world's leading institution that fosters women in STEM who will take the lead in promoting science and technology-based economic growth
Main Functions
Conducting government-commissioned projects on women in STEM
Providing educational/training programs for women in STEM
Operating career development programs
Conducting policy research and analysis on women in STEM
Improving women's representation in STEM and achieving gender equality
Communicating and collaborating with domestic and international organizations
Organization History
Organization Overview
Legal basis of establishment | Article 14 of ACT ON FOSTERING AND SUPPORTING WOMEN SCIENTISTS AND TECHNICIANS
Date of establishment | April 1, 2013
Affiliated organization of the Ministry of Science and ICT
Jan. 2011
Establishment of Center for Women in Science, Engineering and Technology
Jan. 2013
WISET established as a non-profit organization (Director Heisook Lee)
May 2013
Launching Center for Science, Engineering, and Technology Cooperatives (by Ministry of Science and ICT)
Aug. 2014
Launching Seoul Job Center for Women in Science, Engineering, and Technology & Expansion and relocation of WISET Academy (by Ministry of Gender Equality and Family)
Nov. 2022
Aree Moon inaugurated as 4th President of WISET
June. 2021
Changed the name of the organization to Korea Foundation for Women In Science, Engineering and Technology
Jan. 2017
WISET designated as a public organization
WISET

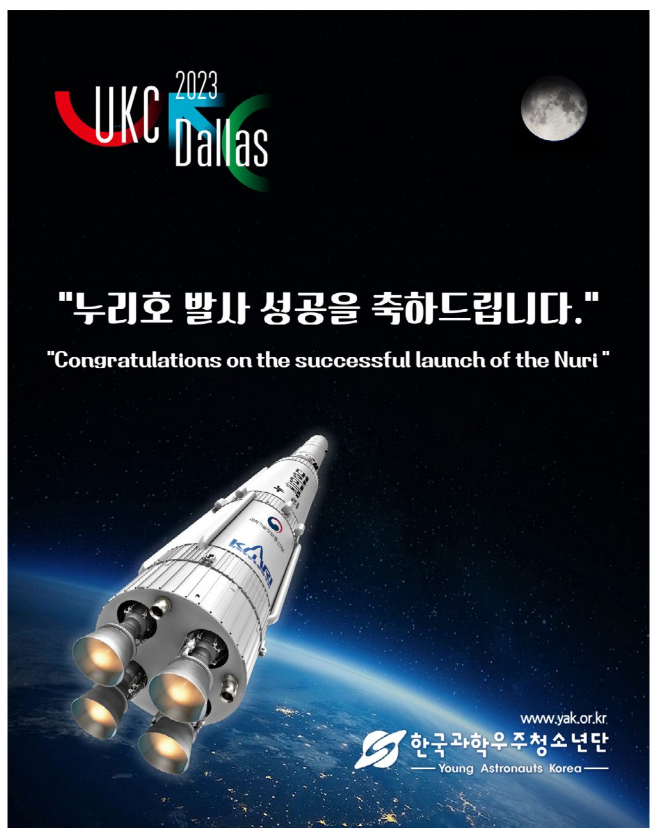

UKC 2023 Dallas
"누리호 발사 성공을 축하드립니다."
"Congratulations on the successful launch of the Nuri"
KARI
www.yak.or.kr
한국과학우주청소년단
Young Astronauts Korea

Conference Venue Map

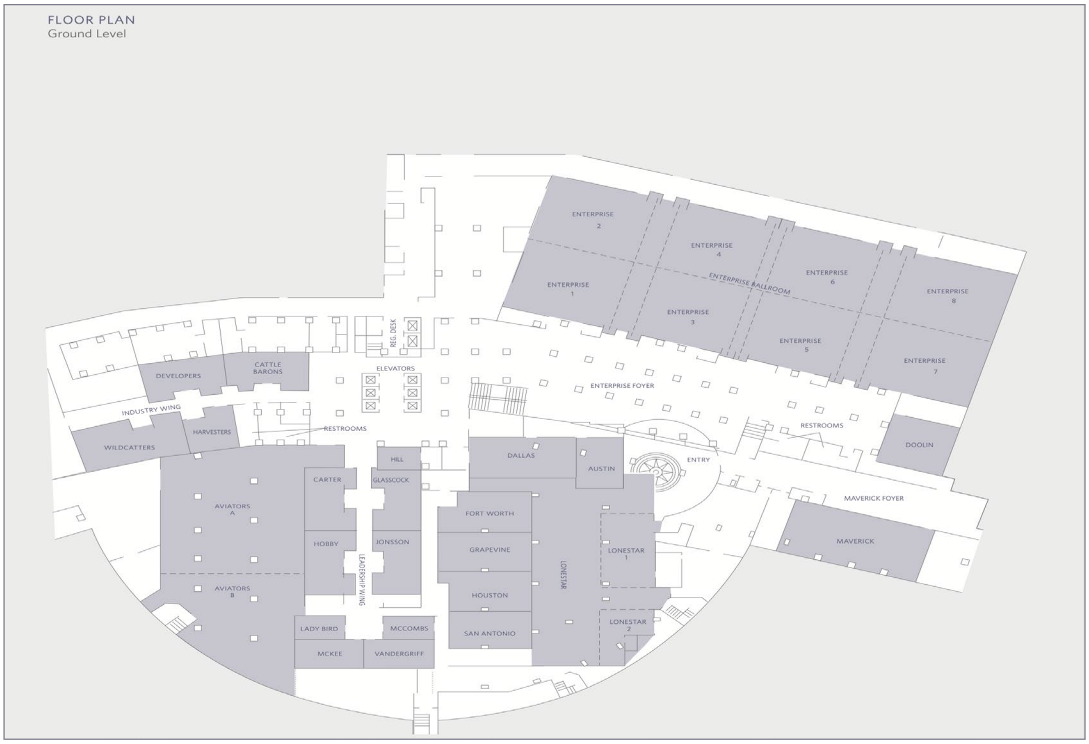

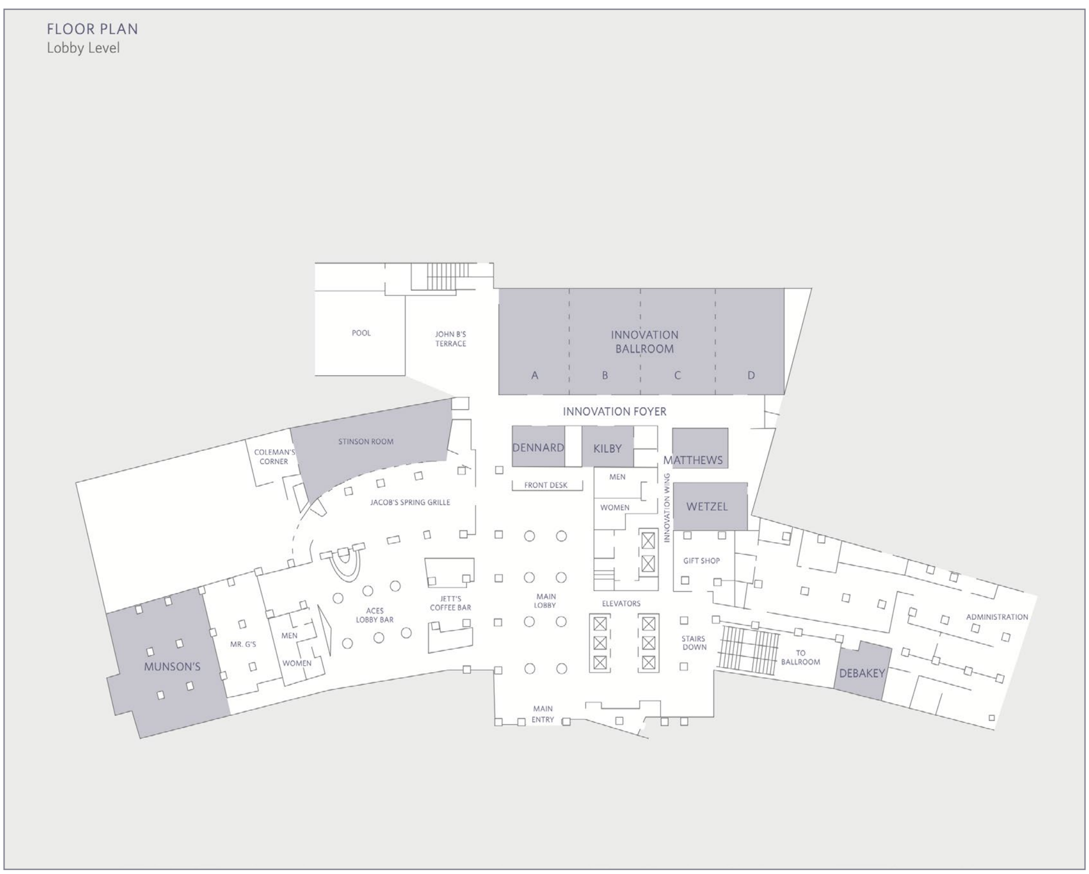

The Hyatt Regency DFW

2334 N International Pkwy, Dallas, TX 75261
(972) 453-1234

Discovery, Innovation and Dissemination for Transformative Impact

UKC 2023
US-KOREA CONFERENCE

Korean-American Scientists and Engineers Association
1952 Gallows Road, Suite 300, Vienna, VA 22182
Tel. 703-748-1221. Fax. 703-748-1331
sejong@ksea.org
www.ksea.org

Front cover image - Freepik.com.
This cover has been designed using assets from Freepik.com